The Dissertation Committee for Arthur Bryan Crawford Certifies that this is the approved version of the following dissertation:

Evaluation of the Impact of Non-Uniform Neutron Radiation Fields on the Dose Received by Glove Box Radiation Workers

Committee:

Steven Biegalski, Supervisor

Sheldon Landsberger

John Howell

Ofodike Ezekoye

Sukesh Aghara

Evaluation of the Impact of Non-Uniform Neutron Radiation Fields on the Dose Received by Glove Box Radiation Workers

by

Arthur Bryan Crawford, B.S., M.S.

Dissertation

Presented to the Faculty of the Graduate School of

The University of Texas at Austin

in Partial Fulfillment

of the Requirements

for the Degree of

Doctor of Philosophy

The University of Texas at Austin

December, 2004

Dedication

I was born to goodly parents

Harvey E. Crawford and Johnnie Lee Young Crawford

Acknowledgements

I would like to express my gratitude to Dr. Sheldon Landsberger for his vision in starting a distance learning program at the University of Texas at Austin and for his support and encouragement on this quest. I would like to thank my advisor, Dr. Steven Biegalski, for his support and encouragement even though the topic area was new to him.

I would like to thank the members of my dissertation committee for finding the time to review this dissertation. To the staff of the Nuclear Engineering Teaching Laboratory I say thank you for your kindness and support during those brief times that I was on campus.

A special thanks to my past and present group leaders, David Seidel, Eric McNamara, and Bill Eisele and my Division Leader, Lee McAtee, at Los Alamos National Laboratory, for their support in being allowed to use time and material resources at the Laboratory and for financial support in the form of tuition reimbursement and travel expenses.

A special thanks to R.T. Perry for the discussions that we had at Los Alamos. To Jim Bland, a friend and mentor, for his insights and encouragement, a profound thanks of gratitude.

And to my family for their moral support and prayers, may they be blessed in all of their endeavors.

Evaluation of the Impact of Non-Uniform Neutron Radiation Fields on the Dose Received by Glove Box Radiation Workers

Publication No._____

Arthur Bryan Crawford, PhD.

The University of Texas at Austin, 2004

Supervisor: Steven Biegalski

The effort to estimate the radiation dose received by an occupationally exposed worker is a complex task. Regulatory guidance assumes that the stochastic risks from uniform and non-uniform whole-body irradiations are equal. An ideal uniform irradiation of the whole body would require a broad parallel radiation field of relatively high-energy radiation, which many occupationally exposed workers do not experience. In reality, workers are exposed to a non-uniform irradiation of the whole body such as a radiation field with one or more types of radiation, each with varying energies and/or fluence rates, incident on the worker.

Most occupational radiation exposure at LANL is due to neutron radiation. Many of these exposures originate from activities performed in glove boxes with nuclear materials. A standard Los Alamos 2x2x2 glove box is modeled with the source material being clean weapons grade plutonium. Dosimeter tally planes were modeled to stimulate the various positions that a dosimeter can be worn. An anthropomorphic phantom was used to determine whole body dose. Various geometries of source position and phantom

location were used to determine the effects of streaming on the radiation dose a worker may receive.

Based on computational and experimental results, the effects of a non-uniform radiation field have on radiation dose received by a worker in a glove box environment are: 1) Dosimeter worn at chest level can overestimate the whole body dose between a factor of two to six depending on location of the phantom with the source material close to the front of the glove box, 2) Dosimeter should be worn at waist level instead of chest level to more accurately reflect the whole body dose received, 3) Dose can be significantly higher for specific locations of the worker relative to the position of the source, 4) On the average the testes contribute almost 44% of the whole body dose for a male, and 5) Appropriate design considerations such as more shielding on the bottom of the glove box and controls such as the use of internal or external shielding can reduce the effects on dose from these non-uniform fields.

Table of Contents

List of Tables

List of Figures

Chapter 1: Introduction

1.1 Estimation of Radiation Dose Received by a Glove Box Worker and its Associated Problems

The effort to estimate the radiation dose received by an occupationally exposed worker is a complex task. The earliest efforts were directed towards medical radiologists and technicians operating x-ray machines and the system of protection developed was based on the "tolerance dose concept" (Taylor 1981; Poston 2000). The dose estimate was based on physical observations, e.g., reddening of the skin, and the unit of measurement, threshold erythema dose (TED), was the amount of radiation that would cause this reddening of the skin. The "tolerance dose", i.e., a dose that could be tolerated, was set at 0.01 TED/month. With the establishment of the Roentgen (R) as the unit of exposure in 1924, it was determined that TED was approximately 300 to 600 R and the tolerance dose was approximately 0.1 to 0.2 R/day of exposure. A tolerance dose of 0.1 R/day was adopted as the standard. The main assumption in the use of the tolerance dose concept was the existence of a threshold value below which no injury was expected to result. This concept was abandoned in 1948 upon recognition that there may be no threshold for gene mutation effects.

The concept of "permissible dose - …the dose of ionizing radiation that, in light of present knowledge, is not expected to cause appreciable body injury to a person at any time in his lifetime." became the basis of regulatory protection regulations from the late 1940's thru the 1970's into the early 1990's (Taylor 1979). A maximum permissible dose (MPD) of 0.3 R/week was established as the new dose limit. Since the Roentgen was originally defined as a measure of the amount of ionization produced in a given volume of air by x-ray or gamma-ray radiation, it is really a unit of measurement of exposure

because it does not express the direct interaction between the radiation and the material irradiated. The rad became the new unit for absorbed dose and was defined as the amount of radiation required to cause absorption of 100 ergs of energy per gram of material. As it was realized that different radiations had varying effects on the human body, another unit, the rem, was defined to permit comparison of radiation doses from different types of radiation that produce different amounts of damage. The concept of relative biological effectiveness (RBE), i.e., the ratio of the absorbed doses of different radiations required to produce the same damage, was developed. This lead to defining a quality factor (Q), for a given radiation, that would be a conservative upper limit of the RBE for the biological effect of greatest interest. Thus the product of absorbed dose (rads) and quality factor Q is known as the dose equivalent in units of rem (Healy 1970).

In the early 1970's, the transition from radiation protection standards based on thresholds, safety factors, and permissible dose to standards based on quantitative risk assessment began. A linear, no threshold dose-response relationship was assumed for carcinogenic and genetic effects (1×10^{-04}/rem whole body for malignant illnesses and 4×10^{-05}/rem for hereditary effects) whereas absolute thresholds were assumed for all other radiation effects. Based on occupations with a high standard of safety, acceptable risk was taken as 50 deaths per million workers or a 40-year occupational lifetime risk of two fatalities per 1000 workers. Using an upper limit of 10 times this value for any individual worker, this resulted in an annual whole body dose limit of 5 rem/yr. Similarly, the effective dose equivalent H_E is the weighted sum of the mean dose equivalents for all the relevant tissues and organs and thus takes into account the different mortality risks from cancer and the risk of hereditary effects associated with irradiations of different tissues and organs. This concept of risk-based dose limits provided the rationale for the 1977 ICRP recommendations (ICRP 1977).

In the early 1990s, the Nuclear Regulatory Commission (NRC) and Department of Energy (DOE) adopted the methodology of ICRP Publication 26 (1977) used in determining the dose of occupationally exposed workers. The intent of the ICRP Publication 26, NRC's regulation 10 CFR 20 and DOE's regulation 10 CFR 835 is to prevent non-stochastic effects and minimize the occurrence of stochastic effects to an acceptable level (ICRP 1977; NRC 1991; DOE 1999). The basis of these recommendations and regulations assume that the stochastic risk from uniform and non-uniform whole-body irradiations are equal. An ideal uniform irradiation of the whole body would require a broad parallel radiation field of relatively high-energy radiation, which many occupationally exposed workers do not experience. A non-uniform irradiation of the whole body could be created by a broad parallel beam of low energy radiation incident on one side of the worker, partial shielding of the body, or a radiation field with one or more types of radiation, each with varying energies or fluence rates, incident on the worker.

There is no dosimetry device for the direct radiation dose measurement received by a worker's whole body or a specific tissue or organ. Instead, the dose from an external source of radiation can be estimated by one or more monitoring devices positioned somewhere on the surface of the worker's clothing or body. Commonly used monitoring devices, called dosimeters, can measure the type, fluence, and energy of the radiation incident on the worker's body. The Los Alamos National Laboratory (LANL) Model 8823 whole body dosimeter has been designed to perform accurate dose estimates for beta, photon, and neutron radiations that are encountered in typical field radiation conditions (Hoffman and Mallett 1999). For high-energy neutron radiation, the LANL track etch dosimeter (TED) provides better quality measurements than the Model 8823 (Hoffman 1998). The response of the dosimeter with associated dose algorithm, the

location of the dosimeter(s), and the number of dosimeters on the surface of the worker are the main components in estimating the radiation dose received by a worker.

The primary task of computational dosimetry is to simulate or model radiation environments and find methods to enhance the accuracy of the determination of absorbed dose and dose equivalent (Siebert and Thomas 1997). Monte Carlo techniques are used extensively for these models and simulations in computational dosimetry. Appendix A provides an overview of Monte Carlo methods. It is important to remember that the models and simulations are an approximation to reality; the results are only as good as the assumptions, input data, and model for any given computational condition. These analyses can provide important insights into streaming problems, shielding options, dosimetry requirements, layout or work area, and potential radiological conditions not anticipated.

In conjunction with the models or simulations of radiation environments, anthropomorphic computational phantoms are used to estimate the absorbed dose in specific organs or tissues of the body. BodyBuilder phantoms, developed from the mathematical phantom work at Oak Ridge National Laboratory (ORNL), allows the modeling of a human body with respect to the sex, selection of organs of interest, age, height, and weight including additional torso fat if desired (Van Riper 2002; Cristy and Eckerman 2003).

1.2 CURRENT PROBLEM STATEMENT

Most occupational radiation exposure at LANL is due to neutron radiation (Hoffman and Mallett 1999). Almost always, the neutron radiation fields are part of a mixed radiation field. These exposures originate from isotropic sources, nuclear materials handling, sub-critical and critical assemblies, and accelerators. Many of the research and development activities connected with nuclear materials are performed in glove boxes.

The primary purpose of a glove box is to contain radioactive and other hazardous materials and prevent the inhalation or ingestion these materials by the workers (Dooley and Kornreich 1998). The glove box isolates the material and prevents direct contact with the worker as well as the spread of contamination in the workplace. Many different materials may be used in the construction of a glove box, depending on the radioactive and hazardous materials involved (AGS 1998). A standard glove box is constructed of stainless steel with transparent viewing windows and access ports with attached gloves. The glove box has airtight seals around penetrations or interfaces between the stainless steel and viewing windows, glove port gloves, and exhaust ventilation system which creating a negative pressure atmosphere of air or an inert gas. A properly sealed and ventilated glove box will contain the hazardous material, but in the case of radioactive material, the radiation (photons and neutrons) can penetrate the walls of the stainless steel glove box, viewing windows and glove ports.

There are several methods used to reduce the radiation penetrating the stainless steel glove box walls, viewing windows, and glove ports, depending on the type and energy of radiation. Since the nominal -ray energy is low, the photons may be reduced with a relatively thin high Z material (i.e., a few millimeters to centimeters thickness of tungsten, lead or stainless steel). The high Z material may be placed around the source inside the glove box or incorporated into the structure of the glove box. Lead, when used, is usually sandwiched between plates of stainless steel that form the outer and inner surfaces of the glove box walls, excluding the glove ports and viewing windows. The viewing windows can be covered with leaded glass, but the glove ports do not normally have additional shielding for the photons, except when glove port gloves contain lead or other high Z materials. The unshielded or partially shielded glove port gloves or viewing

windows potentially create streaming paths for photons creating a non-uniform radiation field with varying fluence rates and energy distribution.

The shielding for neutrons requires different types of material than used for photon shielding. Low Z materials, several inches thick, are used for neutron shields. It is common for the entire external surface of the glove box to be covered with four to six-inch thick transparent Lucite™ and Plexiglas™, except the glove ports or other penetrations. This transparent shield permits glove box workers to look into the glove box to perform work or inspect the contents or process. The non-shielded or partially shielded portions of the glove box give rise to a neutron-streaming path and thus create a non-uniform radiation field external to the glove box.

The estimation of radiation dose is performed in accordance with ICRP 26. The ICRP 26 risk-based dosimetry system deals with tissue risk coefficients and corresponding tissue weighting factors to assess tissue dose equivalent and to calculate effective dose equivalent. This system is based on the assumption that the stochastic risk is the same for a uniform whole body irradiation and the sum of individual weighted tissue irradiations (ICRP 1977). The risk factors for different tissues are based upon the estimated likelihood of inducing fatal malignant disease, non-stochastic changes, or substantial genetic defects in descendants. Table 1.1 provides the risk factors for each tissue or organ with their corresponding weighting factors that represent the proportion of the stochastic risk resulting from tissue T.

Effective dose equivalent (H_E) is calculated using $H_E = \sum_T w_T \cdot H_T$ where H_T is the dose equivalent in tissue and w_T is the weighting factor for each tissue. This is then compared to the whole body dose limit of 50 mSv (5 rem). This methodology is used because it forms the current basis of federal law (NRC 1991), which is the basis for DOE regulatory requirements. This risk-based dosimetry system was modified by the most

recent comprehensive recommendations of ICRP (Publication 60) (ICRP 1991). Although the use of this "new" system has been questioned at length (Dietze 1998; Thomas 1997; Thomas 1998), this methodology is being adopted by many countries (not including the United States) in their regulatory requirements. Since it has not been codified into federal law, calculations or estimates of radiation dose in accordance with these new recommendations will only be provided for comparison to ICRP 26 values.

Table 1.1: Weighting Factor Determination Based on ICRP 26.

Tissue	Effect	Risk coefficient (Sv^{-1})	w_T
Gonads	Hereditary (1^{st} and 2^{nd})	4×10^{-3}	0.25
Breast	Cancer	2.5×10^{-3}	0.15
Red Bone Marrow	Leukemia	2.0×10^{-3}	0.12
Lung	Cancer	2×10^{-3}	0.12
Thyroid	Cancer	5×10^{-4}	0.03
Bone Surface	Cancer	5×10^{-4}	0.03
Remainder	Cancer	5×10^{-3}	0.3 *
		1.65×10^{-2} (1.25×10^{-2} without gonads)	

* Limit for any single tissue in remainder category is 0.06. Rank order remainder organs/tissues and apply 0.06 to the first five organs/tissues. Note: Lens of eye, skin, hands and forearms, feet and ankles are not to be included in the "Remainder".

ICRP acknowledges the use of dose equivalent as determined by dosimeters worn by the occupational worker as an acceptable means to determine the effective dose equivalent (HPS 1997). The current practice for most radiation fields is the use of a single dosimeter. Radiological glove box workers are trained to wear the whole-body dosimeter on the front of their body between their shoulders and their waist. The dosimeter may be worn on a lanyard or clipped to the worker's clothing. Wearing the dosimeter on a lanyard will usually locate the dosimeter mid-chest to upper abdomen; however, it also permits the dosimeter to rotate out of position even when the glove box worker is facing the radiation source.

The criteria for determining the type and number of dosimeters worn by occupational workers should be determined as a result of radiological surveys to assess the workplace radiation field variability (Brown 1997) coupled with computational modeling of the workplace conditions. The HPS N13.41-1997 standard lists several conditions that may indicate a need for multiple dosimetry. These can be summarized as two main conditions: 1) non-uniform radiation field due to partial shielding or streaming, and 2) variability in radiation field. Thus, a major concern is whether dose equivalent is correctly being estimated by the dosimeter(s) worn so that a viable estimate of effective dose equivalent can be determined, especially in a glove box environment where the radiation source will produce a non-uniform mixed radiation field.

The radiation source term of interest is either weapons-grade plutonium (> 90% ^{239}Pu or heat source plutonium (^{238}Pu). The age and purity of the plutonium will determine the composition of the radionuclides that make up the source, and in conjunction with the surrounding materials, will dictate the initial photon and neutron energy spectrums and the fluence rate for each radiation in the mixed field (Brown 1997). The neutron component of the source term is from the spontaneous fission of certain plutonium nuclides and ^{241}Am and (α,n) reactions with low Z materials within the glove box. The photon component arises from radioactive decay, spontaneous fission, fission products, and (n,γ) reactions. The radiation sources for this modeling are generated using ORIGEN-S (Gauld, Hermann, and Westfall 2002) to calculate nuclide decay and photon energy spectra and SOURCES (Wilson *et al.* 2002) to calculate the neutron energy spectra. The radiation fields are evaluated using Monte Carlo transport code MCNPX™ (Hendricks *et al.* 2003). MCNPX was created by combining the capabilities of LAHET™ (Prael and Lichtenstein 1989) and MCNP™ (Briesmeister 2000) into one code and was accomplished by extending the capabilities of MCNP (Monte Carlo Neutral Particle) to

all particles and energies and including physics models where table-based data was not available. Radiation dose is estimated using MCNPX (Monte Carlo Neutron Particle Extended) and anthropomorphic phantoms for various irradiation geometries.

Additionally, a dosimeter tally plane can be modeled to simulate the various positions that a dosimeter can be worn. This will allow for the estimated dose at each location to be compared to the whole-body dose calculated using the phantom. Also, additional "dosimeters" could be modeled to simulate whether multiple dosimetry provides a better estimate of dose.

1.3 PREVIOUS STUDIES INVOLVING ESTIMATION OF DOSE RECEIVED IN NON-UNIFORM RADIATION FIELDS

1.3.1 Overview

In the past, the major concern of dosimetry in radiation protection has been the external exposure of the workforce to gamma radiation while the realm of high LET radiations, particularly neutrons, has been considered to be in a state of disarray (Thomas 1998). This is evidenced in the literature by a preponderance of articles pertaining to photon dosimetry with few pertaining to neutron dosimetry. Thus, this review will include appropriate articles dealing with photon dosimetry.

There are many factors influencing the assessment or estimation of tissue dose equivalent and effective dose equivalent for externally irradiated workers. The major factors are the methodology used to calculate tissue dose equivalent and effective dose equivalent, the radiation field geometry including the orientation of the worker to the radiation and the distance between the worker and the radiation source(s), the location of a single or multiple dosimeters worn by the worker, fluence to dose conversion coefficients, partial irradiation of the worker's body caused by streaming or created by

structures, equipment or shielding material, and the uniformity or lack thereof of the energy and fluence rate of the radiation field.

1.3.2 Photons

Until 1991, the recommendations of ICRP 26 represent the methodology to calculate tissue dose equivalent and effective dose equivalent (Kramer and Drexler 1982; Drexler, Williams, and Zankl 1985). Since 1991, the recommendations of ICRP 60 have started to replace ICRP 26 as the methodology to calculate effective dose (Zankl, Petoussi, and Drexler 1992; Zankl and Drexler 1995). There have been several computational studies dealing with the relationship of the radiation field incident on a worker's body and the estimation of dose equivalent for various tissues and of whole-body effective dose equivalent (Reece, Poston, and Xu 1994; Kim, Reece, and Poston 1998; Kim, Reece, and Poston 1999). These studies dealt with the proposed methodology and conversion coefficients to estimate tissue dose equivalents and effective dose equivalent or effective dose the worker might receive for a given irradiation scenario. The radiation fields evaluated were from broad parallel beams or disk floor sources or point source geometries that would approximate a uniform field utilizing Monte Carlo transport codes and anthropomorphic computational phantoms to evaluate the radiation dose for the various geometries.

The radiation dose quantities from external irradiation cannot be directly measured, so the measurement of the radiation dose is made at the surface of the body with the use of conversion coefficients and algorithms to estimate the tissue dose and whole body dose. (Kim, Reece, and Poston 1999). Fluence-to-dose conversion coefficients have been established by Monte Carlo transport codes calculations for various irradiation geometries. ANSI/ANS-6.1.1-1991 (ANS 1991) established and used ICRP 51 (ICRP 1987) fluence-to-dose factors for photons incident on an

anthropomorphic phantom for a range of photon energies and the following geometries: anterior-posterior, posterior-anterior, lateral, rotational and isotropic exposures. ICRP 74 (ICRP 1996) developed external radiation fluence-to-dose conversion coefficients that incorporated the concept of individual ICRP 60 tissues of highest risk for the following irradiation conditions: anterior-posterior, posterior-anterior, right lateral, left lateral rotational and isotropic exposure.

Typically, the radiation field is assumed uniform for most work conditions or studies with respect to fluence rate, energy distribution, and conversion coefficients corresponding to the external irradiation scenario. The anterior-posterior irradiation condition of a parallel-broad photon beam creates the highest effective dose equivalent (effective dose) than the other irradiation projections (Reece, Poston, and Xu 1994; Kim, Reece, and Poston 1999). The studies performed on other types of uniform radiation fields, such as point or disk photon sources, demonstrate relationships of estimated effective dose equivalent (effective dose) dose for certain locations of the radiation source and orientation to a male or female. The irradiation orientation to phantoms suggest individuals, males and females, will receive a higher effective dose equivalent from a frontal irradiation than from the lateral or posterior-anterior, at least for photon energies with 1 MeV or less (Reece, Poston, and Xu 1994; Kim, Reece, and Poston 1998).

When the body shields the dosimeter, the individual's effective dose equivalent could be underestimated by as much as 60% to 90% for photon energies ranging from 1 MeV to 0.08 MeV (Reece and Xu 1997). Fluence-to-dose conversion factors can vary significantly depending on the location and orientation of the dosimeter, and the direction of the irradiation incident on the body. The location of a dosimeter on the front torso and

a given incident photon geometry can impact the measured absorbed dose on the surface of the body (Zankl 1999).

While a personal dosimeter on the chest can significantly underestimate worker dose, using an extra dosimeter on the back and taking a weighted average of these two dosimeter readings can fix the underestimation problem (Kim and Reece 2000). However, this approach can overestimate the effective dose for the lateral, over-head and underfoot beam directions.

1.3.3 Neutrons

Until 1991, the recommendations of ICRP 26 represent the methodology to calculate tissue dose equivalent and effective dose equivalent (Endres *et al*. 1987; Tanner *et al*. 1992). Since 1991, the recommendations of ICRP 60 have started to replace ICRP 26 as the methodology to calculate effective dose (Hollnagel, Alberts and Dietze 1994; Meinhold 1992; Portal and Dietze 1992; Morstin, Kopec and Schmitz 1992). There have been several computational studies dealing with the relationship of the radiation field incident on a worker's body and the estimation of dose equivalent for various tissues and of whole-body effective dose equivalent (Hollnagel 1992; Drake and Bartlett 1997; Shores 1999; George and Shores 2000). These studies dealt with the proposed methodology and conversion coefficients to estimate tissue dose equivalents and effective dose equivalent or effective dose the worker might receive for a given irradiation scenario. The radiation fields evaluated were from broad parallel beams, PuBe neutron sources, and from typical working environments found at nuclear power reactors.

One of these studies (George and Shores 2000) illustrates at least three different methods to calculate the effective dose equivalent (EDE or H_E). The first method used to calculate H_E was based on pre-calculated fluence-to-dose conversion factors. The fluence was determined at a plane having the same horizontal and vertical dimensions as the

computational phantom in method 3 in addition to a volume element having the same dimensions as the LANL TLD. The second method was based on calculating the energy deposition in a computational anthropomorphic phantom and folding in appropriate quality factors and tissue weighting factors. Method 3 employed pre-calculated fluence-to-dose conversion factors to calculate Deep Dose Equivalent (DDE) in mathematical shapes that simulate the human body. The DDE values were then weighted by compartment factors specified in ANSI N13.41 to calculate an H_E. The calculated neutron EDE rates based on pre-calculated fluence-to-dose conversion factors yielded results similar to the energy deposition method. The neutron EDE rate based on the simulated human body compartment's DDE was significantly higher than the energy deposition model.

As with photons, fluence-to-dose conversion coefficients have been established by Monte Carlo transport codes calculations for various irradiation geometries with ANSI/ANS-6.1.1-1991 (ANS 1991) and ICRP 74 (ICRP 1996) as the primary sources. Unlike photons, fluence-to-dose conversion factors are dependent upon the relative biological effectiveness (RBE) of neutrons and its variation with energy and how quality factors are determined (Cross and Ing 1985; Sinclair 1990; Van Dam *et al*. 1992; Hall and Brenner 1992). Although conversion coefficients relating neutron fluence to dose equivalent have been tabulated in many different formats and have been specified for many different phantoms and despite the significant changes in the definitions of the radiation protection quantities that have taken place, interestingly, the neutron conversion coefficients have remained nearly invariant for more than 40 years (McDonald, Schwartz, and Thomas 1998).

Plutonium glove box workers usually wear a minimum of two dosimeters, a torso dosimeter and a wrist dosimeter (in lieu of a finger dosimeter). The torso dosimeter is a

custom designed Model 8823 whole-body TLD dosimeter that contains two Harshaw/Bicron-NE TLD cards and accurately measures dose equivalent estimates for beta, gamma and neutron radiations (Hoffman 1998, and Hoffman and Mallett 1999). The Model 8823 whole-body dosimeter's physical design and accompanying computational dose algorithm will determine the tissue dose equivalent at 7 mg/cm^2 (shallow- dose equivalent), 300 mg/cm^2 (lens-of-the-eye dose equivalent) and 1000 mg/cm^2 (deep dose equivalent). This dosimeter meets the requirements in 10CFR835 *Occupational Radiation Protection* (DOE 1999) and is accredited for all performance testing categories in the Department of Energy Laboratory Accreditation Program (DOELAP) for external dosimetry.

1.4 OBJECTIVES

Since most worker occupational exposure at LANL is due to neutron radiation, it is important to understand the differences in calculating dose using either ICRP 26 or ICRP 60 and which one is more conservative. If the dose calculated is too conservative, this has both a psychological impact as well as a productivity impact. If the dose calculated is not conservative, then a true safety concern exists. This research will evaluate the impact of non-uniform neutron radiation fields on assessing the tissue dose equivalents (equivalent dose) and effective dose equivalent (effective dose) of individuals working at a glove box workstation or in the vicinity of glove boxes. To accomplish this, a computational analysis for a typical LANL glove box will be performed with the following objectives:

i. Evaluate the neutron radiation field distribution at various distances from a glove box for various radiation source locations inside the glove box.

ii. Evaluate the tissue dose equivalent and effective dose equivalent received by anthropomorphic computational phantoms at various distances and locations from a glove box containing neutron emitting radiation sources.

iii. Evaluate the fluence rate and neutron energy field incident on pseudo-dosimeter tally cells positioned at various surface locations of the phantom.

iv. Compare results of i - iii.

Chapter 2: Monte Carlo Calculations for Estimating Dose Received

2.1 MONTE CARLO METHOD

2.1.1 Use of Random Sampling

The Monte Carlo method is distinguished from other techniques in numerical analysis by the use of random sampling to construct the solution of a physical or mathematical problem (Carter and Cashwell 1975). In its simplest form, Monte Carlo consists of simulating a finite number of histories through the use of random numbers, or more appropriately a pseudorandom number generator. In each history, random numbers are generated and used to sample suitable probability distributions that describe the physical or mathematical problem at hand (Lewis and Miller 1993).

Perhaps the earliest documented use of random sampling to find the solution to a mathematical problem was that of Comte de Buffon in 1777 (Kalos and Whitlock 1986). Although random sampling has been used to solve different mathematical problems since then, the Monte Carlo method is generally attributed to scientists working on the development of nuclear weapons at Los Alamos during the 1940's (Briesmeister 2000).

For the neutron, photon, electron, or coupled neutron/photon/electron transport, this method has evolved with digital computers and at Los Alamos, it is known today as the Monte Carlo N-Particle (MCNP) method. There are two different versions available: the standard version, MCNP5 (X-5 Monte Carlo Team 2003) and an extended version MCNPX (Hendricks 2003) that allows for the transport of more energetic neutrons, photons, and electrons as well as other particles. Quite often, either version is often referred to as just MCNP.

2.1.2 Probability Density Function and the Cumulative Distribution Function

"Life" of a neutron or photon, from its birth to its death, is governed by nature via many random processes (Lux and Koblinger 1991). Indeed, for an individual particle, neither the "birth" of the particle nor its location (if the source cannot be represented as a point source), nor its initial flight direction or energy or flight distance to its next interaction (collision) or the type of interaction and whether it is scattered or absorbed can be determined in advance. However, probability distributions can be determined for these random variables that describe the life of a particle.

Typically, x represents some property of a particle history, such as flight distance, that may take on a range of values. If the probability that x will have a value between a and b is $P(a \le x \le b)$, a probability density function (PDF) f(x) can be defined as the limit of

$$f(\mathrm{x})\Delta\mathrm{x} = P(\mathrm{x} \le \mathrm{x}' \le \mathrm{x} + \Delta\mathrm{x}) \tag{2.1}$$

as $\Delta\mathrm{x} \to 0$. Thus $f(\mathrm{x})\Delta\mathrm{x}$ represents the probability that x' will take on a value between x and x + Δx . Since probability is a number between 0 and 1, then f(x) •0, and

$$\int_a^b f(x)dx = P(a \le x \le b) \tag{2.2}$$

with the requirement that f(x) be normalized; i.e.

$$\int_{-\infty}^{\infty} f(x)dx = 1 \tag{2.3}$$

if x can take on any real value between -• and •. If the domain values are restricted between x^- and x^+, then

$$\int_{x^-}^{x^+} f(x)dx = 1. \tag{2.4}$$

The probability that the random variable x' is less than or equal to x is given by the cumulative probability distribution function (CDF)

$$F(x) = P(x' \le x) = \int_{-\infty}^{x} f(x')dx'. \tag{2.5}$$

From equation 2.5 it is clear that

$$\lim_{x\to\infty} F(x) = F(\infty) = 1, \tag{2.6}$$

$$\lim_{x\to 0} F(x) = F(0) = 0. \tag{2.7}$$

Using equations 2.2 and 2.5

$$P(a \le x' \le b) = F(b) - F(a). \tag{2.8}$$

Often, it is more convenient to write equation 2.5 in differential form

$$\frac{dF(x)}{dx} = f(x). \tag{2.9}$$

2.1.3 Transformation of Random Variables

Often in Monte Carlo calculations, it is desirable to transform from one random variable to another, such as from speed to energy distribution for neutrons. Let *f(x)* be the PDF for the random variable *x* and let *g(y)* be the PDF for the random variable y, then $f(x)dx$ is the probability that *x* is between *x* and $x + dx$ and $g(y)dy$ is the probability that y is between *y* and *y+dy*. Since it is desired that the probability not change because of the transformation, then the following condition must be satisfied

$$\left| f(x)dx \right| = \left| g(y)dy \right|, \tag{2.10}$$

or since f(x) > 0 and g(y) > 0,

$$g(y) = f(x)\left|\frac{dx}{dy}\right|. \tag{2.11}$$

In particular, consider the case *y=F(x)*, the CDF of the random variable x. Then equation 2.11 becomes

$$g(F) = f(x)\left|\frac{dx}{dF}\right|. \tag{2.12}$$

Using equation 2.9 to evaluate the derivative above

$$g(F) = 1, \qquad 0 \le F \le 1. \tag{2.13}$$

Since *g(F)* is the PDF of the random variable *F*, equation 2.13 states that the probability of F taking on a value between F and $F + dF$ is just dF. Thus, F is uniformly distributed between zero and one.

Using a pseudorandom number generator that produces sequences of numbers that are uniformly distributed between zero and one, *F(x)* is then sampled in an unbiased manner by setting

$$F(x) = \xi . \tag{2.14}$$

However, it is the distribution of *x* that needs to be sampled. Therefore the inversion

$$x = F(\xi)^{-1} \tag{2.15}$$

must be performed. There are many techniques that can be used to perform this inversion.

2.1.4 Pseudorandom Number Generator

The selection of the path length, angle of scattering, and many other parameters is made using a pseudorandom number generator. MCNP uses the linear congruential scheme of Lehmer (1951) though the mechanics of implementation have been modified for portability to different computer platforms (X-5 Monte Carlo Team 2003).

The modified Lehmer's scheme generates a pseudorandom sequence of integers I_n by

$$I_{n+1} = (GI_n + C) \bmod 2^M, n = 0,1,... \tag{2.16}$$

where G is the random number multiplier, I_0 is the initial random seed, C is an additive constant, and M-bit integers and M-bit floating point mantissas are assumed. The random number is then

$$R_n = 2^{-M} I_n . \tag{2.17}$$

where MCNP implements the above algorithm using either 48-bit integers (the default) or 63-bit integers. The starting random number for history *k* is

$$I_0^k = [G^{kS} I_0 + C(G^{kS} - 1)/(G - 1)] \bmod 2^M \tag{2.18}$$

where S is the random number stride, that is, the number of random numbers allocated to each single history. Successive random numbers for history k are then

$$I_{n+1}^{k} = (GI_{n}^{k} + C) \bmod 2^{M} \tag{2.19}$$

where the default values of G, M, I_0, S, and C, which can be changed with the RAND card, are

$$\begin{aligned} G &= 5^{19} = 19{,}073{,}486{,}328{,}125 \\ M &= 48 \\ C &= 0 \\ S &= 152{,}917 \\ I_0 &= 1 \end{aligned} \tag{2.20}$$

2.2 MONTE CARLO SAMPLING TECHNIQUES

2.2.1 Sampling Techniques

There are many techniques to perform the inversion of equation 2.15. These include sampling distribution transformations (discrete or continuous), transformation of random variables, numerical transformations, rejection techniques, composition of random variable transformations, multivariate distributions, the Metropolis, Rosenbluth, Rosenbluth, Teller and Teller M(RT)^2 algorithm (Kalos and Whitlock 1986). The first four techniques are the most relevant to particle transport.

2.2.2 Sampling of Discrete Probability Distribution

The way in which a random number between 0 and 1 is used to choose an event from a discrete probability distribution is as follows. Consider the selection of whether a neutron is supposed to interact by one of the following six types of reactions:

1. (n, n), elastic scattering with cross section σ_s and probability p_1
2. (n, n'), inelastic scattering with cross section σ_I and probability p_2

3. (n,γ), radiative capture with cross section σ_γ and probability p_3
4. (n,α), (n, p), …, charged particle with cross section $\sigma_4 = \sigma_\alpha + \sigma_p$ … and probability p_4
5. (n, 2n), (n, 3n), …, n producing with cross section $\sigma_5 = \sigma_{2n} + \sigma_{3n}$… and probability p_5
6. (n, f), fission with cross section σ_f and probability p_6

where the total microscopic cross section is the sum of the possible reaction cross sections

$$\sigma_t = (\sigma_s + \sigma_I + \sigma_\gamma + \sigma_\alpha + \ldots + \sigma_{2n} + \ldots + \sigma_f) \tag{2.21}$$

and the probabilities are defined by

$$\begin{aligned} p_1 &= \sigma_s/\sigma_t, \\ p_2 &= \sigma_i/\sigma_t, \\ p_3 &= \sigma_\gamma/\sigma_t, \\ p_4 &= \sigma_\alpha/\sigma_t + \sigma_p/\sigma_t + \ldots, \\ p_5 &= \sigma_{2n}/\sigma_t + \sigma_{3n}/\sigma_t + \ldots, \text{ and} \\ p_6 &= \sigma_f/\sigma_t \end{aligned} \tag{2.22}$$

respectively with $p_1 + \ldots + p_6 = 1$.

This case of discrete probabilities can be illustrated graphically by assigning a variable x on the interval $0 \le x < n$ (n = 6 in this case) to the above events $E_1, \ldots, E_n$ with the agreement that $j-1 \le x < j$ represents the event E_j. A probability density function p(x) can be constructed by the definition $p(x) = p_i$ where $i-1 \le x < i$ for i = 1, 2, … , n. Thus, p(x) is a step function similar to that shown in Fig. 2.1.

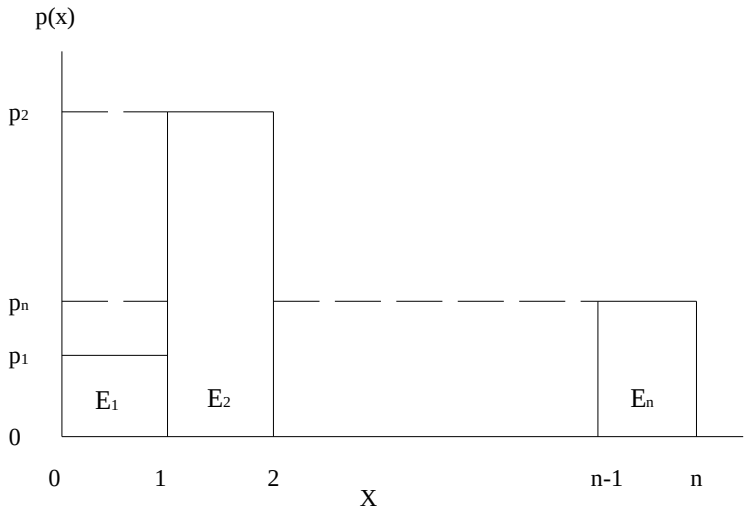

Figure 2.1: Discrete Probability Density Function.

The CDF P(x) for the above PDF p(x) is shown in Fig. 2.2, a monotone increasing broken-line function.

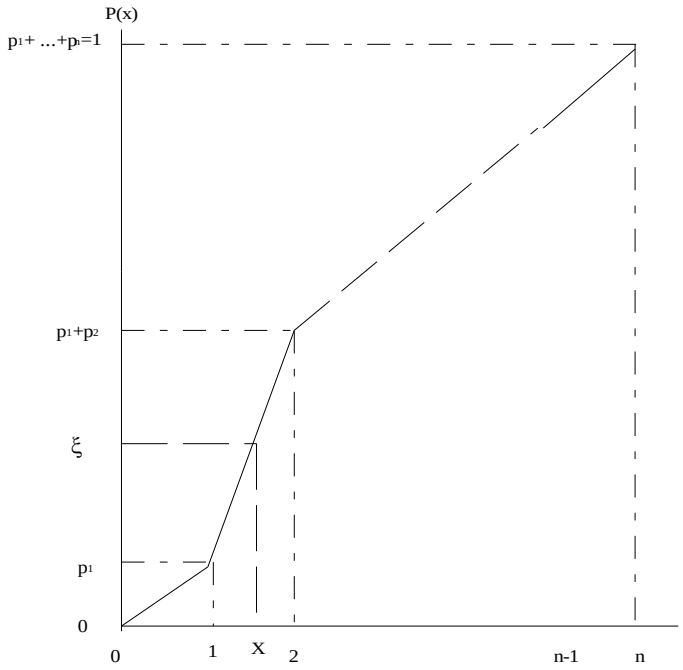

Figure 2.2: Discrete Cumulative Probability Density Function.

Thus, P(x) can be interpreted as the probability of the inequality $x \leq i$, for i = 1, 2, …, n. For a random number ξ distributed uniformly over the interval, $0 \leq \xi < 1$, and if x falls on the interval $j-1 \leq x < j$, i.e., x such that $P(j-1) \leq \xi < P(j)$, then $\xi = P(x)$ determines the event E_j.

2.2.3 Sampling of an Invertible Continuous Probability Distribution Function

Consider sampling the distance to collision of a particle. The probability of a first collision between *s* and $s + ds$ along the flight path is given by

$$p(l)dl = e^{-\Sigma_t l}\Sigma_t dl \tag{2.23}$$

Setting

$$\xi = P(s) = \int_0^s p(l)dl = 1 - e^{-\Sigma_t s}, \tag{2.24}$$

it follows that

$$s = -\frac{1}{\Sigma_t}\ln(1-\xi). \tag{2.25}$$

Since $1-\xi$ is distributed as ξ, then

$$s = -\frac{1}{\Sigma_t}\ln(\xi). \tag{2.26}$$

That is, a random variable transformed as the natural logarithm of a uniform random variable is distributed exponentially.

All cumulative probability distribution functions that arise from properly defined probability distribution functions are invertible, numerically if not analytically (Bielajew 2001).

2.2.4 Histogram or Tabulated Values Technique for a Continuous PDF

Although $\xi = P(x) = \int_a^x p(t)dt$ determines x uniquely, it is often difficult to find the inverse $x = P^{-1}(\xi)$. Sometimes the CDF *P(x)* can be computed for specific values; other times the PDF *p(t)* is given as numerical data. In either of these cases, one can

subdivide the interval [a, b] such that $x_0 = a < x_1 < ... < x_n = b$ and then use tabulated values of $P_i = P(x_i)$ at the points of subdivision. Thus, for a random number ξ, uniformly distributed over [0,1], the interval $[x_{j-1}, x_j]$ that x falls into can be determined. By interpolation, if j is the first value of the index for which $\xi - P_j$ is negative, then the value of the parameter x is determined to be

$$x = x_j - \frac{P_j - \xi}{P_j - P_{j-1}}\left(x_j - x_{j-1}\right). \tag{2.27}$$

This is basically the same method used for the discrete PDF and is a common numerical transformation.

2.2.5 Rejection Techniques

An alternate method of sampling makes use of the fact that the CDF (equation 2.5) represents the area under the curve of *f(x)* over the interval from -• to x. The simplest rejection technique is illustrated by considering a PDF *f(x)* such that:

$0 \bullet f(x) \bullet M$ for all $x \in (a, b)$, and (2.28)

$f(x) = 0$ for $f(x)$ outside of (a, b). (2.29)

Therefore the area under the curve of *f(x)* is enclosed within the rectangle defined by $0 \le y \le M$ and $a < x < b$.

To find a point (x, y) distributed uniformly within the rectangle, two random numbers, $_1$ and $_2$ are chosen. The x value is selected uniformly within (a, b) by

$$x = a + (b - a)\xi_1, \tag{2.30}$$

and the y value is selected uniformly within [0, M] by

$$y = M\xi_2. \tag{2.31}$$

If $y > f(x)$, the point is rejected and another point is selected. If $y < f(x)$, the point is accepted and the random variable is set to *x*.

The efficiency of this technique is just the area below the graph to that of the rectangle. Since the area under the graph is one by definition of the PDF, then the efficiency is just

$$E = \frac{1}{M(b-a)}. \tag{2.32}$$

Although in principle this technique will work for any PDF, the efficiency may be too low in a given case for practical use. It should be note that one does not need to find the inverse of the CDF in this technique.

More general rejection techniques involve finding a trial value of a random variable and then subjecting this value to one or more tests involving one or more random variables. It may then be accepted or rejected. If rejected, the cycle of choosing and testing another trial value is repeated until an acceptance takes place (Kalos and Whitlock 1986).

2.3 ANALOG MONTE CARLO SAMPLING

2.3.1 Monte Carlo Modeling of Neutron Motion

The movement of neutrons in a material is simulated by analog Monte Carlo by mimicking as precisely as possible the physical phenomena involved in such movement. First, the problem must be defined including such factors as the geometry and the neutron source. Once defined, the random walk of the neutrons through the geometry may be executed. The results of each random walk are used to calculate the detector response that is modeled by the calculation (Profio 1979; Dupree and Fraley 2002).

2.3.2 Problem Definition

The physical description of the problem geometry and the material constituents is essential; all flight paths, particle interactions or escapes are based on this description. Describing a complex geometry accurately and ensuring that all regions are defined with

respect to the bounding surfaces is one of the most arduous tasks in preparing input for a Monte Carlo problem (Profio 1979). To help in this task, interactive geometry editors/viewers, such as MORITZ, have been developed for MCNP (Van Riper 2002).

The physical description of the source may be a PDF that describes the source geometry and the distribution of neutrons within the source region or may be a specific set of start points with associated directions and energies. The initial starting neutron for each history arises from this definition and not from prior interactions.

2.3.3 Random Walk

The random walk (Dupree and Fraley 2002) begins with a neutron being selected from the source distribution and assigned an initial position, energy, and direction of travel. Normally a weight of 1.0 is initially assigned to the neutron.

The path length or distance to next collision, i.e. the collision site, is determined from the exponential distribution of collisions along the flight path. The probability of collision per unit path length is determined from the cross sections of the materials through which the neutron travels (Section 2.2.3).

At the collision site, the specific nuclide involved in the collision is determined based on a proportionate division of the total cross section among the nuclides present. The specific interaction is determined based on the cross section of the nuclide chosen (Section 2.2.2). Alternative techniques include averaging or mixing the cross sections of the nuclides present to form one set of cross sections that contain all the features of all the nuclides present or doing a multi group formulation where a table of group averaged cross sections is used in connection with a set of discrete energy bins.

Results of the interaction selected include one or more of the following alternatives: death of the neutron (reduction of the weight by the non-absorption probability); scattering of the neutron with scattering angle determined from the

scattering characteristics of the nuclide encountered; or production of secondary particles, including fission.

The initial neutron and all secondary particles (or a statistically valid sample from them) are tracked similarly. This process continues until the initial neutron and all secondary particles produced die or escape from the geometry.

The detector response that is modeled is usually calculated during the random walk. The number of histories, i.e. initial starting neutrons, is chosen so that the relative error is less than 0.1 and preferably less than 0.05 (Briesmeister 2000; X-5 Monte Carlo Team 2003).

2.3.4 Detector Response

During the random walk the expected value or the mean of some random variable, most often related to scalar flux, current distribution, or another variable sought from the solution of the transport equation, is calculated. Results are obtained by assigning a score x_i (x_i = particle flux, particle track length, particle energy deposition or particle heating etc., associated with the i^{th} random walk) to each random walk.

Suppose *f(x)* is the PDF for selecting a random walk that scores *x* to the tally being estimated. The true mean is

$$E(x) = \int x f(x) dx \tag{2.33}$$

and is estimated by the sample mean

$$x_N = \bar{x} = \frac{1}{N} \sum_{i=1}^{N} x_i \tag{2.34}$$

where x_i is the value of *x* selected from *f(x)* for the i^{th} history and N is the number of histories. The Monte Carlo mean $\bar{x}$ is the average value of the score x_i for all the histories in the problem and is called a tally. Thus as the Monte Carlo calculation proceeds, we

tally the x_i due to each history in order to calculate the sample mean at the end of the calculation.

In MCNP, there are six tally types for neutrons: F1:n for surface current, F2:n for surface fluence, F4:n for cell fluence, F5:n for fluence at point or ring detector, F6:n for energy deposition, and F7:n for fission energy deposition. For these tally types, Table 2.1 gives the tally type, what estimator is used for calculating the tally, and the units that the tally is given in.

Table 2.1: Tally Types.

Tally Type	Estimator	Units (per source particle)
F1:n Surface Current	W	#
F2:n Surface Fluence	$W/(\lvert\mu\rvert * A)$	#/cm^2
F4:n Cell Fluence	$W * \lambda/V$	#/cm^2
F5:n Detector Fluence	$W*p(\mu)*exp(-s)/2\ R^2$	#/cm^2
F6:n Energy Deposition	$W* * {}_T(E)*H(E)* {}_a/m$	Mev/gm
F7:n Fission Energy Deposition	$W* * {}_f(E)*Q* {}_a/m$	Mev/gm

where

W = particle weight,

E = energy of particle (MeV),

p(μ) = probability density function,

μ= cosine of angle between surface normal and trajectory of particle,

= track length (cm),

S = total mean free path to detector (cm),

R = distance to detector (cm),

$_T$(E) = microscopic total cross section (barns),

$_f$(E) = microscopic fission cross section (barns),

H(E) = heating number (MeV/collision),

Q = fission heating Q-value (MeV),

$_a$ = atom density (atoms/barn-cm),

M = cell mass (gm),

A = surface area (cm^2), and

V = cell volume (cm^3).

All MCNP tallies (except in criticality problems) are normalized to one starting source particle. Each tally must be scaled to the desired source strength. The fluence (particles/cm^2) is of paramount importance because it can be converted into absorbed dose or dose equivalent if the differential energy distribution is known.

2.3.5 MCNP Precision

The results from the Monte Carlo simulations represent averages of contributions from many histories sampled during the calculations; therefore MCNP (Briesmeister 2000) does ten statistical checks of the tallies to verify the stochastic behavior of the sampling and to provide assurance that the confidence interval for each tally is acceptable. The quantities involved in these checks are the estimated mean, relative error (R), variance of the variance (VOV), figure of merit (FOM), and the large history score behavior of *f(x).*These ten statistical checks are printed in the Tally Fluctuation Chart (TFC) at the end of the output file.

MEAN $x_n \, or \, \bar{x}$

1. Random behavior should be exhibited; i.e., a non-monotonic behavior (no up or down trend) in the estimated mean as a function of the number histories n for the last half of the problem.

RELATIVE ERROR *R*

The measure of how close the mean is to the true physical quantity being estimated (accuracy, systematic error, or bias) cannot directly be estimated by MCNP. Factors that affect the accuracy are: physics models used in the code, physical modeling of source and geometry, and user errors and abuse of the code.

The uncertainty in the estimated mean $\bar{x} = x_n$ caused by the statistical fluctuations in the sampled $x_i's$ is estimated by MCNP and reported as the relative error

$$R \equiv \sigma_s / x_n = \left[\frac{1}{n} \left(\frac{\overline{x^2}}{x_n^2} - 1 \right) \right]^{1/2} . \tag{2.35}$$

where $_s$ is the standard deviation of the mean x_n and $\overline{x^2} = \frac{1}{n} \sum_{i=1}^{n} x_i^2$, the average of the sum of the squares of the tally scores x_i. Thus, the following checks are made on the estimated relative error R:

2. Acceptable magnitude of R < 0:05 for a point detector tally or < 0:10 for a non-point detector tally);
3. R should be monotonically decreasing as a function of the number histories n for the last half of the problem; and
4. Specifically, R should decrease as $1/\sqrt{n}$ for the last half of the problem.

VARIANCE OF VARIANCE (VOV)

The VOV is

$$\sum_{i=1}^{n} (x - \bar{x})^4 / \left[n (\sum_{i=1}^{n} (x - \bar{x})^2)^2 \right] - 1/n \tag{2.36}$$

and involves the first four history score moments. It should decrease as 1/n. The following checks are made on the VOV:

5. The magnitude of the estimated VOV should be less than 0.10 for all types of tallies;

6. VOV should be monotonically decreasing as a function of n for the last half of the problem; and
7. Specifically, VOV should decrease as 1/n for the last half of the problem.

FIGURE OF MERIT (FOM)

Since $R^2 \propto 1/n$ and the computational time $T \propto n$, then the figure of merit

$$FOM = 1/R^2T \tag{2.37}$$

should be constant with n. The measure of how quickly the desired precision is achieved is called the efficiency and increases with larger FOM values. The following checks are made on the FOM:

8. FOM should approach a statistically constant value as a function of n for the last half of the problem; and
9. FOM should exhibit non-monotonic behavior as a function of n for the last half of the problem.

HISTORY SCORE PDF

A history score PDF is generated using a logarithmic score grid for accumulating history scores. Six hundred bins are established (60 decades with 10 log bins per decade) and the probability for each bin j is calculated as follows:

$$f(x_j) = \frac{number\ of\ scores\ in\ bin\ j}{(N)(\Delta x)} \tag{2.38}$$

where N is the number of histories and x is the bin width. MCNP applies a curve fitting routine to the 201 largest history scores. If *f(x)* is unbounded, then it must decrease faster than $1/x^3$ for the second moment of f(x) to exist. Otherwise, the variance becomes infinite. The curve fitting routine assumes a Pareto shape for the PDF tail

$$f(x) = a^{-1}(1 + kx/a)^{-(1/k)-1} \tag{2.39}$$

where the slope

$$m \equiv (1/k) + 1. \tag{2.40}$$

The following check in made on the history score PDF:

10. The SLOPE m of the history scores x should be greater than 3.0 so that the second moment will exist if the SLOPE is extrapolated to infinity.

The seven N-dependent checks for the TFC bin are for the last half of the problem. The last half of the problem should be well behaved (in the sense of the Central Limit Theorem) to form the most valid confidence intervals. “Monotonically decreasing" in checks 3 and 5, allows for some increases in both R and the VOV. Such increases in adjacent TFC entries are acceptable and usually do not, by themselves, cause poor confidence intervals. A TFC bin R that does not pass check 3, by definition, does not pass check 4. Similarly, a TFC bin VOV that does not pass check 6, by definition, does not pass check 7.

2.4 MODIFICATIONS TO ANALOG MONTE CARLO SAMPLING

2.4.1 Problems with Analog Monte Carlo Sampling

Since analog Monte Carlo is based on mimicking as precisely as possible the physical processes of neutron transport (i.e. what nature does), it can suffer the same problems as an actual physical experiment. In an actual experiment, only a fraction of the emitted particles may reach the region of interest. This can result in low count rates in the detector necessitating longer count times or many repetitions of the experiment in order to obtain good statistics. In the equivalent numerical experiment one is forced to increase the number of particle histories or simulations in order to have good statistics (i.e. reducing the variance); however, the computational time may be prohibitive.

Thus variance reduction techniques have been developed to modify the analog simulation process in such a way that more particle simulations have non-zero

contributions to the detector response or score while keeping the expected results of the analog and modified simulations identical (Lux and Koblinger 1990).

2.4.2 Variance Reduction Techniques

Variance reduction techniques that have been developed (Booth 1985) include:

- Geometry Splitting/Russian Roulette;
- Energy splitting/Roulette
- Implicit Capture and Weight Cutoff
- Forced Collisions
- Angle Biasing
- Source Biasing
- Point vs. Ring Detector
- Weight Window – Space-Energy Dependent Splitting/Roulette
- Exponential Transform

For this dissertation, the variance reduction techniques used were Source Biasing and Implicit Capture.

Source biasing maintains the physics of an isotropic distribution while aiming more particles in the preferred direction but with reduced weight. This is accomplished by sampling from an exponential function in the cosine of the angle with respect to a specified reference direction. Weights assigned to particles are adjusted so as to preserve the weight that would have been assigned without source biasing in place. Thus, more particles are sent toward the region of interest.

Implicit capture is synonymous with absorption by weight reduction. Instead of allowing a particle to be absorbed, the particle always survives the collision but with a weight *w* modified by the survival probability shown in equation 2.41

$$w = w\,(1 - \frac{\sigma_{ai}}{\sigma_{ti}}) \tag{2.41}$$

where $_{ai}$ and $_{ti}$ are the microscopic absorption cross section and total microscopic cross section for nuclide i respectively. This allows for more particles to reach the region of interest instead of being killed off before getting there.

Chapter 3: Computational Experiment for Typical LANL Glove Box

3.1 OBJECTIVES

The computational experiment for a typical LANL glove box consisted of the following:

i. Construct a model of a typical LANL glove box.

ii. Evaluate the neutron radiation field distribution at various distances from a glove box for various radiation source locations inside the glove box.

iii. Evaluate the tissue dose equivalent and effective dose equivalent received by anthropomorphic computational phantoms at various distances and locations from a glove box containing neutron emitting radiation sources.

iv. Evaluate the fluence rate and neutron energy field incident on pseudo-dosimeter tally cells positioned at various surface locations of the phantom.

v. Compare results of ii - iv.

3.2 EXPERIMENTAL SETUP

3.2.1 Description of Glove Box

A standard 2x2x2 LANL glove box is two workstations deep, two stations wide and two stations high where a typical workstation represents one pair of glove ports or about 71.12 to 81.28 cm (28 to 32 inches) in depth and width per workstation. The body of the glove box is approximately 152.4 cm x 162.6 cm x 114.3 cm (60• x 64" x 45") and the bottom of the glove box is approximately 106.7 cm (42•) above the floor. The sides of the shell of the glove box is constructed of an inner layer of 0.47625 cm ($^{3}/_{16}$•) type 304 stainless steel, a middle layer of 0.635 cm (¼") lead, an outer layer of 0.3175 cm ($^{1}/_{8}$")

stainless steel while the top and bottom of the shell were constructed of 0.47625 cm ($^{3}/_{16}$") stainless steel. The windows were constructed of 0.79 cm ($^{5}/_{16}$") boroscillate glass.

This standard glove box needs to be modified if the source term has a significant neutron and/or photon components. If the glove box already exists, then it is easier to hang shielding materials on the outside of the glove box in the thickness required to reduce the dose to acceptable levels. This is usually done using low Z materials such as polyethylene for neutrons, lead blankets for photons, or using movable shields. If possible, it is better to design the required shielding into the glove box before it is built. Normally, the box is designed to attenuate the photons first and then designed to attenuate the neutrons. This is because in normal operations, the dose from photons can be orders of magnitude higher than that from neutrons.

In designing the shell of a glove box, there are two approaches that are normally taken as depicted in Figs. 3-1 and 3-2.

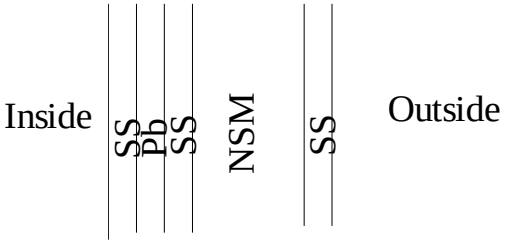

Figure 3-1: Shell Design A.

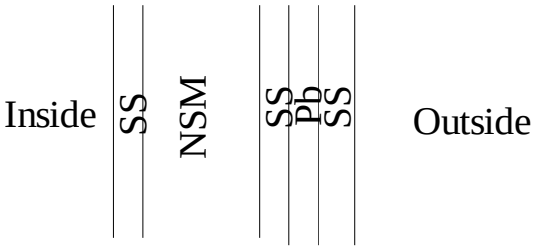

Figure 3-2: Shell Design B.

Both of these designs add another layer of stainless steel and a layer of neutron shielding material (NSM). Historically, shell design A depicted above has been used with no documentation as to why. Shell design B with the lead (Pb) layer closest to the outside was chosen for this glove box. This provides for shielding of the photons created by neutrons interactions in the neutron shielding material. Layers of stainless steel 304 (SS) is used on both sides of the Pb and the NSM layers.

The thickness of the NSM layer and the material used is dependent on many factors with the primary factor being the reduced reach inside the glove box by the worker for increasing shell thicknesses. Most glove box workers can tolerate a shell thickness between two and three inches and still perform work inside the box. For this glove box, a 5.08 cm (2 in.) thickness of the NSM was chosen with a resulting total shell thickness of 6.67 cm ($2^{10}/_{16}$").

The choice of neutron shielding material was based on the attenuation of dose due to neutrons provided by the material. Appendix A provides the methodology used to determine the attenuation for several different neutron shielding materials. The material chosen was a mixture of NS-3, Pb, and B_4C (34% NS-3, 65% Pb, and 1% B_4C) (Dargis 2003) that has actually been used before and is not just a theoretical composition. The half-value thickness for this material is 2.4 cm (0.95 in).

The upper and lower panels on each long side contain four glove ports, each with a radius of 10.16 cm (4"). Between each pair of glove ports is a small viewing window 16 cm x 26.67 cm (6.3" x 10.5"). In the slanted middle panel of the glove box are two large viewing windows between the upper and lower glove ports on the left and right side. For each pair of glove ports, the centers of the glove ports are 43.18 cm (17") apart.

The base of the glove box was 2.54 cm (1 in.) stainless steel while the top was 0.47625 cm ($^3/_{16}$") stainless steel. The bottom of the glove box is 103.99 cm (40.94") off

the floor. The floor was taken to be 30.5 cm (1 ft) of concrete. The top of the glove box is 220.35 cm (86.75") above floor level. The glove box legs were not modeled.

The vertical dimension 'z' was taken so that z = 0 was floor level. The 'x' dimension was taken such that positive 'x' pointed out from the glove box. The glove box has mirror symmetry about the vertical plane containing x=0 and y = 0. Figs. 3-3 to 3-5 depict the typical 2x2x2 LANL glove box as modified above to provide more neutron shielding. A computational phantom is shown at the middle of the glove box.

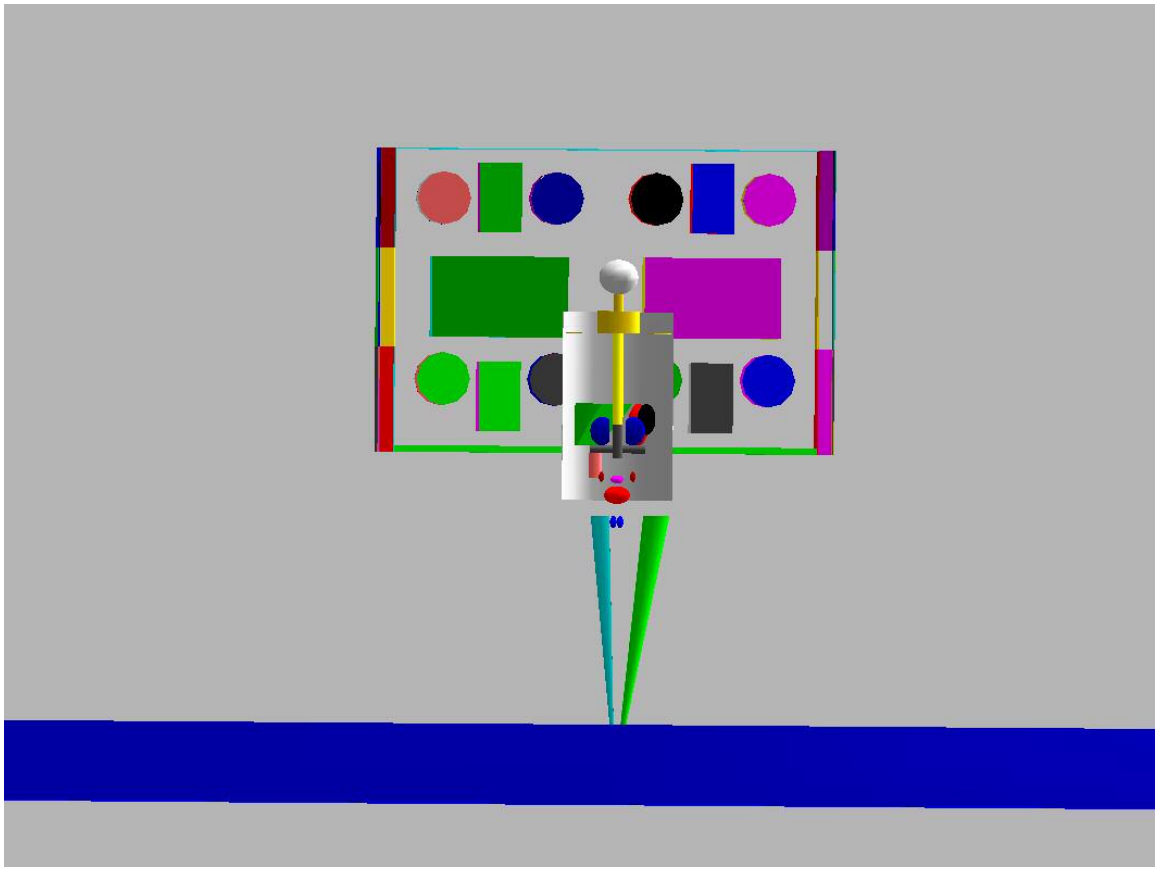

Figure 3-3: Typical 2x2x2 LANL Glove box – Front View.

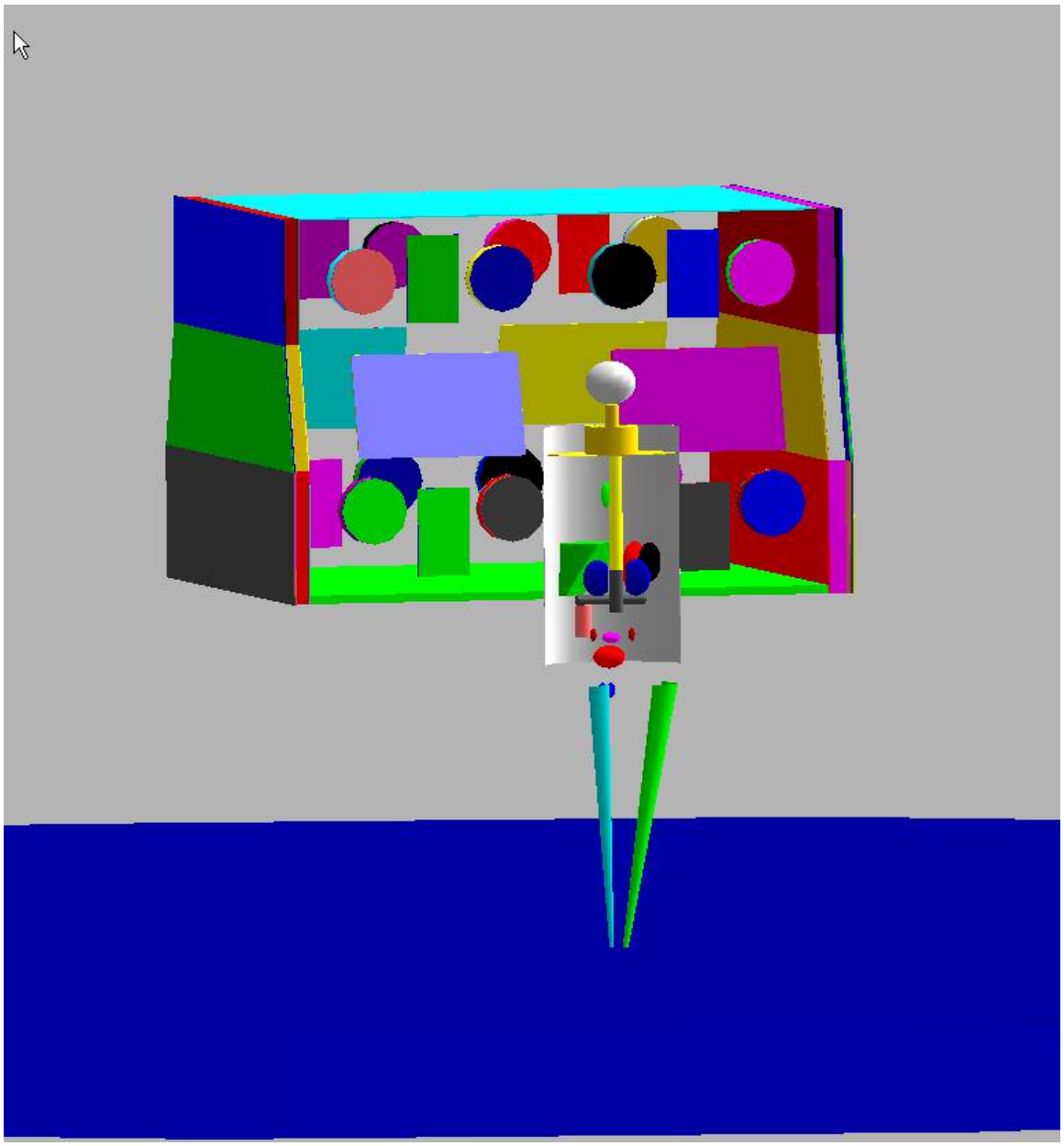

Figure 3-4: Typical 2x2x2 LANL Glove box – 3D View.

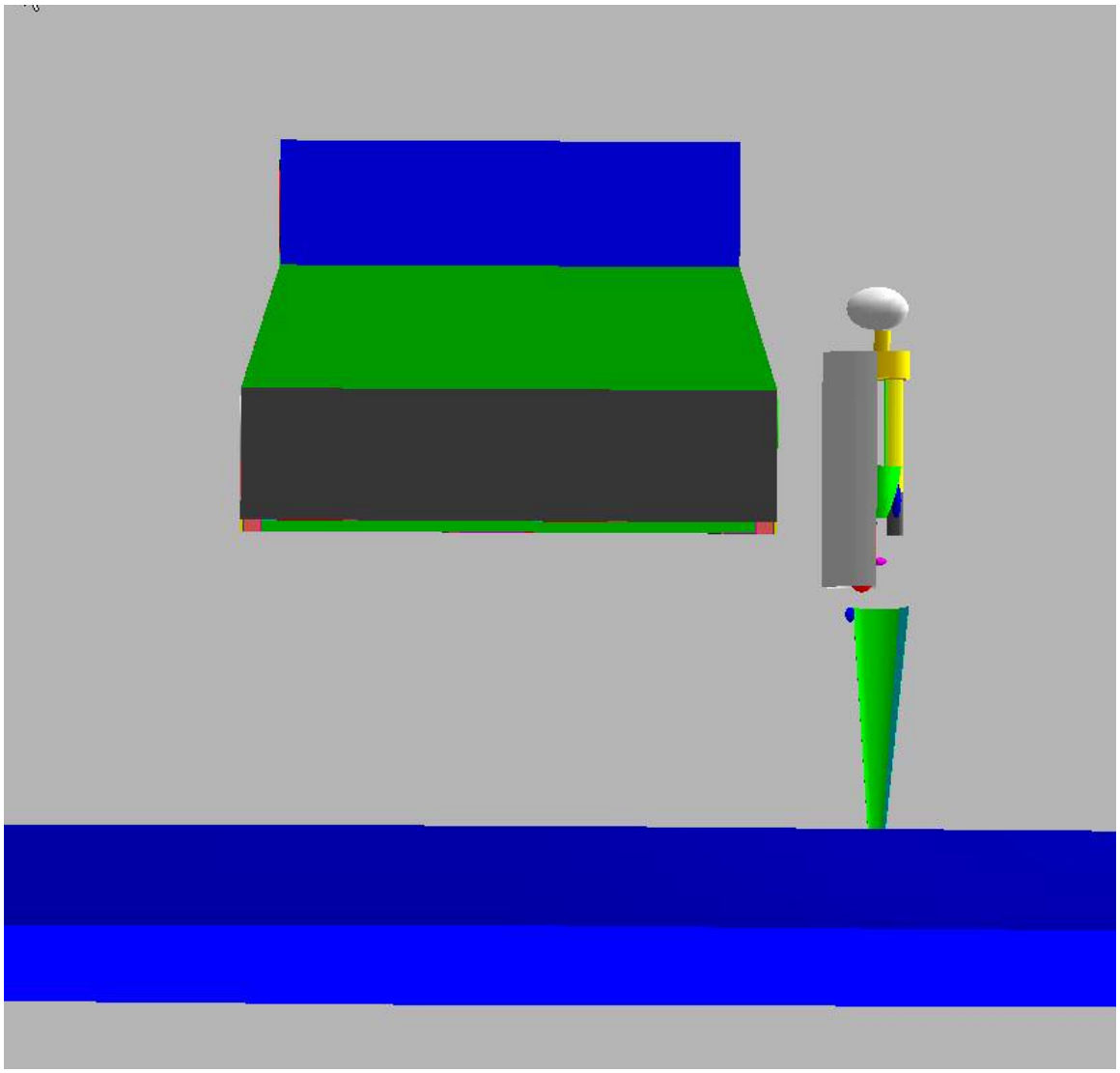

Figure 3-5: Typical 2x2x2 LANL Glove box – Side View.

3.2.2 Description of Computational Phantom

In conjunction with the glove box model developed above and the desire to simulate the radiation environment around the glove box, an anthropomorphic computational phantom is used to estimate the absorbed dose in specific organs or tissues of the body. BodyBuilder phantoms, developed from the mathematical phantom work at

ORNL, allows the modeling of a human body with respect to the sex, selection of organs of interest, age, height, and weight including additional torso fat if desired (Van Riper 2002; Cristy and Eckerman 2003).

The phantom was 179 cm (70.5 ") tall and had a weight of 73.54 kg (161.8 pounds). In Figs. 3-3 to 3-5, the gray shield in front of the phantom is the dosimeter tally surface used to simulate the different positions a dosimeter can be worn on the body between neck and waist level. This surface is a cylindrical surface 16.8 cm from the centerline of the phantom. Fig.3-6 provides a longitudinal medial view of the phantom. Beside it is the dosimeter lattice that is placed over and around the torso of the phantom. The lattice consists of 8 cm x 8 cm squares, each represents a dosimeter location. The highlighted tally represents the middle of the torso where the dosimeter is most likely worn.

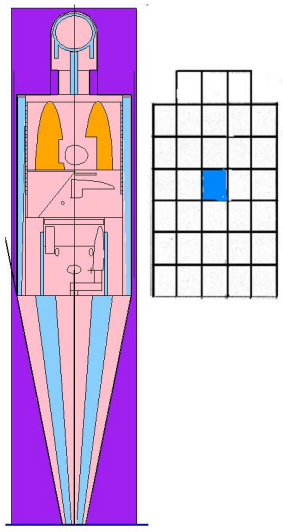

Figure 3-6: Longitudinal Medial View of Phantom and Dosimeter Tally Plane.

3.2.3 Neutron Source

The neutron energy spectrum for 1 kg of clean Weapons Grade (WG) Pu with isotopic content given in Table 3-1 was calculated using Sources 4C. The total neutron emission was 6.359 x 10^{+04} neutrons/s per kg of Pu and had a mean energy of 1.94 MeV. The neutron energy spectrum is given in Table 3-2 and Fig. 3-7.

Table 3-1: Isotopic Content of Neutron Source.

Nuclide	Pu-238	Pu-239	Pu-240	Pu-241	Pu-242	Am-241
Wt%	0.03	93.71	5.96	0.25	0.03	0.02

Table 3-2: Neutron Energy Spectrum.

Energy (MeV)	n/s/kg	Energy (MeV)	n/s/kg
1.000E-08	0	3.000E+00	2.965E+03
1.000E-02	2.649E+01	3.300E+00	2.454E+03
2.000E-02	4.820E+01	3.600E+00	2.013E+03
5.000E-02	2.180E+02	4.000E+00	2.113E+03
1.000E-01	5.232E+02	4.400E+00	1.588E+03
2.000E-01	1.424E+03	5.000E+00	1.650E+03
4.000E-01	3.716E+03	6.000E+00	1.501E+03
6.000E-01	4.309E+03	7.000E+00	6.667E+02
8.000E-01	4.535E+03	8.000E+00	2.864E+02
1.000E+00	4.545E+03	9.000E+00	1.198E+02
1.300E+00	6.550E+03	1.000E+01	4.898E+01
1.700E+00	7.862E+03	1.200E+01	2.743E+01
2.100E+00	6.656E+03	1.500E+01	4.633E+00
2.400E+00	4.189E+03	2.000E+01	2.651E-01
2.700E+00	3.546E+03	Total	6.359E+04

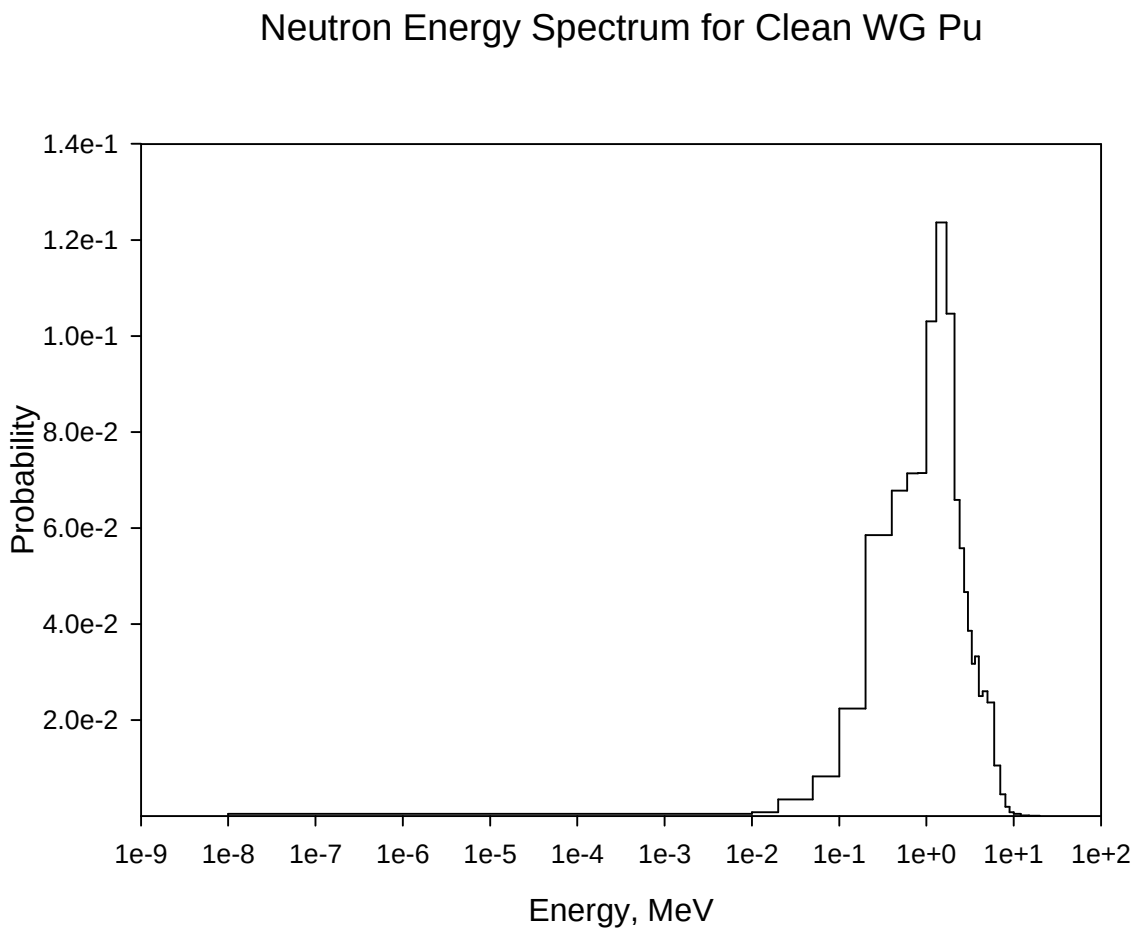

Figure 3-7: Neutron Energy Spectrum for Clean WG Pu.

3.2.4 Setup to Determine Neutron Radiation Field and Associated Dose at Selected Locations

Mesh tallies at 30.5 cm and 91.5 cm (1 ft and 3 ft) from the front of the glove box were used to determine the neutron radiation field for different source locations. The source locations were determined by a grid within the glove box. The grid was formed three lines parallel to the x-axis and 11 lines parallel to the y-axis. The line S is 6 cm from the left side of the glove box while the lines V and M went through the gloveport

viewing window (V) and the middle (M) of the glove box. The numbers labeling the lines parallel to the y-axis represent the distance in cm from the inside surface of the front of the glove box. The 33 source locations were the intersections of these lines.

A computational phantom representing a worker was located at one of six places determined by the intersection of the lines S, V, and M with the mesh tally lines at 30.5 cm and 91.5 cm (1 ft and 3 ft). Besides calculating the whole body dose using the computational phantom, each phantom had a dosimeter tally lattice associated with it as described above that allowed the calculation of the dose a dosimeter would measure at various locations on the torso of a worker. Fig. 3-8 shows a phantom located at the intersection of M and 30.5 cm (1 ft) lines and the source (marked by 'x') at the intersection of the lines labeled V and 15.

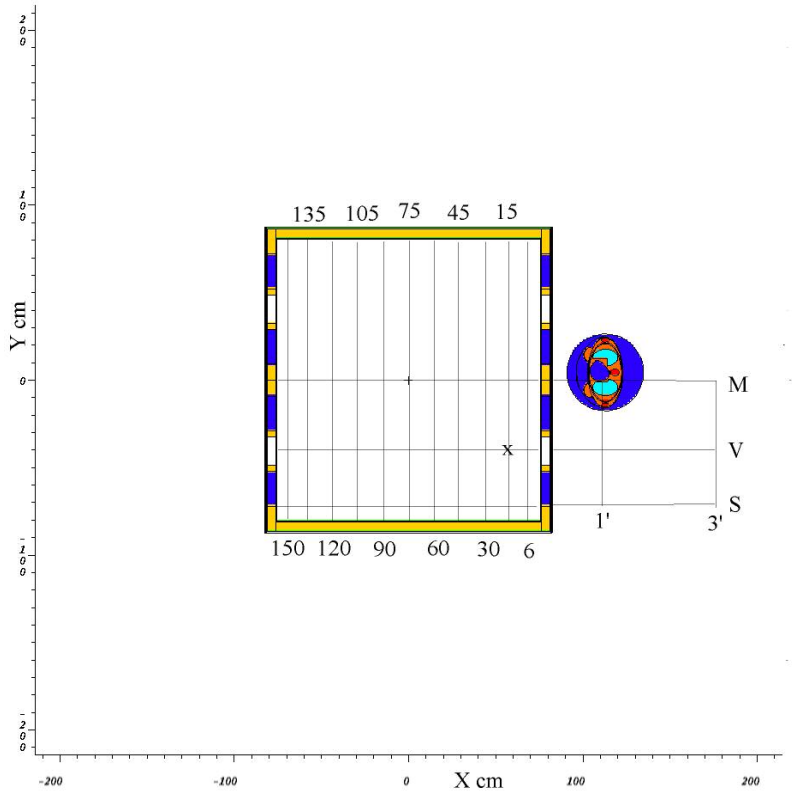

Figure 3-8: Setup to Determine Neutron Radiation Field.

3.2.5 Estimating Whole Body Dose Using Computational Phantom and F6 Tally

By the nature of the simulation, MCNP builds up a picture of the radiation field and determines the fluence (particles/cm^2) at a desired tally location. All MCNP tallies (except in criticality problems) are normalized to one starting source particle. Each tally must be scaled to the desired source strength. Fluence is of paramount importance since it can be converted into absorbed dose or dose equivalent if the differential energy distribution is known.

For calculating the whole body dose, an F6 – Energy Deposition – tally type was used for each organ/tissue of interest. MCNP returns for each F6 tally some number X with units of Mev/g per source particle. To convert to absorbed dose D,

*D = X Mev/g/src-part * 1 rad/6.242E+7 Mev/g =X * 1.6E-08 rad/src-part.* (3.1)

To convert to dose equivalent,

H_T *= Q (rem/rad) * D_T (rad/src-part) = Q*D_T rem/src-part* (3.2)

where Q is the mean quality factor. Since Q depends on the energy of the particle, a differential distribution of Q can be input by using the *de* and *df* cards. Thus, in addition to X, MCNP returns some number Y representing the value of Q. Thus, the dose equivalent per source particle for a given organ/tissue is

H_T *= X Mev/g/src-part * Y (rem/rad) * [1 rad/6.242E+7 Mev/g] * [1000 mrem/rem] = 1.602E-5 * XY mrem/src part.* (3.3)

Then the effective dose equivalent for the whole body is

$$H_E = \sum_T w_T \cdot H_T \quad (3.4)$$

where w_T is a weighting factor representing the proportion of stochastic risk resulting from organ/tissue *T* to the total risk.

The above methodology for calculating effective dose equivalent is based on ICRP 26 (1977) and can be used with either the ANSI-1977 set of quality factors or the

ICRP 51 (1987) set of quality factors. ICRP 60 (1991) changed the methodology to calculate whole body dose. This defined three principal protection quantities:

D_T, mean absorbed dose in an organ or tissue,

H_T, equivalent dose in an organ or tissue, and

E, effective dose.

These protection quantities are related by the following:

$D_T = {}_T / m_T$, where ${}_T$ and m_T are the energy deposited in a tissue of mass m,

$H_T = w_R D_{T,R}$, where $D_{T,R}$ is the averaged absorbed dose from radiation R and tissue T, and w_R is the radiation weighting factor for radiation R, and

$E = w_T H_T$, where w_T is the weighting factor for tissue T. (3.5)

In calculating the effective dose with MCNP, the radiation weighting factor depends on energy and can be input as a differential distribution by using the *de* and *df* cards. For calculational purposes,

$$w_R = 5 + 17e^{-(\ln(2E))^2/6} \quad (3.4)$$

where E is the neutron energy in MeV (ICRP 1991). Likewise, MCNP will output XY and

H_T = *1.602E-5 * XY mrem/src part.* (3.5)

Since MCNP returns only the value *XY*, a tally multiplier card was used to input the value *1.602E-5*. Table 3-3 provides the quality factors or radiation weighting factors that were used.

A spreadsheet format (see Appendix B for an example) was created to take the dose equivalent data for each organ/tissue and apply the appropriate tissue weighting factors to come up with effective dose equivalent (Equation 3-4) or the effective dose (Equation 3-5).

Table 3-3: Neutron Quality Factors and Radiation Weighting Factors.

Energy	ANSI 1977	ANSI 1991		Energy	ANSI 1977	ANSI 1991	
	ICRP 26	ICRP 51	ICRP 60		ICRP 26	ICRP 51	ICRP 60
E (MeV)	Q	Q	W_R	E (MeV)	Q	Q	W_R
1.00E-09			5.0	2.00E-01		24.8	19.8
1.00E-08			5.0	3.00E-01			21.3
2.50E-08	2	6.56	5.0	5.00E-01	11	25.4	22.0
1.00E-07	2	6.32	5.0	7.00E-01			21.7
2.00E-07			5.0	9.00E-01			21.0
5.00E-07			5.0	1.00E+00	11	23.6	20.7
1.00E-06	2	6.02	5.0	1.20E+00			20.0
2.00E-06			5.0	1.50E+00		21.2	
5.00E-06			5.0	2.00E+00		19.78	17.3
1.00E-05	2	5.82	5.0	2.50E+00	9		
2.00E-05			5.0	3.00E+00		18	15.0
5.00E-05			5.0	4.00E+00		17.1	13.3
1.00E-04	2	5.7	5.0	5.00E+00	8	15.7	12.0
2.00E-04			5.0	6.00E+00		14.86	11.1
5.00E-04			5.0	7.00E+00	7	14.6	10.3
1.00E-03	2	5.48	5.0	8.00E+00		14.6	9.7
2.00E-03			5.1	9.00E+00			9.2
5.00E-03			5.5	1.00E+01	6.5	14.82	8.8
1.00E-02	2.5	5.54	6.3	1.20E+01			8.2
2.00E-02			8.0	1.40E+01	7.5	15.08	7.7
3.00E-02			9.5	1.50E+01			7.5
5.00E-02		14.46	12.0	1.60E+01			7.3
7.00E-02			13.9	1.70E+01		14.88	
1.00E-01	7.5	20.2	16.0	1.80E+01			7.0
1.50E-01			18.4	2.00E+01	8	15.48	6.8

For determining effective dose equivalent (ICRP 26 1977), the remainder is distributed as a tissue weighting factor $w_T = 0.05$ to each of the five organs or tissues of the remainder receiving the highest dose equivalents. For determining effective dose

(ICRP 60 1991), the weighting factor of 0.05 is applied to the sum of the dose equivalents for all of the remainder tissues (adrenals, brain, upper large intestine, small intestine, kidney, muscle, pancreas, spleen, thymus, and uterus). Table 3-4 provides the tissue weighting factors that were used.

Table 3-4: Tissue Weighting Factors.

Tissue	ICRP 26 w_T	ICRP 60 w_T
Gonads	0.25	0.20
Red bone marrow	0.12	0.12
Colon		0.12
Lung	0.12	0.12
Stomach		0.12
Bladder		0.05
Breast	0.15	0.05
Liver		0.05
Esophagus		0.05
Thyroid	0.03	0.05
Skin		0.01
Bone surfaces	0.03	0.01
Remainder	0.30	0.05

3.2.6 Estimating Dose that a Dosimeter Would Measure h4

For estimating the dose that a dosimeter would measure, an F2 – Surface Fluence – type tally was used for each dosimeter location in the dosimeter lattice. This tally return a number *X tally particles/(source neutron cm^2)*. To convert this to dose, neutron flux-to dose conversion factors were input as a differential distribution by using the *de* and *df* cards. With this addition, a number

*X Y tally neutrons/(source_neutrons-cm^2) * E-12 Sv-cm^2/tally neutron*

is returned. To convert this number to dose (mrem/h-kg), the following conversion is made

(6.359E+04 src_neuts/s) / (kg Pu) x (100 rem/Sv) x (3600 s/h) x (1000 mrem/rem)

** X Y tally neutrons/ (source_neutrons-cm^2) * E-12 Sv-cm^2/tally neutron*

*= 2.28924E+1*XY mrem/h-kg.*

Thus, a tally multiplier card with the value *2.28924E+1* is used so that MCNP outputs the dose in the units desired (mrem/h-kg).

Tables 3-5, 3-6, and 3-7 provide the flux-to-dose conversion factors that were used. Fig. 3-9 provides a graphical comparison of the dose conversion factors used.

Table 3-5: ANSI-1977 Neutron Flux-to-Dose Conversion Factors.

Neutron Flux-to-Dose-Rate Conversion Factors				
ANSI/ANS-6.1.1-1977 (Basis: NCRP)				
E	DFn(E)			
MeV	(rem/hr) / (n/cm^2-s)	rem-cm^2 / n	Sv-cm^2 / n	pSv-cm^2 / n
2.50E-08	3.67E-06	1.019E-09	1.019E-11	1.02E+01
1.00E-07	3.67E-06	1.019E-09	1.019E-11	1.02E+01
1.00E-06	4.46E-06	1.239E-09	1.239E-11	1.24E+01
1.00E-05	4.54E-06	1.261E-09	1.261E-11	1.26E+01
1.00E-04	4.18E-06	1.161E-09	1.161E-11	1.16E+01
1.00E-03	3.76E-06	1.044E-09	1.044E-11	1.04E+01
1.00E-02	3.56E-06	9.889E-10	9.889E-12	9.89E+00
1.00E-01	2.17E-05	6.028E-09	6.028E-11	6.03E+01
5.00E-01	9.26E-05	2.572E-08	2.572E-10	2.57E+02
1.00E+00	1.32E-04	3.667E-08	3.667E-10	3.67E+02
2.50E+00	1.25E-04	3.472E-08	3.472E-10	3.47E+02
5.00E+00	1.56E-04	4.333E-08	4.333E-10	4.33E+02
7.00E+00	1.47E-04	4.083E-08	4.083E-10	4.08E+02
1.00E+01	1.47E-04	4.083E-08	4.083E-10	4.08E+02
1.40E+01	2.08E-04	5.778E-08	5.778E-10	5.78E+02
2.00E+01	2.27E-04	6.306E-08	6.306E-10	6.31E+02

Table 3-6: ANSI 1991 Neutron Flux-to-Dose Conversion Factors.

Neutron Flux-to-Dose-Rate Conversion Factors			
ANSI/ANS-6.1.1-1991 (Basis: ICRP 51)			
E	DFn(E)		
MeV	(rem/hr) / (n/cm^2-s)	Sv-cm^2 / n	pSv-cm^2 / n
2.50E-08	1.44E-06	4.00E-12	4.00
1.00E-07	1.58E-06	4.40E-12	4.40
1.00E-06	1.74E-06	4.82E-12	4.82
1.00E-05	1.61E-06	4.46E-12	4.46
1.00E-04	1.59E-06	4.41E-12	4.41
1.00E-03	1.38E-06	3.83E-12	3.83
1.00E-02	1.63E-06	4.53E-12	4.53
2.00E-02	2.11E-06	5.87E-12	5.87
5.00E-02	3.92E-06	1.09E-11	10.90
1.00E-01	7.13E-06	1.98E-11	19.80
2.00E-01	1.39E-05	3.86E-11	38.60
5.00E-01	3.13E-05	8.70E-11	87.00
1.00E+00	5.15E-05	1.43E-10	143.00
1.50E+00	6.59E-05	1.83E-10	183.00
2.00E+00	7.70E-05	2.14E-10	214.00
3.00E+00	9.50E-05	2.64E-10	264.00
4.00E+00	1.08E-04	3.00E-10	300.00
5.00E+00	1.18E-04	3.27E-10	327.00
6.00E+00	1.25E-04	3.47E-10	347.00
7.00E+00	1.31E-04	3.65E-10	365.00
8.00E+00	1.37E-04	3.80E-10	380.00
1.00E+01	1.48E-04	4.10E-10	410.00
1.40E+01	1.73E-04	4.80E-10	480.00

Table 3-7: ICRP 74 Neutron Flux-to-Dose Conversion Factors.

Neutron Flux-to-Dose-Rate Conversion Factors							
ICRP 74				ICRP 74			
E	DFn(E)			E	DFn(E)		
MeV	(rem/hr) / (n/cm^2-s)	Sv-cm^2 / n	pSv-cm^2 / n	MeV	(rem/hr) / (n/cm^2-s)	Sv-cm^2 / n	pSv-cm^2 / n
1.00E-09	1.89E-06	5.24E-12	5.24E+00	5.00E-01	6.77E-05	1.88E-10	1.88E+02
1.00E-08	2.25E-06	6.25E-12	6.25E+00	7.00E-01	8.32E-05	2.31E-10	2.31E+02
2.50E-08	2.74E-06	7.60E-12	7.60E+00	9.00E-01	9.61E-05	2.67E-10	2.67E+02
1.00E-07	3.58E-06	9.95E-12	9.95E+00	1.00E+00	1.02E-04	2.82E-10	2.82E+02
2.00E-07	4.03E-06	1.12E-11	1.12E+01	1.20E+00	1.12E-04	3.10E-10	3.10E+02
5.00E-07	4.61E-06	1.28E-11	1.28E+01	2.00E+00	1.38E-04	3.83E-10	3.83E+02
1.00E-06	4.97E-06	1.38E-11	1.38E+01	3.00E+00	1.56E-04	4.32E-10	4.32E+02
2.00E-06	5.22E-06	1.45E-11	1.45E+01	4.00E+00	1.65E-04	4.58E-10	4.58E+02
5.00E-06	5.40E-06	1.50E-11	1.50E+01	5.00E+00	1.71E-04	4.74E-10	4.74E+02
1.00E-05	5.44E-06	1.51E-11	1.51E+01	6.00E+00	1.74E-04	4.83E-10	4.83E+02
2.00E-05	5.44E-06	1.51E-11	1.51E+01	7.00E+00	1.76E-04	4.90E-10	4.90E+02
5.00E-05	5.33E-06	1.48E-11	1.48E+01	8.00E+00	1.78E-04	4.94E-10	4.94E+02
1.00E-04	5.26E-06	1.46E-11	1.46E+01	9.00E+00	1.79E-04	4.97E-10	4.97E+02
2.00E-04	5.18E-06	1.44E-11	1.44E+01	1.00E+01	1.80E-04	4.99E-10	4.99E+02
5.00E-04	5.11E-06	1.42E-11	1.42E+01	1.20E+01	1.80E-04	4.99E-10	4.99E+02
1.00E-03	5.11E-06	1.42E-11	1.42E+01	1.40E+01	1.79E-04	4.96E-10	4.96E+02
2.00E-03	5.18E-06	1.44E-11	1.44E+01	1.50E+01	1.78E-04	4.94E-10	4.94E+02
5.00E-03	5.65E-06	1.57E-11	1.57E+01	1.60E+01	1.77E-04	4.91E-10	4.91E+02
1.00E-02	6.59E-06	1.83E-11	1.83E+01	1.80E+01	1.75E-04	4.86E-10	4.86E+02
2.00E-02	8.57E-06	2.38E-11	2.38E+01	2.00E+01	1.73E-04	4.80E-10	4.80E+02
3.00E-02	1.04E-05	2.90E-11	2.90E+01	3.00E+01	1.65E-04	4.58E-10	4.58E+02
5.00E-02	1.39E-05	3.85E-11	3.85E+01	5.00E+01	1.57E-04	4.37E-10	4.37E+02
7.00E-02	1.70E-05	4.72E-11	4.72E+01	7.50E+01	1.54E-04	4.29E-10	4.29E+02
1.00E-01	2.15E-05	5.98E-11	5.98E+01	1.00E+02	1.54E-04	4.29E-10	4.29E+02
1.50E-01	2.89E-05	8.02E-11	8.02E+01	1.30E+02	1.56E-04	4.32E-10	4.32E+02
2.00E-01	3.56E-05	9.90E-11	9.90E+01	1.50E+02	1.58E-04	4.38E-10	4.38E+02
3.00E-01	4.79E-05	1.33E-10	1.33E+02	1.80E+02	1.60E-04	4.45E-10	4.45E+02

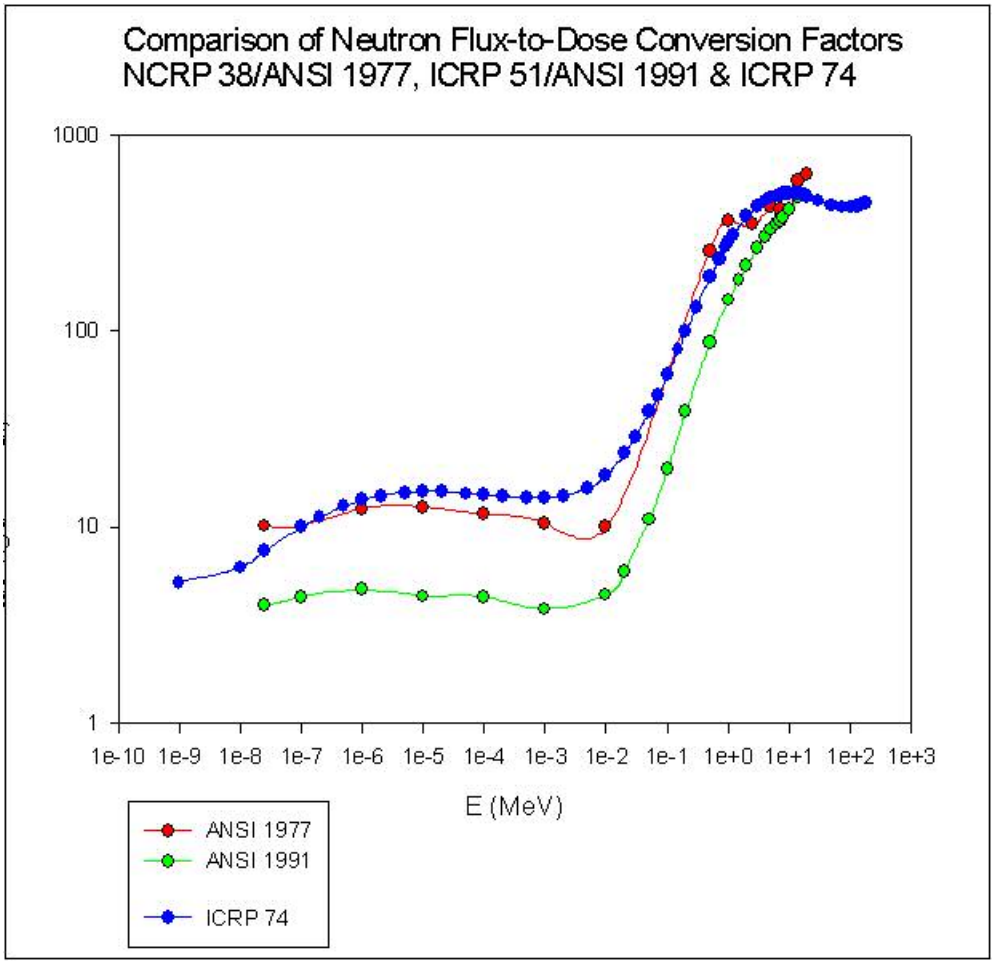

Figure 3-9: Comparison of Neutron Flux-to-Dose Conversion Factors.

3.2.7 Determining the Neutron Radiation Field

For determining the neutron radiation field, a mesh tally (Type 1) that allows for the setup of a large Cartesian, cylindrical, or spherical mesh in which to score track averaged data such as flux. The average fluence is particle weight times track length divided by volume in units of number/cm^2. If the source is considered to be steady state in particles per second, then the value becomes flux in number/cm^2/second. This may be converted to dose by the same methodology as above.

The mesh was setup to provide the neutron dose field in a 400 cm by 440 cm YZ plane at distances 30.5 cm, 91.5 cm and 183 cm (1 ft, 91.5 cm and 6 ft) in front of the glove box. It was 1 cm deep in the X direction. The grid points in the YZ plane were 8 cm apart. This mesh then simulated the placing of 2750 dosimeters in a plane parallel to the front of the glove box.

3.3 COMPUTATIONAL RESULTS

3.3.1 Neutron Radiation Field

Appendix C provides the plots of the neutron radiation field at distances 30.5 cm, 91.5 cm, and 183 cm (1 ft, 3 ft, and 6 ft) in front of the glove box for 33 different source locations (11 on the side, 11 in front of the viewing window, and 11 in the middle). ANSI 1977 fluence-to-dose conversion factors were used. The outline of the front of the glove box is shown on each plot for reference.

3.3.2 Estimated Dose using Phantom's Dosimeter Lattice

Appendix D provides a summary of the calculations of the estimated dose using the phantom’s dosimeter lattice at 30.5 cm (1 ft) and 91.5 cm (3 ft) for each of the different conversion factor sets. For each phantom position, it provides the maximum, minimum, average, and reference position values in the dosimeter tally plane along with the respective dosimeter positions. For ANSI 1977 conversion factors, the dosimeter positions were labeled between 402 and 722 while they were labeled between 2 and 322 for ANSI 1991 conversion factors and between 802 and 1122 for ICRP-74 conversion factors (refer to Table 3-8).

Table 3-8: ANSI 1991 Neutron Flux-to-Dose Conversion Factors.

Relative	Y (cm) for Phantom Tally Plane				
Z (cm)	-16	-8	0	8	16
		2	12	22	
		402	412	422	
74		802	812	822	
	32	42	52	62	72
	432	442	452	462	472
66	832	842	852	862	872
	82	92	102	112	122
	482	492	502	512	522
58	882	892	902	912	922
	132	142	152	162	172
	532	542	552	562	572
50	932	942	952	962	972
	182	192	202	212	222
	582	592	602	612	622
42	982	992	1002	1012	1022
	232	242	252	262	272
	632	642	652	662	672
34	1032	1042	1052	1062	1072
	282	292	302	312	322
	682	692	702	712	722
26	1082	1092	1102	1112	1122

3.3.3 Estimated Whole Body Dose Using the Computational Phantom

Appendix E provides a summary of the whole body dose for each combination of 6 phantom positions and 33 source positions in mrem/hr/kg for a male with breasts, male without breasts, and a female for each methodology ICRP-26 and ICRP-60. Estimates for the phantom at the 30.5 cm (1 ft) positions using quality factors from ANSI 1977, ANSI 1991, and ICRP-74 are provided in Tables E-1 through E-3 respectively while Tables E-4 through E-6 provide estimates with the phantom at the 91.5 cm (3 ft) positions.

3.3.4 Comparison of Different Conversion Factors using Dosimeter Reference Position 4

Appendix F provides a comparison the using ANSI 1977, ANSI 1991, and ICRP-74 conversion factors at the reference dosimeter position. Appendices F.1 and F.2 provide tabular comparisons at 30.5 cm and 91.5 cm (1 ft and 3 ft) respectively while Appendices F.3 and F.4 provide a graphical comparison. Nine comparisons were made in each. Each consisted of considering the phantom at one of the given three locations (side, viewing window, or middle) and letting the source position vary from the front of the glove box to the back of the glove box (source distance within glove box from 6 cm to 150 cm measured from the inside front of the glove box).

3.3.5 Comparison of Whole Body Dose with Dosimeter Tally Plane Dose

Appendix G provides a graphical comparison of the whole body dose estimates to the reference dosimeter dose for a male with breasts, for a male without breasts, and for a female. This comparison is given for the phantom at 30.5 cm and at 91.5 cm (1 ft and 3 ft) for the following cases: ICRP 26 methodology with ANSI 1977 dose conversion factors, ICRP 26 methodology with ANSI 1991 dose conversion factors, ICRP 60 methodology with ANSI 1991 dose conversion factors, and ICRP 60 methodology with ICRP 74 dose conversion factors.

In addition, Appendix G provides comparisons of the whole body doses with the average dose of all the dosimeters located on the phantom dosimeter plan and the maximum and minimum doses from any of the dosimeters. Appendix H provides tables that give the distribution of the average, maximum, and minimum of the dosimeter readings on the dosimeter tally plane for all source locations and phantom locations (side, viewing window, and middle) for both 30.5 cm and at 91.5 cm (1 ft and 3 ft) phantom distances from the glove box.. These tables are given for each of the dosimetry

methodologies. Appendix H.1 provides detailed tables that provide the dosimeter location of the average, maximum, and minimum values for each configuration. Appendices H.2 through H.4 provide summary tables for each dosimetry methodology.

3.4 DISCUSSION OF RESULTS

3.4.1 Neutron Radiation Field

To get a feel for what the neutron radiation field is like without a glove box present or with an unshielded glove box (i.e., no specific neutron shielding material in the shell), Figures 3-10 through 3-15 compare the neutron radiation field at 30.5 cm, 91.5 cm, and 183cm (1 ft, 3ft, and 6 ft) for these two cases with the source at 60 cm inside on line V that goes from the front to the back of the glove box on a line centered on the left viewing window.

With no glove box present, the calculation shows the typical circular patterns that would be expected with a more uniform field the farther the dosimeter plane is away from the source. For the unshielded glove box, the circular pattern is changed to reflect the neutron scattering that occurs within the shell of the glove box. The pattern changes are due to streaming. This shows that there is little attenuation of the field by a glove box with no neutron shielding material.

In fact, since there is little attenuation, the dose in the streaming areas actually increases due to the contribution of the secondary (scattered) neutrons to those areas which the primary (streaming) neutrons affect. The farther the dose plane from the glove box the more distinct the streaming pattern becomes.

For the unshielded cases, just below Z=100 cm, one sees the dose pattern change dramatically. These patterns are due to the neutrons coming from the source and traversing the bottom stainless steel plate of the glove box. The sharp line is for those

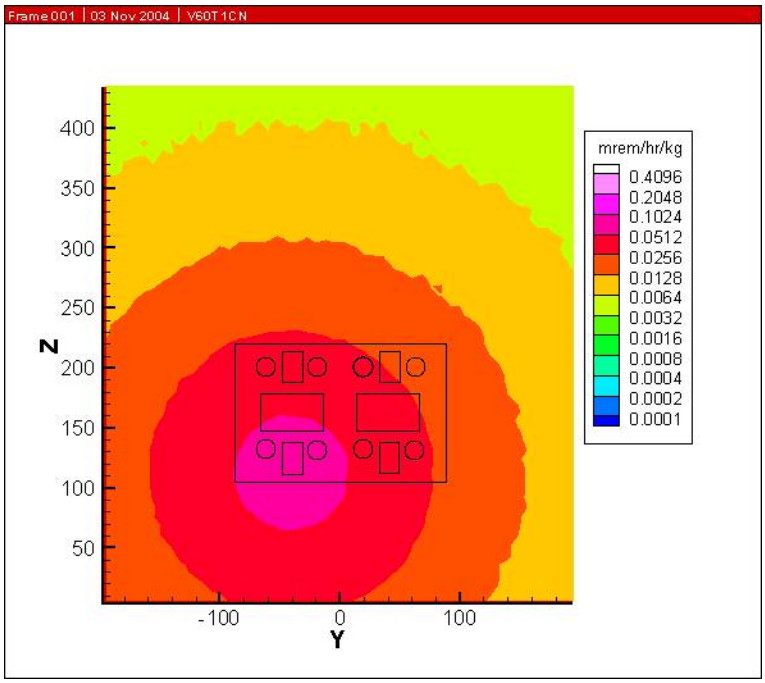

Figure 3-10: Field at 30.5 cm with No Glove Box.

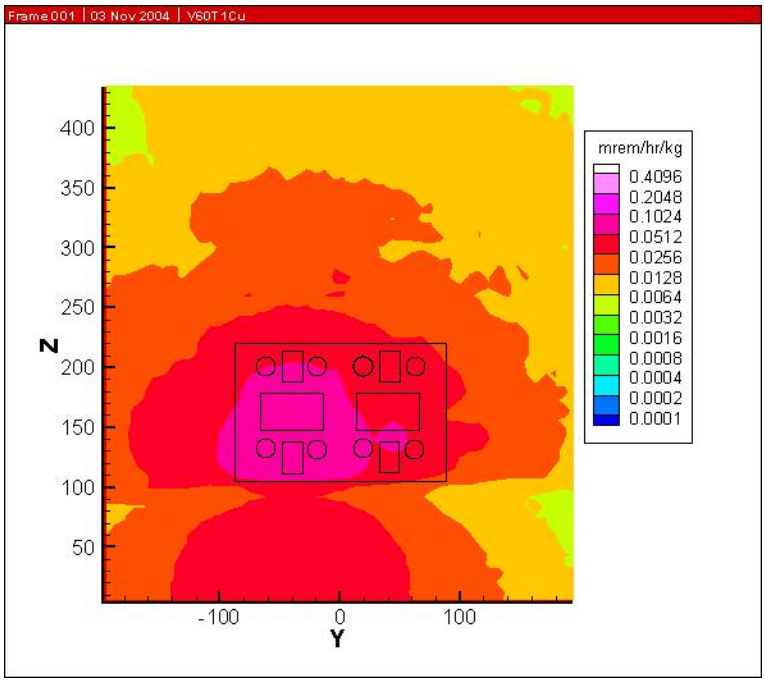

Figure 3-11: Field at 30.5 cm with No Shielding Material in Glove Box.

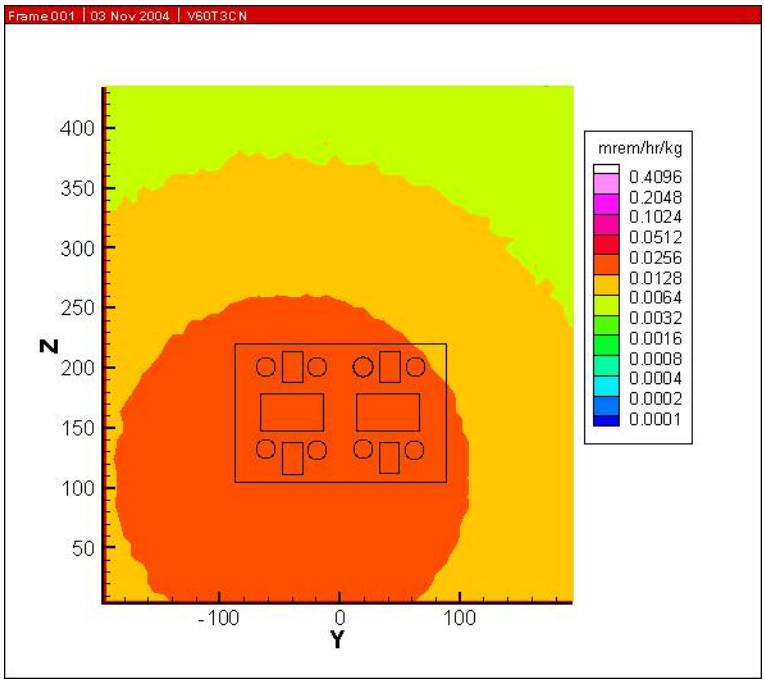

Figure 3-12: Field at 91.5 cm with No Glove Box.

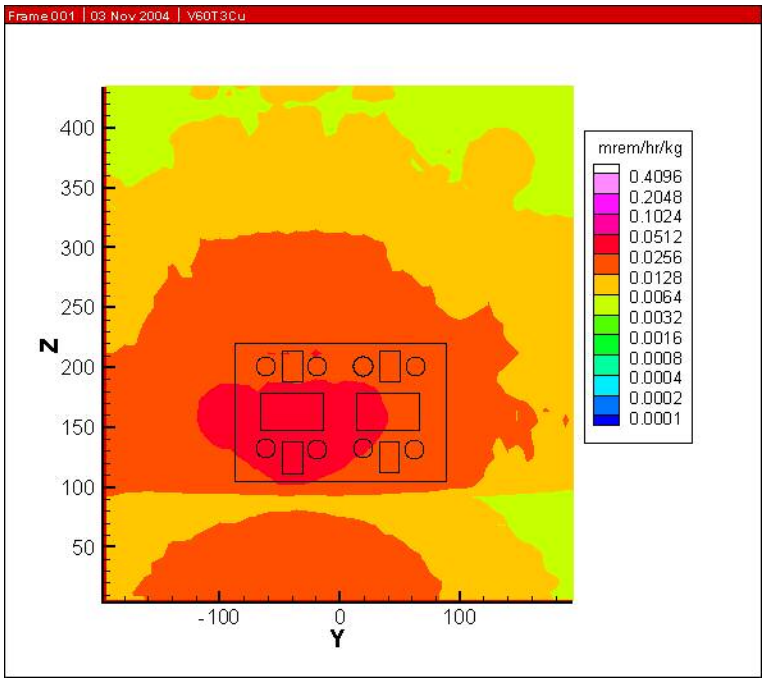

Figure 3-13: Field at 91.5 cm with No Shielding Material in Glove Box.

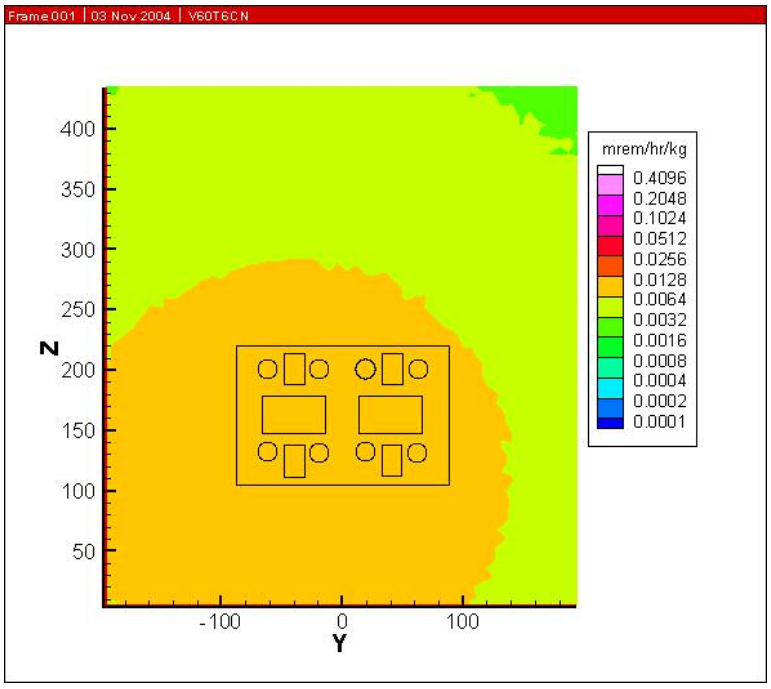

Figure 3-14: Field at 183 cm with No Glove Box.

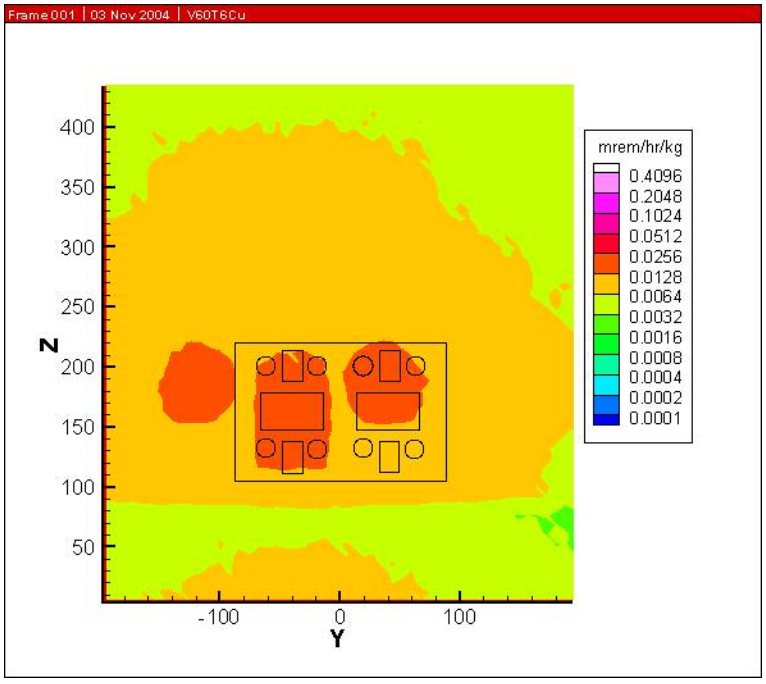

Figure 3-15: Field at 183 cm with No Shielding Material in Glove Box.

neutrons that leave the source at a small angle of incidence to the bottom plate and thus have to traverse through more of the bottom plate. The round ball shape drops lower the farther the dose plane is from the glove box. These neutrons have to travel through less of the bottom plate.

The pattern in front of the left workstation at 30.5 cm (1 ft) is smeared together due to the streaming paths intersecting one another. As one moves to 91.5 cm (3 ft), the pattern takes on a “Mickey Mouse” shape while at 183 cm (6 ft) it shows distinctly the glove ports and viewing windows. The jagged patterns on the outside of the previous circular shapes are due to streaming from the other ports or windows of the glove box.

Since the predominant position of a worker will be at the 1 foot position in front of the glove box, the discussion of results for the neutron radiation field will concentrate on this position for the worker with the source on line V. The source positions considered are 6, 15 30, 45, 60, 75, 90, 105, 120, 135, and 150 cm as measured from the front of the inside of the glove box going toward the back of the glove box.

To better understand the effects of streaming, two figures are presented. The first is with the glove box completely shielded; i.e., the ports and windows are filled in with the same shielding materials as the shell. This will provide the field with no streaming paths. The second is with the regular glove box with glove ports open and windows in place as if a worker or workers were present. The normal glove box cases show the effects of streaming due to no viable shielding in the glove ports and with windows in place that do not offer the same degree of shielding as the shell. Each set of figures will be presented in the left column with a discussion of each in the right column. Since there are many commonalities, those will be discussed here. The change going from the shielded case to the regular case is described. For the examples discussed here, the source

location is six cm off the bottom of the glove box and goes back on a line through the middle of the viewing window of the left workstation.

- The magnitude of the dose field is throughout the plane relative to the same location in the shielded case. Depending on location, the magnitude of the change can be a factor of four or more. This is in keeping with the attenuation properties of the two inches of neutron shielding material in the shell (34% NS-3 + 1% B_4C + 65% Pb whose half value thickness is 2.4 cm).
- Consider the region in the dose plane from the floor level to the level of the bottom of the glove box. This region does not have any streaming paths. However, the pattern of the dose field is determined by where the source is located. At the same height above the floor, the magnitude of the dose field decreases the farther the source is inside the glove box. This is due to two factors: first, the neutrons have to traverse more material to reach the same external point and are attenuated more as a result, and secondly, the distance from the source as increased.
- With the source close in to the front of the glove box, the streaming patterns are smeared together in many cases. As the source is moved farther back into the box, the streaming patterns become more distinct and knowing the source location, the windows or ports through which the streaming occurred are more easily identified.
- These streaming paths are important considerations for co-located workers since they may easily be in a higher dose field than they thought they were in.

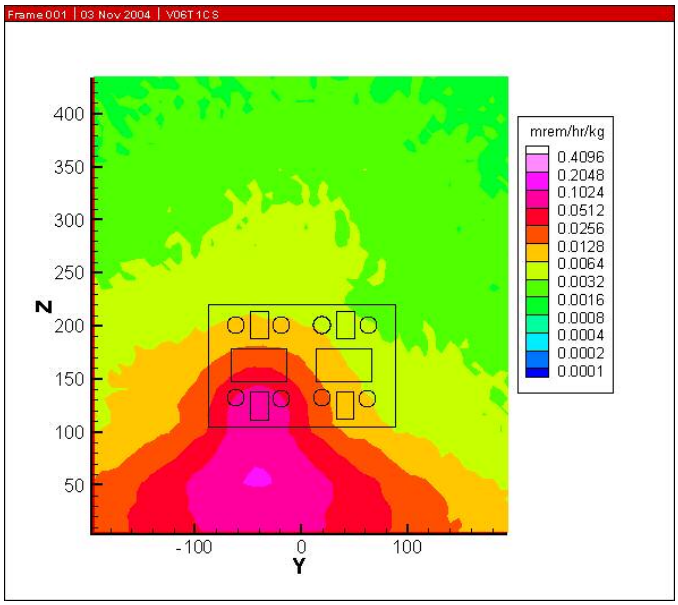

Figure 3-16: Windows and Glove Ports Shielded with Source at 6 cm.

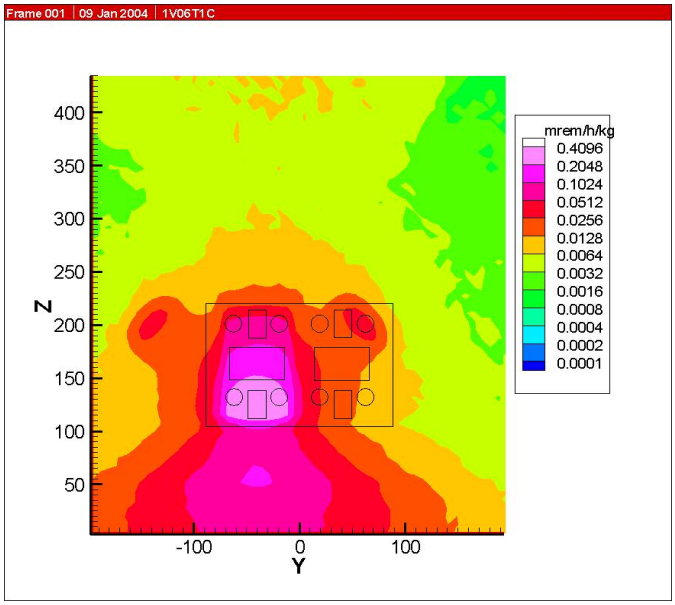

Figure 3-17: Windows and Glove Ports Unshielded with Source at 6 cm.

With the source just 6 cm inside the glove box, the primary streaming paths are directed up to chest level through the window and to the sides of and at head level of the worker through the glove ports. Some streaming through the middle window is identified at the region above Z=400.

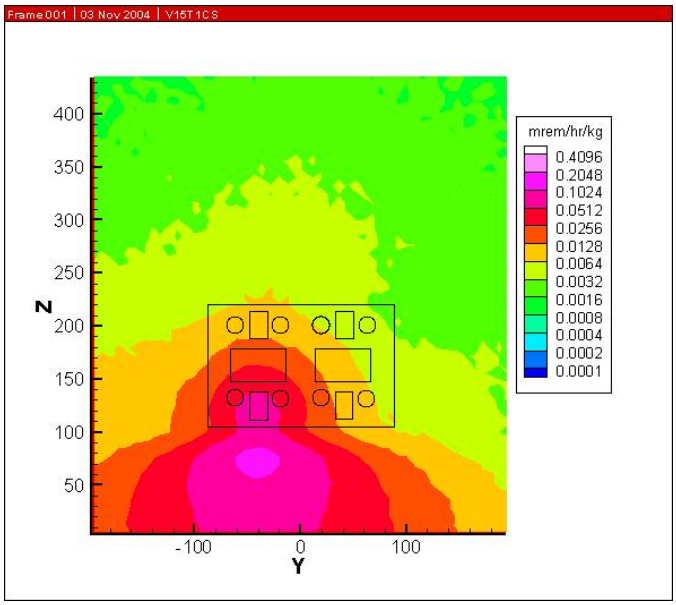

Figure 3-18: Windows and Glove Ports Shielded with Source at 15 cm.

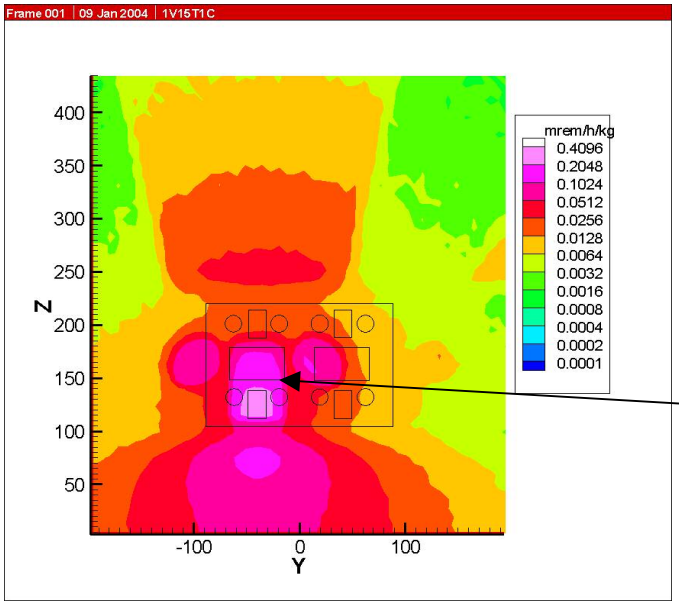

Figure 3-19: Windows and Glove Ports Unshielded with Source at 15 cm.

As the source has moved back to 15 cm, the smeared shape in the middle of the glove box starts looking like "Mickey Mouse". Streaming through the middle window is plainly evident above Z=200. This could be a concern to any maintenance personnel that need to be above the glove box.

To the right of the glove box, streaming from the right lower workstation and from the right middle window can be seen.

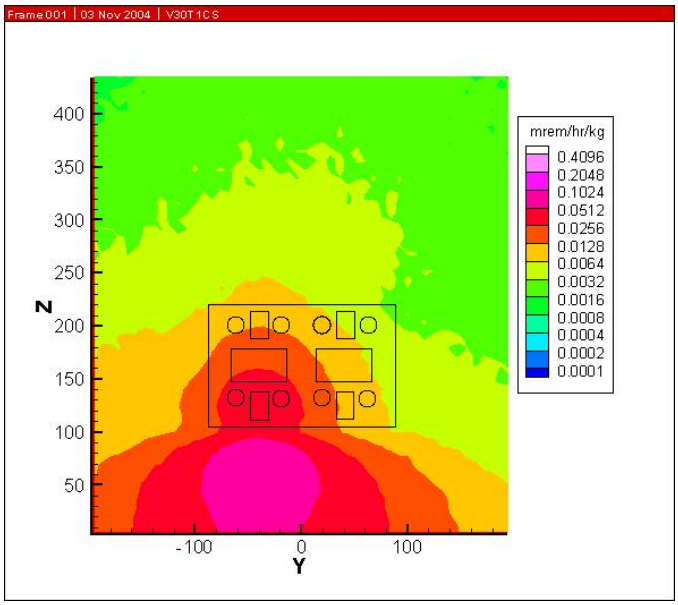

Figure 3-20: Windows and Glove Ports Shielded with Source at 30 cm.

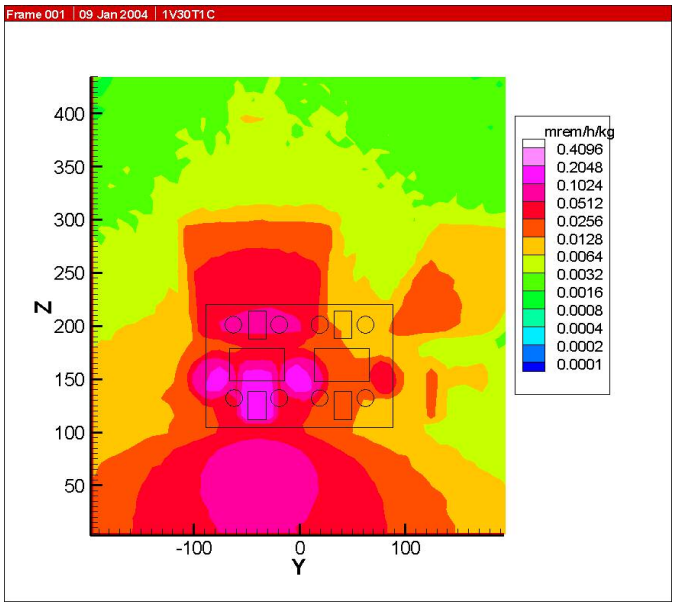

Figure 3-21: Windows and Glove Ports Unshielded with Source at 30 cm.

As the source is moved back to 30 cm, the "Mickey Mouse" shape gets narrower. The streaming above the glove box is more easily identified with the middle window

At about Z=150 on the right hand side of the glove box, the streaming from the left glove port and associated viewing window of the lower right workstation are identified. Above that is the streaming pattern from the middle right window.

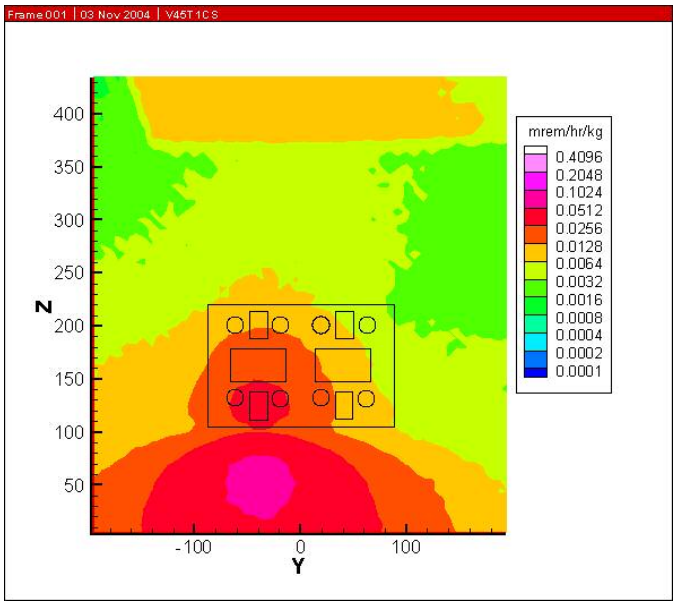

Figure 3-22: Windows and Glove Ports Shielded with Source at 45 cm.

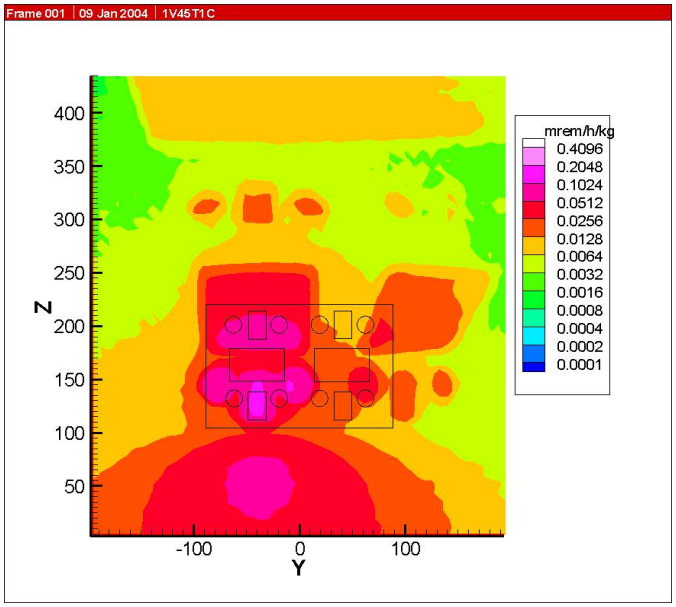

Figure 3-23: Windows and Glove Ports Unshielded with Source at 45 cm.

As the source is moved back to 45 cm, the dose field of the neutrons going through the top of the glove box becomes visible in the dose plane. Streaming through the upper left workstation ports and window, lower right workstation ports and window, and the middle window are easily identified.

At about Z=300 and Y=100, streaming through the left glove port of the upper right workstation can now be identified.

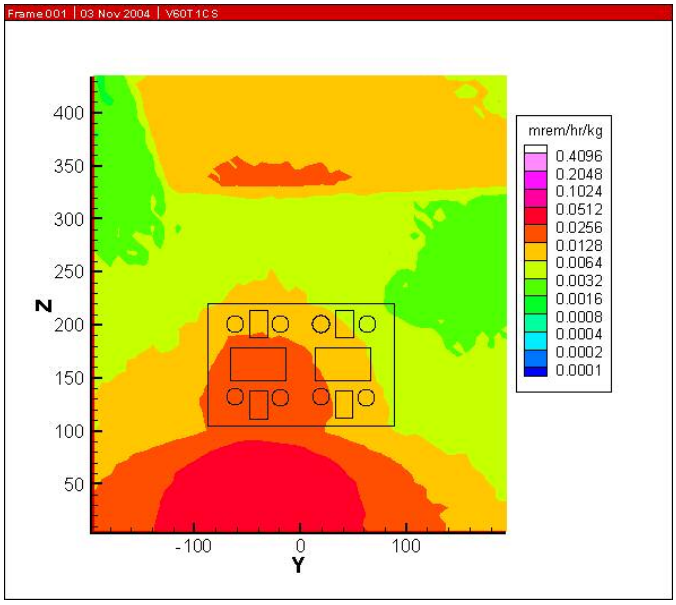

Figure 3-24: Windows and Glove Ports Shielded with Source at 60 cm.

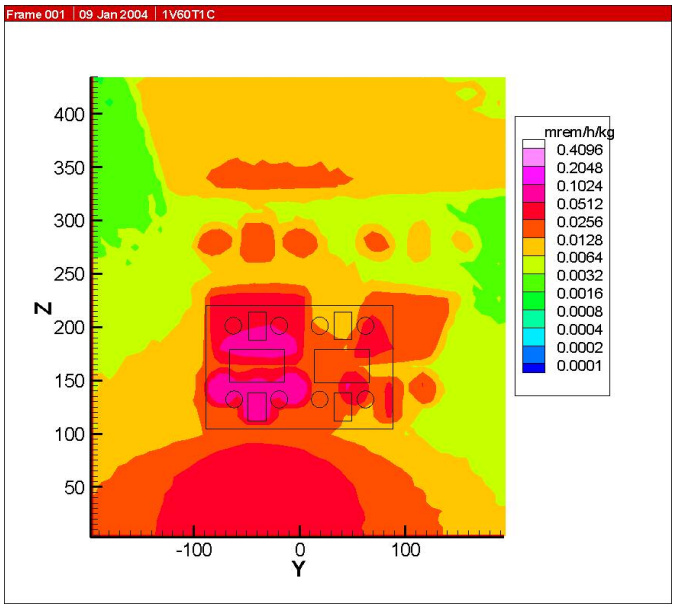

Figure 3-25: Windows and Glove Ports Unshielded with Source at 60 cm.

Above Z=300, the dose field is that coming from neutrons going through the top of the glove box. Below that level, streaming from all of the glove ports and windows is clearly identified.

The "Mickey Mouse" shape is getting smaller and now appears to be detached from its body below.

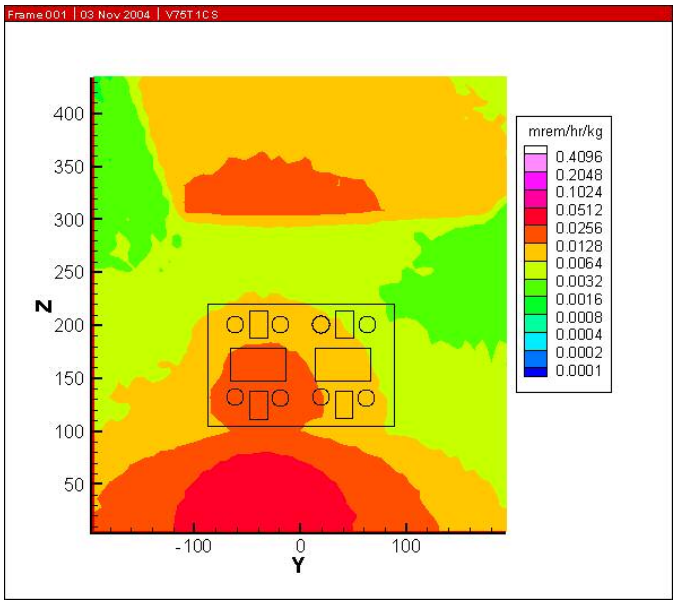

Figure 3-26: Windows and Glove Ports Shielded with Source at 75 cm.

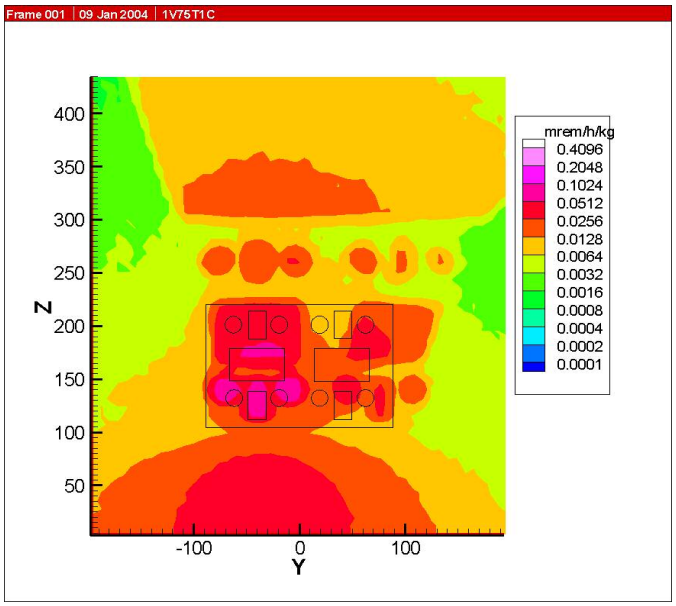

Figure 3-27: Windows and Glove Ports Unshielded with Source at 75 cm.

Above Z=300, the dose field is that coming from neutrons going through the top of the glove box. Below that level, streaming from all of the glove ports and windows is clearly identified.

The "Mickey Mouse" shape is getting smaller and now is more detached from its body below.

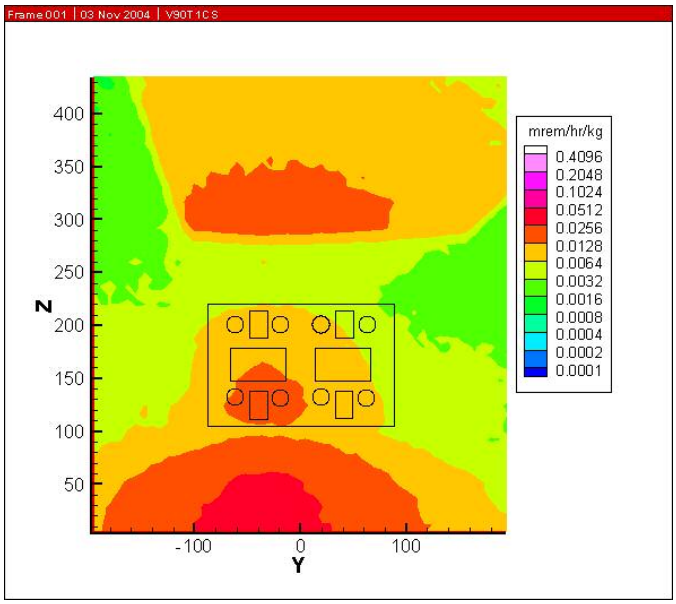

Figure 3-28: Windows and Glove Ports Shielded with Source at 90 cm.

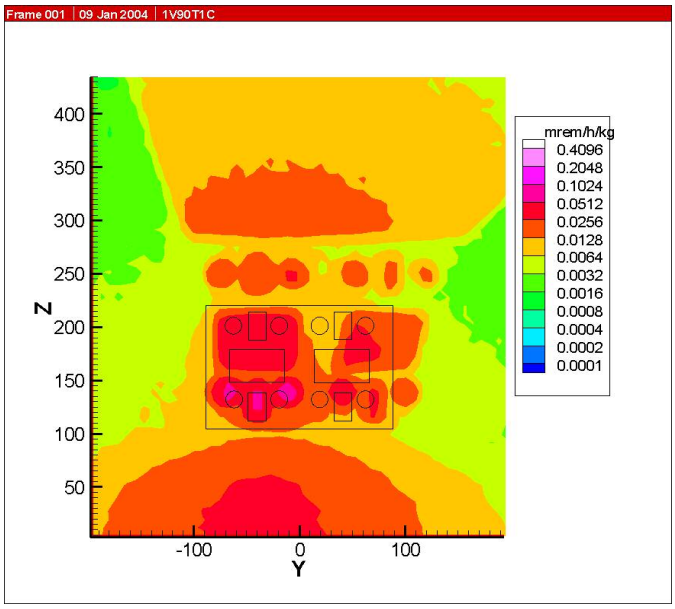

Figure 3-29: Windows and Glove Ports Unshielded with Source at 90 cm.

Above Z=300, the dose field is that coming from neutrons going through the top of the glove box. Below that level, streaming from all of the glove ports and windows is clearly identified.

The "Mickey Mouse" shape is getting smaller and now is more detached from its body below.

The dose field in the middle of the glove box due to streaming is not as smeared and is getting more localized.

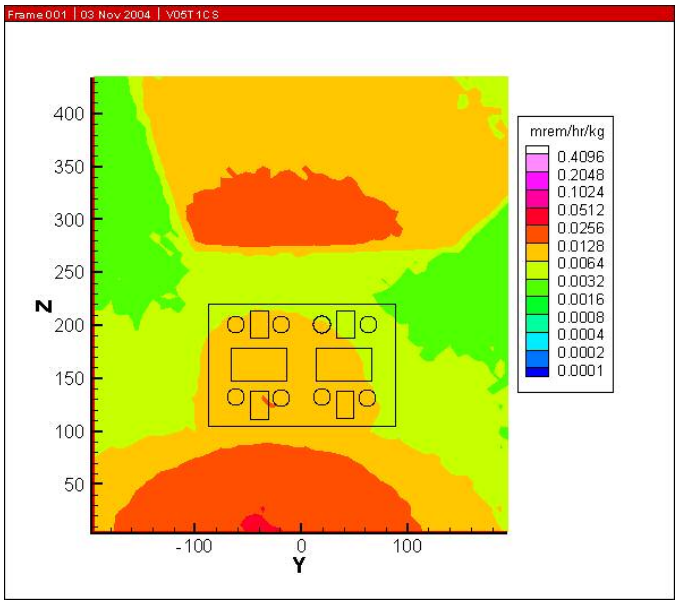

Figure 3-30: Windows and Glove Ports Shielded with Source at 105 cm.

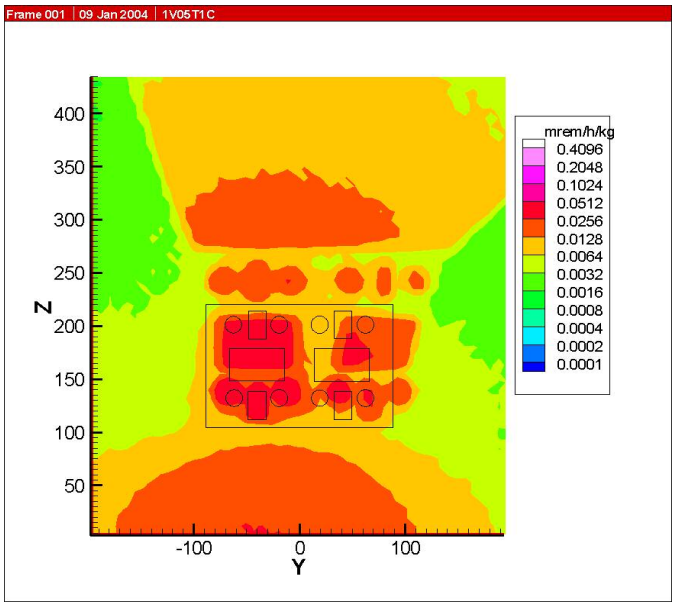

Figure 3-31: Windows and Glove Ports Unshielded with Source at 105 cm.

Above Z=300, the dose field is that coming from neutrons going through the top of the glove box. Below that level, streaming from all of the glove ports and windows is clearly identified.

The "Mickey Mouse" shape is getting smaller and now is more detached from its body below.

The dose field in the middle of the glove box due to streaming is less smeared and is almost localized into portions from the left and right workstations.

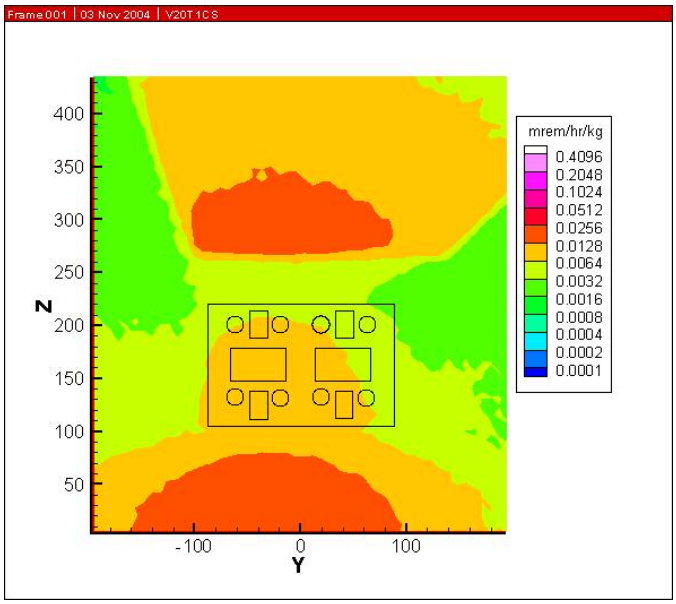

Figure 3-32: Windows and Glove Ports Shielded with Source at 120 cm.

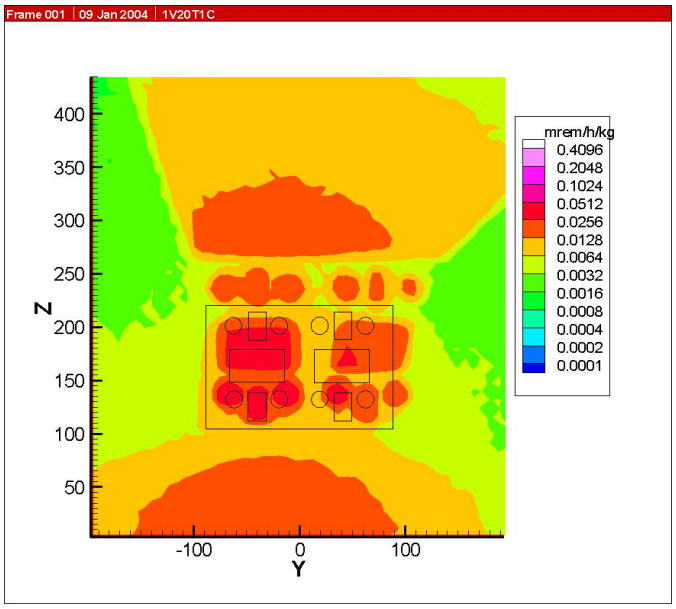

Figure 3-33: Windows and Glove Ports Unshielded with Source at 120 cm.

Above Z=300, the dose field is that coming from neutrons going through the top of the glove box. Below that level, streaming from all of the glove ports and windows is clearly identified.

The "Mickey Mouse" shape is getting smaller and now is more detached from its body below.

The dose field in the middle of the glove box due to streaming is not smeared and is localized into portions from the right and left workstations.

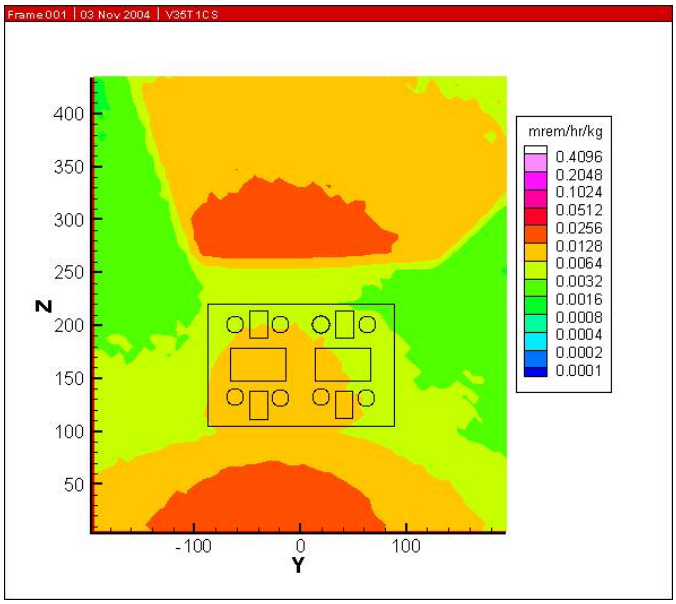

Figure 3-34: Shielded with Source at 135 cm.

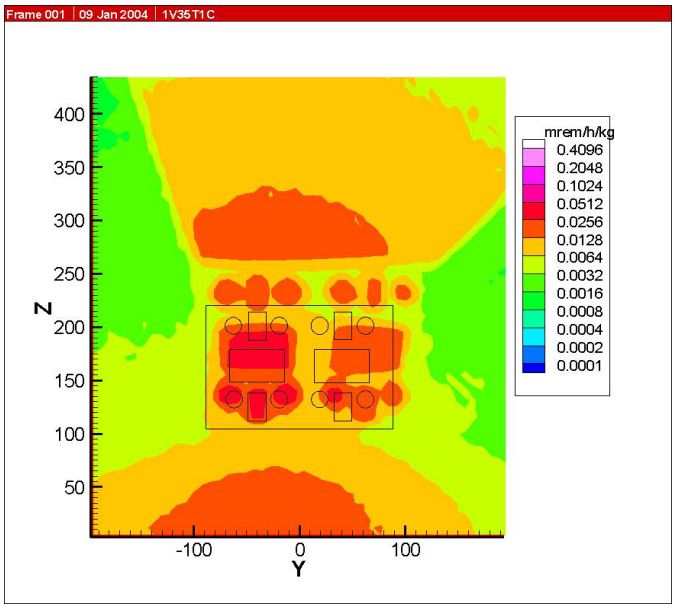

Figure 3-35: Windows and Glove Ports Unshielded with Source at 135 cm.

Above Z=300, the dose field is that coming from neutrons going through the top of the glove box. Below that level, streaming from all of the glove ports and windows is clearly identified.

The "Mickey Mouse" shape is getting smaller and now is more detached from its body below.

The dose field in the middle of the glove box due to streaming is not smeared and is localized into portions from the right and left workstations.

Overall, with the source is farther away, the dose field due to streaming is getting smaller in size while the remaining field is starting to become more uniform.

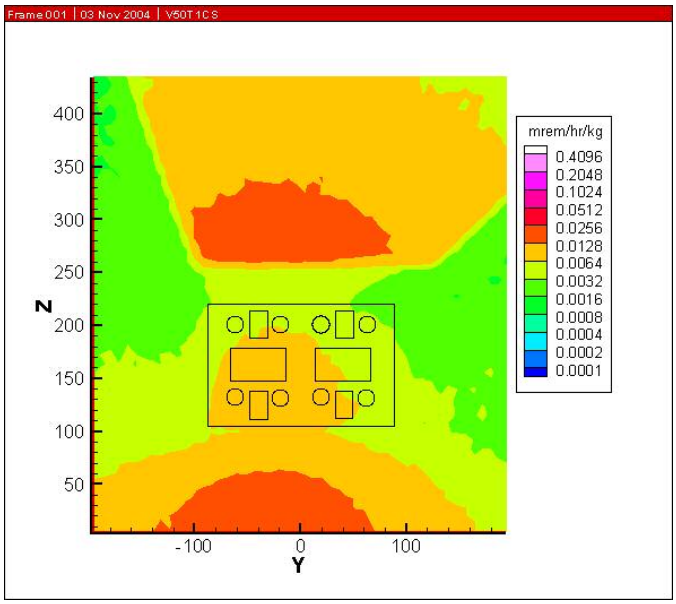

Figure 3-36: Windows and Glove Ports Shielded with Source at 150 cm.

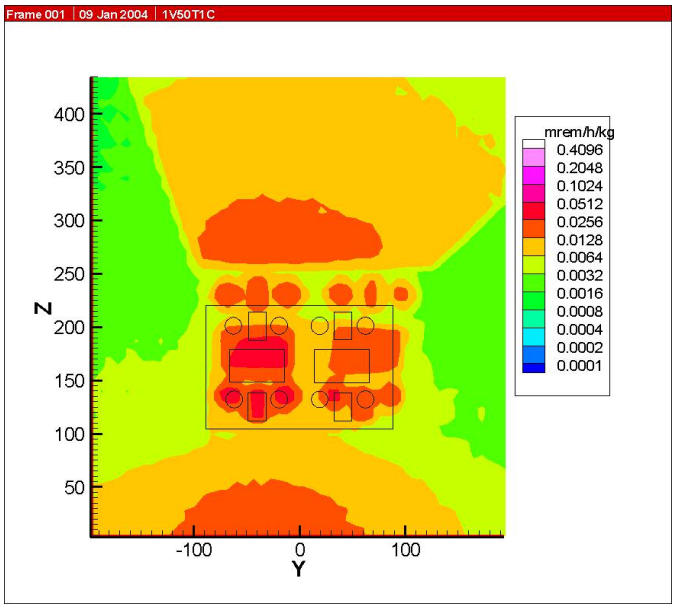

Figure 3-37: Windows and Glove Ports Unshielded with Source at 150 cm.

Above Z=300, the dose field is that coming from neutrons going through the top of the glove box. Below that level, streaming from all of the glove ports and windows is clearly identified.

The "Mickey Mouse" shape is getting smaller and now is more detached from its body below.

The dose field in the middle of the glove box due to streaming is not smeared and is localized into portions from the right and left workstations.

Overall, with the source is farther away, the dose field due to streaming is more localized while the remaining field is becoming more uniform.

Appendix C provides the comparison between the shielded and normal cases at 30.5 cm, 91.5 cm, and 183 cm (1 ft, 3 ft, and 6 ft) distances from the front of the glove box for each of the 33 different source positions. The discussion provided above for the cases where the source in on the line V and the dose plane at 30.5 cm (1 ft) applies to all of the other case. For the dose plane moves farther from the glove box, the more quickly the dose field tends to a more uniform field; especially as the source is moved farther back into the glove box.

3.4.2 Comparison of Whole Body Dose with Dosimeter Tally Plane Reference Position Dose

First, before performing a comparison of the whole body dose as determined from the computational phantom, it is desirable to compare the reference position doses using the different conversion factors from ANSI 1977, ANSI 1991, and ICRP 74. For a worker working in the glove box, the discussion will center on the phantom at the 30.5 cm (1 ft) location. There are three possible phantom positions and 33 possible source positions. With M, S, and V representing the middle of the glove box, S the line 6 cm to the right of the left side, and V in front of the viewing window of the lower left workstation and 1 representing the phantom distance from the glove box, the data is presented in curves for a given phantom position and the source moving back along one of the lines M, S, or V. Thus, MxxM1 represents the source position xx on the line M with the phantom at M1. In Figures 3-38 to 3-46 it is shown that ANSI 1977 conversion factors provide a more conservative estimate of the dose with ICRP 74 dose values just slightly lower than those obtained using ANSI 1977. This same conclusion is reached for the phantom at 91.5 cm (3 ft) (see Appendix F).

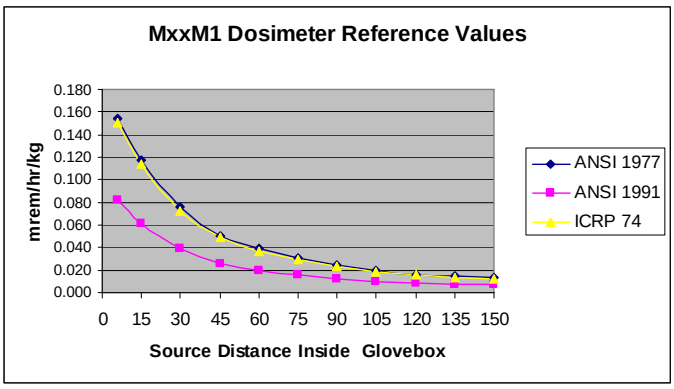

Figure 3-38: MxxM1.

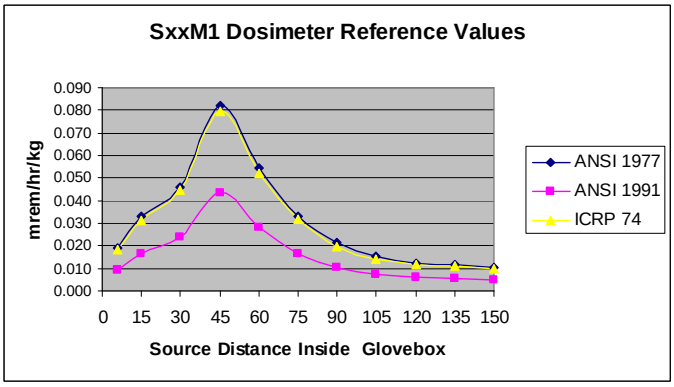

Figure 3-39: SxxM1.

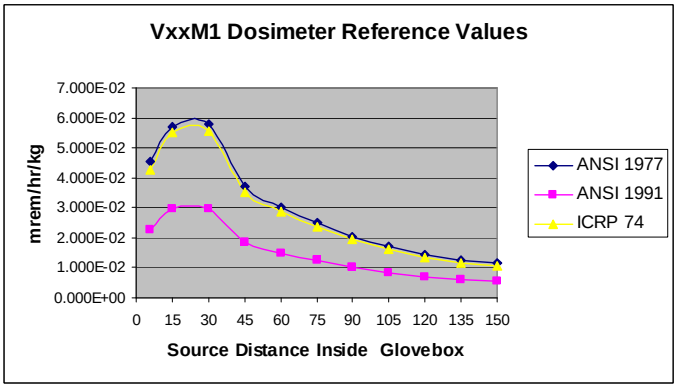

Figure 3-40: VxxM1.

The shape of the curve is to be expected since the streaming paths either go to the side of the worker since the worker is not in front of a workstation.

As distance along S increases, streaming through the left workstation glove ports and viewing window causes the dose to increase while moving the source farther back in the glove box results in the dose decreasing.

Streaming effects through the right glove port of the left workstation only affect the dose for distances close to the front of the glove box.

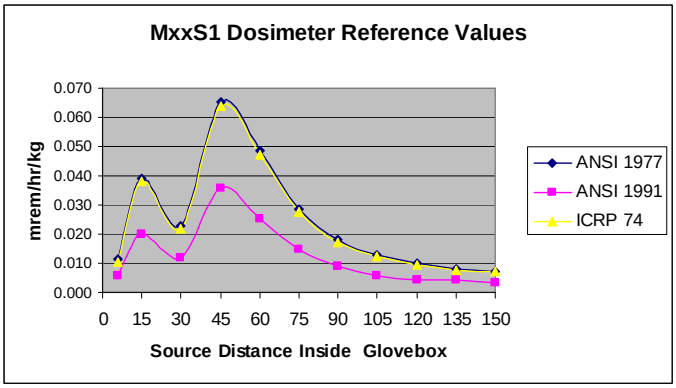

The first hump shows the streaming through the left glove port of the left workstation while the larger bump reflects the streaming through the viewing window.

Figure 3-41: MxxS1.

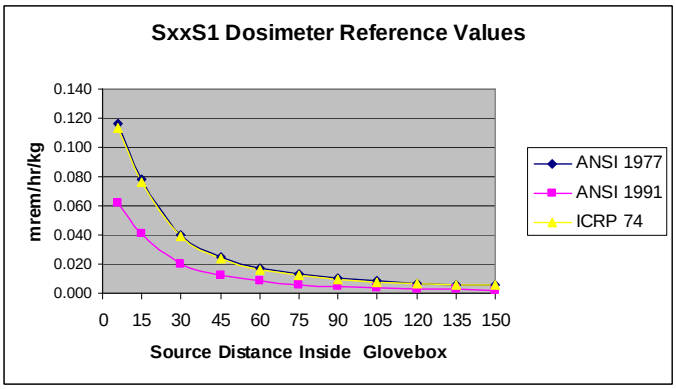

The shape of the curve is to be expected since the streaming paths either go to the side of the worker since the worker is not in front of a workstation.

Figure 3-42: SxxS1.

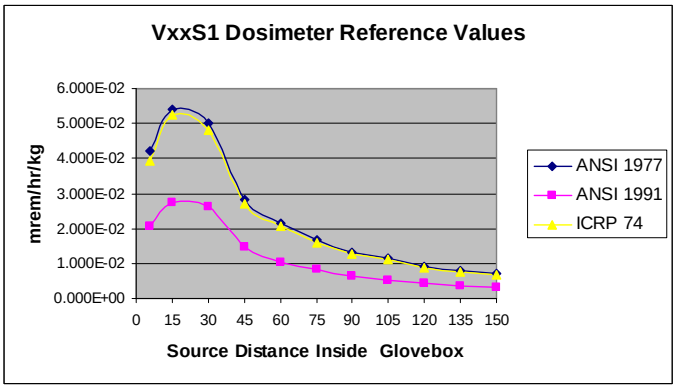

Streaming effects through the left glove port of the left workstation only affect the dose for distances close to the front of the glove box.

Figure 3-43: VxxS1.

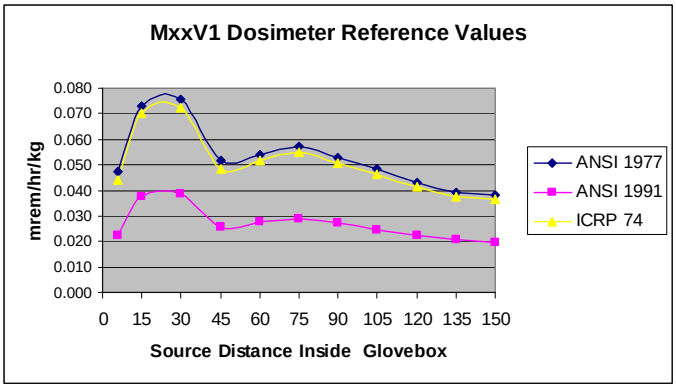

Figure 3-44: MxxV1.

Streaming effects through the right glove port of the left workstation only affect the dose for distances close to the front of the glove box. The smaller broader hump is due to the viewing window.

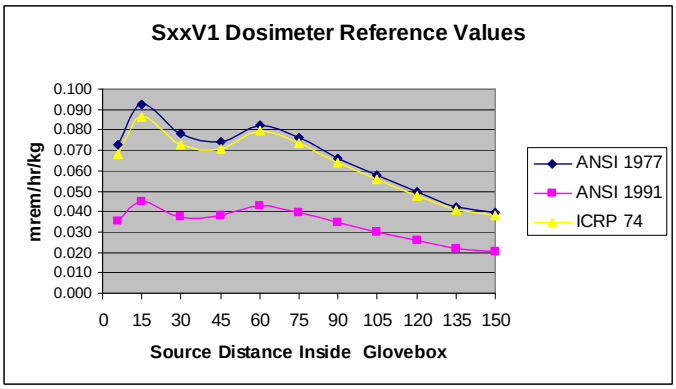

Figure 3-45: SxxV1.

There is relatively constant streaming through either the left glove port or the viewing window with the phantom in this position and the source on the side.

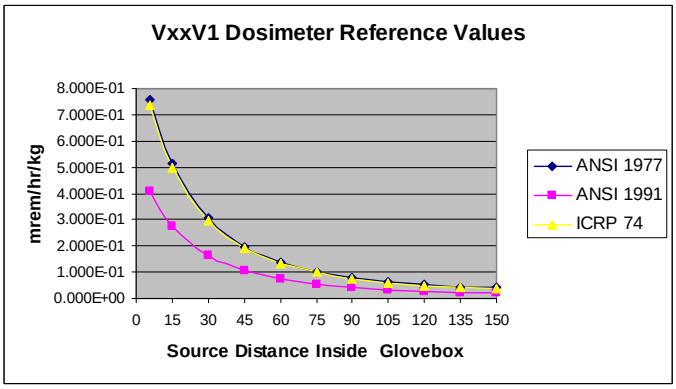

Figure 3-46: VxxV1.

Since the phantom is within the streaming pattern for all distances, the curve reflects the change in distance as the source moves toward the back of the glove box.

For each of the cases described above, the whole body dose was compared to the reference position dosimeter. The whole body dose in this case was calculated according to ICRP 26 methodology with neutron quality factors determined from ANSI 1977. This case was chosen since it is the regulatory position taken at Los Alamos. Other cases were looked at and are reported in Appendix G.

The whole body dose was calculated for a “male with breasts”, a normal male (without breasts), and for a female. The calculations for a “male with breasts” account for the breast tissue that a male has. Although the breast tissue volume for a male is small compared to a female, computational models show that that there is an increase in effective dose equivalent for low energy photons for smaller breast tissue volumes (Kramer and Drexler 1982).

The whole body dose for a male with breasts was greater than that of a male without breasts. In most cases the dose to a male without breasts was larger than the dose for a female. This is predominantly due to the dose that the testes receive. Table 3-9 provides the percentage of the whole body dose that comes from the dose received by the testes. Figures 3-47 to 3-55 provide the comparisons of the reference dosimeter with the different whole body doses calculated. In general, the whole body dose curves do not follow the reference position dosimeter. From a streaming point of view, the streaming paths will hit different parts of the body and the reference dosimeter may not be in all the paths.

Table 3-9: Contribution of Testes to Male Whole Body Dose.

	ANSI 1977	Testes % Contribution			ANSI 1977	Testes % Contribution	
Run	ICRP 26	MwB	MwoB	Run	ICRP 26	MwB	MwoB
1M06M1A	2.43E-02	47.2	58.3	1S75V1A	4.27E-03	21.9	39.4
1M06S1A	2.50E-03	39.3	48.4	1S90M1A	2.21E-03	21.5	33.1
1M06V1A	1.01E-02	45.9	55.8	1S90S1A	2.79E-03	46.9	56.2
1M15M1A	2.68E-02	52.5	62.2	1S90V1A	3.14E-03	19.8	34.3
1M15S1A	3.80E-03	36.0	51.7	1S05M1A	2.11E-03	23.8	36.6
1M15V1A	1.37E-02	44.0	51.0	1S05S1A	2.06E-03	44.5	54.2
1M30M1A	1.73E-02	51.1	60.5	1S05V1A	2.40E-03	18.3	30.9
1M30S1A	3.59E-03	26.2	38.4	1S20M1A	1.56E-03	22.7	37.2
1M30V1A	1.04E-02	30.2	41.5	1S20S1A	1.78E-03	45.7	55.9
1M45M1A	1.11E-02	46.9	58.0	1S20V1A	1.97E-03	18.0	29.8
1M45S1A	3.28E-03	27.4	39.4	1S35M1A	1.28E-03	22.6	39.2
1M45V1A	7.64E-03	25.8	40.0	1S35S1A	1.36E-03	42.9	53.6
1M60M1A	7.13E-03	40.0	54.6	1S35V1A	1.62E-03	17.5	28.8
1M60S1A	2.76E-03	24.2	32.2	1S50M1A	1.09E-03	21.8	38.9
1M60V1A	5.92E-03	26.1	45.3	1S50S1A	1.14E-03	40.3	50.8
1M75M1A	5.12E-03	36.0	53.0	1S50V1A	1.41E-03	16.3	27.1
1M75S1A	2.15E-03	21.2	30.7	1V06M1A	8.89E-03	37.8	47.3
1M75V1A	4.09E-03	23.6	42.1	1V06S1A	8.82E-03	37.8	46.6
1M90M1A	3.78E-03	33.4	51.0	1V06V1A	2.32E-02	18.6	30.3
1M90S1A	1.67E-03	20.3	30.8	1V15M1A	1.25E-02	44.6	51.8
1M90V1A	3.05E-03	22.0	39.4	1V15S1A	1.24E-02	45.8	52.5
1M05M1A	2.74E-03	30.0	47.9	1V15V1A	2.68E-02	26.0	39.4
1M05S1A	1.55E-03	21.5	32.9	1V30M1A	1.03E-02	31.8	43.0
1M05V1A	2.32E-03	19.9	35.2	1V30S1A	9.71E-03	31.5	42.5
1M20M1A	2.20E-03	28.6	46.4	1V30V1A	1.73E-02	26.5	39.1
1M20S1A	1.18E-03	20.1	32.0	1V45M1A	7.25E-03	28.6	41.8
1M20V1A	1.90E-03	18.7	32.3	1V45S1A	6.97E-03	29.1	42.3
1M35M1A	1.91E-03	28.6	46.8	1V45V1A	1.11E-02	26.6	37.7
1M35S1A	1.09E-03	22.1	37.1	1V60M1A	5.54E-03	31.4	49.2
1M35V1A	1.66E-03	18.3	30.9	1V60S1A	5.05E-03	31.9	50.1

	ANSI 1977	Testes % Contribution			ANSI 1977	Testes % Contribution	
Run	ICRP 26	MwB	MwoB	Run	ICRP 26	MwB	MwoB
1M50M1A	1.43E-03	24.5	42.2	1V60V1A	7.47E-03	26.7	37.4
1M50S1A	9.18E-04	20.7	36.6	1V75M1A	3.97E-03	30.0	48.8
1M50V1A	1.43E-03	17.0	28.8	1V75S1A	3.87E-03	32.8	52.6
1S06M1A	3.21E-03	38.8	48.7	1V75V1A	4.99E-03	24.8	34.6
1S06S1A	2.06E-02	46.4	57.1	1V90M1A	3.39E-03	31.7	49.9
1S06V1A	1.29E-02	43.9	54.5	1V90S1A	2.51E-03	29.7	49.3
1S15M1A	4.93E-03	30.3	43.3	1V90V1A	3.69E-03	24.8	34.2
1S15S1A	2.42E-02	55.5	63.6	1V05M1A	2.53E-03	29.8	47.7
1S15V1A	1.71E-02	42.0	49.8	1V05S1A	2.04E-03	29.9	49.1
1S30M1A	4.85E-03	29.9	42.9	1V05V1A	2.69E-03	22.6	31.4
1S30S1A	1.49E-02	55.5	62.9	1V20M1A	1.99E-03	28.7	46.4
1S30V1A	1.25E-02	29.7	43.0	1V20S1A	1.59E-03	29.5	48.0
1S45M1A	4.26E-03	26.9	36.4	1V20V1A	2.13E-03	21.9	30.2
1S45S1A	9.24E-03	53.8	61.5	1V35M1A	1.65E-03	28.3	45.3
1S45V1A	9.29E-03	28.1	48.0	1V35S1A	1.39E-03	30.7	48.7
1S60M1A	3.36E-03	22.9	31.7	1V35V1A	1.78E-03	21.5	29.8
1S60S1A	6.21E-03	52.7	60.9	1V50M1A	1.31E-03	25.6	42.6
1S60V1A	6.08E-03	24.5	44.0	1V50S1A	1.27E-03	30.6	48.6
1S75M1A	2.89E-03	22.5	33.5	1V50V1A	1.47E-03	19.7	27.6
1S75S1A	4.29E-03	51.0	59.8	Average		30.9	43.8

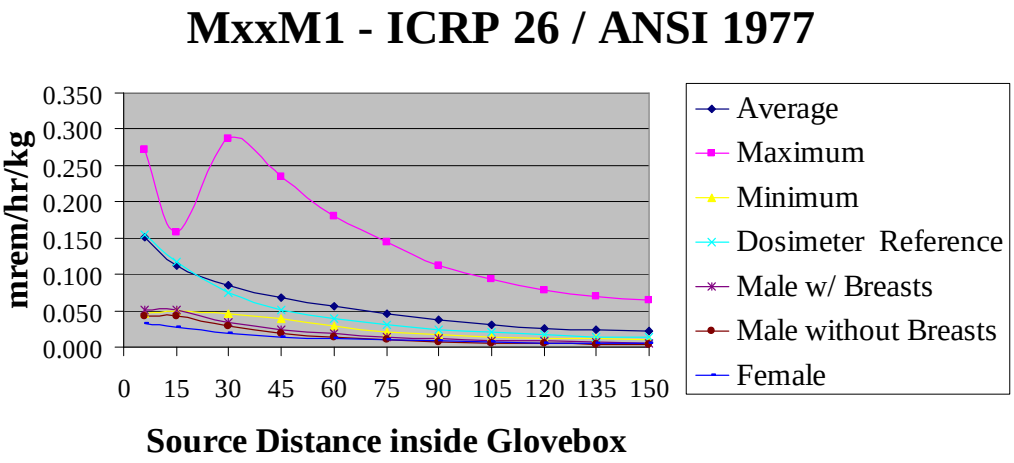

Figure 3-47: MxxM1- ICRP 26 – ANSI 1977.

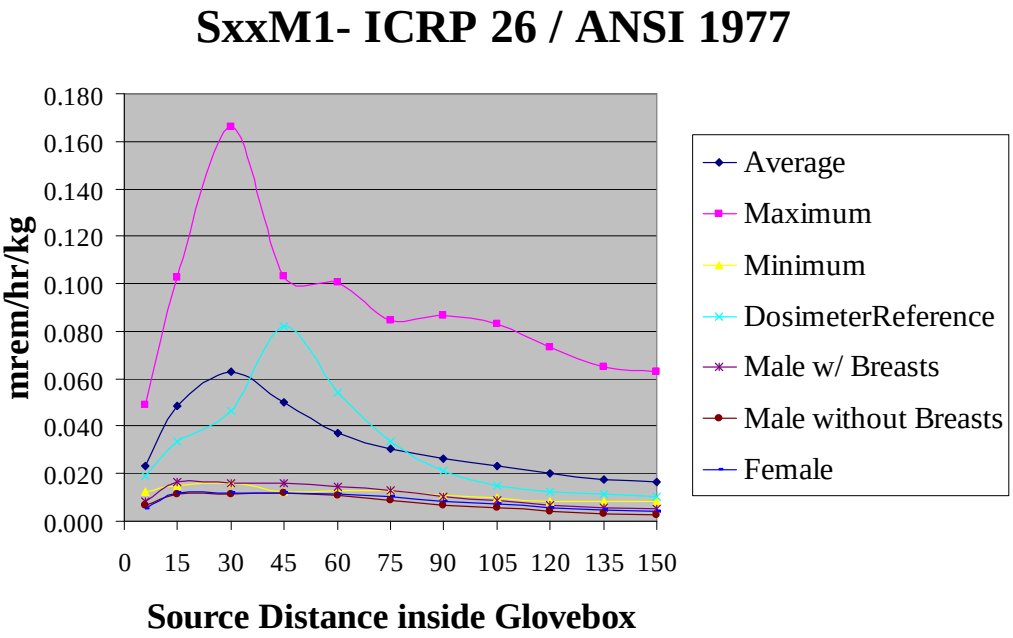

Figure 3-48: SxxM1- ICRP 26 – ANSI 1977.

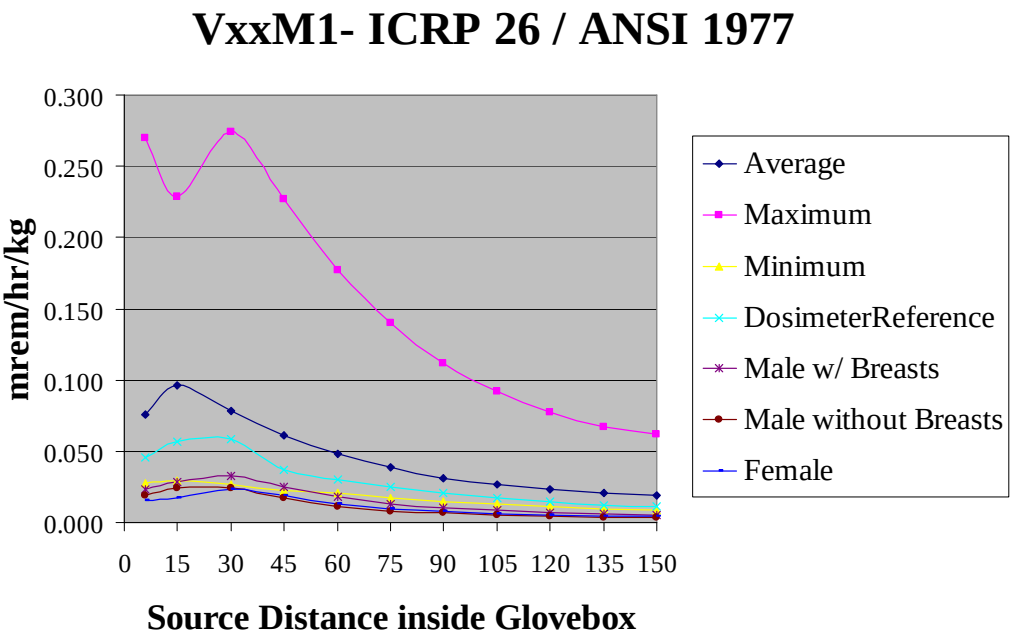

Figure 3-49: VxxM1- ICRP 26 – ANSI 1977.

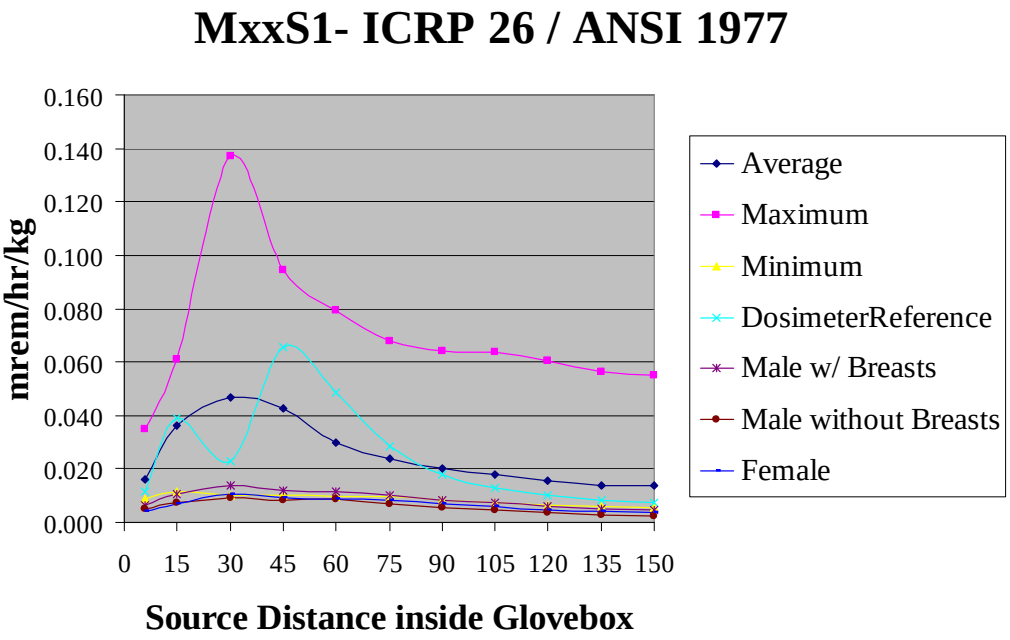

Figure 3-50: MxxS1- ICRP 26 – ANSI 1977.

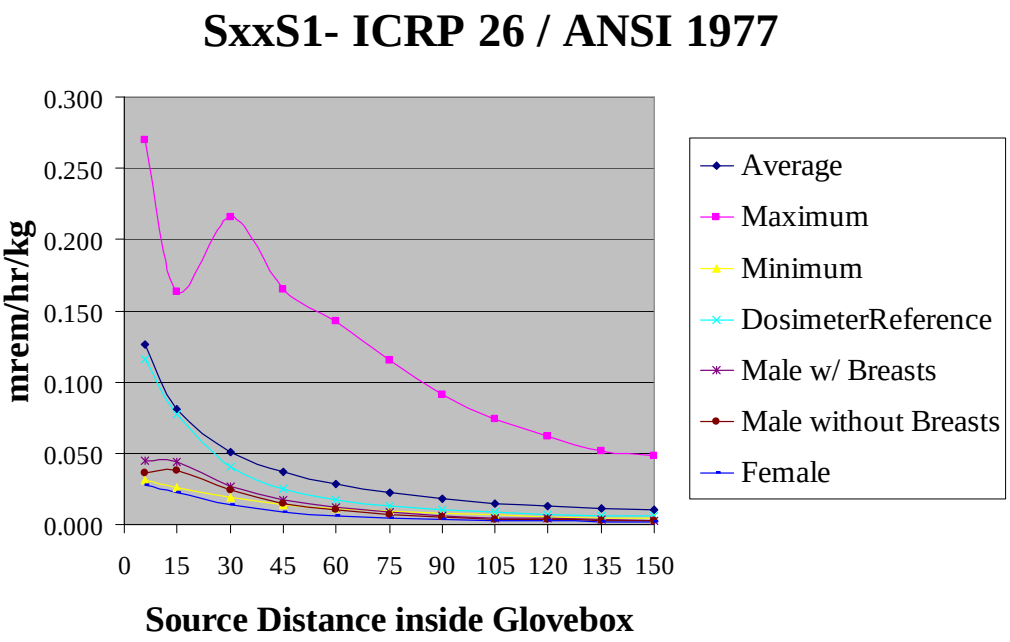

Figure 3-51: SxxS1- ICRP 26 – ANSI 1977.

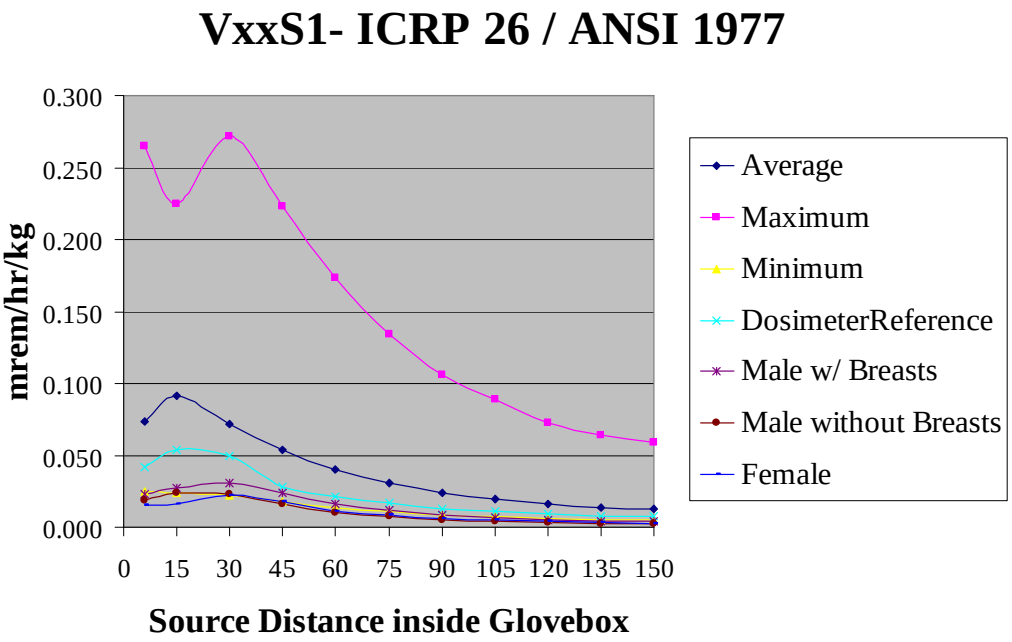

Figure 3-52: VxxS1- ICRP 26 – ANSI 1977.

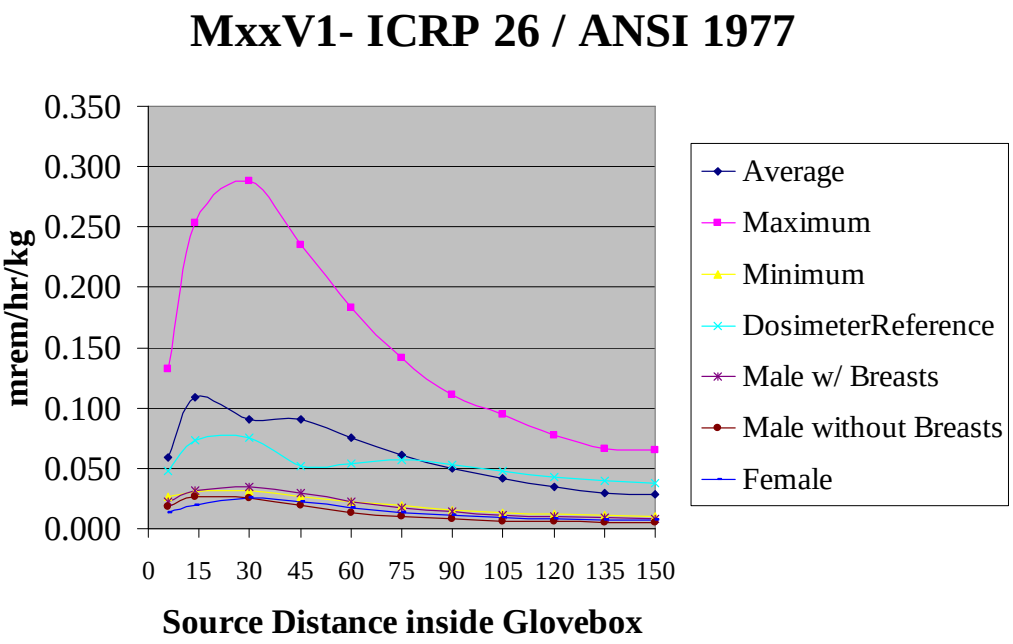

Figure 3-53: MxxV1- ICRP 26 – ANSI 1977.

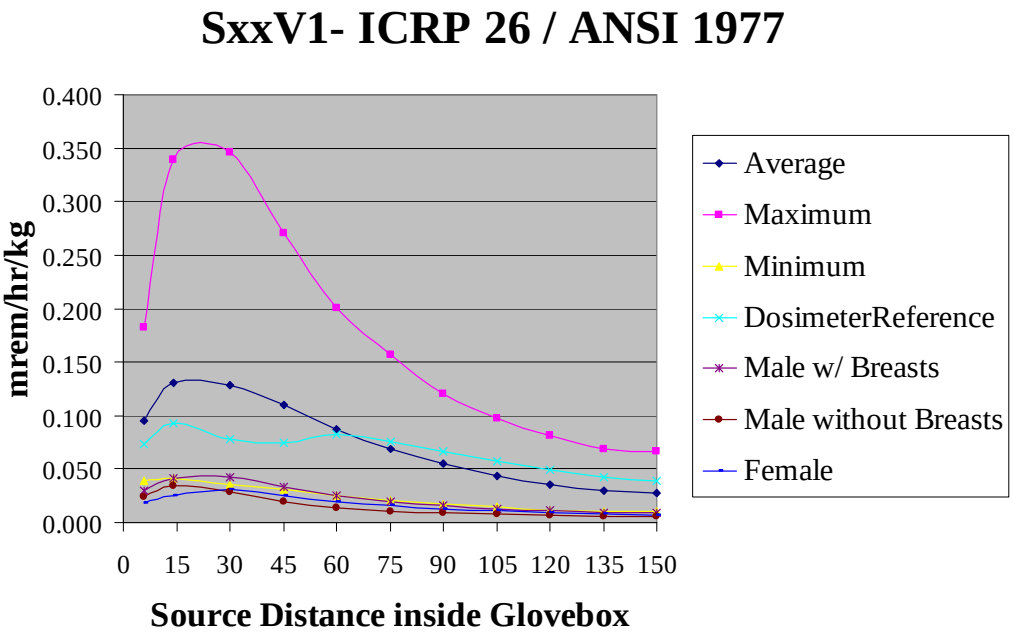

Figure 3-54: SxxV1- ICRP 26 – ANSI 1977.

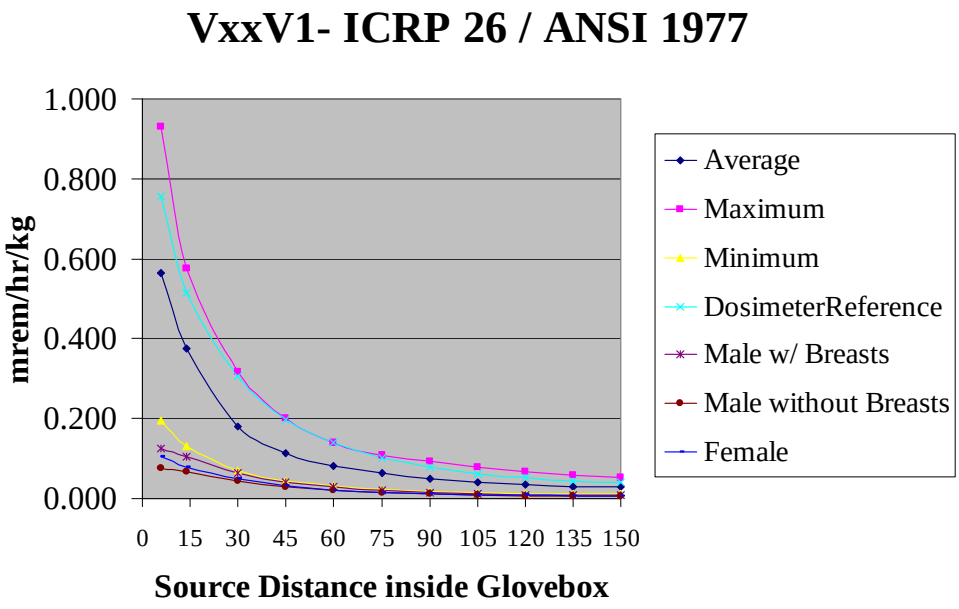

Figure 3-55: VxxV1- ICRP 26 – ANSI 1977.

3.4.3 Comparison of Whole Body Dose with Various Dosimeter Tally Plane Doses

For each configuration, the average, maximum, and minimum values that occurred on the dosimeter tally plane were determined. These were compared with the whole body doses that were calculated using the phantom. For the case of ICRP 26 methodology using ANSI 1977 data, Figures 3-47 to 3-55 above show the comparison. Appendix G provides the comparison for other cases. For this case it is seen that the minimum value tracks very well with the whole body doses that were calculated. From Table H.3-1, it is seen that 77% of the time, the dosimeter with the minimum value is one that is worn at waist level. When the phantom is at one of the 91.5 cm (3 ft) locations, the dosimeter with the minimum value is worn at the waist level 74% of the time.

Chapter 4: Conclusions and Recommendations

4.1 GENERAL DISCUSSION

Shielding problems can be among the most difficult to solve. Coupled with the task of estimating the dose that a worker receives makes it even more difficult. Because of the traditional way shielding is taught, most people do not understand that there are realistic issues dealing with non-uniform radiation fields resulting from streaming of radiation from an experiment, process, or operation through areas that are less shielded than others; especially when the work involves "shielded" glove boxes. This study with the following conclusions and recommendations is the author's attempt to clarify some of these issues.

4.2 CONCLUSIONS AND RECOMMENDATIONS

4.2.1 Conclusions

The followings conclusions are made:

1) The neutron radiation field and associated dose field are very dependent on the streaming paths available. In the case considered here, the magnitude of the change of the dose field relative to the same location in the shielded case can be a factor or 4 or more. This is in keeping with the attenuation properties of the two inches of neutron shielding material in the shell (34% NS-3 + 1% B_4C + 65% Pb whose half value thickness is 2.4 cm). Thus, in streaming areas, the radiation field is as if there were no shielding present.
2) With the source close in to the front of the glove box, the streaming patterns are smeared together in many cases. As the source is moved

farther back into the box, the streaming patterns are more collimated. Thus, depending on the location of the worker and where the source material is, the dose received can be significantly higher.

3) ANSI 1977 conversion factors provide a more conservative estimate of the dose with ICRP 74 dose values just slightly lower than those obtained using ANSI 1977.
4) The whole body dose for a male with breasts was greater than that of a male without breasts or a female. In most cases the dose to a male without breasts was larger than the dose for a female. This is predominantly due to the dose that the testes receive. The testes contribute almost 44% to the total whole body dose on the average for a male without breasts with a range of 27% to 64%.
5) Consider the region in the dose plane from the floor level to the level of the bottom of the glove box. Although this region does not have any streaming paths due to glove ports or windows, the non-uniform field in this region is due to the varying thicknesses of the bottom shell that the radiation has to traverse. Thus, the pattern of the dose field is determined by where the source is located. At the same height above the floor, the magnitude of the dose field decreases the farther the source is inside the glove box. Thus, for normal working conditions where the source is close to the front of the glove box, the dose to the testes is higher.
6) In the dosimeter tally plane, the dosimeter with the minimum value tracks the whole body dose very well. The dosimeter with the minimum value is one that is worn at waist level 77% of the time. When the phantom is at

one of the 3 ft locations, the dosimeter with the minimum value is worn at the waist level 74% of the time.

7) The reference dosimeter position can overestimate the whole body dose between a factor of two to six depending on location of the phantom and with the source material close to the front of the glove box.

4.2.2 Recommendations

1) Experimental validation and benchmarking of MCNP models of glove boxes is needed.
2) Since the LANL TLD can be in a significantly varying radiation field (i.e., each element is not seeing the same uniform field), a reevaluation of the dose algorithms should be performed. In addition, further studies of the angular dependence of the dosimeter should be made with the dosimeter in a highly varying radiation field.
3) Collaboration with experimenters conducting similar photon studies is needed. Most radiation sources of interest are photon sources in addition to neutron sources.
4) Streaming paths are important considerations for co-located workers since they may easily be in a higher dose field than they thought they were in. These paths should be determined for all glove boxes so that a proper ALARA (As Low As Reasonably Achievable) evaluation can be made. These evaluations focus on the different methods that reduce dose: increase shielding (type of shielding, internal or external, thickness required, and cost), minimize time (as relates to productivity and operational concerns relative to potential dose received), and maximize

distance between source material and worker. These methods are not independent of each other.

5) Currently, dosimeters are required to be worn between waist and neck level. The reference position in the middle of the chest provides an overly conservative estimate of the whole body dose by a factor of two to six depending on location of material and where the worker stands. Consideration should be given to requiring dosimeters to be worn at waist level. This should provide a better estimate of the whole body dose 75% of the time. Experimental validation of this recommendation is needed.
6) Internal shielding around source material that is not being handled or processed in some fashion should be considered. This would reduce the dose from this material for all streaming paths of interest.
7) Glove ports and windows in workstations that are not being used should be provided with external shielding to reduce the dose from these streaming paths.
8) Additional shielding from waist level down and under the glove box should be provided either in the design and construction of new glove boxes or externally if they are already built. This is needed in order to reduce the dose to the testes for male workers.
9) Estimates of whole body dose should include males with breasts. Males have about 8% of all breast cancers. Since males have a smaller breast tissue volume, a higher dose is received by the male compared to the female who has a larger breast tissue volume.

Appendix A: Neutron Attenuation Provided By Several Different Materials

METHODOLOGY FOR DETERMINING THE ATTENUATION OF DIFFERENT NEUTRON SHIELDING MATERIALS

A point source of clean weapons grade (WG) Pu was placed at the origin. At a distance of 45 cm from the source, a spherical shell ranging between 2 and 20 cm was placed that contained the material of interest. At a distance of 100 cm, the dose (mrem/hr/kg of WG Pu) and spectra (n/s/kg of WG Pu)) were determined.

For each material, runs were made for shell thicknesses of 0, 2, 4, 6, 8, 10, 12, 14, 16, 18, and 20 cm. The dose at thickness t, D_t, was divided by the dose at 0 cm, D_0. A plot of ln (D_t/ D_0) vs thickness was made for each material. The attenuation coefficient is the negative of the value of the slope. The half value layer and tenth value layer were then determined from the attenuation coefficient. Table D-1 provides the attenuation coefficient based on dose and the corresponding half-and tenth-value layers for many shielding materials of interest. Table D-2 provides the same except that it was based on the spectra.

Table A-1: Attenuation Coefficients for Various Materials Based on Dose

Material	Material	Att. Coef.	$X_{1/2}$ (cm)	$X_{1/10}$ (cm)
Nylon	m702	0.3028	2.289	7.604
NS-3 + 1% B4C + 65% Pb	m516	0.2874	2.412	8.012
NS-4 + 56% B4c + 32% Pb	m521	0.2850	2.432	8.079
NS-4-FR + 15% Pb	m524	0.2698	2.569	8.534
NS-4 + 88% Pb	m520	0.2563	2.704	8.984
NS-1 + 50% B4C + 34% Pb	m511	0.2514	2.757	9.159
NS-3 + 11.25% B4C + 70.75% Pb	m517	0.2493	2.780	9.236
NS-4-FR + 6.5% B4C + 8.5% Pb	m525	0.2321	2.986	9.921
NS-3 + 82% Pb	m515	0.2120	3.270	10.861
NS-1 + 84% Pb	m510	0.1893	3.662	12.164
PVC	m703	0.1885	3.677	12.215

Material	Material	Att. Coef.	$X_{1/2}$ (cm)	$X_{1/10}$ (cm)
NS-4 + 56% B4C	m519	0.1848	3.751	12.460
Paraffin	m526	0.1824	3.800	12.624
Lithium Hydride	m543	0.1784	3.885	12.907
Polyethylene	m528	0.1762	3.934	13.068
Rx #213	m534	0.1761	3.936	13.075
Krafton-XP3	m506	0.1713	4.046	13.442
NS-4-FR + 6.5% B4C	m523	0.1698	4.082	13.561
Krafton-N5	m505	0.1697	4.085	13.569
WEP	m541	0.1693	4.094	13.601
Rx #207	m532	0.1679	4.128	13.714
Rx #259	m539	0.1678	4.131	13.722
Rx #210	m533	0.1676	4.136	13.739
NS-4-FR	m522	0.1664	4.166	13.838
Krafton-C1	m504	0.1660	4.176	13.871
Premadex	m530	0.1578	4.393	14.592
Rx #201	m531	0.1558	4.449	14.779
NS-3 + 11.25% B4C	m514	0.1520	4.560	15.149
NS-4	m518	0.1503	4.612	15.320
NS-3 + 4% B4C	m513	0.1498	4.627	15.371
Plexiglas (Lucite)	m527	0.1478	4.690	15.579
Borated Water	m003	0.1469	4.718	15.675
Heavy Water	m004	0.1469	4.718	15.675
NS-3	m512	0.1461	4.744	15.760
Water	m002	0.1452	4.774	15.858
Rx #215	m535	0.1451	4.777	15.869
Bisco	m500	0.1395	4.969	16.506
Rx #244	m538	0.1365	5.078	16.869
NS-1 + 50% B4C	m509	0.1345	5.154	17.120
Kynar	m701	0.1343	5.161	17.145
Rx #237	m537	0.1304	5.316	17.658
Boron Carbide	m503	0.1296	5.348	17.767
Rx #217	m536	0.1293	5.361	17.808
Lexan	m507	0.1209	5.733	19.045
Borobond 4.1	m501	0.1117	6.205	20.614
Rx #277	m540	0.1084	6.394	21.242

Material	Material	Att. Coef.	$X_{1/2}$ (cm)	$X_{1/10}$ (cm)
NS-1	m508	0.1055	6.570	21.825
Cadmium Glass	m401	0.0993	6.980	23.188
Liquid Hydrogen	m542	0.0860	8.060	26.774
Silicon Rubber	m704	0.0757	9.157	30.417
Teflon	m705	0.0733	9.456	31.413
Leaded Glass 6.0	m403	0.0732	9.469	31.456
Boral	m502	0.0657	10.550	35.047
Graphite	m005	0.0549	12.626	41.941
Leaded Glass 3.8	m402	0.0548	12.649	42.018
Compacted Tuff	m800	0.0548	12.649	42.018
Fiberglass	m700	0.0513	13.512	44.885
Borosilicate Glass	m400	0.0470	14.748	48.991
Ordinary Concrete	m200	0.0457	15.167	50.385
Iconel	m303	0.0433	16.008	53.177
316SS	m301	0.0382	18.145	60.277
304SS	m300	0.0366	18.938	62.912
Pyrex	m404	0.0364	19.043	63.258
Carbon Steel	m302	0.0266	26.058	86.563
Polyurethane	m529	0.0004	1732.868	5756.463
Air	m001	0.0000	346573.590	1151292.546

Table A-2: Attenuation Coefficients for Various Materials

Material	Number	Att. Coef.	$X_{1/2}$ (cm)	$X_{1/10}$ (cm)
NS-4 + 56% B4c + 32% Pb	m521	0.2847	2.435	8.088
NS-3 + 1% B4C + 65% Pb	m516	0.2841	2.440	8.105
NS-1 + 50% B4C + 34% Pb	m511	0.2485	2.789	9.266
NS-3 + 11.25% B4C + 70.75% Pb	m517	0.2456	2.822	9.375
NS-4-FR + 15% Pb	m524	0.2375	2.919	9.695
NS-4-FR + 6.5% B4C + 8.5% Pb	m525	0.2318	2.990	9.933
Nylon	m702	0.2197	3.155	10.481
NS-4 + 88% Pb	m520	0.2027	3.420	11.360
NS-4 + 56% B4C	m519	0.1840	3.767	12.514
PVC	m703	0.1800	3.851	12.792
NS-4-FR + 6.5% B4C	m523	0.1661	4.173	13.863
Rx #210	m533	0.1661	4.173	13.863
Lithium Hydride	m543	0.1654	4.191	13.921
WEP	m541	0.1629	4.255	14.135
Rx #259	m539	0.1622	4.273	14.196
Rx #207	m532	0.1608	4.311	14.320
Rx #201	m531	0.1514	4.578	15.209
Premadex	m530	0.1504	4.609	15.310
NS-3 + 82% Pb	m515	0.1499	4.624	15.361
NS-3 + 11.25% B4C	m514	0.1481	4.680	15.548
Paraffin	m526	0.1481	4.680	15.548
NS-3 + 4% B4C	m513	0.1440	4.814	15.990
Polyethylene	m528	0.1408	4.923	16.354
Rx #213	m534	0.1407	4.926	16.365
Borated Water	m003	0.1388	4.994	16.589
Rx #215	m535	0.1355	5.115	16.993
Bisco	m500	0.1338	5.180	17.209
NS-1 + 50% B4C	m509	0.1305	5.311	17.644
Rx #244	m538	0.1293	5.361	17.808
Krafton-C1	m504	0.1290	5.373	17.849
Krafton-N5	m505	0.1275	5.436	18.059
NS-4-FR	m522	0.1257	5.514	18.318

Material	Number	Att. Coef.	$X_{1/2}$ (cm)	$X_{1/10}$ (cm)
Krafton-XP3	m506	0.1234	5.617	18.660
NS-1 + 84% Pb	m510	0.1232	5.626	18.690
Boron Carbide	m503	0.1231	5.631	18.705
Rx #237	m537	0.1202	5.767	19.156
NS-4	m518	0.1137	6.096	20.251
Water	m002	0.1090	6.359	21.125
Plexiglas (Lucite)	m527	0.1036	6.691	22.226
Borobond 4.1	m501	0.1019	6.802	22.597
NS-3	m512	0.1009	6.870	22.820
Rx #277	m540	0.0968	7.161	23.787
Rx #217	m536	0.0827	8.381	27.843
Lexan	m507	0.0700	9.902	32.894
Kynar	m701	0.0676	10.254	34.062
Silicon Rubber	m704	0.0616	11.252	37.380
NS-1	m508	0.0588	11.788	39.160
Liquid Hydrogen	m542	0.0537	12.908	42.879
Boral	m502	0.0519	13.355	44.366
Cadmium Glass	m401	0.0374	18.533	61.566
Borosilicate Glass	m400	0.0226	30.670	101.884
Fiberglass	m700	0.0211	32.851	109.127
Iconel	m303	0.0174	39.836	132.332
Pyrex	m404	0.0122	56.815	188.736
316SS	m301	0.0092	75.342	250.281
304SS	m300	0.0075	92.420	307.011
Ordinary Concrete	m200	0.0064	108.304	359.779
Leaded Glass 6.0	m403	0.0055	126.027	418.652
Leaded Glass 3.8	m402	0.0032	216.608	719.558
Carbon Steel	m302	0.0027	256.721	852.809
Teflon	m705	0.0009	770.164	2558.428
Compacted Tuff	m800	0.0007	990.210	3289.407
Heavy Water	m004	0.0004	1732.868	5756.463
Graphite	m005	0.0004	1732.868	5756.463
Polyurethane	m529	0.0000	34657.359	115129.255
Air	m001	0.0000	173286.795	575646.273

Appendix B: Example Of Spreadsheet Format For Calculating Phantom Dose Estimates

Table B-1: Sheet 1: Input

Phantom ANSI 1977 Neutron Tally		**Date:**	23 Dec 2003		
Neutron		**Preparer:**	ABC		
1 kg Pu (clean)		**fm:**	2.29E+08	src particle / hr-basis	
Phantom 1 ft from GB		6.359E+04 sp/s-kg * 3600 s/hr			
1940	keV	**Average of neutron energy spectrum**			
Tally Cell	mrem/sp	sp/hr-basis	mrem/hr-basis		
306	8.29808E-11	2.29E+08	1.90E-02		
316	5.86938E-10	2.29E+08	1.34E-01		
326	8.23482E-10	2.29E+08	1.89E-01		
336	3.88792E-12	2.29E+08	8.90E-04		
346	8.39152E-14	2.29E+08	1.92E-05		
356	1.07729E-10	2.29E+08	2.47E-02		
366	6.26512E-11	2.29E+08	1.43E-02		
376	4.11304E-10	2.29E+08	9.42E-02		
386	8.39152E-14	2.29E+08	1.92E-05		
396	2.66822E-10	2.29E+08	6.11E-02		
406	1.52873E-10	2.29E+08	3.50E-02		
416	2.92987E-10	2.29E+08	6.71E-02		
426	5.12470E-10	2.29E+08	1.17E-01		
436	7.42672E-11	2.29E+08	1.70E-02		
446	9.23479E-11	2.29E+08	2.11E-02		
456	9.62839E-11	2.29E+08	2.20E-02		
466	7.87520E-11	2.29E+08	1.80E-02		
476	9.37811E-15	2.29E+08	2.15E-06		
486	2.07578E-10	2.29E+08	4.75E-02		
496	4.68944E-10	2.29E+08	1.07E-01		
506	3.74382E-10	2.29E+08	8.57E-02		
516	2.63250E-10	2.29E+08	6.03E-02		
526	1.14310E-10	2.29E+08	2.62E-02		
536	1.02074E-09	2.29E+08	2.34E-01		
546	5.54599E-11	2.29E+08	1.27E-02		
556	7.95029E-11	2.29E+08	1.82E-02		

Table B-2: Sheet 2 – Phantom plus ICRP 26 Remainder

Androgynous Phantom:					
ICRP 26			ICRP 60		
Cell	Tissue	mrem/hr-basis	Cell	Tissue	mrem/hr-basis
6	Brain	1.90E-02	6	Brain	1.90E-02
16	Thyroid	1.34E-01	16	Thyroid	1.34E-01
26	Thymus	1.89E-01	26	Thymus	1.89E-01
36	Lungs	8.90E-04	36	Lungs	8.90E-04
46	Heart	1.92E-05	46	Heart	1.92E-05
56	Adrenals	2.47E-02	56	Adrenals	2.47E-02
66	Kidneys	1.43E-02	66	Kidneys	1.43E-02
76	Liver	9.42E-02	76	Liver	9.42E-02
86	Gall Bladder	1.92E-05	86	Gall Bladder	1.92E-05
96	Pancreas	6.11E-02	96	Pancreas	6.11E-02
106	Spleen	3.50E-02	106	Spleen	3.50E-02
116	Esophagus	6.71E-02	116	Esophagus	6.71E-02
126	Stomach	1.17E-01	126	Stomach	1.17E-01
136	Small Intestine	1.70E-02	136	Small	1.70E-02
146	Ascending Colon	2.11E-02	146	Ascending	2.11E-02
156	Transverse Colon	2.20E-02	156	Transverse	2.20E-02
166	Descending Colon	1.80E-02	166	Descending	1.80E-02
176	Sigmoid	2.15E-06	176	Sigmoid	2.15E-06
186	Bladder	4.75E-02	186	Bladder	4.75E-02
196	Testes	1.07E-01	196	Testes	1.07E-01
206	Gentalia	8.57E-02	206	Gentalia	8.57E-02
216	Skin	6.03E-02	216	Skin	6.03E-02
226	Bone	2.62E-02	226	Bone	2.62E-02
236	Breast	2.34E-01	236	Breast	2.34E-01
246	Ovaries	1.27E-02	246	Ovaries	1.27E-02
256	Uterus	1.82E-02	256	Uterus	1.82E-02
Sheet 4	Red Bone Marrow	2.73E-02		Red Bone	2.73E-02
Sheet 4	NBS	2.60E-02		NBS	2.60E-02
Sheet 3	Colon	1.76E-02		Colon	1.76E-02
Sheet 3	ULI	1.76E-02		ULI	1.76E-02
			Male	Remainder	2.02E-02
			Female	Remainder	2.05E-02

Determination of Reminder Tissues			Top 5 Remainder Tissues				
Rank	Tissue	mrem/hr-basis	1	2	3	4	5
16	Brain	1.90E-02	Thymus	Stomach	Liver	Gentalia	Esophagus
1	Thymus	1.89E-01	1.89E-01	1.17E-01	9.42E-02	8.57E-02	6.71E-02
20	Heart	1.92E-05					
13	Adrenals	2.47E-02					
19	Kidneys	1.43E-02					
3	Liver	9.42E-02					
20	Gall Bladder	1.92E-05					
6	Pancreas	6.11E-02					
9	Spleen	3.50E-02					
5	Esophagus	6.71E-02					
2	Stomach	1.17E-01					
18	Small	1.70E-02					
15	Ascending	2.11E-02					
14	Transverse	2.20E-02					
17	Descending	1.80E-02					
22	Sigmoid	2.15E-06					
8	Bladder	4.75E-02					
4	Gentalia	8.57E-02					
7	Skin	6.03E-02					
11	Bone	2.62E-02					
10	Colon	2.73E-02					
12	ULI	2.60E-02					

Table B-3: Sheet 3: Colon-ULI

Tissue Sum of Fractions						
	Colon dose rate mrem/hr-basis	fraction	weighted mrem/hr-basis	ULI dose rate mrem/hr-basis	fraction	weighted mrem/hr-basis
Ascending	2.11E-02	0.253	5.35E-03	2.11E-02	0.253	5.35E-03
Transverse	2.20E-02	0.340	7.49E-03	2.20E-02	0.340	7.49E-03
Descending	1.80E-02	0.263	4.74E-03	1.80E-02	0.263	4.74E-03
Sigmoid 1	2.15E-06	0.144	3.09E-07			
Sum			1.76E-02			1.76E-02

Table B-4: Sheet 4: Red Bone Marrow – Near Bone Surface

	Ratio BM to Bone	
E (keV)	RBM	NBS
60	0.2794	1.0197
100	0.519	1.0088
300	0.9481	1.0052
500	1.0004	1.0049
1000	1.0192	1.0051
1940	1.04E+00	9.93E-01

Bone	Ratio BM to Bone		mrem/hr-basis	
mrem/hr-basis	RBM	NBS	RBM	NBS
2.62E-02	1.04E+00	9.93E-01	2.73E-02	2.60E-02

Equations	
Red Bone Marrow	$y = 1.043\left(1 - e^{-0.006629x}\right)$
Near Bone Surface	$y = 1.0127 - 0.0000102x$
where x = E (keV) and y = Ratio BM to Bone	

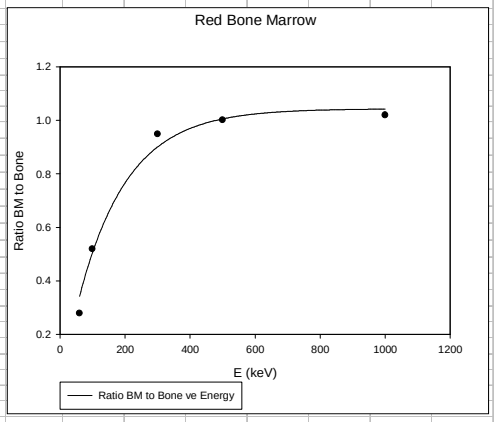

$y = 1.043\left(1 - e^{-0.006629x}\right)$

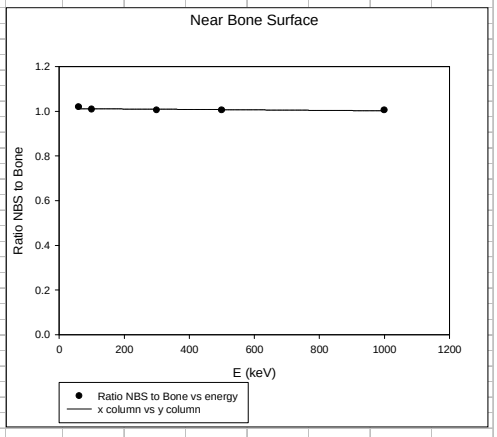

$y = 1.0127 - 0.0000102x$

Table B-5: Sheet 5: ICRP 60 Remainder

ICRP 60: Male and Female Remainder Determination				
Tissue	Fraction	mrem/hr-basi	Male mrem/hr-basis	Female mrem/hr-basis
Adrenal	0.00422	2.47E-02	1.04E-04	1.04E-04
Brain	0.36803	1.90E-02	6.99E-03	6.99E-03
ULI	0.16817	1.76E-02	2.96E-03	2.96E-03
SI	0.28476	1.70E-02	4.84E-03	4.84E-03
Kidney	0.07737	1.43E-02	1.11E-03	1.11E-03
Pancreas	0.02437	6.11E-02	1.49E-03	1.49E-03
Spleen	0.04728	3.50E-02	1.65E-03	1.65E-03
Thymus	0.0054	1.89E-01	1.02E-03	1.02E-03
Uterus	0.02042	1.82E-02		3.72E-04
Remainder			2.0164E-02	2.0536E-02

Table B-6: Sheet: EDE and ED

ICRP 26												
Male with breasts												
Tissue	Testes	Breast	RBM	Lungs	Thyroid	NBS	Thymus	Stomach	Liver	Gentalia	Esophagu	EDE
mrem/hr-b	1.07E-01	2.34E-01	2.73E-02	8.90E-04	1.34E-01	2.60E-02	1.89E-01	1.17E-01	9.42E-02	8.57E-02	6.71E-02	
fraction	0.25	0.15	0.12	0.12	0.03	0.03	0.06	0.06	0.06	0.06	0.06	
mrem/hr-b	2.68E-02	3.51E-02	3.28E-03	1.07E-04	4.03E-03	7.79E-04	1.13E-02	7.04E-03	5.65E-03	5.14E-03	4.02E-03	1.03E-01
Male without breasts												
Tissue	Testes	Breast	RBM	Lungs	Thyroid	NBS	Thymus	Stomach	Liver	Gentalia	Esophagu	EDE
mrem/hr-b	1.07E-01	2.34E-01	2.73E-02	8.90E-04	1.34E-01	2.60E-02	1.89E-01	1.17E-01	9.42E-02	8.57E-02	6.71E-02	
fraction	0.25	0	0.12	0.12	0.03	0.03	0.06	0.06	0.06	0.06	0.06	
mrem/hr-b	2.68E-02	0.00E+00	3.28E-03	1.07E-04	4.03E-03	7.79E-04	1.13E-02	7.04E-03	5.65E-03	5.14E-03	4.02E-03	6.82E-02
Female												
Tissue	Ovaries	Breast	RBM	Lungs	Thyroid	NBS	Thymus	Stomach	Liver	Gentalia	Esophagu	EDE
mrem/hr-b	1.27E-02	2.34E-01	2.73E-02	8.90E-04	1.34E-01	2.60E-02	1.89E-01	1.17E-01	9.42E-02	8.57E-02	6.71E-02	
fraction	0.25	0.15	0.12	0.12	0.03	0.03	0.06	0.06	0.06	0.06	0.06	
mrem/hr-b	3.17E-03	3.51E-02	3.28E-03	1.07E-04	4.03E-03	7.79E-04	1.13E-02	7.04E-03	5.65E-03	5.14E-03	4.02E-03	7.96E-02
ICRP 60												
Male with breasts												
Tissue	Testes	RBM	Colon	Lungs	Stomach	Bladder	Breast	Liver	Esophagu	Thyroid	Skin	NBS	Remainde	ED
mrem/hr-b	1.07E-01	2.73E-02	1.76E-02	8.90E-04	1.17E-01	4.75E-02	2.34E-01	9.42E-02	6.71E-02	1.34E-01	6.03E-02	2.60E-02	2.02E-02	
fraction	0.2	0.12	0.12	0.12	0.12	0.05	0.05	0.05	0.05	0.05	0.01	0.01	0.05	
mrem/hr-b	2.15E-02	3.28E-03	2.11E-03	1.07E-04	1.41E-02	2.38E-03	1.17E-02	4.71E-03	3.35E-03	6.72E-03	6.03E-04	2.60E-04	1.01E-03	7.18E-02
Male without breasts														
Tissue	Testes	RBM	Colon	Lungs	Stomach	Bladder	Breast	Liver	Esophagu	Thyroid	Skin	NBS	Remainde	ED
mrem/hr-b	1.07E-01	2.73E-02	1.76E-02	8.90E-04	1.17E-01	4.75E-02	2.34E-01	9.42E-02	6.71E-02	1.34E-01	6.03E-02	2.60E-02	2.02E-02	
fraction	0.2	0.12	0.12	0.12	0.12	0.05	0	0.05	0.05	0.05	0.01	0.01	0.05	
mrem/hr-b	2.15E-02	3.28E-03	2.11E-03	1.07E-04	1.41E-02	2.38E-03	0.00E+00	4.71E-03	3.35E-03	6.72E-03	6.03E-04	2.60E-04	1.01E-03	6.01E-02
Female														
Tissue	Ovaries	RBM	Colon	Lungs	Stomach	Bladder	Breast	Liver	Esophagu	Thyroid	Skin	NBS	Remainde	ED
mrem/hr-b	1.27E-02	2.73E-02	1.76E-02	8.90E-04	1.17E-01	4.75E-02	2.34E-01	9.42E-02	6.71E-02	1.34E-01	6.03E-02	2.60E-02	2.05E-02	
fraction	0.2	0.12	0.12	0.12	0.12	0.05	0.05	0.05	0.05	0.05	0.01	0.01	0.05	
mrem/hr-b	2.54E-03	3.28E-03	2.11E-03	1.07E-04	1.41E-02	2.38E-03	1.17E-02	4.71E-03	3.35E-03	6.72E-03	6.03E-04	2.60E-04	1.03E-03	5.28E-02

Appendix C: Neutron Radiation Field

APPENDIX C.1:

ANSI 1977 AT 1 FOOT WITH SOURCE ON LINE S

The neutron dose field is determined using ANSI 1977 flux-to-dose conversion factors and a mesh tally that is 1 ft in front of the glove box. Figures C.1-1 thru C.1-11 show the changes in the field as the source is moved from 6 cm from the front inside surface of the box to 150 cm from the inside surface on a line that is 6 cm from the left edge of the box (S). The source is 6 cm above the glove box floor. The outline of the front of glove box is shown in each Figure.

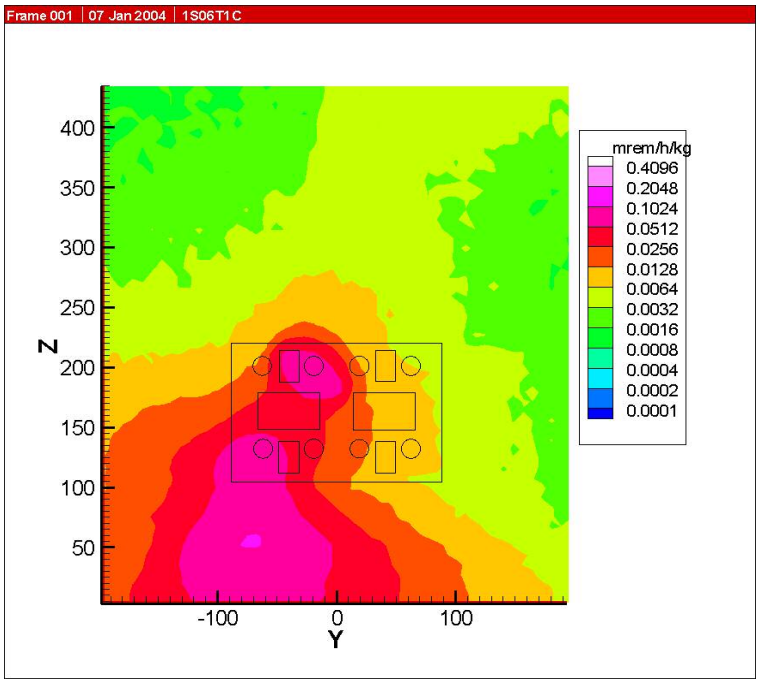

Figure C.1-1: Source at 6 cm.

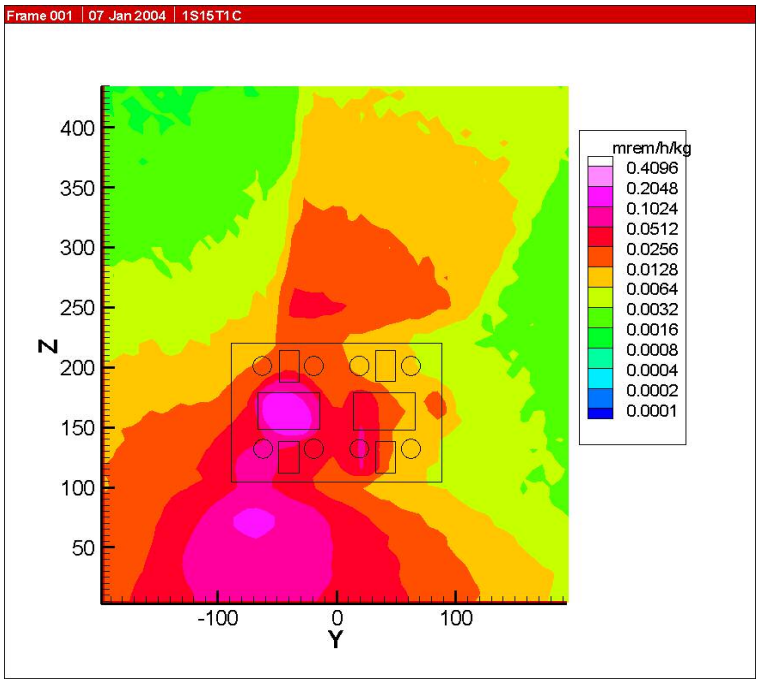

Figure C.1-2: Source at 15 cm.

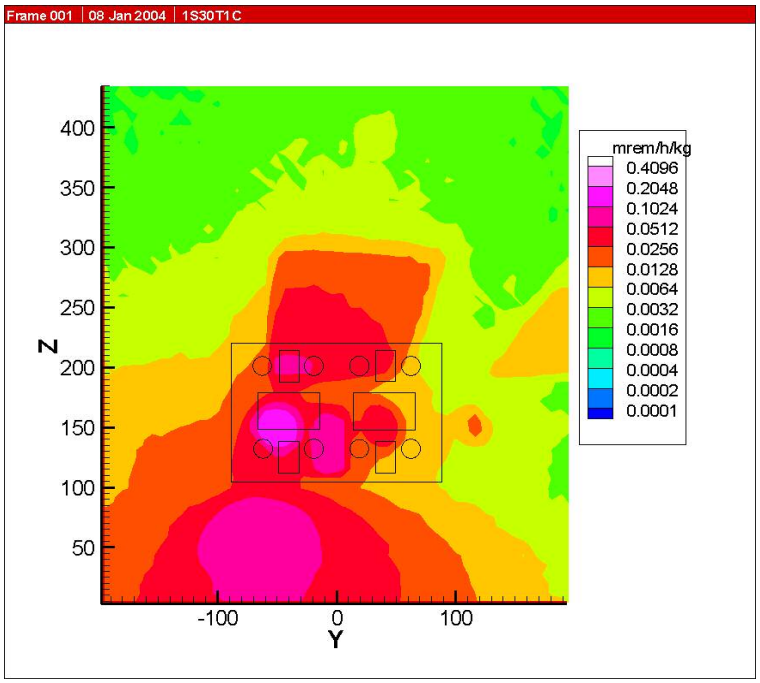

Figure C.1-3: Source at 30 cm.

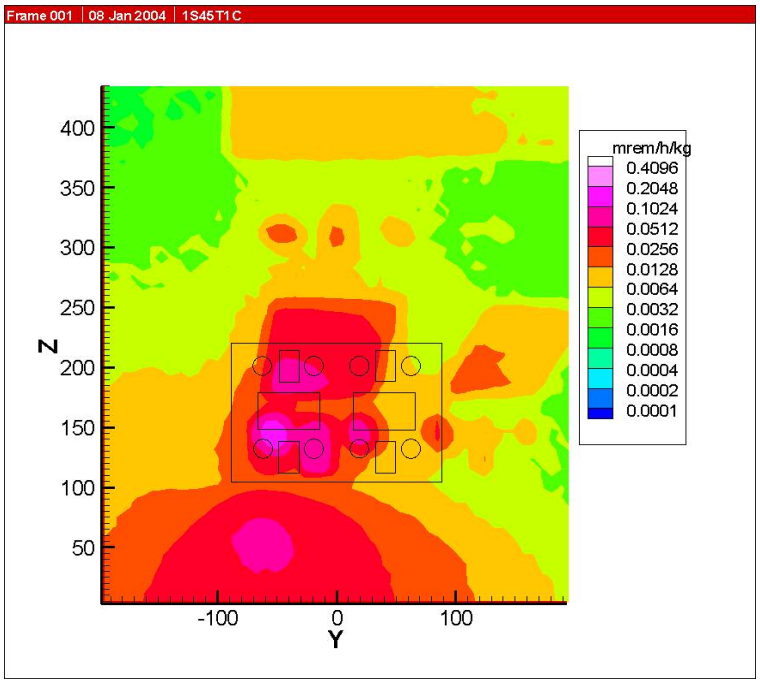

Figure C.1-4: Source at 45 cm.

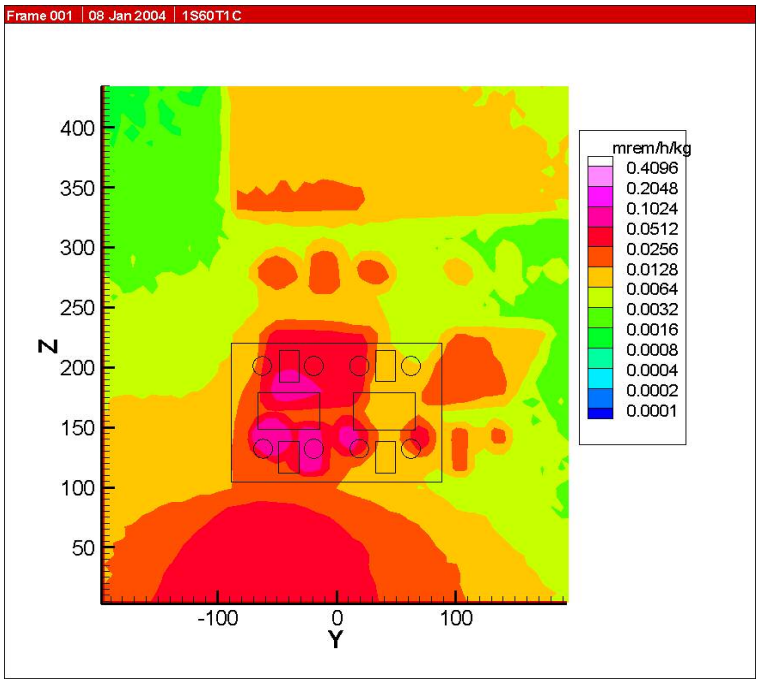

Figure C.1-5: Source at 60 cm.

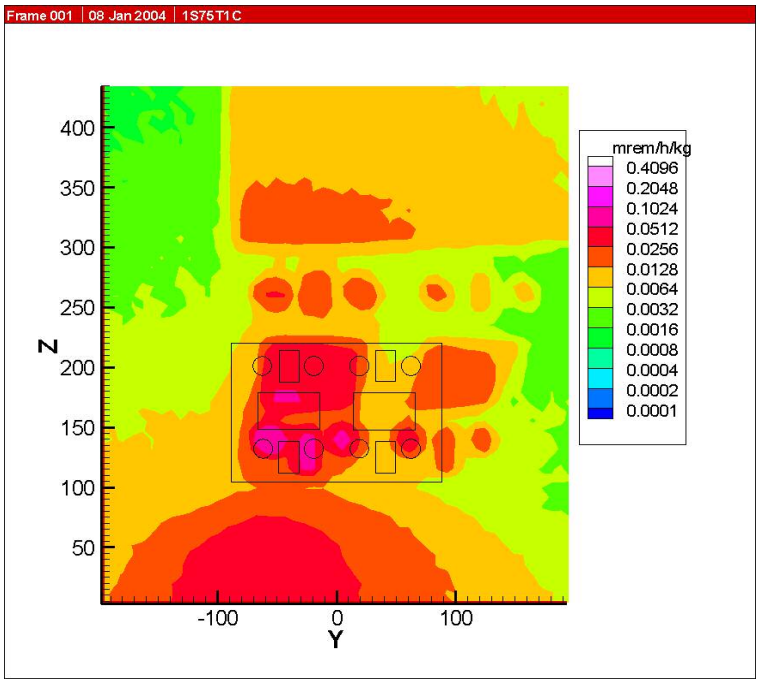

Figure C.1-6: Source at 75 cm.

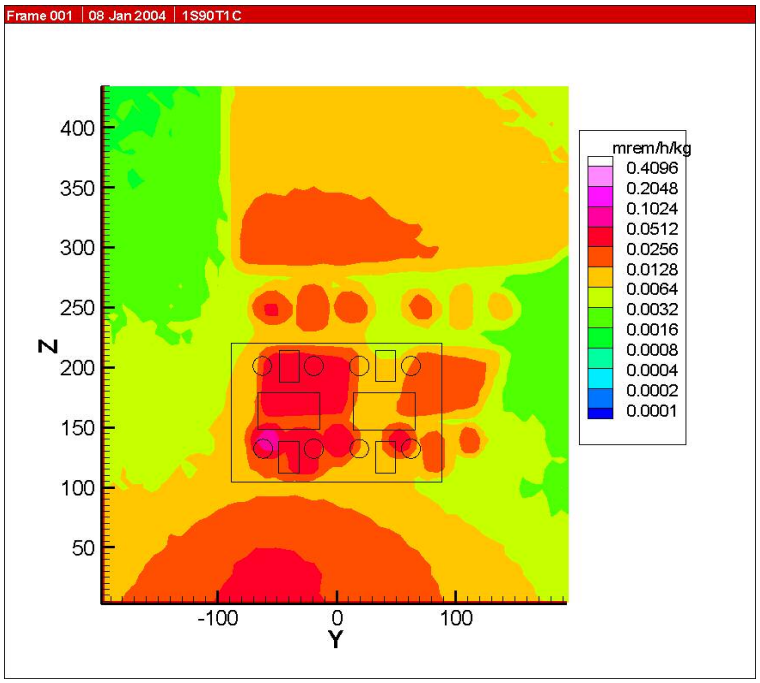

Figure C.1-7: Source at 90 cm.

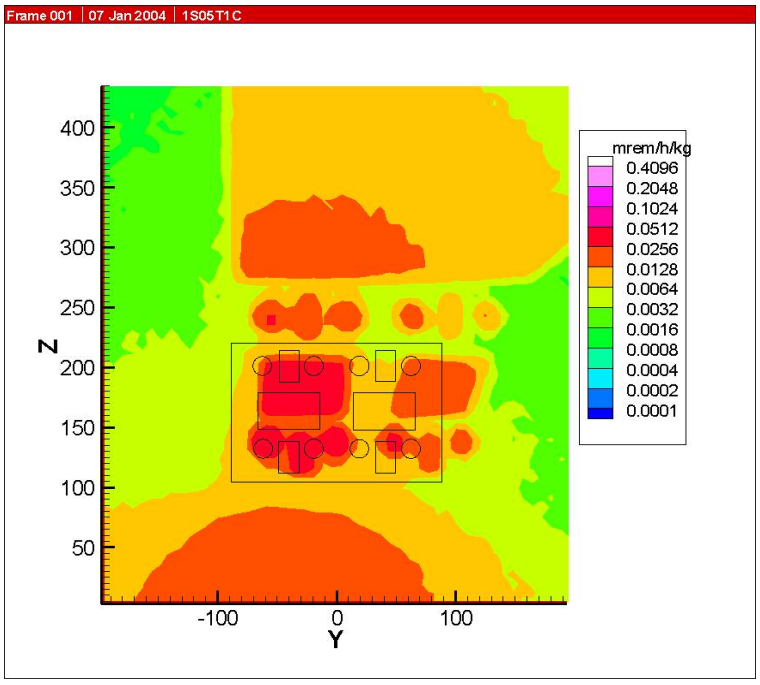

Figure C.1-8: Source at 105 cm.

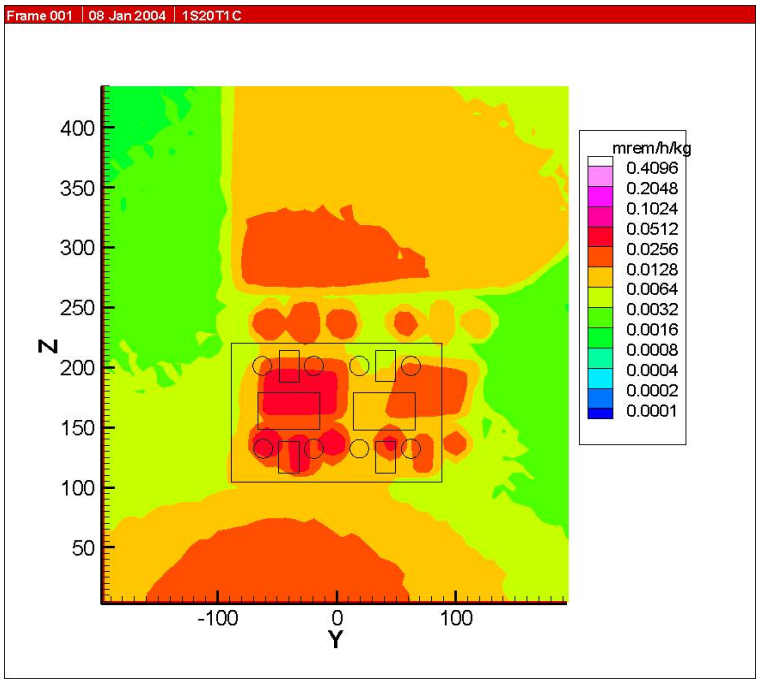

Figure C.1-9: Source at 120 cm.

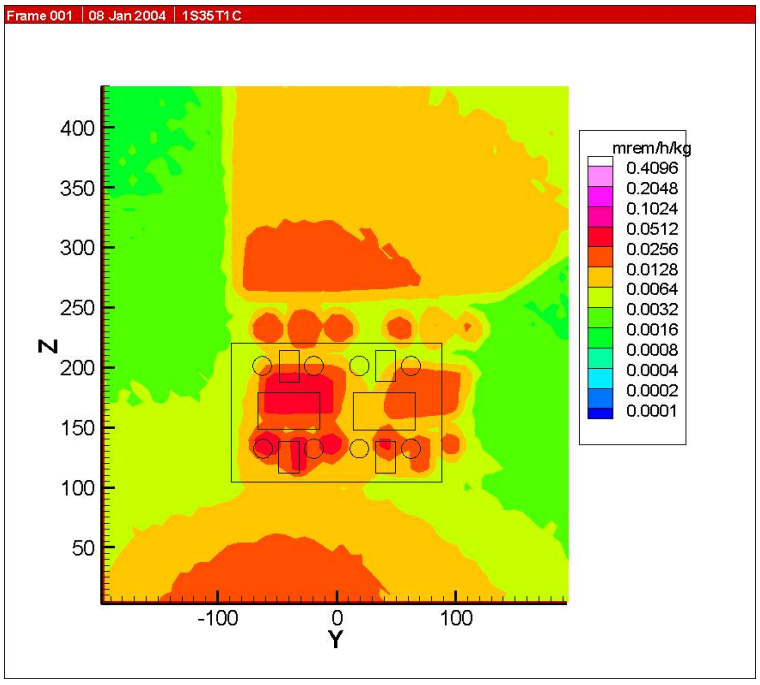

Figure C.1-10: Source at 135 cm.

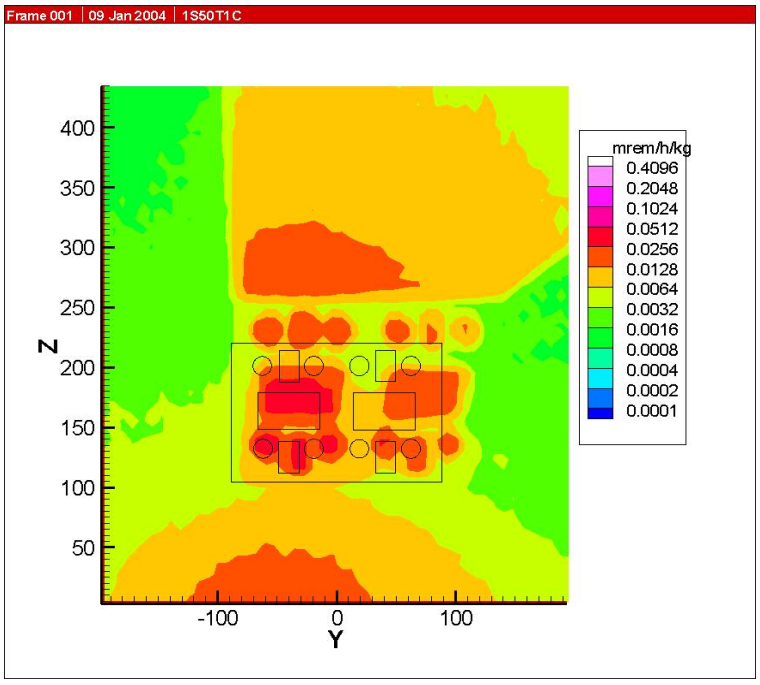

Figure C.1-11: Source at 150 cm.

APPENDIX C.2:

ANSI 1977 AT 1 FOOT WITH SOURCE ON LINE V

The neutron dose field is determined using ANSI 1977 flux-to-dose conversion factors and a mesh tally that is 1 ft in front of the glove box. Figures C.2-1 thru C.2-11 show the changes in the field as the source is moved from 6 cm from the front inside surface of the box to 150 cm from the inside surface on a line that corresponds to the middle of the left pair of gloveports (V). The source is 6 cm above the glove box floor. The outline of the front of glove box is shown in each Figure.

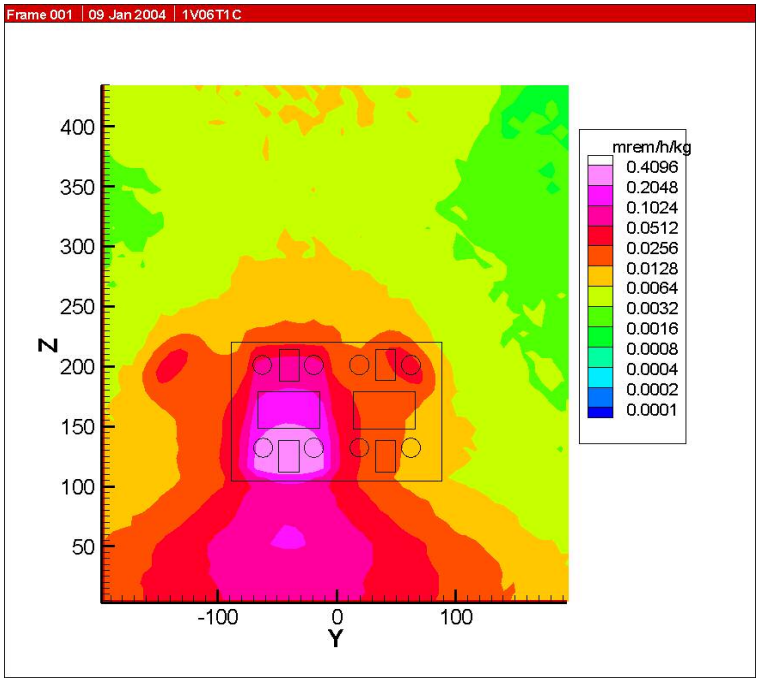

Figure C.2-1: Source at 6 cm.

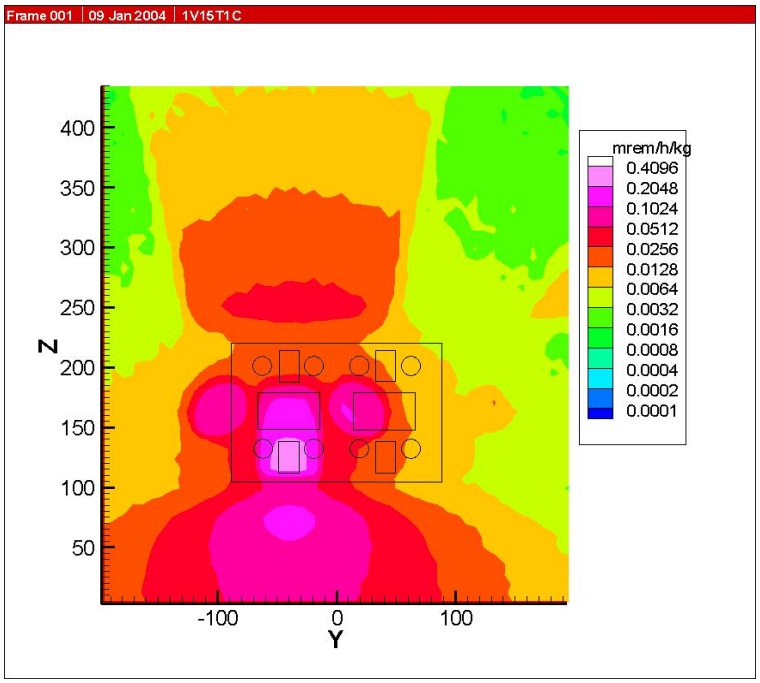

Figure C.2-2: Source at 15 cm.

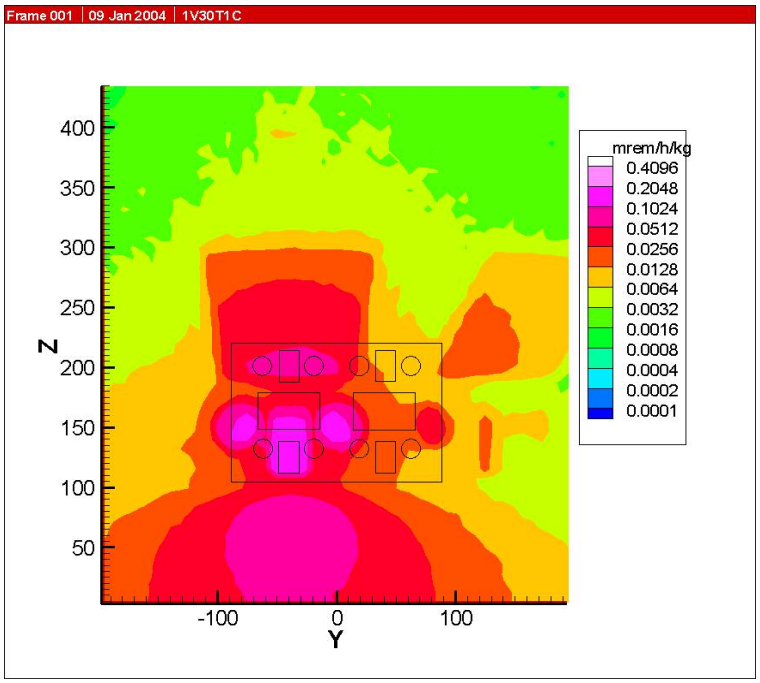

Figure C.2-3: Source at 30 cm.

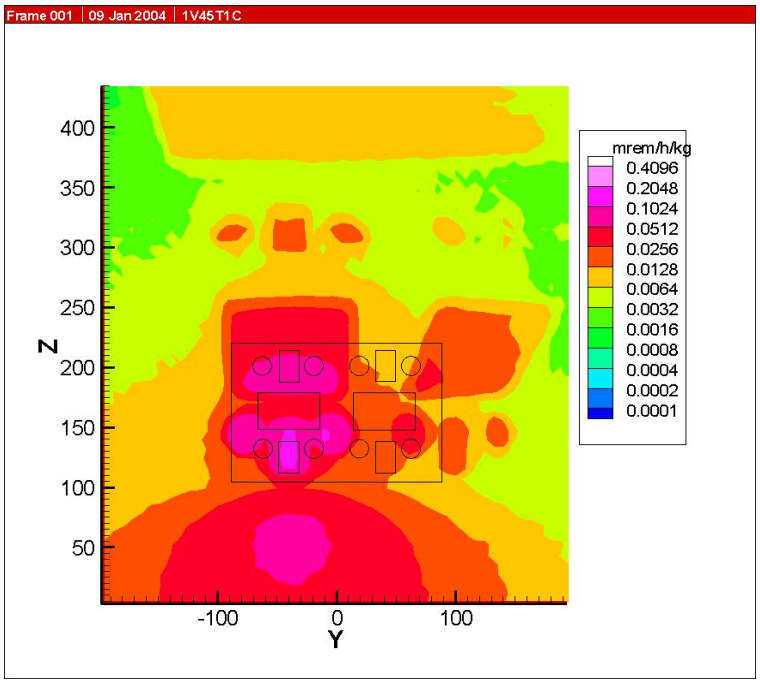

Figure C.2-4: Source at 45 cm.

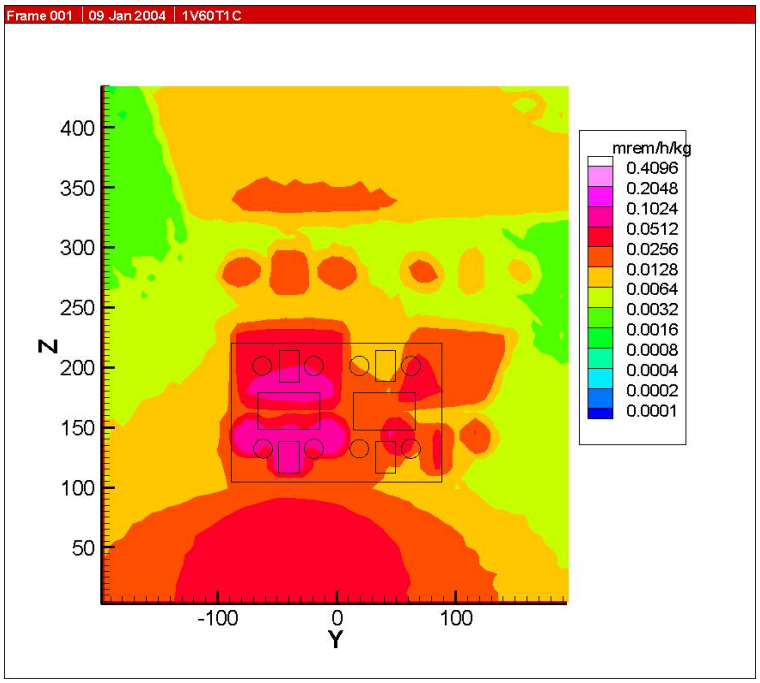

Figure C.2-5: Source at 60 cm.

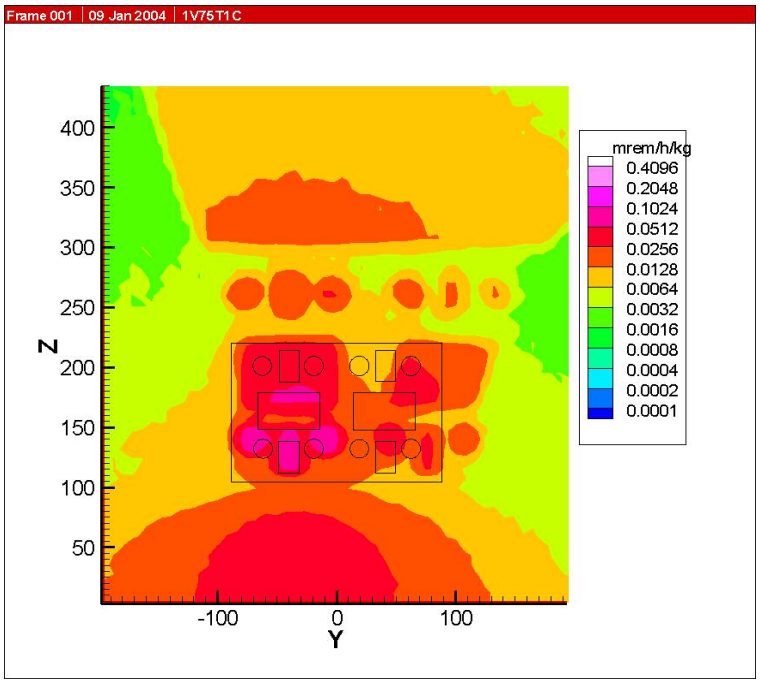

Figure C.2-6: Source at 75 cm.

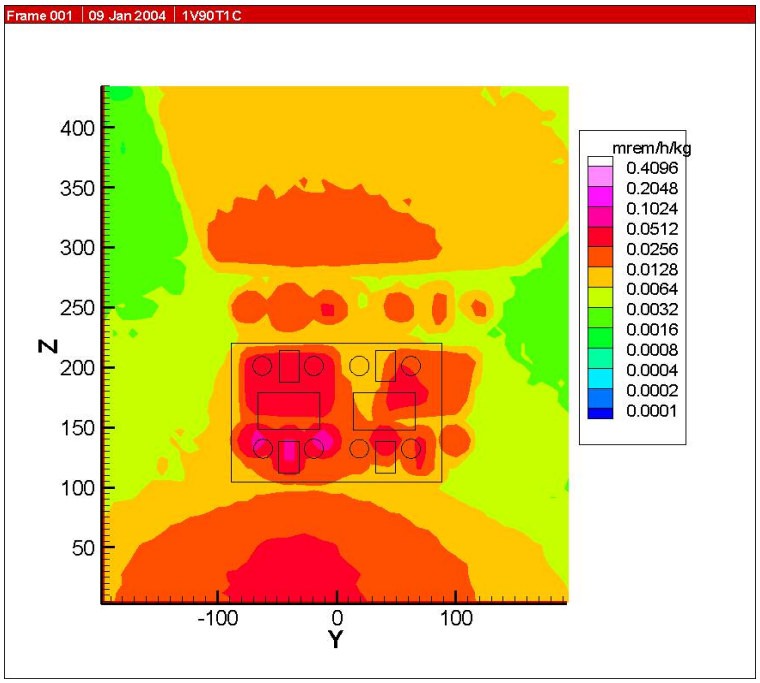

Figure C.2-7: Source at 90 cm.

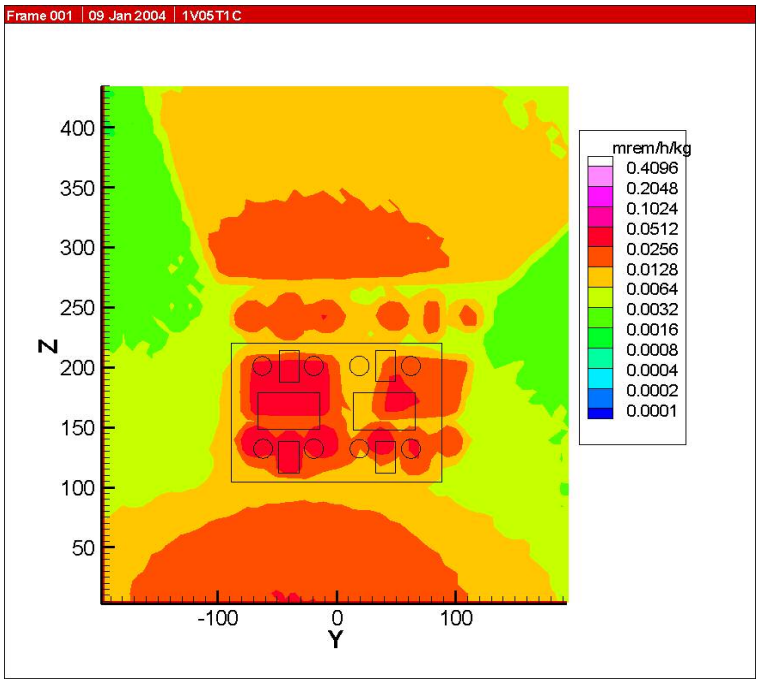

Figure C.2-8: Source at 105 cm.

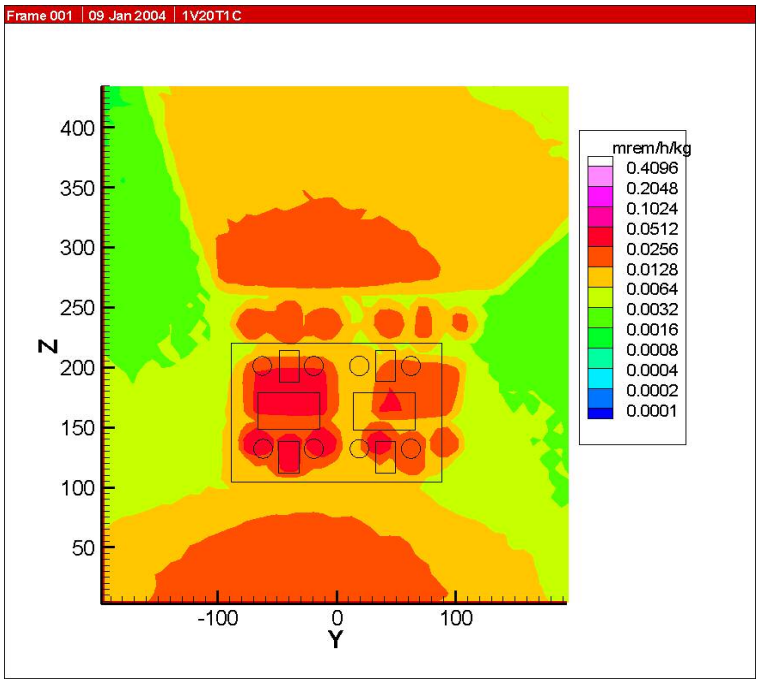

Figure C.2-9: Source at 120 cm.

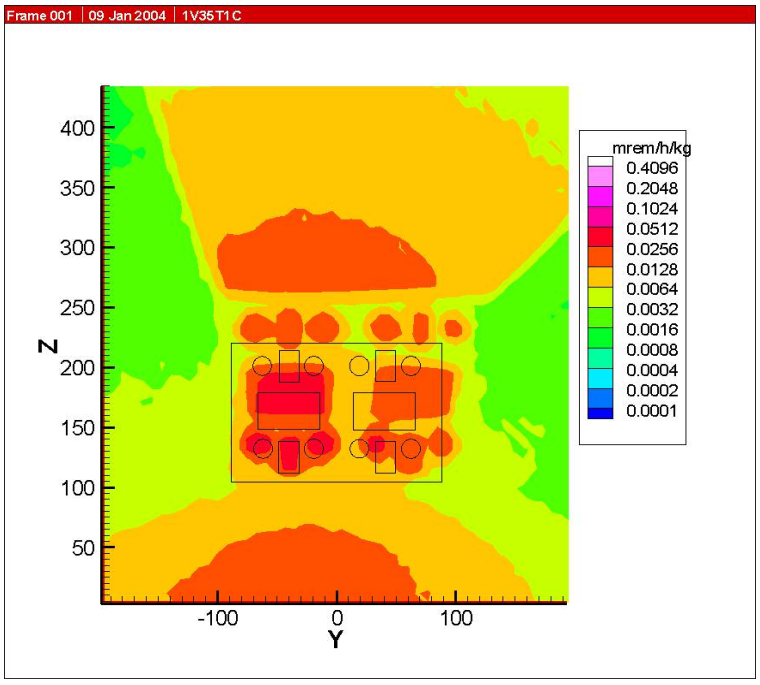

Figure C.2-10: Source at 135 cm.

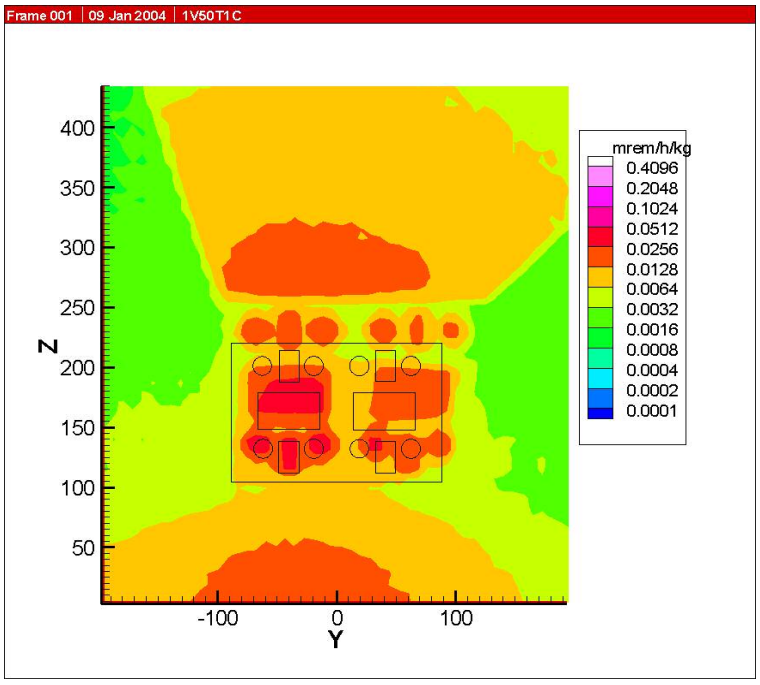

Figure C.2-11: Source at 150 cm.

APPENDIX C.3:

ANSI 1977 AT 1 FOOT WITH SOURCE ON LINE M

The neutron dose field is determined using ANSI 1977 flux-to-dose conversion factors and a mesh tally that is 1 ft in front of the glove box. Figures C.3-1 thru C.3-11 show the changes in the field as the source is moved from 6 cm from the front inside surface of the box to 150 cm from the inside surface on a line that corresponds to the middle of the glove box (M). The source is 6 cm above the glove box floor. The outline of the front of glove box is shown in each Figure.

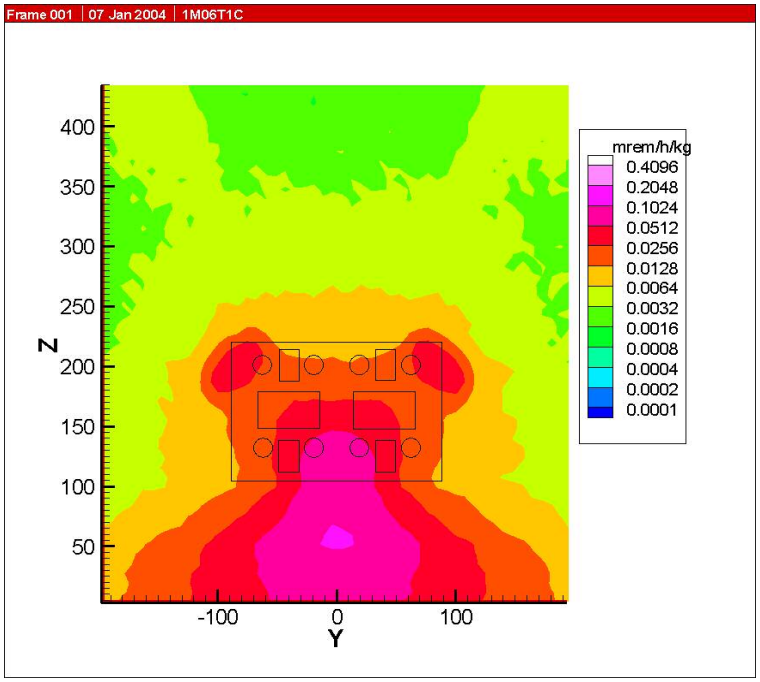

Figure C.3-1: Source at 6 cm.

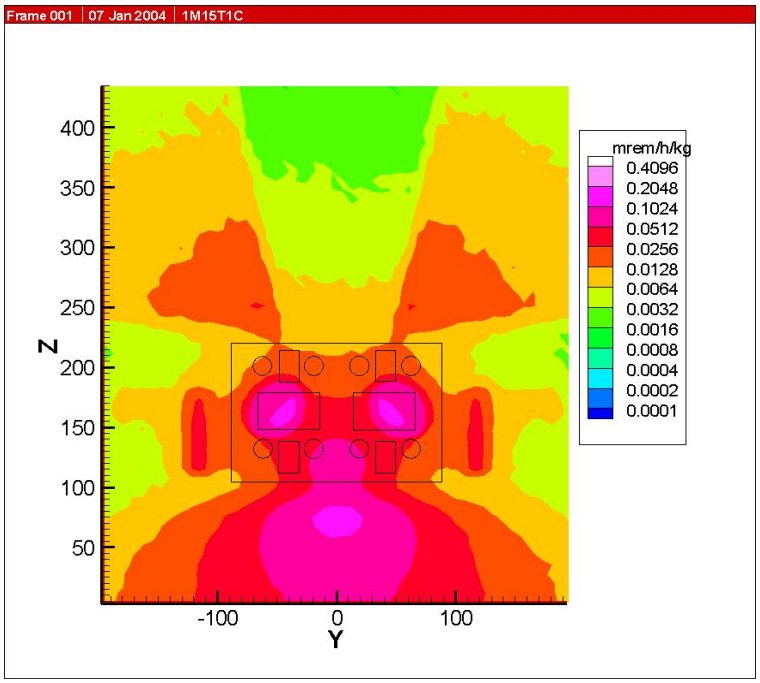

Figure C.3-2: Source at 15 cm.

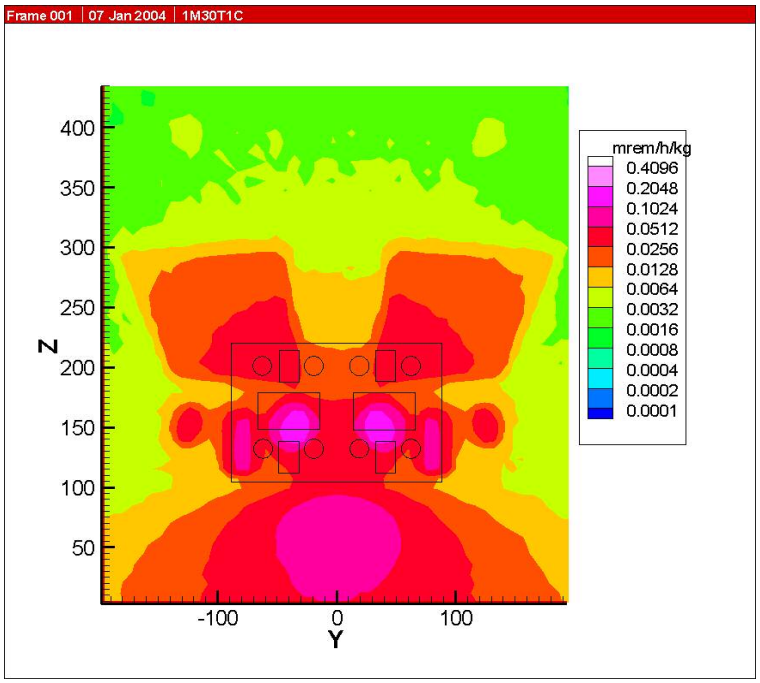

Figure C.3-3: Source at 30 cm.

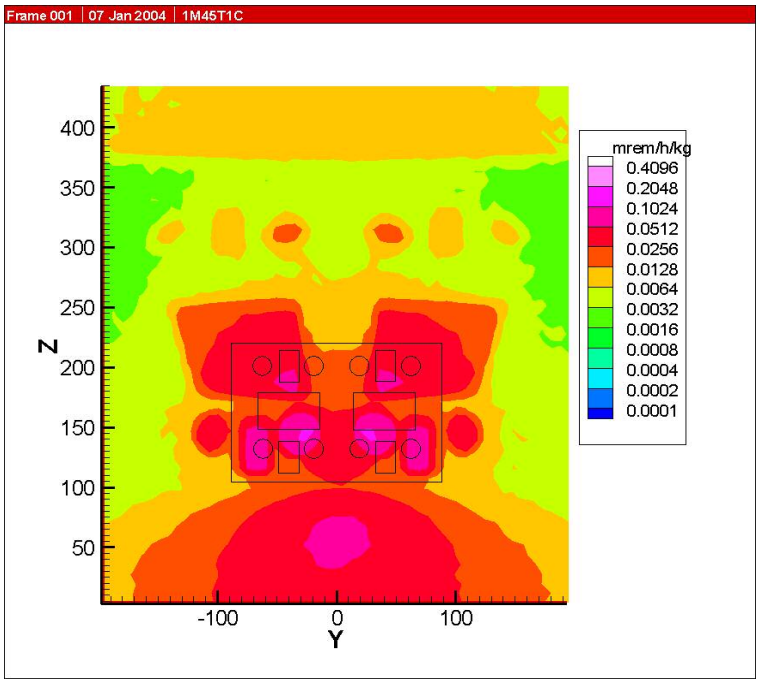

Figure C.3-4: Source at 45 cm.

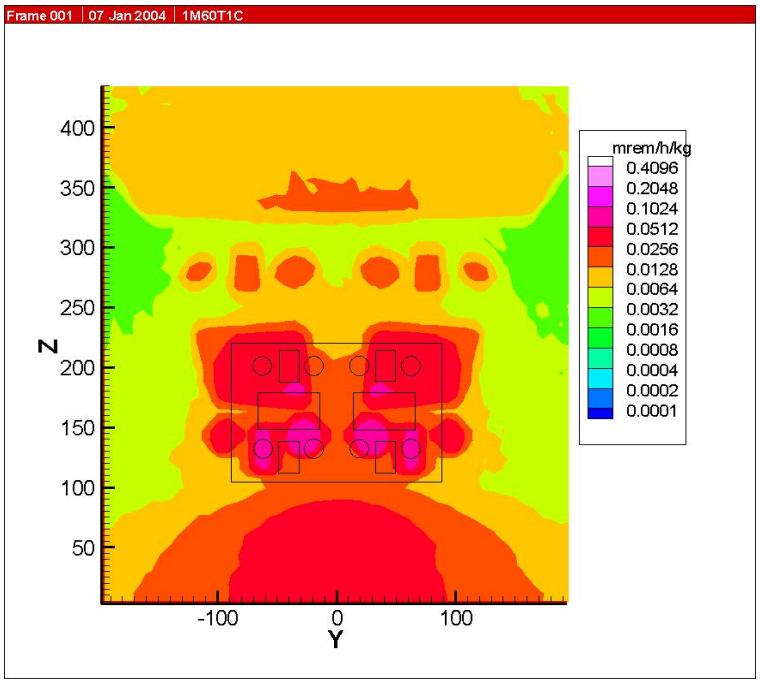

Figure C.3-5: Source at 60 cm.

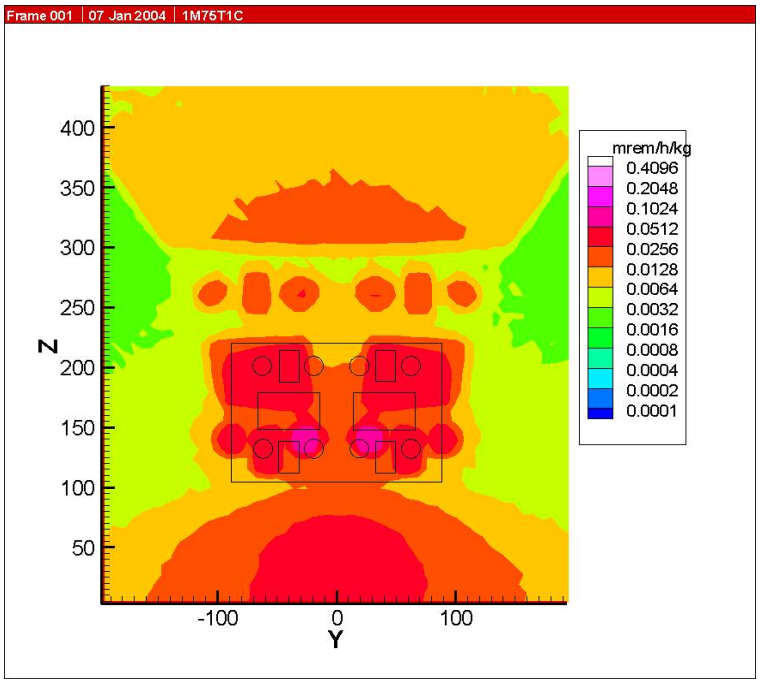

Figure C.3-6: Source at 75 cm.

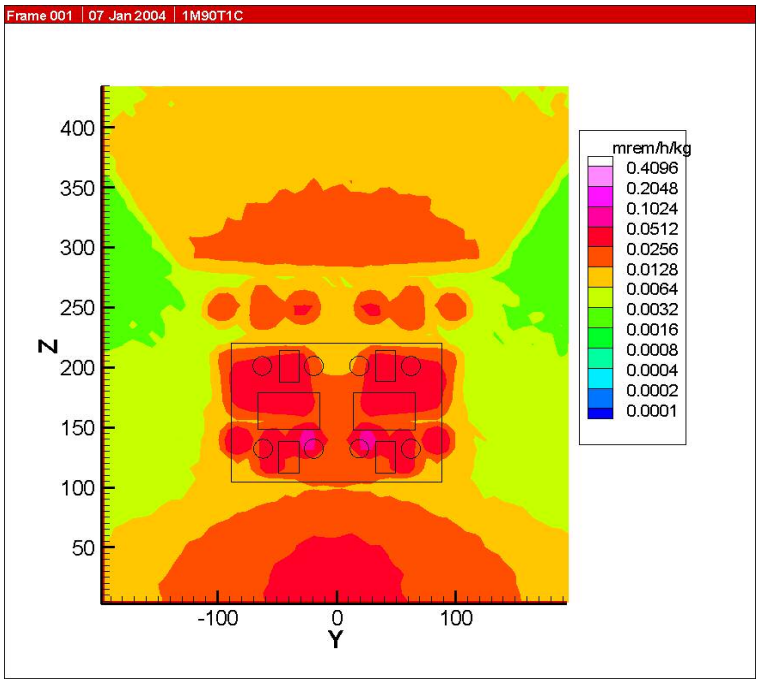

Figure C.3-7: Source at 90 cm.

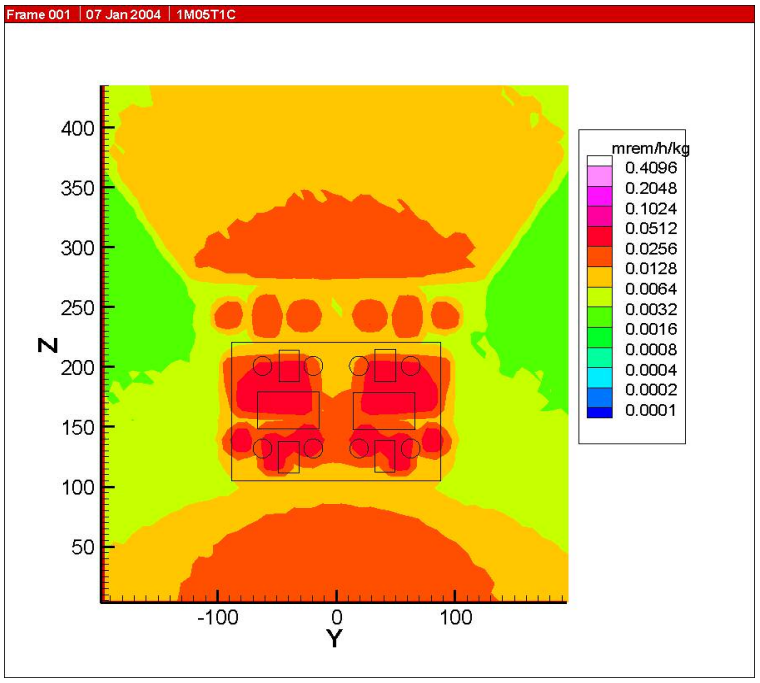

Figure C.3-8: Source at 105 cm.

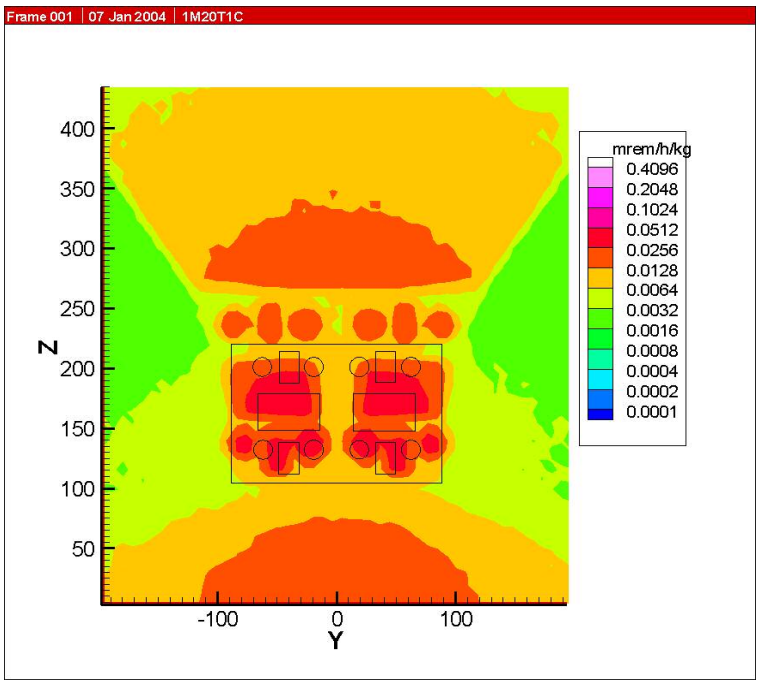

Figure C.3-9: Source at 120 cm.

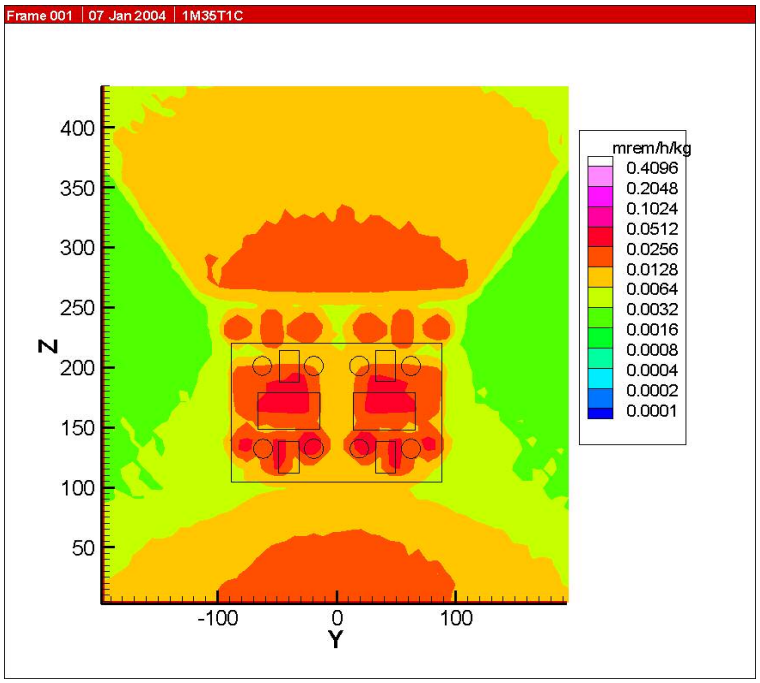

Figure C.3-10: Source at 135 cm.

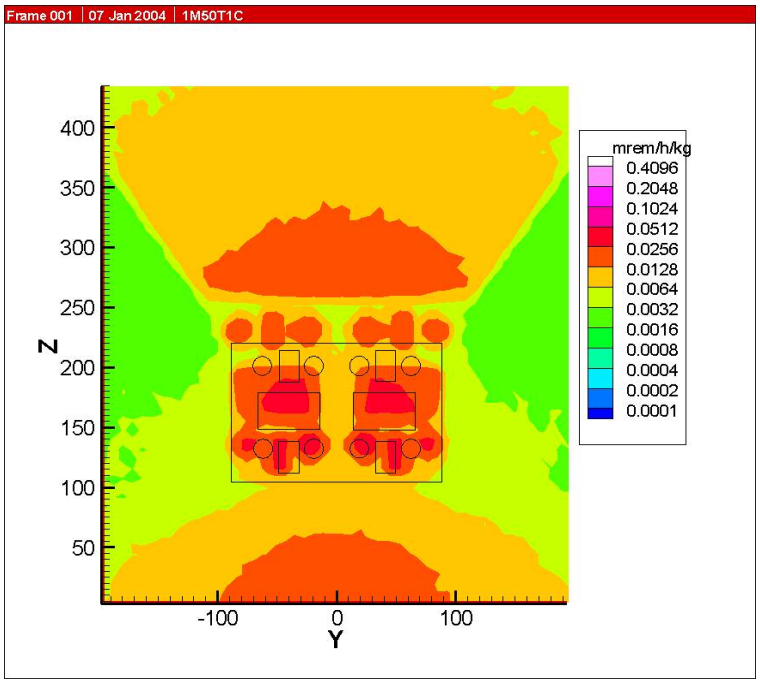

Figure C.3-11: Source at 150 cm.

APPENDIX C.4:

ANSI 1977 AT 3 FOOT WITH SOURCE ON LINE S

The neutron dose field is determined using ANSI 1977 flux-to-dose conversion factors and a mesh tally that is 3 ft in front of the glove box. Figures C.4-1 thru C.4-11 show the changes in the field as the source is moved from 6 cm from the front inside surface of the box to 150 cm from the inside surface on a line that is 6 cm from the left edge of the box (S). The source is 6 cm above the glove box floor. The outline of the front of glove box is shown in each Figure.

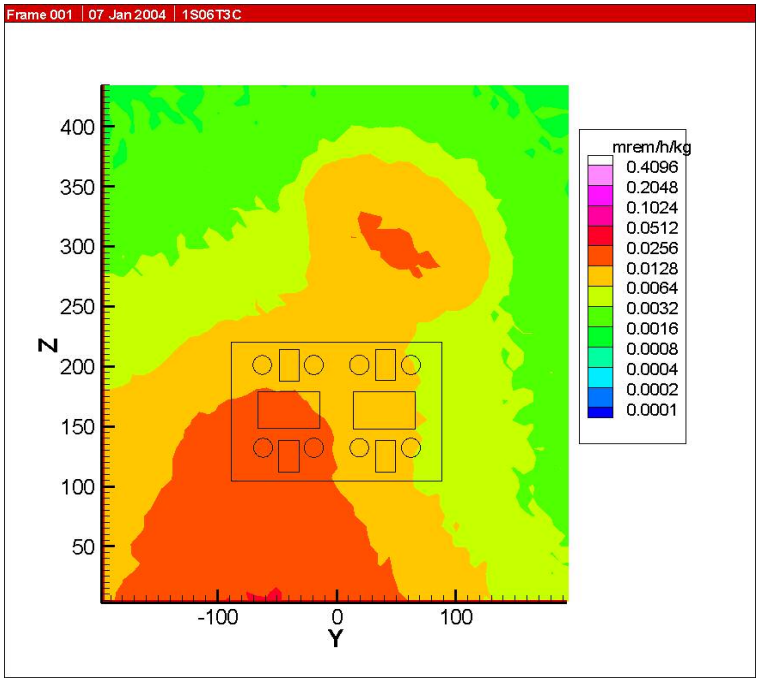

Figure C.4-1: Source at 6 cm.

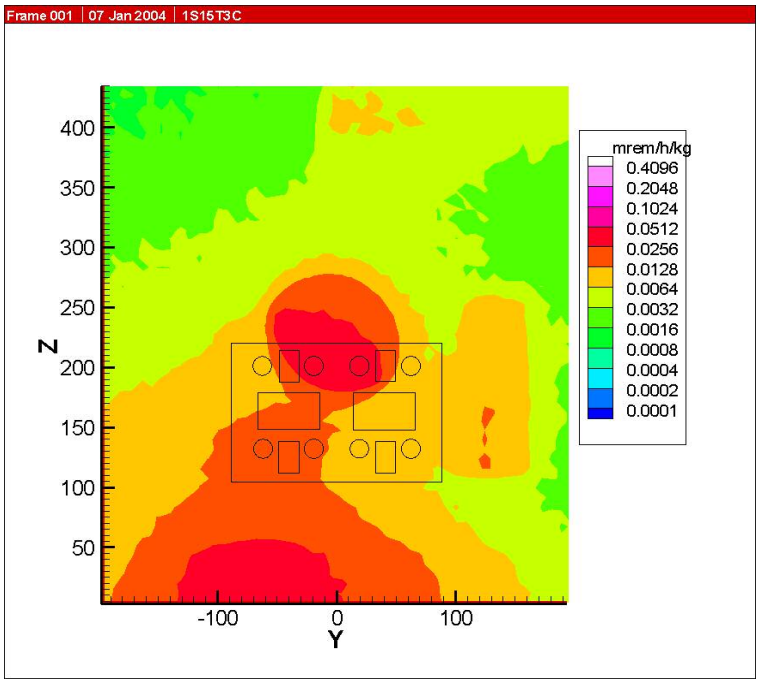

Figure C.4-2: Source at 15 cm.

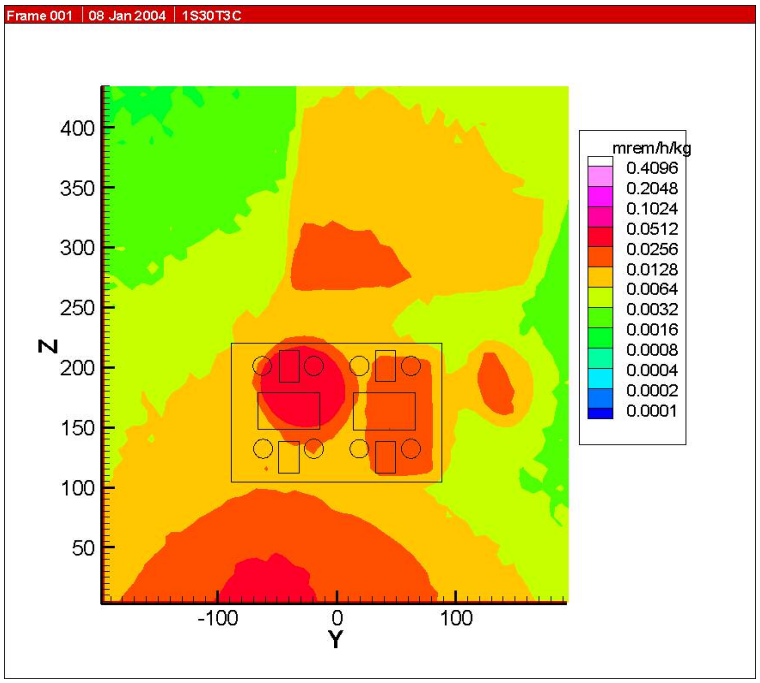

Figure C.4-3: Source at 30 cm.

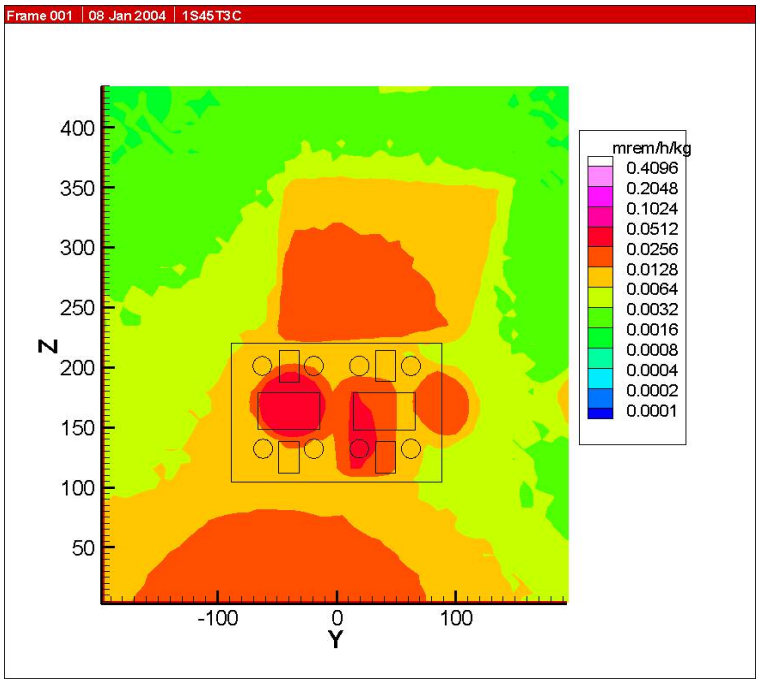

Figure C.4-4: Source at 45 cm.

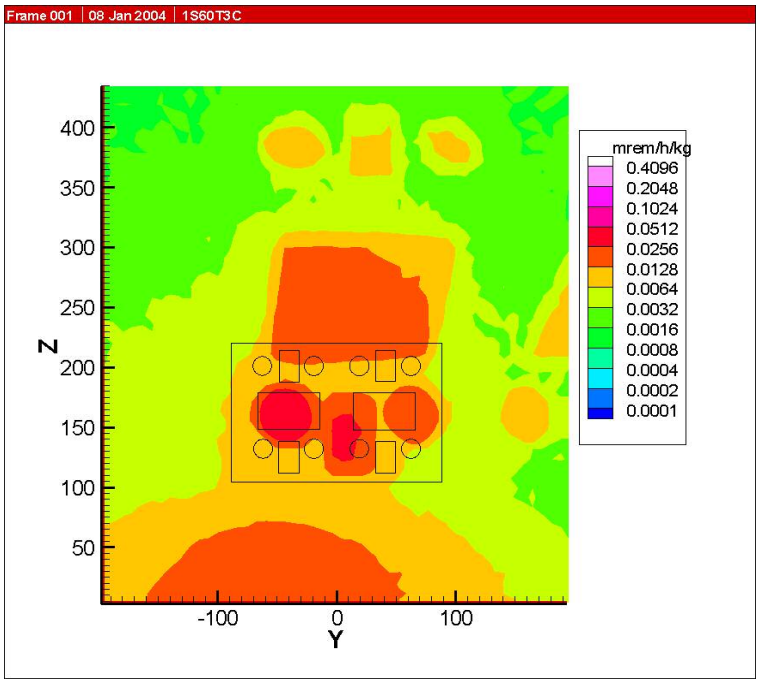

Figure C.4-5: Source at 60 cm.

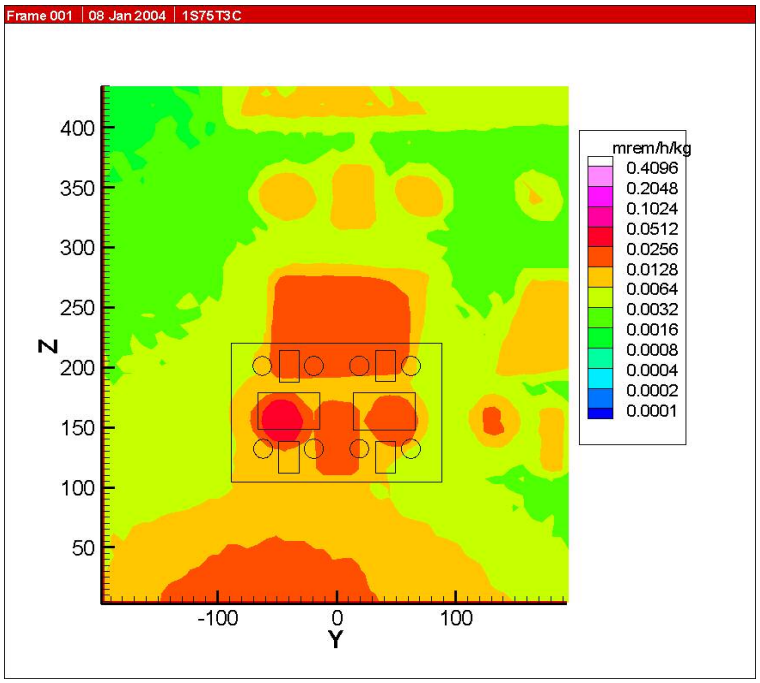

Figure C.4-6: Source at 75 cm.

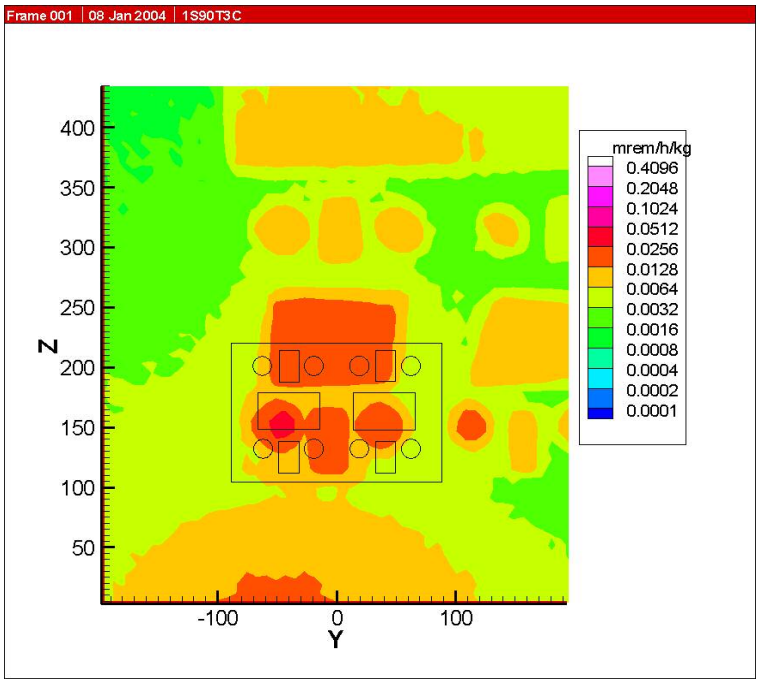

Figure C.4-7: Source at 90 cm.

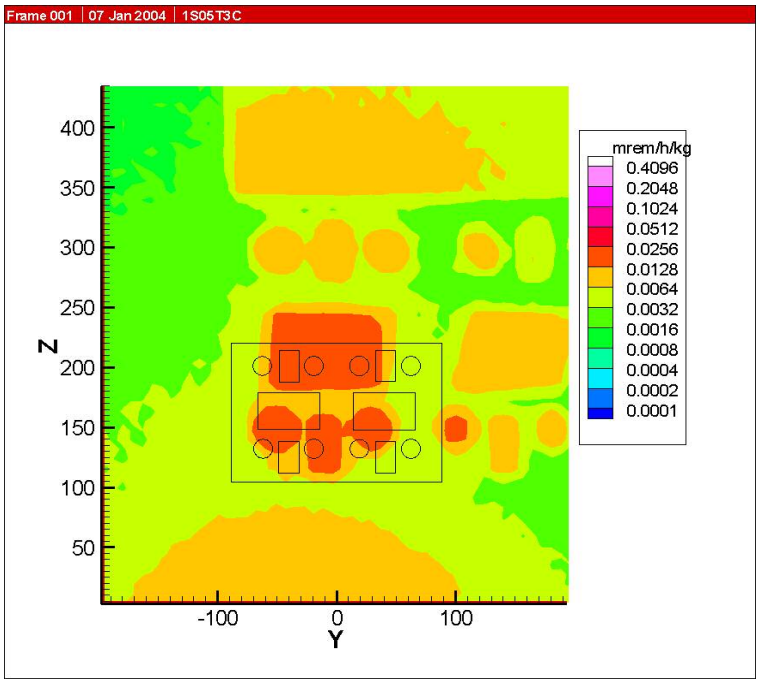

Figure C.4-8: Source at 105 cm.

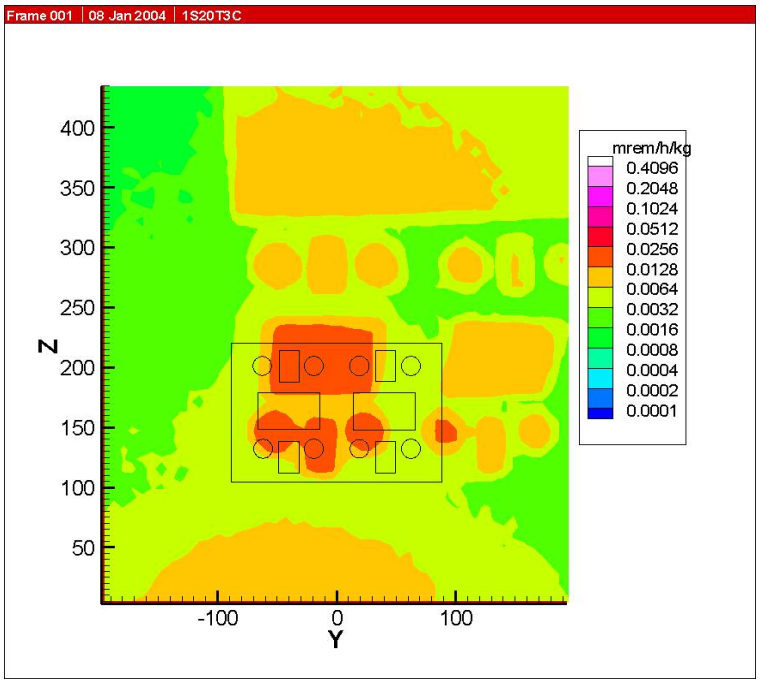

Figure C.4-9: Source at 120 cm.

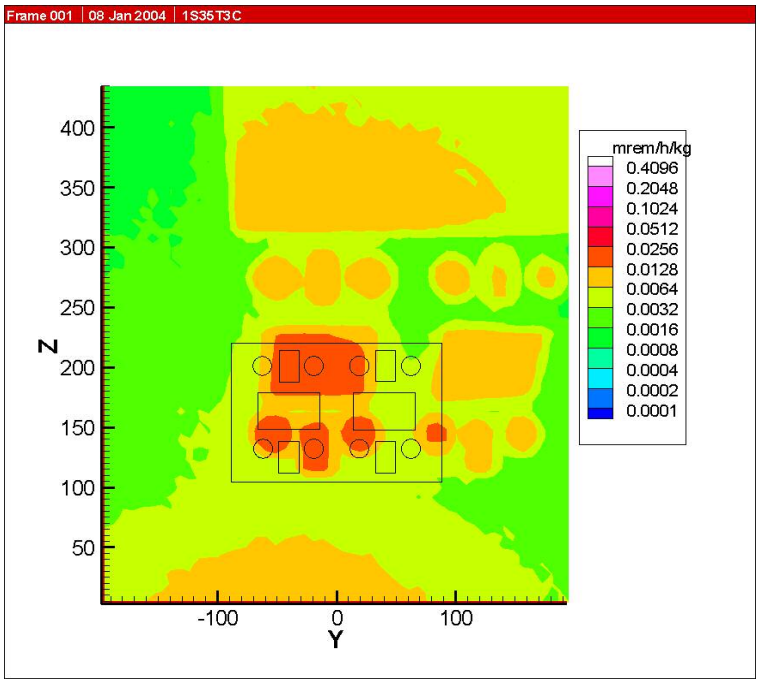

Figure C.4-10: Source at 135 cm.

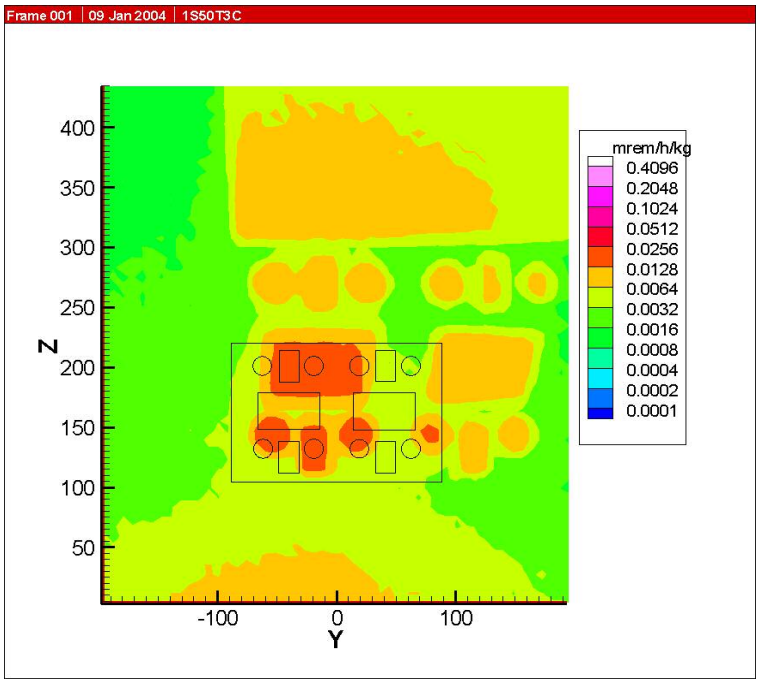

Figure C.4-11: Source at 150 cm.

APPENDIX C.5:

ANSI 1977 AT 3 FOOT WITH SOURCE ON LINE V

The neutron dose field is determined using ANSI 1977 flux-to-dose conversion factors and a mesh tally that is 3 ft in front of the glove box. Figures C.2-1 thru C.2-11 show the changes in the field as the source is moved from 6 cm from the front inside surface of the box to 150 cm from the inside surface on a line that corresponds to the middle of the left pair of gloveports (V). The source is 6 cm above the glove box floor. The outline of the front of glove box is shown in each Figure.

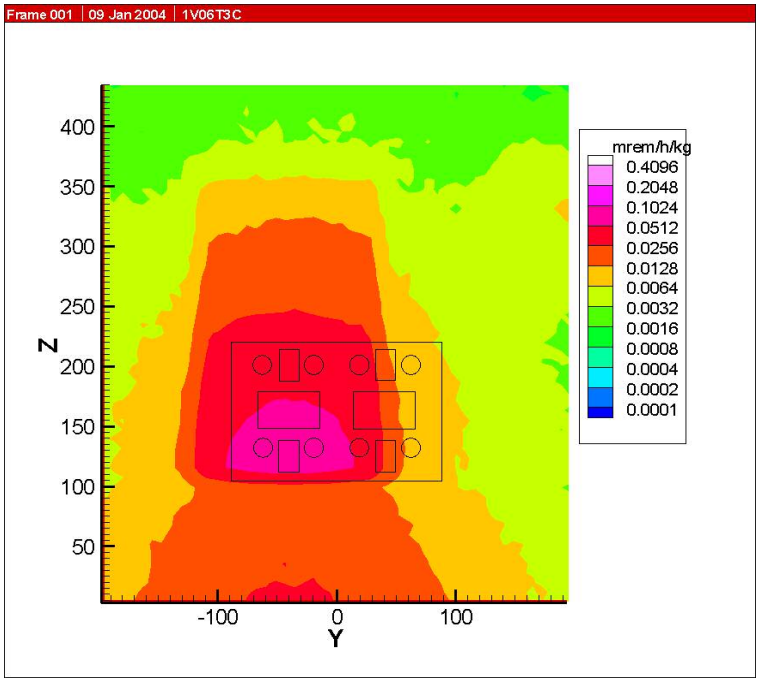

Figure C.5-1: Source at 6 cm.

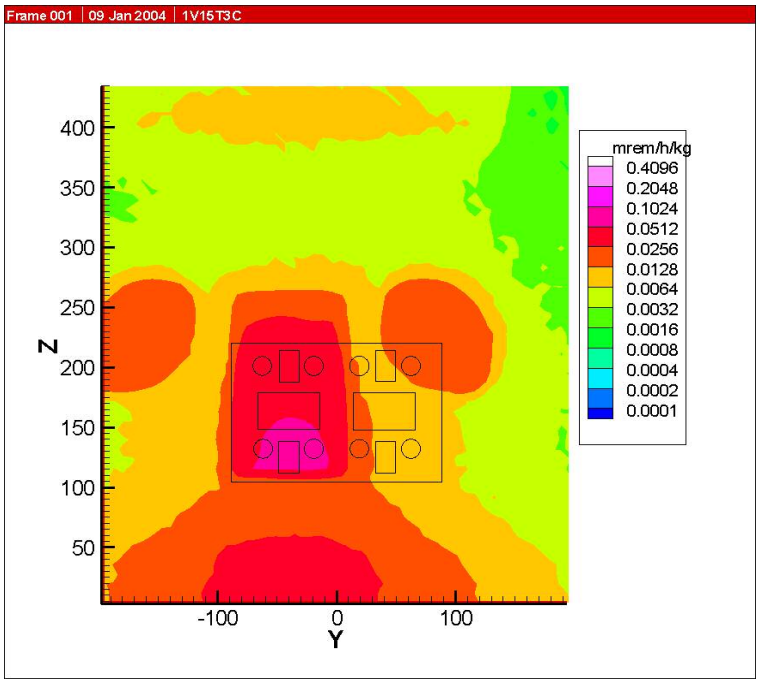

Figure C.5-2: Source at 15 cm.

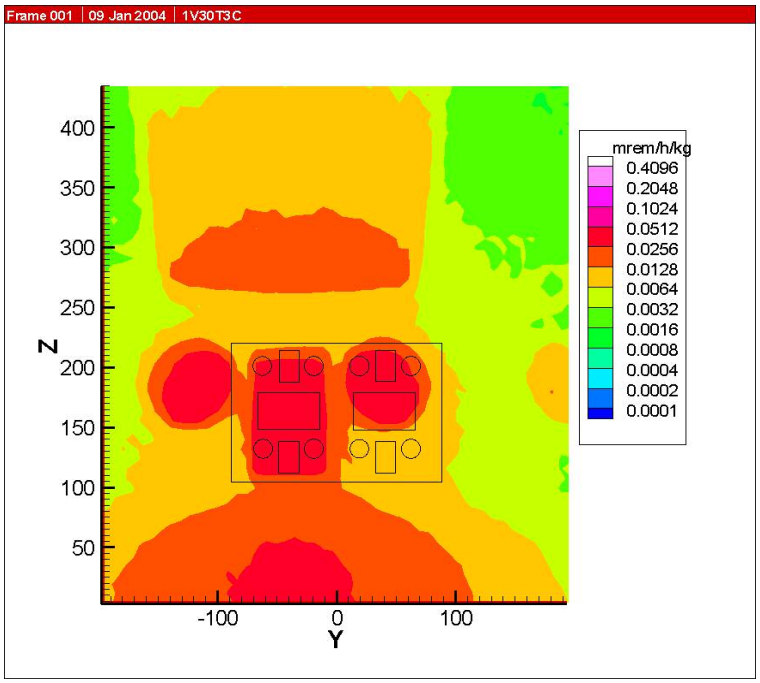

Figure C.5-3: Source at 30 cm.

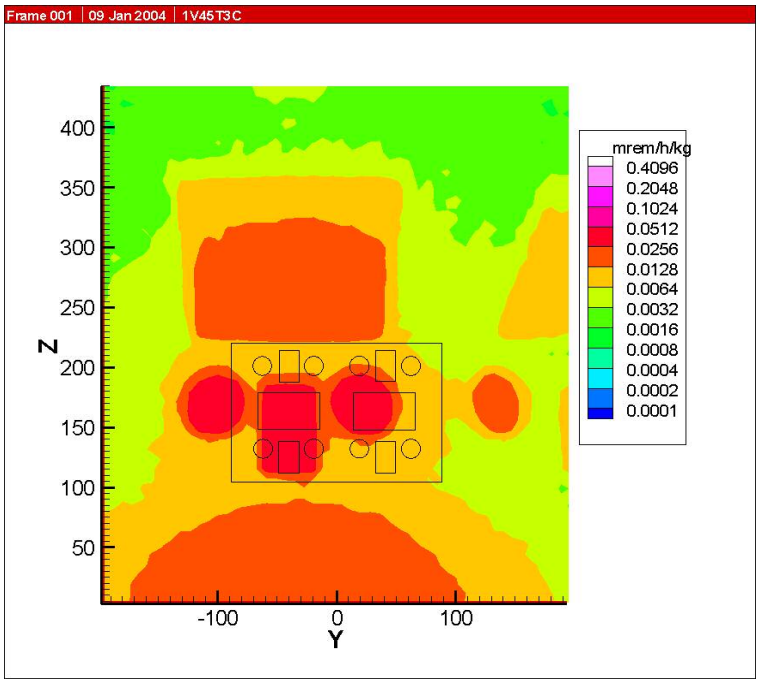

Figure C.5-4: Source at 45 cm.

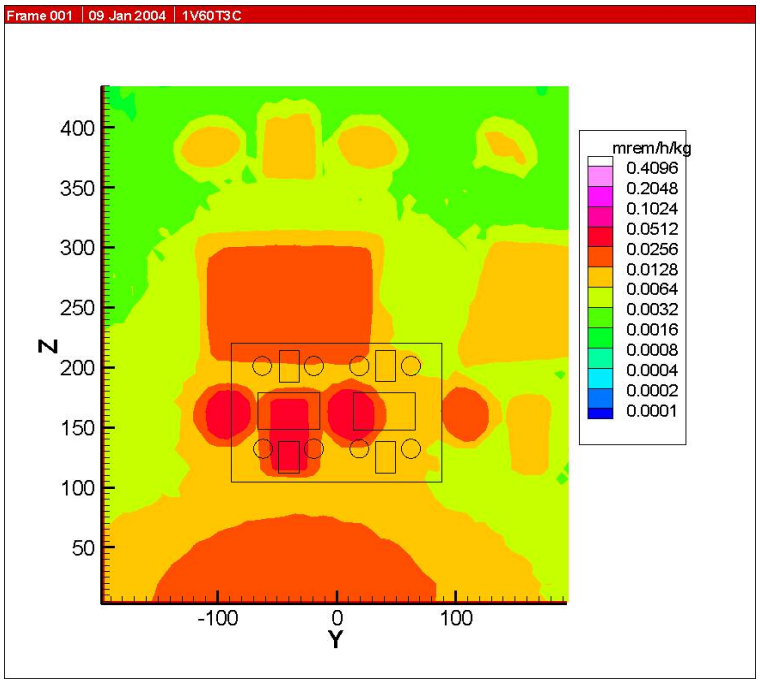

Figure C.5-5: Source at 60 cm.

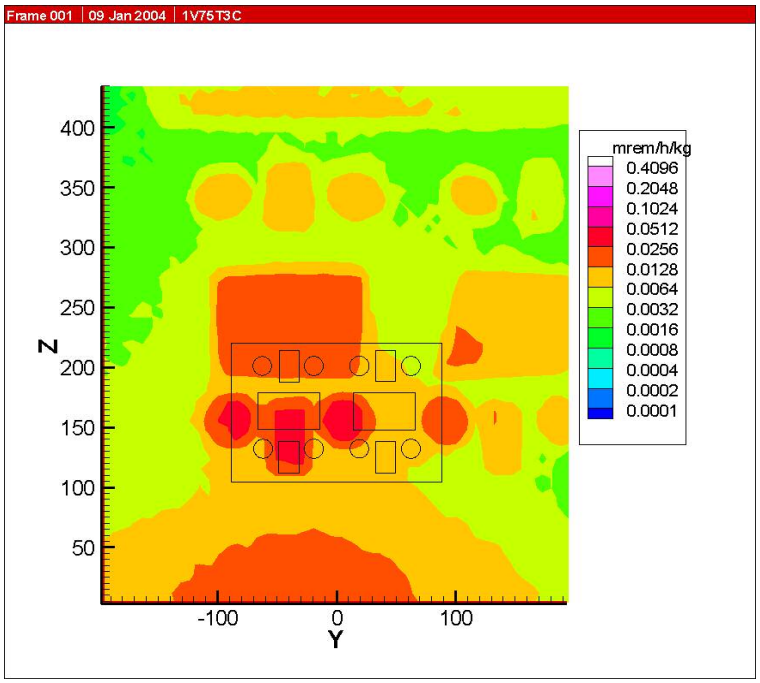

Figure C.5-6: Source at 75 cm.

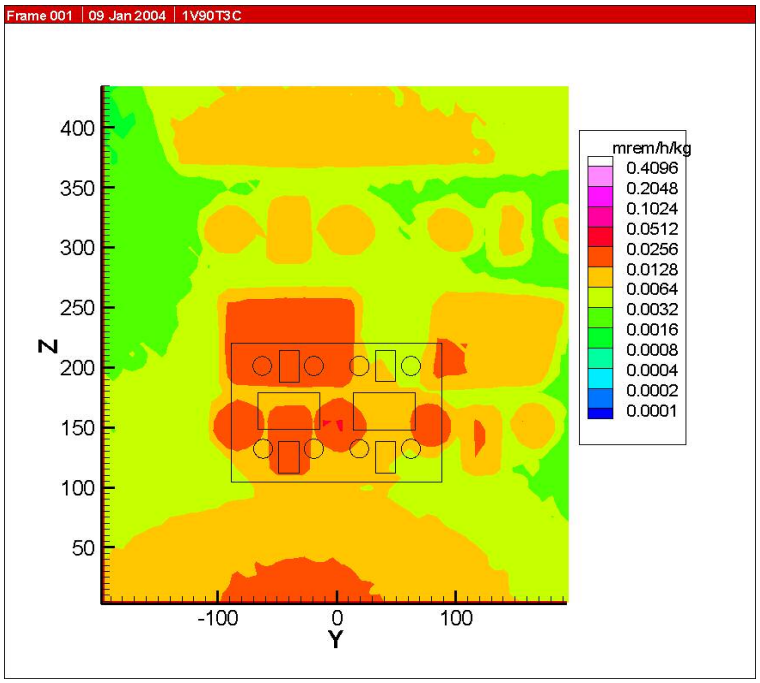

Figure C.5-7: Source at 90 cm.

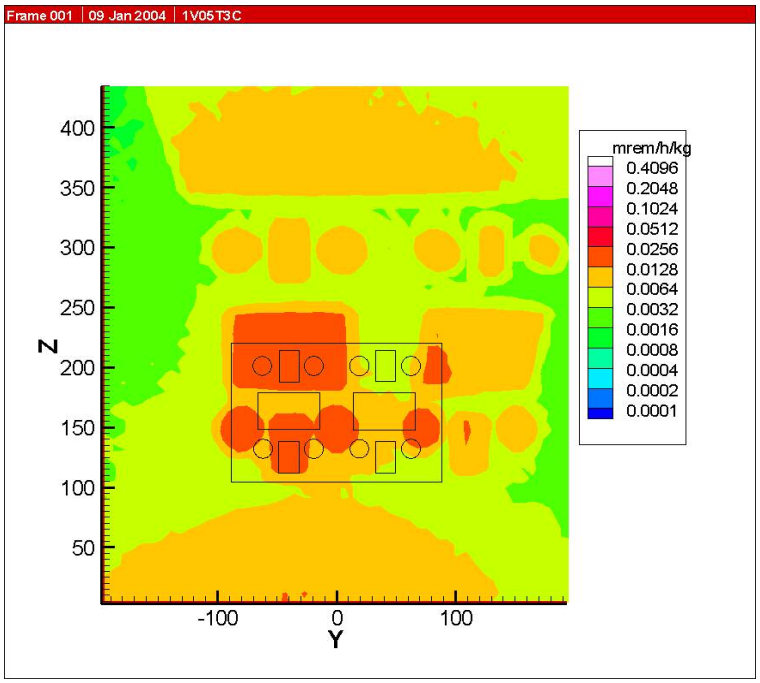

Figure C.5-8: Source at 105 cm.

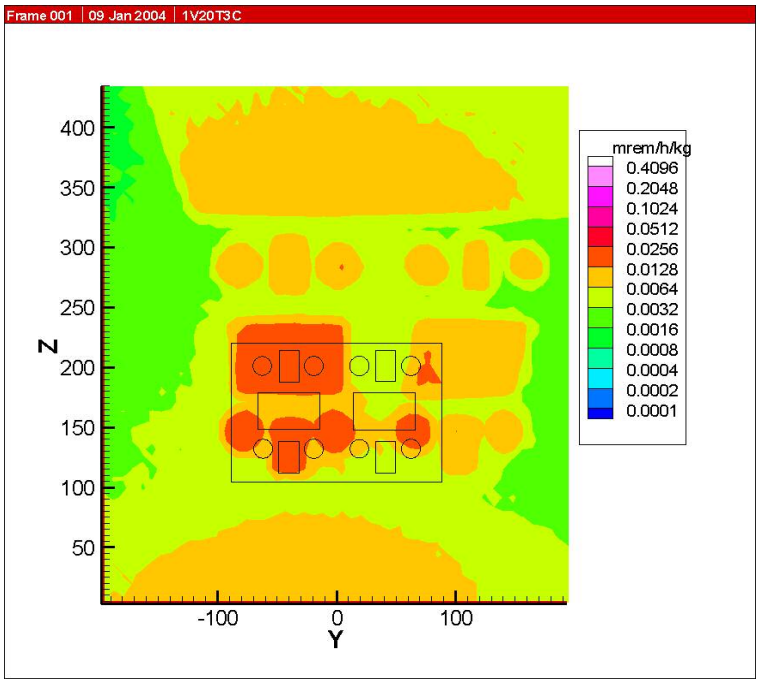

Figure C.5-9: Source at 120 cm.

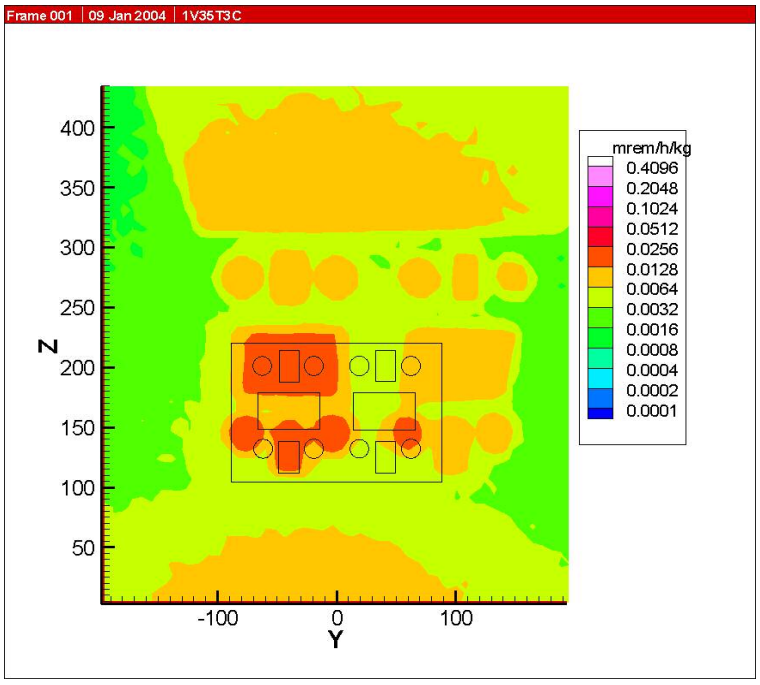

Figure C.5-10: Source at 135 cm.

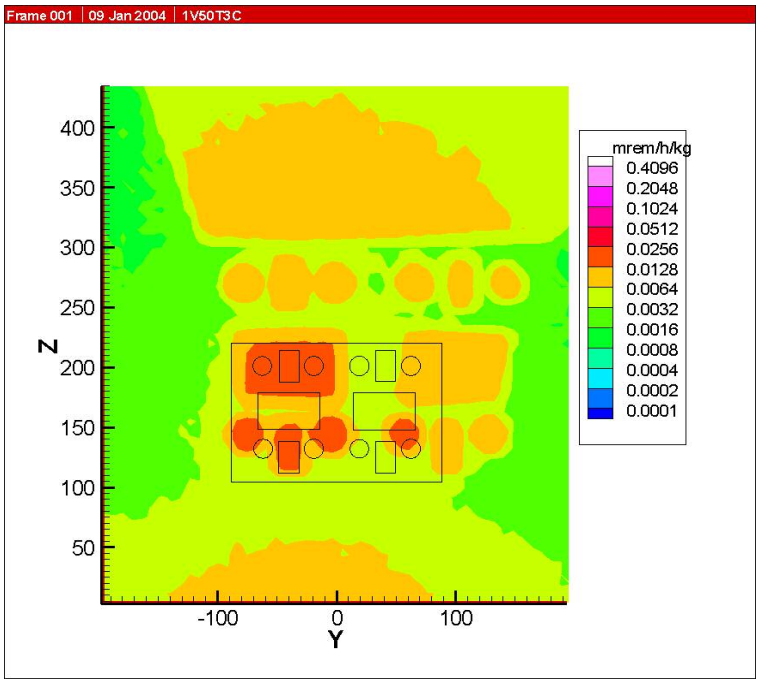

Figure C.5-11: Source at 150 cm.

APPENDIX C.6:

ANSI 1977 AT 3 FOOT WITH SOURCE ON LINE M

The neutron dose field is determined using ANSI 1977 flux-to-dose conversion factors and a mesh tally that is 3 ft in front of the glove box. Figures C.3-1 thru C.3-11 show the changes in the field as the source is moved from 6 cm from the front inside surface of the box to 150 cm from the inside surface on a line that corresponds to the middle of the glove box (M). The source is 6 cm above the glove box floor. The outline of the front of glove box is shown in each Figure.

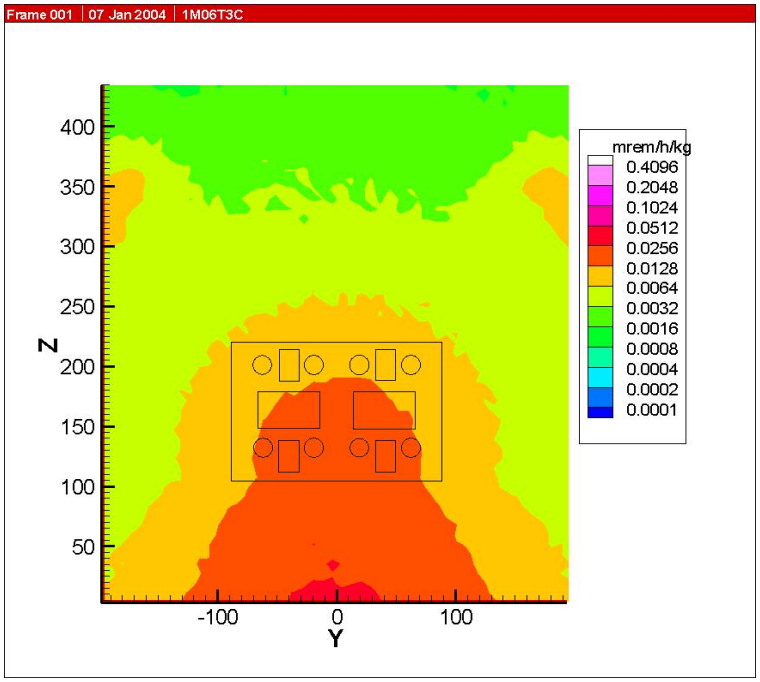

Figure C.6-1: Source at 6 cm.

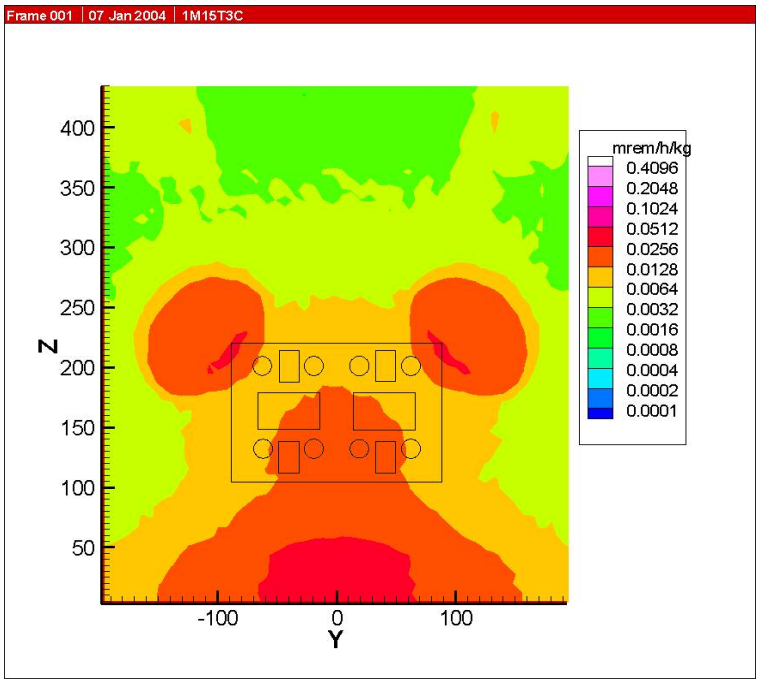

Figure C.6-2: Source at 15 cm.

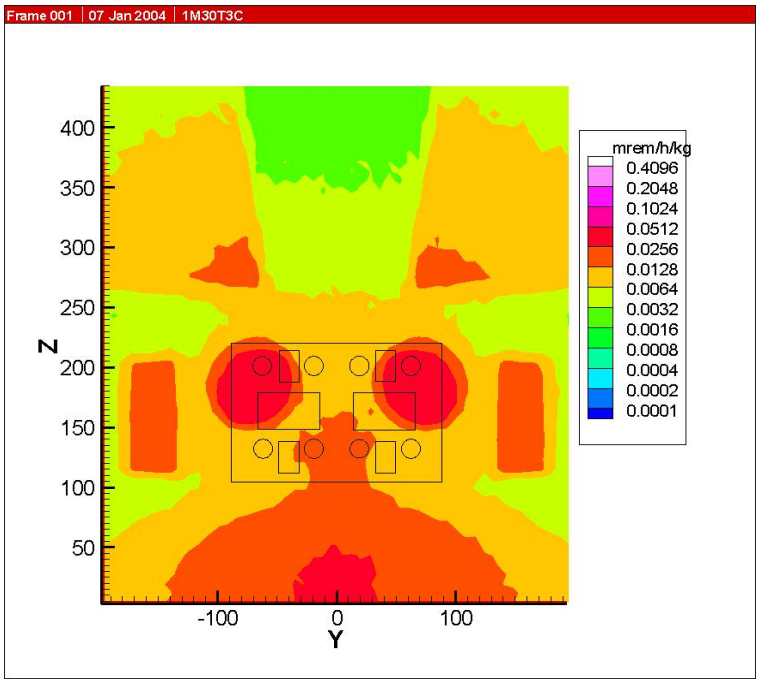

Figure C.6-3: Source at 30 cm.

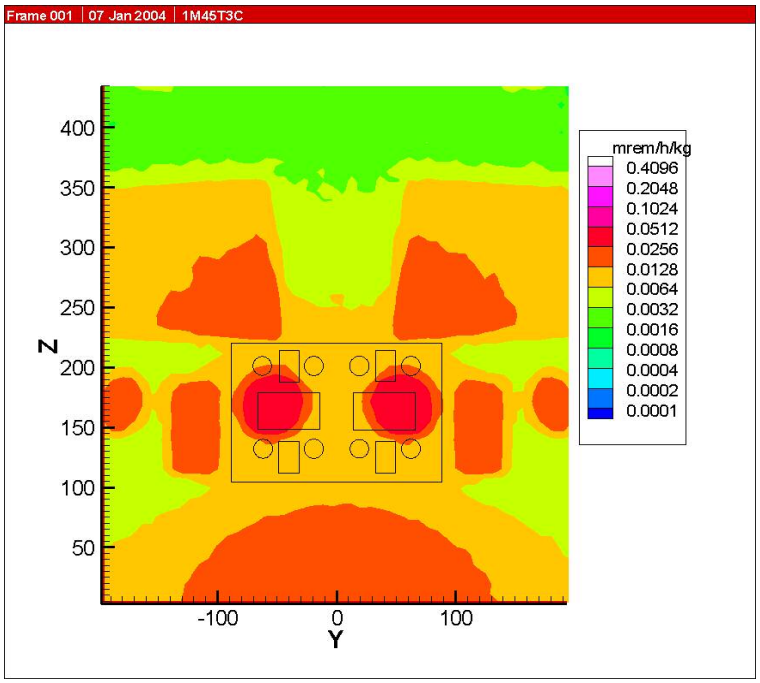

Figure C.6-4: Source at 45 cm.

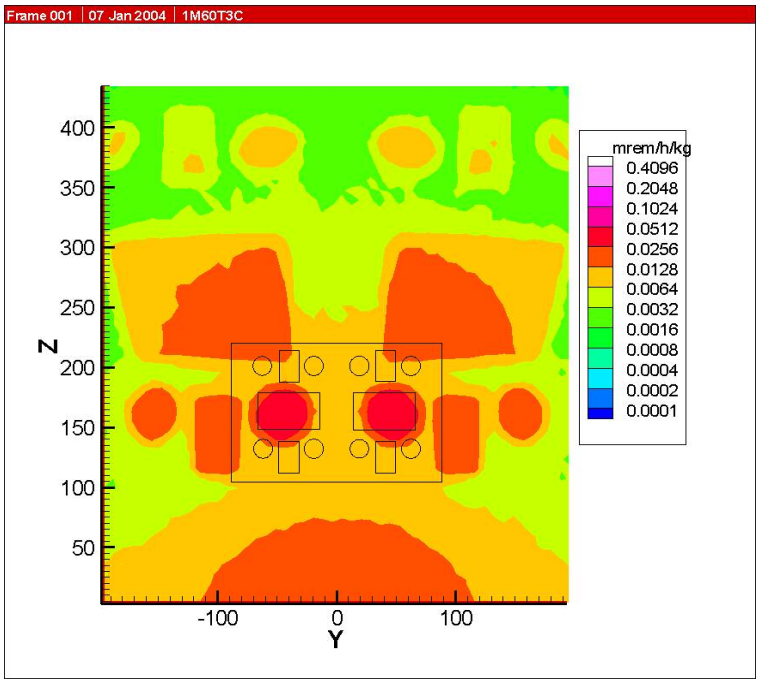

Figure C.6-5: Source at 60 cm.

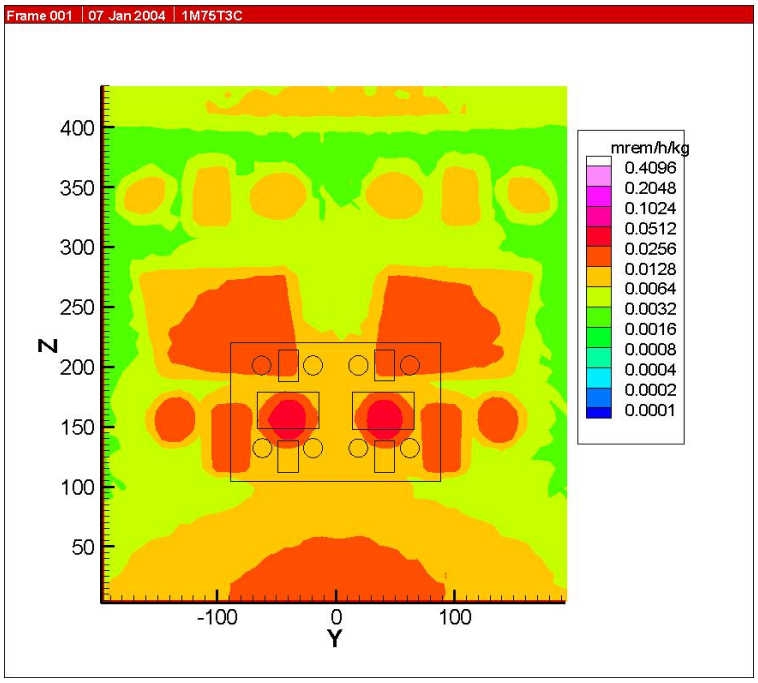

Figure C.6-6: Source at 75 cm.

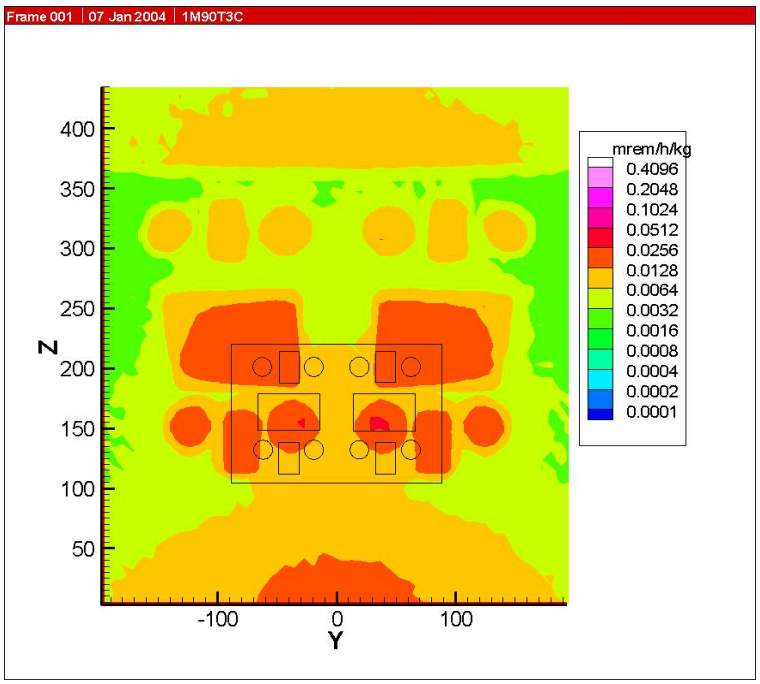

Figure C.6-7: Source at 90 cm.

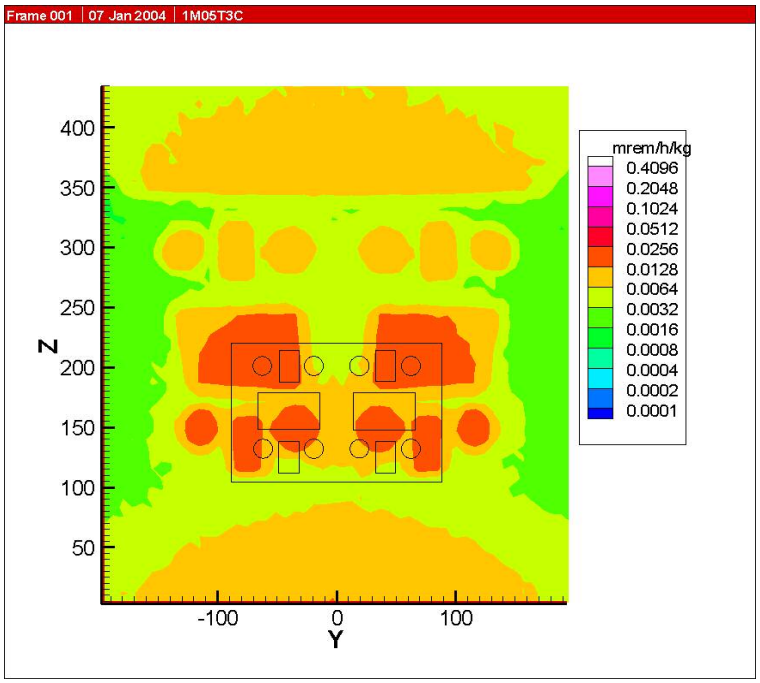

Figure C.6-8: Source at 105 cm.

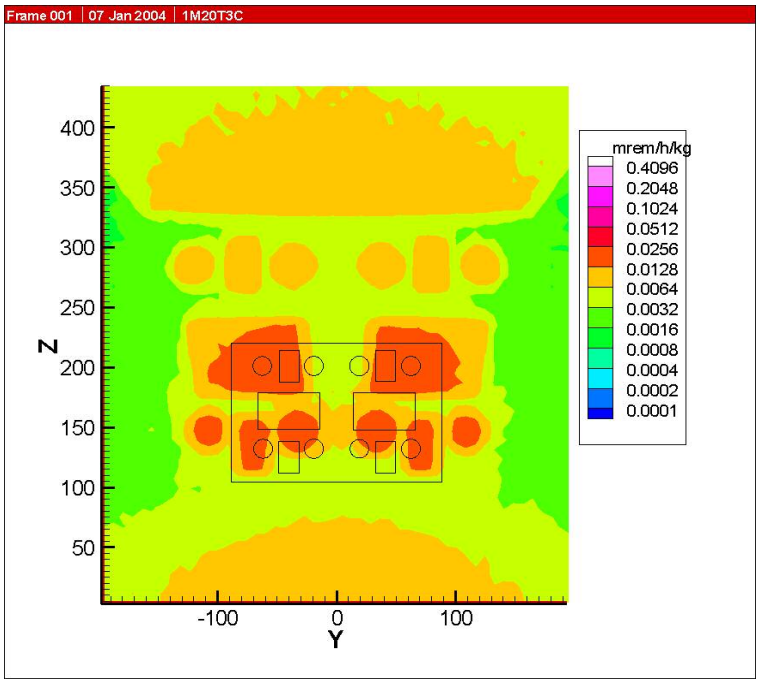

Figure C.6-9: Source at 120 cm.

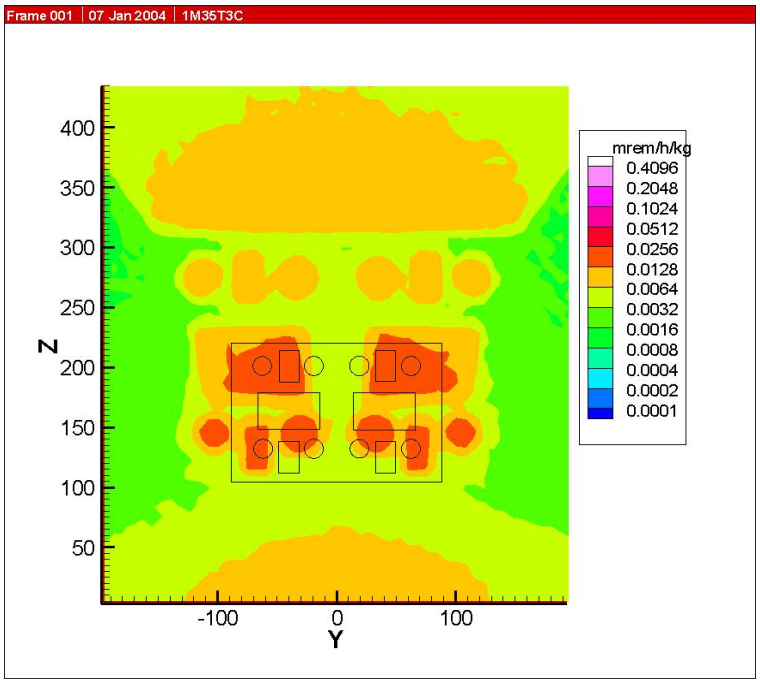

Figure C.6-10: Source at 135 cm.

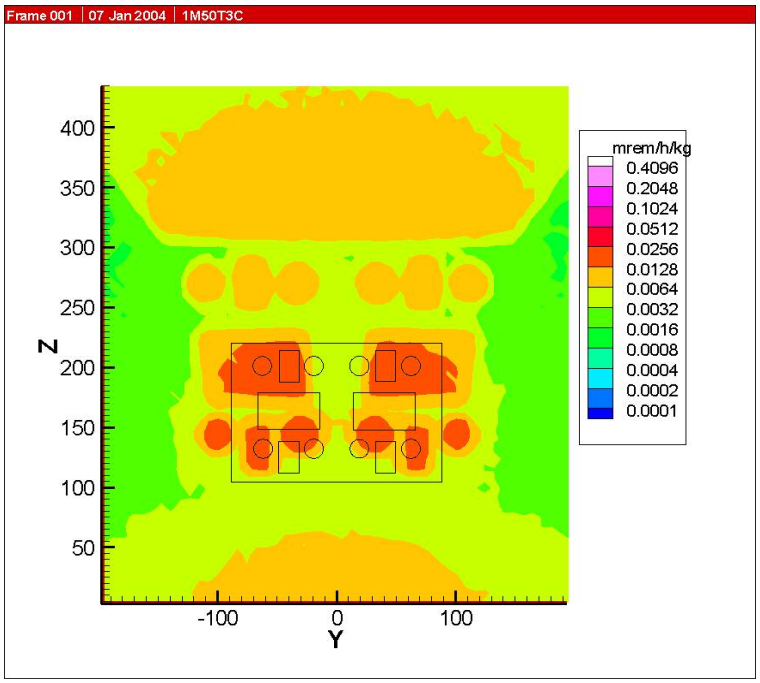

Figure C.6-11: Source at 150 cm.

APPENDIX C.7:

ANSI 1977 AT 6 FOOT WITH SOURCE ON LINE S

The neutron dose field is determined using ANSI 1977 flux-to-dose conversion factors and a mesh tally that is 6 ft in front of the glove box. Figures C.1-1 thru C.1-11 show the changes in the field as the source is moved from 6 cm from the front inside surface of the box to 150 cm from the inside surface on a line that is 6 cm from the left edge of the box (S). The source is 6 cm above the glove box floor. The outline of the front of glove box is shown in each Figure.

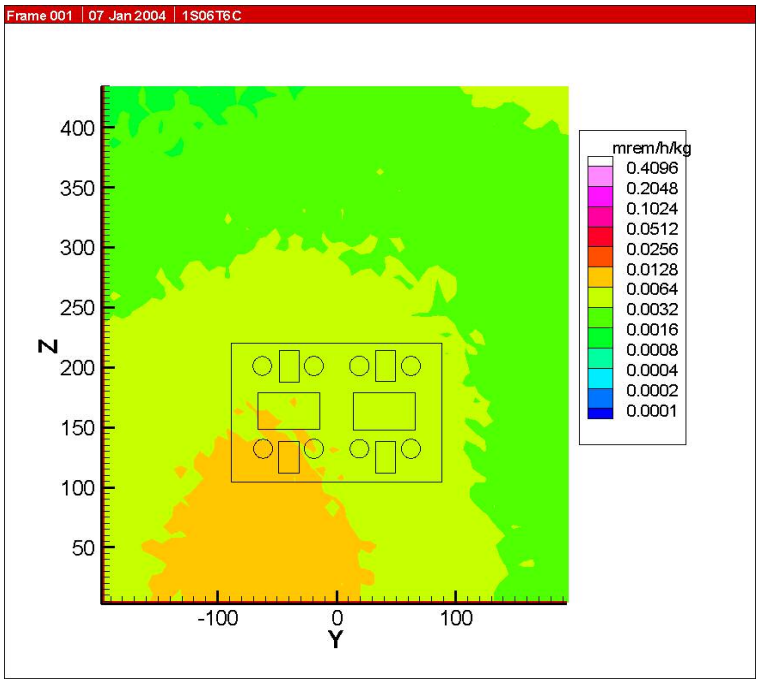

Figure C.7-1: Source at 6 cm.

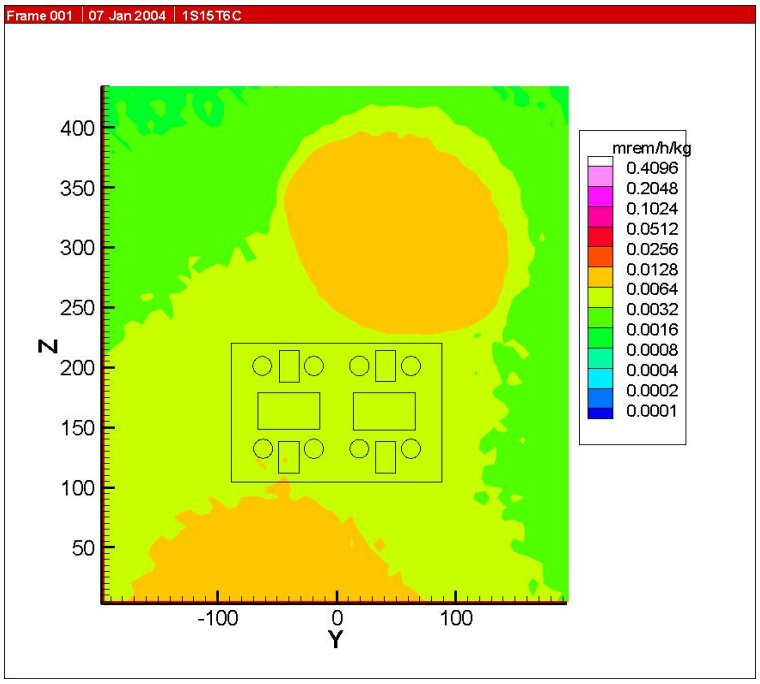

Figure C.7-2: Source at 15 cm.

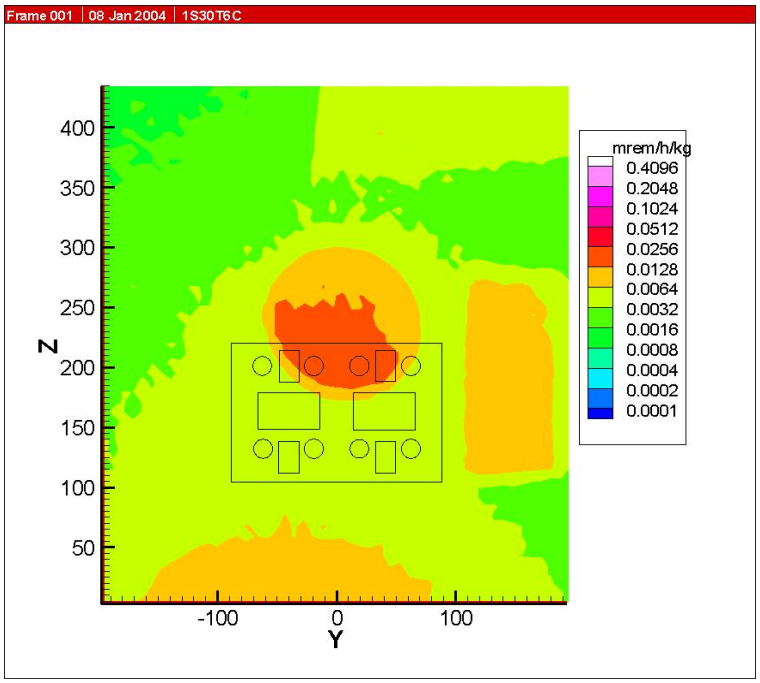

Figure C.7-3: Source at 30 cm.

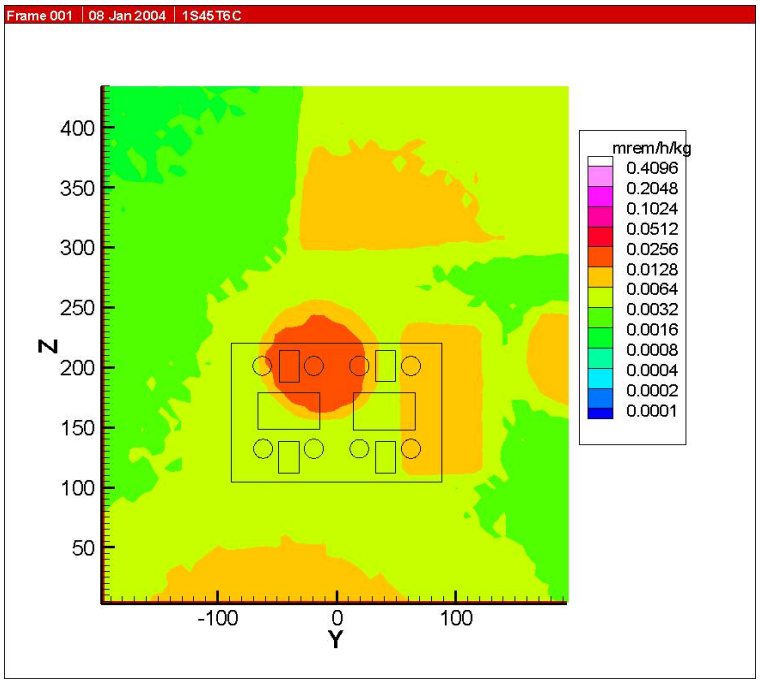

Figure C.7-4: Source at 45 cm.

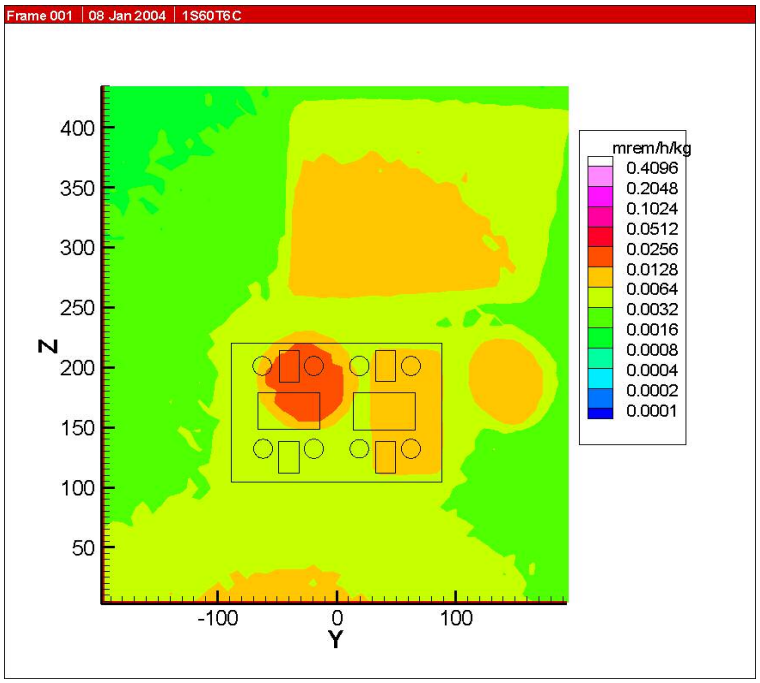

Figure C.7-5: Source at 60 cm.

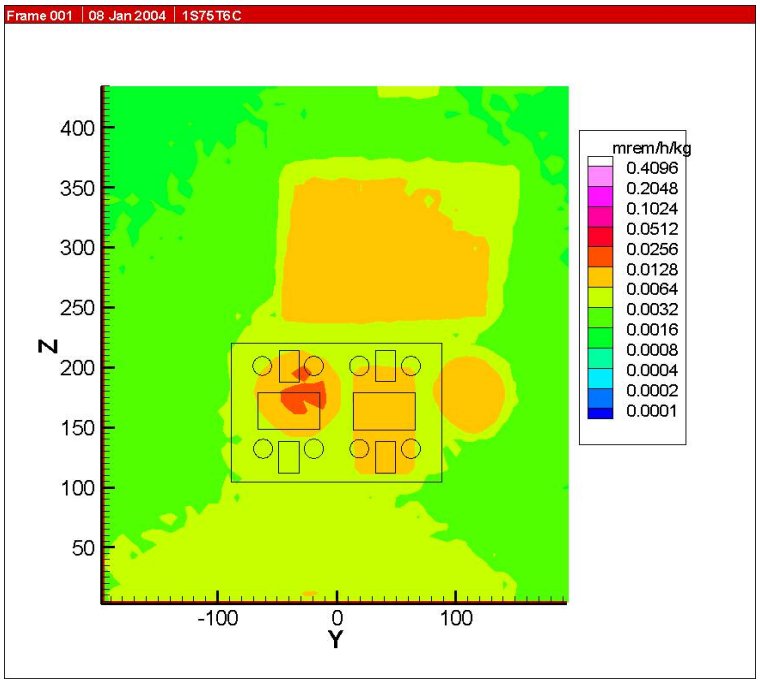

Figure C.7-6: Source at 75 cm.

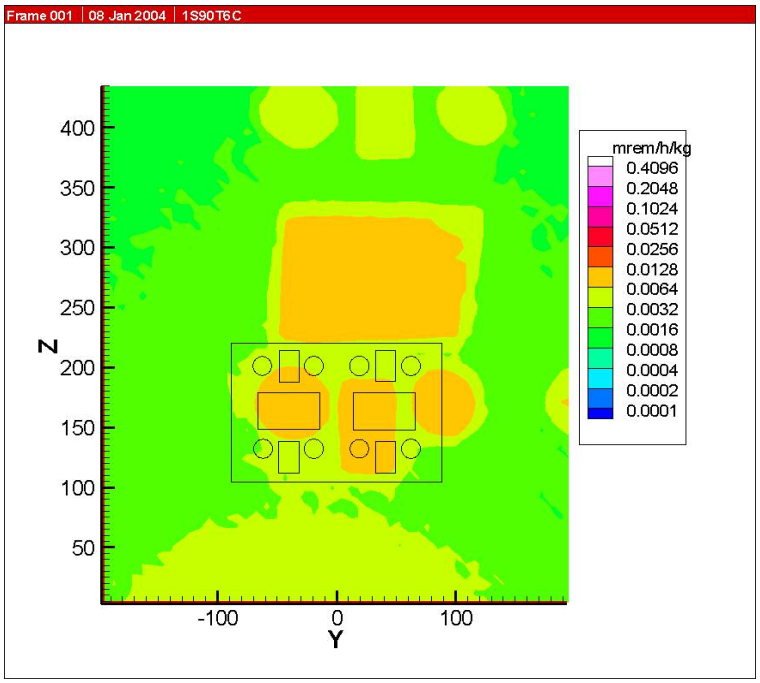

Figure C.7-7: Source at 90 cm.

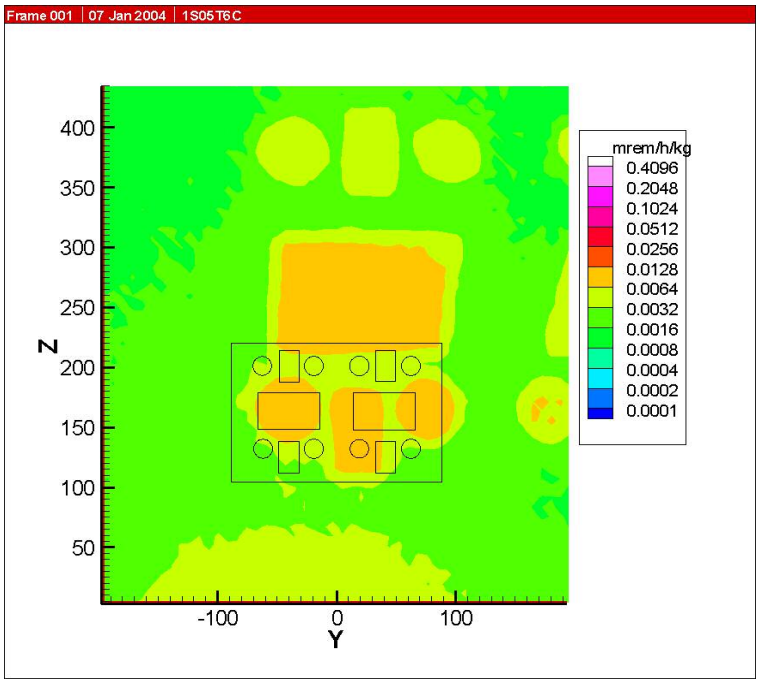

Figure C.7-8: Source at 105 cm.

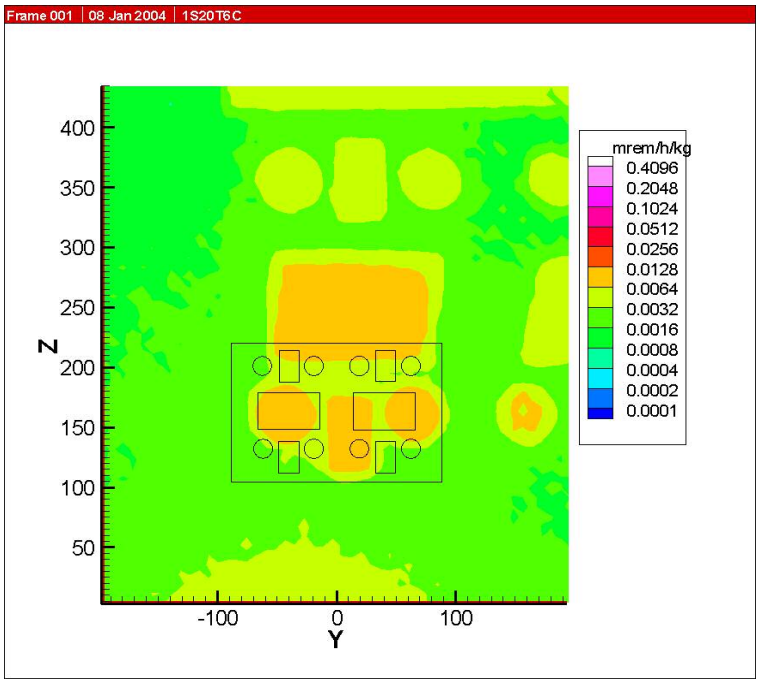

Figure C.7-9: Source at 120 cm.

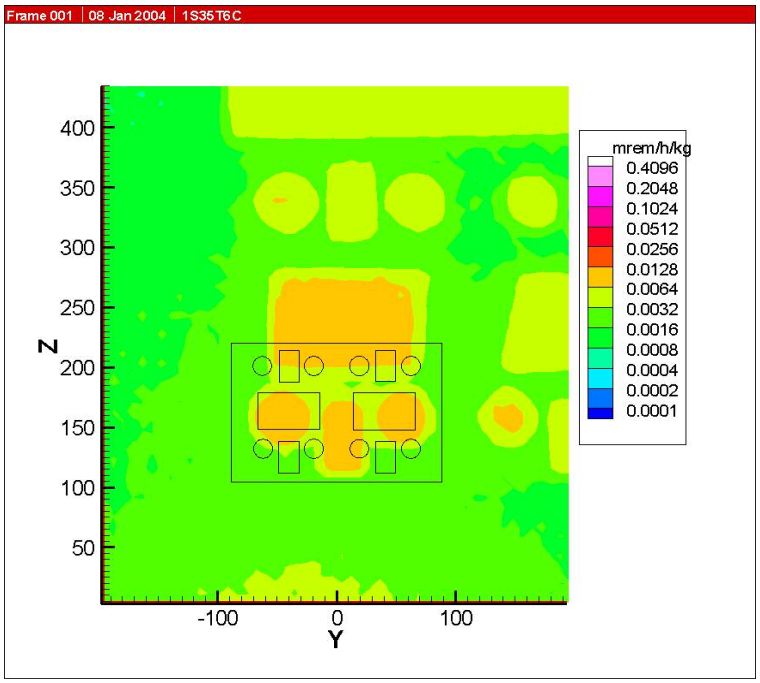

Figure C.7-10: Source at 135 cm.

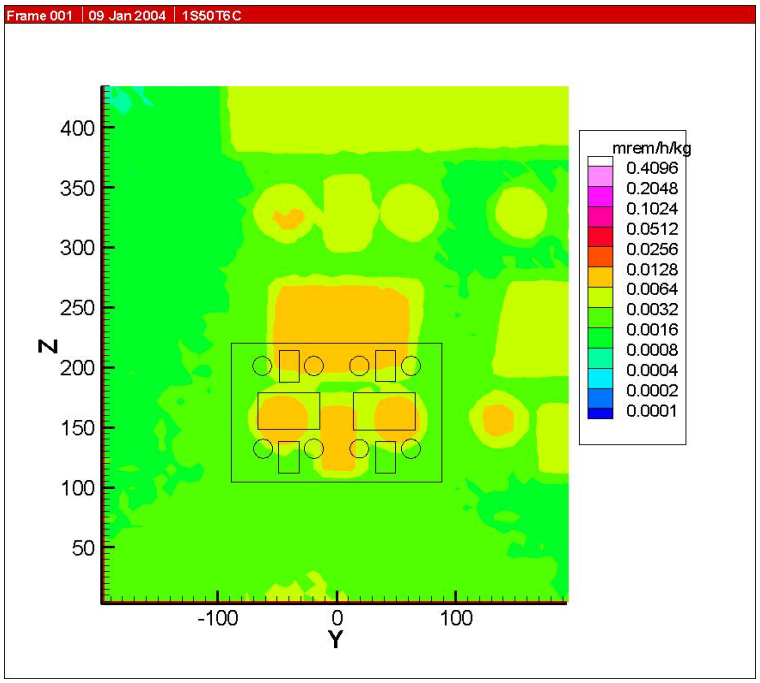

Figure C.7-11: Source at 150 cm.

APPENDIX C.8:

ANSI 1977 AT 6 FOOT WITH SOURCE ON LINE V

The neutron dose field is determined using ANSI 1977 flux-to-dose conversion factors and a mesh tally that is 6 ft in front of the glove box. Figures C.2-1 thru C.2-11 show the changes in the field as the source is moved from 6 cm from the front inside surface of the box to 150 cm from the inside surface on a line that corresponds to the middle of the left pair of gloveports (V). The source is 6 cm above the glove box floor. The outline of the front of glove box is shown in each Figure.

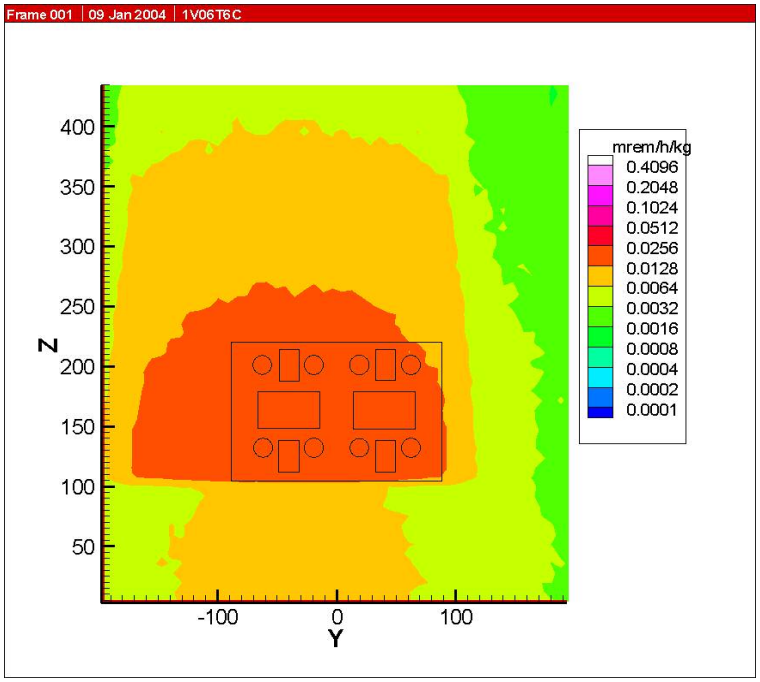

Figure C.8-1: Source at 6 cm.

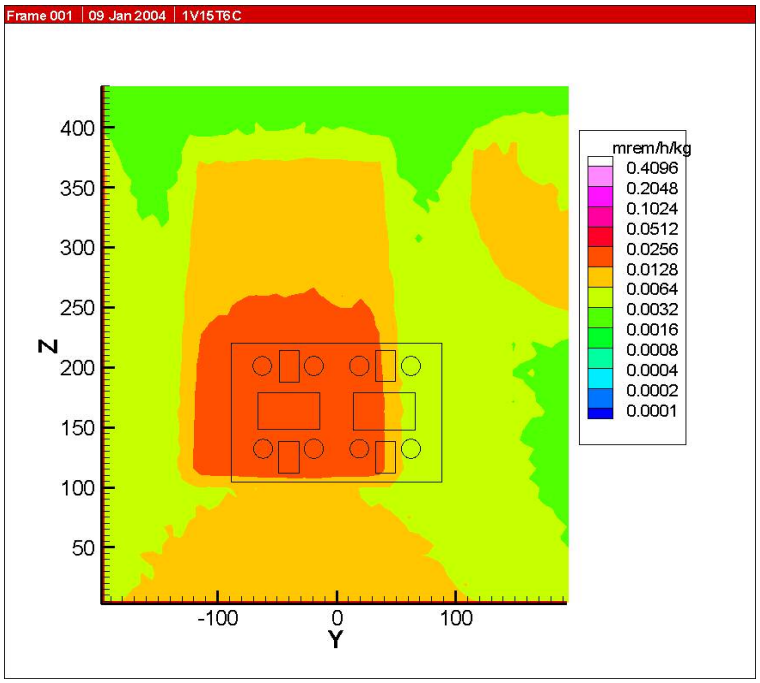

Figure C.8-2: Source at 15 cm.

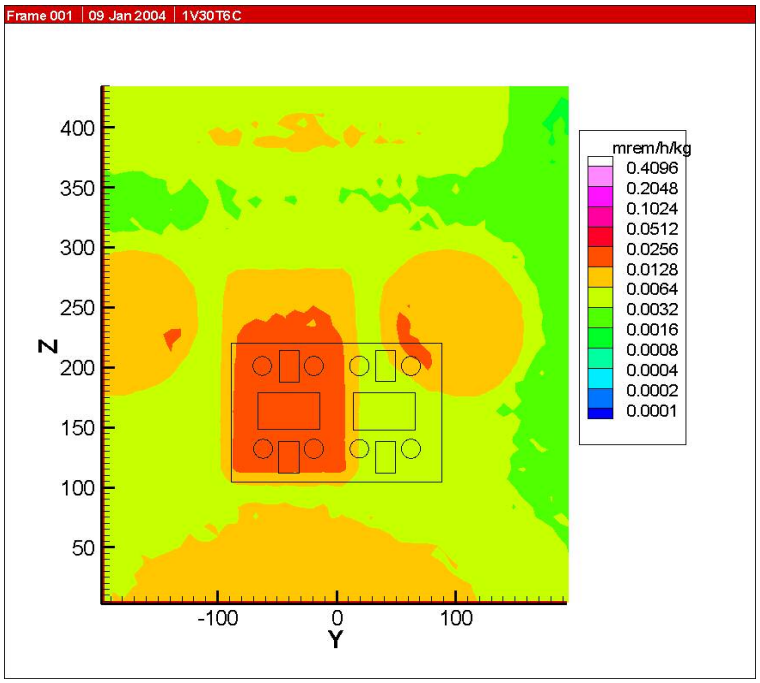

Figure C.8-3: Source at 30 cm.

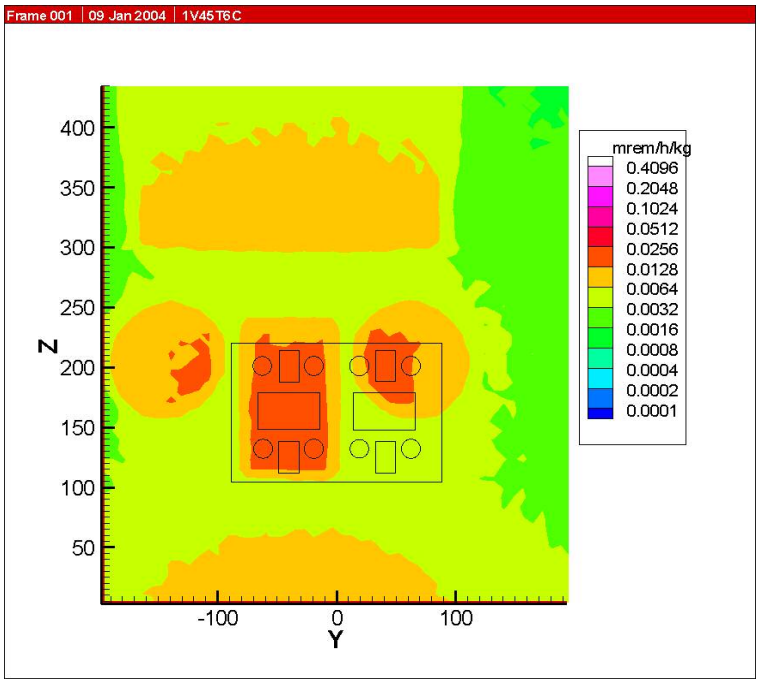

Figure C.8-4: Source at 45 cm.

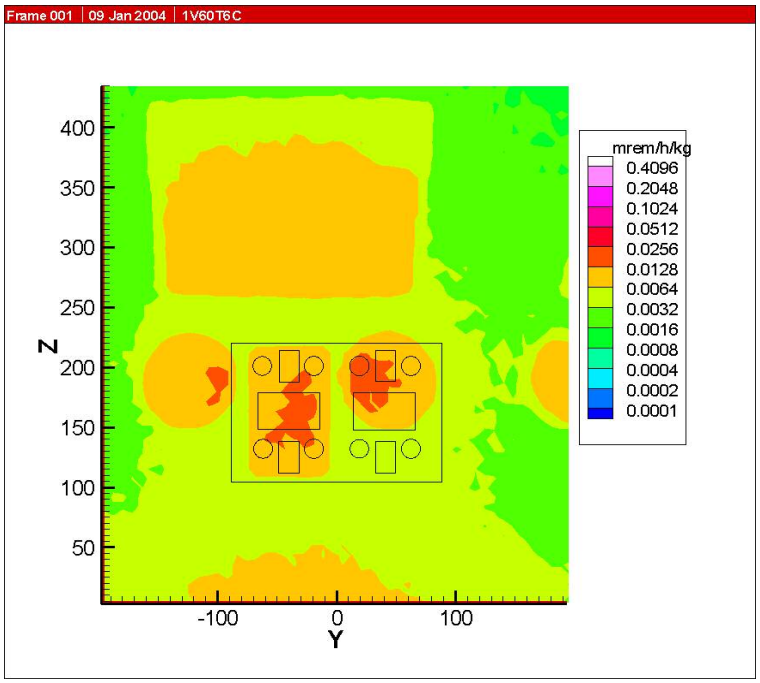

Figure C.8-5: Source at 60 cm.

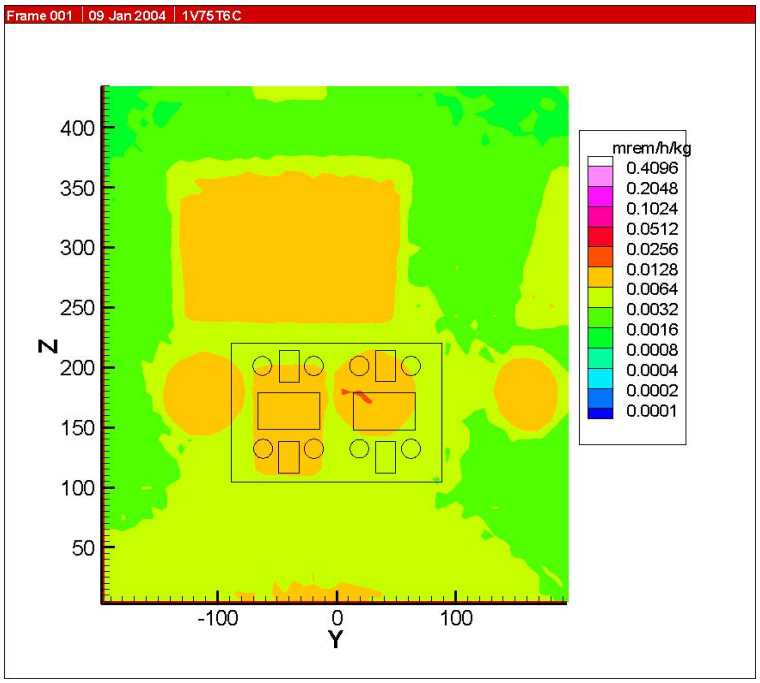

Figure C.8-6: Source at 75 cm.

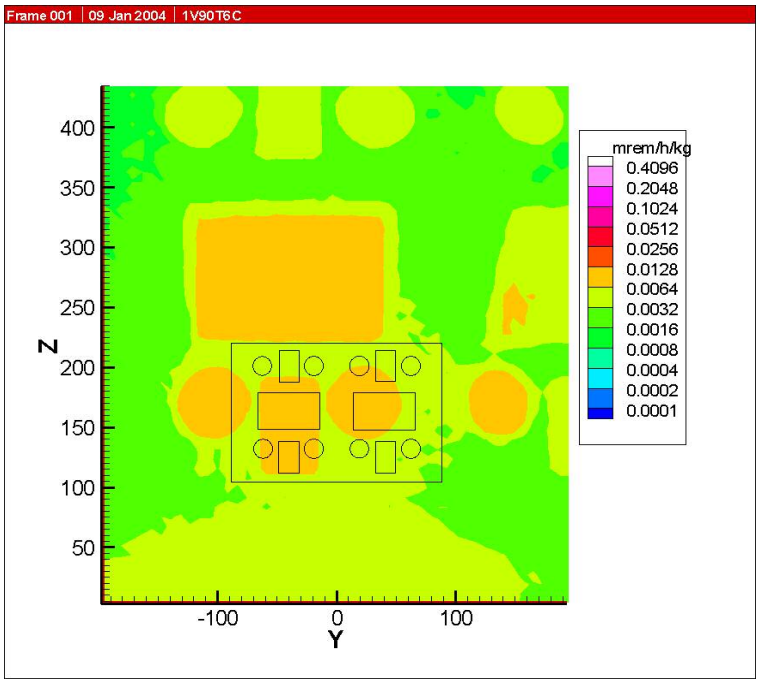

Figure C.8-7: Source at 90 cm.

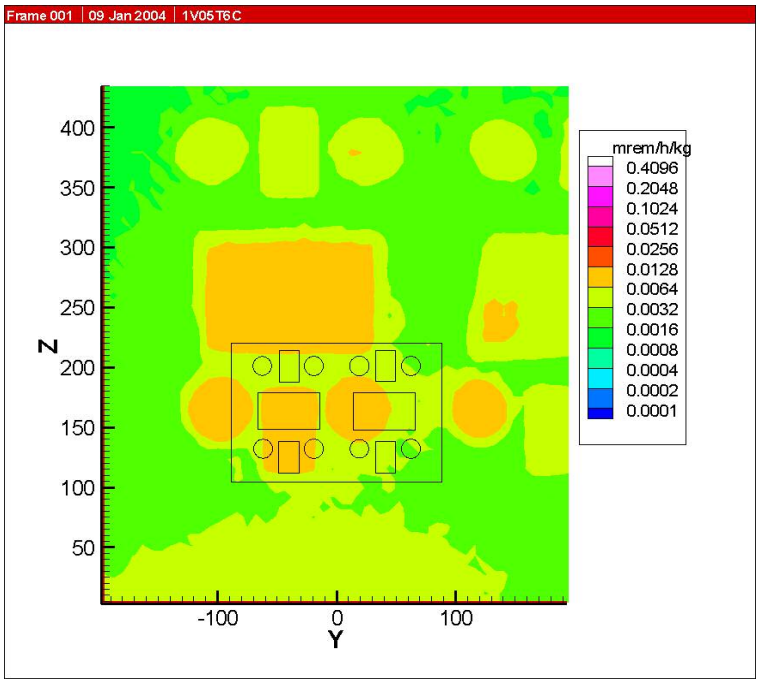

Figure C.8-8: Source at 105 cm.

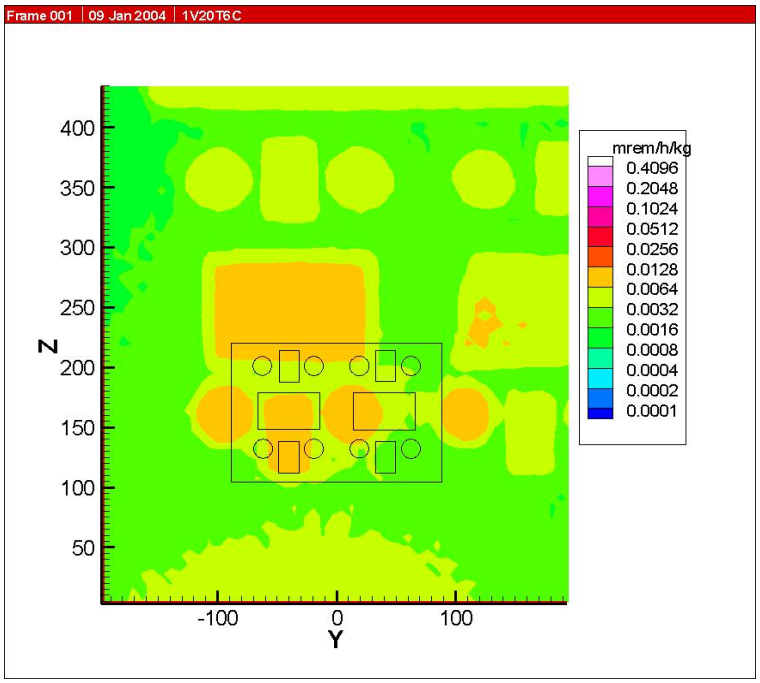

Figure C.8-9: Source at 120 cm.

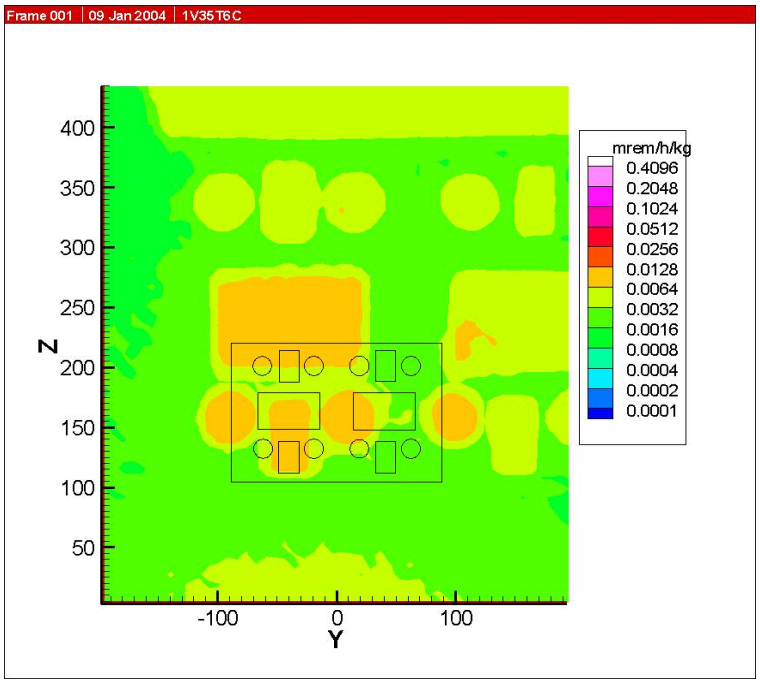

Figure C.8-10: Source at 135 cm.

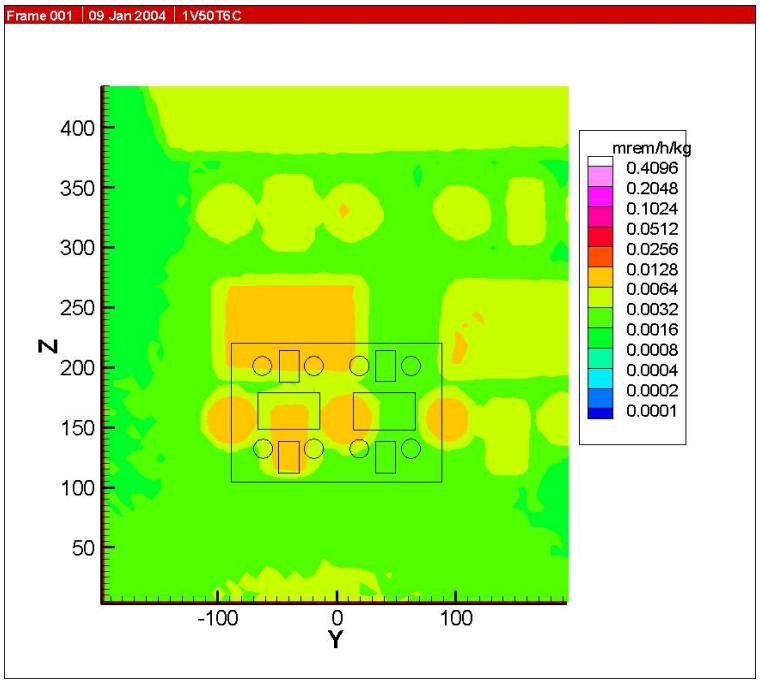

Figure C.8-11: Source at 150 cm.

APPENDIX C.9:

ANSI 1977 AT 6 FOOT WITH SOURCE ON LINE M

The neutron dose field is determined using ANSI 1977 flux-to-dose conversion factors and a mesh tally that is 6 ft in front of the glove box. Figures C.9-1 thru C.9-11 show the changes in the field as the source is moved from 6 cm from the front inside surface of the box to 150 cm from the inside surface on a line that corresponds to the middle of the glove box (M). The source is 6 cm above the glove box floor. The outline of the front of glove box is shown in each Figure.

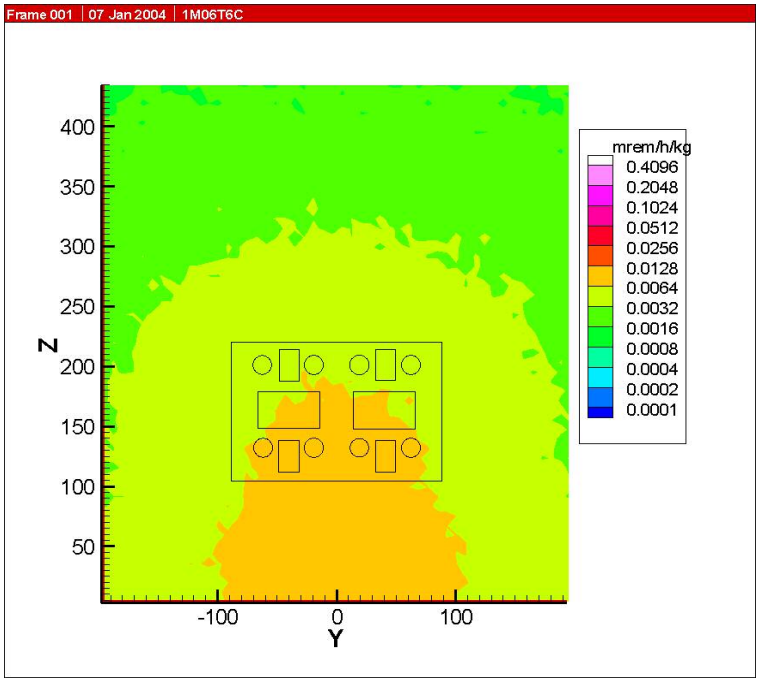

Figure C.9-1: Source at 6 cm.

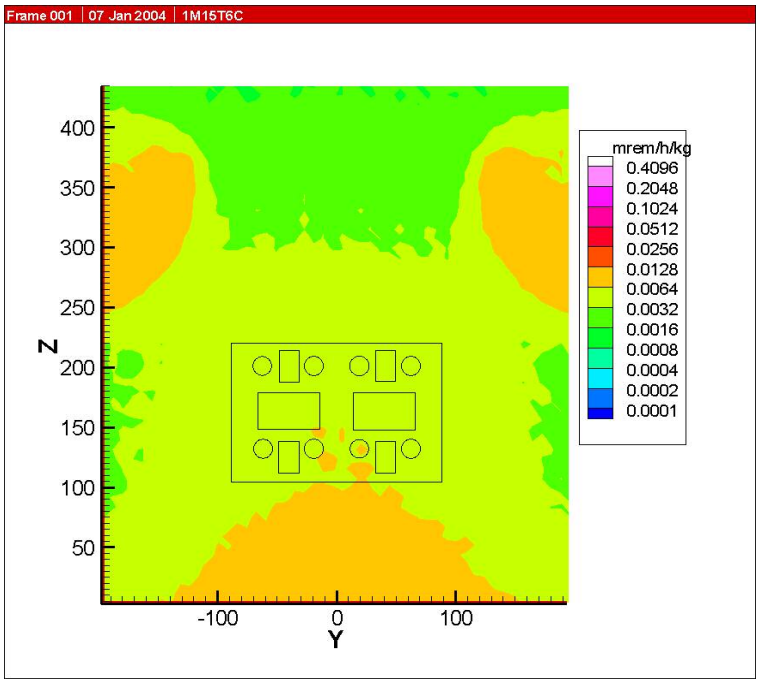

Figure C.9-2: Source at 15 cm.

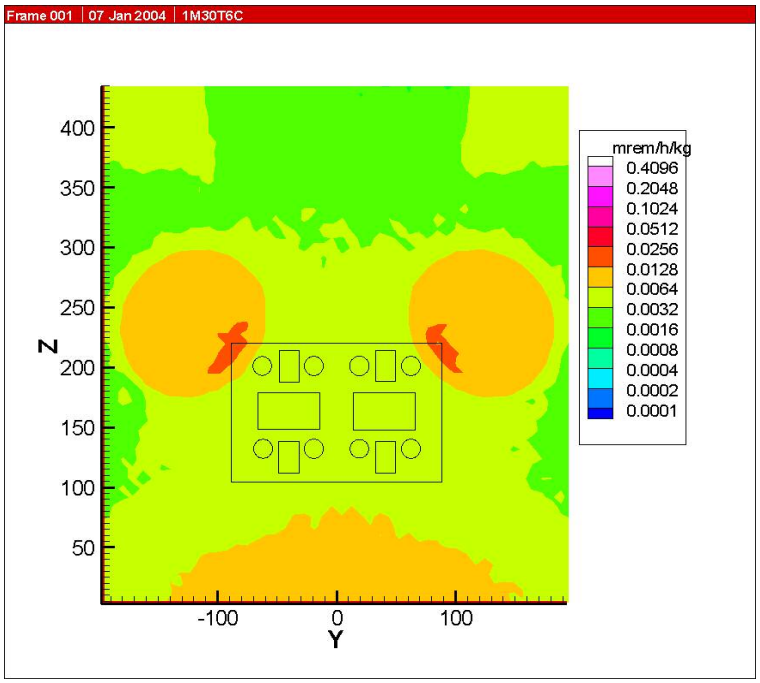

Figure C.9-3: Source at 30 cm.

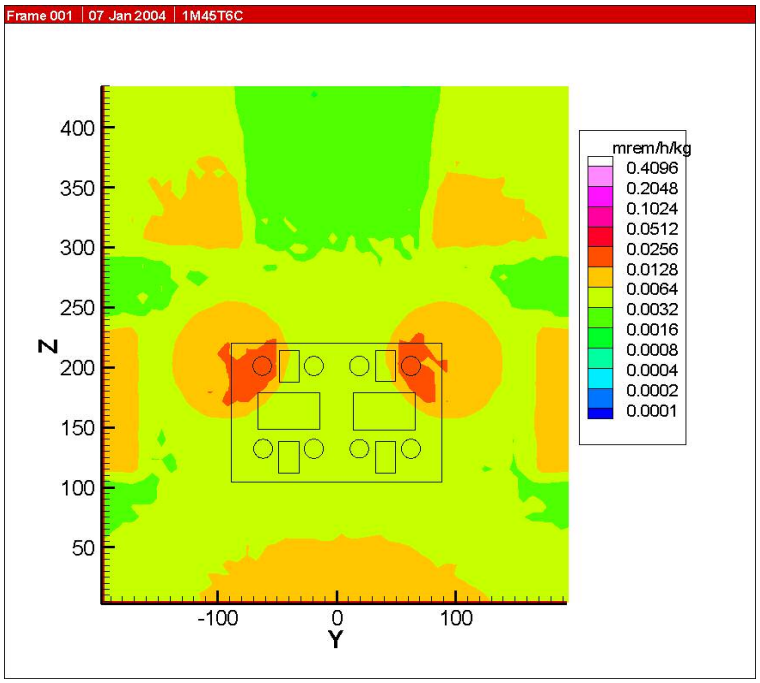

Figure C.9-4: Source at 45 cm.

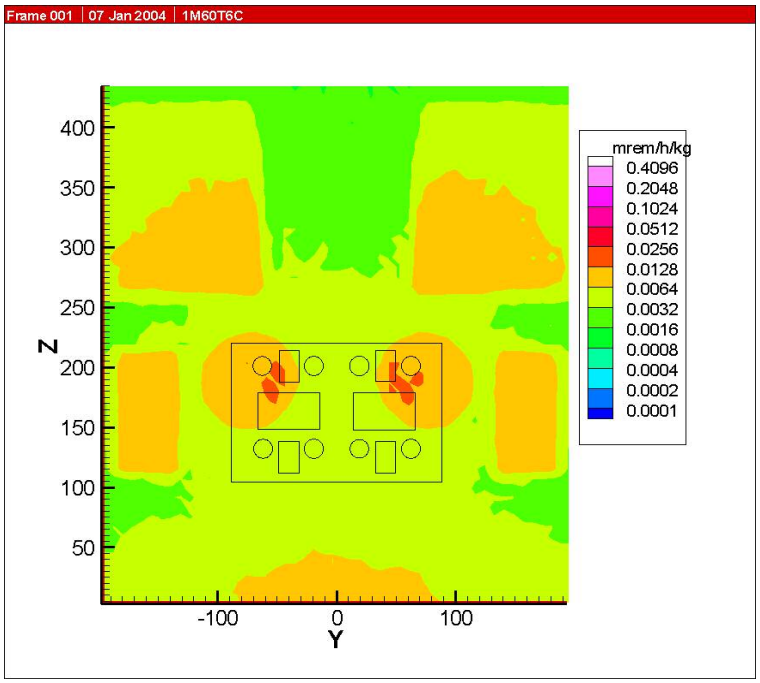

Figure C.9-5: Source at 60 cm.

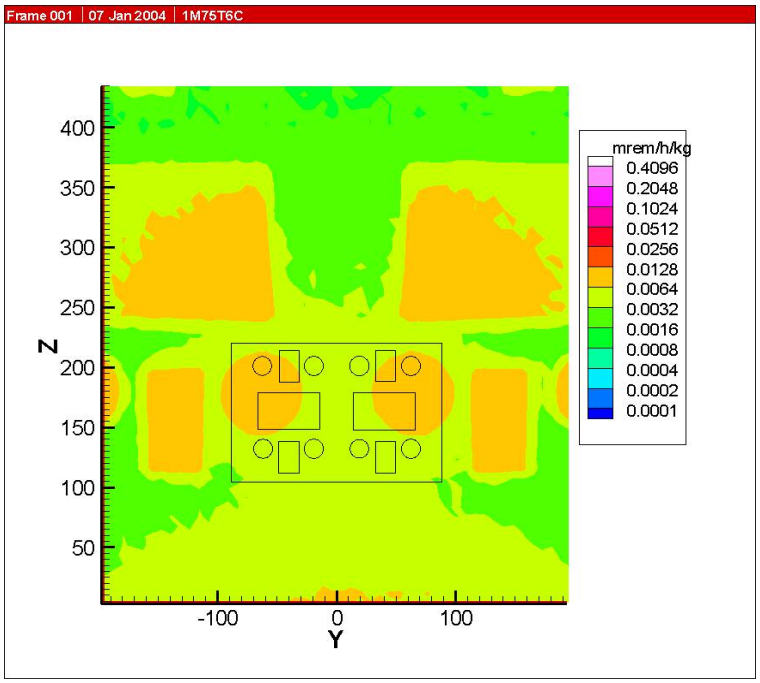

Figure C.9-6: Source at 75 cm.

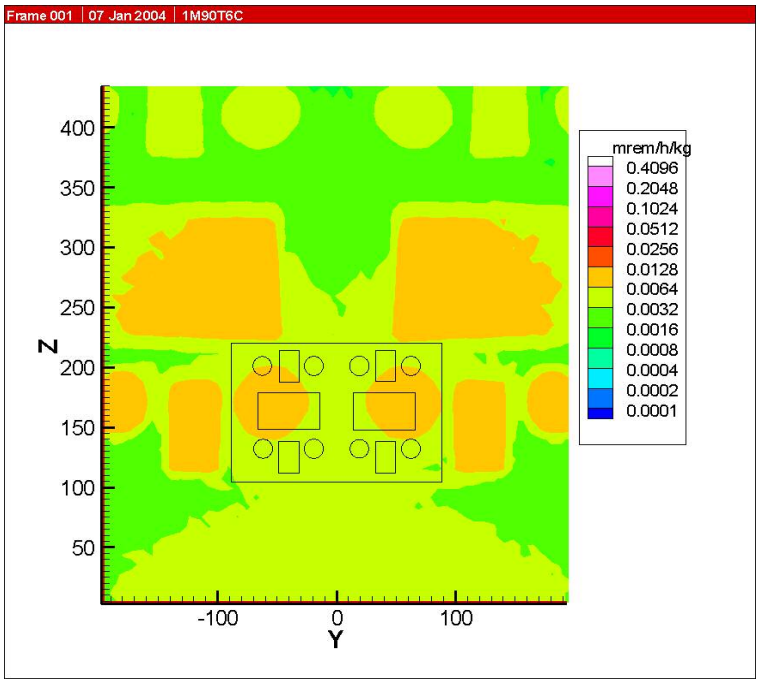

Figure C.9-7: Source at 90 cm.

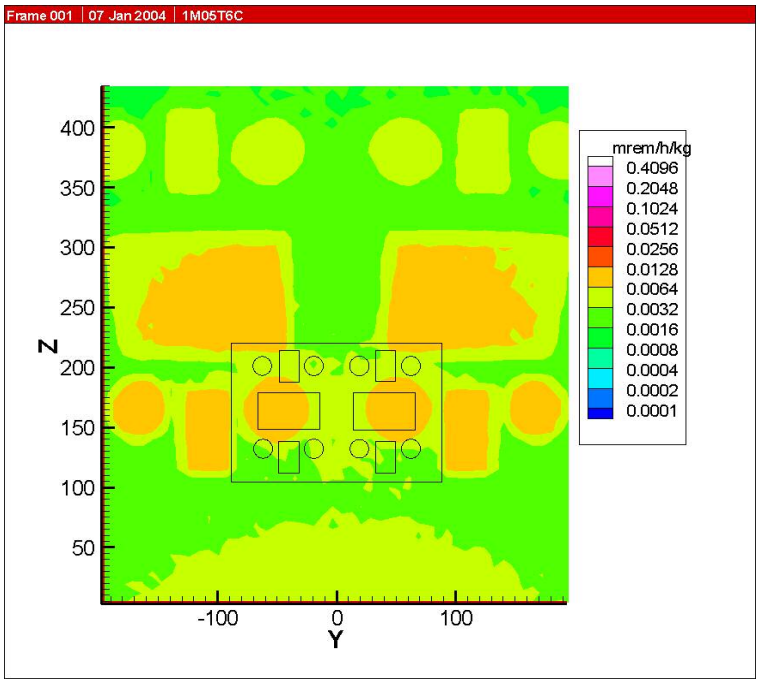

Figure C.9-8: Source at 105 cm.

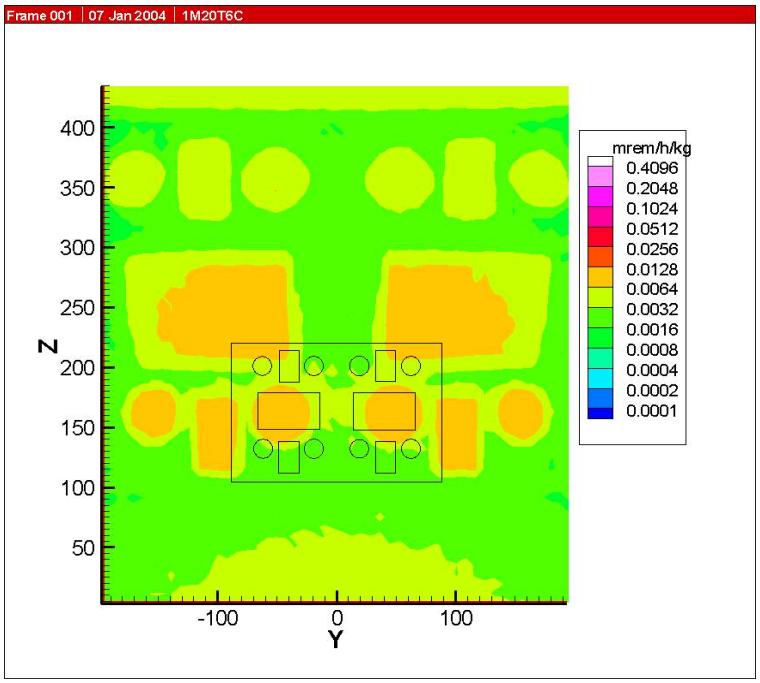

Figure C.9-9: Source at 120 cm.

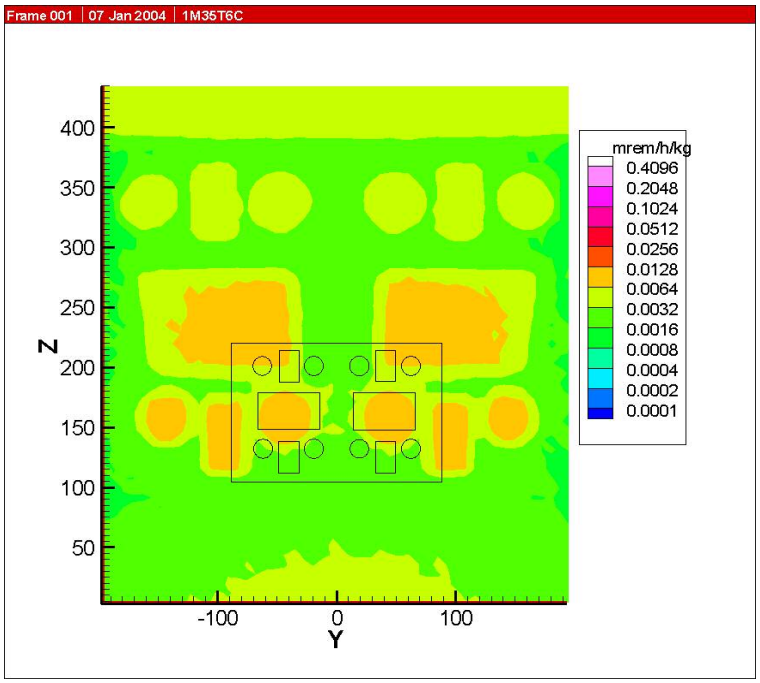

Figure C.9-10: Source at 135 cm.

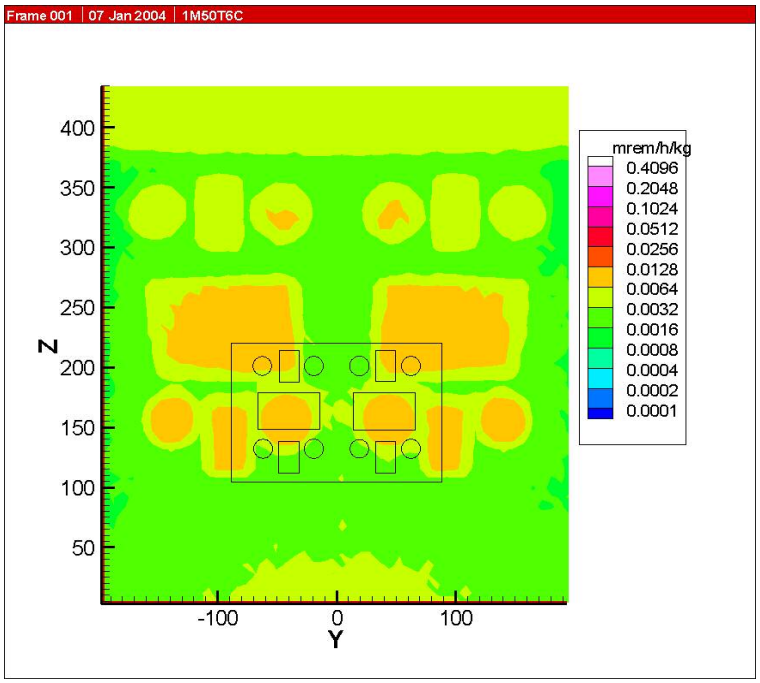

Figure C.9-11: Source at 150 cm.

Appendix D: Summary Of Estimated Doses Using Phantom's Dosimeter Lattice

Table D-1: Summary Phantom Dosimeter Tally Plane using ANSI 1977 at 1 Ft

	Tally Total (mrem/hr/kg)				Dosimeter Position for		
Configuration	Ave	Max	Min	Reference	Ave	Max	Min
1M06M1Z	1.51E-01	2.72E-01	4.60E-02	1.55E-01	552	652	412
1M06S1Z	1.61E-02	3.51E-02	8.66E-03	1.15E-02	612	522	692
1M06V1Z	5.94E-02	1.32E-01	2.61E-02	4.74E-02	412	672	692
1M15M1Z	1.11E-01	1.58E-01	4.98E-02	1.17E-01	572	652	412
1M15S1Z	3.60E-02	6.10E-02	1.16E-02	3.89E-02	412	562	692
1M15V1Z	1.08E-01	2.54E-01	3.09E-02	7.29E-02	622	462	692
1M30M1Z	8.53E-02	2.87E-01	4.65E-02	7.54E-02	482	472	412
1M30S1Z	4.66E-02	1.37E-01	1.00E-02	2.28E-02	502	572	692
1M30V1Z	9.10E-02	2.88E-01	3.14E-02	7.57E-02	622	472	692
1M45M1Z	6.86E-02	2.34E-01	3.87E-02	5.03E-02	482	522	412
1M45S1Z	4.24E-02	9.43E-02	1.00E-02	6.54E-02	562	572	692
1M45V1Z	9.08E-02	2.35E-01	2.67E-02	5.15E-02	442	522	692
1M60M1Z	5.57E-02	1.79E-01	2.88E-02	3.87E-02	562	522	712
1M60S1Z	3.00E-02	7.93E-02	9.71E-03	4.86E-02	722	512	692
1M60V1Z	7.53E-02	1.83E-01	2.20E-02	5.40E-02	642	522	702
1M75M1Z	4.56E-02	1.44E-01	2.08E-02	3.06E-02	532	522	702
1M75S1Z	2.38E-02	6.77E-02	9.65E-03	2.85E-02	672	512	642
1M75V1Z	6.13E-02	1.42E-01	1.94E-02	5.72E-02	642	522	702
1M90M1Z	3.68E-02	1.12E-01	1.66E-02	2.40E-02	622	522	702
1M90S1Z	2.00E-02	6.40E-02	8.08E-03	1.80E-02	612	522	692
1M90V1Z	4.95E-02	1.11E-01	1.55E-02	5.27E-02	642	522	702
1M05M1Z	3.08E-02	9.33E-02	1.40E-02	1.99E-02	462	522	702
1M05S1Z	1.77E-02	6.39E-02	7.22E-03	1.28E-02	672	522	692
1M05V1Z	4.20E-02	9.42E-02	1.36E-02	4.82E-02	642	522	702
1M20M1Z	2.63E-02	7.77E-02	1.22E-02	1.64E-02	462	522	702
1M20S1Z	1.56E-02	6.04E-02	6.62E-03	1.02E-02	422	522	692
1M20V1Z	3.46E-02	7.76E-02	1.23E-02	4.30E-02	622	522	712
1M35M1Z	2.34E-02	6.97E-02	1.11E-02	1.44E-02	582	522	692
1M35S1Z	1.40E-02	5.66E-02	5.80E-03	8.29E-03	672	522	592
1M35V1Z	2.97E-02	6.64E-02	1.09E-02	3.92E-02	562	572	702
1M50M1Z	2.21E-02	6.40E-02	9.98E-03	1.33E-02	432	522	702
1M50S1Z	1.36E-02	5.49E-02	5.45E-03	7.37E-03	462	522	492

Configuration	Tally Total (mrem/hr/kg)				Dosimeter Position for		
	Ave	Max	Min	Reference	Ave	Max	Min
1M50V1Z	2.83E-02	6.47E-02	1.03E-02	3.81E-02	402	572	702
1S06M1Z	2.33E-02	4.90E-02	1.24E-02	1.92E-02	592	482	702
1S06S1Z	1.27E-01	2.70E-01	3.11E-02	1.16E-01	642	672	402
1S06V1Z	9.48E-02	1.82E-01	3.94E-02	7.30E-02	542	632	712
1S15M1Z	4.84E-02	1.02E-01	1.51E-02	3.33E-02	472	542	712
1S15S1Z	8.04E-02	1.63E-01	2.57E-02	7.77E-02	512	672	402
1S15V1Z	1.30E-01	3.39E-01	4.15E-02	9.24E-02	632	432	712
1S30M1Z	6.30E-02	1.66E-01	1.59E-02	4.62E-02	562	532	712
1S30S1Z	5.10E-02	2.16E-01	1.90E-02	4.01E-02	512	472	402
1S30V1Z	1.29E-01	3.46E-01	3.54E-02	7.80E-02	502	482	712
1S45M1Z	5.01E-02	1.03E-01	1.21E-02	8.23E-02	462	492	712
1S45S1Z	3.72E-02	1.65E-01	1.39E-02	2.52E-02	462	472	402
1S45V1Z	1.11E-01	2.70E-01	3.13E-02	7.44E-02	462	482	712
1S60M1Z	3.72E-02	1.01E-01	1.29E-02	5.42E-02	452	492	712
1S60S1Z	2.83E-02	1.43E-01	1.14E-02	1.70E-02	462	522	402
1S60V1Z	8.74E-02	2.01E-01	2.50E-02	8.25E-02	442	482	702
1S75M1Z	3.05E-02	8.48E-02	1.27E-02	3.33E-02	632	492	702
1S75S1Z	2.26E-02	1.15E-01	9.26E-03	1.30E-02	662	522	402
1S75V1Z	6.92E-02	1.57E-01	2.06E-02	7.61E-02	532	472	702
1S90M1Z	2.63E-02	8.67E-02	1.09E-02	2.12E-02	502	482	712
1S90S1Z	1.78E-02	9.11E-02	7.42E-03	1.07E-02	612	522	442
1S90V1Z	5.49E-02	1.21E-01	1.71E-02	6.63E-02	472	482	692
1S05M1Z	2.30E-02	8.28E-02	9.88E-03	1.51E-02	632	482	702
1S05S1Z	1.50E-02	7.38E-02	6.77E-03	8.40E-03	612	522	492
1S05V1Z	4.34E-02	9.74E-02	1.44E-02	5.78E-02	652	482	692
1S20M1Z	2.02E-02	7.31E-02	8.47E-03	1.25E-02	632	482	712
1S20S1Z	1.26E-02	6.20E-02	5.07E-03	6.74E-03	662	522	402
1S20V1Z	3.54E-02	8.10E-02	1.20E-02	4.97E-02	672	482	702
1S35M1Z	1.76E-02	6.51E-02	8.46E-03	1.15E-02	442	482	712
1S35S1Z	1.10E-02	5.17E-02	4.51E-03	5.76E-03	512	522	442
1S35V1Z	3.00E-02	6.93E-02	1.06E-02	4.23E-02	582	482	702
1S50M1Z	1.67E-02	6.28E-02	8.18E-03	1.03E-02	632	482	702
1S50S1Z	1.02E-02	4.85E-02	4.61E-03	5.73E-03	662	522	492
1S50V1Z	2.81E-02	6.64E-02	1.03E-02	3.95E-02	422	482	702

Configuration	Tally Total (mrem/hr/kg)				Dosimeter Position for		
	Ave	Max	Min	Reference	Ave	Max	Min
1V06M1Z	7.60E-02	2.70E-01	2.75E-02	4.52E-02	542	582	712
1V06S1Z	7.39E-02	2.65E-01	2.44E-02	4.20E-02	562	622	692
1V06V1Z	5.63E-01	9.30E-01	1.96E-01	7.56E-01	492	602	722
1V15M1Z	9.61E-02	2.29E-01	2.88E-02	5.72E-02	632	442	712
1V15S1Z	9.15E-02	2.25E-01	2.43E-02	5.39E-02	672	462	692
1V15V1Z	3.76E-01	5.76E-01	1.32E-01	5.15E-01	522	602	722
1V30M1Z	7.80E-02	2.74E-01	2.66E-02	5.81E-02	582	432	712
1V30S1Z	7.20E-02	2.72E-01	2.24E-02	5.00E-02	622	472	692
1V30V1Z	1.81E-01	3.18E-01	6.99E-02	3.05E-01	462	602	712
1V45M1Z	6.09E-02	2.27E-01	2.26E-02	3.70E-02	582	482	712
1V45S1Z	5.38E-02	2.23E-01	1.83E-02	2.83E-02	622	522	692
1V45V1Z	1.13E-01	2.00E-01	4.42E-02	1.97E-01	432	602	692
1V60M1Z	4.77E-02	1.77E-01	2.05E-02	3.03E-02	582	482	712
1V60S1Z	4.01E-02	1.74E-01	1.40E-02	2.16E-02	672	522	692
1V60V1Z	8.20E-02	1.39E-01	3.10E-02	1.39E-01	452	552	702
1V75M1Z	3.83E-02	1.40E-01	1.69E-02	2.51E-02	632	482	702
1V75S1Z	3.08E-02	1.34E-01	1.15E-02	1.68E-02	672	522	692
1V75V1Z	6.30E-02	1.07E-01	2.37E-02	1.02E-01	642	522	702
1V90M1Z	3.10E-02	1.12E-01	1.47E-02	2.05E-02	632	482	712
1V90S1Z	2.39E-02	1.06E-01	8.48E-03	1.32E-02	462	522	402
1V90V1Z	4.97E-02	9.27E-02	1.82E-02	7.72E-02	662	522	702
1V05M1Z	2.64E-02	9.20E-02	1.27E-02	1.71E-02	572	482	702
1V05S1Z	1.96E-02	8.92E-02	7.31E-03	1.15E-02	722	522	492
1V05V1Z	4.10E-02	7.71E-02	1.51E-02	6.15E-02	662	482	702
1V20M1Z	2.33E-02	7.73E-02	1.16E-02	1.44E-02	632	482	692
1V20S1Z	1.61E-02	7.29E-02	6.24E-03	9.03E-03	722	522	402
1V20V1Z	3.48E-02	6.60E-02	1.29E-02	5.11E-02	662	522	692
1V35M1Z	2.07E-02	6.73E-02	9.85E-03	1.24E-02	632	482	712
1V35S1Z	1.38E-02	6.40E-02	5.13E-03	8.01E-03	722	522	402
1V35V1Z	3.01E-02	5.71E-02	1.13E-02	4.37E-02	412	522	702
1V50M1Z	1.93E-02	6.21E-02	8.64E-03	1.15E-02	542	482	702
1V50S1Z	1.27E-02	5.91E-02	5.02E-03	7.28E-03	722	522	402
1V50V1Z	2.78E-02	5.35E-02	1.03E-02	4.07E-02	432	482	702

Table D-2: Summary Phantom Dosimeter Tally Plane using ANSI 1991 at 1 Ft

	Tally Total (mrem/hr/kg)				Dosimeter Position for		
Configuration	Ave	Max	Min	Reference	Ave	Max	Min
1M06M1A	7.93E-02	1.44E-01	2.27E-02	8.16E-02	152	252	12
1M06S1A	7.70E-03	1.69E-02	4.01E-03	5.50E-03	212	122	192
1M06V1A	2.97E-02	6.97E-02	1.24E-02	2.24E-02	112	272	292
1M15M1A	5.79E-02	8.35E-02	2.48E-02	6.13E-02	322	252	12
1M15S1A	1.85E-02	3.28E-02	4.80E-03	2.01E-02	222	162	292
1M15V1A	5.67E-02	1.37E-01	1.45E-02	3.75E-02	272	62	292
1M30M1A	4.43E-02	1.55E-01	2.34E-02	3.91E-02	192	72	12
1M30S1A	2.42E-02	7.37E-02	4.71E-03	1.18E-02	102	172	292
1M30V1A	4.70E-02	1.53E-01	1.39E-02	3.86E-02	222	72	292
1M45M1A	3.55E-02	1.25E-01	1.97E-02	2.59E-02	82	122	12
1M45S1A	2.19E-02	4.98E-02	4.33E-03	3.55E-02	162	122	292
1M45V1A	4.73E-02	1.24E-01	1.19E-02	2.55E-02	42	122	292
1M60M1A	2.87E-02	9.48E-02	1.45E-02	1.97E-02	162	122	312
1M60S1A	1.51E-02	4.21E-02	4.32E-03	2.53E-02	82	112	302
1M60V1A	3.90E-02	9.61E-02	1.04E-02	2.78E-02	242	122	292
1M75M1A	2.34E-02	7.60E-02	1.05E-02	1.54E-02	132	122	302
1M75S1A	1.16E-02	3.58E-02	3.80E-03	1.49E-02	272	112	292
1M75V1A	3.14E-02	7.48E-02	8.46E-03	2.89E-02	242	122	292
1M90M1A	1.88E-02	5.88E-02	8.16E-03	1.19E-02	222	122	302
1M90S1A	9.77E-03	3.30E-02	3.41E-03	9.24E-03	212	122	292
1M90V1A	2.53E-02	5.77E-02	7.05E-03	2.73E-02	32	122	292
1M05M1A	1.57E-02	4.88E-02	6.85E-03	9.78E-03	222	122	302
1M05S1A	8.62E-03	3.32E-02	2.87E-03	5.88E-03	22	122	292
1M05V1A	2.12E-02	4.85E-02	5.97E-03	2.48E-02	242	122	302
1M20M1A	1.33E-02	4.07E-02	5.85E-03	8.16E-03	62	122	302
1M20S1A	7.57E-03	3.14E-02	2.87E-03	4.45E-03	22	122	292
1M20V1A	1.75E-02	4.05E-02	5.36E-03	2.23E-02	162	122	292
1M35M1A	1.18E-02	3.60E-02	5.36E-03	7.06E-03	182	122	292
1M35S1A	6.72E-03	2.95E-02	2.45E-03	4.07E-03	22	122	292
1M35V1A	1.48E-02	3.43E-02	4.82E-03	2.04E-02	22	122	302
1M50M1A	1.07E-02	3.25E-02	4.49E-03	6.74E-03	32	122	292
1M50S1A	6.36E-03	2.80E-02	2.29E-03	3.36E-03	22	122	292

	Tally Total (mrem/hr/kg)				Dosimeter Position for		
Configuration	Ave	Max	Min	Reference	Ave	Max	Min
1M50V1A	1.40E-02	3.32E-02	4.20E-03	1.96E-02	2	122	302
1S06M1A	1.12E-02	2.36E-02	5.66E-03	9.48E-03	192	82	302
1S06S1A	6.68E-02	1.42E-01	1.57E-02	6.16E-02	242	272	2
1S06V1A	4.83E-02	9.70E-02	1.82E-02	3.56E-02	142	12	312
1S15M1A	2.51E-02	5.56E-02	7.15E-03	1.66E-02	72	142	312
1S15S1A	4.17E-02	8.53E-02	1.22E-02	4.07E-02	112	272	2
1S15V1A	6.75E-02	1.83E-01	2.00E-02	4.50E-02	182	32	312
1S30M1A	3.28E-02	8.84E-02	7.26E-03	2.41E-02	162	132	312
1S30S1A	2.59E-02	1.16E-01	8.95E-03	2.02E-02	62	72	2
1S30V1A	6.71E-02	1.84E-01	1.90E-02	3.76E-02	102	82	312
1S45M1A	2.56E-02	5.41E-02	5.56E-03	4.35E-02	62	92	312
1S45S1A	1.85E-02	8.76E-02	6.33E-03	1.21E-02	62	72	2
1S45V1A	5.70E-02	1.41E-01	1.49E-02	3.78E-02	62	82	312
1S60M1A	1.87E-02	5.25E-02	5.95E-03	2.81E-02	52	92	312
1S60S1A	1.38E-02	7.57E-02	4.76E-03	8.26E-03	62	122	2
1S60V1A	4.50E-02	1.05E-01	1.15E-02	4.27E-02	42	82	312
1S75M1A	1.53E-02	4.41E-02	6.12E-03	1.68E-02	182	92	302
1S75S1A	1.09E-02	6.13E-02	3.99E-03	6.09E-03	212	122	292
1S75V1A	3.53E-02	8.15E-02	9.34E-03	3.97E-02	142	82	302
1S90M1A	1.31E-02	4.49E-02	5.10E-03	1.04E-02	102	82	312
1S90S1A	8.43E-03	4.80E-02	3.16E-03	4.68E-03	112	122	292
1S90V1A	2.80E-02	6.27E-02	7.47E-03	3.45E-02	72	82	302
1S05M1A	1.15E-02	4.29E-02	4.53E-03	7.33E-03	232	82	302
1S05S1A	6.92E-03	3.83E-02	2.69E-03	3.67E-03	112	122	42
1S05V1A	2.19E-02	5.03E-02	6.13E-03	3.01E-02	252	82	302
1S20M1A	1.01E-02	3.80E-02	3.92E-03	6.13E-03	232	82	312
1S20S1A	5.85E-03	3.22E-02	2.25E-03	3.12E-03	112	122	92
1S20V1A	1.78E-02	4.22E-02	5.48E-03	2.56E-02	272	82	292
1S35M1A	8.79E-03	3.35E-02	4.05E-03	5.57E-03	42	82	302
1S35S1A	5.03E-03	2.70E-02	2.03E-03	2.64E-03	162	122	192
1S35V1A	1.50E-02	3.60E-02	4.67E-03	2.19E-02	92	82	302
1S50M1A	8.00E-03	3.17E-02	3.54E-03	4.80E-03	232	82	312
1S50S1A	4.72E-03	2.51E-02	1.79E-03	2.27E-03	62	122	42
1S50V1A	1.39E-02	3.44E-02	4.15E-03	2.03E-02	122	132	302

	Tally Total (mrem/hr/kg)				Dosimeter Position for		
Configuration	Ave	Max	Min	Reference	Ave	Max	Min
1V06M1A	3.92E-02	1.46E-01	1.32E-02	2.25E-02	192	182	312
1V06S1A	3.83E-02	1.43E-01	1.18E-02	2.05E-02	212	222	292
1V06V1A	3.05E-01	5.05E-01	9.89E-02	4.08E-01	102	202	322
1V15M1A	5.05E-02	1.24E-01	1.40E-02	2.98E-02	232	42	312
1V15S1A	4.81E-02	1.22E-01	1.21E-02	2.76E-02	272	62	292
1V15V1A	2.02E-01	3.11E-01	6.79E-02	2.76E-01	122	202	282
1V30M1A	4.05E-02	1.46E-01	1.31E-02	2.98E-02	182	32	312
1V30S1A	3.71E-02	1.44E-01	1.03E-02	2.61E-02	222	72	292
1V30V1A	9.51E-02	1.71E-01	3.61E-02	1.62E-01	182	202	292
1V45M1A	3.13E-02	1.20E-01	1.12E-02	1.84E-02	182	82	312
1V45S1A	2.76E-02	1.18E-01	8.72E-03	1.46E-02	222	122	292
1V45V1A	5.86E-02	1.06E-01	2.21E-02	1.05E-01	72	202	312
1V60M1A	2.44E-02	9.33E-02	9.83E-03	1.50E-02	182	82	312
1V60S1A	2.03E-02	9.13E-02	6.43E-03	1.05E-02	222	122	292
1V60V1A	4.21E-02	7.35E-02	1.51E-02	7.31E-02	52	202	302
1V75M1A	1.94E-02	7.34E-02	8.20E-03	1.24E-02	232	82	302
1V75S1A	1.54E-02	7.09E-02	4.89E-03	8.29E-03	272	122	292
1V75V1A	3.22E-02	5.53E-02	1.09E-02	5.36E-02	172	122	302
1V90M1A	1.57E-02	5.86E-02	7.07E-03	1.03E-02	42	82	312
1V90S1A	1.18E-02	5.56E-02	3.70E-03	6.50E-03	272	122	292
1V90V1A	2.51E-02	4.79E-02	8.20E-03	4.03E-02	242	122	302
1V05M1A	1.33E-02	4.80E-02	6.05E-03	8.41E-03	172	82	302
1V05S1A	9.48E-03	4.64E-02	3.23E-03	5.28E-03	272	122	292
1V05V1A	2.07E-02	3.96E-02	7.02E-03	3.24E-02	262	82	292
1V20M1A	1.18E-02	4.02E-02	5.52E-03	7.13E-03	72	82	312
1V20S1A	7.78E-03	3.77E-02	2.40E-03	4.27E-03	322	122	242
1V20V1A	1.74E-02	3.43E-02	5.73E-03	2.66E-02	12	122	302
1V35M1A	1.04E-02	3.49E-02	4.64E-03	6.11E-03	232	82	312
1V35S1A	6.53E-03	3.33E-02	2.27E-03	3.64E-03	322	122	2
1V35V1A	1.50E-02	2.93E-02	5.13E-03	2.25E-02	2	122	302
1V50M1A	9.45E-03	3.18E-02	3.70E-03	5.47E-03	142	82	302
1V50S1A	5.94E-03	3.03E-02	2.13E-03	3.35E-03	322	122	292
1V50V1A	1.38E-02	2.73E-02	4.66E-03	2.09E-02	32	82	302

Table D-3: Summary Phantom Dosimeter Tally Plane using ICRP-74 at 1 Ft

	Tally Total (mrem/hr/kg)				Dosimeter Position for		
Configuration	Ave	Max	Min	Reference	Ave	Max	Min
1M06M1Z	1.47E-01	2.65E-01	4.33E-02	1.50E-01	952	1052	812
1M06S1Z	1.49E-02	3.26E-02	8.03E-03	1.07E-02	1012	922	1092
1M06V1Z	5.66E-02	1.29E-01	2.45E-02	4.43E-02	862	1072	1092
1M15M1Z	1.08E-01	1.54E-01	4.70E-02	1.13E-01	1122	1052	812
1M15S1Z	3.47E-02	5.98E-02	1.07E-02	3.79E-02	812	962	1092
1M15V1Z	1.05E-01	2.47E-01	2.89E-02	7.00E-02	1072	862	1092
1M30M1Z	8.21E-02	2.79E-01	4.41E-02	7.28E-02	992	872	812
1M30S1Z	4.51E-02	1.34E-01	9.23E-03	2.20E-02	902	972	1092
1M30V1Z	8.74E-02	2.78E-01	2.96E-02	7.23E-02	1022	872	1092
1M45M1Z	6.58E-02	2.26E-01	3.69E-02	4.84E-02	882	922	812
1M45S1Z	4.09E-02	9.13E-02	9.12E-03	6.39E-02	962	972	1092
1M45V1Z	8.75E-02	2.26E-01	2.51E-02	4.85E-02	842	922	1092
1M60M1Z	5.33E-02	1.73E-01	2.75E-02	3.70E-02	962	922	1112
1M60S1Z	2.87E-02	7.66E-02	9.01E-03	4.70E-02	1122	912	1092
1M60V1Z	7.24E-02	1.76E-01	2.04E-02	5.18E-02	1042	922	1092
1M75M1Z	4.36E-02	1.39E-01	1.99E-02	2.91E-02	932	922	1102
1M75S1Z	2.26E-02	6.54E-02	9.11E-03	2.75E-02	1072	912	1102
1M75V1Z	5.87E-02	1.36E-01	1.81E-02	5.48E-02	1042	922	1102
1M90M1Z	3.51E-02	1.08E-01	1.56E-02	2.27E-02	1022	922	1102
1M90S1Z	1.90E-02	6.14E-02	7.54E-03	1.72E-02	1012	922	1092
1M90V1Z	4.74E-02	1.07E-01	1.44E-02	5.07E-02	832	922	1102
1M05M1Z	2.93E-02	8.94E-02	1.32E-02	1.87E-02	862	922	1102
1M05S1Z	1.68E-02	6.12E-02	6.60E-03	1.21E-02	1072	922	1092
1M05V1Z	4.02E-02	9.05E-02	1.27E-02	4.63E-02	1042	922	1102
1M20M1Z	2.50E-02	7.46E-02	1.14E-02	1.56E-02	862	922	1102
1M20S1Z	1.48E-02	5.78E-02	6.06E-03	9.57E-03	822	922	1092
1M20V1Z	3.30E-02	7.46E-02	1.13E-02	4.14E-02	962	922	1102
1M35M1Z	2.22E-02	6.65E-02	1.04E-02	1.36E-02	982	922	1092
1M35S1Z	1.32E-02	5.43E-02	5.41E-03	7.83E-03	1072	922	992
1M35V1Z	2.83E-02	6.36E-02	1.00E-02	3.77E-02	962	972	1102
1M50M1Z	2.09E-02	6.10E-02	9.27E-03	1.25E-02	832	922	1102
1M50S1Z	1.28E-02	5.24E-02	5.06E-03	6.96E-03	862	922	892

1M50V1Z	2.68E-02	6.16E-02	9.52E-03	3.64E-02	802	922	1102
1S06M1Z	2.17E-02	4.57E-02	1.13E-02	1.81E-02	992	882	1102
1S06S1Z	1.23E-01	2.62E-01	2.96E-02	1.13E-01	1042	1072	802
1S06V1Z	9.08E-02	1.77E-01	3.72E-02	6.84E-02	942	1032	1112
1S15M1Z	4.64E-02	1.00E-01	1.41E-02	3.15E-02	872	942	1112
1S15S1Z	7.78E-02	1.58E-01	2.42E-02	7.58E-02	952	1072	802
1S15V1Z	1.25E-01	3.29E-01	3.93E-02	8.66E-02	932	832	1112
1S30M1Z	6.04E-02	1.61E-01	1.44E-02	4.44E-02	962	932	1112
1S30S1Z	4.90E-02	2.09E-01	1.75E-02	3.86E-02	912	872	802
1S30V1Z	1.24E-01	3.34E-01	3.38E-02	7.27E-02	902	882	1112
1S45M1Z	4.78E-02	9.88E-02	1.12E-02	7.94E-02	862	892	1112
1S45S1Z	3.56E-02	1.60E-01	1.28E-02	2.39E-02	862	872	802
1S45V1Z	1.06E-01	2.59E-01	2.96E-02	7.07E-02	862	882	1112
1S60M1Z	3.53E-02	9.63E-02	1.18E-02	5.20E-02	852	892	1112
1S60S1Z	2.69E-02	1.37E-01	1.05E-02	1.60E-02	862	922	802
1S60V1Z	8.37E-02	1.93E-01	2.35E-02	7.93E-02	842	882	1102
1S75M1Z	2.89E-02	8.11E-02	1.19E-02	3.17E-02	1032	892	1102
1S75S1Z	2.14E-02	1.11E-01	8.42E-03	1.22E-02	1012	922	802
1S75V1Z	6.62E-02	1.50E-01	1.93E-02	7.31E-02	932	872	1102
1S90M1Z	2.48E-02	8.28E-02	1.01E-02	1.99E-02	902	882	1112
1S90S1Z	1.68E-02	8.78E-02	6.81E-03	9.92E-03	1012	922	842
1S90V1Z	5.26E-02	1.16E-01	1.61E-02	6.38E-02	872	882	1092
1S05M1Z	2.17E-02	7.91E-02	9.06E-03	1.41E-02	1032	882	1102
1S05S1Z	1.41E-02	7.10E-02	6.04E-03	7.86E-03	1012	922	892
1S05V1Z	4.14E-02	9.33E-02	1.36E-02	5.58E-02	1052	882	1102
1S20M1Z	1.91E-02	7.01E-02	7.84E-03	1.18E-02	1032	882	1112
1S20S1Z	1.19E-02	5.96E-02	4.66E-03	6.31E-03	1062	922	802
1S20V1Z	3.38E-02	7.77E-02	1.11E-02	4.78E-02	1072	882	1102
1S35M1Z	1.67E-02	6.20E-02	7.92E-03	1.08E-02	842	882	1112
1S35S1Z	1.03E-02	4.98E-02	4.11E-03	5.27E-03	912	922	842
1S35V1Z	2.85E-02	6.62E-02	9.75E-03	4.06E-02	982	882	1102
1S50M1Z	1.57E-02	5.96E-02	7.58E-03	9.71E-03	1032	882	1102
1S50S1Z	9.60E-03	4.65E-02	4.20E-03	5.32E-03	1062	922	892
1S50V1Z	2.67E-02	6.39E-02	9.50E-03	3.79E-02	822	932	1102
1V06M1Z	7.28E-02	2.63E-01	2.55E-02	4.27E-02	992	982	1112
1V06S1Z	7.08E-02	2.59E-01	2.27E-02	3.93E-02	1012	1022	1092
1V06V1Z	5.50E-01	9.09E-01	1.87E-01	7.36E-01	902	1002	1122

1V15M1Z	9.25E-02	2.22E-01	2.69E-02	5.51E-02	1032	842	1112
1V15S1Z	8.84E-02	2.19E-01	2.29E-02	5.23E-02	1072	862	1092
1V15V1Z	3.66E-01	5.61E-01	1.27E-01	5.00E-01	922	1002	1122
1V30M1Z	7.48E-02	2.65E-01	2.51E-02	5.56E-02	982	832	1112
1V30S1Z	6.92E-02	2.63E-01	2.11E-02	4.81E-02	1022	872	1092
1V30V1Z	1.75E-01	3.08E-01	6.72E-02	2.95E-01	862	1002	1112
1V45M1Z	5.81E-02	2.19E-01	2.14E-02	3.51E-02	982	882	1112
1V45S1Z	5.16E-02	2.15E-01	1.75E-02	2.71E-02	1022	922	1092
1V45V1Z	1.08E-01	1.94E-01	4.21E-02	1.91E-01	872	1002	1092
1V60M1Z	4.55E-02	1.70E-01	1.90E-02	2.87E-02	982	882	1112
1V60S1Z	3.84E-02	1.67E-01	1.32E-02	2.06E-02	1072	922	1092
1V60V1Z	7.86E-02	1.35E-01	2.93E-02	1.34E-01	852	1002	1102
1V75M1Z	3.64E-02	1.34E-01	1.58E-02	2.37E-02	1032	882	1102
1V75S1Z	2.94E-02	1.30E-01	1.08E-02	1.60E-02	1072	922	1092
1V75V1Z	6.03E-02	1.03E-01	2.22E-02	9.87E-02	972	922	1102
1V90M1Z	2.94E-02	1.07E-01	1.38E-02	1.96E-02	1032	882	1112
1V90S1Z	2.27E-02	1.02E-01	7.95E-03	1.26E-02	862	922	802
1V90V1Z	4.75E-02	8.87E-02	1.70E-02	7.45E-02	1042	922	1102
1V05M1Z	2.50E-02	8.81E-02	1.18E-02	1.61E-02	972	882	1102
1V05S1Z	1.86E-02	8.60E-02	6.80E-03	1.09E-02	1122	922	892
1V05V1Z	3.91E-02	7.38E-02	1.41E-02	5.94E-02	1062	882	1102
1V20M1Z	2.21E-02	7.39E-02	1.08E-02	1.37E-02	872	882	1092
1V20S1Z	1.52E-02	7.00E-02	5.84E-03	8.56E-03	1122	922	802
1V20V1Z	3.31E-02	6.32E-02	1.20E-02	4.93E-02	1062	922	1092
1V35M1Z	1.96E-02	6.44E-02	9.11E-03	1.17E-02	1032	882	1112
1V35S1Z	1.30E-02	6.15E-02	4.73E-03	7.59E-03	1122	922	802
1V35V1Z	2.86E-02	5.46E-02	1.06E-02	4.19E-02	812	922	1102
1V50M1Z	1.83E-02	5.93E-02	8.06E-03	1.09E-02	942	882	1102
1V50S1Z	1.19E-02	5.65E-02	4.61E-03	6.89E-03	1122	922	802
1V50V1Z	2.64E-02	5.11E-02	9.62E-03	3.91E-02	832	882	1102

Table D-4: Summary Phantom Dosimeter Tally Plane using ANSI 1977 at 3 Ft

	Tally Total (mrem/hr/kg)				Dosimeter Position for		
Configuration	Ave	Max	Min	Reference	Ave	Max	Min
1M06M3Z	3.40E-02	4.41E-02	2.53E-02	3.06E-02	662	582	412
1M06S3Z	1.51E-02	2.42E-02	1.05E-02	1.27E-02	662	622	402
1M06V3Z	2.71E-02	3.98E-02	1.85E-02	2.30E-02	662	672	402
1M15M3Z	2.84E-02	3.69E-02	2.15E-02	2.65E-02	642	572	412
1M15S3Z	1.49E-02	2.32E-02	1.12E-02	1.26E-02	532	572	402
1M15V3Z	2.36E-02	3.47E-02	1.73E-02	2.00E-02	612	722	402
1M30M3Z	2.22E-02	2.81E-02	1.86E-02	1.95E-02	562	522	402
1M30S3Z	1.58E-02	4.45E-02	9.47E-03	1.18E-02	582	422	692
1M30V3Z	2.08E-02	4.20E-02	1.56E-02	1.67E-02	532	402	692
1M45M3Z	1.87E-02	2.43E-02	1.50E-02	1.63E-02	512	572	702
1M45S3Z	2.17E-02	4.36E-02	9.49E-03	1.53E-02	522	432	702
1M45V3Z	2.47E-02	6.39E-02	1.37E-02	1.48E-02	622	432	702
1M60M3Z	1.62E-02	2.10E-02	1.28E-02	1.40E-02	512	472	702
1M60S3Z	2.52E-02	4.04E-02	8.51E-03	3.04E-02	612	432	692
1M60V3Z	2.46E-02	5.58E-02	1.12E-02	1.37E-02	572	432	702
1M75M3Z	1.49E-02	3.55E-02	1.08E-02	1.20E-02	462	472	702
1M75S3Z	2.21E-02	3.03E-02	8.18E-03	2.66E-02	672	512	702
1M75V3Z	2.27E-02	4.89E-02	9.63E-03	1.81E-02	482	472	702
1M90M3Z	1.36E-02	4.26E-02	9.28E-03	1.03E-02	672	472	702
1M90S3Z	1.84E-02	3.80E-02	7.47E-03	1.88E-02	552	572	702
1M90V3Z	1.99E-02	4.69E-02	8.39E-03	1.81E-02	562	472	692
1M05M3Z	1.28E-02	4.10E-02	8.58E-03	9.73E-03	622	472	702
1M05S3Z	1.67E-02	3.39E-02	6.58E-03	9.31E-03	492	522	692
1M05V3Z	1.77E-02	4.26E-02	7.76E-03	1.59E-02	402	472	692
1M20M3Z	1.18E-02	3.80E-02	7.90E-03	9.04E-03	622	472	692
1M20S3Z	1.55E-02	3.16E-02	5.50E-03	7.74E-03	562	432	702
1M20V3Z	1.72E-02	3.77E-02	6.86E-03	1.43E-02	442	472	702
1M35M3Z	1.13E-02	3.46E-02	6.87E-03	8.39E-03	632	472	702
1M35S3Z	1.44E-02	2.94E-02	4.98E-03	9.02E-03	542	482	702
1M35V3Z	1.66E-02	3.54E-02	6.50E-03	1.27E-02	412	522	702
1M50M3Z	1.09E-02	3.41E-02	6.53E-03	8.19E-03	622	472	702

Configuration	Tally Total (mrem/hr/kg)				Dosimeter Position for		
	Ave	Max	Min	Reference	Ave	Max	Min
1M50S3Z	1.41E-02	2.82E-02	4.50E-03	1.05E-02	412	482	702
1M50V3Z	1.64E-02	3.52E-02	6.27E-03	1.24E-02	502	522	702
1S06M3Z	1.76E-02	2.67E-02	1.35E-02	1.46E-02	492	682	412
1S06S3Z	2.97E-02	4.05E-02	2.08E-02	2.61E-02	432	622	412
1S06V3Z	2.76E-02	3.87E-02	2.08E-02	2.55E-02	542	582	412
1S15M3Z	1.72E-02	2.55E-02	1.27E-02	1.46E-02	492	482	712
1S15S3Z	2.26E-02	3.11E-02	1.55E-02	1.96E-02	712	522	402
1S15V3Z	2.34E-02	3.03E-02	1.84E-02	1.98E-02	542	682	412
1S30M3Z	1.86E-02	2.87E-02	1.24E-02	1.49E-02	442	522	712
1S30S3Z	1.64E-02	2.35E-02	1.25E-02	1.46E-02	482	622	412
1S30V3Z	2.48E-02	6.05E-02	1.60E-02	1.77E-02	482	422	712
1S45M3Z	3.14E-02	5.31E-02	1.17E-02	3.71E-02	652	522	712
1S45S3Z	1.31E-02	1.94E-02	1.02E-02	1.17E-02	632	622	492
1S45V3Z	2.72E-02	5.92E-02	1.29E-02	1.57E-02	492	472	702
1S60M3Z	3.25E-02	4.41E-02	1.11E-02	3.65E-02	672	572	712
1S60S3Z	1.09E-02	1.70E-02	7.97E-03	9.83E-03	512	472	442
1S60V3Z	2.56E-02	6.12E-02	1.06E-02	1.55E-02	522	432	702
1S75M3Z	2.47E-02	4.73E-02	9.40E-03	2.98E-02	652	432	702
1S75S3Z	9.92E-03	2.68E-02	6.76E-03	8.71E-03	462	472	402
1S75V3Z	2.28E-02	5.61E-02	9.62E-03	1.62E-02	472	432	702
1S90M3Z	2.14E-02	4.31E-02	8.83E-03	1.36E-02	642	432	712
1S90S3Z	8.84E-03	3.12E-02	5.89E-03	8.13E-03	562	472	492
1S90V3Z	2.13E-02	4.77E-02	8.42E-03	1.40E-02	542	432	702
1S05M3Z	1.95E-02	3.99E-02	7.31E-03	9.81E-03	592	482	702
1S05S3Z	8.26E-03	2.96E-02	5.17E-03	6.27E-03	422	472	442
1S05V3Z	2.00E-02	4.23E-02	7.84E-03	1.23E-02	542	482	712
1S20M3Z	1.76E-02	3.48E-02	6.70E-03	9.85E-03	562	482	702
1S20S3Z	7.54E-03	2.68E-02	4.78E-03	5.80E-03	532	472	492
1S20V3Z	1.85E-02	4.01E-02	6.92E-03	1.12E-02	542	482	702
1S35M3Z	1.60E-02	3.21E-02	6.03E-03	1.43E-02	552	522	702
1S35S3Z	6.97E-03	2.60E-02	4.09E-03	5.22E-03	512	472	402
1S35V3Z	1.71E-02	3.54E-02	6.08E-03	1.03E-02	452	432	702
1S50M3Z	1.53E-02	3.13E-02	5.47E-03	1.60E-02	442	472	702
1S50S3Z	6.57E-03	2.51E-02	3.91E-03	4.85E-03	722	472	642

Configuration	Tally Total (mrem/hr/kg)				Dosimeter Position for		
	Ave	Max	Min	Reference	Ave	Max	Min
1S50V3Z	1.65E-02	3.38E-02	5.41E-03	8.86E-03	612	432	702
1V06M3Z	8.03E-02	1.24E-01	3.14E-02	7.67E-02	442	582	702
1V06S3Z	7.87E-02	1.21E-01	3.02E-02	7.57E-02	462	622	692
1V06V3Z	9.86E-02	1.31E-01	4.17E-02	9.79E-02	492	582	702
1V15M3Z	4.27E-02	1.05E-01	1.94E-02	2.60E-02	682	582	422
1V15S3Z	4.06E-02	1.02E-01	1.79E-02	2.49E-02	722	622	442
1V15V3Z	8.08E-02	1.10E-01	2.56E-02	8.11E-02	642	622	692
1V30M3Z	2.40E-02	5.11E-02	1.53E-02	1.75E-02	622	482	662
1V30S3Z	2.15E-02	4.92E-02	1.39E-02	1.49E-02	722	522	692
1V30V3Z	6.34E-02	8.89E-02	1.89E-02	6.30E-02	422	572	702
1V45M3Z	2.45E-02	6.28E-02	1.31E-02	1.52E-02	482	472	702
1V45S3Z	2.18E-02	5.59E-02	1.17E-02	1.24E-02	522	432	702
1V45V3Z	5.13E-02	7.24E-02	1.51E-02	5.19E-02	422	522	702
1V60M3Z	2.49E-02	5.66E-02	1.21E-02	1.33E-02	482	472	652
1V60S3Z	2.20E-02	5.15E-02	9.39E-03	1.14E-02	572	432	702
1V60V3Z	4.10E-02	5.57E-02	1.28E-02	4.36E-02	602	572	702
1V75M3Z	2.31E-02	4.73E-02	9.86E-03	1.83E-02	522	472	702
1V75S3Z	2.04E-02	4.36E-02	8.37E-03	1.66E-02	482	432	642
1V75V3Z	3.21E-02	3.94E-02	1.10E-02	3.72E-02	582	512	702
1V90M3Z	2.02E-02	4.68E-02	9.35E-03	1.78E-02	542	432	702
1V90S3Z	1.78E-02	4.50E-02	7.48E-03	1.61E-02	562	472	702
1V90V3Z	2.60E-02	3.29E-02	1.02E-02	3.14E-02	662	422	702
1V05M3Z	1.75E-02	4.22E-02	8.33E-03	1.60E-02	512	432	712
1V05S3Z	1.52E-02	3.90E-02	6.57E-03	1.38E-02	492	472	702
1V05V3Z	2.19E-02	2.89E-02	8.93E-03	2.70E-02	522	512	702
1V20M3Z	1.54E-02	3.95E-02	7.28E-03	1.31E-02	462	432	702
1V20S3Z	1.32E-02	3.51E-02	5.78E-03	1.18E-02	442	472	702
1V20V3Z	1.88E-02	2.54E-02	8.03E-03	2.38E-02	642	462	702
1V35M3Z	1.36E-02	3.53E-02	6.16E-03	1.10E-02	412	482	702
1V35S3Z	1.16E-02	3.26E-02	5.26E-03	9.93E-03	412	472	702
1V35V3Z	1.66E-02	2.29E-02	6.57E-03	2.16E-02	642	512	702
1V50M3Z	1.26E-02	3.41E-02	5.83E-03	1.01E-02	412	482	712
1V50S3Z	1.09E-02	3.17E-02	4.69E-03	8.72E-03	622	472	702
1V50V3Z	1.55E-02	2.15E-02	6.48E-03	2.04E-02	652	512	692

Table H-5: Summary Phantom Dosimeter Tally Plane using ANSI 1991 at 3 Ft

	Tally Total (mrem/hr/kg)				Dosimeter Position for		
Configuration	Ave	Max	Min	Reference	Max	Min	Ave
1M06M3A	1.74E-02	2.29E-02	1.28E-02	1.58E-02	262	182	12
1M06S3A	6.98E-03	1.15E-02	4.99E-03	5.75E-03	162	222	142
1M06V3A	1.32E-02	2.01E-02	9.10E-03	1.12E-02	312	222	2
1M15M3A	1.38E-02	1.77E-02	1.07E-02	1.27E-02	242	82	12
1M15S3A	7.24E-03	1.13E-02	5.45E-03	6.10E-03	282	222	2
1M15V3A	1.18E-02	1.73E-02	8.81E-03	1.00E-02	162	322	2
1M30M3A	1.06E-02	1.36E-02	8.70E-03	9.68E-03	162	122	12
1M30S3A	7.82E-03	2.40E-02	4.60E-03	5.74E-03	182	22	292
1M30V3A	1.04E-02	2.27E-02	7.65E-03	8.19E-03	82	2	292
1M45M3A	8.73E-03	1.16E-02	7.02E-03	7.59E-03	92	172	302
1M45S3A	1.13E-02	2.35E-02	4.56E-03	7.76E-03	122	32	302
1M45V3A	1.26E-02	3.44E-02	6.70E-03	7.18E-03	222	32	302
1M60M3A	7.46E-03	9.93E-03	5.50E-03	6.57E-03	142	72	302
1M60S3A	1.32E-02	2.16E-02	4.07E-03	1.62E-02	252	32	292
1M60V3A	1.26E-02	2.94E-02	5.45E-03	6.67E-03	172	32	302
1M75M3A	6.76E-03	1.77E-02	4.87E-03	5.66E-03	62	72	302
1M75S3A	1.16E-02	1.61E-02	3.88E-03	1.42E-02	272	112	302
1M75V3A	1.16E-02	2.56E-02	4.63E-03	9.11E-03	82	72	302
1M90M3A	6.30E-03	2.22E-02	4.04E-03	4.55E-03	232	72	302
1M90S3A	9.49E-03	2.00E-02	3.49E-03	9.90E-03	152	172	302
1M90V3A	1.01E-02	2.47E-02	3.99E-03	9.14E-03	162	72	292
1M05M3A	5.89E-03	2.17E-02	3.73E-03	4.41E-03	222	72	302
1M05S3A	8.63E-03	1.79E-02	3.05E-03	4.55E-03	92	122	292
1M05V3A	8.98E-03	2.23E-02	3.75E-03	8.12E-03	2	72	292
1M20M3A	5.44E-03	1.94E-02	3.36E-03	3.94E-03	182	72	292
1M20S3A	7.92E-03	1.66E-02	2.56E-03	3.67E-03	162	32	302
1M20V3A	8.76E-03	1.97E-02	3.27E-03	7.18E-03	42	72	302
1M35M3A	5.14E-03	1.76E-02	2.98E-03	3.67E-03	132	72	302
1M35S3A	7.37E-03	1.53E-02	2.37E-03	4.47E-03	142	82	302
1M35V3A	8.39E-03	1.83E-02	3.12E-03	6.37E-03	12	122	292
1M50M3A	5.00E-03	1.69E-02	2.70E-03	3.57E-03	222	72	302
1M50S3A	6.89E-03	1.41E-02	2.24E-03	5.25E-03	12	122	292

	Tally Total (mrem/hr/kg)				Dosimeter Position for		
Configuration	Ave	Max	Min	Reference	Max	Min	Ave
1M50V3A	7.95E-03	1.77E-02	2.67E-03	5.63E-03	162	122	302
1S06M3A	8.65E-03	1.33E-02	6.56E-03	6.99E-03	92	282	12
1S06S3A	1.49E-02	1.99E-02	1.04E-02	1.31E-02	312	272	12
1S06V3A	1.35E-02	1.89E-02	9.97E-03	1.22E-02	142	132	22
1S15M3A	7.95E-03	1.25E-02	6.00E-03	6.83E-03	192	82	262
1S15S3A	1.16E-02	1.59E-02	8.05E-03	1.01E-02	262	222	2
1S15V3A	1.18E-02	1.55E-02	9.16E-03	1.01E-02	142	182	22
1S30M3A	8.73E-03	1.48E-02	5.42E-03	6.63E-03	112	122	312
1S30S3A	8.20E-03	1.17E-02	6.24E-03	7.37E-03	262	122	12
1S30V3A	1.26E-02	3.23E-02	7.86E-03	8.85E-03	122	22	312
1S45M3A	1.58E-02	2.74E-02	5.24E-03	1.96E-02	252	122	312
1S45S3A	6.42E-03	9.60E-03	4.96E-03	5.87E-03	112	222	92
1S45V3A	1.39E-02	3.11E-02	6.28E-03	7.81E-03	92	72	302
1S60M3A	1.65E-02	2.22E-02	4.81E-03	1.88E-02	182	172	312
1S60S3A	5.27E-03	8.47E-03	3.69E-03	4.87E-03	312	72	42
1S60V3A	1.26E-02	3.26E-02	4.96E-03	6.88E-03	112	32	292
1S75M3A	1.23E-02	2.46E-02	4.23E-03	1.52E-02	252	82	302
1S75S3A	4.75E-03	1.39E-02	3.16E-03	4.22E-03	62	72	2
1S75V3A	1.12E-02	2.89E-02	4.39E-03	7.34E-03	112	32	312
1S90M3A	1.05E-02	2.19E-02	3.64E-03	6.22E-03	242	132	312
1S90S3A	4.24E-03	1.64E-02	2.71E-03	3.99E-03	62	72	92
1S90V3A	1.06E-02	2.45E-02	3.49E-03	6.80E-03	142	32	302
1S05M3A	9.51E-03	1.98E-02	3.14E-03	4.45E-03	2	82	302
1S05S3A	3.94E-03	1.56E-02	2.36E-03	3.01E-03	22	72	42
1S05V3A	1.03E-02	2.21E-02	3.74E-03	6.07E-03	142	82	292
1S20M3A	8.63E-03	1.76E-02	2.84E-03	4.73E-03	162	82	312
1S20S3A	3.58E-03	1.40E-02	2.17E-03	2.73E-03	62	72	92
1S20V3A	9.48E-03	2.08E-02	3.31E-03	5.44E-03	142	82	302
1S35M3A	7.86E-03	1.62E-02	2.54E-03	6.96E-03	152	122	302
1S35S3A	3.32E-03	1.33E-02	1.87E-03	2.40E-03	112	72	92
1S35V3A	8.75E-03	1.84E-02	2.87E-03	4.98E-03	162	32	302
1S50M3A	7.49E-03	1.59E-02	2.22E-03	7.94E-03	42	72	302
1S50S3A	2.82E-03	1.21E-02	1.53E-03	1.61E-03	62	72	92
1S50V3A	8.15E-03	1.72E-02	2.41E-03	4.00E-03	212	32	302

	Tally Total (mrem/hr/kg)				Dosimeter Position for		
Configuration	Ave	Max	Min	Reference	Max	Min	Ave
1V06M3A	4.32E-02	6.75E-02	1.61E-02	4.16E-02	42	182	302
1V06S3A	4.20E-02	6.53E-02	1.52E-02	4.06E-02	252	272	292
1V06V3A	5.26E-02	7.06E-02	2.11E-02	5.26E-02	252	232	302
1V15M3A	2.17E-02	5.58E-02	8.75E-03	1.29E-02	282	182	312
1V15S3A	2.14E-02	5.56E-02	8.80E-03	1.27E-02	322	222	242
1V15V3A	4.30E-02	5.88E-02	1.20E-02	4.33E-02	62	222	302
1V30M3A	1.14E-02	2.61E-02	7.16E-03	8.11E-03	72	182	302
1V30S3A	1.09E-02	2.61E-02	6.77E-03	7.36E-03	322	122	292
1V30V3A	3.33E-02	4.65E-02	8.67E-03	3.37E-02	2	172	302
1V45M3A	1.19E-02	3.21E-02	5.89E-03	6.96E-03	32	72	302
1V45S3A	1.12E-02	3.00E-02	5.73E-03	6.09E-03	72	32	242
1V45V3A	2.68E-02	3.77E-02	7.17E-03	2.73E-02	52	122	302
1V60M3A	1.22E-02	3.02E-02	5.34E-03	6.19E-03	132	72	252
1V60S3A	1.13E-02	2.76E-02	4.60E-03	5.55E-03	172	32	302
1V60V3A	2.12E-02	2.86E-02	5.78E-03	2.28E-02	202	172	302
1V75M3A	1.13E-02	2.44E-02	4.42E-03	8.86E-03	122	72	302
1V75S3A	1.05E-02	2.31E-02	4.03E-03	8.48E-03	82	32	302
1V75V3A	1.63E-02	2.04E-02	5.04E-03	1.91E-02	262	112	302
1V90M3A	9.80E-03	2.45E-02	4.09E-03	8.91E-03	142	32	292
1V90S3A	9.11E-03	2.39E-02	3.55E-03	8.31E-03	162	72	292
1V90V3A	1.30E-02	1.74E-02	4.30E-03	1.61E-02	82	62	302
1V05M3A	8.45E-03	2.18E-02	3.54E-03	7.63E-03	22	32	302
1V05S3A	7.77E-03	2.06E-02	3.11E-03	7.08E-03	92	72	302
1V05V3A	1.08E-02	1.50E-02	3.74E-03	1.38E-02	72	112	302
1V20M3A	7.39E-03	2.04E-02	3.08E-03	6.51E-03	62	32	302
1V20S3A	6.68E-03	1.84E-02	2.75E-03	5.95E-03	152	72	302
1V20V3A	9.27E-03	1.30E-02	3.47E-03	1.20E-02	12	92	292
1V35M3A	6.52E-03	1.80E-02	2.78E-03	5.27E-03	12	82	302
1V35S3A	5.85E-03	1.71E-02	2.53E-03	4.86E-03	12	72	302
1V35V3A	8.11E-03	1.15E-02	2.95E-03	1.11E-02	252	92	302
1V50M3A	6.02E-03	1.71E-02	2.70E-03	4.81E-03	12	82	312
1V50S3A	5.16E-03	1.61E-02	1.93E-03	4.07E-03	12	72	302
1V50V3A	7.52E-03	1.12E-02	2.81E-03	1.03E-02	252	112	312

Table H-6: Summary Phantom Dosimeter Tally Plane using ICRP-74 at 3 Ft

	Tally Total (mrem/hr/kg)				Dosimeter Position for		
Configuration	Ave	Max	Min	Reference	Ave	Max	Min
1M06M3Z	3.26E-02	4.25E-02	2.41E-02	2.95E-02	1062	982	812
1M06S3Z	1.42E-02	2.28E-02	9.79E-03	1.18E-02	1112	1022	802
1M06V3Z	2.58E-02	3.81E-02	1.75E-02	2.20E-02	1112	1072	802
1M15M3Z	2.71E-02	3.48E-02	2.04E-02	2.53E-02	1042	972	812
1M15S3Z	1.39E-02	2.17E-02	1.04E-02	1.18E-02	932	972	802
1M15V3Z	2.24E-02	3.27E-02	1.65E-02	1.90E-02	1012	1122	802
1M30M3Z	2.11E-02	2.66E-02	1.76E-02	1.86E-02	962	922	802
1M30S3Z	1.48E-02	4.33E-02	8.90E-03	1.10E-02	982	822	1092
1M30V3Z	1.97E-02	4.09E-02	1.46E-02	1.57E-02	932	802	1092
1M45M3Z	1.77E-02	2.28E-02	1.42E-02	1.54E-02	892	972	1102
1M45S3Z	2.09E-02	4.24E-02	8.83E-03	1.45E-02	922	832	1102
1M45V3Z	2.35E-02	6.21E-02	1.28E-02	1.38E-02	1022	832	1102
1M60M3Z	1.52E-02	1.96E-02	1.20E-02	1.32E-02	912	872	1102
1M60S3Z	2.42E-02	3.91E-02	7.89E-03	2.95E-02	1052	832	1092
1M60V3Z	2.34E-02	5.36E-02	1.05E-02	1.28E-02	972	832	1102
1M75M3Z	1.39E-02	3.40E-02	1.01E-02	1.14E-02	862	872	1102
1M75S3Z	2.13E-02	2.93E-02	7.57E-03	2.58E-02	1072	912	1102
1M75V3Z	2.16E-02	4.69E-02	8.99E-03	1.71E-02	882	872	1102
1M90M3Z	1.27E-02	4.10E-02	8.62E-03	9.63E-03	1122	872	1102
1M90S3Z	1.76E-02	3.66E-02	6.89E-03	1.81E-02	952	972	1102
1M90V3Z	1.88E-02	4.52E-02	7.78E-03	1.71E-02	962	872	1092
1M05M3Z	1.20E-02	3.93E-02	7.94E-03	9.11E-03	1022	872	1102
1M05S3Z	1.60E-02	3.28E-02	6.02E-03	8.69E-03	892	922	1092
1M05V3Z	1.68E-02	4.08E-02	7.26E-03	1.52E-02	802	872	1092
1M20M3Z	1.11E-02	3.65E-02	7.24E-03	8.43E-03	1022	872	1092
1M20S3Z	1.47E-02	3.03E-02	5.05E-03	7.14E-03	962	832	1102
1M20V3Z	1.64E-02	3.61E-02	6.35E-03	1.35E-02	842	872	1102
1M35M3Z	1.06E-02	3.32E-02	6.33E-03	7.77E-03	912	872	1102
1M35S3Z	1.37E-02	2.80E-02	4.61E-03	8.50E-03	942	882	1102
1M35V3Z	1.57E-02	3.38E-02	6.06E-03	1.20E-02	812	922	1102
1M50M3Z	1.02E-02	3.24E-02	5.99E-03	7.66E-03	932	872	1102
1M50S3Z	1.34E-02	2.70E-02	4.21E-03	1.01E-02	812	882	1102

	Tally Total (mrem/hr/kg)				Dosimeter Position for		
Configuration	Ave	Max	Min	Reference	Ave	Max	Min
1M50V3Z	1.55E-02	3.36E-02	5.77E-03	1.16E-02	902	922	1102
1S06M3Z	1.66E-02	2.53E-02	1.26E-02	1.36E-02	892	1082	812
1S06S3Z	2.86E-02	3.90E-02	2.00E-02	2.52E-02	832	1022	812
1S06V3Z	2.64E-02	3.72E-02	1.98E-02	2.42E-02	992	982	812
1S15M3Z	1.61E-02	2.40E-02	1.18E-02	1.37E-02	892	882	1112
1S15S3Z	2.17E-02	2.98E-02	1.50E-02	1.88E-02	1112	1022	802
1S15V3Z	2.23E-02	2.91E-02	1.74E-02	1.90E-02	1122	1082	822
1S30M3Z	1.74E-02	2.72E-02	1.15E-02	1.38E-02	802	922	1112
1S30S3Z	1.55E-02	2.22E-02	1.18E-02	1.39E-02	1082	1022	812
1S30V3Z	2.36E-02	5.85E-02	1.51E-02	1.68E-02	922	822	1112
1S45M3Z	3.01E-02	5.14E-02	1.09E-02	3.60E-02	1052	922	1112
1S45S3Z	1.23E-02	1.83E-02	9.58E-03	1.12E-02	912	1022	892
1S45V3Z	2.60E-02	5.70E-02	1.21E-02	1.49E-02	892	872	1102
1S60M3Z	3.12E-02	4.18E-02	1.03E-02	3.51E-02	1072	972	1112
1S60S3Z	1.02E-02	1.61E-02	7.31E-03	9.29E-03	962	872	842
1S60V3Z	2.44E-02	5.93E-02	9.98E-03	1.46E-02	922	832	1102
1S75M3Z	2.36E-02	4.56E-02	8.77E-03	2.86E-02	1052	832	1102
1S75S3Z	9.23E-03	2.57E-02	6.21E-03	8.15E-03	862	872	802
1S75V3Z	2.17E-02	5.38E-02	8.96E-03	1.51E-02	872	832	1102
1S90M3Z	2.04E-02	4.12E-02	8.17E-03	1.27E-02	1042	832	1112
1S90S3Z	8.23E-03	3.00E-02	5.41E-03	7.66E-03	962	872	892
1S90V3Z	2.03E-02	4.59E-02	7.76E-03	1.32E-02	942	832	1102
1S05M3Z	1.86E-02	3.82E-02	6.82E-03	9.09E-03	992	882	1102
1S05S3Z	7.67E-03	2.85E-02	4.73E-03	5.86E-03	822	872	842
1S05V3Z	1.91E-02	4.06E-02	7.29E-03	1.16E-02	942	882	1092
1S20M3Z	1.67E-02	3.34E-02	6.16E-03	9.34E-03	962	882	1102
1S20S3Z	6.98E-03	2.57E-02	4.35E-03	5.38E-03	862	872	892
1S20V3Z	1.76E-02	3.83E-02	6.45E-03	1.04E-02	942	882	1102
1S35M3Z	1.52E-02	3.09E-02	5.61E-03	1.37E-02	952	922	1102
1S35S3Z	6.47E-03	2.46E-02	3.75E-03	4.78E-03	912	872	802
1S35V3Z	1.63E-02	3.39E-02	5.61E-03	9.58E-03	962	832	1102
1S50M3Z	1.45E-02	2.98E-02	5.00E-03	1.53E-02	842	872	1102
1S50S3Z	6.09E-03	2.39E-02	3.52E-03	4.31E-03	1122	872	1042
1S50V3Z	1.57E-02	3.24E-02	5.05E-03	8.28E-03	1012	832	1102

	Tally Total (mrem/hr/kg)				Dosimeter Position for		
Configuration	Ave	Max	Min	Reference	Ave	Max	Min
1V06M3Z	7.82E-02	1.21E-01	3.01E-02	7.51E-02	842	982	1102
1V06S3Z	7.68E-02	1.19E-01	2.89E-02	7.42E-02	1002	1022	1092
1V06V3Z	9.62E-02	1.28E-01	4.01E-02	9.57E-02	952	1022	1102
1V15M3Z	4.11E-02	1.02E-01	1.82E-02	2.48E-02	1082	982	822
1V15S3Z	3.93E-02	1.00E-01	1.68E-02	2.37E-02	1122	1022	1042
1V15V3Z	7.87E-02	1.07E-01	2.43E-02	7.91E-02	862	1022	1092
1V30M3Z	2.27E-02	4.92E-02	1.43E-02	1.65E-02	1022	882	1062
1V30S3Z	2.05E-02	4.76E-02	1.30E-02	1.40E-02	1122	922	1092
1V30V3Z	6.15E-02	8.61E-02	1.77E-02	6.13E-02	802	972	1102
1V45M3Z	2.32E-02	6.02E-02	1.22E-02	1.41E-02	832	872	1102
1V45S3Z	2.09E-02	5.42E-02	1.10E-02	1.16E-02	922	832	1042
1V45V3Z	4.97E-02	7.00E-02	1.41E-02	5.04E-02	852	922	1102
1V60M3Z	2.37E-02	5.47E-02	1.13E-02	1.25E-02	882	872	1052
1V60S3Z	2.10E-02	4.99E-02	8.80E-03	1.06E-02	972	832	1102
1V60V3Z	3.96E-02	5.36E-02	1.20E-02	4.23E-02	1002	972	1102
1V75M3Z	2.19E-02	4.55E-02	9.19E-03	1.74E-02	922	872	1102
1V75S3Z	1.95E-02	4.21E-02	7.83E-03	1.58E-02	882	832	1102
1V75V3Z	3.09E-02	3.81E-02	1.03E-02	3.59E-02	982	912	1102
1V90M3Z	1.92E-02	4.50E-02	8.68E-03	1.71E-02	942	832	1102
1V90S3Z	1.69E-02	4.35E-02	6.93E-03	1.54E-02	962	872	1092
1V90V3Z	2.49E-02	3.17E-02	9.37E-03	3.02E-02	1062	912	1102
1V05M3Z	1.66E-02	4.05E-02	7.73E-03	1.52E-02	912	832	1112
1V05S3Z	1.45E-02	3.76E-02	6.10E-03	1.32E-02	892	872	1102
1V05V3Z	2.09E-02	2.78E-02	8.20E-03	2.61E-02	972	912	1102
1V20M3Z	1.45E-02	3.77E-02	6.73E-03	1.24E-02	862	832	1102
1V20S3Z	1.25E-02	3.37E-02	5.35E-03	1.12E-02	952	872	1102
1V20V3Z	1.79E-02	2.44E-02	7.42E-03	2.29E-02	1052	862	1102
1V35M3Z	1.28E-02	3.37E-02	5.67E-03	1.04E-02	812	832	1102
1V35S3Z	1.10E-02	3.13E-02	4.92E-03	9.28E-03	812	872	1102
1V35V3Z	1.58E-02	2.19E-02	6.11E-03	2.09E-02	922	912	1102
1V50M3Z	1.19E-02	3.24E-02	5.38E-03	9.50E-03	812	882	1112
1V50S3Z	1.03E-02	3.04E-02	4.37E-03	8.18E-03	1022	872	1102
1V50V3Z	1.47E-02	2.06E-02	6.00E-03	1.96E-02	1052	912	1092

Appendix E: Estimated Dose Using Phantom's Dosimeter Lattice

Table E-1: Summary Whole Body Dose using ANSI 1977 at 1 Ft

	ICRP 26			ICRP 60		
Configuration	M w B	M w/oB	Female	M w B	M w/o B	Female
1M06M1A	5.14E-02	4.17E-02	3.15E-02	3.97E-02	3.64E-02	2.37E-02
1M06S1A	6.36E-03	5.16E-03	4.12E-03	4.35E-03	3.96E-03	2.57E-03
1M06V1A	2.19E-02	1.81E-02	1.33E-02	1.66E-02	1.53E-02	9.70E-03
1M15M1A	5.10E-02	4.31E-02	2.76E-02	3.78E-02	3.51E-02	1.91E-02
1M15S1A	1.06E-02	7.34E-03	7.05E-03	6.77E-03	5.70E-03	3.97E-03
1M15V1A	3.11E-02	2.68E-02	1.89E-02	2.38E-02	2.24E-02	1.41E-02
1M30M1A	3.38E-02	2.86E-02	1.85E-02	2.47E-02	2.30E-02	1.25E-02
1M30S1A	1.37E-02	9.36E-03	1.05E-02	1.06E-02	9.19E-03	8.06E-03
1M30V1A	3.45E-02	2.51E-02	2.51E-02	2.23E-02	1.91E-02	1.47E-02
1M45M1A	2.37E-02	1.91E-02	1.37E-02	1.70E-02	1.55E-02	9.04E-03
1M45S1A	1.20E-02	8.31E-03	8.98E-03	7.58E-03	6.36E-03	5.19E-03
1M45V1A	2.96E-02	1.91E-02	2.27E-02	1.79E-02	1.44E-02	1.24E-02
1M60M1A	1.78E-02	1.31E-02	1.14E-02	1.22E-02	1.06E-02	7.07E-03
1M60S1A	1.14E-02	8.59E-03	8.83E-03	7.20E-03	6.25E-03	5.13E-03
1M60V1A	2.27E-02	1.31E-02	1.73E-02	1.34E-02	1.02E-02	9.07E-03
1M75M1A	1.42E-02	9.67E-03	9.63E-03	9.49E-03	7.97E-03	5.80E-03
1M75S1A	1.02E-02	7.02E-03	8.16E-03	5.91E-03	4.87E-03	4.31E-03
1M75V1A	1.74E-02	9.71E-03	1.36E-02	1.02E-02	7.69E-03	7.25E-03
1M90M1A	1.13E-02	7.41E-03	7.86E-03	7.43E-03	6.13E-03	4.66E-03
1M90S1A	8.24E-03	5.42E-03	6.72E-03	4.46E-03	3.52E-03	3.25E-03
1M90V1A	1.39E-02	7.73E-03	1.11E-02	8.18E-03	6.13E-03	5.96E-03
1M05M1A	9.12E-03	5.72E-03	6.71E-03	5.86E-03	4.73E-03	3.93E-03
1M05S1A	7.22E-03	4.70E-03	5.76E-03	3.89E-03	3.05E-03	2.72E-03
1M05V1A	1.17E-02	6.58E-03	9.54E-03	6.72E-03	5.03E-03	5.02E-03
1M20M1A	7.70E-03	4.75E-03	5.92E-03	4.93E-03	3.95E-03	3.51E-03
1M20S1A	5.88E-03	3.70E-03	4.79E-03	3.22E-03	2.50E-03	2.35E-03
1M20V1A	1.02E-02	5.90E-03	8.39E-03	5.72E-03	4.29E-03	4.29E-03
1M35M1A	6.67E-03	4.08E-03	4.92E-03	4.30E-03	3.44E-03	2.90E-03
1M35S1A	4.92E-03	2.94E-03	3.97E-03	2.86E-03	2.20E-03	2.10E-03

Configuration	ICRP 26			ICRP 60		
	M w B	M w/oB	Female	M w B	M w/o B	Female
1M35V1A	9.05E-03	5.37E-03	7.49E-03	5.07E-03	3.84E-03	3.82E-03
1M50M1A	5.85E-03	3.40E-03	4.52E-03	3.72E-03	2.90E-03	2.66E-03
1M50S1A	4.42E-03	2.51E-03	3.63E-03	2.64E-03	2.00E-03	2.00E-03
1M50V1A	8.44E-03	4.98E-03	7.18E-03	4.70E-03	3.55E-03	3.69E-03
1S06M1A	8.28E-03	6.60E-03	5.33E-03	5.41E-03	4.85E-03	3.05E-03
1S06S1A	4.44E-02	3.60E-02	2.75E-02	3.52E-02	3.24E-02	2.17E-02
1S06V1A	2.93E-02	2.36E-02	1.84E-02	2.06E-02	1.87E-02	1.19E-02
1S15M1A	1.63E-02	1.14E-02	1.18E-02	1.06E-02	8.93E-03	7.01E-03
1S15S1A	4.35E-02	3.80E-02	2.20E-02	3.27E-02	3.09E-02	1.55E-02
1S15V1A	4.08E-02	3.44E-02	2.53E-02	2.93E-02	2.72E-02	1.69E-02
1S30M1A	1.62E-02	1.13E-02	1.18E-02	1.06E-02	8.92E-03	7.02E-03
1S30S1A	2.69E-02	2.38E-02	1.34E-02	1.98E-02	1.87E-02	8.99E-03
1S30V1A	4.21E-02	2.91E-02	3.09E-02	2.63E-02	2.20E-02	1.74E-02
1S45M1A	1.58E-02	1.17E-02	1.19E-02	9.71E-03	8.33E-03	6.57E-03
1S45S1A	1.72E-02	1.50E-02	8.79E-03	1.25E-02	1.18E-02	5.83E-03
1S45V1A	3.31E-02	1.94E-02	2.47E-02	2.02E-02	1.56E-02	1.35E-02
1S60M1A	1.47E-02	1.06E-02	1.16E-02	9.16E-03	7.80E-03	6.68E-03
1S60S1A	1.18E-02	1.02E-02	6.04E-03	8.56E-03	8.03E-03	3.96E-03
1S60V1A	2.48E-02	1.38E-02	1.94E-02	1.57E-02	1.20E-02	1.13E-02
1S75M1A	1.28E-02	8.64E-03	1.01E-02	7.25E-03	5.86E-03	5.08E-03
1S75S1A	8.41E-03	7.18E-03	4.39E-03	6.08E-03	5.67E-03	2.86E-03
1S75V1A	1.95E-02	1.08E-02	1.56E-02	1.24E-02	9.53E-03	9.31E-03
1S90M1A	1.03E-02	6.67E-03	8.28E-03	5.52E-03	4.31E-03	3.90E-03
1S90S1A	5.95E-03	4.97E-03	3.38E-03	4.29E-03	3.96E-03	2.23E-03
1S90V1A	1.58E-02	9.15E-03	1.29E-02	9.80E-03	7.58E-03	7.47E-03
1S05M1A	8.87E-03	5.76E-03	7.09E-03	4.81E-03	3.77E-03	3.38E-03
1S05S1A	4.63E-03	3.80E-03	2.73E-03	3.33E-03	3.05E-03	1.81E-03
1S05V1A	1.32E-02	7.77E-03	1.10E-02	8.06E-03	6.27E-03	6.31E-03
1S20M1A	6.87E-03	4.19E-03	5.47E-03	3.97E-03	3.08E-03	2.85E-03
1S20S1A	3.89E-03	3.18E-03	2.28E-03	2.79E-03	2.55E-03	1.51E-03
1S20V1A	1.10E-02	6.61E-03	9.17E-03	6.84E-03	5.39E-03	5.41E-03

Configuration	ICRP 26			ICRP 60		
	M w B	M w/oB	Female	M w B	M w/o B	Female
1S35M1A	5.67E-03	3.27E-03	4.48E-03	3.37E-03	2.57E-03	2.42E-03
1S35S1A	3.18E-03	2.55E-03	1.90E-03	2.27E-03	2.06E-03	1.24E-03
1S35V1A	9.25E-03	5.62E-03	7.76E-03	5.78E-03	4.57E-03	4.58E-03
1S50M1A	5.00E-03	2.80E-03	4.02E-03	2.99E-03	2.26E-03	2.22E-03
1S50S1A	2.82E-03	2.24E-03	1.85E-03	2.00E-03	1.80E-03	1.22E-03
1S50V1A	8.64E-03	5.19E-03	7.37E-03	5.39E-03	4.24E-03	4.37E-03
1V06M1A	2.35E-02	1.88E-02	1.59E-02	1.63E-02	1.47E-02	1.02E-02
1V06S1A	2.33E-02	1.89E-02	1.57E-02	1.71E-02	1.57E-02	1.10E-02
1V06V1A	1.25E-01	7.66E-02	1.05E-01	8.56E-02	6.96E-02	7.03E-02
1V15M1A	2.81E-02	2.42E-02	1.69E-02	2.06E-02	1.93E-02	1.17E-02
1V15S1A	2.70E-02	2.36E-02	1.59E-02	2.08E-02	1.97E-02	1.19E-02
1V15V1A	1.03E-01	6.82E-02	7.96E-02	7.18E-02	6.01E-02	5.28E-02
1V30M1A	3.25E-02	2.40E-02	2.31E-02	2.05E-02	1.77E-02	1.30E-02
1V30S1A	3.08E-02	2.28E-02	2.21E-02	1.99E-02	1.73E-02	1.30E-02
1V30V1A	6.53E-02	4.43E-02	5.00E-02	4.56E-02	3.86E-02	3.34E-02
1V45M1A	2.53E-02	1.73E-02	1.88E-02	1.54E-02	1.27E-02	1.02E-02
1V45S1A	2.39E-02	1.65E-02	1.76E-02	1.48E-02	1.23E-02	9.73E-03
1V45V1A	4.16E-02	2.94E-02	3.17E-02	2.93E-02	2.52E-02	2.14E-02
1V60M1A	1.76E-02	1.13E-02	1.25E-02	1.09E-02	8.78E-03	6.80E-03
1V60S1A	1.58E-02	1.01E-02	1.11E-02	9.81E-03	7.89E-03	6.05E-03
1V60V1A	2.80E-02	2.00E-02	2.12E-02	1.93E-02	1.66E-02	1.39E-02
1V75M1A	1.32E-02	8.14E-03	9.55E-03	8.20E-03	6.50E-03	5.26E-03
1V75S1A	1.18E-02	7.36E-03	8.20E-03	7.37E-03	5.89E-03	4.48E-03
1V75V1A	2.01E-02	1.44E-02	1.57E-02	1.38E-02	1.19E-02	1.02E-02
1V90M1A	1.07E-02	6.78E-03	7.53E-03	6.74E-03	5.45E-03	4.23E-03
1V90S1A	8.45E-03	5.10E-03	6.20E-03	5.23E-03	4.12E-03	3.43E-03
1V90V1A	1.49E-02	1.08E-02	1.16E-02	1.03E-02	8.91E-03	7.62E-03
1V05M1A	8.49E-03	5.31E-03	6.29E-03	5.39E-03	4.32E-03	3.63E-03
1V05S1A	6.82E-03	4.16E-03	4.98E-03	4.27E-03	3.38E-03	2.80E-03
1V05V1A	1.19E-02	8.57E-03	9.48E-03	8.08E-03	6.98E-03	6.16E-03
1V20M1A	6.93E-03	4.29E-03	5.15E-03	4.44E-03	3.56E-03	3.01E-03

Configuration	ICRP 26			ICRP 60		
	M w B	M w/oB	Female	M w B	M w/o B	Female
1V20S1A	5.40E-03	3.32E-03	3.97E-03	3.41E-03	2.72E-03	2.27E-03
1V20V1A	9.73E-03	7.06E-03	7.78E-03	6.64E-03	5.75E-03	5.08E-03
1V35M1A	5.82E-03	3.63E-03	4.36E-03	3.74E-03	3.01E-03	2.57E-03
1V35S1A	4.53E-03	2.85E-03	3.21E-03	2.86E-03	2.30E-03	1.81E-03
1V35V1A	8.29E-03	5.99E-03	6.68E-03	5.68E-03	4.91E-03	4.39E-03
1V50M1A	5.11E-03	3.07E-03	3.93E-03	3.24E-03	2.56E-03	2.30E-03
1V50S1A	4.13E-03	2.60E-03	2.96E-03	2.65E-03	2.14E-03	1.72E-03
1V50V1A	7.44E-03	5.31E-03	6.08E-03	5.06E-03	4.35E-03	3.97E-03

Table E-2: Summary Whole Body Dose using ANSI 1991 at 1 Ft

	ICRP 26			ICRP 60		
Configuration	M w B	M w/o B	Female	M w B	M w/o B	Female
1M06M1B	1.12E-01	9.07E-02	6.86E-02	8.63E-02	7.92E-02	5.17E-02
1M06S1B	1.33E-02	1.08E-02	8.64E-03	9.14E-03	8.30E-03	5.42E-03
1M06V1B	4.79E-02	3.94E-02	2.92E-02	3.62E-02	3.34E-02	2.12E-02
1M15M1B	1.11E-01	9.39E-02	5.98E-02	8.25E-02	7.69E-02	4.17E-02
1M15S1B	2.30E-02	1.61E-02	1.53E-02	1.48E-02	1.25E-02	8.65E-03
1M15V1B	6.77E-02	5.83E-02	4.11E-02	5.19E-02	4.87E-02	3.06E-02
1M30M1B	7.34E-02	6.20E-02	4.01E-02	5.39E-02	5.01E-02	2.73E-02
1M30S1B	2.98E-02	2.04E-02	2.27E-02	2.31E-02	2.00E-02	1.75E-02
1M30V1B	7.51E-02	5.47E-02	5.45E-02	4.85E-02	4.16E-02	3.20E-02
1M45M1B	5.09E-02	4.12E-02	2.97E-02	3.67E-02	3.34E-02	1.98E-02
1M45S1B	2.61E-02	1.82E-02	1.95E-02	1.66E-02	1.39E-02	1.13E-02
1M45V1B	6.44E-02	4.17E-02	4.93E-02	3.90E-02	3.14E-02	2.69E-02
1M60M1B	3.87E-02	2.83E-02	2.47E-02	2.66E-02	2.32E-02	1.55E-02
1M60S1B	2.49E-02	1.87E-02	1.92E-02	1.57E-02	1.36E-02	1.11E-02
1M60V1B	4.95E-02	2.86E-02	3.76E-02	2.93E-02	2.23E-02	1.98E-02
1M75M1B	3.03E-02	2.05E-02	2.06E-02	2.02E-02	1.70E-02	1.24E-02
1M75S1B	2.22E-02	1.53E-02	1.77E-02	1.29E-02	1.07E-02	9.38E-03
1M75V1B	3.79E-02	2.13E-02	2.96E-02	2.24E-02	1.69E-02	1.58E-02
1M90M1B	2.42E-02	1.58E-02	1.66E-02	1.60E-02	1.32E-02	9.91E-03
1M90S1B	1.80E-02	1.18E-02	1.46E-02	9.76E-03	7.71E-03	7.08E-03
1M90V1B	3.03E-02	1.70E-02	2.42E-02	1.79E-02	1.34E-02	1.30E-02
1M05M1B	1.94E-02	1.21E-02	1.42E-02	1.25E-02	1.01E-02	8.36E-03
1M05S1B	1.58E-02	1.03E-02	1.25E-02	8.52E-03	6.70E-03	5.94E-03
1M05V1B	2.55E-02	1.45E-02	2.08E-02	1.47E-02	1.11E-02	1.10E-02
1M20M1B	1.68E-02	1.04E-02	1.27E-02	1.08E-02	8.63E-03	7.44E-03
1M20S1B	1.29E-02	8.12E-03	1.05E-02	7.08E-03	5.49E-03	5.14E-03
1M20V1B	2.23E-02	1.29E-02	1.83E-02	1.26E-02	9.45E-03	9.38E-03
1M35M1B	1.43E-02	8.75E-03	1.04E-02	9.24E-03	7.39E-03	6.14E-03
1M35S1B	1.08E-02	6.49E-03	8.68E-03	6.31E-03	4.86E-03	4.59E-03

	ICRP 26			ICRP 60		
Configuration	M w B	M w/o B	Female	M w B	M w/o B	Female
1M35V1B	1.98E-02	1.18E-02	1.64E-02	1.11E-02	8.47E-03	8.37E-03
1M50M1B	1.29E-02	7.51E-03	9.92E-03	8.21E-03	6.41E-03	5.83E-03
1M50S1B	9.73E-03	5.54E-03	7.94E-03	5.80E-03	4.41E-03	4.37E-03
1M50V1B	1.85E-02	1.09E-02	1.57E-02	1.03E-02	7.81E-03	8.08E-03
1S06M1B	1.82E-02	1.45E-02	1.17E-02	1.19E-02	1.07E-02	6.74E-03
1S06S1B	9.64E-02	7.82E-02	5.94E-02	7.69E-02	7.08E-02	4.73E-02
1S06V1B	6.40E-02	5.15E-02	4.03E-02	4.50E-02	4.08E-02	2.60E-02
1S15M1B	3.50E-02	2.44E-02	2.53E-02	2.28E-02	1.93E-02	1.50E-02
1S15S1B	9.47E-02	8.27E-02	4.78E-02	7.13E-02	6.73E-02	3.38E-02
1S15V1B	8.90E-02	7.50E-02	5.51E-02	6.38E-02	5.92E-02	3.68E-02
1S30M1B	3.51E-02	2.45E-02	2.54E-02	2.28E-02	1.93E-02	1.51E-02
1S30S1B	5.88E-02	5.19E-02	2.93E-02	4.32E-02	4.09E-02	1.96E-02
1S30V1B	9.17E-02	6.34E-02	6.73E-02	5.74E-02	4.79E-02	3.78E-02
1S45M1B	3.37E-02	2.47E-02	2.58E-02	2.07E-02	1.77E-02	1.44E-02
1S45S1B	3.76E-02	3.29E-02	1.92E-02	2.74E-02	2.58E-02	1.27E-02
1S45V1B	7.22E-02	4.24E-02	5.38E-02	4.42E-02	3.42E-02	2.95E-02
1S60M1B	3.14E-02	2.26E-02	2.48E-02	1.96E-02	1.67E-02	1.44E-02
1S60S1B	2.58E-02	2.23E-02	1.32E-02	1.87E-02	1.76E-02	8.64E-03
1S60V1B	5.42E-02	3.03E-02	4.22E-02	3.42E-02	2.62E-02	2.46E-02
1S75M1B	2.75E-02	1.85E-02	2.19E-02	1.55E-02	1.25E-02	1.10E-02
1S75S1B	1.85E-02	1.58E-02	9.64E-03	1.34E-02	1.25E-02	6.27E-03
1S75V1B	4.26E-02	2.38E-02	3.40E-02	2.71E-02	2.09E-02	2.03E-02
1S90M1B	2.24E-02	1.45E-02	1.80E-02	1.20E-02	9.35E-03	8.47E-03
1S90S1B	1.31E-02	1.10E-02	7.43E-03	9.44E-03	8.71E-03	4.88E-03
1S90V1B	3.45E-02	2.00E-02	2.81E-02	2.14E-02	1.66E-02	1.63E-02
1S05M1B	1.91E-02	1.24E-02	1.48E-02	1.04E-02	8.17E-03	7.01E-03
1S05S1B	1.02E-02	8.38E-03	6.00E-03	7.33E-03	6.72E-03	3.96E-03
1S05V1B	2.87E-02	1.70E-02	2.39E-02	1.76E-02	1.37E-02	1.38E-02
1S20M1B	1.48E-02	9.02E-03	1.19E-02	8.56E-03	6.62E-03	6.22E-03
1S20S1B	8.59E-03	7.02E-03	5.02E-03	6.15E-03	5.63E-03	3.30E-03
1S20V1B	2.40E-02	1.45E-02	2.00E-02	1.50E-02	1.18E-02	1.18E-02

Configuration	ICRP 26			ICRP 60		
	M w B	M w/o B	Female	M w B	M w/o B	Female
1S35M1B	1.26E-02	7.48E-03	9.62E-03	7.59E-03	5.89E-03	5.21E-03
1S35S1B	7.04E-03	5.64E-03	4.18E-03	5.02E-03	4.55E-03	2.73E-03
1S35V1B	2.02E-02	1.23E-02	1.69E-02	1.27E-02	1.00E-02	1.00E-02
1S50M1B	1.10E-02	6.20E-03	8.82E-03	6.59E-03	4.99E-03	4.85E-03
1S50S1B	6.26E-03	4.97E-03	4.09E-03	4.42E-03	3.99E-03	2.68E-03
1S50V1B	1.89E-02	1.14E-02	1.61E-02	1.18E-02	9.31E-03	9.56E-03
1V06M1B	5.13E-02	4.10E-02	3.46E-02	3.55E-02	3.21E-02	2.22E-02
1V06S1B	5.03E-02	4.07E-02	3.44E-02	3.70E-02	3.38E-02	2.42E-02
1V06V1B	2.70E-01	1.66E-01	2.28E-01	1.86E-01	1.51E-01	1.52E-01
1V15M1B	6.11E-02	5.27E-02	3.65E-02	4.49E-02	4.21E-02	2.52E-02
1V15S1B	5.89E-02	5.13E-02	3.45E-02	4.53E-02	4.28E-02	2.58E-02
1V15V1B	2.24E-01	1.48E-01	1.72E-01	1.56E-01	1.30E-01	1.14E-01
1V30M1B	6.98E-02	5.17E-02	4.97E-02	4.42E-02	3.82E-02	2.81E-02
1V30S1B	6.69E-02	4.97E-02	4.79E-02	4.34E-02	3.76E-02	2.81E-02
1V30V1B	1.42E-01	9.63E-02	1.09E-01	9.92E-02	8.40E-02	7.25E-02
1V45M1B	5.48E-02	3.77E-02	4.07E-02	3.34E-02	2.77E-02	2.21E-02
1V45S1B	5.21E-02	3.60E-02	3.83E-02	3.22E-02	2.68E-02	2.11E-02
1V45V1B	9.07E-02	6.40E-02	6.90E-02	6.38E-02	5.49E-02	4.65E-02
1V60M1B	3.79E-02	2.43E-02	2.69E-02	2.35E-02	1.90E-02	1.47E-02
1V60S1B	3.45E-02	2.20E-02	2.42E-02	2.14E-02	1.73E-02	1.32E-02
1V60V1B	6.11E-02	4.36E-02	4.63E-02	4.21E-02	3.63E-02	3.02E-02
1V75M1B	2.84E-02	1.74E-02	2.07E-02	1.76E-02	1.40E-02	1.14E-02
1V75S1B	2.58E-02	1.62E-02	1.79E-02	1.61E-02	1.29E-02	9.76E-03
1V75V1B	4.40E-02	3.16E-02	3.42E-02	3.01E-02	2.60E-02	2.23E-02
1V90M1B	2.23E-02	1.40E-02	1.61E-02	1.41E-02	1.13E-02	9.10E-03
1V90S1B	1.85E-02	1.12E-02	1.35E-02	1.15E-02	9.05E-03	7.51E-03
1V90V1B	3.26E-02	2.36E-02	2.53E-02	2.25E-02	1.95E-02	1.66E-02
1V05M1B	1.81E-02	1.12E-02	1.34E-02	1.15E-02	9.17E-03	7.69E-03
1V05S1B	1.49E-02	9.15E-03	1.09E-02	9.37E-03	7.44E-03	6.10E-03
1V05V1B	2.60E-02	1.88E-02	2.07E-02	1.77E-02	1.53E-02	1.34E-02
1V20M1B	1.49E-02	9.21E-03	1.09E-02	9.53E-03	7.65E-03	6.36E-03

	ICRP 26			ICRP 60		
Configuration	M w B	M w/o B	Female	M w B	M w/o B	Female
1V20S1B	1.19E-02	7.33E-03	8.67E-03	7.51E-03	5.99E-03	4.96E-03
1V20V1B	2.13E-02	1.55E-02	1.70E-02	1.45E-02	1.26E-02	1.11E-02
1V35M1B	1.25E-02	7.85E-03	9.26E-03	8.09E-03	6.53E-03	5.47E-03
1V35S1B	9.98E-03	6.31E-03	7.04E-03	6.30E-03	5.08E-03	3.95E-03
1V35V1B	1.82E-02	1.31E-02	1.46E-02	1.25E-02	1.08E-02	9.60E-03
1V50M1B	1.12E-02	6.78E-03	8.61E-03	7.14E-03	5.65E-03	5.04E-03
1V50S1B	9.08E-03	5.74E-03	6.49E-03	5.83E-03	4.71E-03	3.76E-03
1V50V1B	1.63E-02	1.16E-02	1.33E-02	1.11E-02	9.54E-03	8.68E-03

Table E-3: Summary Whole Body Dose using ICRP-74 at 1 Ft

	ICRP 26			ICRP 60		
Configuration	M w B	M w/o B	Female	M w B	M w/o B	Female
1M06M1B	9.53E-02	7.73E-02	5.84E-02	7.35E-02	6.74E-02	4.39E-02
1M06S1B	1.14E-02	9.22E-03	7.39E-03	7.81E-03	7.09E-03	4.63E-03
1M06V1B	4.09E-02	3.36E-02	2.49E-02	3.08E-02	2.84E-02	1.80E-02
1M15M1B	9.47E-02	8.02E-02	5.10E-02	7.04E-02	6.55E-02	3.54E-02
1M15S1B	1.97E-02	1.38E-02	1.31E-02	1.26E-02	1.07E-02	7.37E-03
1M15V1B	5.78E-02	4.98E-02	3.51E-02	4.42E-02	4.15E-02	2.60E-02
1M30M1B	6.27E-02	5.30E-02	3.42E-02	4.60E-02	4.27E-02	2.32E-02
1M30S1B	2.54E-02	1.74E-02	1.93E-02	1.97E-02	1.70E-02	1.49E-02
1M30V1B	6.41E-02	4.67E-02	4.65E-02	4.13E-02	3.55E-02	2.72E-02
1M45M1B	4.35E-02	3.52E-02	2.54E-02	3.13E-02	2.86E-02	1.68E-02
1M45S1B	2.23E-02	1.55E-02	1.66E-02	1.42E-02	1.19E-02	9.62E-03
1M45V1B	5.49E-02	3.56E-02	4.20E-02	3.33E-02	2.68E-02	2.29E-02
1M60M1B	3.30E-02	2.42E-02	2.11E-02	2.27E-02	1.98E-02	1.32E-02
1M60S1B	2.12E-02	1.60E-02	1.63E-02	1.34E-02	1.16E-02	9.48E-03
1M60V1B	4.23E-02	2.45E-02	3.21E-02	2.50E-02	1.91E-02	1.68E-02
1M75M1B	2.59E-02	1.75E-02	1.76E-02	1.73E-02	1.45E-02	1.06E-02
1M75S1B	1.89E-02	1.31E-02	1.51E-02	1.10E-02	9.10E-03	7.99E-03
1M75V1B	3.24E-02	1.82E-02	2.53E-02	1.91E-02	1.44E-02	1.35E-02
1M90M1B	2.07E-02	1.35E-02	1.42E-02	1.36E-02	1.13E-02	8.45E-03
1M90S1B	1.53E-02	1.01E-02	1.25E-02	8.33E-03	6.58E-03	6.02E-03
1M90V1B	2.59E-02	1.45E-02	2.06E-02	1.53E-02	1.15E-02	1.11E-02
1M05M1B	1.66E-02	1.04E-02	1.21E-02	1.07E-02	8.62E-03	7.12E-03
1M05S1B	1.35E-02	8.81E-03	1.07E-02	7.28E-03	5.73E-03	5.06E-03
1M05V1B	2.18E-02	1.24E-02	1.78E-02	1.26E-02	9.47E-03	9.35E-03
1M20M1B	1.44E-02	8.92E-03	1.08E-02	9.21E-03	7.39E-03	6.36E-03
1M20S1B	1.10E-02	6.95E-03	8.91E-03	6.05E-03	4.70E-03	4.38E-03
1M20V1B	1.90E-02	1.11E-02	1.56E-02	1.07E-02	8.08E-03	8.00E-03
1M35M1B	1.23E-02	7.52E-03	8.92E-03	7.92E-03	6.33E-03	5.24E-03
1M35S1B	9.26E-03	5.56E-03	7.41E-03	5.39E-03	4.16E-03	3.92E-03

	ICRP 26			ICRP 60		
Configuration	M w B	M w/o B	Female	M w B	M w/o B	Female
1M35V1B	1.69E-02	1.01E-02	1.40E-02	9.53E-03	7.25E-03	7.14E-03
1M50M1B	1.10E-02	6.45E-03	8.47E-03	7.03E-03	5.50E-03	4.97E-03
1M50S1B	8.32E-03	4.74E-03	6.78E-03	4.96E-03	3.77E-03	3.73E-03
1M50V1B	1.58E-02	9.35E-03	1.34E-02	8.83E-03	6.67E-03	6.90E-03
1S06M1B	1.56E-02	1.24E-02	1.00E-02	1.02E-02	9.14E-03	5.76E-03
1S06S1B	8.20E-02	6.65E-02	5.05E-02	6.53E-02	6.02E-02	4.02E-02
1S06V1B	5.45E-02	4.39E-02	3.43E-02	3.83E-02	3.47E-02	2.22E-02
1S15M1B	2.98E-02	2.09E-02	2.15E-02	1.94E-02	1.64E-02	1.28E-02
1S15S1B	8.08E-02	7.06E-02	4.07E-02	6.08E-02	5.73E-02	2.87E-02
1S15V1B	7.60E-02	6.40E-02	4.70E-02	5.45E-02	5.05E-02	3.13E-02
1S30M1B	3.00E-02	2.09E-02	2.17E-02	1.95E-02	1.65E-02	1.28E-02
1S30S1B	5.02E-02	4.43E-02	2.49E-02	3.68E-02	3.49E-02	1.66E-02
1S30V1B	7.83E-02	5.42E-02	5.74E-02	4.89E-02	4.09E-02	3.22E-02
1S45M1B	2.88E-02	2.11E-02	2.20E-02	1.77E-02	1.52E-02	1.23E-02
1S45S1B	3.21E-02	2.81E-02	1.64E-02	2.34E-02	2.21E-02	1.08E-02
1S45V1B	6.17E-02	3.63E-02	4.59E-02	3.77E-02	2.93E-02	2.51E-02
1S60M1B	2.68E-02	1.93E-02	2.12E-02	1.68E-02	1.43E-02	1.23E-02
1S60S1B	2.21E-02	1.91E-02	1.13E-02	1.60E-02	1.50E-02	7.36E-03
1S60V1B	4.63E-02	2.59E-02	3.60E-02	2.92E-02	2.24E-02	2.10E-02
1S75M1B	2.35E-02	1.58E-02	1.87E-02	1.33E-02	1.07E-02	9.40E-03
1S75S1B	1.59E-02	1.35E-02	8.23E-03	1.14E-02	1.07E-02	5.34E-03
1S75V1B	3.64E-02	2.03E-02	2.90E-02	2.32E-02	1.78E-02	1.73E-02
1S90M1B	1.91E-02	1.24E-02	1.54E-02	1.02E-02	8.00E-03	7.23E-03
1S90S1B	1.13E-02	9.40E-03	6.35E-03	8.08E-03	7.46E-03	4.16E-03
1S90V1B	2.95E-02	1.71E-02	2.40E-02	1.83E-02	1.42E-02	1.39E-02
1S05M1B	1.63E-02	1.06E-02	1.27E-02	8.92E-03	7.00E-03	5.98E-03
1S05S1B	8.75E-03	7.18E-03	5.14E-03	6.27E-03	5.75E-03	3.38E-03
1S05V1B	2.46E-02	1.46E-02	2.04E-02	1.51E-02	1.18E-02	1.17E-02
1S20M1B	1.27E-02	7.72E-03	1.02E-02	7.32E-03	5.66E-03	5.31E-03
1S20S1B	7.37E-03	6.03E-03	4.29E-03	5.28E-03	4.83E-03	2.81E-03
1S20V1B	2.05E-02	1.24E-02	1.70E-02	1.28E-02	1.01E-02	1.00E-02

	ICRP 26			ICRP 60		
Configuration	M w B	M w/o B	Female	M w B	M w/o B	Female
1S35M1B	1.08E-02	6.41E-03	8.21E-03	6.50E-03	5.04E-03	4.44E-03
1S35S1B	6.04E-03	4.84E-03	3.58E-03	4.30E-03	3.90E-03	2.33E-03
1S35V1B	1.73E-02	1.05E-02	1.44E-02	1.08E-02	8.57E-03	8.52E-03
1S50M1B	9.41E-03	5.31E-03	7.54E-03	5.64E-03	4.27E-03	4.14E-03
1S50S1B	5.37E-03	4.26E-03	3.50E-03	3.79E-03	3.42E-03	2.29E-03
1S50V1B	1.62E-02	9.74E-03	1.37E-02	1.01E-02	7.96E-03	8.15E-03
1V06M1B	4.37E-02	3.50E-02	2.95E-02	3.03E-02	2.74E-02	1.89E-02
1V06S1B	4.28E-02	3.47E-02	2.92E-02	3.15E-02	2.87E-02	2.06E-02
1V06V1B	2.30E-01	1.41E-01	1.94E-01	1.58E-01	1.28E-01	1.29E-01
1V15M1B	5.22E-02	4.50E-02	3.11E-02	3.83E-02	3.59E-02	2.14E-02
1V15S1B	5.02E-02	4.38E-02	2.94E-02	3.86E-02	3.65E-02	2.19E-02
1V15V1B	1.91E-01	1.26E-01	1.47E-01	1.33E-01	1.11E-01	9.73E-02
1V30M1B	5.96E-02	4.41E-02	4.24E-02	3.77E-02	3.26E-02	2.39E-02
1V30S1B	5.71E-02	4.24E-02	4.08E-02	3.70E-02	3.21E-02	2.39E-02
1V30V1B	1.21E-01	8.22E-02	9.24E-02	8.45E-02	7.16E-02	6.17E-02
1V45M1B	4.68E-02	3.22E-02	3.46E-02	2.85E-02	2.36E-02	1.88E-02
1V45S1B	4.44E-02	3.07E-02	3.26E-02	2.74E-02	2.29E-02	1.80E-02
1V45V1B	7.73E-02	5.46E-02	5.88E-02	5.44E-02	4.68E-02	3.96E-02
1V60M1B	3.24E-02	2.08E-02	2.29E-02	2.01E-02	1.62E-02	1.25E-02
1V60S1B	2.95E-02	1.88E-02	2.06E-02	1.83E-02	1.47E-02	1.12E-02
1V60V1B	5.21E-02	3.72E-02	3.94E-02	3.59E-02	3.09E-02	2.58E-02
1V75M1B	2.43E-02	1.49E-02	1.76E-02	1.51E-02	1.20E-02	9.74E-03
1V75S1B	2.21E-02	1.38E-02	1.52E-02	1.38E-02	1.10E-02	8.31E-03
1V75V1B	3.76E-02	2.70E-02	2.92E-02	2.57E-02	2.22E-02	1.90E-02
1V90M1B	1.91E-02	1.20E-02	1.37E-02	1.21E-02	9.69E-03	7.77E-03
1V90S1B	1.58E-02	9.59E-03	1.15E-02	9.80E-03	7.73E-03	6.39E-03
1V90V1B	2.78E-02	2.02E-02	2.16E-02	1.92E-02	1.66E-02	1.41E-02
1V05M1B	1.55E-02	9.62E-03	1.14E-02	9.81E-03	7.85E-03	6.56E-03
1V05S1B	1.28E-02	7.83E-03	9.27E-03	8.00E-03	6.36E-03	5.20E-03
1V05V1B	2.22E-02	1.60E-02	1.76E-02	1.51E-02	1.30E-02	1.14E-02
1V20M1B	1.27E-02	7.90E-03	9.31E-03	8.16E-03	6.55E-03	5.43E-03

Configuration	ICRP 26			ICRP 60		
	M w B	M w/o B	Female	M w B	M w/o B	Female
1V20S1B	1.02E-02	6.28E-03	7.40E-03	6.42E-03	5.13E-03	4.23E-03
1V20V1B	1.82E-02	1.32E-02	1.45E-02	1.24E-02	1.08E-02	9.45E-03
1V35M1B	1.07E-02	6.73E-03	7.92E-03	6.93E-03	5.60E-03	4.68E-03
1V35S1B	8.53E-03	5.41E-03	6.01E-03	5.39E-03	4.35E-03	3.37E-03
1V35V1B	1.55E-02	1.12E-02	1.24E-02	1.06E-02	9.21E-03	8.18E-03
1V50M1B	9.62E-03	5.81E-03	7.36E-03	6.11E-03	4.84E-03	4.30E-03
1V50S1B	7.77E-03	4.92E-03	5.54E-03	4.98E-03	4.03E-03	3.20E-03
1V50V1B	1.39E-02	9.95E-03	1.13E-02	9.48E-03	8.15E-03	7.40E-03

Table E-4: Summary Whole Body Dose using ANSI 1977 at 3 Ft

	ICRP 26			ICRP 60		
Configuration	M w B	M w/o B	Female	M w B	M w/o B	Female
1M06M3Z	1.20E-02	9.47E-03	8.07E-03	9.39E-03	8.56E-03	6.28E-03
1M06S3Z	5.23E-03	4.22E-03	3.24E-03	3.98E-03	3.65E-03	2.40E-03
1M06V3Z	9.24E-03	7.40E-03	6.25E-03	7.20E-03	6.58E-03	4.81E-03
1M15M3Z	1.00E-02	8.01E-03	6.72E-03	7.84E-03	7.17E-03	5.21E-03
1M15S3Z	5.33E-03	4.31E-03	3.31E-03	4.05E-03	3.71E-03	2.44E-03
1M15V3Z	8.64E-03	6.92E-03	5.72E-03	6.62E-03	6.04E-03	4.28E-03
1M30M3Z	8.58E-03	7.06E-03	5.22E-03	6.51E-03	6.00E-03	3.83E-03
1M30S3Z	6.13E-03	5.14E-03	4.32E-03	4.98E-03	4.65E-03	3.53E-03
1M30V3Z	7.72E-03	6.33E-03	4.88E-03	5.85E-03	5.38E-03	3.58E-03
1M45M3Z	6.62E-03	5.31E-03	4.30E-03	4.97E-03	4.54E-03	3.12E-03
1M45S3Z	5.50E-03	3.87E-03	3.87E-03	3.71E-03	3.17E-03	2.41E-03
1M45V3Z	7.70E-03	6.53E-03	5.52E-03	6.46E-03	6.07E-03	4.72E-03
1M60M3Z	5.44E-03	4.31E-03	3.56E-03	4.16E-03	3.78E-03	2.65E-03
1M60S3Z	6.81E-03	4.89E-03	5.42E-03	4.78E-03	4.14E-03	3.67E-03
1M60V3Z	7.30E-03	6.21E-03	5.57E-03	5.63E-03	5.26E-03	4.24E-03
1M75M3Z	4.65E-03	3.71E-03	2.93E-03	3.48E-03	3.17E-03	2.10E-03
1M75S3Z	7.13E-03	4.72E-03	5.98E-03	5.24E-03	4.43E-03	4.31E-03
1M75V3Z	6.67E-03	5.56E-03	5.15E-03	4.95E-03	4.58E-03	3.73E-03
1M90M3Z	3.98E-03	3.17E-03	2.58E-03	3.01E-03	2.74E-03	1.89E-03
1M90S3Z	5.64E-03	4.10E-03	4.72E-03	4.36E-03	3.84E-03	3.62E-03
1M90V3Z	6.09E-03	4.74E-03	4.72E-03	4.41E-03	3.96E-03	3.32E-03
1M05M3Z	3.33E-03	2.58E-03	2.23E-03	2.51E-03	2.27E-03	1.64E-03
1M05S3Z	4.68E-03	3.30E-03	3.88E-03	3.64E-03	3.18E-03	3.00E-03
1M05V3Z	5.38E-03	3.87E-03	4.40E-03	3.80E-03	3.30E-03	3.02E-03
1M20M3Z	3.05E-03	2.36E-03	2.07E-03	2.30E-03	2.07E-03	1.52E-03
1M20S3Z	4.12E-03	2.60E-03	3.27E-03	3.02E-03	2.51E-03	2.34E-03
1M20V3Z	4.95E-03	3.49E-03	4.09E-03	3.48E-03	2.99E-03	2.79E-03
1M35M3Z	2.74E-03	2.11E-03	1.87E-03	2.03E-03	1.81E-03	1.33E-03
1M35S3Z	3.70E-03	2.20E-03	3.03E-03	2.50E-03	2.00E-03	1.97E-03
1M35V3Z	4.73E-03	3.22E-03	4.01E-03	3.22E-03	2.72E-03	2.65E-03

Configuration	ICRP 26			ICRP 60		
	M w B	M w/o B	Female	M w B	M w/o B	Female
1M50M3Z	2.61E-03	1.98E-03	1.85E-03	1.92E-03	1.71E-03	1.31E-03
1M50S3Z	3.71E-03	2.29E-03	3.05E-03	2.43E-03	1.96E-03	1.90E-03
1M50V3Z	4.49E-03	2.96E-03	3.90E-03	3.06E-03	2.55E-03	2.58E-03
1S06M3Z	5.76E-03	4.56E-03	3.83E-03	4.24E-03	3.84E-03	2.70E-03
1S06S3Z	1.04E-02	8.25E-03	6.91E-03	8.24E-03	7.54E-03	5.48E-03
1S06V3Z	9.21E-03	7.21E-03	6.51E-03	7.15E-03	6.49E-03	5.00E-03
1S15M3Z	5.67E-03	4.55E-03	3.83E-03	4.24E-03	3.87E-03	2.77E-03
1S15S3Z	8.50E-03	6.86E-03	5.66E-03	6.57E-03	6.02E-03	4.30E-03
1S15V3Z	8.91E-03	7.15E-03	5.79E-03	6.75E-03	6.16E-03	4.25E-03
1S30M3Z	5.82E-03	4.61E-03	4.02E-03	4.16E-03	3.76E-03	2.73E-03
1S30S3Z	6.96E-03	5.77E-03	4.18E-03	5.25E-03	4.85E-03	3.02E-03
1S30V3Z	8.94E-03	7.48E-03	6.04E-03	7.08E-03	6.59E-03	4.76E-03
1S45M3Z	8.17E-03	5.95E-03	6.43E-03	6.02E-03	5.27E-03	4.62E-03
1S45S3Z	5.38E-03	4.49E-03	3.26E-03	4.02E-03	3.72E-03	2.32E-03
1S45V3Z	8.12E-03	6.86E-03	5.96E-03	6.66E-03	6.23E-03	4.93E-03
1S60M3Z	9.01E-03	5.86E-03	7.66E-03	6.38E-03	5.33E-03	5.31E-03
1S60S3Z	4.40E-03	3.66E-03	2.63E-03	3.29E-03	3.04E-03	1.87E-03
1S60V3Z	7.47E-03	6.33E-03	5.82E-03	5.73E-03	5.35E-03	4.41E-03
1S75M3Z	7.33E-03	5.28E-03	6.01E-03	5.48E-03	4.80E-03	4.43E-03
1S75S3Z	3.52E-03	2.86E-03	2.22E-03	2.58E-03	2.36E-03	1.54E-03
1S75V3Z	6.94E-03	5.50E-03	5.61E-03	5.01E-03	4.53E-03	3.95E-03
1S90M3Z	5.68E-03	4.03E-03	4.70E-03	4.04E-03	3.48E-03	3.25E-03
1S90S3Z	3.01E-03	2.44E-03	1.95E-03	2.23E-03	2.04E-03	1.38E-03
1S90V3Z	5.95E-03	4.34E-03	4.92E-03	4.18E-03	3.65E-03	3.36E-03
1S05M3Z	4.36E-03	2.64E-03	3.63E-03	2.86E-03	2.28E-03	2.27E-03
1S05S3Z	2.44E-03	1.97E-03	1.59E-03	1.82E-03	1.66E-03	1.14E-03
1S05V3Z	5.81E-03	4.04E-03	4.72E-03	4.02E-03	3.43E-03	3.16E-03
1S20M3Z	4.26E-03	2.58E-03	3.52E-03	2.75E-03	2.20E-03	2.17E-03
1S20S3Z	2.08E-03	1.61E-03	1.51E-03	1.52E-03	1.36E-03	1.06E-03
1S20V3Z	5.39E-03	3.53E-03	4.53E-03	3.66E-03	3.04E-03	2.97E-03
1S35M3Z	4.05E-03	2.63E-03	3.53E-03	2.63E-03	2.16E-03	2.22E-03

Configuration	ICRP 26			ICRP 60		
	M w B	M w/o B	Female	M w B	M w/o B	Female
1S35S3Z	2.02E-03	1.59E-03	1.29E-03	1.48E-03	1.34E-03	9.02E-04
1S35V3Z	4.79E-03	2.91E-03	4.07E-03	3.15E-03	2.52E-03	2.58E-03
1S50M3Z	3.89E-03	2.64E-03	3.38E-03	2.58E-03	2.16E-03	2.17E-03
1S50S3Z	1.67E-03	1.31E-03	1.09E-03	1.22E-03	1.10E-03	7.53E-04
1S50V3Z	4.38E-03	2.52E-03	3.81E-03	2.84E-03	2.22E-03	2.39E-03
1V06M3Z	2.02E-02	1.32E-02	1.76E-02	1.48E-02	1.24E-02	1.26E-02
1V06S3Z	1.98E-02	1.30E-02	1.73E-02	1.52E-02	1.29E-02	1.31E-02
1V06V3Z	2.53E-02	1.68E-02	2.18E-02	1.91E-02	1.63E-02	1.63E-02
1V15M3Z	1.29E-02	8.87E-03	1.02E-02	9.12E-03	7.80E-03	6.97E-03
1V15S3Z	1.36E-02	9.70E-03	1.06E-02	1.10E-02	9.65E-03	8.55E-03
1V15V3Z	2.15E-02	1.43E-02	1.87E-02	1.62E-02	1.38E-02	1.39E-02
1V30M3Z	7.40E-03	6.07E-03	4.78E-03	5.53E-03	5.09E-03	3.44E-03
1V30S3Z	7.04E-03	5.77E-03	4.57E-03	5.28E-03	4.86E-03	3.31E-03
1V30V3Z	1.79E-02	1.22E-02	1.46E-02	1.33E-02	1.15E-02	1.07E-02
1V45M3Z	7.59E-03	6.40E-03	5.46E-03	6.27E-03	5.87E-03	4.57E-03
1V45S3Z	7.10E-03	6.04E-03	5.08E-03	5.94E-03	5.58E-03	4.33E-03
1V45V3Z	1.43E-02	9.59E-03	1.20E-02	1.05E-02	8.97E-03	8.71E-03
1V60M3Z	7.11E-03	6.09E-03	5.25E-03	5.58E-03	5.24E-03	4.09E-03
1V60S3Z	6.63E-03	5.69E-03	4.86E-03	5.10E-03	4.78E-03	3.69E-03
1V60V3Z	1.19E-02	8.03E-03	9.99E-03	8.79E-03	7.50E-03	7.26E-03
1V75M3Z	6.50E-03	5.44E-03	5.11E-03	4.72E-03	4.37E-03	3.61E-03
1V75S3Z	6.32E-03	5.37E-03	4.82E-03	4.57E-03	4.25E-03	3.37E-03
1V75V3Z	9.88E-03	6.53E-03	8.35E-03	7.17E-03	6.05E-03	5.95E-03
1V90M3Z	5.80E-03	4.48E-03	4.74E-03	4.18E-03	3.74E-03	3.34E-03
1V90S3Z	5.52E-03	4.34E-03	4.36E-03	3.96E-03	3.57E-03	3.03E-03
1V90V3Z	8.28E-03	5.50E-03	6.84E-03	6.08E-03	5.15E-03	4.93E-03
1V05M3Z	5.32E-03	3.90E-03	4.36E-03	3.77E-03	3.30E-03	3.01E-03
1V05S3Z	5.17E-03	3.82E-03	4.10E-03	3.69E-03	3.24E-03	2.84E-03
1V05V3Z	6.85E-03	4.48E-03	5.85E-03	4.98E-03	4.19E-03	4.18E-03
1V20M3Z	4.97E-03	3.56E-03	4.04E-03	3.49E-03	3.03E-03	2.75E-03
1V20S3Z	4.46E-03	3.17E-03	3.75E-03	3.04E-03	2.61E-03	2.47E-03

Configuration	ICRP 26			ICRP 60		
	M w B	M w/o B	Female	M w B	M w/o B	Female
1V20V3Z	5.96E-03	3.97E-03	5.08E-03	4.40E-03	3.73E-03	3.69E-03
1V35M3Z	4.44E-03	3.16E-03	3.56E-03	3.12E-03	2.70E-03	2.41E-03
1V35S3Z	4.08E-03	2.90E-03	3.35E-03	2.83E-03	2.43E-03	2.24E-03
1V35V3Z	5.31E-03	3.64E-03	4.40E-03	3.97E-03	3.42E-03	3.24E-03
1V50M3Z	3.99E-03	2.80E-03	3.28E-03	2.76E-03	2.36E-03	2.19E-03
1V50S3Z	3.68E-03	2.58E-03	2.99E-03	2.48E-03	2.11E-03	1.93E-03
1V50V3Z	4.77E-03	3.21E-03	4.09E-03	3.55E-03	3.02E-03	3.01E-03

Table E-5: Summary Whole Body Dose using ANSI 1991 at 3 Ft

	ICRP 26			ICRP 60		
Configuration	M w B	M w/o B	Female	M w B	M w/o B	Female
1M06M3A	2.63E-02	2.08E-02	1.77E-02	2.06E-02	1.88E-02	1.37E-02
1M06S3A	1.15E-02	9.29E-03	7.12E-03	8.75E-03	8.01E-03	5.25E-03
1M06V3A	2.03E-02	1.63E-02	1.37E-02	1.58E-02	1.44E-02	1.05E-02
1M15M3A	2.30E-02	1.84E-02	1.52E-02	1.77E-02	1.62E-02	1.15E-02
1M15S3A	1.18E-02	9.51E-03	7.29E-03	8.91E-03	8.17E-03	5.35E-03
1M15V3A	1.83E-02	1.46E-02	1.24E-02	1.42E-02	1.29E-02	9.45E-03
1M30M3A	1.97E-02	1.61E-02	1.21E-02	1.47E-02	1.35E-02	8.62E-03
1M30S3A	1.34E-02	1.13E-02	9.44E-03	1.09E-02	1.02E-02	7.69E-03
1M30V3A	1.64E-02	1.35E-02	1.03E-02	1.25E-02	1.15E-02	7.65E-03
1M45M3A	1.53E-02	1.24E-02	9.85E-03	1.14E-02	1.04E-02	7.00E-03
1M45S3A	1.21E-02	8.54E-03	8.45E-03	8.16E-03	6.98E-03	5.27E-03
1M45V3A	1.62E-02	1.37E-02	1.15E-02	1.35E-02	1.27E-02	9.77E-03
1M60M3A	1.25E-02	9.95E-03	8.15E-03	9.47E-03	8.62E-03	5.99E-03
1M60S3A	1.49E-02	1.07E-02	1.18E-02	1.05E-02	9.07E-03	7.99E-03
1M60V3A	1.53E-02	1.31E-02	1.16E-02	1.19E-02	1.12E-02	8.94E-03
1M75M3A	1.08E-02	8.69E-03	6.86E-03	8.04E-03	7.32E-03	4.86E-03
1M75S3A	1.56E-02	1.03E-02	1.30E-02	1.14E-02	9.70E-03	9.37E-03
1M75V3A	1.44E-02	1.21E-02	1.09E-02	1.07E-02	9.91E-03	7.91E-03
1M90M3A	8.96E-03	7.09E-03	5.79E-03	6.83E-03	6.21E-03	4.30E-03
1M90S3A	1.23E-02	8.94E-03	1.03E-02	9.50E-03	8.38E-03	7.89E-03
1M90V3A	1.29E-02	1.01E-02	1.01E-02	9.39E-03	8.44E-03	7.11E-03
1M05M3A	7.76E-03	6.00E-03	5.23E-03	5.83E-03	5.25E-03	3.81E-03
1M05S3A	1.02E-02	7.24E-03	8.46E-03	7.97E-03	6.97E-03	6.55E-03
1M05V3A	1.13E-02	8.12E-03	9.41E-03	8.00E-03	6.95E-03	6.52E-03
1M20M3A	7.08E-03	5.49E-03	4.85E-03	5.24E-03	4.71E-03	3.45E-03
1M20S3A	9.03E-03	5.73E-03	7.14E-03	6.62E-03	5.52E-03	5.11E-03
1M20V3A	1.04E-02	7.32E-03	8.70E-03	7.29E-03	6.28E-03	5.97E-03
1M35M3A	6.27E-03	4.71E-03	4.43E-03	4.59E-03	4.07E-03	3.12E-03
1M35S3A	8.14E-03	4.87E-03	6.63E-03	5.50E-03	4.42E-03	4.30E-03

	ICRP 26			ICRP 60		
Configuration	M w B	M w/o B	Female	M w B	M w/o B	Female
1M35V3A	1.01E-02	6.90E-03	8.61E-03	6.94E-03	5.88E-03	5.78E-03
1M50M3A	5.81E-03	4.42E-03	4.09E-03	4.28E-03	3.81E-03	2.90E-03
1M50S3A	8.14E-03	5.03E-03	6.67E-03	5.34E-03	4.30E-03	4.16E-03
1M50V3A	9.87E-03	6.51E-03	8.52E-03	6.73E-03	5.61E-03	5.65E-03
1S06M3A	1.27E-02	1.00E-02	8.42E-03	9.31E-03	8.43E-03	5.91E-03
1S06S3A	2.27E-02	1.81E-02	1.51E-02	1.80E-02	1.65E-02	1.19E-02
1S06V3A	2.02E-02	1.59E-02	1.42E-02	1.57E-02	1.42E-02	1.09E-02
1S15M3A	1.30E-02	1.04E-02	8.71E-03	9.58E-03	8.72E-03	6.15E-03
1S15S3A	1.87E-02	1.51E-02	1.24E-02	1.44E-02	1.32E-02	9.37E-03
1S15V3A	1.84E-02	1.48E-02	1.21E-02	1.41E-02	1.29E-02	9.05E-03
1S30M3A	1.30E-02	1.03E-02	9.03E-03	9.24E-03	8.34E-03	6.08E-03
1S30S3A	1.53E-02	1.27E-02	9.15E-03	1.15E-02	1.07E-02	6.60E-03
1S30V3A	1.91E-02	1.59E-02	1.30E-02	1.51E-02	1.41E-02	1.03E-02
1S45M3A	1.86E-02	1.37E-02	1.46E-02	1.36E-02	1.20E-02	1.04E-02
1S45S3A	1.19E-02	9.93E-03	7.18E-03	8.86E-03	8.20E-03	5.09E-03
1S45V3A	1.70E-02	1.44E-02	1.26E-02	1.42E-02	1.33E-02	1.07E-02
1S60M3A	1.99E-02	1.30E-02	1.70E-02	1.41E-02	1.18E-02	1.17E-02
1S60S3A	9.76E-03	8.11E-03	5.81E-03	7.28E-03	6.73E-03	4.12E-03
1S60V3A	1.64E-02	1.39E-02	1.27E-02	1.26E-02	1.17E-02	9.63E-03
1S75M3A	1.62E-02	1.16E-02	1.34E-02	1.20E-02	1.05E-02	9.78E-03
1S75S3A	7.81E-03	6.34E-03	4.91E-03	5.71E-03	5.22E-03	3.39E-03
1S75V3A	1.52E-02	1.21E-02	1.23E-02	1.10E-02	9.93E-03	8.61E-03
1S90M3A	1.29E-02	9.09E-03	1.05E-02	9.11E-03	7.86E-03	7.27E-03
1S90S3A	6.68E-03	5.42E-03	4.32E-03	4.94E-03	4.52E-03	3.05E-03
1S90V3A	1.30E-02	9.53E-03	1.08E-02	9.17E-03	8.00E-03	7.35E-03
1S05M3A	1.03E-02	6.39E-03	8.17E-03	6.70E-03	5.41E-03	5.04E-03
1S05S3A	5.45E-03	4.40E-03	3.52E-03	4.05E-03	3.70E-03	2.51E-03
1S05V3A	1.24E-02	8.63E-03	1.02E-02	8.51E-03	7.27E-03	6.76E-03
1S20M3A	9.56E-03	5.76E-03	8.06E-03	6.22E-03	4.95E-03	5.02E-03
1S20S3A	4.64E-03	3.59E-03	3.34E-03	3.37E-03	3.02E-03	2.33E-03
1S20V3A	1.12E-02	7.32E-03	9.50E-03	7.65E-03	6.34E-03	6.26E-03

	ICRP 26			ICRP 60		
Configuration	M w B	M w/o B	Female	M w B	M w/o B	Female
1S35M3A	9.40E-03	6.20E-03	8.09E-03	6.24E-03	5.17E-03	5.19E-03
1S35S3A	4.49E-03	3.54E-03	2.86E-03	3.29E-03	2.97E-03	1.99E-03
1S35V3A	1.04E-02	6.34E-03	8.79E-03	6.90E-03	5.56E-03	5.65E-03
1S50M3A	8.54E-03	5.80E-03	7.40E-03	5.65E-03	4.74E-03	4.74E-03
1S50S3A	3.72E-03	2.93E-03	2.41E-03	2.71E-03	2.45E-03	1.66E-03
1S50V3A	9.62E-03	5.57E-03	8.32E-03	6.25E-03	4.90E-03	5.21E-03
1V06M3A	4.40E-02	2.89E-02	3.80E-02	3.22E-02	2.71E-02	2.74E-02
1V06S3A	4.30E-02	2.83E-02	3.73E-02	3.30E-02	2.81E-02	2.85E-02
1V06V3A	5.50E-02	3.67E-02	4.73E-02	4.16E-02	3.55E-02	3.54E-02
1V15M3A	2.89E-02	2.01E-02	2.25E-02	2.04E-02	1.75E-02	1.53E-02
1V15S3A	2.97E-02	2.12E-02	2.31E-02	2.39E-02	2.10E-02	1.86E-02
1V15V3A	4.68E-02	3.12E-02	4.04E-02	3.52E-02	3.00E-02	3.01E-02
1V30M3A	1.74E-02	1.43E-02	1.08E-02	1.29E-02	1.19E-02	7.69E-03
1V30S3A	1.55E-02	1.27E-02	1.00E-02	1.16E-02	1.07E-02	7.22E-03
1V30V3A	3.89E-02	2.67E-02	3.17E-02	2.90E-02	2.49E-02	2.33E-02
1V45M3A	1.73E-02	1.45E-02	1.23E-02	1.42E-02	1.33E-02	1.02E-02
1V45S3A	1.56E-02	1.33E-02	1.11E-02	1.30E-02	1.22E-02	9.41E-03
1V45V3A	3.10E-02	2.09E-02	2.60E-02	2.29E-02	1.96E-02	1.89E-02
1V60M3A	1.59E-02	1.33E-02	1.20E-02	1.23E-02	1.15E-02	9.22E-03
1V60S3A	1.46E-02	1.25E-02	1.06E-02	1.12E-02	1.05E-02	8.04E-03
1V60V3A	2.59E-02	1.75E-02	2.17E-02	1.92E-02	1.64E-02	1.58E-02
1V75M3A	1.46E-02	1.21E-02	1.15E-02	1.07E-02	9.82E-03	8.17E-03
1V75S3A	1.39E-02	1.18E-02	1.05E-02	1.00E-02	9.33E-03	7.37E-03
1V75V3A	2.15E-02	1.43E-02	1.81E-02	1.57E-02	1.32E-02	1.29E-02
1V90M3A	1.32E-02	1.02E-02	1.05E-02	9.58E-03	8.59E-03	7.45E-03
1V90S3A	1.21E-02	9.53E-03	9.55E-03	8.69E-03	7.82E-03	6.63E-03
1V90V3A	1.80E-02	1.20E-02	1.49E-02	1.33E-02	1.12E-02	1.07E-02
1V05M3A	1.24E-02	9.11E-03	9.94E-03	8.69E-03	7.61E-03	6.76E-03
1V05S3A	1.13E-02	8.40E-03	8.94E-03	8.12E-03	7.14E-03	6.20E-03
1V05V3A	1.50E-02	9.80E-03	1.27E-02	1.09E-02	9.16E-03	9.09E-03
1V20M3A	1.11E-02	7.85E-03	9.14E-03	7.69E-03	6.62E-03	6.15E-03

	ICRP 26			ICRP 60		
Configuration	M w B	M w/o B	Female	M w B	M w/o B	Female
1V20S3A	9.79E-03	6.98E-03	8.18E-03	6.68E-03	5.75E-03	5.40E-03
1V20V3A	1.30E-02	8.69E-03	1.10E-02	9.62E-03	8.17E-03	8.03E-03
1V35M3A	9.80E-03	6.89E-03	7.98E-03	6.84E-03	5.86E-03	5.38E-03
1V35S3A	8.97E-03	6.40E-03	7.32E-03	6.22E-03	5.36E-03	4.90E-03
1V35V3A	1.16E-02	8.01E-03	9.58E-03	8.71E-03	7.50E-03	7.06E-03
1V50M3A	8.76E-03	6.15E-03	7.18E-03	6.07E-03	5.20E-03	4.80E-03
1V50S3A	8.07E-03	5.66E-03	6.54E-03	5.44E-03	4.64E-03	4.22E-03
1V50V3A	1.04E-02	7.02E-03	8.92E-03	7.75E-03	6.62E-03	6.55E-03

Table E-6: Summary Whole Body Dose using ICRP-74 at 3 Ft

	ICRP 26			ICRP 60		
Configuration	M w B	M w/o B	Female	M w B	M w/o B	Female
1M06M3Z	2.24E-02	1.78E-02	1.50E-02	1.76E-02	1.60E-02	1.17E-02
1M06S3Z	9.86E-03	7.96E-03	6.08E-03	7.49E-03	6.86E-03	4.47E-03
1M06V3Z	1.73E-02	1.39E-02	1.17E-02	1.35E-02	1.23E-02	8.93E-03
1M15M3Z	1.96E-02	1.58E-02	1.29E-02	1.51E-02	1.39E-02	9.78E-03
1M15S3Z	1.01E-02	8.15E-03	6.22E-03	7.63E-03	6.99E-03	4.55E-03
1M15V3Z	1.56E-02	1.25E-02	1.05E-02	1.21E-02	1.10E-02	8.03E-03
1M30M3Z	1.69E-02	1.38E-02	1.03E-02	1.26E-02	1.16E-02	7.34E-03
1M30S3Z	1.15E-02	9.66E-03	8.05E-03	9.31E-03	8.70E-03	6.55E-03
1M30V3Z	1.40E-02	1.15E-02	8.83E-03	1.07E-02	9.83E-03	6.51E-03
1M45M3Z	1.31E-02	1.06E-02	8.41E-03	9.74E-03	8.89E-03	5.96E-03
1M45S3Z	1.03E-02	7.33E-03	7.22E-03	6.99E-03	5.98E-03	4.49E-03
1M45V3Z	1.38E-02	1.17E-02	9.79E-03	1.15E-02	1.08E-02	8.32E-03
1M60M3Z	1.07E-02	8.53E-03	6.97E-03	8.11E-03	7.38E-03	5.12E-03
1M60S3Z	1.27E-02	9.16E-03	1.01E-02	8.93E-03	7.74E-03	6.81E-03
1M60V3Z	1.30E-02	1.12E-02	9.86E-03	1.02E-02	9.55E-03	7.62E-03
1M75M3Z	9.30E-03	7.46E-03	5.87E-03	6.89E-03	6.28E-03	4.15E-03
1M75S3Z	1.33E-02	8.84E-03	1.11E-02	9.76E-03	8.28E-03	7.97E-03
1M75V3Z	1.23E-02	1.04E-02	9.33E-03	9.11E-03	8.47E-03	6.74E-03
1M90M3Z	7.69E-03	6.09E-03	4.95E-03	5.86E-03	5.32E-03	3.67E-03
1M90S3Z	1.05E-02	7.63E-03	8.77E-03	8.11E-03	7.15E-03	6.72E-03
1M90V3Z	1.11E-02	8.64E-03	8.59E-03	8.03E-03	7.22E-03	6.06E-03
1M05M3Z	6.65E-03	5.15E-03	4.47E-03	5.00E-03	4.50E-03	3.26E-03
1M05S3Z	8.74E-03	6.19E-03	7.20E-03	6.81E-03	5.95E-03	5.58E-03
1M05V3Z	9.62E-03	6.95E-03	8.03E-03	6.83E-03	5.94E-03	5.56E-03
1M20M3Z	6.07E-03	4.71E-03	4.15E-03	4.48E-03	4.03E-03	2.95E-03
1M20S3Z	7.73E-03	4.91E-03	6.10E-03	5.66E-03	4.72E-03	4.35E-03
1M20V3Z	8.84E-03	6.26E-03	7.43E-03	6.22E-03	5.36E-03	5.09E-03
1M35M3Z	5.39E-03	4.04E-03	3.80E-03	3.94E-03	3.49E-03	2.67E-03
1M35S3Z	6.96E-03	4.17E-03	5.66E-03	4.70E-03	3.78E-03	3.67E-03

Configuration	ICRP 26			ICRP 60		
	M w B	M w/o B	Female	M w B	M w/o B	Female
1M35V3Z	8.60E-03	5.90E-03	7.35E-03	5.93E-03	5.03E-03	4.93E-03
1M50M3Z	4.98E-03	3.79E-03	3.50E-03	3.66E-03	3.26E-03	2.48E-03
1M50S3Z	6.97E-03	4.31E-03	5.70E-03	4.57E-03	3.69E-03	3.56E-03
1M50V3Z	8.44E-03	5.57E-03	7.28E-03	5.75E-03	4.79E-03	4.82E-03
1S06M3Z	1.08E-02	8.58E-03	7.19E-03	7.96E-03	7.20E-03	5.04E-03
1S06S3Z	1.94E-02	1.54E-02	1.28E-02	1.54E-02	1.41E-02	1.01E-02
1S06V3Z	1.73E-02	1.36E-02	1.21E-02	1.34E-02	1.21E-02	9.27E-03
1S15M3Z	1.11E-02	8.90E-03	7.44E-03	8.18E-03	7.44E-03	5.24E-03
1S15S3Z	1.59E-02	1.29E-02	1.05E-02	1.23E-02	1.13E-02	7.96E-03
1S15V3Z	1.57E-02	1.26E-02	1.03E-02	1.20E-02	1.10E-02	7.70E-03
1S30M3Z	1.11E-02	8.80E-03	7.72E-03	7.90E-03	7.13E-03	5.19E-03
1S30S3Z	1.31E-02	1.09E-02	7.81E-03	9.87E-03	9.12E-03	5.61E-03
1S30V3Z	1.63E-02	1.36E-02	1.11E-02	1.29E-02	1.20E-02	8.78E-03
1S45M3Z	1.59E-02	1.17E-02	1.24E-02	1.16E-02	1.02E-02	8.85E-03
1S45S3Z	1.02E-02	8.52E-03	6.14E-03	7.58E-03	7.02E-03	4.34E-03
1S45V3Z	1.46E-02	1.23E-02	1.08E-02	1.21E-02	1.14E-02	9.10E-03
1S60M3Z	1.70E-02	1.11E-02	1.45E-02	1.20E-02	1.01E-02	1.00E-02
1S60S3Z	8.38E-03	6.97E-03	4.97E-03	6.24E-03	5.77E-03	3.52E-03
1S60V3Z	1.40E-02	1.19E-02	1.09E-02	1.07E-02	1.00E-02	8.21E-03
1S75M3Z	1.38E-02	9.89E-03	1.14E-02	1.03E-02	8.94E-03	8.34E-03
1S75S3Z	6.70E-03	5.45E-03	4.20E-03	4.89E-03	4.48E-03	2.90E-03
1S75V3Z	1.30E-02	1.03E-02	1.05E-02	9.38E-03	8.49E-03	7.34E-03
1S90M3Z	1.10E-02	7.79E-03	9.00E-03	7.80E-03	6.73E-03	6.20E-03
1S90S3Z	5.74E-03	4.66E-03	3.70E-03	4.24E-03	3.88E-03	2.61E-03
1S90V3Z	1.11E-02	8.15E-03	9.18E-03	7.84E-03	6.84E-03	6.27E-03
1S05M3Z	8.77E-03	5.48E-03	6.98E-03	5.74E-03	4.64E-03	4.30E-03
1S05S3Z	4.67E-03	3.77E-03	3.01E-03	3.47E-03	3.17E-03	2.14E-03
1S05V3Z	1.05E-02	7.37E-03	8.67E-03	7.26E-03	6.20E-03	5.76E-03
1S20M3Z	8.18E-03	4.94E-03	6.89E-03	5.32E-03	4.24E-03	4.29E-03
1S20S3Z	3.98E-03	3.09E-03	2.87E-03	2.89E-03	2.59E-03	2.00E-03
1S20V3Z	9.60E-03	6.26E-03	8.11E-03	6.53E-03	5.41E-03	5.33E-03

	ICRP 26			ICRP 60		
Configuration	M w B	M w/o B	Female	M w B	M w/o B	Female
1S35M3Z	8.03E-03	5.30E-03	6.90E-03	5.33E-03	4.42E-03	4.43E-03
1S35S3Z	3.85E-03	3.04E-03	2.45E-03	2.83E-03	2.55E-03	1.70E-03
1S35V3Z	8.85E-03	5.43E-03	7.50E-03	5.90E-03	4.76E-03	4.82E-03
1S50M3Z	7.30E-03	4.96E-03	6.32E-03	4.83E-03	4.05E-03	4.04E-03
1S50S3Z	3.19E-03	2.52E-03	2.06E-03	2.33E-03	2.10E-03	1.42E-03
1S50V3Z	8.22E-03	4.77E-03	7.10E-03	5.34E-03	4.19E-03	4.44E-03
1V06M3Z	3.75E-02	2.46E-02	3.24E-02	2.74E-02	2.31E-02	2.33E-02
1V06S3Z	3.66E-02	2.41E-02	3.17E-02	2.81E-02	2.39E-02	2.42E-02
1V06V3Z	4.69E-02	3.12E-02	4.02E-02	3.54E-02	3.02E-02	3.01E-02
1V15M3Z	2.47E-02	1.72E-02	1.92E-02	1.74E-02	1.49E-02	1.30E-02
1V15S3Z	2.54E-02	1.81E-02	1.96E-02	2.04E-02	1.79E-02	1.58E-02
1V15V3Z	3.98E-02	2.66E-02	3.44E-02	2.99E-02	2.55E-02	2.56E-02
1V30M3Z	1.49E-02	1.22E-02	9.27E-03	1.11E-02	1.02E-02	6.55E-03
1V30S3Z	1.33E-02	1.09E-02	8.56E-03	9.92E-03	9.12E-03	6.15E-03
1V30V3Z	3.31E-02	2.27E-02	2.70E-02	2.47E-02	2.13E-02	1.98E-02
1V45M3Z	1.48E-02	1.24E-02	1.05E-02	1.21E-02	1.13E-02	8.69E-03
1V45S3Z	1.33E-02	1.13E-02	9.47E-03	1.11E-02	1.04E-02	8.01E-03
1V45V3Z	2.65E-02	1.79E-02	2.21E-02	1.96E-02	1.67E-02	1.61E-02
1V60M3Z	1.36E-02	1.14E-02	1.02E-02	1.06E-02	9.83E-03	7.85E-03
1V60S3Z	1.24E-02	1.07E-02	9.06E-03	9.55E-03	8.96E-03	6.85E-03
1V60V3Z	2.21E-02	1.50E-02	1.85E-02	1.63E-02	1.40E-02	1.34E-02
1V75M3Z	1.25E-02	1.04E-02	9.86E-03	9.11E-03	8.39E-03	6.97E-03
1V75S3Z	1.18E-02	1.01E-02	8.99E-03	8.56E-03	7.97E-03	6.28E-03
1V75V3Z	1.84E-02	1.22E-02	1.55E-02	1.34E-02	1.13E-02	1.10E-02
1V90M3Z	1.13E-02	8.73E-03	8.98E-03	8.20E-03	7.35E-03	6.36E-03
1V90S3Z	1.04E-02	8.14E-03	8.14E-03	7.42E-03	6.68E-03	5.65E-03
1V90V3Z	1.54E-02	1.03E-02	1.27E-02	1.13E-02	9.60E-03	9.12E-03
1V05M3Z	1.06E-02	7.81E-03	8.49E-03	7.43E-03	6.51E-03	5.77E-03
1V05S3Z	9.70E-03	7.19E-03	7.63E-03	6.94E-03	6.10E-03	5.29E-03
1V05V3Z	1.28E-02	8.36E-03	1.08E-02	9.28E-03	7.81E-03	7.74E-03
1V20M3Z	9.47E-03	6.73E-03	7.79E-03	6.58E-03	5.67E-03	5.24E-03

	ICRP 26			ICRP 60		
Configuration	M w B	M w/o B	Female	M w B	M w/o B	Female
1V20S3Z	8.36E-03	5.96E-03	6.98E-03	5.71E-03	4.91E-03	4.60E-03
1V20V3Z	1.11E-02	7.42E-03	9.41E-03	8.20E-03	6.97E-03	6.84E-03
1V35M3Z	8.38E-03	5.89E-03	6.81E-03	5.85E-03	5.02E-03	4.59E-03
1V35S3Z	7.67E-03	5.48E-03	6.25E-03	5.32E-03	4.59E-03	4.18E-03
1V35V3Z	9.93E-03	6.84E-03	8.17E-03	7.43E-03	6.40E-03	6.02E-03
1V50M3Z	7.49E-03	5.26E-03	6.13E-03	5.18E-03	4.44E-03	4.10E-03
1V50S3Z	6.90E-03	4.85E-03	5.58E-03	4.66E-03	3.97E-03	3.60E-03
1V50V3Z	8.90E-03	6.00E-03	7.60E-03	6.62E-03	5.65E-03	5.58E-03

Appendix F: Comparison Of Different Conversion Factors Using Dosimeter Reference Position

APPENDIX F.1:

COMPARISON AT 1 FOOT

Table F.1-1: MxxM1

MxxM1	Distance	ANSI 1977	ANSI 1991	ICRP 74
M06M1	6	1.55E-01	8.16E-02	1.50E-01
M15M1	15	1.17E-01	6.13E-02	1.13E-01
M30M1	30	7.54E-02	3.91E-02	7.28E-02
M45M1	45	5.03E-02	2.59E-02	4.84E-02
M60M1	60	3.87E-02	1.97E-02	3.70E-02
M75M1	75	3.06E-02	1.54E-02	2.91E-02
M90M1	90	2.40E-02	1.19E-02	2.27E-02
M05M1	105	1.99E-02	9.78E-03	1.87E-02
M20M1	120	1.64E-02	8.16E-03	1.56E-02
M35M1	135	1.44E-02	7.06E-03	1.36E-02
M50M1	150	1.33E-02	6.74E-03	1.25E-02

Table F.1-2: SxxM1

SxxM1	Distance	ANSI 1977	ANSI 1991	ICRP 74
S06M1	6	1.92E-02	9.48E-03	1.81E-02
S15M1	15	3.33E-02	1.66E-02	3.15E-02
S30M1	30	4.62E-02	2.41E-02	4.44E-02
S45M1	45	8.23E-02	4.35E-02	7.94E-02
S60M1	60	5.42E-02	2.81E-02	5.20E-02
S75M1	75	3.33E-02	1.68E-02	3.17E-02
S90M1	90	2.12E-02	1.04E-02	1.99E-02
S05M1	105	1.51E-02	7.33E-03	1.41E-02
S20M1	120	1.25E-02	6.13E-03	1.18E-02
S35M1	135	1.15E-02	5.57E-03	1.08E-02
S50M1	150	1.03E-02	4.80E-03	9.71E-03

Table F.1-3: VxxM1

VxxM1	Distance	ANSI 1977	ANSI 1991	ICRP 74
V06M1	6	4.52E-02	2.25E-02	4.27E-02
V15M1	15	5.72E-02	2.98E-02	5.51E-02
V30M1	30	5.81E-02	2.98E-02	5.56E-02
V45M1	45	3.70E-02	1.84E-02	3.51E-02
V60M1	60	3.03E-02	1.50E-02	2.87E-02
V75M1	75	2.51E-02	1.24E-02	2.37E-02
V90M1	90	2.05E-02	1.03E-02	1.96E-02
V05M1	105	1.71E-02	8.41E-03	1.61E-02
V20M1	120	1.44E-02	7.13E-03	1.37E-02
V35M1	135	1.24E-02	6.11E-03	1.17E-02
V50M1	150	1.15E-02	5.47E-03	1.09E-02

Table F.1-4: MxxS1

MxxS1	Distance	ANSI 1977	ANSI 1991	ICRP 74
M06S1	6	1.15E-02	5.50E-03	1.07E-02
M15S1	15	3.89E-02	2.01E-02	3.79E-02
M30S1	30	2.28E-02	1.18E-02	2.20E-02
M45S1	45	6.54E-02	3.55E-02	6.39E-02
M60S1	60	4.86E-02	2.53E-02	4.70E-02
M75S1	75	2.85E-02	1.49E-02	2.75E-02
M90S1	90	1.80E-02	9.24E-03	1.72E-02
M05S1	105	1.28E-02	5.88E-03	1.21E-02
M20S1	120	1.02E-02	4.45E-03	9.57E-03
M35S1	135	8.29E-03	4.07E-03	7.83E-03
M50S1	150	7.37E-03	3.36E-03	6.96E-03

Table F.1-5: SxxS1

SxxS1	Distance	ANSI 1977	ANSI 1991	ICRP 74
S06S1	6	1.16E-01	6.16E-02	1.13E-01
S15S1	15	7.77E-02	4.07E-02	7.58E-02
S30S1	30	4.01E-02	2.02E-02	3.86E-02
S45S1	45	2.52E-02	1.21E-02	2.39E-02
S60S1	60	1.70E-02	8.26E-03	1.60E-02
S75S1	75	1.30E-02	6.09E-03	1.22E-02
S90S1	90	1.07E-02	4.68E-03	9.92E-03
S05S1	105	8.40E-03	3.67E-03	7.86E-03
S20S1	120	6.74E-03	3.12E-03	6.31E-03
S35S1	135	5.76E-03	2.64E-03	5.27E-03
S50S1	150	5.73E-03	2.27E-03	5.32E-03

Table F.1-6: VxxS1

VxxS1	Distance	ANSI 1977	ANSI 1991	ICRP 74
V06S1	6	4.20E-02	2.05E-02	3.93E-02
V15S1	15	5.39E-02	2.76E-02	5.23E-02
V30S1	30	5.00E-02	2.61E-02	4.81E-02
V45S1	45	2.83E-02	1.46E-02	2.71E-02
V60S1	60	2.16E-02	1.05E-02	2.06E-02
V75S1	75	1.68E-02	8.29E-03	1.60E-02
V90S1	90	1.32E-02	6.50E-03	1.26E-02
V05S1	105	1.15E-02	5.28E-03	1.09E-02
V20S1	120	9.03E-03	4.27E-03	8.56E-03
V35S1	135	8.01E-03	3.64E-03	7.59E-03
V50S1	150	7.28E-03	3.35E-03	6.89E-03

Table F.1-7: MxxV1

MxxV1	Distance	ANSI 1977	ANSI 1991	ICRP 74
M06V1	6	4.74E-02	2.24E-02	4.43E-02
M15V1	15	7.29E-02	3.75E-02	7.00E-02
M30V1	30	7.57E-02	3.86E-02	7.23E-02
M45V1	45	5.15E-02	2.55E-02	4.85E-02
M60V1	60	5.40E-02	2.78E-02	5.18E-02
M75V1	75	5.72E-02	2.89E-02	5.48E-02
M90V1	90	5.27E-02	2.73E-02	5.07E-02
M05V1	105	4.82E-02	2.48E-02	4.63E-02
M20V1	120	4.30E-02	2.23E-02	4.14E-02
M35V1	135	3.92E-02	2.04E-02	3.77E-02
M50V1	150	3.81E-02	1.96E-02	3.64E-02

Table F.1-8: SxxV1

SxxV1	Distance	ANSI 1977	ANSI 1991	ICRP 74
S06V1	6	7.30E-02	3.56E-02	6.84E-02
S15V1	15	9.24E-02	4.50E-02	8.66E-02
S30V1	30	7.80E-02	3.76E-02	7.27E-02
S45V1	45	7.44E-02	3.78E-02	7.07E-02
S60V1	60	8.25E-02	4.27E-02	7.93E-02
S75V1	75	7.61E-02	3.97E-02	7.31E-02
S90V1	90	6.63E-02	3.45E-02	6.38E-02
S05V1	105	5.78E-02	3.01E-02	5.58E-02
S20V1	120	4.97E-02	2.56E-02	4.78E-02
S35V1	135	4.23E-02	2.19E-02	4.06E-02
S50V1	150	3.95E-02	2.03E-02	3.79E-02

Table F.1-9: VxxV1

VxxV1	Distance	ANSI 1977	ANSI 1991	ICRP 74
V06V1	6	7.56E-01	4.08E-01	7.36E-01
V15V1	15	5.15E-01	2.76E-01	5.00E-01
V30V1	30	3.05E-01	1.62E-01	2.95E-01
V45V1	45	1.97E-01	1.05E-01	1.91E-01
V60V1	60	1.39E-01	7.31E-02	1.34E-01
V75V1	75	1.02E-01	5.36E-02	9.87E-02
V90V1	90	7.72E-02	4.03E-02	7.45E-02
V05V1	105	6.15E-02	3.24E-02	5.94E-02
V20V1	120	5.11E-02	2.66E-02	4.93E-02
V35V1	135	4.37E-02	2.25E-02	4.19E-02
V50V1	150	4.07E-02	2.09E-02	3.91E-02

APPENDIX F.2:

COMPARISON AT 3 FOOT

Table F.2-1: MxxM3

MxxM3	Distance	ANSI 1977	ANSI 1991	ICRP 74
M06M3	6	3.06E-02	1.58E-02	2.95E-02
M15M3	15	2.65E-02	1.27E-02	2.53E-02
M30M3	30	1.95E-02	9.68E-03	1.86E-02
M45M3	45	1.63E-02	7.59E-03	1.54E-02
M60M3	60	1.40E-02	6.57E-03	1.32E-02
M75M3	75	1.20E-02	5.66E-03	1.14E-02
M90M3	90	1.03E-02	4.55E-03	9.63E-03
M05M3	105	9.73E-03	4.41E-03	9.11E-03
M20M3	120	9.04E-03	3.94E-03	8.43E-03
M35M3	135	8.39E-03	3.67E-03	7.77E-03
M50M3	150	8.19E-03	3.57E-03	7.66E-03

Table F.2-2: SxxM3

SxxM3	Distance	ANSI 1977	ANSI 1991	ICRP 74
S06M3	6	1.46E-02	6.99E-03	1.36E-02
S15M3	15	1.46E-02	6.83E-03	1.37E-02
S30M3	30	1.49E-02	6.63E-03	1.38E-02
S45M3	45	3.71E-02	1.96E-02	3.60E-02
S60M3	60	3.65E-02	1.88E-02	3.51E-02
S75M3	75	2.98E-02	1.52E-02	2.86E-02
S90M3	90	1.36E-02	6.22E-03	1.27E-02
S05M3	105	9.81E-03	4.45E-03	9.09E-03
S20M3	120	9.85E-03	4.73E-03	9.34E-03
S35M3	135	1.43E-02	6.96E-03	1.37E-02
S50M3	150	1.60E-02	7.94E-03	1.53E-02

Table F.2-3: VxxM3

VxxM3	Distance	ANSI 1977	ANSI 1991	ICRP 74
V06M3	6	7.67E-02	4.16E-02	7.51E-02
V15M3	15	2.60E-02	1.29E-02	2.48E-02
V30M3	30	1.75E-02	8.11E-03	1.65E-02
V45M3	45	1.52E-02	6.96E-03	1.41E-02
V60M3	60	1.33E-02	6.19E-03	1.25E-02
V75M3	75	1.83E-02	8.86E-03	1.74E-02
V90M3	90	1.78E-02	8.91E-03	1.71E-02
V05M3	105	1.60E-02	7.63E-03	1.52E-02
V20M3	120	1.31E-02	6.51E-03	1.24E-02
V35M3	135	1.10E-02	5.27E-03	1.04E-02
V50M3	150	1.01E-02	4.81E-03	9.50E-03

Table F.2-4: MxxS3

MxxS3	Distance	ANSI 1977	ANSI 1991	ICRP 74
M06S3	6	1.27E-02	5.75E-03	1.18E-02
M15S3	15	1.26E-02	6.10E-03	1.18E-02
M30S3	30	1.18E-02	5.74E-03	1.10E-02
M45S3	45	1.53E-02	7.76E-03	1.45E-02
M60S3	60	3.04E-02	1.62E-02	2.95E-02
M75S3	75	2.66E-02	1.42E-02	2.58E-02
M90S3	90	1.88E-02	9.90E-03	1.81E-02
M05S3	105	9.31E-03	4.55E-03	8.69E-03
M20S3	120	7.74E-03	3.67E-03	7.14E-03
M35S3	135	9.02E-03	4.47E-03	8.50E-03
M50S3	150	1.05E-02	5.25E-03	1.01E-02

Table F.2-5: SxxS3

SxxS3	Distance	ANSI 1977	ANSI 1991	ICRP 74
S06S3	6	2.61E-02	1.31E-02	2.52E-02
S15S3	15	1.96E-02	1.01E-02	1.88E-02
S30S3	30	1.46E-02	7.37E-03	1.39E-02
S45S3	45	1.17E-02	5.87E-03	1.12E-02
S60S3	60	9.83E-03	4.87E-03	9.29E-03
S75S3	75	8.71E-03	4.22E-03	8.15E-03
S90S3	90	8.13E-03	3.99E-03	7.66E-03
S05S3	105	6.27E-03	3.01E-03	5.86E-03
S20S3	120	5.80E-03	2.73E-03	5.38E-03
S35S3	135	5.22E-03	2.40E-03	4.78E-03
S50S3	150	4.85E-03	1.61E-03	4.31E-03

Table F.2-6: VxxS3

VxxS3	Distance	ANSI 1977	ANSI 1991	ICRP 74
V06S3	6	7.57E-02	4.06E-02	7.42E-02
V15S3	15	2.49E-02	1.27E-02	2.37E-02
V30S3	30	1.49E-02	7.36E-03	1.40E-02
V45S3	45	1.24E-02	6.09E-03	1.16E-02
V60S3	60	1.14E-02	5.55E-03	1.06E-02
V75S3	75	1.66E-02	8.48E-03	1.58E-02
V90S3	90	1.61E-02	8.31E-03	1.54E-02
V05S3	105	1.38E-02	7.08E-03	1.32E-02
V20S3	120	1.18E-02	5.95E-03	1.12E-02
V35S3	135	9.93E-03	4.86E-03	9.28E-03
V50S3	150	8.72E-03	4.07E-03	8.18E-03

Table F.2-7: MxxV3

MxxV3	Distance	ANSI 1977	ANSI 1991	ICRP 74
M06V3	6	2.30E-02	1.12E-02	2.20E-02
M15V3	15	2.00E-02	1.00E-02	1.90E-02
M30V3	30	1.67E-02	8.19E-03	1.57E-02
M45V3	45	1.48E-02	7.18E-03	1.38E-02
M60V3	60	1.37E-02	6.67E-03	1.28E-02
M75V3	75	1.81E-02	9.11E-03	1.71E-02
M90V3	90	1.81E-02	9.14E-03	1.71E-02
M05V3	105	1.59E-02	8.12E-03	1.52E-02
M20V3	120	1.43E-02	7.18E-03	1.35E-02
M35V3	135	1.27E-02	6.37E-03	1.20E-02
M50V3	150	1.24E-02	5.63E-03	1.16E-02

Table F.2-8: SxxV3

SxxV3	Distance	ANSI 1977	ANSI 1991	ICRP 74
S06V3	6	2.55E-02	1.22E-02	2.42E-02
S15V3	15	1.98E-02	1.01E-02	1.90E-02
S30V3	30	1.77E-02	8.85E-03	1.68E-02
S45V3	45	1.57E-02	7.81E-03	1.49E-02
S60V3	60	1.55E-02	6.88E-03	1.46E-02
S75V3	75	1.62E-02	7.34E-03	1.51E-02
S90V3	90	1.40E-02	6.80E-03	1.32E-02
S05V3	105	1.23E-02	6.07E-03	1.16E-02
S20V3	120	1.12E-02	5.44E-03	1.04E-02
S35V3	135	1.03E-02	4.98E-03	9.58E-03
S50V3	150	8.86E-03	4.00E-03	8.28E-03

Table F.2-9: VxxV3

VxxV3	Distance	ANSI 1977	ANSI 1991	ICRP 74
V06V3	6	9.79E-02	5.26E-02	9.57E-02
V15V3	15	8.11E-02	4.33E-02	7.91E-02
V30V3	30	6.30E-02	3.37E-02	6.13E-02
V45V3	45	5.19E-02	2.73E-02	5.04E-02
V60V3	60	4.36E-02	2.28E-02	4.23E-02
V75V3	75	3.72E-02	1.91E-02	3.59E-02
V90V3	90	3.14E-02	1.61E-02	3.02E-02
V05V3	105	2.70E-02	1.38E-02	2.61E-02
V20V3	120	2.38E-02	1.20E-02	2.29E-02
V35V3	135	2.16E-02	1.11E-02	2.09E-02
V50V3	150	2.04E-02	1.03E-02	1.96E-02

APPENDIX F.3:

GRAPHICAL COMPARISON AT 1 FOOT

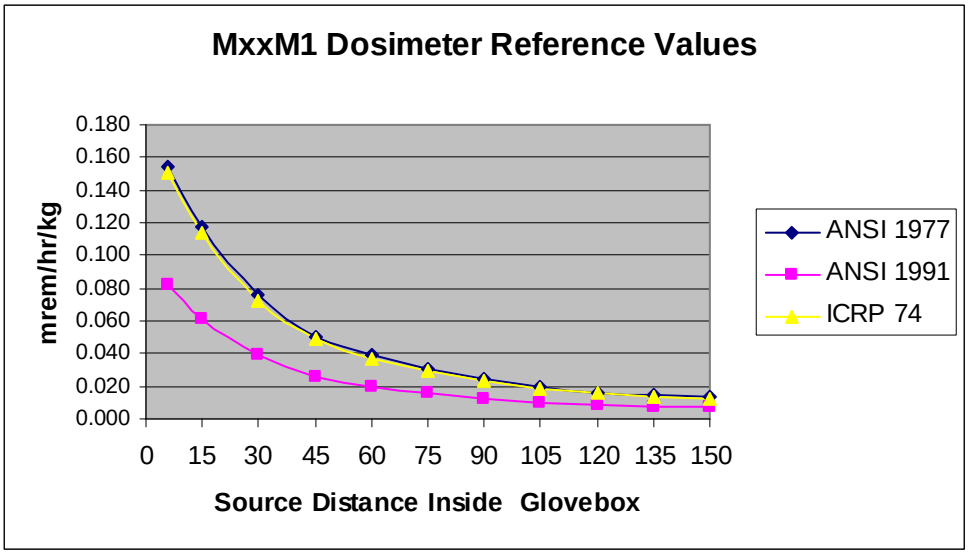

Figure F.3-1: MxxM1.

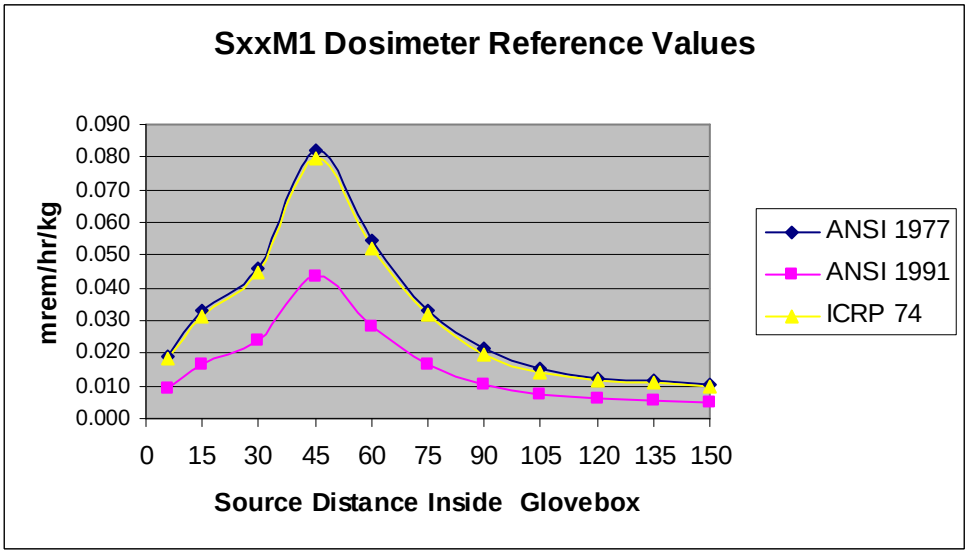

Figure F.3-2: SxxM1.

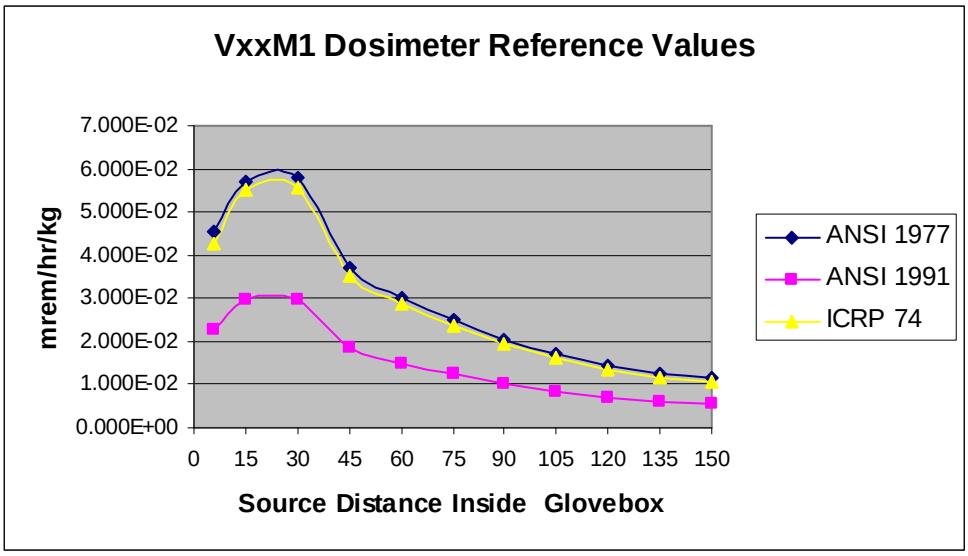

Figure F.3-3: VxxM1.

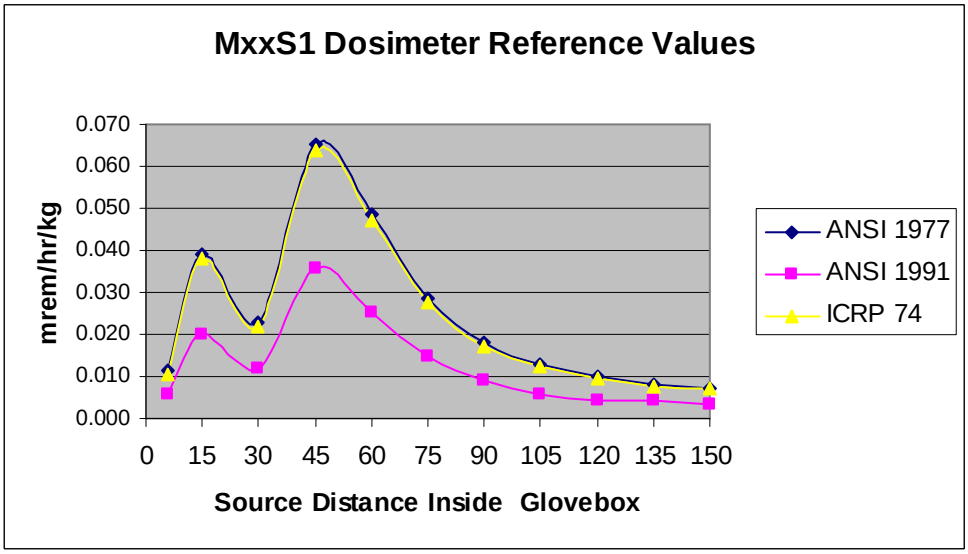

Figure F.3-4: MxxS1.

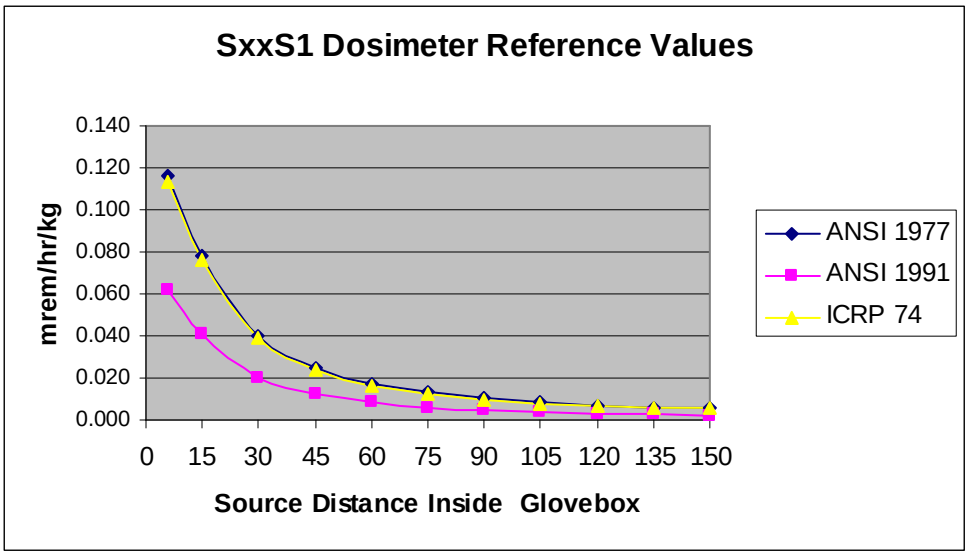

Figure F.3-5: SxxS1.

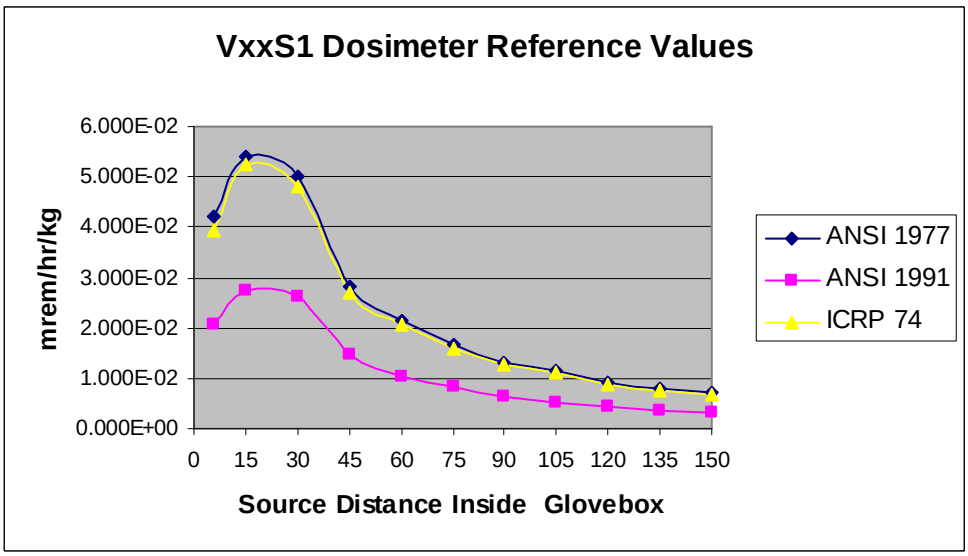

Figure F.3-6: VxxS1.

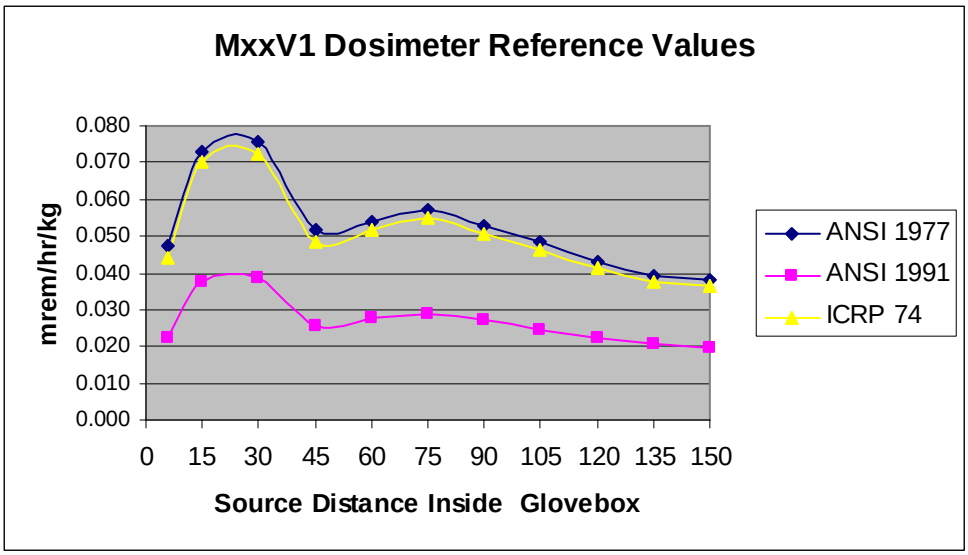

Figure F.3-7: MxxV1.

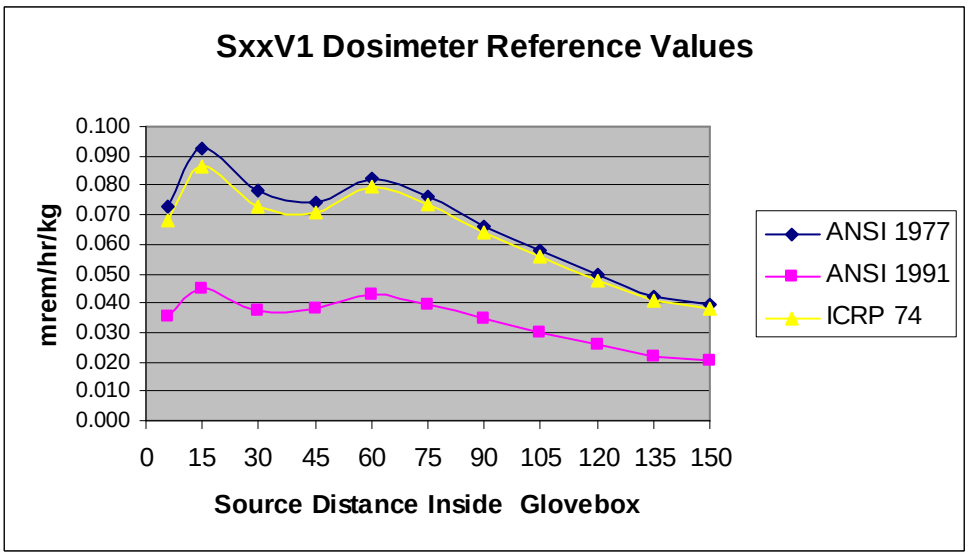

Figure F.3-8: SxxV1.

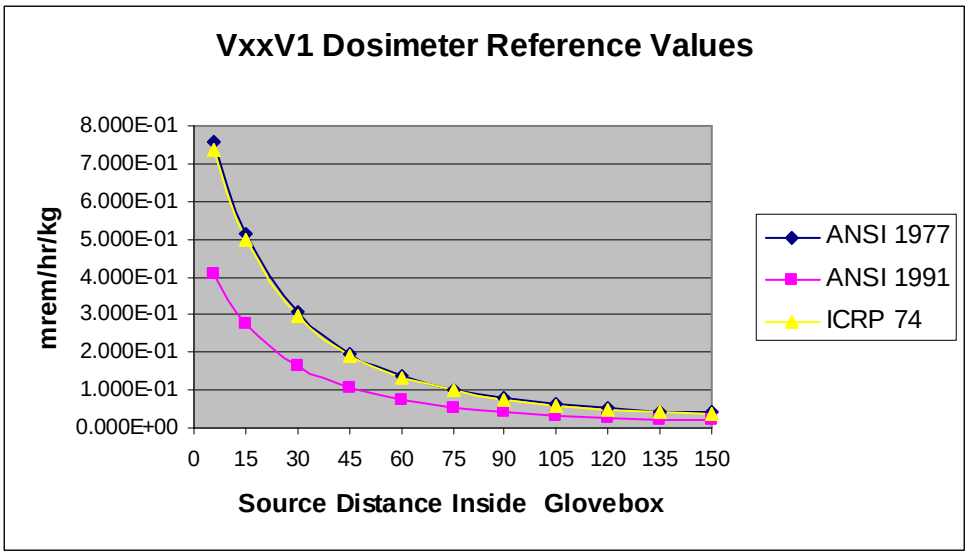

Figure F.3-9: VxxV1.

APPENDIX F.4:

GRAPHICAL COMPARISON AT 3 FOOT

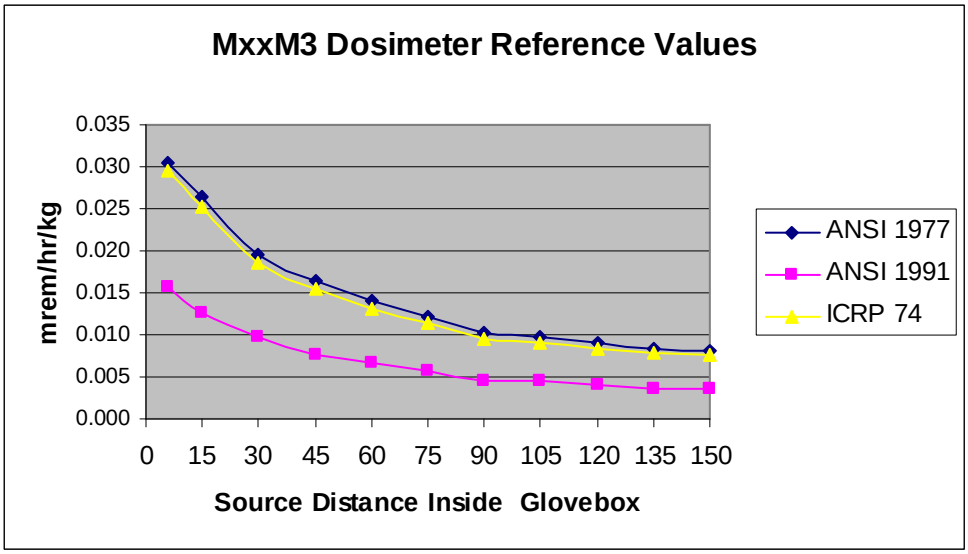

Figure F.4-1: MxxM3.

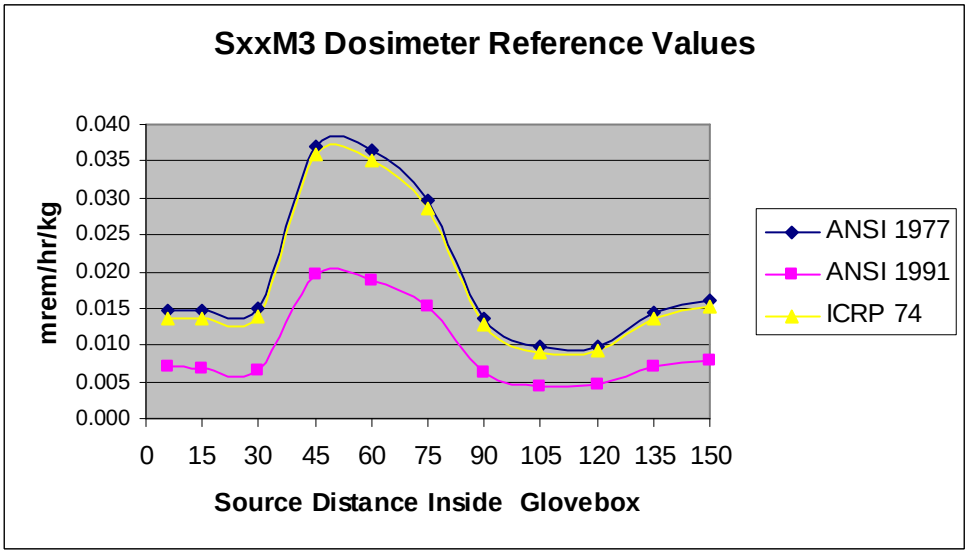

Figure F.4-2: SxxM3.

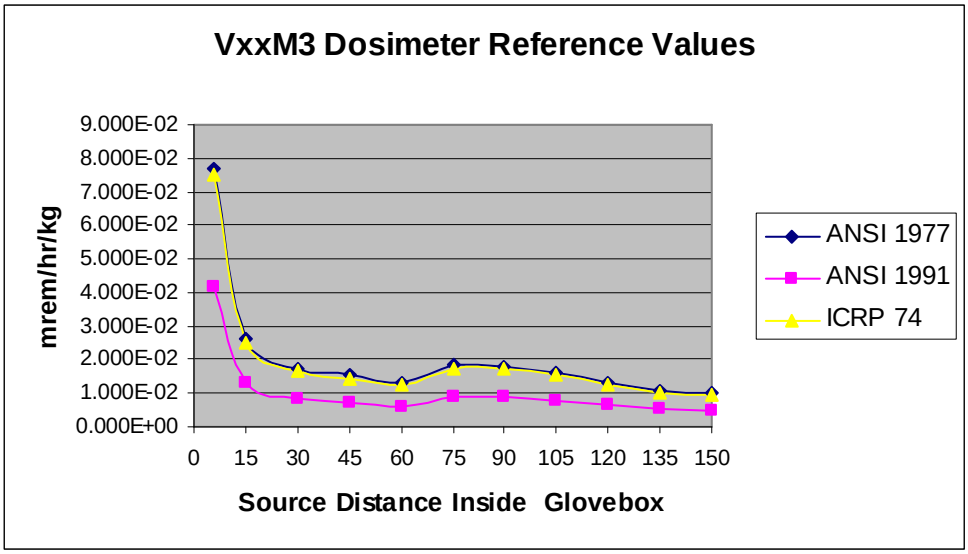

Figure F.4-3: VxxM3.

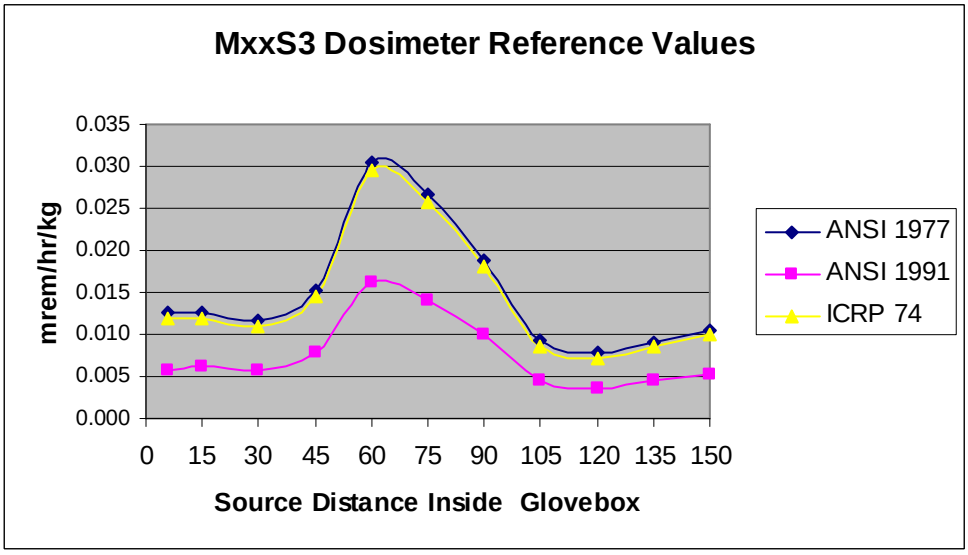

Figure F.4-4: MxxS3.

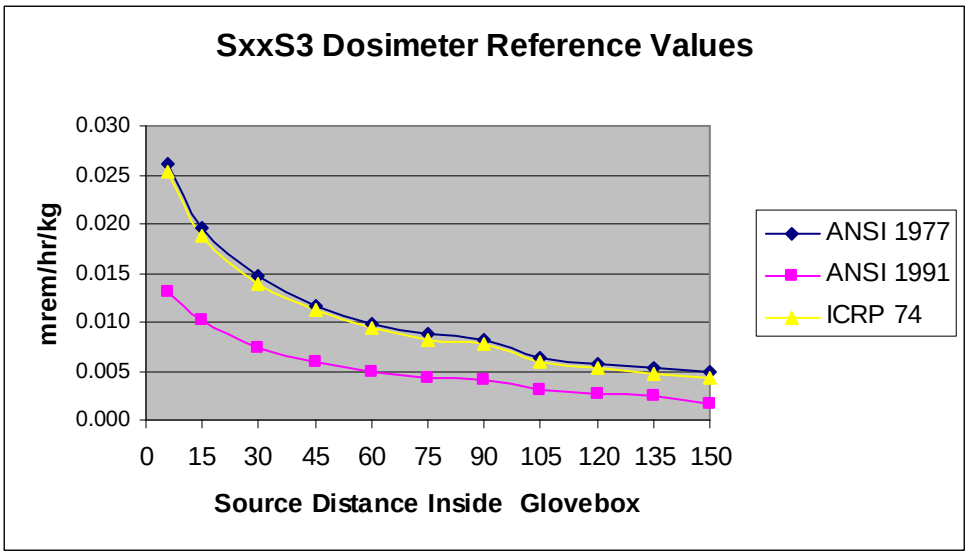

Figure F.4-5: SxxS3.

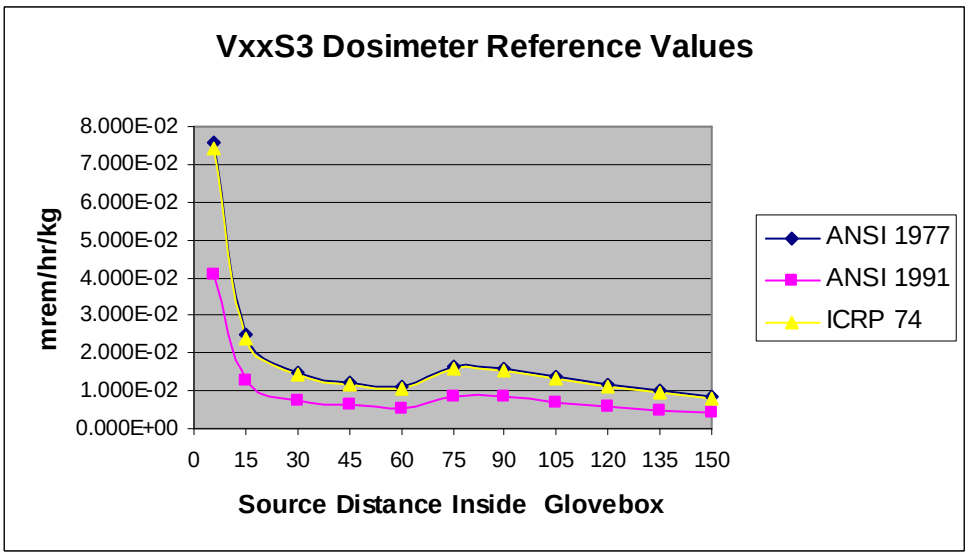

Figure F.4-6: VxxS3.

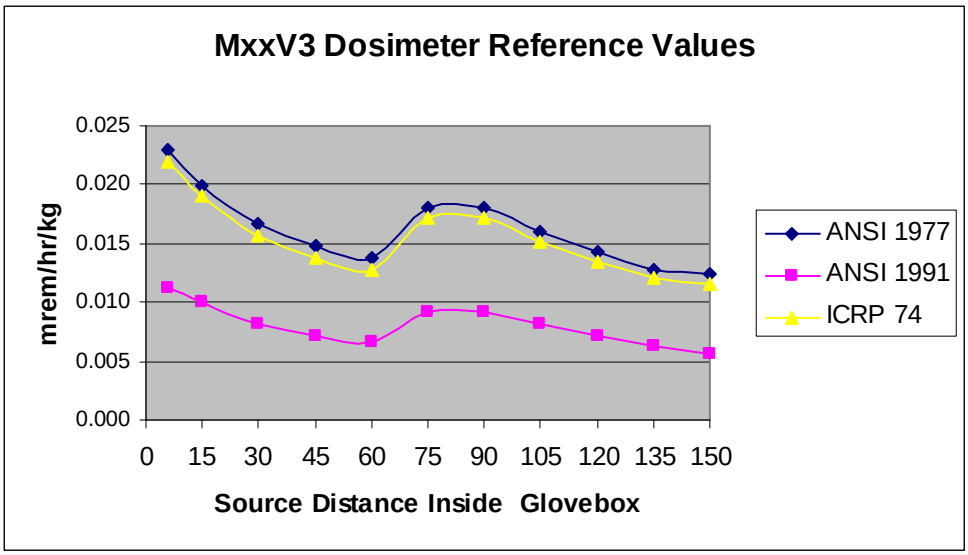

Figure F.4-7: MxxV3.

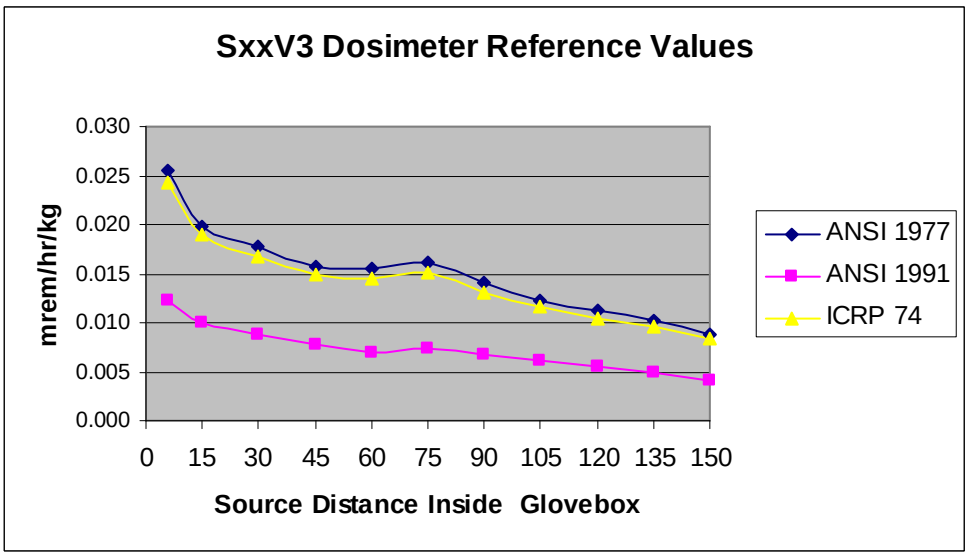

Figure F.4-8: SxxV3.

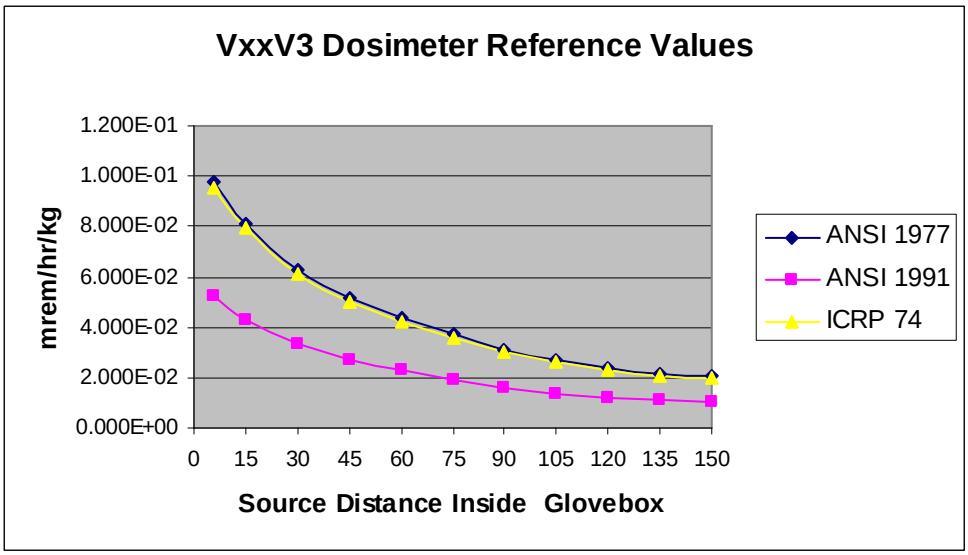

Figure F.4-9: VxxV3.

Appendix G: Comparison Of Whole Body Dose With Dosimeter With Various Tally Plane Doses

APPENDIX G.1:

ICRP 26 – ANSI 1977 AT 1 FOOT

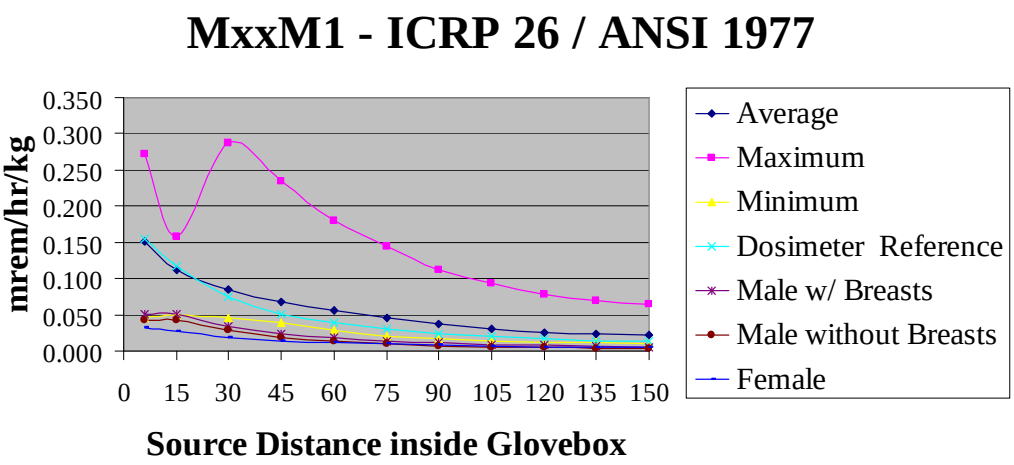

Figure G.1-1: MxxM1- ICRP 26 – ANSI 1977.

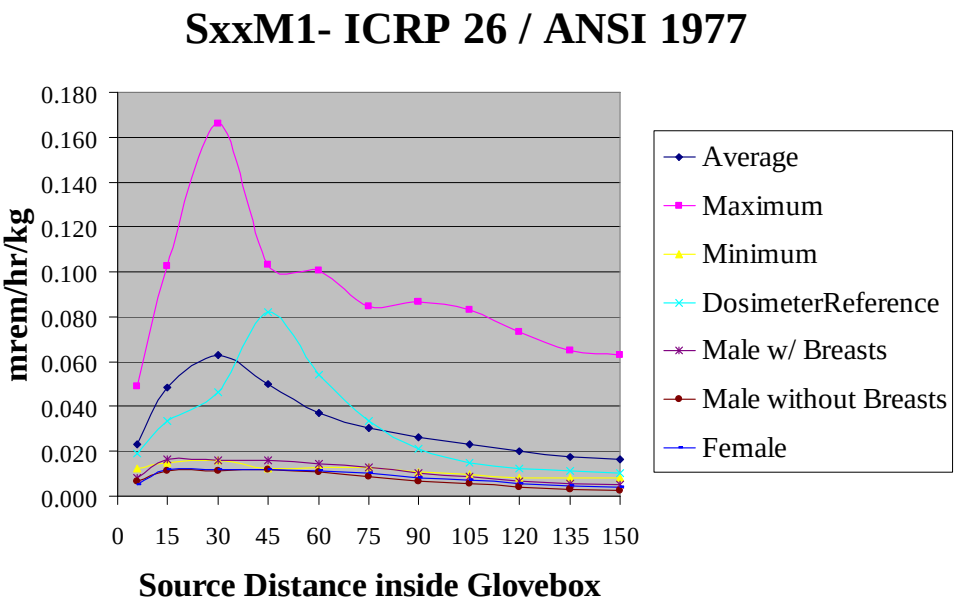

Figure G.1-2: SxxM1- ICRP 26 – ANSI 1977.

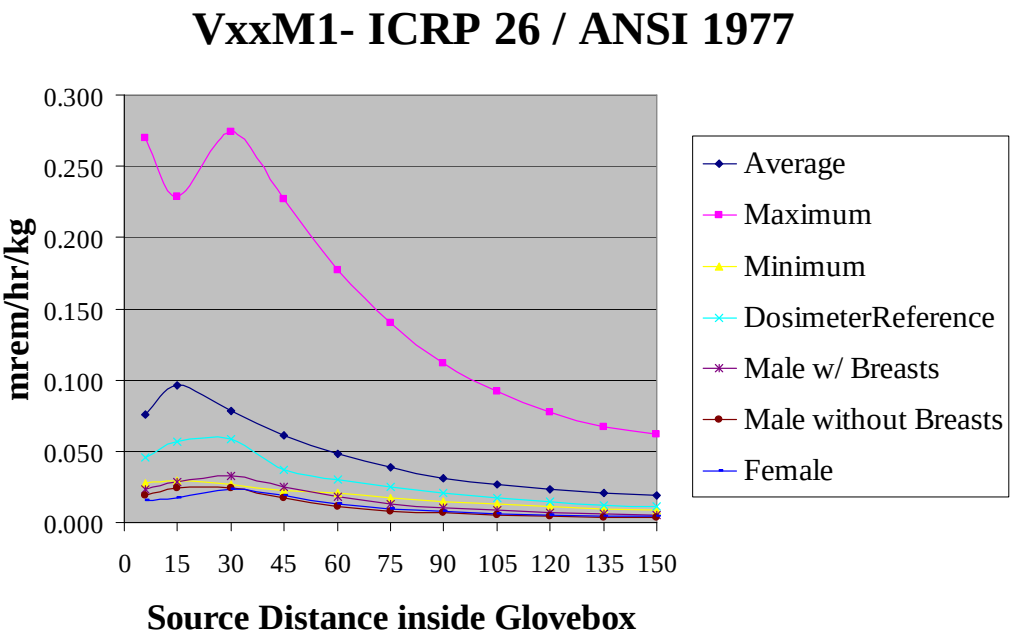

Figure G.1-3: VxxM1- ICRP 26 – ANSI 1977.

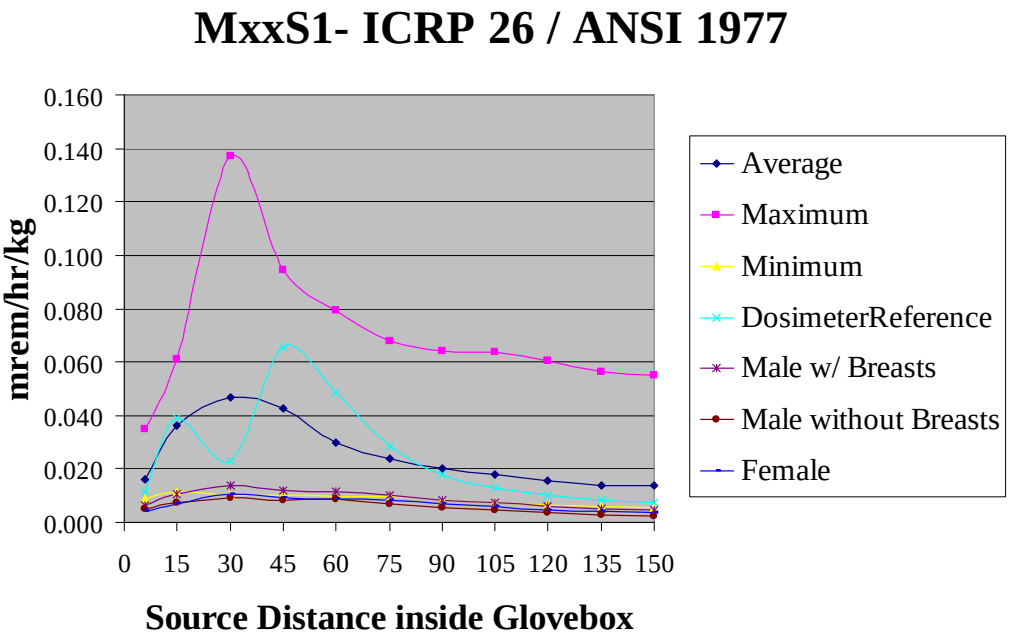

Figure G.1-4: MxxS1- ICRP 26 – ANSI 1977.

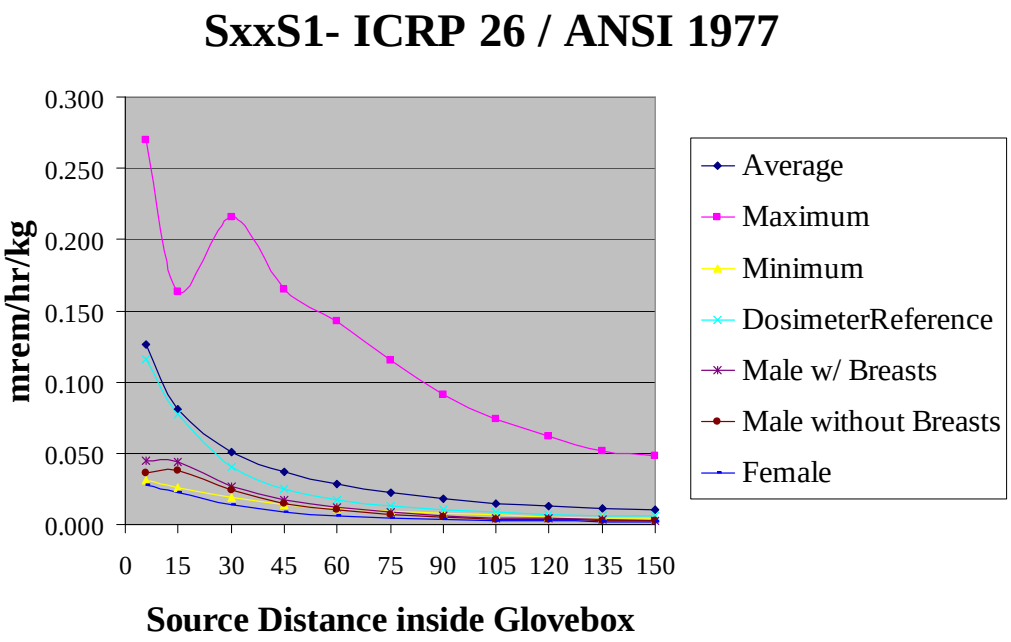

Figure G.1-5: SxxS1- ICRP 26 – ANSI 1977.

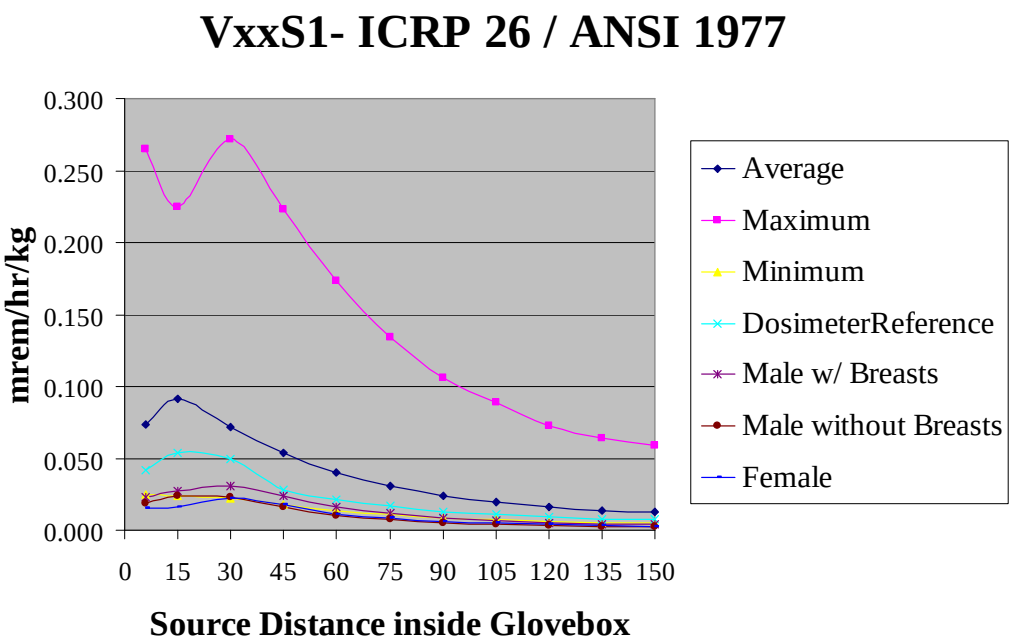

Figure G.1-6: VxxS1- ICRP 26 – ANSI 1977.

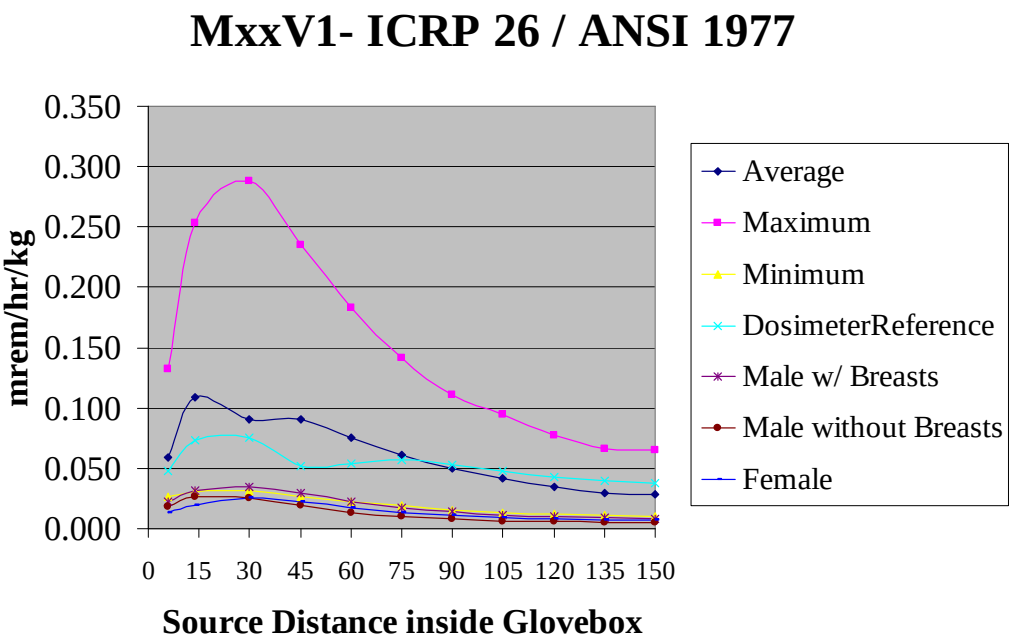

Figure G.1-7: MxxV1- ICRP 26 – ANSI 1977.

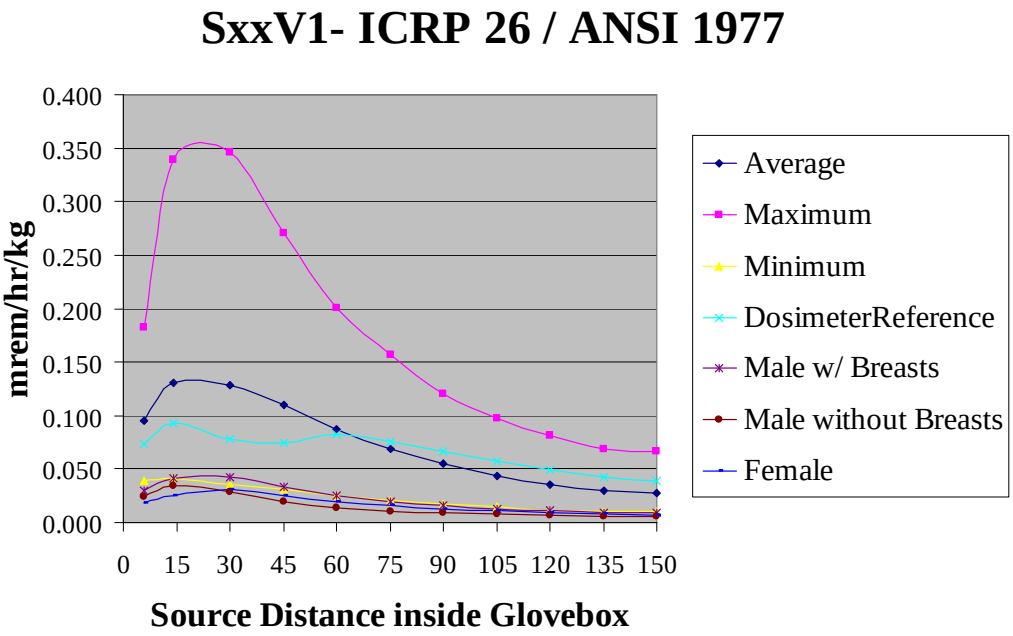

Figure G.1-8: SxxV1- ICRP 26 – ANSI 1977.

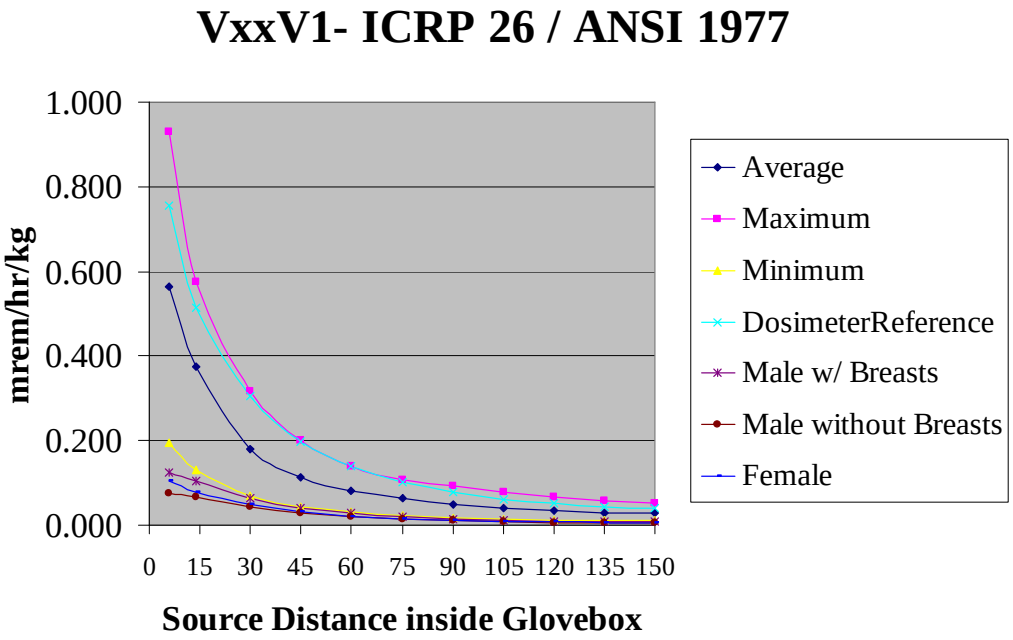

Figure G.1-9: VxxV1- ICRP 26 – ANSI 1977.

APPENDIX G.2:

ICRP 26 – ANSI 1991 AT 1 FOOT

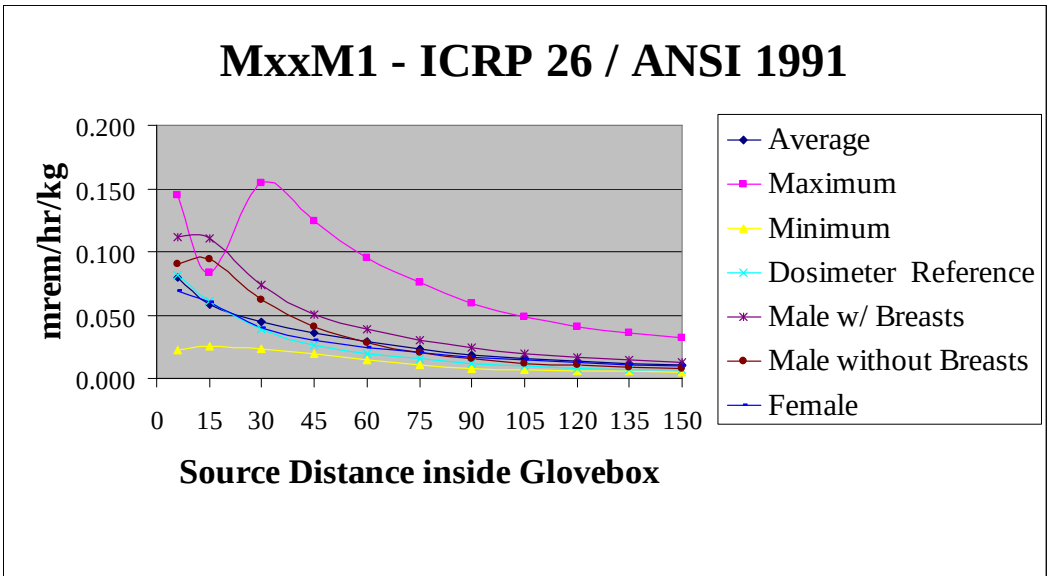

Figure G.2-1: MxxM1- ICRP 26 – ANSI 1991.

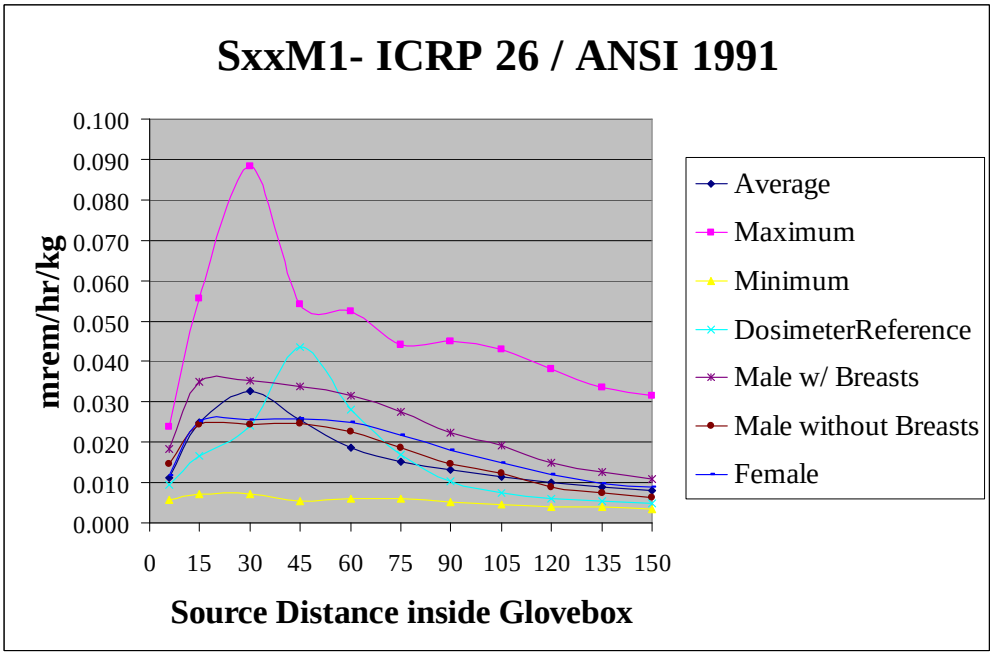

Figure G.2-2: SxxM1- ICRP 26 – ANSI 1991.

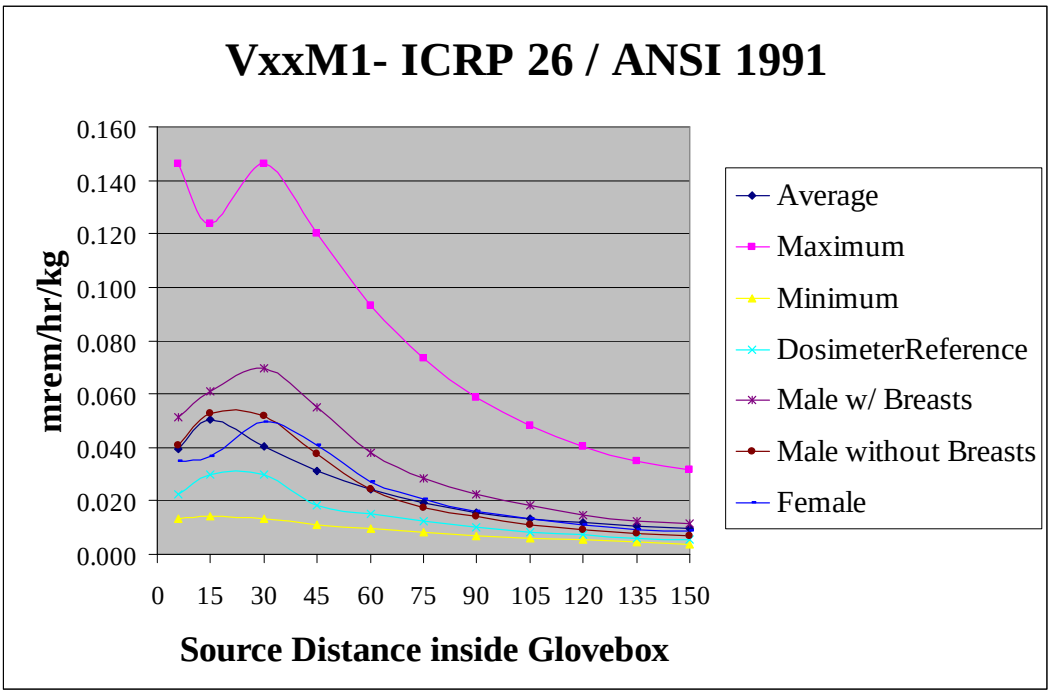

Figure G.2-3: VxxM1- ICRP 26 – ANSI 1991.

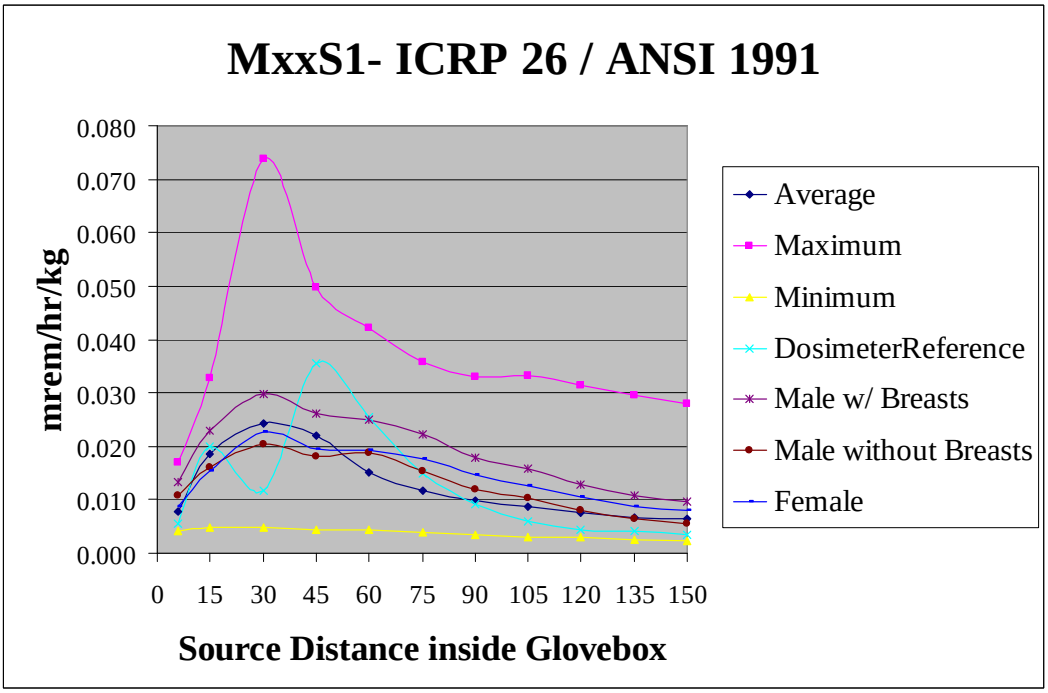

Figure G.2-4: MxxS1- ICRP 26 – ANSI 1991.

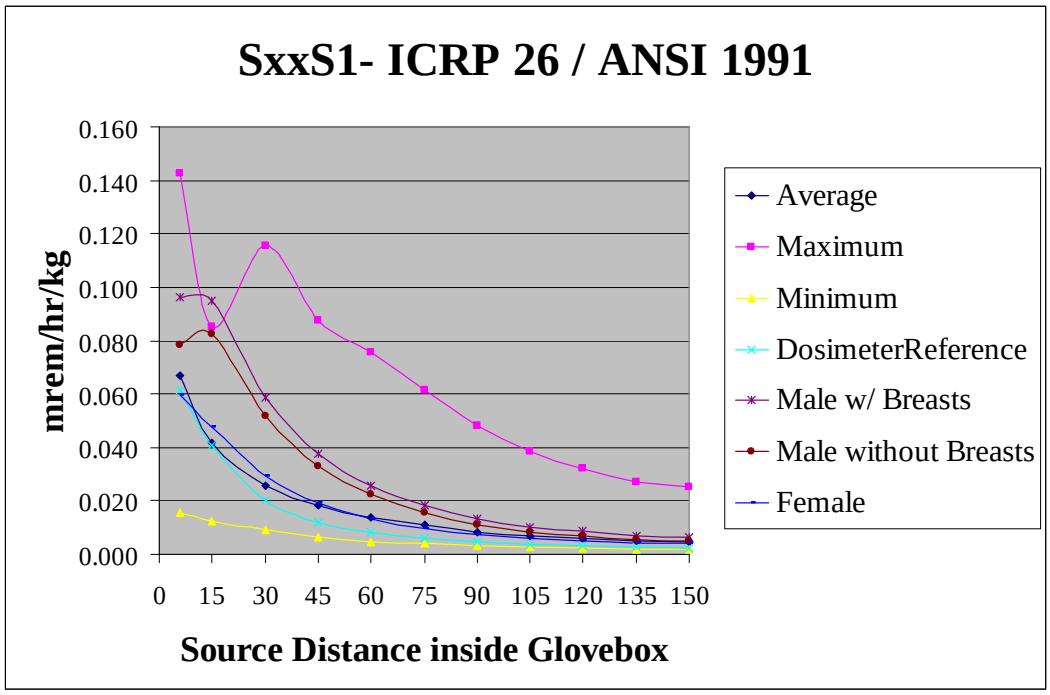

Figure G.2-5: SxxS1- ICRP 26 – ANSI 1991.

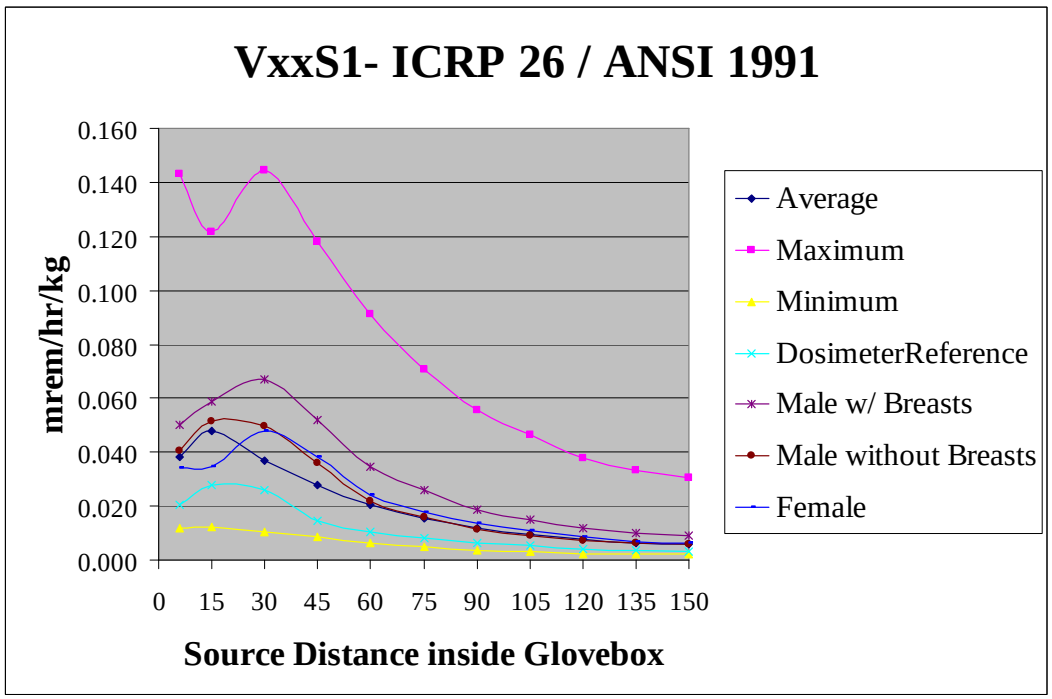

Figure G.2-6: VxxS1- ICRP 26 – ANSI 1991.

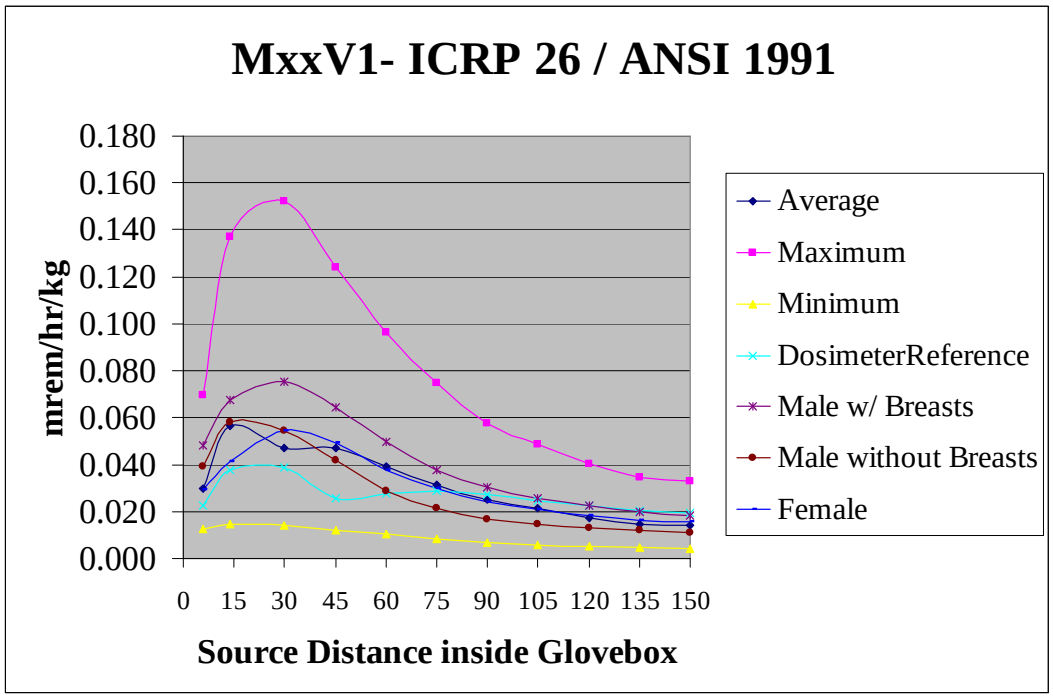

Figure G.2-7: MxxV1- ICRP 26 – ANSI 1991.

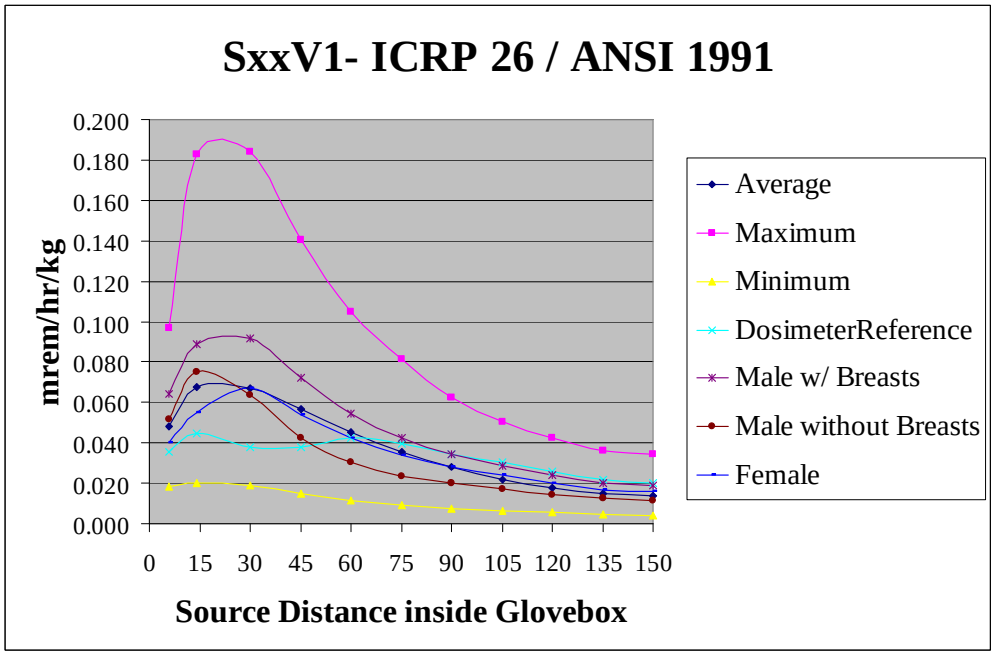

Figure G.2-8: SxxV1- ICRP 26 – ANSI 1991.

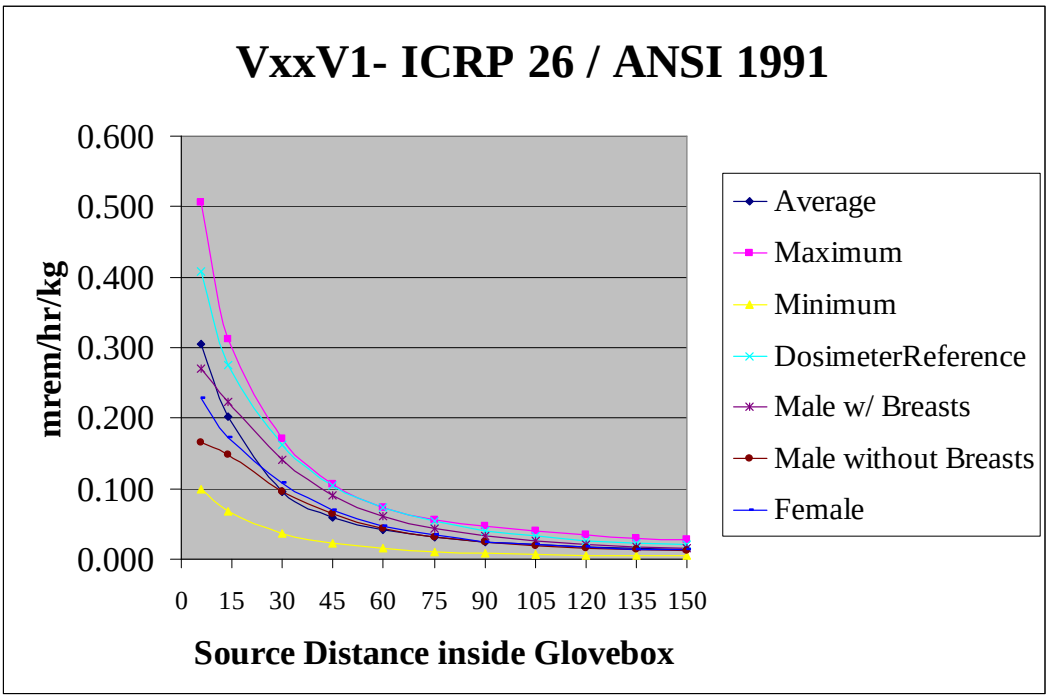

Figure G.2-9: VxxV1- ICRP 26 – ANSI 1991.

APPENDIX G.3:

ICRP 60 – ANSI 1991 AT 1 FOOT

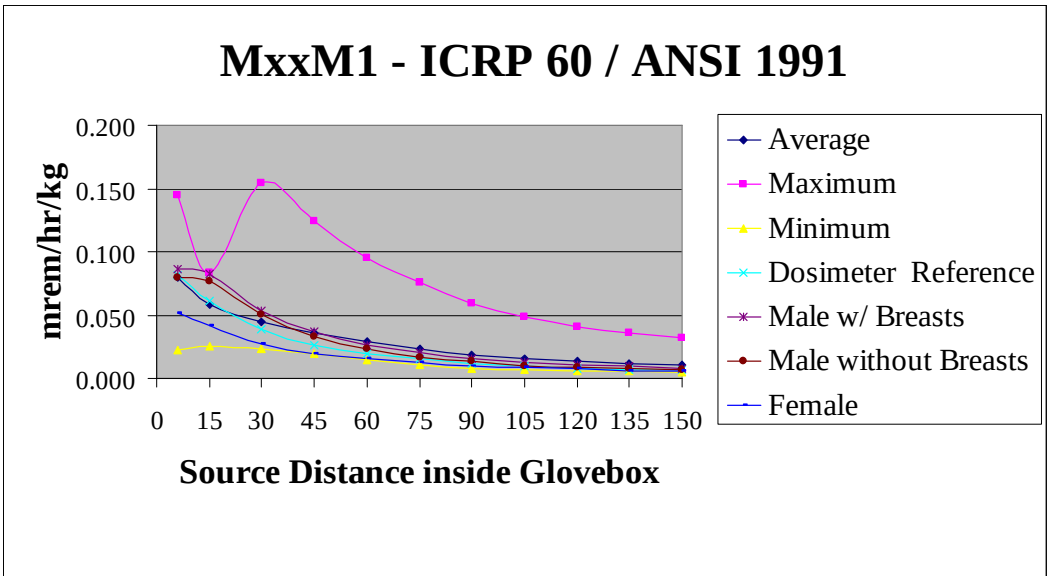

Figure G.3-1: MxxM1- ICRP 60 – ANSI 1991.

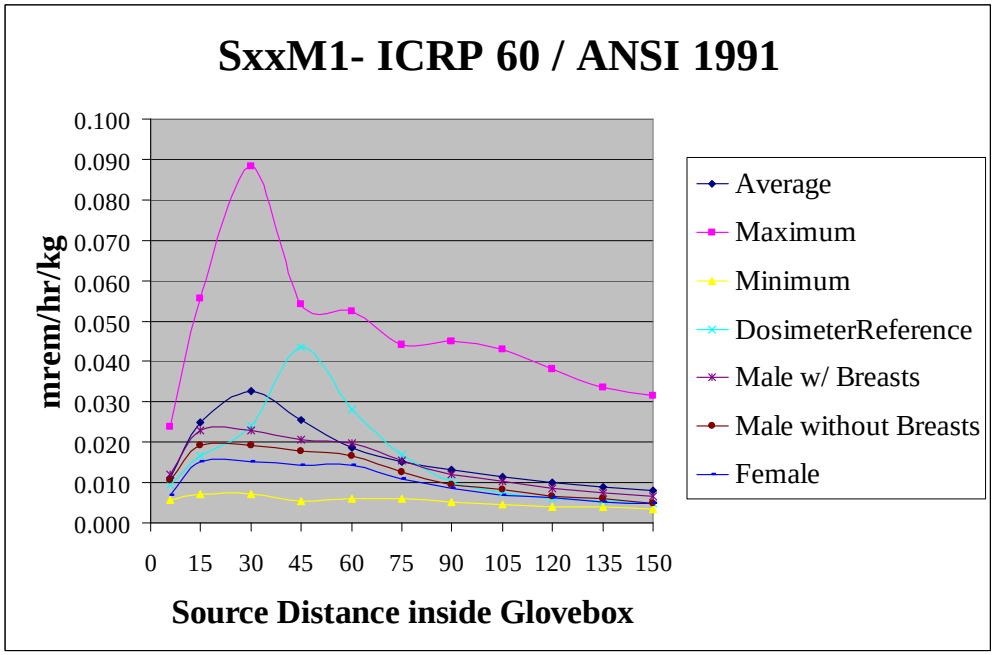

Figure G.3-2: SxxM1- ICRP 60 – ANSI 1991.

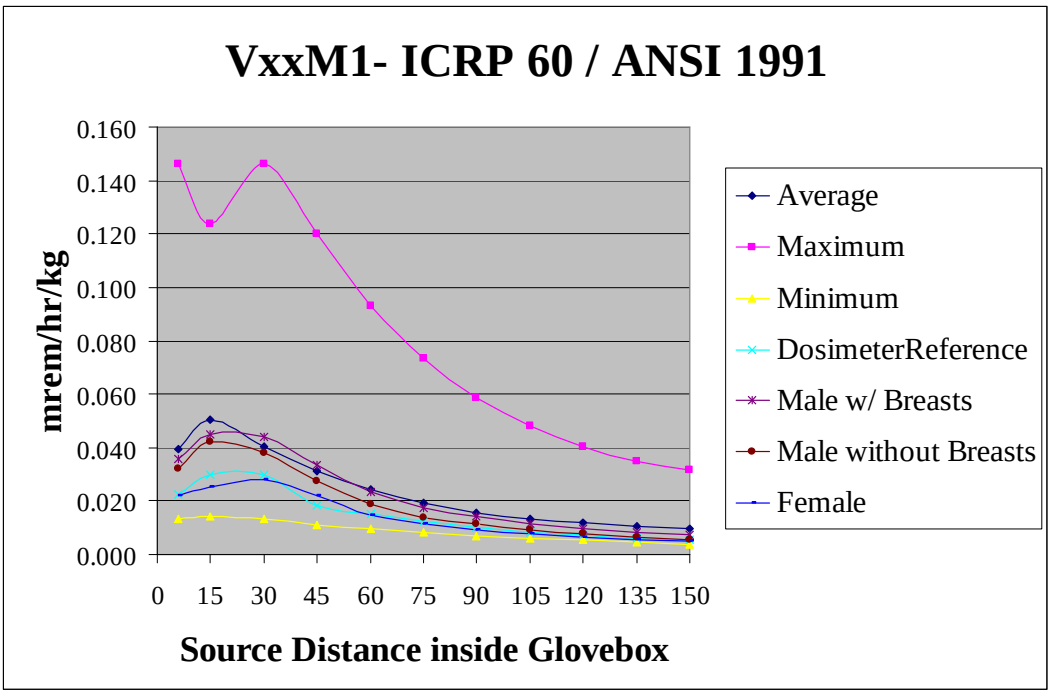

Figure G.3-3: VxxM1- ICRP 60 – ANSI 1991.

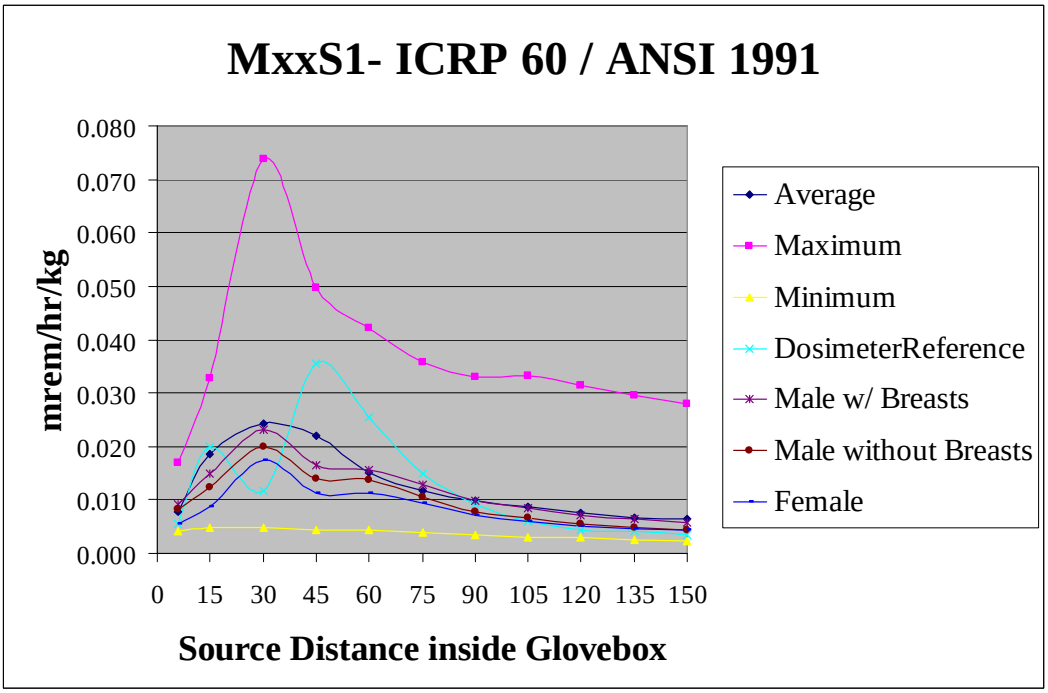

Figure G.3-4: MxxS1- ICRP 60 – ANSI 1991.

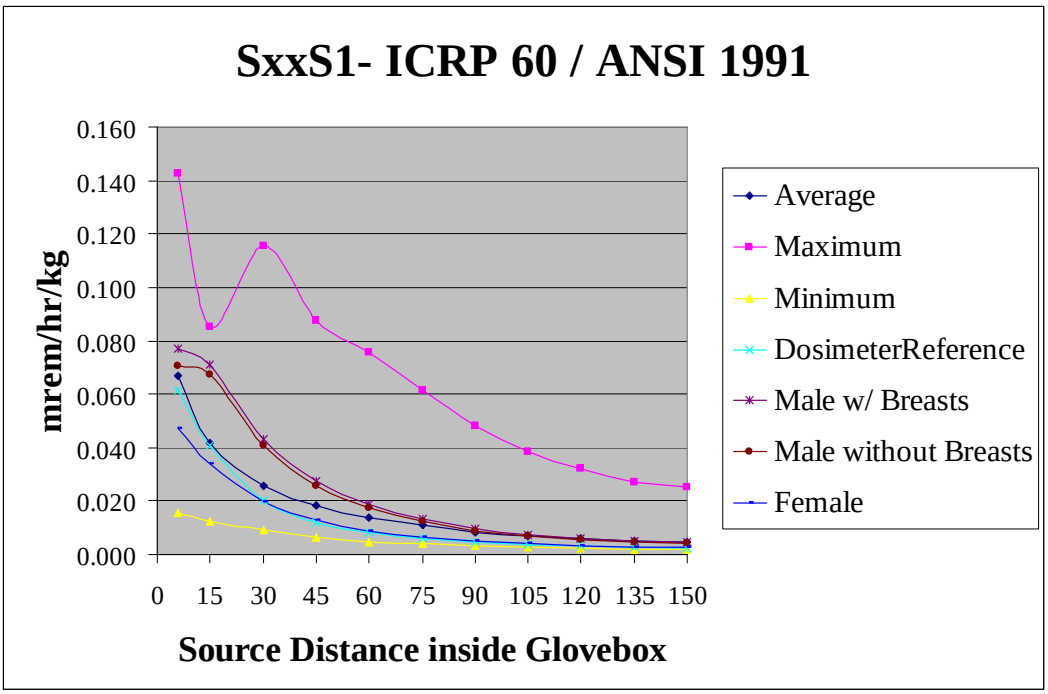

Figure G.3-5: SxxS1- ICRP 60 – ANSI 1991.

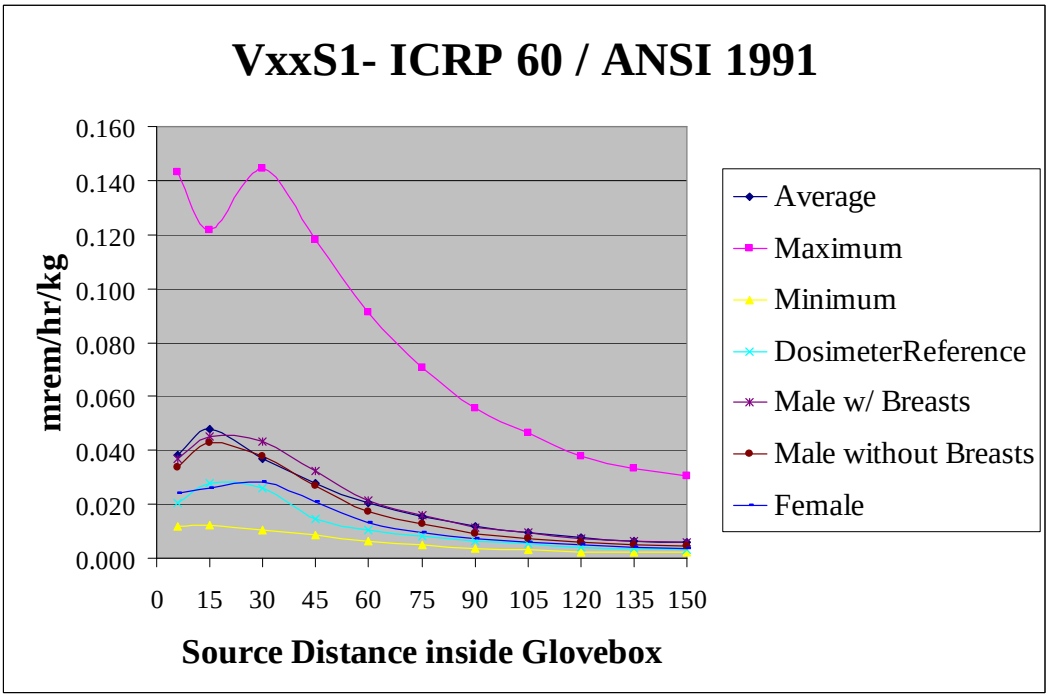

Figure G.3-6: VxxS1- ICRP 60 – ANSI 1991.

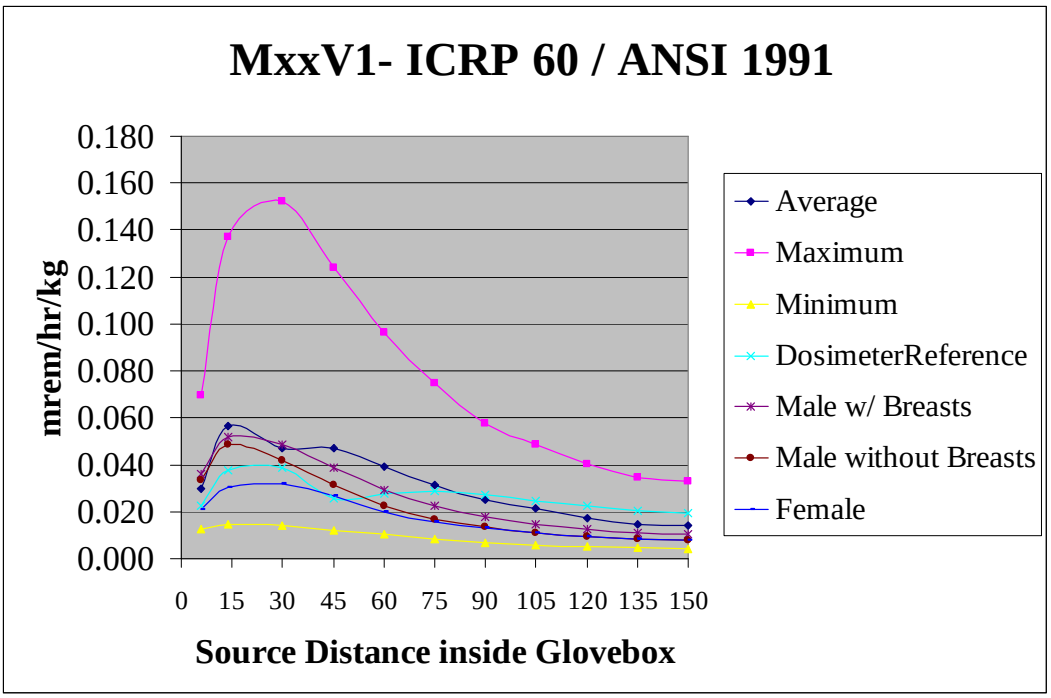

Figure G.3-7: MxxV1- ICRP 60 – ANSI 1991.

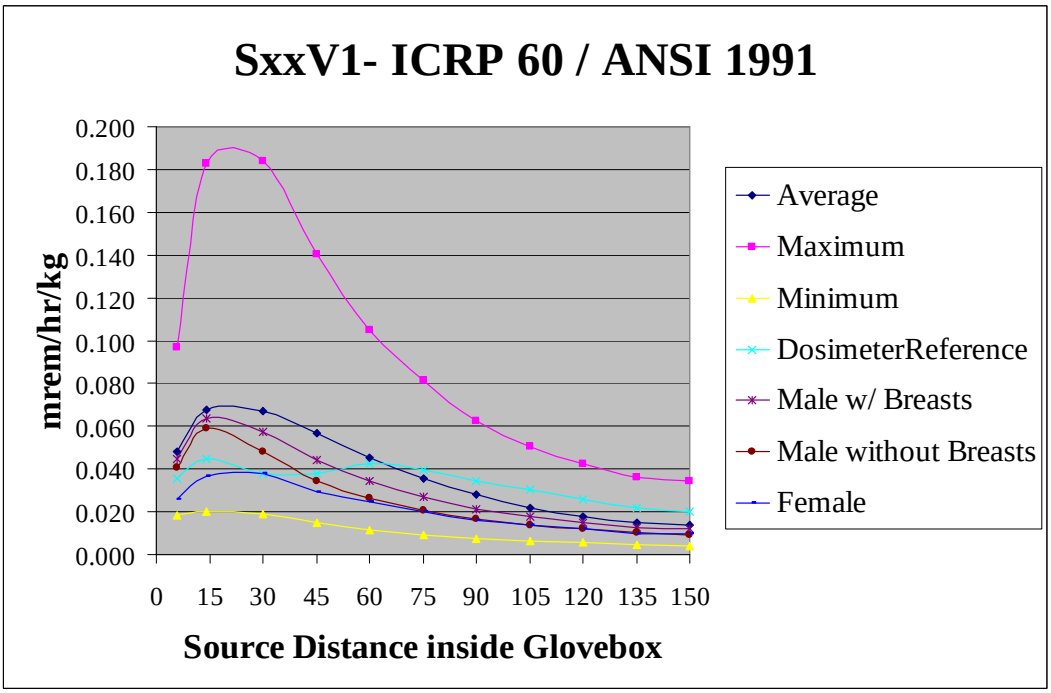

Figure G.3-8: SxxV1- ICRP 60 – ANSI 1991.

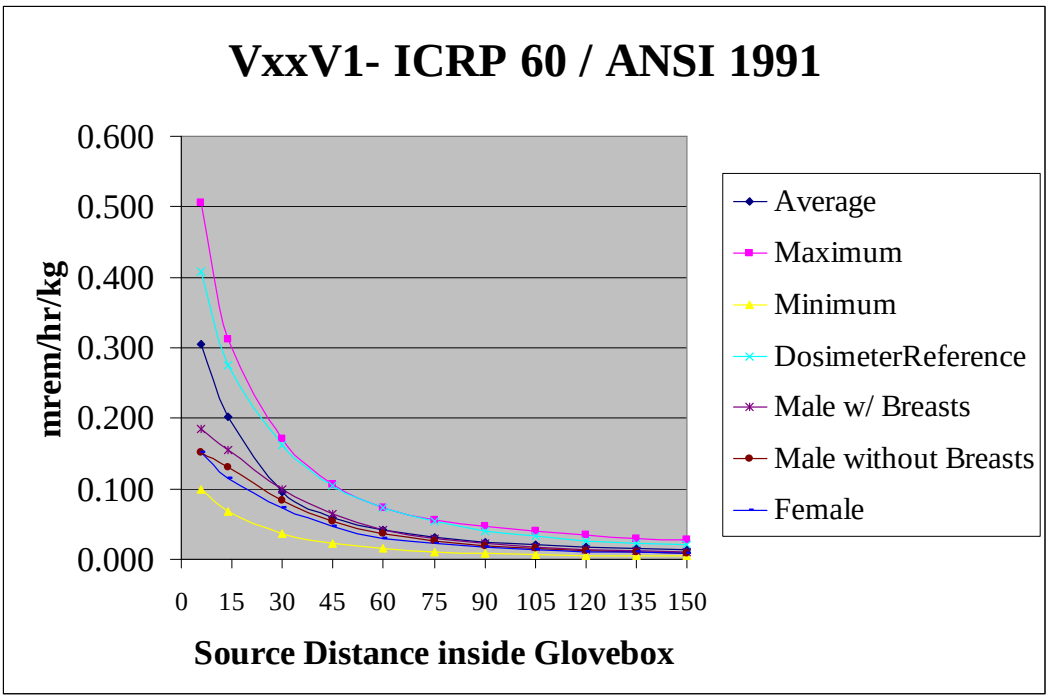

Figure G.3-9: VxxV1- ICRP 60 – ANSI 1991.

APPENDIX G.4:

ICRP 60 – ICRP 74 AT 1 FOOT

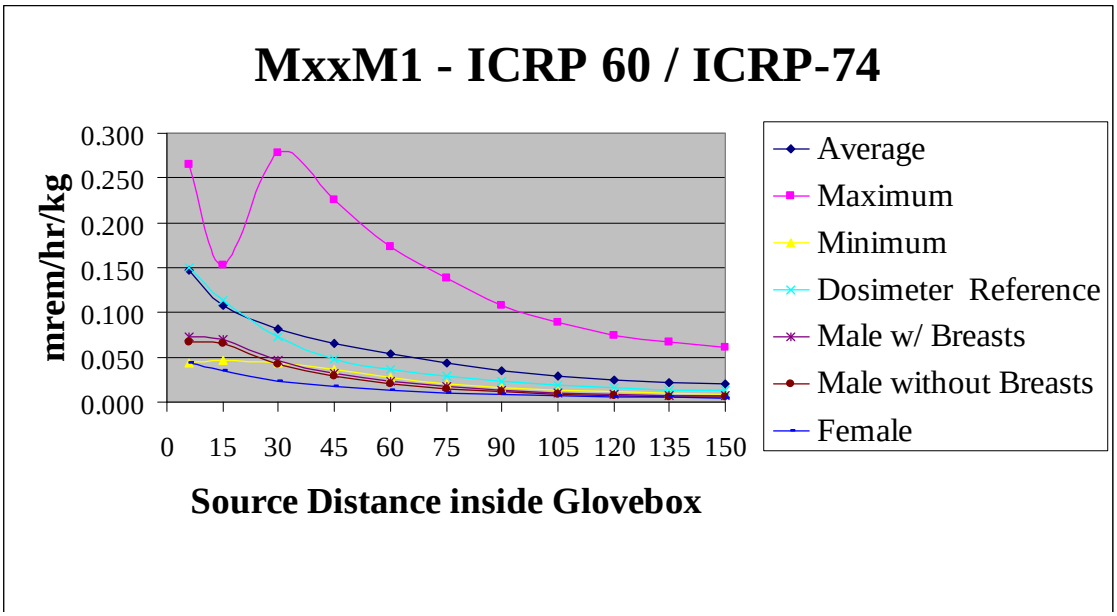

Figure G.4-1: MxxM1- ICRP 60 – ICRP 74.

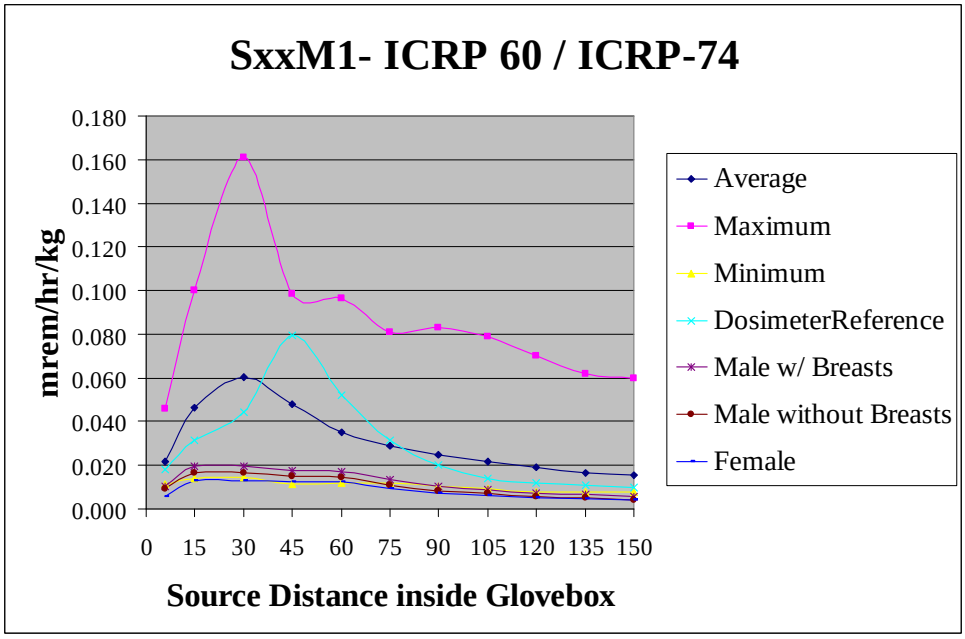

Figure G.4-2: SxxM1- ICRP 60 – ICRP 74.

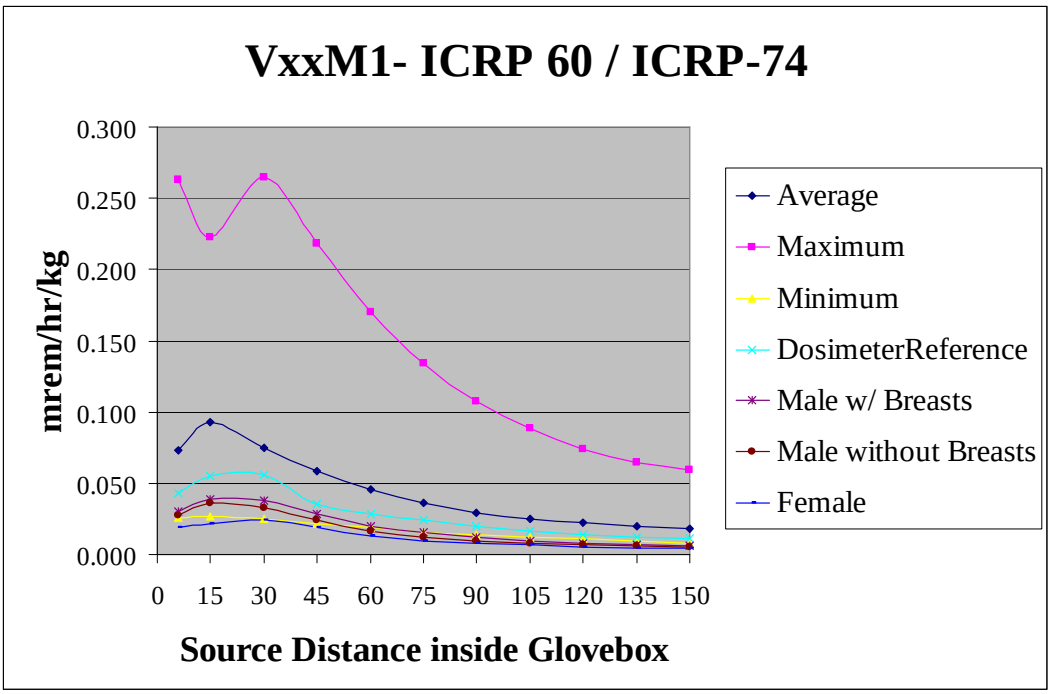

Figure G.4-3: VxxM1- ICRP 60 – ICRP 74.

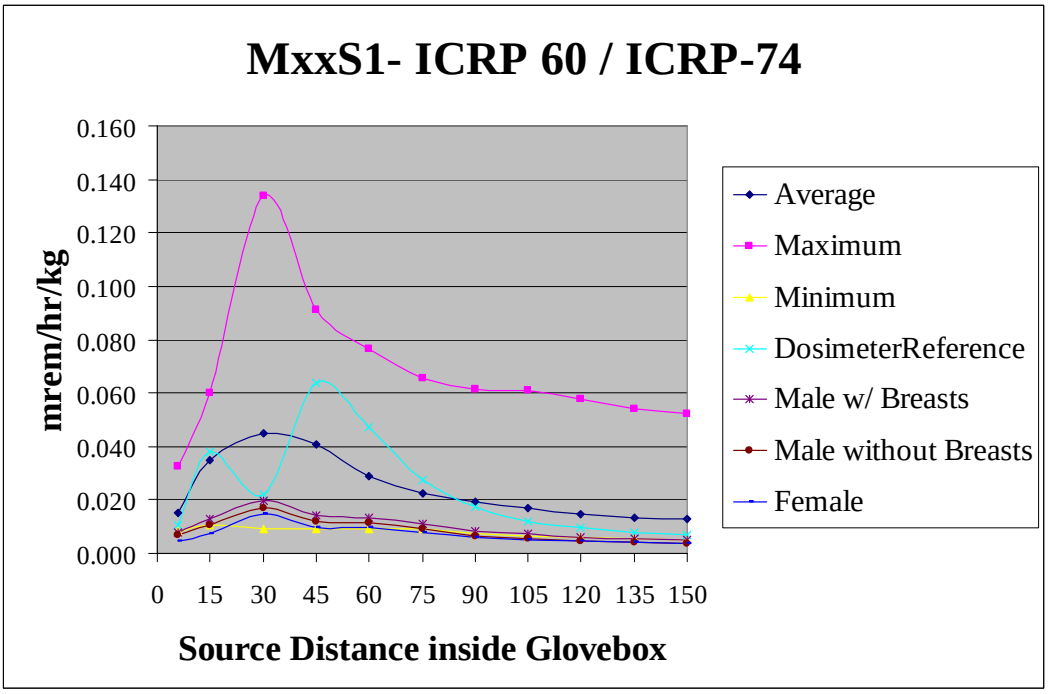

Figure G.4-4: MxxS1- ICRP 60 – ICRP 74.

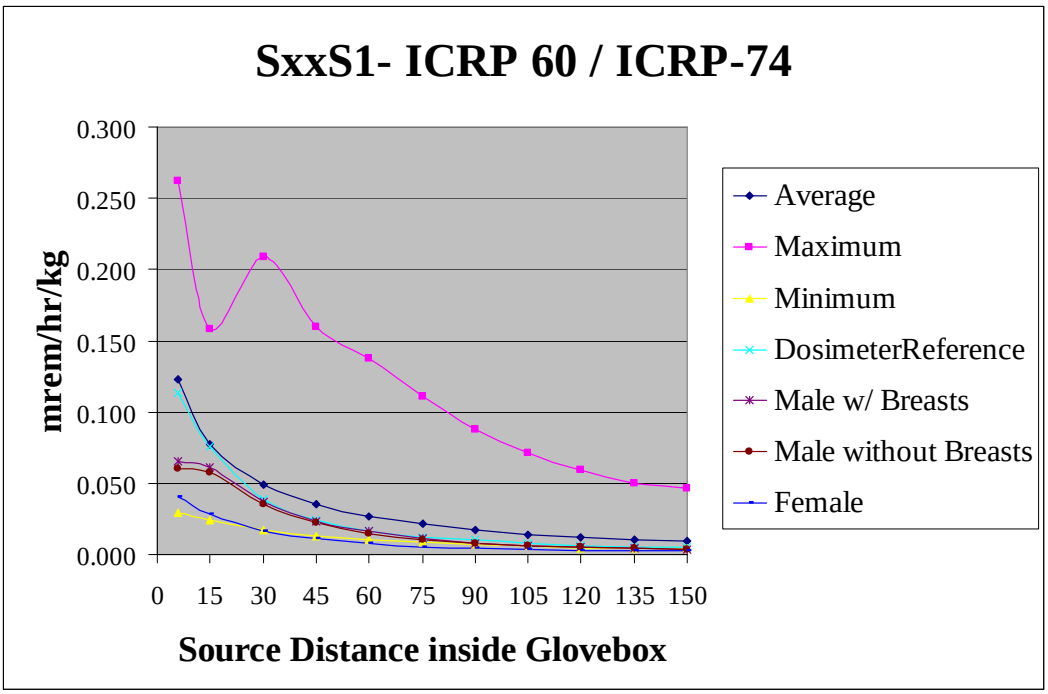

Figure G.4-5: SxxS1- ICRP 60 – ICRP 74.

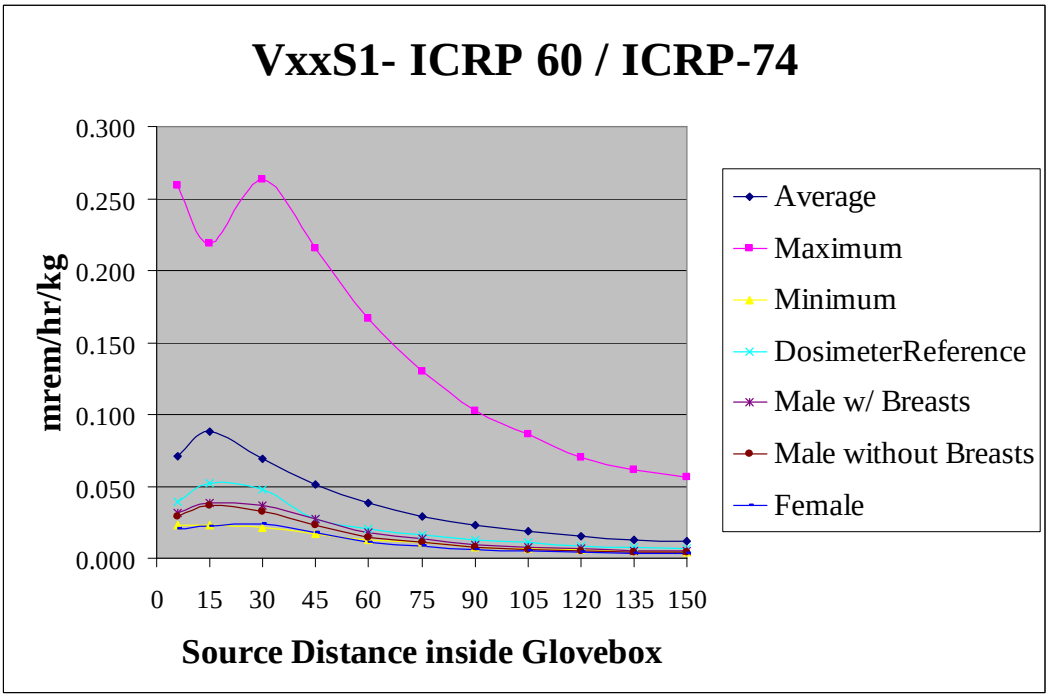

Figure G.4-6: VxxS1- ICRP 60 – ICRP 74.

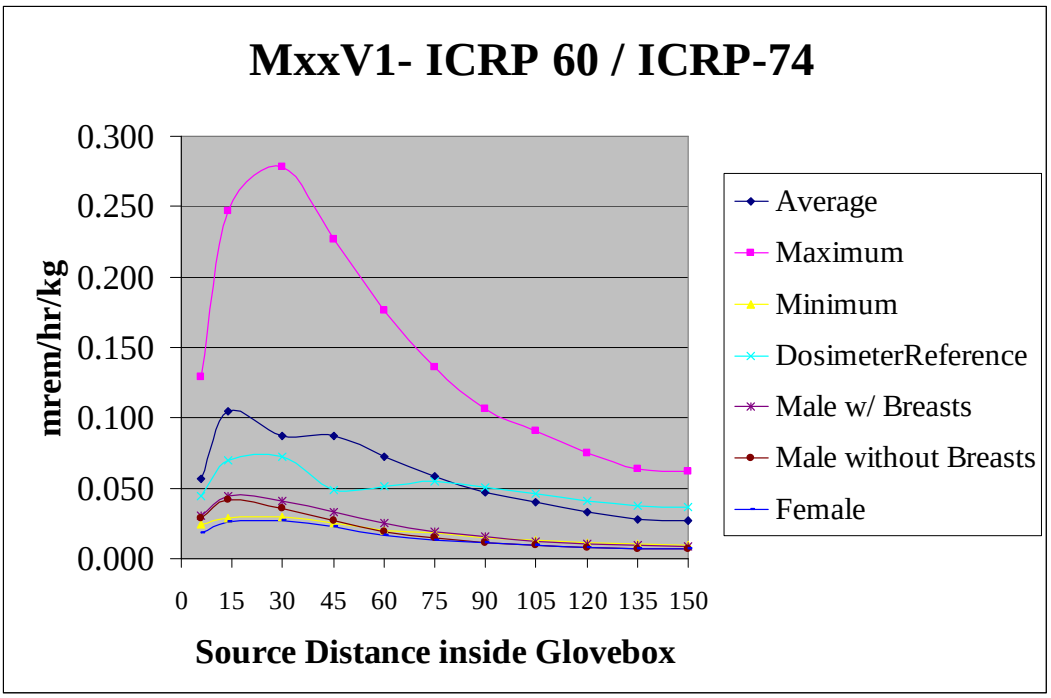

Figure G.4-7: MxxV1- ICRP 60 – ICRP 74.

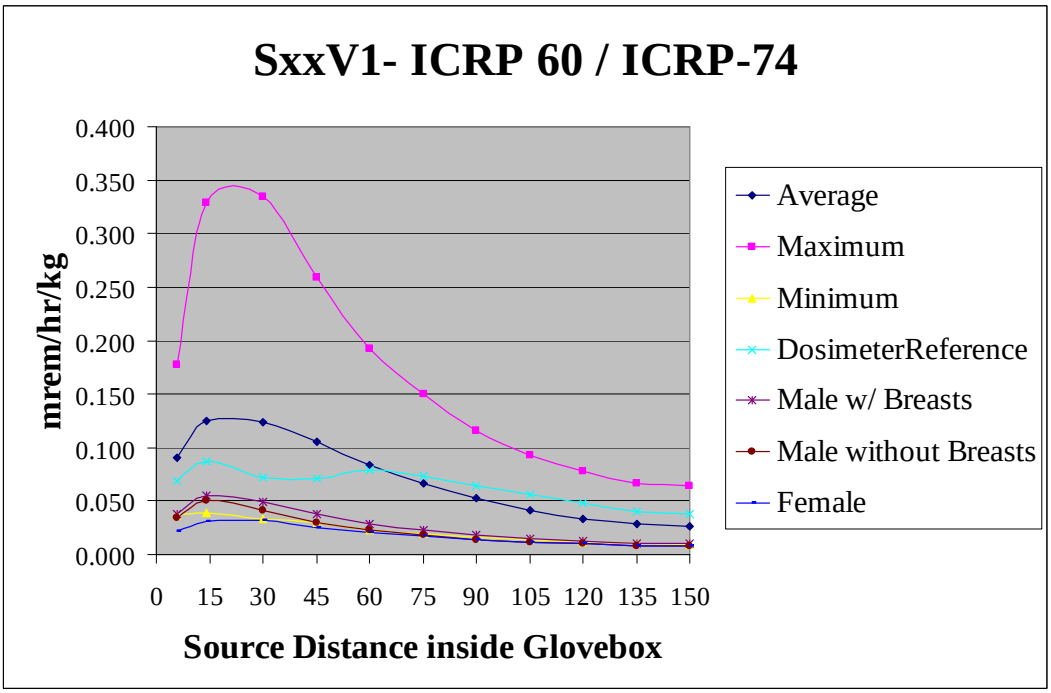

Figure G.4-8: SxxV1- ICRP 60 – ICRP 74.

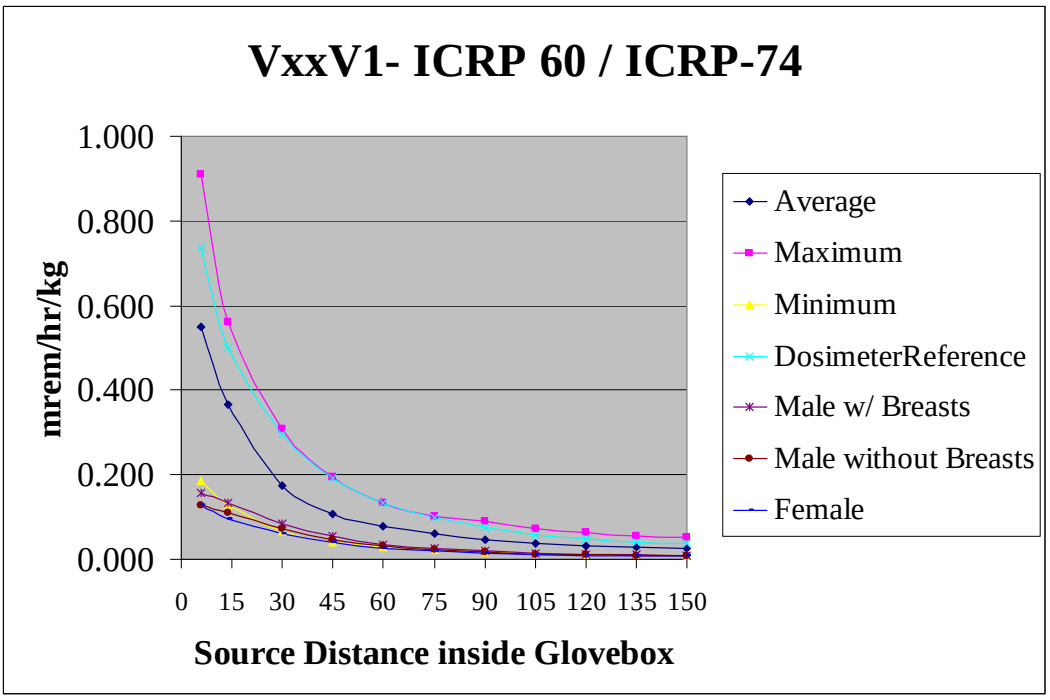

Figure G.4-9: VxxV1 ICRP 60 – ICRP 74.

APPENDIX G.5:

ICRP 26 – ANSI 1977 AT 3 FOOT

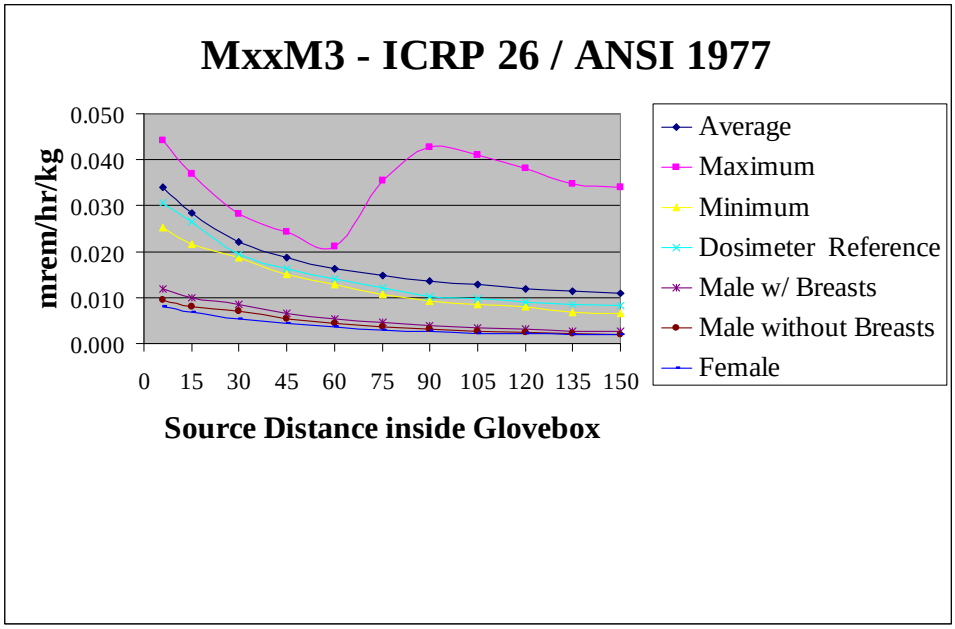

Figure G.5-1: MxxM3- ICRP 26 – ANSI 1977.

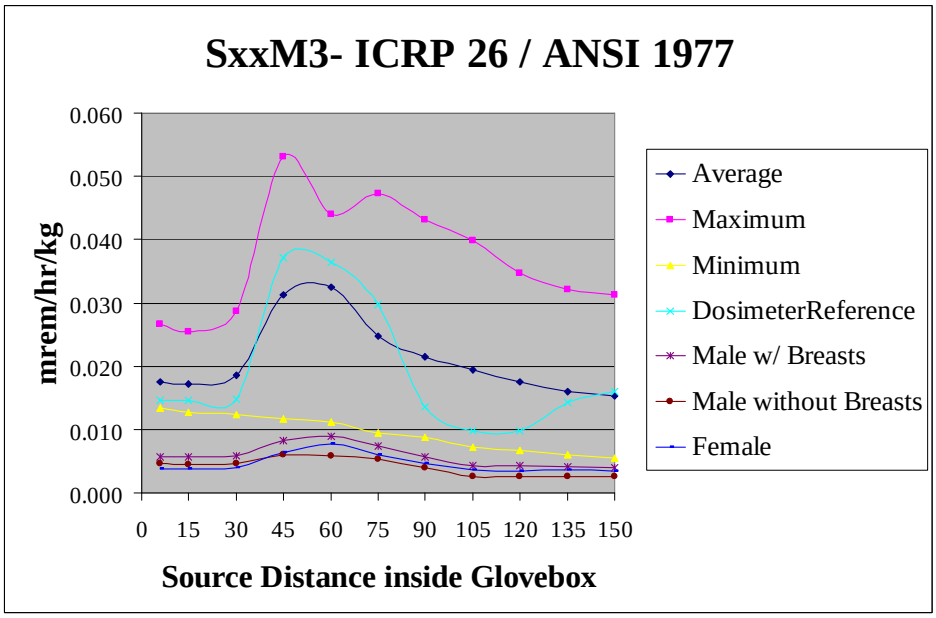

Figure G.5-2: SxxM3- ICRP 26 – ANSI 1977.

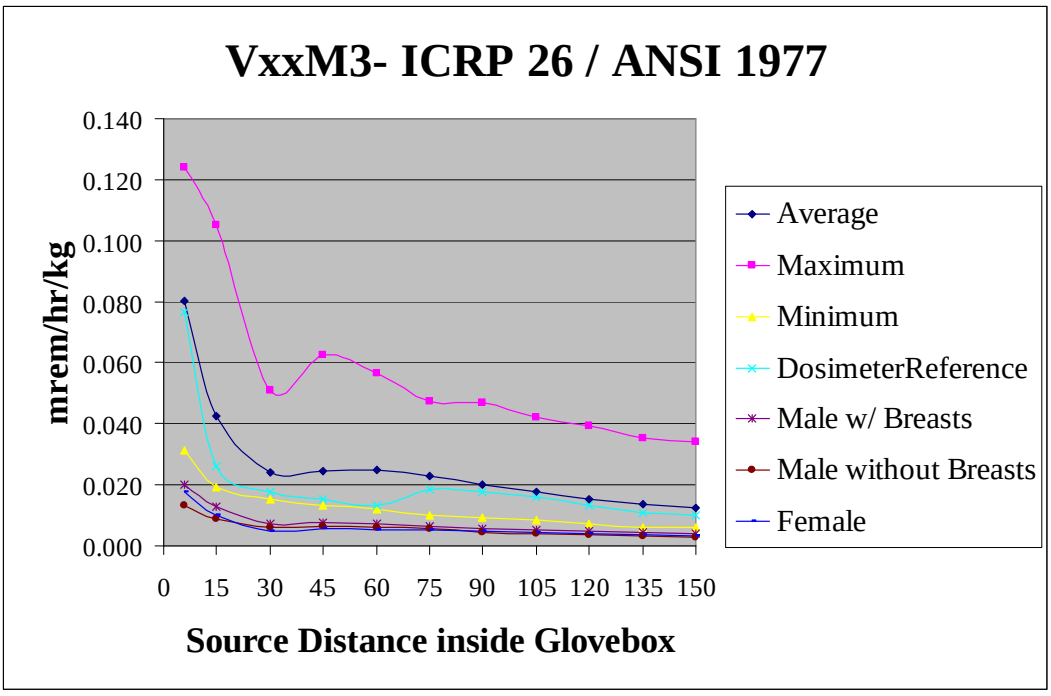

Figure G.5-3: VxxM3- ICRP 26 – ANSI 1977.

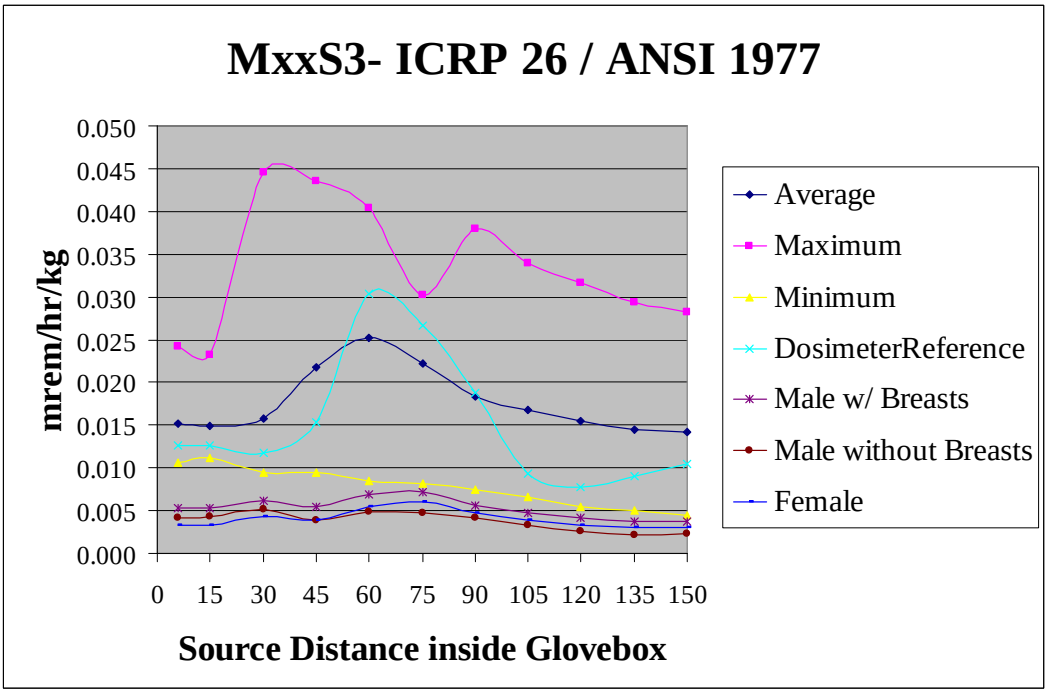

Figure G.5-4: MxxS3- ICRP 26 – ANSI 1977.

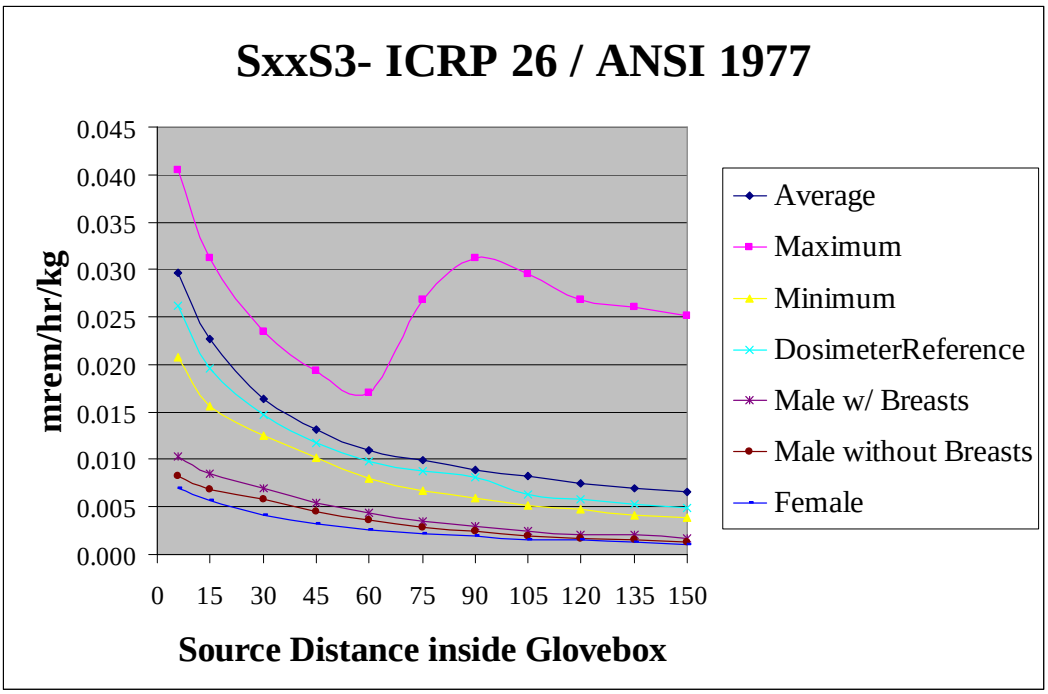

Figure G.5-5: SxxS3- ICRP 26 – ANSI 1977.

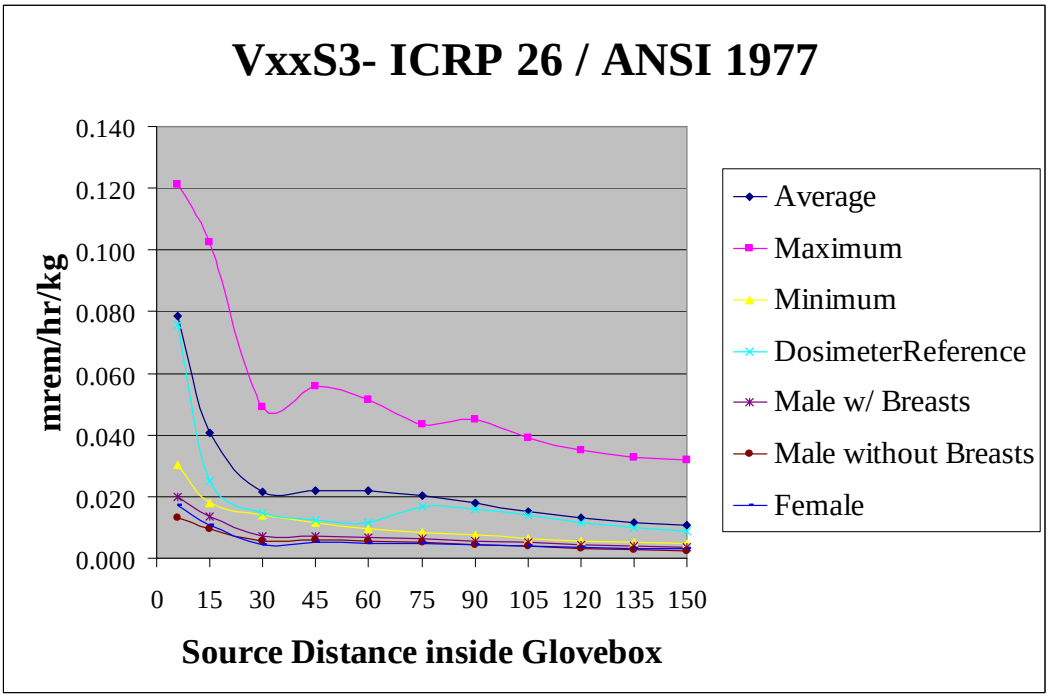

Figure G.5-6: VxxS3- ICRP 26 – ANSI 1977.

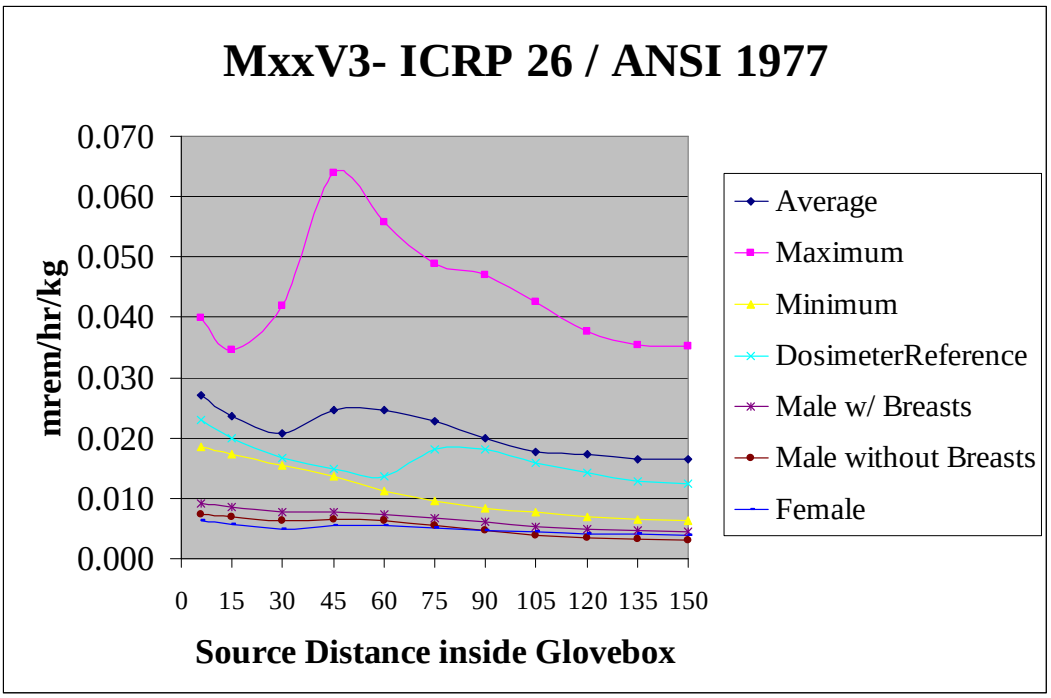

Figure G.5-7: MxxV3- ICRP 26 – ANSI 1977.

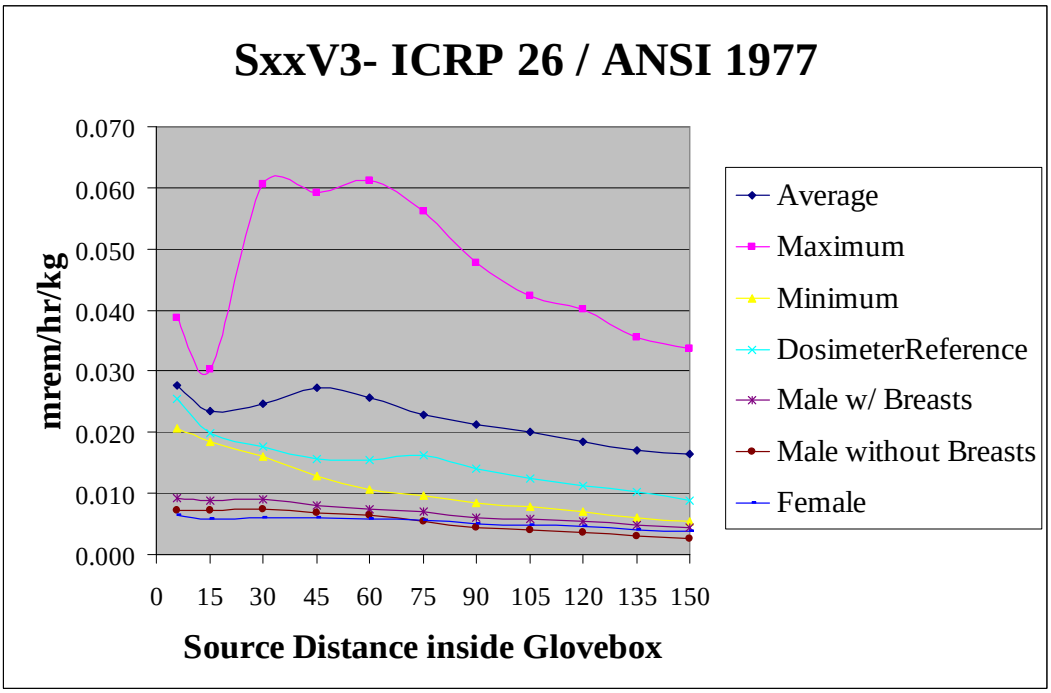

Figure G.5-8: SxxV3- ICRP 26 – ANSI 1977.

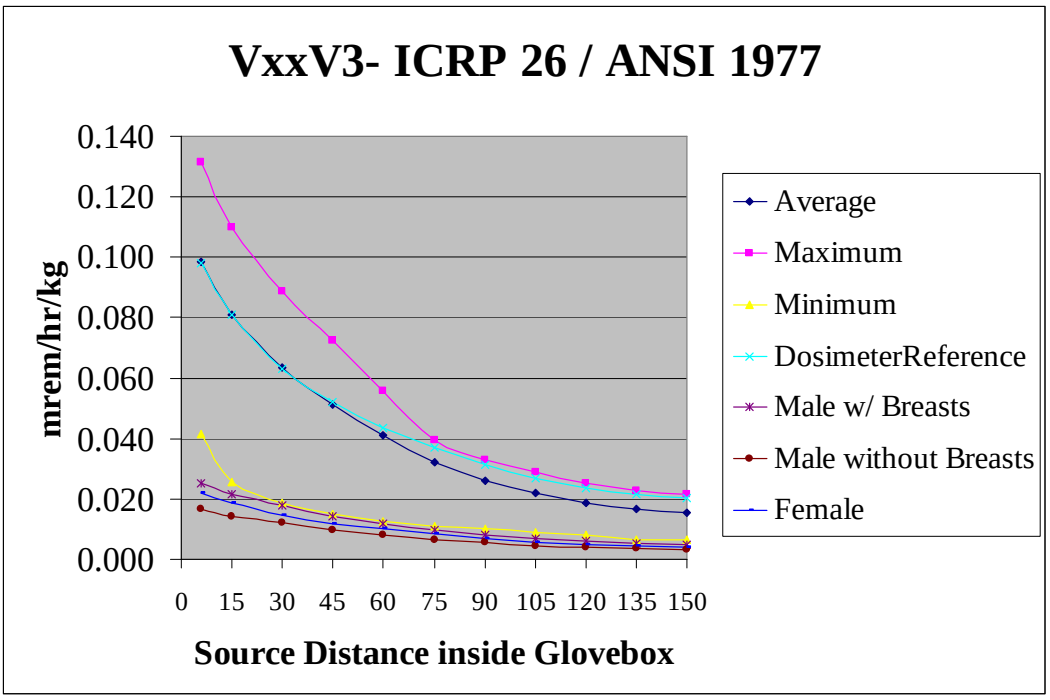

Figure G.5-9: VxxV3- ICRP 26 – ANSI 1977.

APPENDIX G.6:

ICRP 26 – ANSI 1991 AT 3 FOOT

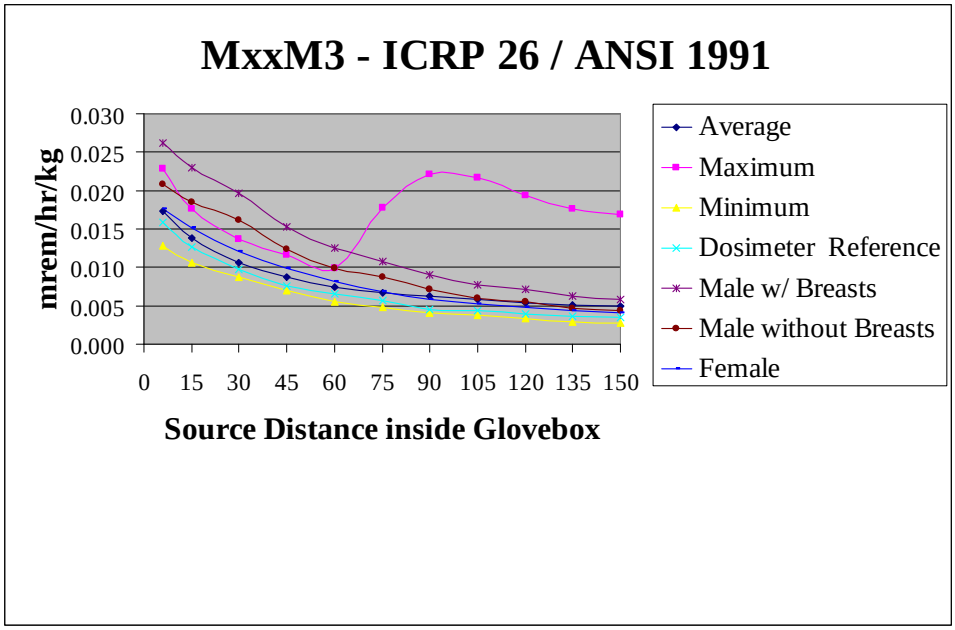

Figure G.6-1: MxxM3- ICRP 26 – ANSI 1991.

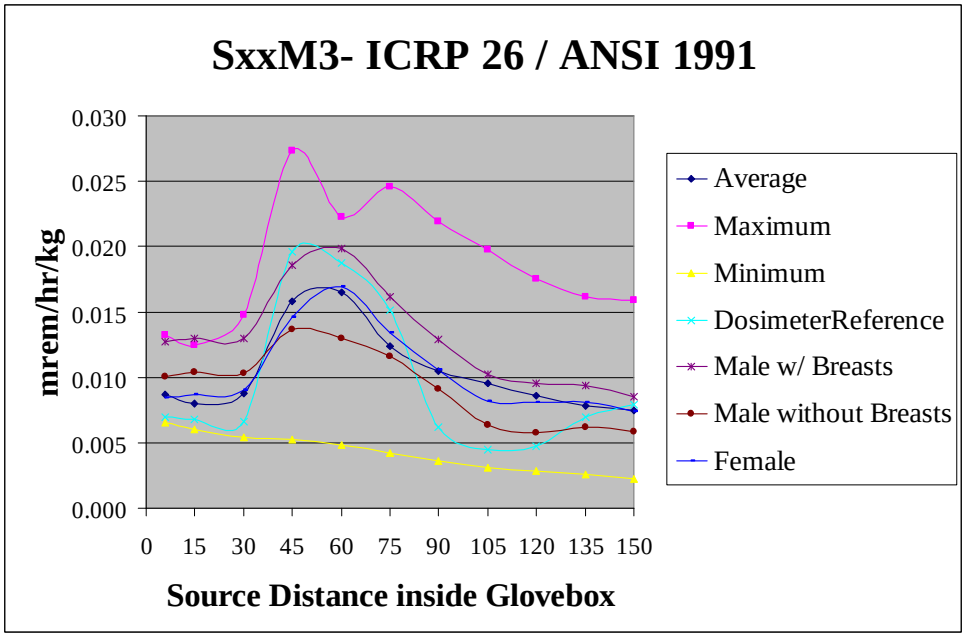

Figure G.6-2: SxxM3- ICRP 26 – ANSI 1991.

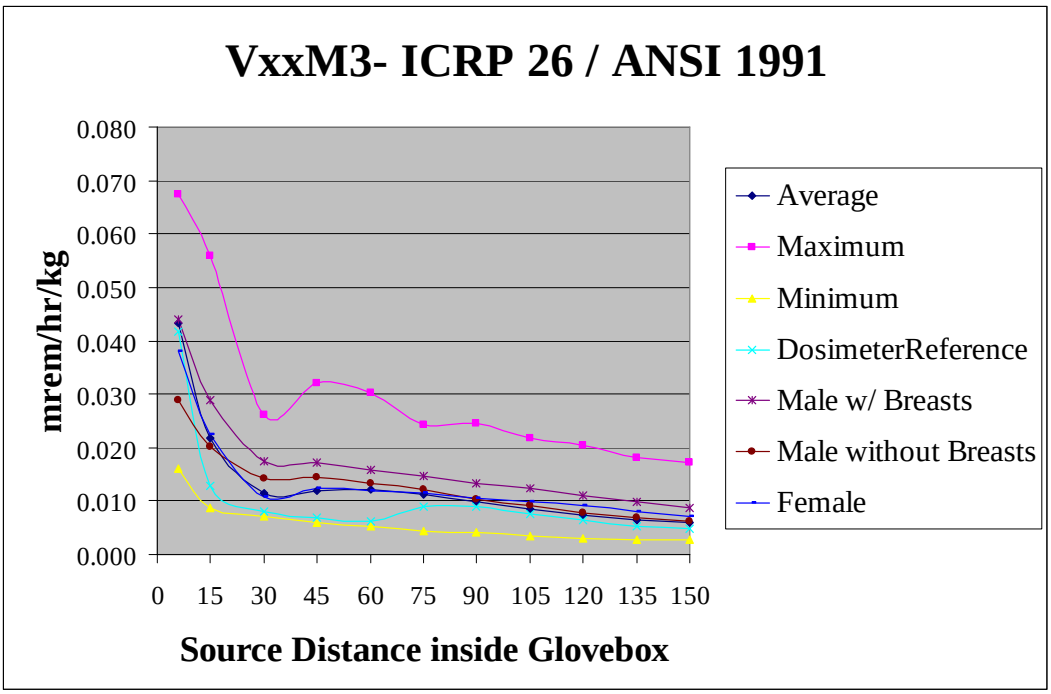

Figure G.6-3: VxxM3- ICRP 26 – ANSI 1991.

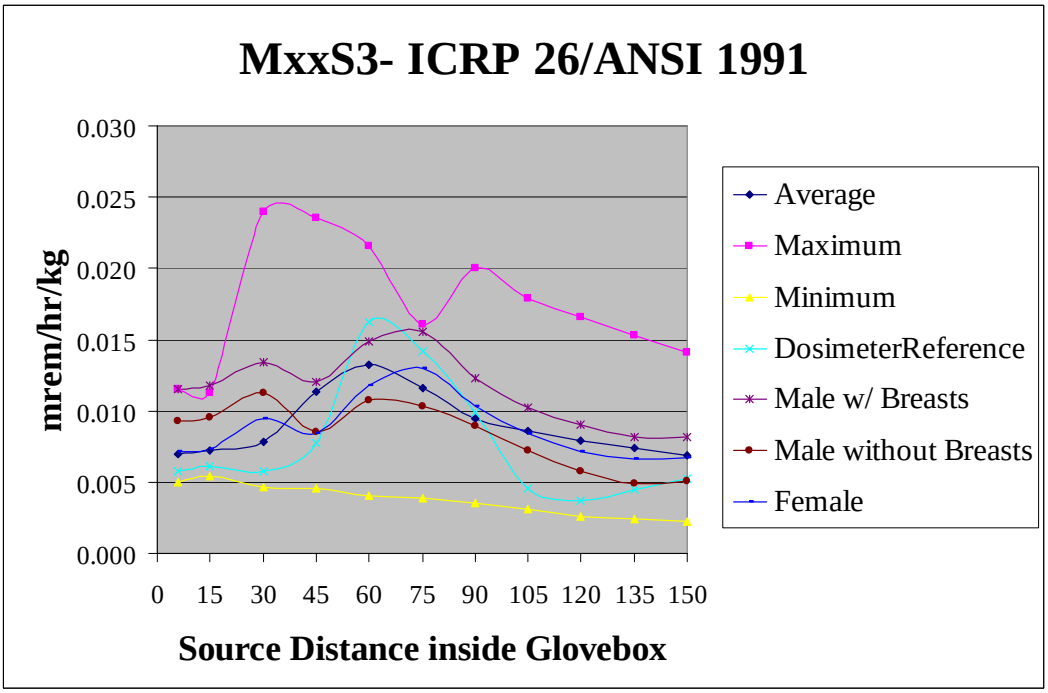

Figure G.6-4: MxxS3- ICRP 26 – ANSI 1991.

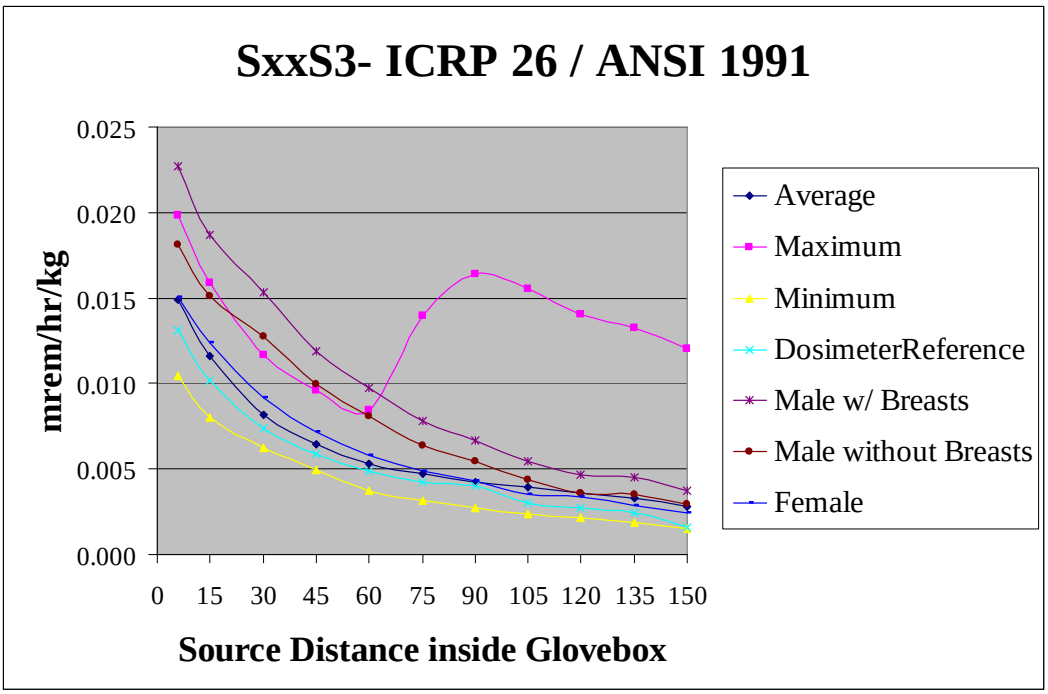

Figure G.6-5: SxxS3- ICRP 26 – ANSI 1991.

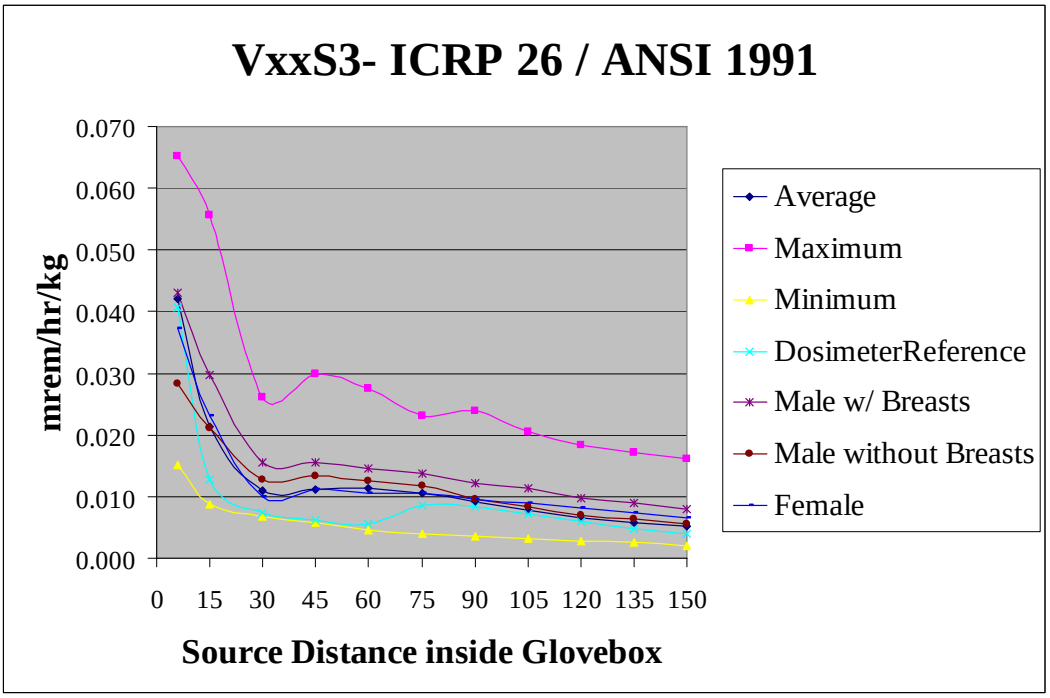

Figure G.6-6: VxxS3- ICRP 26 – ANSI 1991.

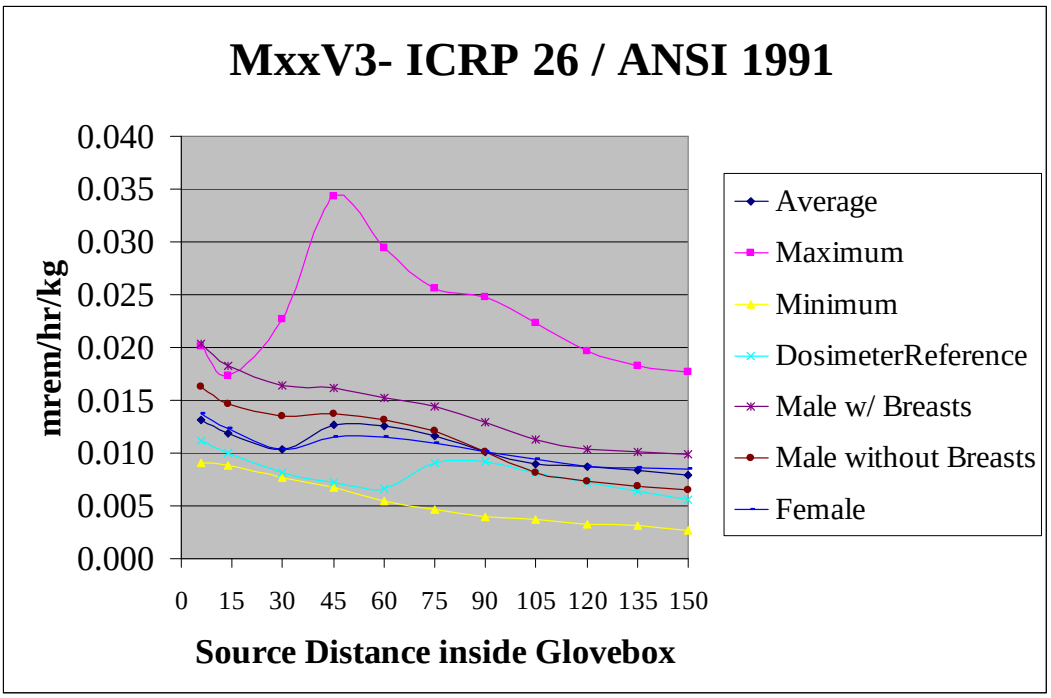

Figure G.6-7: MxxV3- ICRP 26 – ANSI 1991.

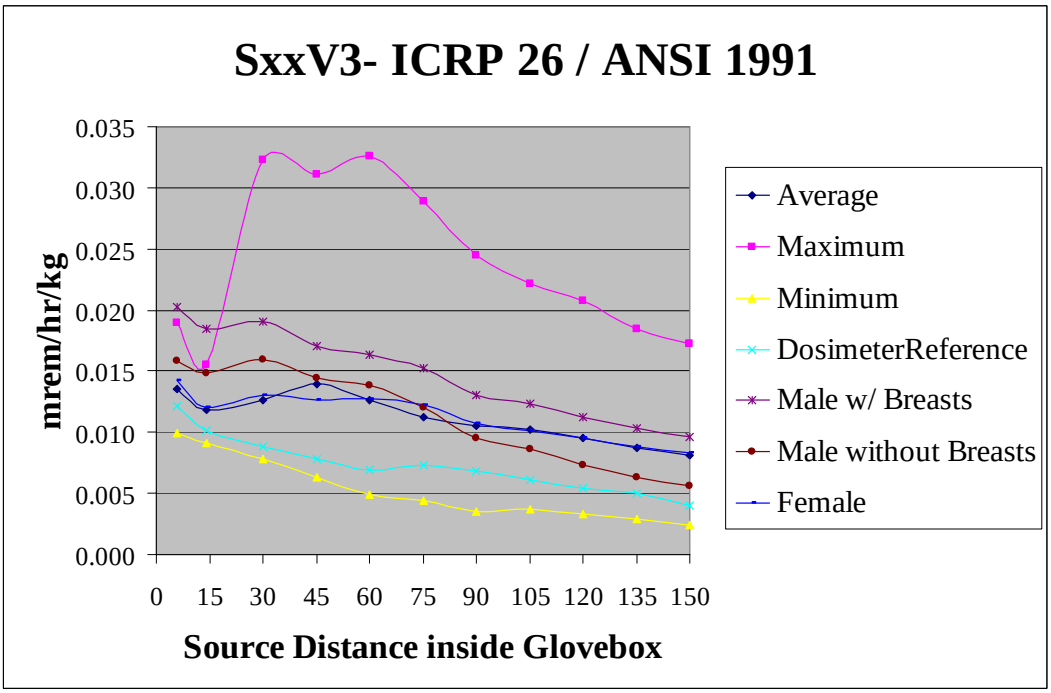

Figure G.6-8: SxxV3- ICRP 26 – ANSI 1991.

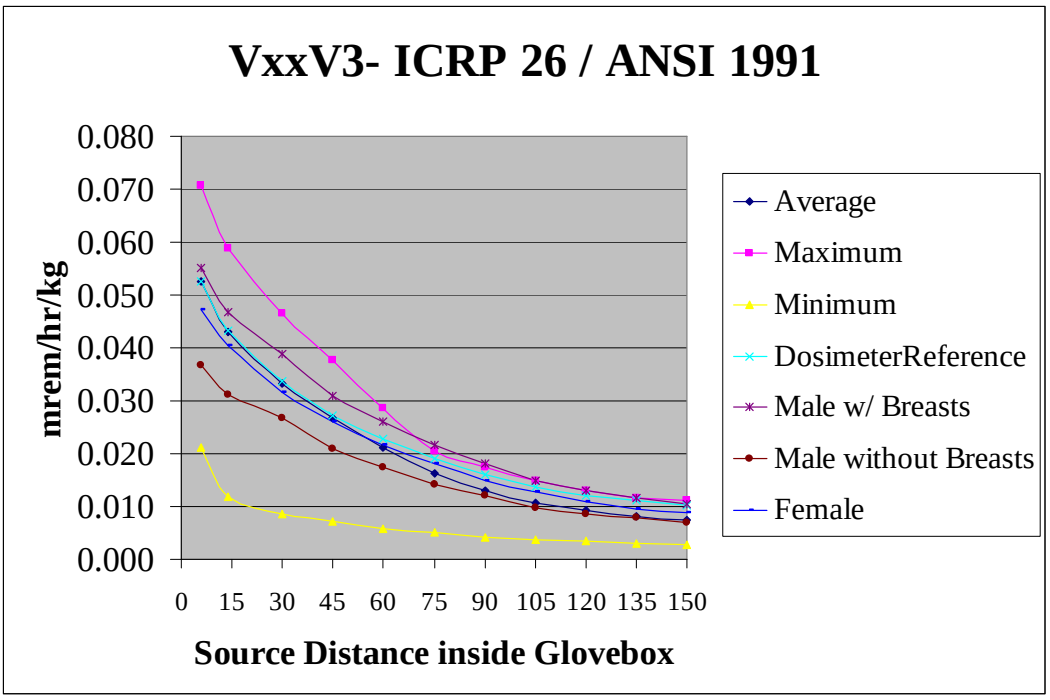

Figure G.6-9: VxxV3- ICRP 26 – ANSI 1991.

APPENDIX G.7:

ICRP 60 – ANSI 1991 AT 3 FOOT

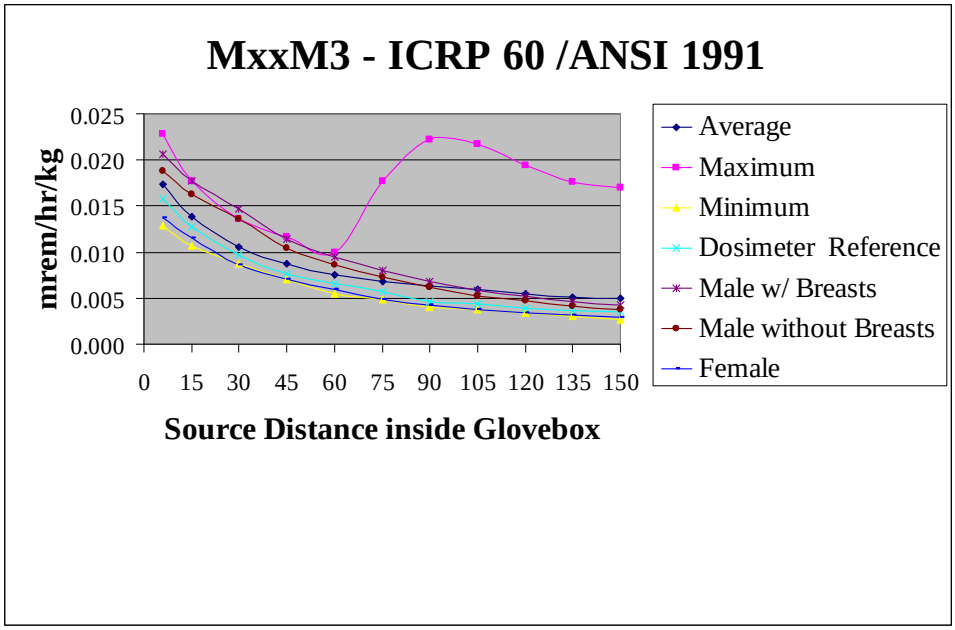

Figure G.7-1: MxxM3- ICRP 60 – ANSI 1991.

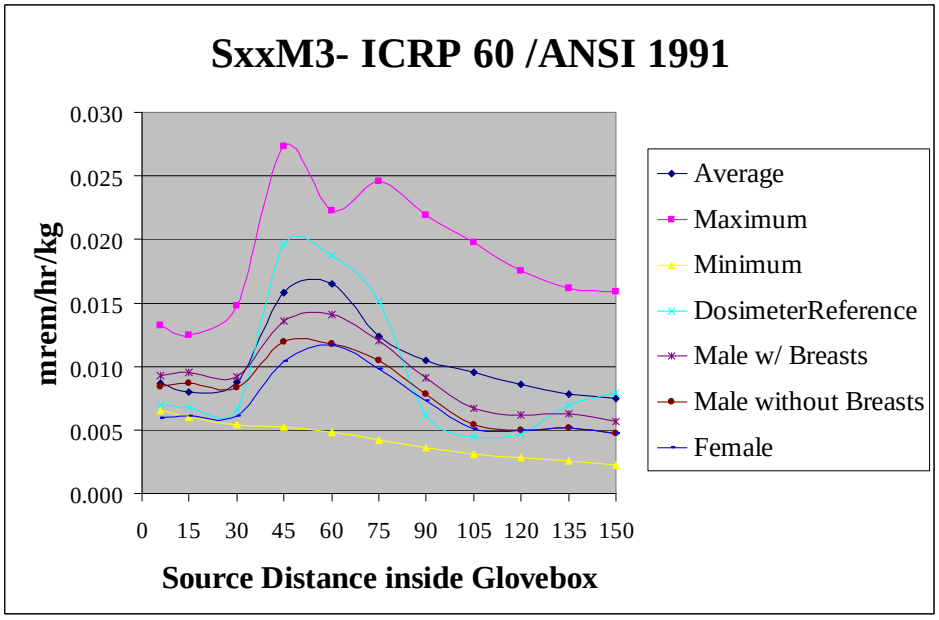

Figure G.7-2: SxxM3- ICRP 60 – ANSI 1991.

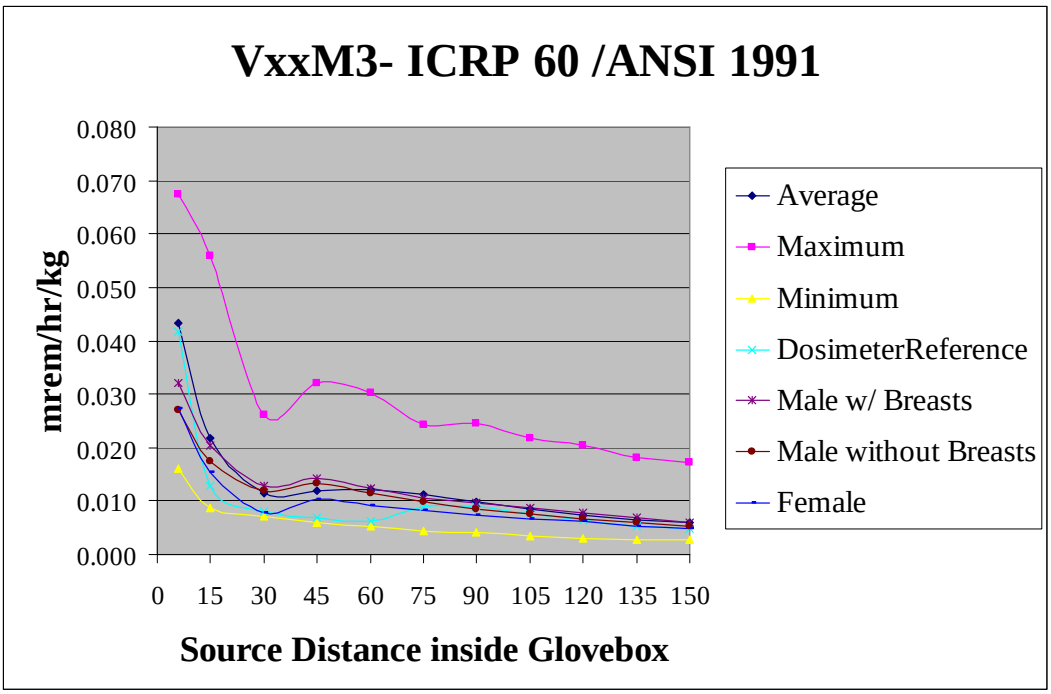

Figure G.7-3: VxxM3- ICRP 60 – ANSI 1991.

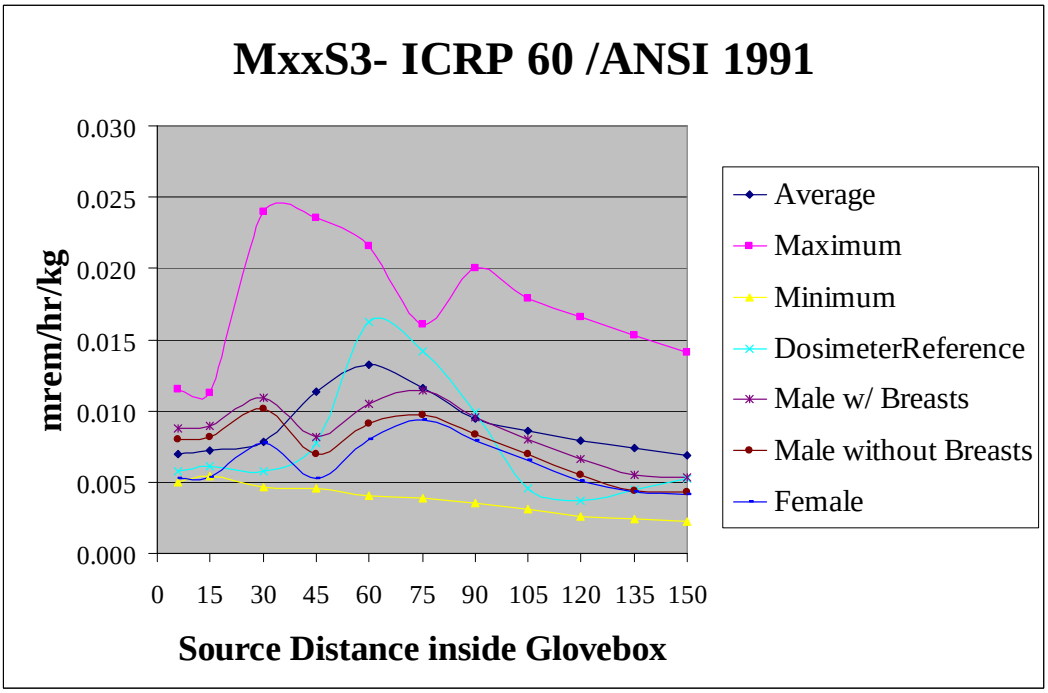

Figure G.7-4: MxxS3- ICRP 60 – ANSI 1991.

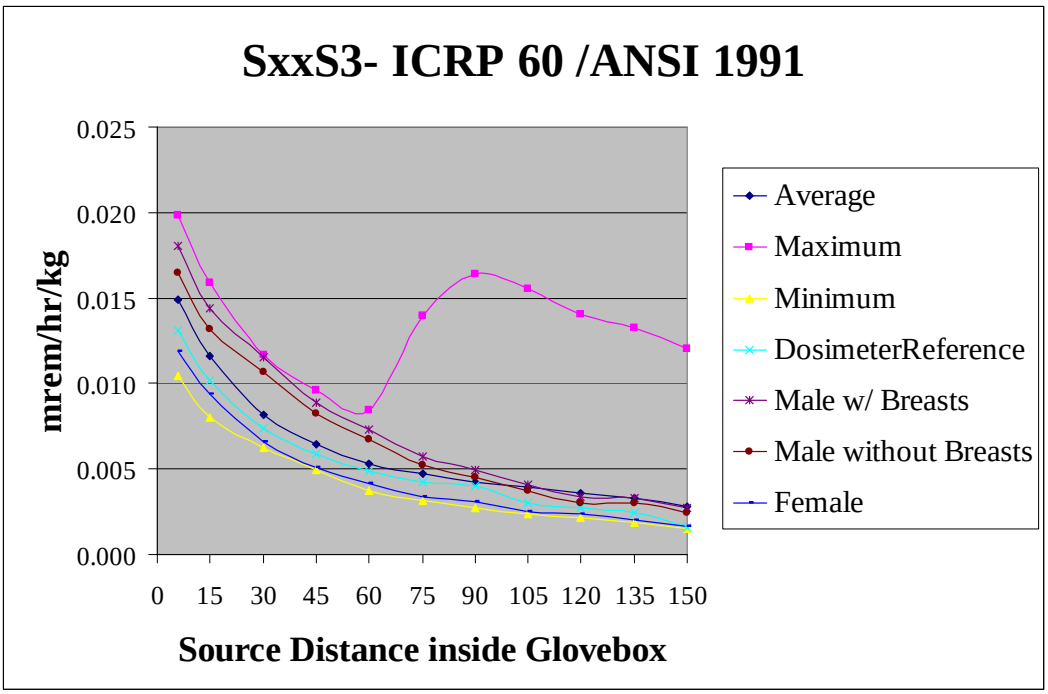

Figure G.7-5: SxxS3- ICRP 60 – ANSI 1991.

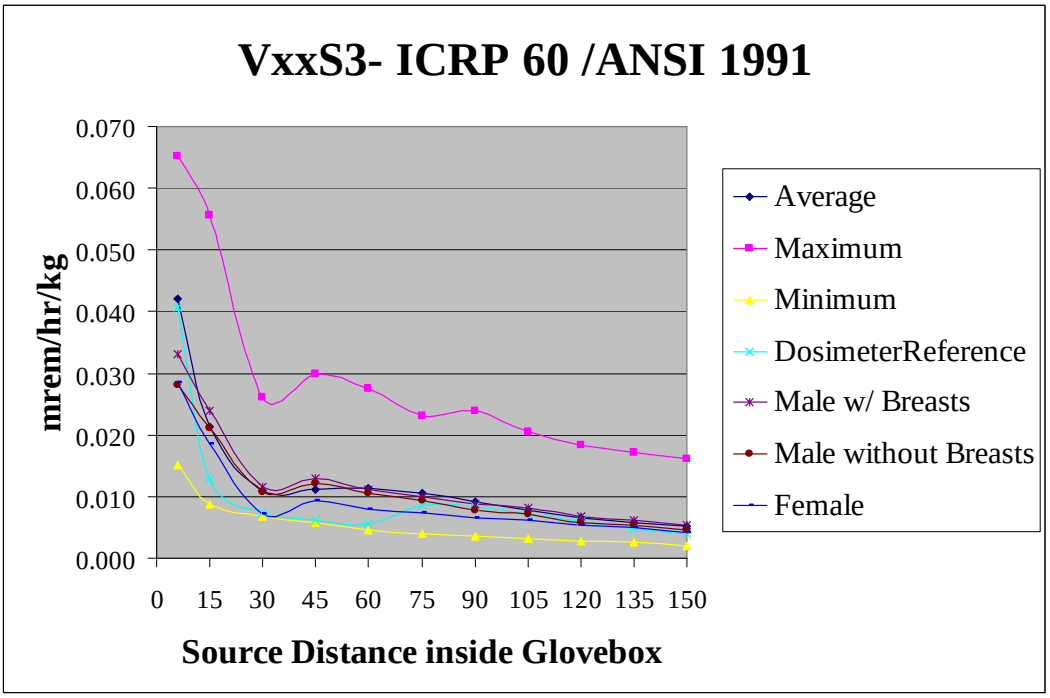

Figure G.7-6: VxxS3- ICRP 60 – ANSI 1991.

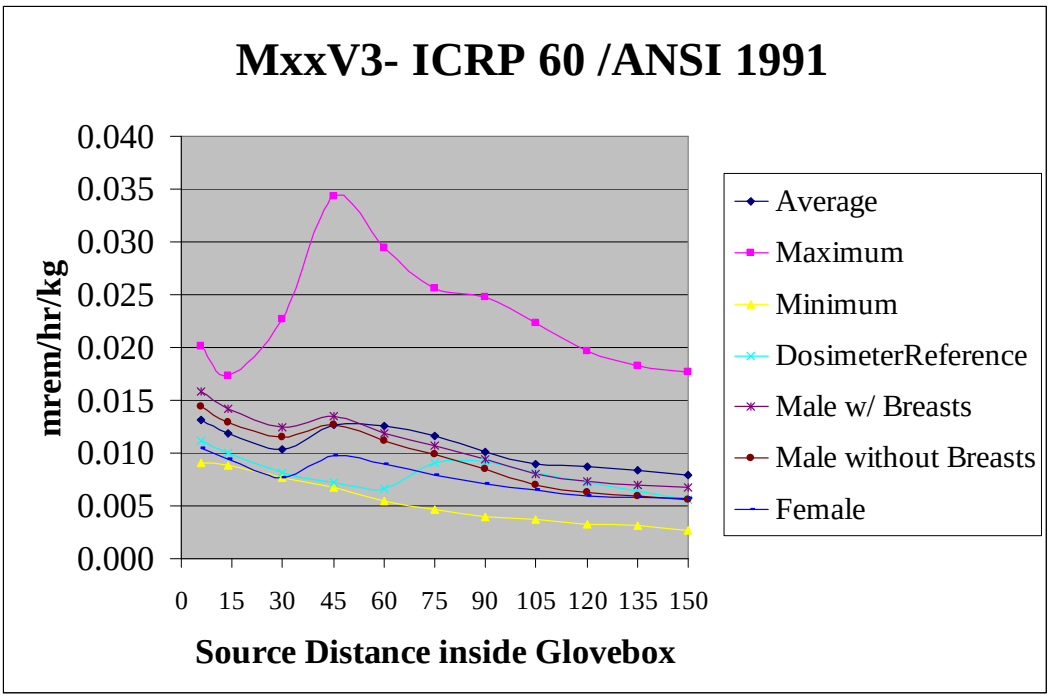

Figure G.7-7: MxxV3- ICRP 60 – ANSI 1991.

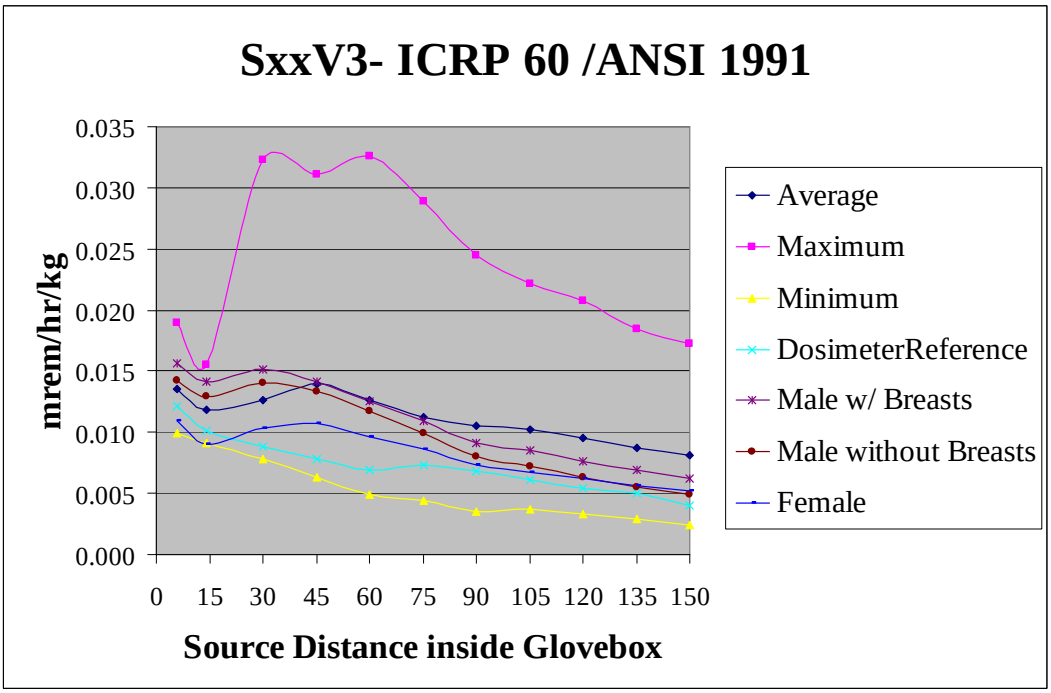

Figure G.7-8: SxxV3- ICRP 60 – ANSI 1991.

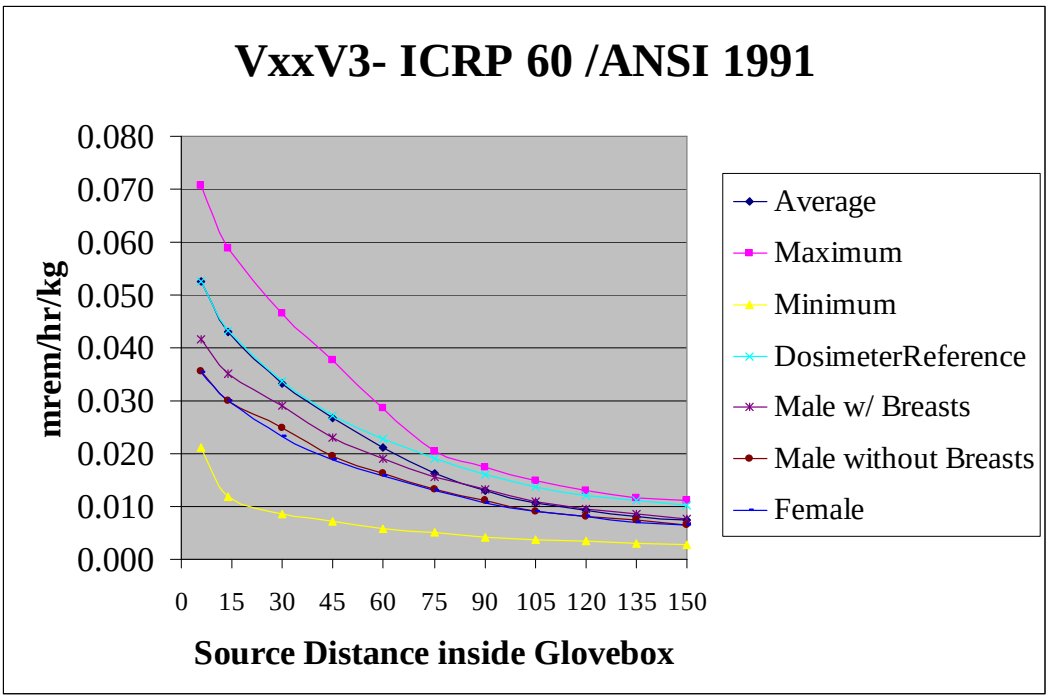

Figure G.7-9: VxxV3- ICRP 60 – ANSI 1991.

APPENDIX G.8:

ICRP 60 – ICRP 74 AT 3 FOOT

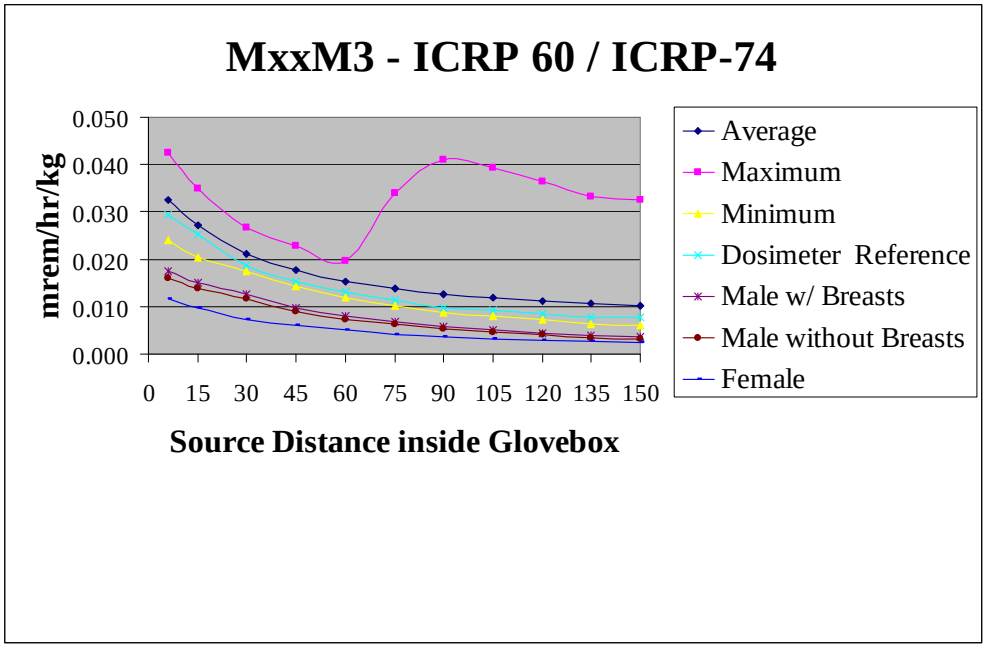

Figure G.8-1: MxxM3- ICRP 60 – ICRP 74.

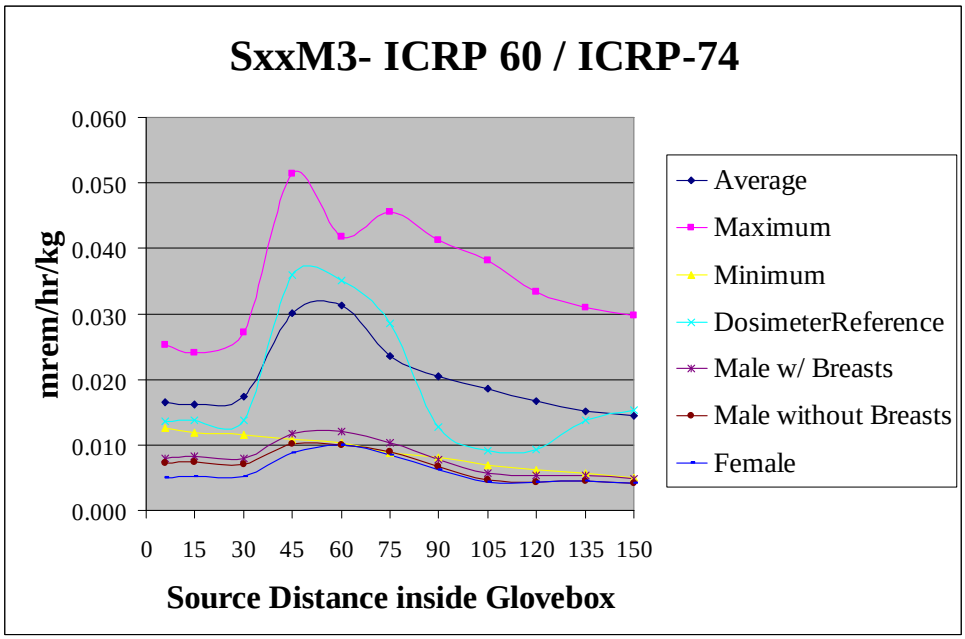

Figure G.8-2: SxxM3- ICRP 60 – ICRP 74.

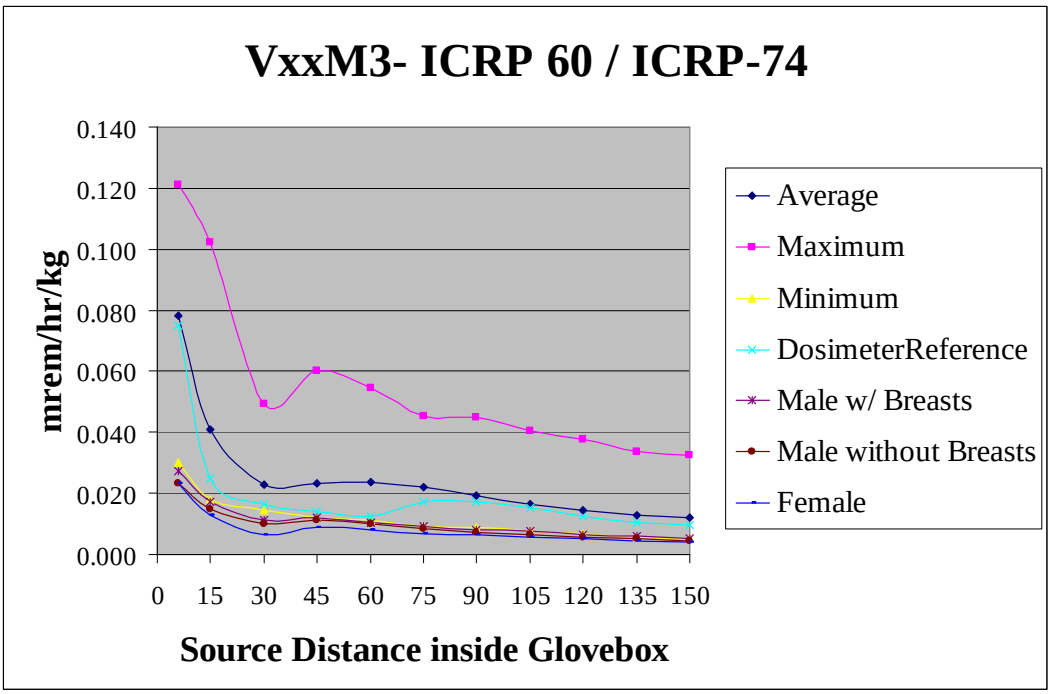

Figure G.8-3: VxxM3- ICRP 60 – ICRP 74.

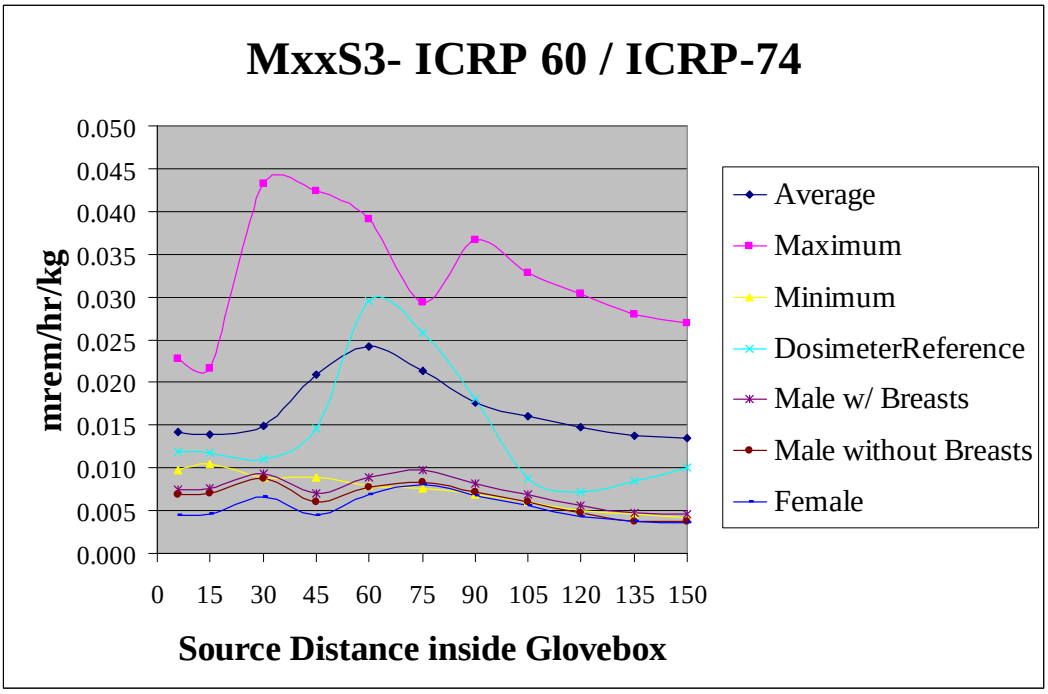

Figure G.8-4: MxxS3- ICRP 60 – ICRP 74.

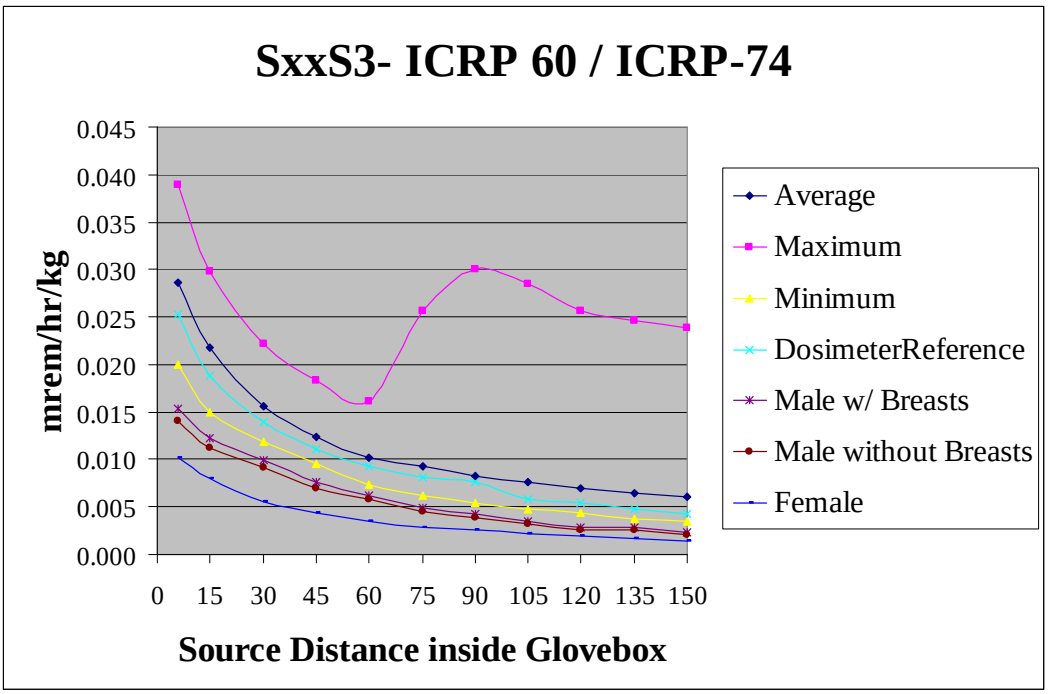

Figure G.8-5: SxxS3- ICRP 60 – ICRP 74.

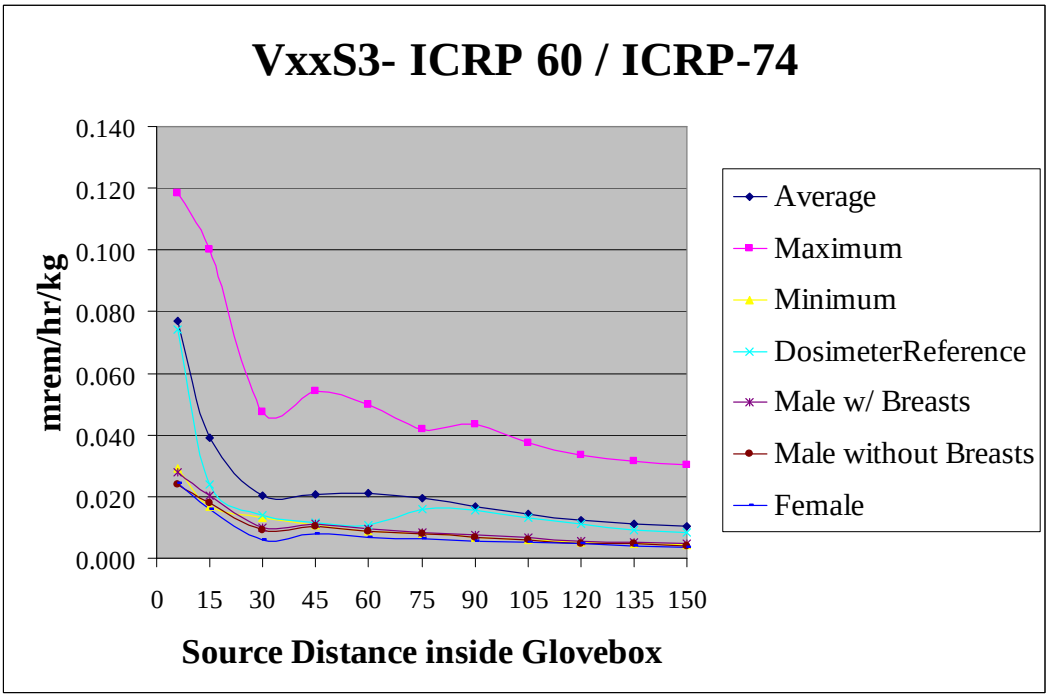

Figure G.8-6: VxxS31- ICRP 60 – ICRP 74.

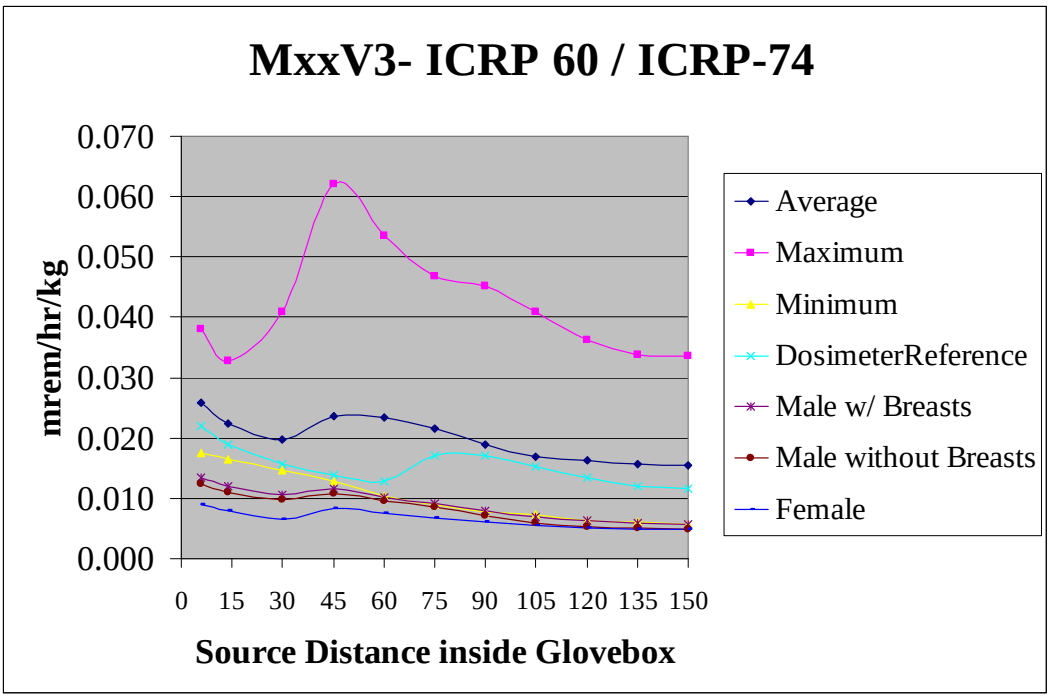

Figure G.8-7: MxxV3- ICRP 60 – ICRP 74.

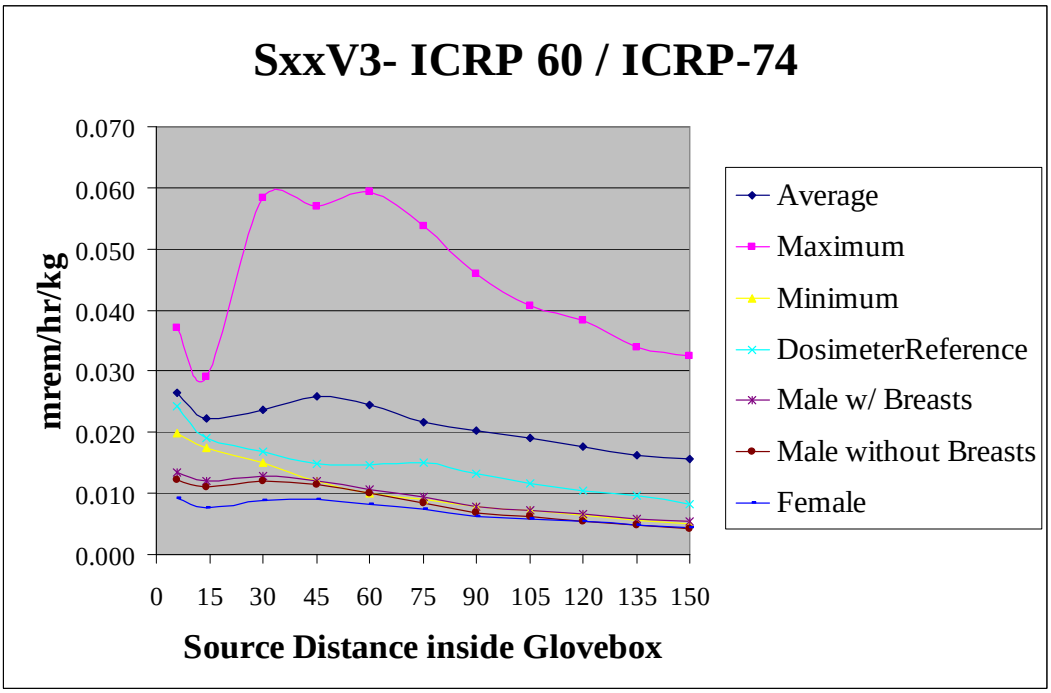

Figure G.8-8: SxxV3- ICRP 60 – ICRP 74.

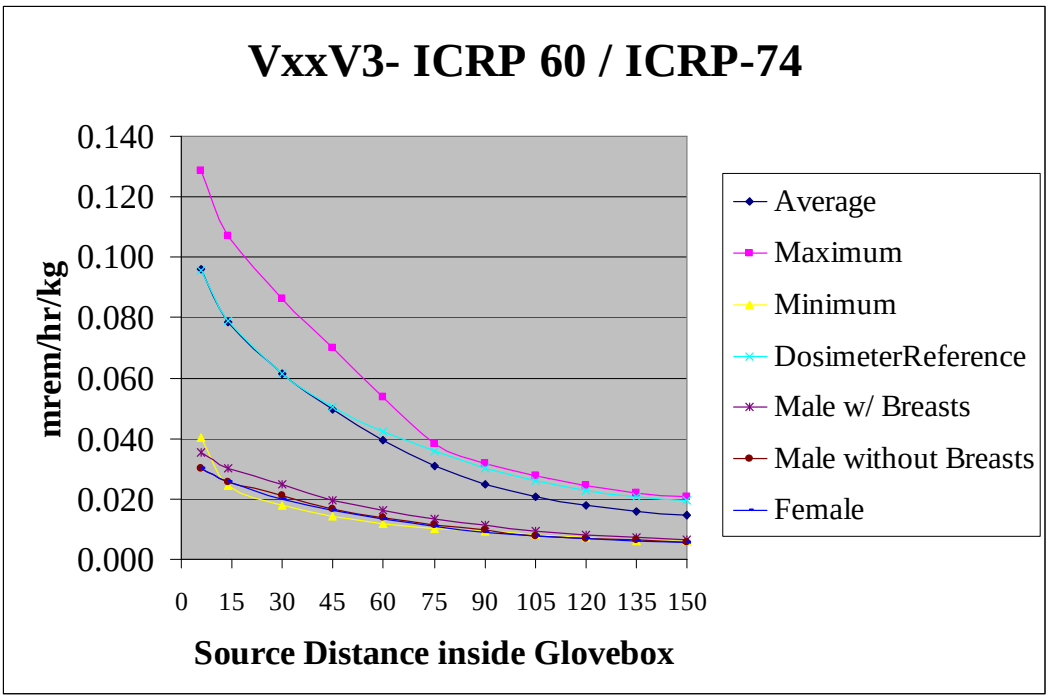

Figure G.8-9: VxxV3 ICRP 60 – ICRP 74.

Appendix H: Distribution Of Average, Maximum, And Minimum Dosimeter Values

APPENDIX H.1: DETAILED TABLES FOR THE LOCATION OF THE AVERAGE, MAXIMUM, AND MINIMUM DOSIMETER VALUES

Table H.1-1: ANSI 1977 at 1 ft - Location of Various Dosimeter Values

ANSI 1977	Location for			ANSI 1977	Location for		
Configuration	Ave	Max	Min	Configuration	Ave	Max	Min
1M06M1Z	552	652	412	1S75V1Z	532	472	702
1M06S1Z	612	522	692	1S90M1Z	502	482	712
1M06V1Z	412	672	692	1S90S1Z	612	522	442
1M15M1Z	572	652	412	1S90V1Z	472	482	692
1M15S1Z	412	562	692	1S05M1Z	632	482	702
1M15V1Z	622	462	692	1S05S1Z	612	522	492
1M30M1Z	482	472	412	1S05V1Z	652	482	692
1M30S1Z	502	572	692	1S20M1Z	632	482	712
1M30V1Z	622	472	692	1S20S1Z	662	522	402
1M45M1Z	482	522	412	1S20V1Z	672	482	702
1M45S1Z	562	572	692	1S35M1Z	442	482	712
1M45V1Z	442	522	692	1S35S1Z	512	522	442
1M60M1Z	562	522	712	1S35V1Z	582	482	702
1M60S1Z	722	512	692	1S50M1Z	632	482	702
1M60V1Z	642	522	702	1S50S1Z	662	522	492
1M75M1Z	532	522	702	1S50V1Z	422	482	702
1M75S1Z	672	512	642	1V06M1Z	542	582	712
1M75V1Z	642	522	702	1V06S1Z	562	622	692
1M90M1Z	622	522	702	1V06V1Z	492	602	722
1M90S1Z	612	522	692	1V15M1Z	632	442	712
1M90V1Z	642	522	702	1V15S1Z	672	462	692
1M05M1Z	462	522	702	1V15V1Z	522	602	722
1M05S1Z	672	522	692	1V30M1Z	582	432	712
1M05V1Z	642	522	702	1V30S1Z	622	472	692
1M20M1Z	462	522	702	1V30V1Z	462	602	712
1M20S1Z	422	522	692	1V45M1Z	582	482	712
1M20V1Z	622	522	712	1V45S1Z	622	522	692
1M35M1Z	582	522	692	1V45V1Z	432	602	692

ANSI 1977	Location for			ANSI 1977	Location for		
Configuration	Ave	Max	Min	Configuration	Ave	Max	Min
1M35S1Z	672	522	592	1V60M1Z	582	482	712
1M35V1Z	562	572	702	1V60S1Z	672	522	692
1M50M1Z	432	522	702	1V60V1Z	452	552	702
1M50S1Z	462	522	492	1V75M1Z	632	482	702
1M50V1Z	402	572	702	1V75S1Z	672	522	692
1S06M1Z	592	482	702	1V75V1Z	642	522	702
1S06S1Z	642	672	402	1V90M1Z	632	482	712
1S06V1Z	542	632	712	1V90S1Z	462	522	402
1S15M1Z	472	542	712	1V90V1Z	662	522	702
1S15S1Z	512	672	402	1V05M1Z	572	482	702
1S15V1Z	632	432	712	1V05S1Z	722	522	492
1S30M1Z	562	532	712	1V05V1Z	662	482	702
1S30S1Z	512	472	402	1V20M1Z	632	482	692
1S30V1Z	502	482	712	1V20S1Z	722	522	402
1S45M1Z	462	492	712	1V20V1Z	662	522	692
1S45S1Z	462	472	402	1V35M1Z	632	482	712
1S45V1Z	462	482	712	1V35S1Z	722	522	402
1S60M1Z	452	492	712	1V35V1Z	412	522	702
1S60S1Z	462	522	402	1V50M1Z	542	482	702
1S60V1Z	442	482	702	1V50S1Z	722	522	402
1S75M1Z	632	492	702	1V50V1Z	432	482	702
1S75S1Z	662	522	402				

Table H.1-2: ANSI 1977 at 1 ft - Location of Various Dosimeter Values

ANSI 1991	Location for			ANSI 1991	Location for		
Configuration	Ave	Max	Min	Configuration	Ave	Max	Min
1M06M1Z	152	252	12	1S75V1Z	142	82	302
1M06S1Z	212	122	192	1S90M1Z	102	82	312
1M06V1Z	112	272	292	1S90S1Z	112	122	292
1M15M1Z	322	252	12	1S90V1Z	72	82	302
1M15S1Z	222	162	292	1S05M1Z	232	82	302
1M15V1Z	272	62	292	1S05S1Z	112	122	42
1M30M1Z	192	72	12	1S05V1Z	252	82	302
1M30S1Z	102	172	292	1S20M1Z	232	82	312
1M30V1Z	222	72	292	1S20S1Z	112	122	92
1M45M1Z	82	122	12	1S20V1Z	272	82	292
1M45S1Z	162	122	292	1S35M1Z	42	82	302
1M45V1Z	42	122	292	1S35S1Z	162	122	192
1M60M1Z	162	122	312	1S35V1Z	92	82	302
1M60S1Z	82	112	302	1S50M1Z	232	82	312
1M60V1Z	242	122	292	1S50S1Z	62	122	42
1M75M1Z	132	122	302	1S50V1Z	122	132	302
1M75S1Z	272	112	292	1V06M1Z	192	182	312
1M75V1Z	242	122	292	1V06S1Z	212	222	292
1M90M1Z	222	122	302	1V06V1Z	102	202	322
1M90S1Z	212	122	292	1V15M1Z	232	42	312
1M90V1Z	32	122	292	1V15S1Z	272	62	292
1M05M1Z	222	122	302	1V15V1Z	122	202	282
1M05S1Z	22	122	292	1V30M1Z	182	32	312
1M05V1Z	242	122	302	1V30S1Z	222	72	292
1M20M1Z	62	122	302	1V30V1Z	182	202	292
1M20S1Z	22	122	292	1V45M1Z	182	82	312
1M20V1Z	162	122	292	1V45S1Z	222	122	292
1M35M1Z	182	122	292	1V45V1Z	72	202	312
1M35S1Z	22	122	292	1V60M1Z	182	82	312
1M35V1Z	22	122	302	1V60S1Z	222	122	292
1M50M1Z	32	122	292	1V60V1Z	52	202	302

ANSI 1991	Location for			ANSI 1991	Location for		
Configuration	Ave	Max	Min	Configuration	Ave	Max	Min
1M50S1Z	22	122	292	1V75M1Z	232	82	302
1M50V1Z	2	122	302	1V75S1Z	272	122	292
1S06M1Z	192	82	302	1V75V1Z	172	122	302
1S06S1Z	242	272	2	1V90M1Z	42	82	312
1S06V1Z	142	12	312	1V90S1Z	272	122	292
1S15M1Z	72	142	312	1V90V1Z	242	122	302
1S15S1Z	112	272	2	1V05M1Z	172	82	302
1S15V1Z	182	32	312	1V05S1Z	272	122	292
1S30M1Z	162	132	312	1V05V1Z	262	82	292
1S30S1Z	62	72	2	1V20M1Z	72	82	312
1S30V1Z	102	82	312	1V20S1Z	322	122	242
1S45M1Z	62	92	312	1V20V1Z	12	122	302
1S45S1Z	62	72	2	1V35M1Z	232	82	312
1S45V1Z	62	82	312	1V35S1Z	322	122	2
1S60M1Z	52	92	312	1V35V1Z	2	122	302
1S60S1Z	62	122	2	1V50M1Z	142	82	302
1S60V1Z	42	82	312	1V50S1Z	322	122	292
1S75M1Z	182	92	302	1V50V1Z	32	82	302
1S75S1Z	212	122	292				

Table H.1-3: ICRP 74 at 1 ft - Location of Various Dosimeter Values

ICRP 74	Location for			ICRP 74	Location for		
Configuration	Ave	Max	Min	Configuration	Ave	Max	Min
1M06M1Z	952	1052	812	1S75V1Z	932	872	1102
1M06S1Z	1012	922	1092	1S90M1Z	902	882	1112
1M06V1Z	862	1072	1092	1S90S1Z	1012	922	842
1M15M1Z	1122	1052	812	1S90V1Z	872	882	1092
1M15S1Z	812	962	1092	1S05M1Z	1032	882	1102
1M15V1Z	1072	862	1092	1S05S1Z	1012	922	892
1M30M1Z	992	872	812	1S05V1Z	1052	882	1102
1M30S1Z	902	972	1092	1S20M1Z	1032	882	1112
1M30V1Z	1022	872	1092	1S20S1Z	1062	922	802
1M45M1Z	882	922	812	1S20V1Z	1072	882	1102
1M45S1Z	962	972	1092	1S35M1Z	842	882	1112
1M45V1Z	842	922	1092	1S35S1Z	912	922	842
1M60M1Z	962	922	1112	1S35V1Z	982	882	1102
1M60S1Z	1122	912	1092	1S50M1Z	1032	882	1102
1M60V1Z	1042	922	1092	1S50S1Z	1062	922	892
1M75M1Z	932	922	1102	1S50V1Z	822	932	1102
1M75S1Z	1072	912	1102	1V06M1Z	992	982	1112
1M75V1Z	1042	922	1102	1V06S1Z	1012	1022	1092
1M90M1Z	1022	922	1102	1V06V1Z	902	1002	1122
1M90S1Z	1012	922	1092	1V15M1Z	1032	842	1112
1M90V1Z	832	922	1102	1V15S1Z	1072	862	1092
1M05M1Z	862	922	1102	1V15V1Z	922	1002	1122
1M05S1Z	1072	922	1092	1V30M1Z	982	832	1112
1M05V1Z	1042	922	1102	1V30S1Z	1022	872	1092
1M20M1Z	862	922	1102	1V30V1Z	862	1002	1112
1M20S1Z	822	922	1092	1V45M1Z	982	882	1112
1M20V1Z	962	922	1102	1V45S1Z	1022	922	1092
1M35M1Z	982	922	1092	1V45V1Z	872	1002	1092
1M35S1Z	1072	922	992	1V60M1Z	982	882	1112
1M35V1Z	962	972	1102	1V60S1Z	1072	922	1092
1M50M1Z	832	922	1102	1V60V1Z	852	1002	1102

ICRP 74	Location for			ICRP 74	Location for		
Configuration	Ave	Max	Min	Configuration	Ave	Max	Min
1M50S1Z	862	922	892	1V75M1Z	1032	882	1102
1M50V1Z	802	922	1102	1V75S1Z	1072	922	1092
1S06M1Z	992	882	1102	1V75V1Z	972	922	1102
1S06S1Z	1042	1072	802	1V90M1Z	1032	882	1112
1S06V1Z	942	1032	1112	1V90S1Z	862	922	802
1S15M1Z	872	942	1112	1V90V1Z	1042	922	1102
1S15S1Z	952	1072	802	1V05M1Z	972	882	1102
1S15V1Z	932	832	1112	1V05S1Z	1122	922	892
1S30M1Z	962	932	1112	1V05V1Z	1062	882	1102
1S30S1Z	912	872	802	1V20M1Z	872	882	1092
1S30V1Z	902	882	1112	1V20S1Z	1122	922	802
1S45M1Z	862	892	1112	1V20V1Z	1062	922	1092
1S45S1Z	862	872	802	1V35M1Z	1032	882	1112
1S45V1Z	862	882	1112	1V35S1Z	1122	922	802
1S60M1Z	852	892	1112	1V35V1Z	812	922	1102
1S60S1Z	862	922	802	1V50M1Z	942	882	1102
1S60V1Z	842	882	1102	1V50S1Z	1122	922	802
1S75M1Z	1032	892	1102	1V50V1Z	832	882	1102
1S75S1Z	1012	922	802				

Table H.1-4: ANSI 1977 at 3 ft - Location of Various Dosimeter Values

ANSI 1977	Location for			ANSI 1977	Location for		
Configuration	Ave	Max	Min	Configuration	Ave	Max	Min
1M06M3Z	662	582	412	1S75V3Z	472	432	702
1M06S3Z	662	622	402	1S90M3Z	642	432	712
1M06V3Z	662	672	402	1S90S3Z	562	472	492
1M15M3Z	642	572	412	1S90V3Z	542	432	702
1M15S3Z	532	572	402	1S05M3Z	592	482	702
1M15V3Z	612	722	402	1S05S3Z	422	472	442
1M30M3Z	562	522	402	1S05V3Z	542	482	712
1M30S3Z	582	422	692	1S20M3Z	562	482	702
1M30V3Z	532	402	692	1S20S3Z	532	472	492
1M45M3Z	512	572	702	1S20V3Z	542	482	702
1M45S3Z	522	432	702	1S35M3Z	552	522	702
1M45V3Z	622	432	702	1S35S3Z	512	472	402
1M60M3Z	512	472	702	1S35V3Z	452	432	702
1M60S3Z	612	432	692	1S50M3Z	442	472	702
1M60V3Z	572	432	702	1S50S3Z	722	472	642
1M75M3Z	462	472	702	1S50V3Z	612	432	702
1M75S3Z	672	512	702	1V06M3Z	442	582	702
1M75V3Z	482	472	702	1V06S3Z	462	622	692
1M90M3Z	672	472	702	1V06V3Z	492	582	702
1M90S3Z	552	572	702	1V15M3Z	682	582	422
1M90V3Z	562	472	692	1V15S3Z	722	622	442
1M05M3Z	622	472	702	1V15V3Z	642	622	692
1M05S3Z	492	522	692	1V30M3Z	622	482	662
1M05V3Z	402	472	692	1V30S3Z	722	522	692
1M20M3Z	622	472	692	1V30V3Z	422	572	702
1M20S3Z	562	432	702	1V45M3Z	482	472	702
1M20V3Z	442	472	702	1V45S3Z	522	432	702
1M35M3Z	632	472	702	1V45V3Z	422	522	702
1M35S3Z	542	482	702	1V60M3Z	482	472	652
1M35V3Z	412	522	702	1V60S3Z	572	432	702
1M50M3Z	622	472	702	1V60V3Z	602	572	702

ANSI 1977	Location for			ANSI 1977	Location for		
Configuration	Ave	Max	Min	Configuration	Ave	Max	Min
1M50S3Z	412	482	702	1V75M3Z	522	472	702
1M50V3Z	502	522	702	1V75S3Z	482	432	642
1S06M3Z	492	682	412	1V75V3Z	582	512	702
1S06S3Z	432	622	412	1V90M3Z	542	432	702
1S06V3Z	542	582	412	1V90S3Z	562	472	702
1S15M3Z	492	482	712	1V90V3Z	662	422	702
1S15S3Z	712	522	402	1V05M3Z	512	432	712
1S15V3Z	542	682	412	1V05S3Z	492	472	702
1S30M3Z	442	522	712	1V05V3Z	522	512	702
1S30S3Z	482	622	412	1V20M3Z	462	432	702
1S30V3Z	482	422	712	1V20S3Z	442	472	702
1S45M3Z	652	522	712	1V20V3Z	642	462	702
1S45S3Z	632	622	492	1V35M3Z	412	482	702
1S45V3Z	492	472	702	1V35S3Z	412	472	702
1S60M3Z	672	572	712	1V35V3Z	642	512	702
1S60S3Z	512	472	442	1V50M3Z	412	482	712
1S60V3Z	522	432	702	1V50S3Z	622	472	702
1S75M3Z	652	432	702	1V50V3Z	652	512	692
1S75S3Z	462	472	402				

Table H.1-5: ANSI 1991 at 3 ft - Location of Various Dosimeter Values

ANSI 1991	Location for			ANSI 1991	Location for		
Configuration	Ave	Max	Min	Configuration	Ave	Max	Min
1M06M3Z	262	182	12	1S75V3Z	112	32	312
1M06S3Z	162	222	142	1S90M3Z	242	132	312
1M06V3Z	312	222	2	1S90S3Z	62	72	92
1M15M3Z	242	82	12	1S90V3Z	142	32	302
1M15S3Z	282	222	2	1S05M3Z	2	82	302
1M15V3Z	162	322	2	1S05S3Z	22	72	42
1M30M3Z	162	122	12	1S05V3Z	142	82	292
1M30S3Z	182	22	292	1S20M3Z	162	82	312
1M30V3Z	82	2	292	1S20S3Z	62	72	92
1M45M3Z	92	172	302	1S20V3Z	142	82	302
1M45S3Z	122	32	302	1S35M3Z	152	122	302
1M45V3Z	222	32	302	1S35S3Z	112	72	92
1M60M3Z	142	72	302	1S35V3Z	162	32	302
1M60S3Z	252	32	292	1S50M3Z	42	72	302
1M60V3Z	172	32	302	1S50S3Z	62	72	92
1M75M3Z	62	72	302	1S50V3Z	212	32	302
1M75S3Z	272	112	302	1V06M3Z	42	182	302
1M75V3Z	82	72	302	1V06S3Z	252	272	292
1M90M3Z	232	72	302	1V06V3Z	252	232	302
1M90S3Z	152	172	302	1V15M3Z	282	182	312
1M90V3Z	162	72	292	1V15S3Z	322	222	242
1M05M3Z	222	72	302	1V15V3Z	62	222	302
1M05S3Z	92	122	292	1V30M3Z	72	182	302
1M05V3Z	2	72	292	1V30S3Z	322	122	292
1M20M3Z	182	72	292	1V30V3Z	2	172	302
1M20S3Z	162	32	302	1V45M3Z	32	72	302
1M20V3Z	42	72	302	1V45S3Z	72	32	242
1M35M3Z	132	72	302	1V45V3Z	52	122	302
1M35S3Z	142	82	302	1V60M3Z	132	72	252
1M35V3Z	12	122	292	1V60S3Z	172	32	302
1M50M3Z	222	72	302	1V60V3Z	202	172	302

ANSI 1991	Location for			ANSI 1991	Location for		
Configuration	Ave	Max	Min	Configuration	Ave	Max	Min
1M50S3Z	12	122	292	1V75M3Z	122	72	302
1M50V3Z	162	122	302	1V75S3Z	82	32	302
1S06M3Z	92	282	12	1V75V3Z	262	112	302
1S06S3Z	312	272	12	1V90M3Z	142	32	292
1S06V3Z	142	132	22	1V90S3Z	162	72	292
1S15M3Z	192	82	262	1V90V3Z	82	62	302
1S15S3Z	262	222	2	1V05M3Z	22	32	302
1S15V3Z	142	182	22	1V05S3Z	92	72	302
1S30M3Z	112	122	312	1V05V3Z	72	112	302
1S30S3Z	262	122	12	1V20M3Z	62	32	302
1S30V3Z	122	22	312	1V20S3Z	152	72	302
1S45M3Z	252	122	312	1V20V3Z	12	92	292
1S45S3Z	112	222	92	1V35M3Z	12	82	302
1S45V3Z	92	72	302	1V35S3Z	12	72	302
1S60M3Z	182	172	312	1V35V3Z	252	92	302
1S60S3Z	312	72	42	1V50M3Z	12	82	312
1S60V3Z	112	32	292	1V50S3Z	12	72	302
1S75M3Z	252	82	302	1V50V3Z	252	112	312
1S75S3Z	62	72	2				

Table H.1-6: ICRP 74 at 3 ft - Location of Various Dosimeter Values

ICRP 74	Location for			ICRP 74	Location for		
Configuration	Ave	Max	Min	Configuration	Ave	Max	Min
1M06M3Z	1062	982	812	1S75V3Z	872	832	1102
1M06S3Z	1112	1022	802	1S90M3Z	1042	832	1112
1M06V3Z	1112	1072	802	1S90S3Z	962	872	892
1M15M3Z	1042	972	812	1S90V3Z	942	832	1102
1M15S3Z	932	972	802	1S05M3Z	992	882	1102
1M15V3Z	1012	1122	802	1S05S3Z	822	872	842
1M30M3Z	962	922	802	1S05V3Z	942	882	1092
1M30S3Z	982	822	1092	1S20M3Z	962	882	1102
1M30V3Z	932	802	1092	1S20S3Z	862	872	892
1M45M3Z	892	972	1102	1S20V3Z	942	882	1102
1M45S3Z	922	832	1102	1S35M3Z	952	922	1102
1M45V3Z	1022	832	1102	1S35S3Z	912	872	802
1M60M3Z	912	872	1102	1S35V3Z	962	832	1102
1M60S3Z	1052	832	1092	1S50M3Z	842	872	1102
1M60V3Z	972	832	1102	1S50S3Z	1122	872	1042
1M75M3Z	862	872	1102	1S50V3Z	1012	832	1102
1M75S3Z	1072	912	1102	1V06M3Z	842	982	1102
1M75V3Z	882	872	1102	1V06S3Z	1002	1022	1092
1M90M3Z	1122	872	1102	1V06V3Z	952	1022	1102
1M90S3Z	952	972	1102	1V15M3Z	1082	982	822
1M90V3Z	962	872	1092	1V15S3Z	1122	1022	1042
1M05M3Z	1022	872	1102	1V15V3Z	862	1022	1092
1M05S3Z	892	922	1092	1V30M3Z	1022	882	1062
1M05V3Z	802	872	1092	1V30S3Z	1122	922	1092
1M20M3Z	1022	872	1092	1V30V3Z	802	972	1102
1M20S3Z	962	832	1102	1V45M3Z	832	872	1102
1M20V3Z	842	872	1102	1V45S3Z	922	832	1042
1M35M3Z	912	872	1102	1V45V3Z	852	922	1102
1M35S3Z	942	882	1102	1V60M3Z	882	872	1052
1M35V3Z	812	922	1102	1V60S3Z	972	832	1102
1M50M3Z	932	872	1102	1V60V3Z	1002	972	1102

ICRP 74	Location for			ICRP 74	Location for		
Configuration	Ave	Max	Min	Configuration	Ave	Max	Min
1M50S3Z	812	882	1102	1V75M3Z	922	872	1102
1M50V3Z	902	922	1102	1V75S3Z	882	832	1102
1S06M3Z	892	1082	812	1V75V3Z	982	912	1102
1S06S3Z	832	1022	812	1V90M3Z	942	832	1102
1S06V3Z	992	982	812	1V90S3Z	962	872	1092
1S15M3Z	892	882	1112	1V90V3Z	1062	912	1102
1S15S3Z	1112	1022	802	1V05M3Z	912	832	1112
1S15V3Z	1122	1082	822	1V05S3Z	892	872	1102
1S30M3Z	802	922	1112	1V05V3Z	972	912	1102
1S30S3Z	1082	1022	812	1V20M3Z	862	832	1102
1S30V3Z	922	822	1112	1V20S3Z	952	872	1102
1S45M3Z	1052	922	1112	1V20V3Z	1052	862	1102
1S45S3Z	912	1022	892	1V35M3Z	812	832	1102
1S45V3Z	892	872	1102	1V35S3Z	812	872	1102
1S60M3Z	1072	972	1112	1V35V3Z	922	912	1102
1S60S3Z	962	872	842	1V50M3Z	812	882	1112
1S60V3Z	922	832	1102	1V50S3Z	1022	872	1102
1S75M3Z	1052	832	1102	1V50V3Z	1052	912	1092
1S75S3Z	862	872	802				

APPENDIX H.2: SUMMARY TABLES FOR THE LOCATION OF THE AVERAGE DOSIMETER VALUES

Table H.2-1: ANSI 1977 at 1 ft - Location of Average Dosimeter Values

Relative	Y (cm) for Phantom Tally Plane				
Z (cm)	-16	-8	0	8	16
74		1	3	2	
66	3	3	2	9	2
58	2	1	3	3	1
50	2	3	1	5	2
42	5	1	0	4	6
34	10	6	1	6	7
26	0	0	0	0	5

Table H.2-2: ANSI 1991 at 1 ft - Location of Average Dosimeter Values

Relative	Y (cm) for Phantom Tally Plane				
Z (cm)	-16	-8	0	8	16
74		2	1	5	
66	3	4	2	7	4
58	2	1	4	5	2
50	1	3	1	5	2
42	7	3	0	4	7
34	6	5	1	1	7
26	0	0	0	0	4

Table H.2-3: ICRP 74 at 1 ft - Location of Average Dosimeter Values

Relative	Y (cm) for Phantom Tally Plane				
Z (cm)	-16	-8	0	8	16
74		1	2	2	
66	3	3	2	10	4
58	1	0	4	2	1
50	3	2	2	5	2
42	5	3	0	6	4
34	8	5	1	4	8
26	0	0	0	0	6

Table H.2-4: ANSI 1977 at 3 ft - Location of Average Dosimeter Values

Relative	Y (cm) for Phantom Tally Plane				
Z (cm)	-16	-8	0	8	16
74		1	5	3	
66	1	5	1	4	1
58	6	6	1	5	5
50	3	7	2	6	2
42	2	1	1	3	6
34	2	5	3	4	3
26	1	0	0	1	3

Table H.2-5: ANSI 1991 at 3 ft - Location of Average Dosimeter Values

Relative	Y (cm) for Phantom Tally Plane				
Z (cm)	-16	-8	0	8	16
74		3	7	2	
66	1	3	1	7	3
58	4	5	0	5	3
50	2	8	3	9	2
42	3	1	1	1	3
34	1	2	7	4	1
26	2	0	0	3	2

Table H.2-6: ICRP 74 at 3 ft - Location of Average Dosimeter Values

Relative	Y (cm) for Phantom Tally Plane				
Z (cm)	-16	-8	0	8	16
74		3	5	1	
66	2	3	1	5	1
58	3	6	1	5	6
50	3	5	4	8	3
42	2	2	2	2	5
34	0	2	5	2	2
26	2	0	0	3	5

APPENDIX H.3: SUMMARY TABLES FOR THE LOCATION OF THE MAXIMUM DOSIMETER VALUES

Table H.3-1: ANSI 1977 at 1 ft - Location of Maximum Dosimeter Values

Relative	Y (cm) for Phantom Tally Plane				
Z (cm)	-16	-8	0	8	16
74		0	0	0	
66	2	1	0	2	6
58	24	3	0	2	39
50	1	1	1	1	4
42	1	0	4	0	1
34	1	0	2	0	3
26	0	0	0	0	0

Table H.3-2: ANSI 1991 at 1 ft - Location of Maximum Dosimeter Values

Relative	Y (cm) for Phantom Tally Plane				
Z (cm)	-16	-8	0	8	16
74		0	1	0	
66	2	1	0	2	5
58	24	3	0	2	42
50	2	1	0	1	1
42	1	0	5	0	1
34	0	0	2	0	3
26	0	0	0	0	0

Table H.3-3: ICRP 74 at 1 ft - Location of Maximum Dosimeter Values

Relative	Y (cm) for Phantom Tally Plane				
Z (cm)	-16	-8	0	8	16
74		0	0	0	
66	2	1	0	2	6
58	23	3	0	2	40
50	2	1	0	1	3
42	1	0	5	0	1
34	1	0	2	0	3
26	0	0	0	0	0

Table H.3-4: ANSI 1977 at 3 ft - Location of Maximum Dosimeter Values

Relative	Y (cm) for Phantom Tally Plane				
Z (cm)	-16	-8	0	8	16
74		1	0	3	
66	18	0	0	1	28
58	10	0	0	5	10
50	0	0	0	0	7
42	5	0	0	0	7
34	0	0	0	0	1
26	2	0	0	0	1

Table H.3-5: ANSI 1991 at 3 ft - Location of Maximum Dosimeter Values

Relative	Y (cm) for Phantom Tally Plane				
Z (cm)	-16	-8	0	8	16
74		1	0	2	
66	16	0	0	1	28
58	10	2	0	4	11
50	2	0	0	0	5
42	5	0	0	0	7
34	1	0	0	0	2
26	1	0	0	0	1

Table H.3-6: ICRP 74 at 3 ft - Location of Maximum Dosimeter Values

Relative	Y (cm) for Phantom Tally Plane				
Z (cm)	-16	-8	0	8	16
74		1	0	2	
66	19	0	0	1	28
58	9	0	0	6	9
50	0	0	0	0	7
42	4	0	0	0	9
34	0	0	0	0	1
26	2	0	0	0	1

APPENDIX H.4: SUMMARY TABLES FOR THE LOCATION OF THE MINIMUM DOSIMETER VALUES

Table H.4-1: ANSI 1977 at 1 ft - Location of Minimum Dosimeter Values

Relative	Y (cm) for Phantom Tally Plane				
Z (cm)	-16	-8	0	8	16
74		11	4	0	
66	0	2	0	0	0
58	0	4	0	0	0
50	0	0	0	0	0
42	0	1	0	0	0
34	0	1	0	0	0
26	0	24	29	21	2

Table H.4-2: ANSI 1991 at 1 ft - Location of Minimum Dosimeter Values

Relative	Y (cm) for Phantom Tally Plane				
Z (cm)	-16	-8	0	8	16
74		6	4	0	
66	0	2	0	0	0
58	0	1	0	0	0
50	0	0	0	0	0
42	0	2	0	0	0
34	0	1	0	0	0
26	1	33	26	22	1

Table H.4-3: ICRP 74 at 1 ft - Location of Minimum Dosimeter Values

Relative	Y (cm) for Phantom Tally Plane				
Z (cm)	-16	-8	0	8	16
74		11	4	0	
66	0	2	0	0	0
58	0	4	0	0	0
50	0	0	0	0	0
42	0	1	0	0	0
34	0	0	0	0	0
26	0	24	31	20	2

Table H.4-4: ANSI 1977 at 3 ft - Location of Minimum Dosimeter Values

Relative	Y (cm) for Phantom Tally Plane				
Z (cm)	-16	-8	0	8	16
74		8	7	1	
66	0	3	0	0	0
58	0	3	0	0	0
50	0	0	0	0	0
42	0	0	0	0	0
34	0	2	1	1	0
26	0	11	53	9	0

Table H.4-5: ANSI 1991 at 3 ft - Location of Minimum Dosimeter Values

Relative	Y (cm) for Phantom Tally Plane				
Z (cm)	-16	-8	0	8	16
74		5	6	2	
66	0	2	0	0	0
58	0	5	0	0	0
50	0	1	0	0	0
42	0	0	0	0	0
34	0	2	1	1	0
26	0	16	48	10	0

Table H.4-6: ICRP 74 at 3 ft - Location of Minimum Dosimeter Values

Relative	Y (cm) for Phantom Tally Plane				
Z (cm)	-16	-8	0	8	16
74		8	6	2	
66	0	2	0	0	0
58	0	3	0	0	0
50	0	0	0	0	0
42	0	0	0	0	0
34	0	3	1	1	0
26	0	13	52	8	0

Appendix I: Glove box Experiment at NETL

GLOVE BOX EXPERIMENT AT NETL

Objectives

The glove box experiment at Nuclear Engineering Teaching Laboratory (NETL) at the University of Texas consisted of the following:

Setup of the glove box located in the reactor bay at NETL with a given neutron source and a field of LANL dosimeters arranged in specific locations around the glove box. Expose dosimeters for 24 hours.

Measure the neutron radiation field at various locations using a He-3 proportional counter.

Construct an MCNP model of the above glove box setup and calculate the neutron radiation dose field at the various dosimeter locations.

Compare results of the computational analysis (iii.) with that of the experiment (i. & ii.).

Repeat steps iii and iv. using an anthropomorphic computational phantom in place of the field of LANL dosimeters.

EXPERIMENTAL SETUP

Description of Glove box

The glove box (Fig. I-1) used was located on the 2nd level of the reactor bay at NETL. The body of the glove box was approximately 182.88 cm x 116.84 cm x 81.76 cm (72• x 46" x $32\frac{3}{16}$") and the bottom of the glove box was 90.17 cm (35½•) above the floor. The glove box was constructed of 0.3175 cm ($\frac{1}{8}$•) stainless steel while the viewing windows were 0.3175 cm ($\frac{1}{8}$•) leaded glass.

The lower viewing window was 155.89 cm x 22.86 cm (61⅜" x 9") and contained four glove ports, each with an inner diameter of 20.96 cm (8¼"). The lower viewing window was symmetrically placed within a panel 40.64 cm x 182.9 cm (16" x 72"). Each pair of glove ports was centered 55.88 cm (22") from the nearest side edge with the centers of each gloveport in a pair 38.10 cm (15") apart.

Figure I-1: Glove Box Used for Experiment

On the floor of the glove box against the front inside surface was a row of lead bricks across the width of the glove box and wrapped in yellow tape, which also covered the floor of the glove box.

Neutron Source

A plutonium-beryllium ($PuBe_{13}$) neutron source, M-797, made by Monsanto Research Corporation (Hertz 1961) was chosen since it was the smallest activity source available. It contained 7.86 g of Be and 15.97 g of Pu uniformly mixed and doubly encapsulated as shown in Fig. I-2 (Profio 1976) with dimensions given in inches. The dimensions of the outer container were 1.02" outer diameter x 1.46" high (2.5908 cm x 3.7084 cm). The source strength was listed as 1.81 x 10^6 n/s. The neutron source was placed on the floor of the glove box on the centerline of the right-hand pair of glove ports 15 cm from the inside surface of the glove box (Fig. I-3).

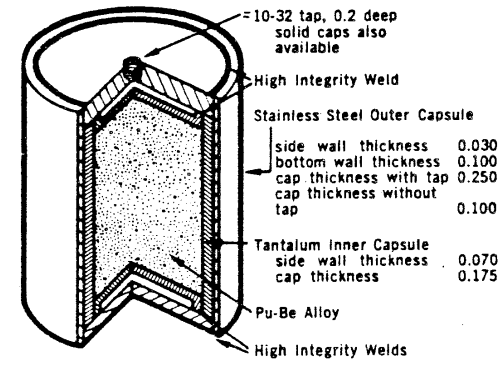

Figure I-2: Plutonium-Beryllium Neutron Source

Figure I-3: Source Positioned Within Glove box

Description of Dosimeters

Los Alamos utilizes Model 8823 whole-body thermoluminescent dosimeter (TLD) to measure personnel exposure to beta, gamma, and neutron sources of radiation. This is a dual card dosimeter. The upper card in the dosimeter contains four TLD elements and is used for estimating the beta and gamma doses. The lower card with four TLD elements is surrounded on all sides by a cadmium box except on the anterior side of two of the elements and posterior to the other two elements. The anterior side represents an anti-albedo detector that measures the thermal energy neutrons incident on the front of the detector while the posterior side represents a classic albedo detector measuring the thermal energy neutrons exiting the body. There is a severe angular dependence for neutrons when the angle of incidence greater than 30º. This dependence can reduce the dose measured to 25% or less of the dose measured at 0º (Mallett 1997).

For radiation environments with high-energy neutron radiation fields, a track-etch dosimeter (TED) is used in conjunction with the Model 8823 dosimeter. The TED

is sensitive to neutron radiations only. A TED consists of a hemispherical-shaped plastic case that contains a triangular polystyrene pyramid with sides that are inclined 40° to the base. A track-etch plastic foil is placed on each side of the pyramid and the base. The purpose of this arrangement is to minimize the angular dependence of the TED.

Setup of Dosimeter Field

A small metal table was placed in front of the pair of glove ports on the right-hand side of the glove box. On the table, two slabs of 5.1 cm (2 in.) thick polyethylene (poly) were setup – the first 30.5 cm (1 ft) away from the glove box and the second 91.5 cm (3 ft) from the glove box. On each an array of dosimeters were taped on as shown in Fig. I-4.

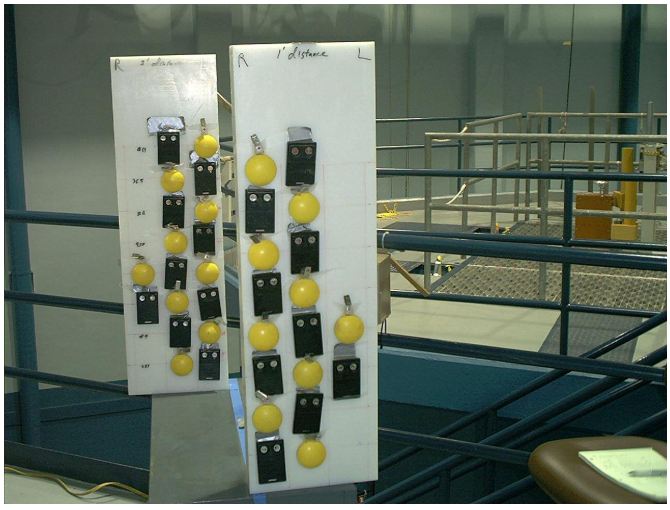

Figure I-4: Setup of Dosimeters in Front of the Glove box

The round yellow dosimeters are the LANL track edge dosimeters (TED) while the rectangular black dosimeters are the LANL 8823 TLDs. Twenty two TEDs, #1-#22, were used with #8 and #10 used as controls. Twenty two TLDs were used, numbers 386, 413,

464, 607, 754, 283, 286, 310, 328, 336, 365, 831, 833, 950, 954, 956, 988, 998, 091, 128 with 372 and 074 used as controls. The dosimeters were placed in squares 8 cm x 8cm that were marked on the poly slabs.

The relative positions of the dosimeters on the poly slabs facing the front of the glove box with their identification number are shown in Table I-1. Each dosimeter occupied an 8 cm x 8 cm square with the center of the dosimeter at the position shown relative to the bottom of the poly block. Absolute positions for the center of each dosimeter are also provided.

Table I-1: Setup of Dosimeters in Front of the Glove box.

	Y (cm) for Poly Slab at 91.5 cm (3 ft)				Y (cm) for Poly Slab at 30.5 cm (1 ft)		
Z (cm)	Relative	-20	-12	-4	4	12	20
Relative	Absolute	55.56	47.56	39.56	31.56	23.56	15.56
64	6.85		336	15	16	286	
56	-1.15		20	365	413	19	
48	-9.15		91	11	18	833	
40	-17.15		13	950	464	17	
32	-25.15	3	954	5	21	831	22
24	-33.15	328	1	988	998	9	956
16	-41.15		128	4	2	754	
8	-49.15		14	283	310	7	

On the left-hand side, one poly block was placed on top of another against the left-hand side with one TLD, #607, and one TED, #12, placed at about floor level of the glove box. On the right-hand side, a poly block was placed on a stool against the right-hand side with one TLD, #386, and one TED, #6, placed at about floor level of the glove box. Fig. I-5 shows the setup of all of the poly slabs in relation to the glove box.

The left edge of the blue line down the middle of the table represents the centerline of the right-hand glove ports on which the source was placed inside the glove box.

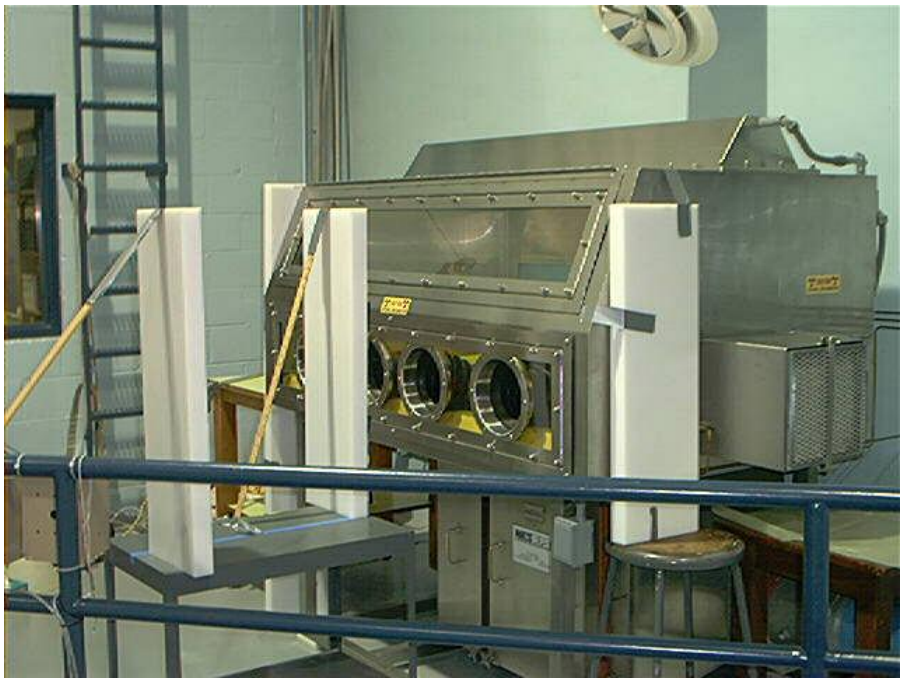

Figure I-5: Setup of Dosimeters Around the Glove box

Setup to Measure Neutron Radiation Field

To measure the neutron radiation field, a RSN-105S-M9, a miniature Helium-3 filled detector welded to the end of a stainless steel cable sheath (Fig. I-6), was used (Richards 2003). The small size permits accurate flux plotting without excessive counting times and with small error from flux perturbation by the detector. It provides high sensitivity while permitting operation at low voltage.

The basic radiation counting system consisted of the He-3 proportional counter, a high voltage power supply feeding a preamplifier, an amplifier with output to an

oscilloscope, a single channel analyzer, a scaler, and a counter. A block diagram for this system is shown in Fig. I-7

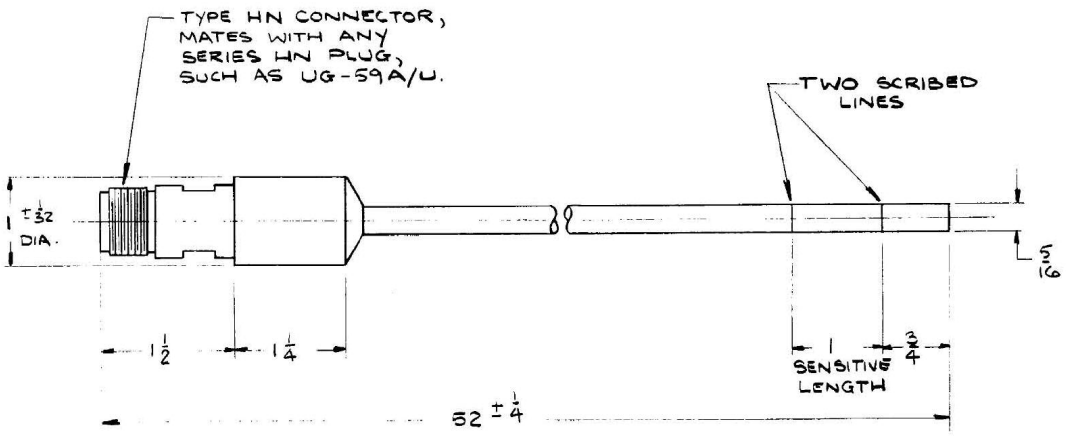

Figure I-6: Helium-3 Proportional Counter

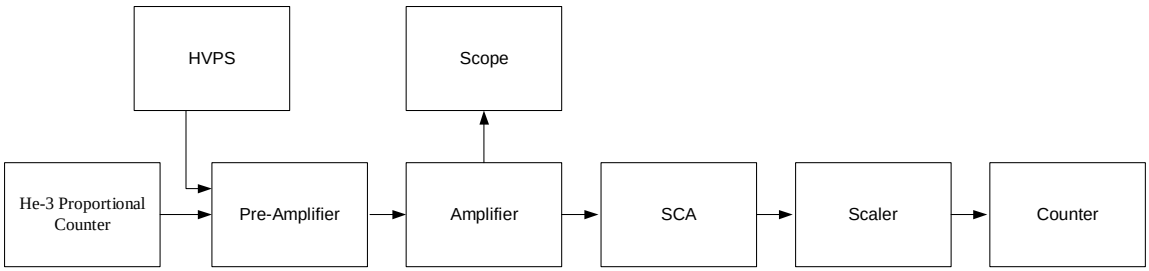

Figure I-7: Block Diagram of Counting System

When the detector element absorbs energy from an incident neutron, it produces a pulse current whose integral is proportional to the absorbed energy. This integrated pulse is converted to a voltage pulse, and then shaped by the preamplifier. The shaping amplifier provides additional amplification. The output pulses from this amplifier go to a single channel analyzer which coupled with the

scaler allows for the counting of all neutrons above a desired energy threshold. Figure I-8 shows the counting system while Fig. I-9 shows the setup for the counting at one of the specified dosimeter positions.

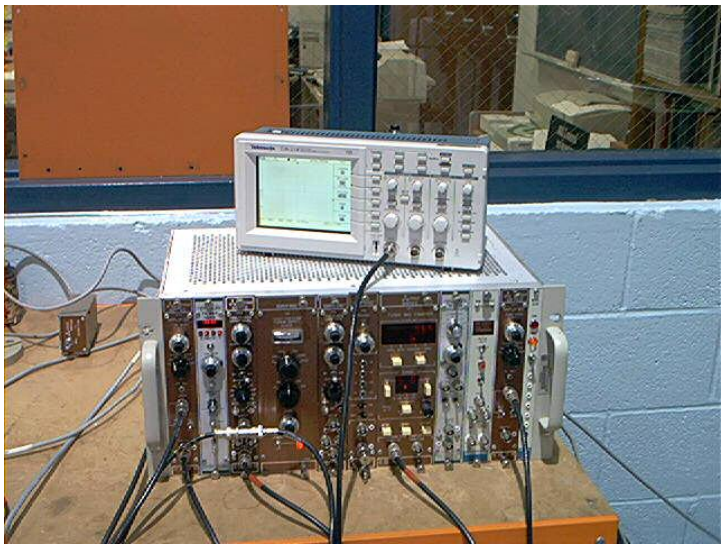

Figure I-8: Setup of Counting System

Figure I-9: Setup of Proportional Counter at a Given Dosimeter Position

EXPERIMENTAL RESULTS

Radiation Dose Field Determined by Dosimeters

Before the experiment, all of the dosimeters were kept together. Two TLDs and two TEDs were kept back as controls. The remaining dosimeters were exposed for 24 hours to the neutron field from the M-797 neutron source. After the experiment and upon return to Los Alamos, the dosimeters were taken to HSR-4, Health Physics Measurements Group, and read. The data files received from HSR-4 are provided in Appendix J. Table I-2 provides the dosimeter readings in mrem by TLD badge number. For the dosimeters placed on the poly slabs in front of the glove box, Table I-3 provides the TLD readings in mrem by location. Table I-4 provides the dosimeter readings in mrem by TED badge number while Tables I-5 and I3-6 provide the readings (mean and base) for the TEDs by location while Table I-7 provides a summary of the dosimeter readings.

Table I-2: TLD Readings in mrem by Badge Number.

Badge	Neutron	Badge	Neutron
74	0.000	413	44.000
91	14.000	464	51.000
128	20.000	607	14.000
283	12.000	754	62.000
286	31.000	831	57.000
310	44.000	833	45.000
328	19.000	950	14.000
336	14.000	954	17.000
365	19.000	956	46.000
372	0.000	988	13.000
386	39.000	998	67.000

Table I-3: TLD Readings in mrem by location.

	Y (cm) for Poly Slab at 91.5 cm				Y (cm) for Poly Slab at 30.5 cm		
Z (cm)	Relative	-20	-12	-4	4	12	20
Relative	Absolute	55.56	47.56	39.56	31.56	23.56	15.56
64	6.85		14			31	
56	-1.15			19	44		
48	-9.15		14			45	
40	-17.15			14	51		
32	-25.15		17			57	
24	-33.15	19		13	67		46
16	-41.15		20			62	
8	-49.15			12	44		

Table I-4: TED Readings in mrem by Dosimeter Number.

Dosimeter Number	Mean Pyramidal	Base Foil	Dosimeter Number	Mean Pyramidal	Base Foil
1	36	71	12	17	22
2	169	300	13	32	60
3	31	57	14	31	55
4	35	59	15	24	48
5	26	61	16	69	106
6	123	183	17	114	195
7	116	191	18	85	144
8	-6	-7	19	79	107
9	138	245	20	29	45
10	-6	-8	21	146	257
11	26	48	22	119	181

Table I-5: TED (Mean) Readings in mrem by Location.

		Y (cm) for Poly Slab at 91.5 cm			Y (cm) for Poly Slab at 30.5 cm		
Z (cm)	Relative	-20	-12	-4	4	12	20
Relative	Absolute	55.56	47.56	39.56	31.56	23.56	15.56
64	6.85			24	69		
56	-1.15		29			79	
48	-9.15			26	85		
40	-17.15		32			114	
32	-25.15	31		26	146		119
24	-33.15		36			138	
16	-41.15			35	169		
8	-49.15		31			116	

Table I-6: TED (Base) Readings in mrem by Location.

		Y (cm) for Poly Slab at 91.5 cm			Y (cm) for Poly Slab at 30.5 cm		
Z (cm)	Relative	-20	-12	-4	4	12	20
Relative	Absolute	55.56	47.56	39.56	31.56	23.56	15.56
64	6.85			48	106		
56	-1.15		45			107	
48	-9.15			48	144		
40	-17.15		60			195	
32	-25.15	57		61	257		181
24	-33.15		71			245	
16	-41.15			59	300		
8	-49.15		55			191	

Table I-7: Summary of Dosimeter Readings in mrem.

	30.5 cm (1 ft)			91.5 cm (3 ft)		
	TLD	TED (mean)	TED (base)	TLD	TED (mean)	TED (base)
Max	67	169	300	20	36	71
Min	44	79	107	12	26	45
Ave	50	115	192	16	30	56

Radiation Dose Field Determined by He-3 Proportional Counter

The neutron radiation field was measured at several of the dosimeter locations at 30.5 cm (1 ft) and 91.5 cm (3 ft). Most were recorded with the poly slabs in place. The proportional counter was held in place by a clamp on a ring stand (Figure I-9). The sensitive portion of the detector was placed approximately where the middle of the dosimeter had been located based on the grids that had been drawn on the poly slabs. In a few cases, the poly slab was removed after the detector was setup and measurements made. A count time of 5 minutes was used. For various dosimeter positions, the measured counts are listed in Table I-8.

To determine the background, the source was removed from the glove box, put into a shielded container, and moved to a far corner of the reactor bay. The detector was placed at position 831 at 30.5 cm (1 ft). A five minute count yielded 198 counts. An overnight run was then begun; however, through a miscommunication, the equipment was removed the next morning before the data could be recorded. According to Associate Director of NETL, Sean O'Kelly (2003), the background in the reactor bay is 40 ct/min.

Table I-8: Neutron Radiation Field Measurements in ct/min by Location.

		Y (cm) for Poly Slab at 91.5 cm			Y (cm) for Poly Slab at 30.5 cm		
Z (cm)	Relative	-20	-12	-4	4	12	20
Relative	Absolute	55.56	47.56	39.56	31.56	23.56	15.56
64	6.85		28			39.4	
56	-1.15					48.6	
48	-9.15					58.4	
40	-17.15					71.2	
32	-25.15		38.3		59.8	69.2	70.4
24	-33.15					81.4	
16	-41.15					79	
8	-49.15		29.6			71.8	

MCNP MODEL OF NETL EXPERIMENT

An MCNP model of the glove box was constructed based on the materials of construction and dimensional measurements taken. Each polyethylene slab was modeled with a simulated dosimeter field corresponding to the experimental setup. The gloves for the glove ports were not modeled based on the fact that gloves contribute little to the attenuation of neutrons due to the thickness of the gloves and the location of the source. The neutron energy spectrum for the M-797 neutron source was calculated using SOURCES 4C (Wilson 2002). A mesh tally was used to simulate the dosimeter field that was setup for the experiment.

The second computational model involved inserting a computational phantom in place of a poly slab and removing the remaining poly slabs from the model. Each phantom also has a dosimeter lattice in front of the torso to simulate the possible positions that a dosimeter can be worn. It is a planar lattice projected onto a vertical cylindrical surface that lies just off the surface of the torso (within ~ 5 cm of the torso depending on location on the cylindrical surface). Figure I-10

provides a longitudinal medial view of the phantom. Beside it is the dosimeter lattice that is placed over and around the torso of the phantom. The highlighted tally represents the middle of the torso where the dosimeter is most likely worn. Table I-9 provides the tally number associated with the positions on the lattice. Sample input decks are provided in Appendix K.

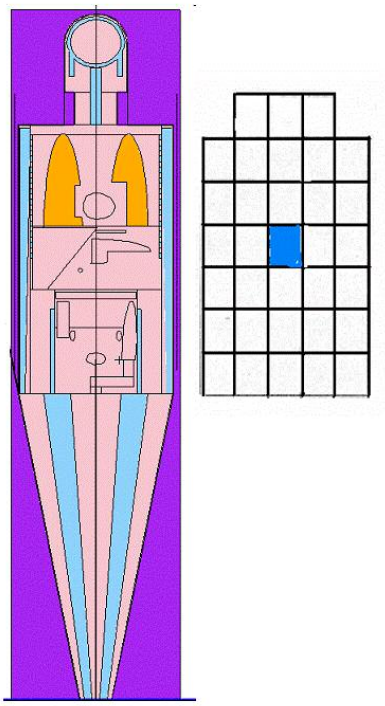

Figure I-10: Computational Phantom with Dosimeter Lattice.

COMPUTATIONAL RESULTS

Calculated Dose Using Mesh Tally

When a mesh tally is used, an output file "mdata" is created with the tally results. Using an auxiliary program called "gridconv", the data in this file is converted from a binary format into a text format that can be used in a spreadsheet or by a graphics package to plot the data. Table I.10 provides the calculated dose in mrem by location.

Table I-9: Tally Number in Dosimeter Lattice by Location.

Relative Z (cm)	Relative Y (cm) for Phantom Tally Plane				
	-16	-8	0	8	16
74		2	12	22	
66	32	42	52	62	72
58	82	92	102	112	122
50	132	142	152	162	172
42	182	192	202	212	222
34	232	242	252	262	272
26	282	292	302	312	322

Table I-10: Calculated Dose by Location on Poly Slabs in mrem per 24 hr.

Relative	Relative Y (cm) for Poly Slab at 91.5 cm			Relative Y (cm) for Poly Slab at 30.5 cm		
Z (cm)	-20	-12	-4	4	12	20
64	47.7	49.4	47.8	112.2	109.1	105.1
56	50.6	51.9	50.4	134.0	129.8	123.8
48	48.9	51.4	49.6	160.3	154.7	144.3
40	39.5	41.0	39.9	191.3	183.2	168.1
32	24.7	26.4	25.2	221.8	210.7	191.7
24	16.6	17.6	16.9	195.8	183.4	163.3
16	16.3	17.0	16.0	114.9	105.3	89.9
8	16.6	17.2	16.1	76.5	69.7	57.9

In the following figures, the dose field is given in mrem per the 24 hour exposure of the experiment. Figure I-11 provides the dose field for the dosimeter locations on the poly slab at 30.5 cm while Figure I-12 provides a planar view that includes the dosimeter grid shown in relation to the outline of the glove box with glove ports and the neutron dose field in that plane. Figures 3-13 through 3-18 provide the same views for the dosimeter grids located on the other poly slabs.

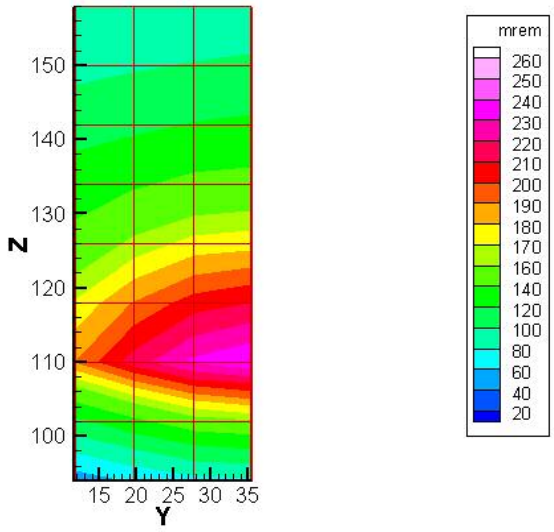

Figure I-11: Grid View of Field on Poly Slab at 30.5 cm. in Front of Glove Box.

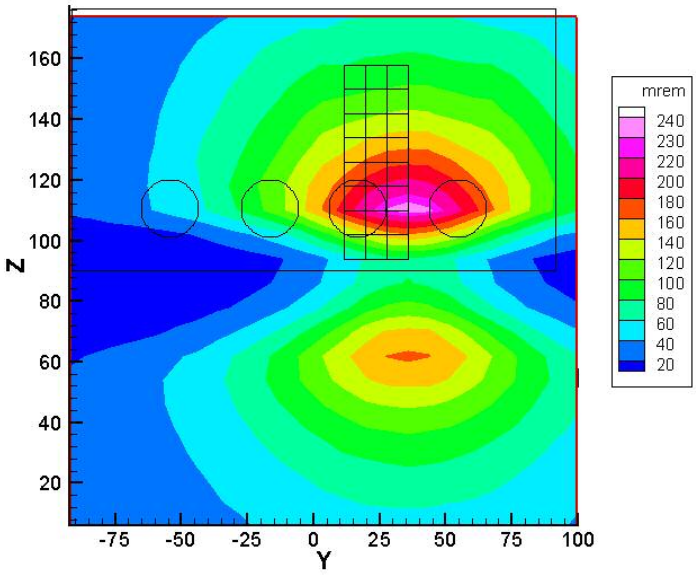

Figure I-12: Planar View of Field at 30.5 cm. in Front of Glove Box.

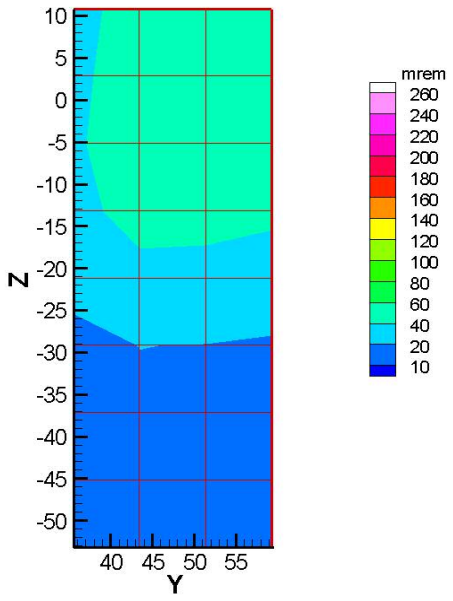

Figure I-13: Grid View of Field on Poly Slab at 91.5 cm. in Front of Glove Box.

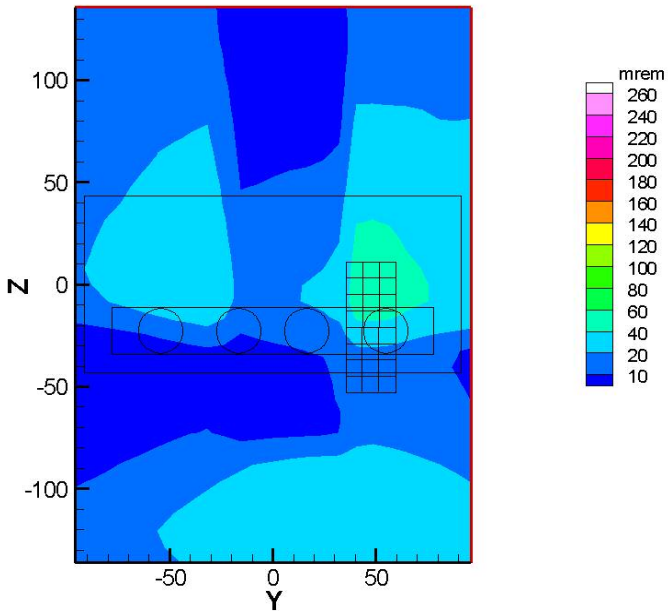

Figure I-14: Planar View of Field at 91.5 cm. in Front of Glove Box.

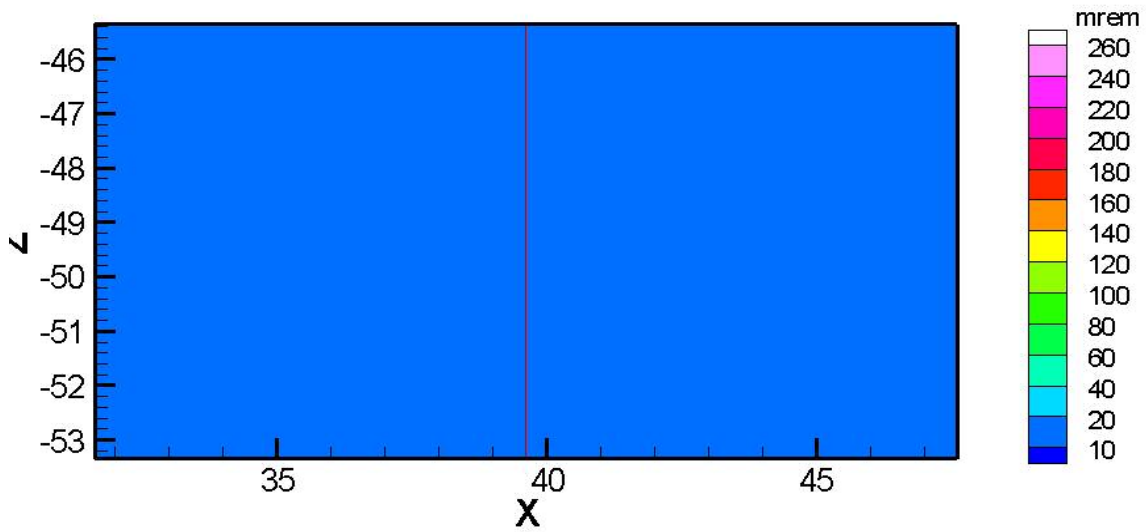

Figure I-15: Grid View of Field on Poly Slab on Left Side of Glove Box.

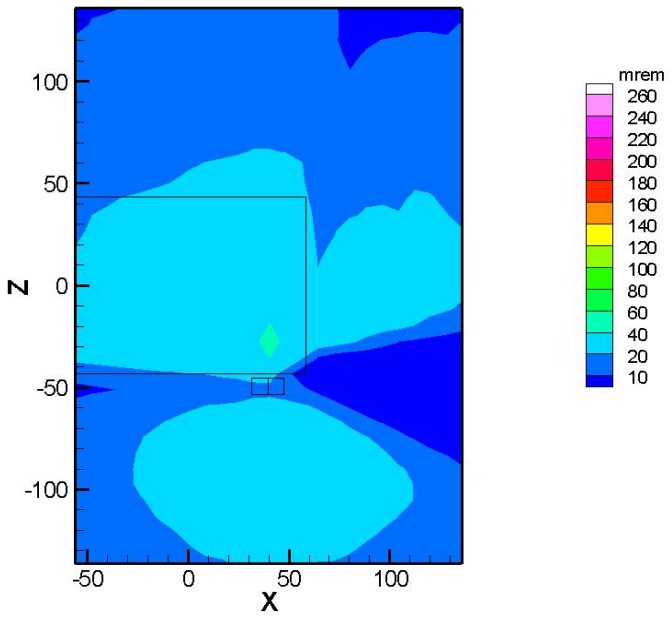

Figure I-16: Planar View of Field on Poly Slab on Left Side of Glove Box.

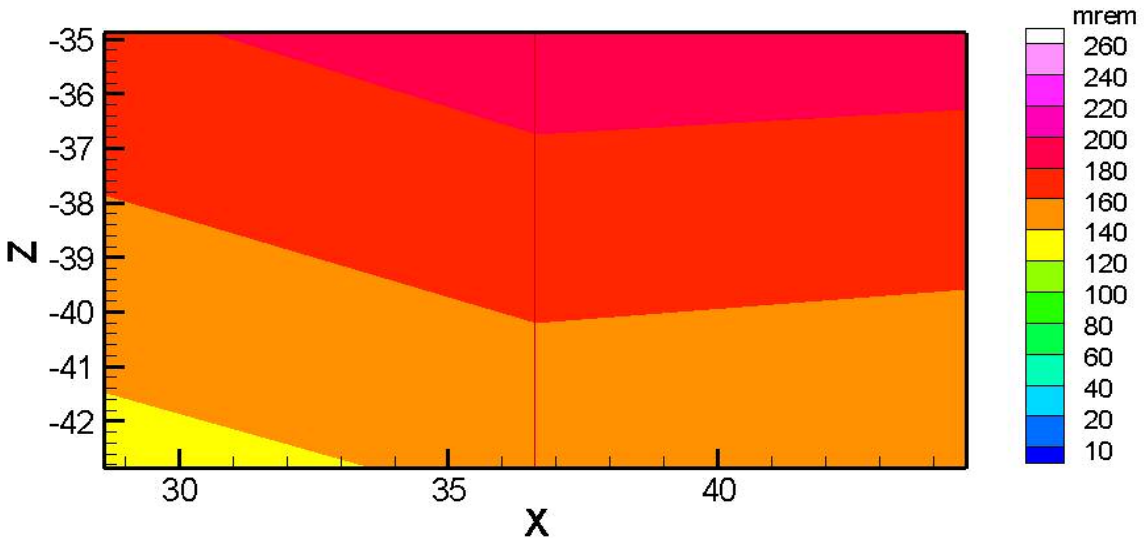

Figure I-17: Grid View of Field on Poly Slab on Right Side of Glove Box.

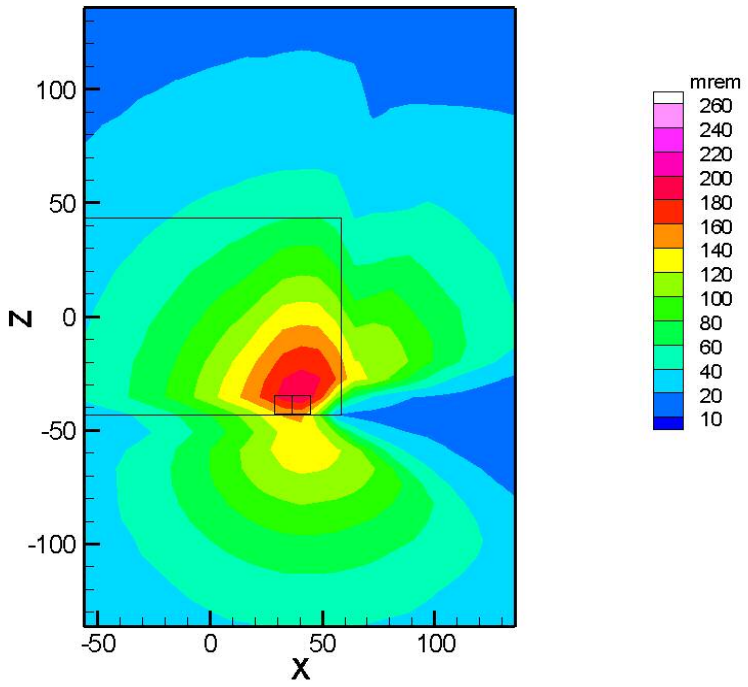

Figure I-18: Planar View of Field on Poly Slab on Right Side of Glove Box.

Estimated Dose Using Computational Phantom with its Dosimeter Lattice

The computational phantom was placed with its center either 30.5 cm or 91.5 cm (1 ft or 3 ft) in front of the glove box. This places the dosimeter lattice about 17 cm closer to the source than the centerline of the phantom. Tables I-11 and I-12 provide these dose estimates using the dosimeter lattice for the phantom at 30.5 cm or 91.5 cm (1 ft or 3 ft) respectively while Figures I-19 and I-20 provide the radiation field at the same location as the phantom dosimeter lattice.

Table I-11: Estimated Dose (mrem) with Dosimeter Lattice at 30.5 cm

Relative	Relative Y (cm) for Phantom Tally Plane & Phantom at 30.5 cm				
Z (cm)	-16	-8	0	8	16
74		129.8	121.8	127.9	
66	215.3	168.7	160.7	169.4	212.5
58	256.9	212.8	208.9	213.6	257.0
50	314.6	274.6	268.8	273.3	318.7
42	382.4	347.6	353.2	349.1	379.5
34	452.9	443.1	460.7	445.1	458.7
26	499.2	538.8	580.3	542.3	497.5

Table I-12: Estimated Dose (mrem) using Dosimeter Lattice of Phantom at 91.5

Relative	Relative Y (cm) for Phantom Tally Plane & Phantom at 91.5 cm				
Z (cm)	-16	-8	0	8	16
74		51.4	49.7	52.1	
66	76.4	57.2	54.2	56.6	73.9
58	82.3	62.2	59.6	62.0	81.9
50	85.8	66.3	63.4	67.0	87.5
42	84.7	68.5	65.6	68.2	85.0
34	65.6	55.6	54.6	54.6	65.8
26	38.3	32.1	31.3	31.9	37.5

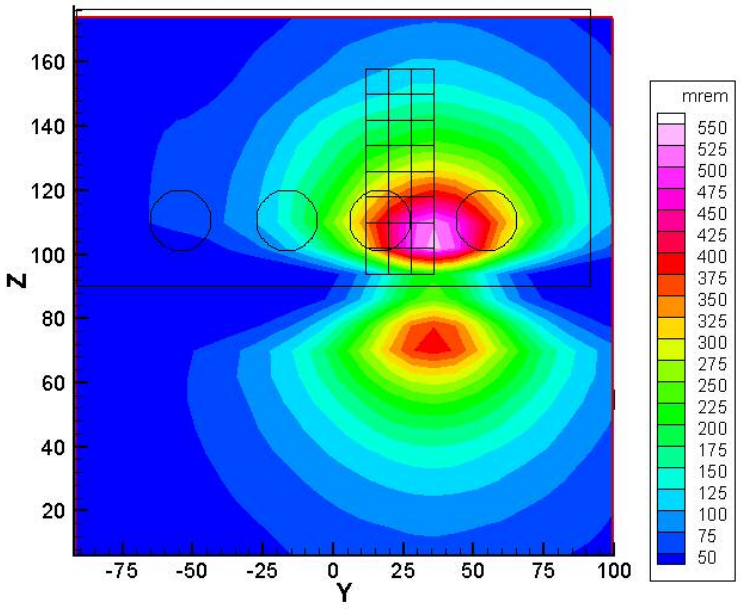

Figure I-19: Estimated Dose Field with Phantom Dosimeter Lattice at 30.5 cm.

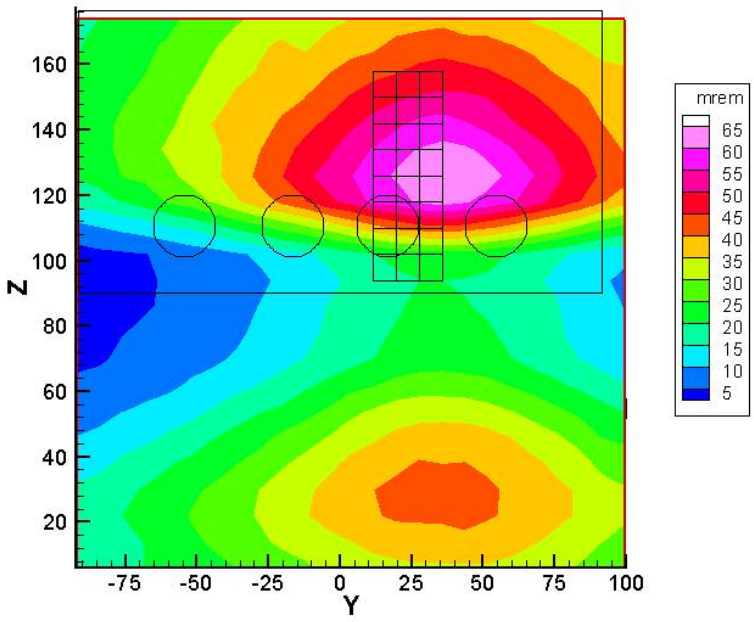

Figure I-20: Estimated Dose Field with Phantom Dosimeter Lattice at 91.5 cm.

In accordance with ICRP 26 (1977), the effective dose equivalent was calculated based on the organ and tissue doses. For comparison, the effective dose was calculated based on ICRP 60 (1991). Table I-13 provides a summary of the dose estimates in mrem based on the estimated dose received by the tissues and organs.

Table I-13: Estimated Dose from Computational Phantom in mrem.

	30.5 cm (1 ft)		91.5 cm (3 ft)	
	EDE (ICRP 26)	ED (ICRP 60)	EDE (ICRP 26)	ED (ICRP 60)
Male with breasts	117.0	97.9	22.1	17.2
Male w/o breasts	92.4	89.6	15.2	14.9
Female	85.1	72.3	19.5	15.1

COMPARISON OF COMPUTATIONAL AND EXPERIMENTAL RESULTS

Comparison of Neutron Radiation Field Measurements with TLD and TED Readings

A comparison of the TED (base), TED (mean), and TLD readings normalized to the Y=12, Z=24 position compared to the normalized field measurements made by the neutron probe is provided in Table I-14.

Table I-14: Comparison of Field Measurements with TLD and TED Readings.

Relative	Neutron probe		TED (mean)		TED (base)		TLD	
Z with Y=12	cts/min	Norm.	(mrem)	norm	(mrem)	norm	(mrem)	norm
64	39.4	0.48					31	0.49
56	48.6	0.60	79	0.60	107	0.44		
48	58.4	0.72					45	0.70
40	71.2	0.87	114	0.87	195	0.80		
32	69.2	0.85					57	0.89
24	81.4	1.00	138	1.00	245	1.00		
16	79	0.97					62	0.97
8	71.8	0.88	116	0.88	191	0.78		

Thus, using normalized data, the field as determined by neutron probe matches closely with the field as determined by the dosimeters. This shows the validity of using dosimeter tally planes to provide the characteristics of the neutron radiation field.

At the 1 ft plane, the radiation field varies by over a factor of 4 across the field. The field pattern in Fig. I-12 is primarily concentric circles except for that portion near the bottom of the glove box. This portion of the field shows the attenuation provided by Pb bricks that were in front of the source in the glove box. At 91.5 cm, the field is more uniform which should be expected since the distance has increased between the plane and the source.

Comparison of TLD and TED Readings with Dosimeter Grids on Poly Slabs

From Table I-3 and Table I-5, for the most part, the TLD readings are about half of the TED (mean) readings. A one-to-one comparison cannot be made because of the way the TLDs and TEDs were put onto the poly slabs – they were next to each other and thus did not provide a measurement for the same location. Likewise, from Table I-4 and Table I-6, the TED (base) readings were greater than the TED (mean) readings by almost a factor of about $1^{1}/_{2}$. When compared with Table I-10, the estimated dose from the dosimeter grids more closely corresponded to the TED (base) readings than to the TED (mean) readings and was about a factor of two to three greater than the TLD readings in general.

The TLD readings can be expected to be low because they are not designed to measure the dose received from a fast neutron spectrum whereas the TEDs are designed for fast neutrons. The chips in the TEDs formed a pyramid. Due to the way they were placed on the poly and due their specific location, the orientation of the faces of the pyramid to the source location varied. Thus, there is no specific

relationship between the TED readings and the dose from the dosimeter girds on the poly slabs except that the variation is in general agreement.

This indicates that there may be a problem using the TLDs for determining dose when the neutron source is a fast spectrum than a thermal spectrum.

Comparison of Dosimeter Grids on Poly Slabs with Phantom Dosimeter Lattice

In comparing Tables I-10 and I-1, the values at the same location are similar except for the bottom three rows of the phantom dosimeter lattice. These values are larger than the corresponding values for the dosimeter grids at 30.5 cm. The predominant reason for this is that the dosimeter lattice is located about 17 cm in front of the centerline of the phantom, which is used as the location of the dosimeter grid. Thus, as shown in Figure I-19, the radiation field is more collimated than at the dosimeter grid as shown in Figure I-12. The collimation produces higher doses in the lower part of the lattice than in the upper half because of the location of the source relative to the grid and lattice. With the grid moved back, the radiation field broadens which results in higher doses in the upper half than in the bottom half of the grid.

Comparison of Phantom Whole Body Dose with Other Estimates

The phantom whole body dose at 30.5 cm was 92.4 mrem for a male without breasts. The TLD estimates were between 44 and 67 mrem with an average of 50 mrem, the TED (mean) estimates were between 70 and 169 with an average of 115 mrem, and the TED (base) estimates were between 107 and 300 mrem with an average of 192 mrem.

At 91.5 cm, the phantom whole body was 19.5 mrem for a male without breasts. The TLD estimates were between 12 and 20 mrem with an average of 16 mrem,

the TED (mean) estimates were between 26 and 36 with an average of 30 mrem, and the TED (base) estimates were between 45 and 71 mrem with an average of 56 mrem.

Thus, the TED (mean) readings came closer to the whole body estimate at a ft. while the TLD readings came closer to the whole body estimate at 91.5 cm.

The computational estimates using dosimeter tally planes are closer to the TED (base) readings and thus are about a factor of 2 to 3 greater than the whole body dose estimates.

Conclusions

The whole body dose was better approximated by the TED (mean) readings than the TLD reading. This is to be expected since the mean energy of the neutron source was 4.85 MeV and TLDs were not designed for higher energy spectrums. Also, since there is a severe angular dependence based on the angle of incidence of the neutron on the TLD, the TLD readings may be low by a factor of four or more.

The computational estimates using dosimeter tally planes or lattices were up to a factor of two to three higher than the whole body estimates. Since a dosimeter can be anywhere between waist and neck, this implies that the dose of record could easily be different depending on where the dosimeter is worn.

Because of the way the experiment was setup, a direct comparison between many different estimates was not possible. Examples include

TLDs and TEDs side by side,

The dosimeter grid on the poly slabs was not filled with dosimeters in every position, and

The dosimeter grid was setup offset from what the phantom tally lattice,

Bullet 3 is typical of the real world. It takes much thought to design an experiment that can be effectively modeled using MCNP. Most of the time, there are no experimental data that can be used to validate a given model. To model an existing operation and measure the radiation dose field to validate it is time consuming and something that no one is usually willing to pay for.

Appendix J: HSR-4 DOSIMETER DATA

APPENDIX J.1

Track Edge Dosimeter (Pn3 Or Ted) Data

Good afternoon Art. Below are the results from the dosimeters you requested.
Please bear in mind our LLD is 20 mRem. Also our Response Factor,
tracks per square centimeter per mRem, is developed using foils exposed in the holder.
When in the holder the foils are held at approximately a forty degree angle to the phantom.
The base foil exposures included here have not been corrected for this.

If you have any questions please contact me.

Rich McKeever

PN3 Data
Date Read 7-May-03
Calc Date 7-May-03

Foil Number	Wheel Position	Area Read	Zone 1	Zone 2	Pixelsum	Foil Position	Foil Exposure (mRem)	BGRD Tracks * cm^-2	Response Factor Tr * cm^-2 * mRem ^-1	Dosimeter Number	Mean Pyramidal Exposure	Base Foil Exposure
869316	4	1.6	63	68	3219456	PL	33	28	1.65	#1	36	71
869317	5	1.6	78	76	3369557	PR	41	28	1.65			
869296	6	1.6	63	74	3384157	PB	35	28	1.65			
869295	7	1.6	114	119	3658399	Base	71	28	1.65			
869264	8	1.6	255	280	3932340	PL	186	28	1.65	#2	169	300
869286	9	1.6	233	237	3854497	PR	161	28	1.65			
869307	10	1.6	234	236	3729920	PB	161	28	1.65			
869328	11	1.6	419	419	4285039	Base	300	28	1.65			
869232	12	1.6	45	48	2911387	PL	18	28	1.65	#3	31	57
869253	13	1.6	78	93	3548035	PR	48	28	1.65			

Foil Number	Wheel Position	Area Read	Zone 1	Zone 2	Pixelsum	Foil Position	Foil Exposure (mRem)	BGRD Tracks * cm^-2	Response Factor Tr * cm^-2 * mRem ^-1	Dosimeter Number	Mean Pyramidal Exposure	Base Foil Exposure
869274	14	1.6	62	57	3124783	PB	28	28	1.65			
869315	15	1.6	93	103	3432379	Base	57	28	1.65			
869222	16	1.6	74	66	3301020	PL	36	28	1.65	#4	35	59
869242	17	1.6	67	75	3188059	PR	37	28	1.65			
869243	18	1.6	70	61	3082452	PB	33	28	1.65			
869221	19	1.6	103	98	3172420	Base	59	28	1.65			
869252	20	1.6	59	55	3312930	PL	26	28	1.65	#5	26	61
869273	21	1.6	53	50	3110743	PR	22	28	1.65			
869294	22	1.6	61	63	3219699	PB	30	28	1.65			
869231	23	1.6	106	100	2970940	Base	61	28	1.65			
869241	24	1.6	203	169	3138027	PL	124	28	1.65	#6	123	183
869262	25	1.6	255	214	3568770	PR	161	28	1.65			
869283	26	1.6	143	124	3238521	PB	84	28	1.65			
869220	27	1.6	260	269	3541795	Base	183	28	1.65			
869293	28	1.6	293	248	3580025	PL	188	28	1.65	#7	116	191
869314	29	1.6	140	129	3121766	PR	85	28	1.65			
869251	30	1.6	142	98	3038811	PB	74	28	1.65			
869272	31	1.6	253	296	3805816	Base	191	28	1.65			
869292	32	1.6	17	13	3209615	PL	-6	28	1.65	#8	-6	-7
869313	33	1.6	15	17	2988182	PR	-5	28	1.65			
869230	34	1.6	10	13	2941882	PB	-8	28	1.65			
869271	35	1.6	15	12	2872014	Base	-7	28	1.65			
869240	36	1.6	270	234	3719170	PL	174	28	1.65	#9	138	245
869261	37	1.6	129	108	3329267	PR	73	28	1.65			
869282	38	1.6	247	242	3611236	PB	168	28	1.65			

Foil Number	Wheel Position	Area Read	Zone 1	Zone 2	Pixelsum	Foil Position	Foil Exposure (mRem)	BGRD Tracks * cm^-2	Response Factor Tr * cm^-2 * mRem ^-1	Dosimeter Number	Mean Pyramidal Exposure	Base Foil Exposure
869219	39	1.6	320	371	4032150	Base	245	28	1.65			
869216	40	1.6	17	14	2920809	PL	-5	28	1.65	#10	-6	-8
869217	41	1.6	13	12	2944344	PR	-8	28	1.65			
869218	42	1.6	20	14	3173403	PB	-4	28	1.65			
869215	43	1.6	14	10	2924985	Base	-8	28	1.65			
869312	44	1.6	45	46	2992532	PL	18	28	1.65	#11	26	48
869229	45	1.6	50	41	3157799	PR	18	28	1.65			
869250	46	1.6	73	86	3132155	PB	43	28	1.65			
869291	47	1.6	98	74	2946605	Base	48	28	1.65			
869237	48	1.6	52	35	3034040	PL	16	28	1.65	#12	17	22
869238	49	1.6	61	48	3268286	PR	24	28	1.65			
869239	50	1.6	42	34	3173680	PB	12	28	1.65			
869236	51	1.6	58	44	3080934	Base	22	28	1.65			
869228	52	1.6	49	39	2902643	PL	16	28	1.65	#13	32	60
869249	53	1.6	67	59	3185543	PR	31	28	1.65			
869270	54	1.6	79	98	3454198	PB	50	28	1.65			
869311	55	1.6	115	88	3297031	Base	60	28	1.65			
869247	21	1.6	52	70	3017569	PL	29	28	1.65	#14	31	55
869248	22	1.6	68	55	3041854	PR	30	28	1.65			
869269	23	1.6	64	71	3420175	PB	34	28	1.65			
869268	24	1.6	95	96	3192079	Base	55	28	1.65			
869289	25	1.6	45	49	3096132	PL	19	28	1.65	#15	24	48
869284	26	1.6	40	42	3217983	PR	14	28	1.65			
869263	27	1.6	74	76	3227690	PB	40	28	1.65			
869310	28	1.6	75	96	3131948	Base	48	28	1.65			

Foil Number	Wheel Position	Area Read	Zone 1	Zone 2	Pixelsum	Foil Position	Foil Exposure (mRem)	BGRD Tracks * cm^-2	Response Factor Tr * cm^-2 * mRem ^-1	Dosimeter Number	Mean Pyramidal Exposure	Base Foil Exposure
869303	29	1.6	81	75	3127587	PL	42	28	1.65	#16	69	106
869304	30	1.6	63	46	2900150	PR	24	28	1.65			
869305	31	1.6	207	207	3637125	PB	140	28	1.65			
869325	32	1.6	179	145	3355048	Base	106	28	1.65			
869259	33	1.6	168	159	3313327	PL	107	28	1.65	#17	114	195
869260	34	1.6	100	78	3159456	PR	50	28	1.65			
869265	35	1.6	260	275	3993458	PB	186	28	1.65			
869258	36	1.6	280	279	3965586	Base	195	28	1.65			
869279	37	1.6	128	104	3449046	PL	71	28	1.65	#18	85	144
869280	38	1.6	72	41	3212134	PR	26	28	1.65			
869281	39	1.6	251	211	3681560	PB	158	28	1.65			
869278	40	1.6	216	208	3558515	Base	144	28	1.65			
869285	41	1.6	113	116	3387793	PL	70	28	1.65	#19	79	107
869326	42	1.6	65	50	3133253	PR	27	28	1.65			
869306	43	1.6	221	195	3487215	PB	141	28	1.65			
869327	44	1.6	154	173	3396949	Base	107	28	1.65			
869300	45	1.6	56	36	3021095	PL	18	28	1.65	#20	29	45
869301	46	1.6	68	60	3035411	PR	32	28	1.65			
869302	47	1.6	72	72	3055297	PB	38	28	1.65			
869299	48	1.6	77	87	3055491	Base	45	28	1.65			
869322	49	1.6	178	194	3317090	PL	124	28	1.65	#21	146	257
869323	50	1.6	150	140	3240845	PR	93	28	1.65			
869324	51	1.6	329	302	3910636	PB	222	28	1.65			
869321	52	1.6	362	361	3784971	Base	257	28	1.65			
869244	53	1.6	239	235	3657592	PL	163	28	1.65	#22	119	181

Foil Number	Wheel Position	Area Read	Zone 1	Zone 2	Pixelsum	Foil Position	Foil Exposure (mRem)	BGRD Tracks * cm^-2	Response Factor Tr * cm^-2 * mRem ^-1	Dosimeter Number	Mean Pyramidal Exposure	Base Foil Exposure
869266	54	1.6	94	104	3124036	PR	58	28	1.65			
869245	55	1.6	195	210	3431066	PB	136	28	1.65			
869223	56	1.6	246	277	3510288	Base	181	28	1.65			

APPENDIX J.2

TLD Data

U T AUSTIN EXPERIMENT TLD Data Read Date 5 May 2003 Calc Date 5 May 2003

Badge	Shallow	Deep	Neutron	Lens	NCR1	NCR2	NCR3	NCR4	NCR5	NCR6	NCR7	NCR8
36386	0	0	39.000	43.000	1.905	-1.567	1.334	8.067	41.121	8.207	6.333	83.432
36413	0	0	44.000	45.000	-6.185	2.575	-4.792	1.125	23.983	2.004	0.620	72.995
36464	0	0	51.000	52.000	-3.731	-3.286	-6.421	-0.617	30.125	3.113	2.213	87.948
36607	0	0	14.000	14.000	-5.167	-6.566	-12.037	-1.851	13.365	0.704	-0.211	27.906
36754	0	0	62.000	63.000	-0.216	-2.538	-7.374	3.519	31.578	5.442	1.198	96.431
37283	0	0	12.000	12.000	-7.407	34.222	-12.830	-1.137	20.078	-0.739	-0.938	29.439
37286	0	0	31.000	32.000	-4.996	-4.795	-5.675	0.067	29.074	3.232	1.152	62.359
37310	0	0	44.000	46.000	-2.544	-1.587	-5.210	1.907	26.534	4.733	3.043	74.639
37328	0	0	19.000	19.000	-8.160	-6.675	-13.099	-2.885	18.740	0.781	0.470	39.327
37336	0	0	14.000	14.000	-5.300	-6.433	-8.857	-1.317	17.364	0.349	0.079	31.321
37365	0	0	19.000	19.000	-7.036	-3.078	-9.718	-1.197	22.626	13.608	0.484	31.116
37372	0	0	0.000	0.000	-9.810	-6.005	-4.232	-3.663	1.100	0.784	-0.171	0.691
37831	0	0	57.000	57.000	-2.138	-1.805	-7.039	0.678	31.428	1.842	0.692	95.181
37833	0	0	45.000	47.000	-1.465	-4.557	-11.616	1.638	35.332	3.376	2.074	86.528
37950	0	0	14.000	14.000	-7.351	-3.811	-11.401	-2.669	24.529	0.177	-0.638	35.297
37954	0	0	17.000	17.000	-4.763	-3.252	-7.713	-3.925	25.689	0.374	0.663	41.204
37956	0	0	46.000	47.000	-2.416	0.242	-4.613	-1.359	35.360	3.124	2.518	88.132

Badge	Shallow	Deep	Neutron	Lens	NCR1	NCR2	NCR3	NCR4	NCR5	NCR6	NCR7	NCR8
37988	0	0	13.000	13.000	-0.218	5.481	-5.728	-0.326	22.341	-0.098	-0.062	32.503
37998	0	0	67.000	69.000	-5.055	-9.044	-5.343	0.101	34.929	4.217	2.484	108.889
38074	0	0	0.000	0.000	-6.310	-5.800	-10.654	-3.379	0.472	-1.616	0.110	1.733
38091	0	0	14.000	14.000	-0.362	0.144	-11.814	-2.822	18.278	-0.645	-1.764	32.564
38128	0	0	20.000	20.000	-2.079	-4.174	-3.345	-0.080	20.397	8.642	-0.046	34.426

Appendix K: SOURCES 4C and MCNP Input Files

APPENDIX K.1

SOURCES 4C Input File For Calculation of Neutron Spectrum of M-797

```
m-797 PuBe Source
1  2  1
3  0
  004 0.92883861
  094 0.07113660
  095 0.00002470
-63  50.0 0.0
5.000E+01
4.500E+01
4.000E+01
3.500E+01
3.000E+01
2.750E+01
2.500E+01
2.250E+01
2.000E+01
1.750E+01
1.690E+01
1.490E+01
1.350E+01
1.160E+01
1.000E+01
8.610E+00
7.410E+00
6.070E+00
4.970E+00
3.680E+00
2.870E+00
2.230E+00
1.740E+00
1.350E+00
1.110E+00
8.210E-01
6.390E-01
4.980E-01
3.880E-01
3.020E-01
1.830E-01
1.110E-01
6.740E-02
4.090E-02
2.550E-02
1.990E-02
1.500E-02
9.120E-03
```

5.530E-03
3.350E-03
2.840E-03
2.400E-03
2.030E-03
1.230E-03
7.490E-04
4.540E-04
2.750E-04
1.670E-04
1.010E-04
6.140E-05
3.720E-05
2.260E-05
1.370E-05
8.310E-06
5.040E-06
3.060E-06
1.860E-06
1.130E-06
6.830E-07
4.140E-07
2.510E-07
1.520E-07
9.240E-08
5
 0942380 1.73E+18
 0942390 5.24E+21
 0942400 2.78E+20
 0942410 2.20E+19
 0952410 1.92E+18
1 4000
 0040090 0.9288

APPENDIX K.2

MCNP Input File: NETL Glove box with Dosimeter Mesh Tally

```
UTGB
c
c Glove box at University of Texas
c Model of experiment conducted during trip of 4/22/03 - 5/01/03
c Source PuBe source M-797
c Mesh tally for dosimeters located on poly block 1' in front of GB with
c right edge of poly block on center line between right glove port pair
c
c ******************************************************************************
c     CELL CARDS
c ******************************************************************************
c
c Inside Glove box
c
1     1 -0.001 2 -5 32 -34 54 -59 #2 imp:n=1 $ Air inside GB
2     2 -11.35 2 -5 33 -34 54 -55    imp:n=1 $ Pb bricks inside GB
c
c Shell
c
3     3 -8.00 1 -6 31- 35 53 -54          imp:n=1 $ Bottom
4     3 -8.00 1 -6 31- 3559   -60         imp:n=1 $ Top
5     3 -8.00 5 -6 31- 35 54 -59          imp:n=1 $ Right
6     3 -8.00 1 -2 31- 35 54 -59          imp:n=1 $ Left
7     3 -8.00 (2 -5 34 -35 54 -59) (-3:4:-34:35:-56:57)       imp:n=1 $ Front
8     3 -8.00 2 -5 31 -32 54 -59          imp:n=1 $ Back
c
c Window  and Gloveports
c
9     4 -3.76 3 -4 34- 35 56 -57 #10 #11 #12 #13    imp:n=1 $ Window
10    0       34 -35 -21                imp:n=1 $ Left Glovepport
11    0       34 -35 -22                imp:n=1 $ Middle Left Glovepport
12    0       34 -35 -23                imp:n=1 $ Middle Right Glovepport
13    0       34 -35 -24                imp:n=1 $ Right Glovepport
c
c
c Poly Slabs
c
14    5 -0.92 7 -8 36 -37 51 -58          imp:n=1 $PL - Poly on left side
15    5 -0.92 9 -10 38 -39 52 -58         imp:n=1 $PR - Poly on right side
16    5 -0.92 11 -12 40 -41 52 -58          imp:n=1 $PL - Poly on left side
17    5 -0.92 12 -13 42 -43 52 -58          imp:n=1 $PL - Poly on left side
c
c Universe
c
98    1 -0.001 -99 (-1:6:-31:35:-53:60)#14 #15 #16 #17   imp:n=1 $
```

```
99     0 99 imp:n=0 $ Outside world
c
c ********************************************************************************
c     END OF CELL CARDS
c ********************************************************************************

c ********************************************************************************
c     SURFACE CARDS
c ********************************************************************************
c
c Y
c
1  py  -91.44
2  py  -91.1225
3  py  -78.105
4  py  78.105
5  py  91.1225
6  py  91.44
7  py  -98.7425
8  py  -93.6625
9  py  93.6625
10 py  98.7425
11 py  8.89
12 py  35.56
13 py  62.23
c
c Glove Ports - Front
21 c/x -54.61 -22.86 10.795
22 c/x -16.61 -22.86 10.795
23 c/x  16.61 -22.86 10.795
24 c/x  54.61 -22.86 10.795
c
c X
c
31 px  -58.42
32 px  -58.102
33 px  47.9425
34 px  58.1025
35 px  58.42
36 px  28.575
37 px  55.245
38 px  25.40
39 px  52.07
40 px  88.90
41 px  93.98
42 px  149.86
43 px  154.94
c
c Z
c
51 pz  -133.35
52 pz  -57.15
53 pz  -43.18
```

```
54 pz  -42.8625
55 pz  -37.7825
56 pz  -34.29
57 pz  -11.43
58 pz  39.37
59 pz  42.8625
60 pz  43.18
c
c Universe
c
99 so  1000
c
c ********************************************************************************
c     END OF SURFACE CARDS
c ********************************************************************************
c

c
c ********************************************************************************
c     MATERIAL CARDS
c ********************************************************************************
c
c
c     Dry air (density = 0.00098 g/cc at Los Alamos)
c     Reference: CRC Handbook of Chemistry and Physics and
c                CRC Handbook of tables for Applied Engineering Science
c     Nuclide composition in ATOM FRACTION
m1     7014     0.782315 $ Nitrogen  N14
       7015     0.002905 $ Nitrogen  N15
       8016     0.209966 $ Oxygen    O16
       8017     0.000080 $ Oxygen    O17
      18000.59c 0.004734 $ Argon     Ar-nat
      nlib=60c plib=02p elib=03e cond=0
c
c
c
c
c     Lead (density = 11.35 g/cc)
c     Nuclide composition in ATOM FRACTION
c     Reference:
c
m2    82000.42c 1.00     $lead       Pb-nat
      nlib=60c plib=02p elib=01e cond=0
c
c
c     Stainless Steel Type 304 Stainless Steel (density = 8.0 g/cc).
c     Nuclide composition in ATOM FRACTION
c     Reference: METALS HANDBOOK Tenth Edition pp. 843 & 871
m3     6000  0.003635  $ Carbon       C-nat
      14000  0.019431  $ Silicon      Si-nat
      15031  0.000793  $ Phosphorus   P31
      16000  0.000511  $ Sulfur       S-nat
      24050  0.008665  $ Chromium     Cr50
```

```
     24052  0.167091  $ Chromium     Cr52
     24053  0.018947  $ Chromium     Cr53
     24054  0.004716  $ Chromium     Cr54
     25055  0.019867  $ Manganese    Mn55
     26054  0.039181  $ Iron         Fe54
     26056  0.615060  $ Iron         Fe56
     26057  0.014204  $ Iron         Fe57
     26058  0.001890  $ Iron         Fe58
     28058  0.058551  $ Nickel       Ni58
     28060  0.022554  $ Nickel       Ni60
     28061  0.000980  $ Nickel       Ni61
     28062  0.003126  $ Nickel       Ni62
     28064  0.000796  $ Nickel       Ni64
     nlib=60c plib=02p elib=03e cond=1
c
c
c    Leaded Glass (density = 3.76 g/cc)
c    Nuclide composition in ATOM FRACTION
c    Reference: Askeland, Donald R., The Science and Engineering of Materials,
c               3rd ed., Table 14-2, p. 449 (1994) composition data
c              Dean, John A., Lange's Handbook of Chemistry, 14th ed.,
c               Table 3.2, pp. 3.12-3.63, McGraw-Hill Inc.(1992) density data
c    Approximate Thickness of glass (mm) per mm lead equivalent = 1.9
m4     8016     0.610814  $ oxygen     O16
       8017     0.000244  $ oxygen     O17
      11023     0.047148  $ sodium     Na23
      14000     0.271543  $ silicon    Si-nat
      19000     0.051704  $ potassium  K-nat
      82000.42c 0.018547  $lead        Pb-nat
     nlib=60c plib=02p elib=01e cond=0
c
c
c    Polyethylene (density = 0.92 g/cc).
c    Nuclide composition in ATOM FRACTION
c    Reference:Harmon II, Charles D., et al., "Criticality Calculations with
c              MCNP: A Primer", Appendix C, LANL, LA-12827-M, August 1994.
m5     1001  0.666584  $ Hydrogen     H1
       1002  0.000100  $ Hydrogen     H2
       6000  0.333316  $ Carbon       C-nat
      nlib=60c plib=02p elib=03e cond=-1
c
c
c
c ***************************************************************************
c    END OF MATERIAL CARDS
c ***************************************************************************
c
c
c ***************************************************************************
c    SOURCE CARDS
c ***************************************************************************
c
c
```

```
mode    n
phys:n  20
cut:n   j 0
phys:p  100
cut:p   j 0.01
c
c      Neutron energy spectra for M-797 PuBe neutron source
c      Be - 7.86 g
c      Pu - 15.97 g
c      Dimensions of container: 1.02" o.d. x 1.46" high
c      Container material: Ta and SS
c      Thickness: Ta -
c      Calibrated 07 Nov 1961
c      Total neutron emission = 1.75E+06 neutrons/s
c
sdef   par=1 pos= 43.1025 35.56 -39.1541 erg=d8
#       si8      sp8
        h        d
       1.00E-11  0.
       1.00E-02  1.47E+00
       2.00E-02  4.25E+00
       5.00E-02  2.53E+01
       1.00E-01  7.62E+01
       2.00E-01  2.29E+02
       4.00E-01  3.81E+03
       6.00E-01  1.57E+04
       8.00E-01  2.39E+04
       1.00E+00  2.59E+04
       1.30E+00  3.83E+04
       1.70E+00  3.87E+04
       2.10E+00  4.67E+04
       2.40E+00  4.65E+04
       2.70E+00  5.67E+04
       3.00E+00  9.16E+04
       3.30E+00  1.17E+05
       3.60E+00  1.10E+05
       4.00E+00  1.35E+05
       4.40E+00  1.23E+05
       5.00E+00  1.65E+05
       6.00E+00  1.65E+05
       7.00E+00  1.53E+05
       8.00E+00  1.73E+05
       9.00E+00  1.30E+05
       1.00E+01  7.86E+04
       1.20E+01  1.08E+04
       1.50E+01  7.41E-02
       2.00E+01  4.22E-03
c      Total     1.75E+06
c
c
c ***************************************************************************
c      END OF SOURCE CARDS
c ***************************************************************************
```

```
c
c
c
c ********************************************************************************
c     TALLY CARDS
c ********************************************************************************
c
c
c Multiplier for dose-rate conversion =
c [(1.75E+06 src_neutrons/s)/(kg Pu)] x [X tally_neutrons/(src_neutron*cm^2)] x
c [(Y*E-12 Sv cm^2)/(tally neutron)]x(100 rem/Sv)x(3600 s/h)x(1000 mrem/rem) x
c  24 h = 1.512E+4*XY mrem
c c  ********************************************************************************
c
c   AP - Neutron Fluence-to Effective-Dose-Equivalent Conversion factors vs
c   Energy from ANSI/ANS-6.1.1-1977 for AP exposure geomertry.  Energy units
c   in MeV and conversion-factors units are 1.0e-12Sv-cm^2.
c
de0   2.50e-8 1.00e-7 1.00e-6 1.00e-5 1.00e-4 1.00e-3 1.00e-2 1.00e-1
     5.00e-1 1.00e+0 2.50e+0 5.00e+0 7.00e+0 1.00e+1 1.40e+1 2.00e+1
c
df0   1.02e+1 1.02e+1 1.24e+1 1.26e+1 1.16e+1 1.04e+1 9.89e+0 6.03e+1
     2.57e+2 3.67e+2 3.47e+2 4.33e+2 4.08e+2 4.08e+2 5.78e+2 6.31e+2
c
tmesh
rmesh1:n
  cora1  87.4 88.4
  corb1 -100 24i 100
  corc1 -140 34i 140
endmd
fm1 1.512E+4
c
c
c
c ********************************************************************************
c     END OF TALLY CARDS
c ********************************************************************************
c
dbcn   12j 137753
prdmp  j 5e7 j 1
ctme   9999
nps    1e8
print  10 40 50 60 110 140 160 161 162 170
```

APPENDIX K.3

MCNP Input File: NETL Glove box with Phantom and Dosimeter Tally Plane

```
UTP1
c
c Glove box at University of Texas
c Model of experiment conducted during trip of 4/22/03 - 5/01/03
c Source PuBe source M-797
c Phantom at 1 ft in front of glove box on centerline of source
c
c
*****************************************************************************
******
c     CELL CARDS
c
*****************************************************************************
******
c
c Inside Glove box
c
1001   1 -0.001 1002 -1005 1032 -1034 1054 -1059 #1002 $ Air inside GB
1002   2 -11.35 1002 -1005 1033 -1034 1054 -1055       $ Pb bricks inside GB
c
c Shell
c
1003   3 -8.00 1001 -1006 1031 -1035 1053 -1054    $ Bottom
1004   3 -8.00 1001 -1006 1031 -1035 1059 -1060    $ Top
1005   3 -8.00 1005 -1006 1031 -1035 1054 -1059    $ Right
1006   3 -8.00 1001 -1002 1031 -1035 1054 -1059    $ Left
1007   3 -8.00 (1002 -1005 1034 -1035 1054 -1059)
     (-1003:1004:-1034:1035:-1056:1057)         $ Front
1008   3 -8.00 1002 -1005 1031 -1032 1054 -1059    $ Back
c
c Window  and Gloveports
c
1009   4 -3.76 1003 -1004  1034 -1035 1056 -1057
     #1010 #1011 #1012 #1013   $ Window
1010   0       1034 -1035 -1021  $ Left Glovepport
1011   0       1034 -1035 -1022  $ Middle Left Glovepport
1012   0       1034 -1035 -1023  $ Middle Right Glovepport
1013   0       1034 -1035 -1024  $ Right Glovepport
```

```
c
c
c Poly Slabs
c
c 1014   5 -0.92 1007 -1008 1036 -1037 1051 -1058     $PL - Poly on left side
c 1015   5 -0.92 1009 -1010 1038 -1039 1052 -1058     $PR - Poly on right side
c 1016   5 -0.92 1011 -1012 1040 -1041 1052 -1058     $PL - Poly on left side
c 1017   5 -0.92 1012 -1013 1042 -1043 1052 -1058     $PL - Poly on left side
c
c Universe
c
1098   1 -0.001 -1099 (-1001:1006:-1031:1035:-1053:1060) #900   $
c
c
c
************************************************************************
******
c      Male Phanton cells Body Builder
c      Height: 179 cm , Weight 73.54 kg, 0 cm extra torso fat
c
************************************************************************
******
c      SkeletonVolume = 7218.700000, skel_vol = 7142.857143
c
c      LEG BONES
50     11 -1.40   -4   53  (-51  : -52 ) u=2 vol=2800.00
c
c      ARM BONES
70     11 -1.40   4  -73  (-71  : -72 )  u=2 vol=956.00
c
c      PELVIS
90     11 -1.40   91  -92   93   4  -101  ( 95  : -94 ) u=2 vol=606.00
c
c      SPINE ( Total Spine vol=983.00 )
100    11 -1.40 -100 -103 101  u=2 vol=206.14
101    11 -1.40 -100 -8   103  u=2 vol=554.90
102    11 -1.40 -105 -102 8    u=2 vol=221.96
c
c      SKULL & FACE
110    11 -1.40  (111 -110):(121 -120 122 -1 -123 110) u=2 vol=923.00
c
c      RIBS
130    11 -1.40  132 -131 ((134 -133):(136 -135):(138 -137):(74 -139):
            (76 -75):(78 -77):(80 -79):(82 -81):(332 -83):
```

```
          (86 -85):(88 -87):(98 -89)) u=2 vol=694.00
c
c     CLAVICLES
140    11 -1.40  -140 ((141 -143):(-142 144)) u=2 vol=54.70
c
c     SCAPULAE
150    11 -1.40  131 -156 154 -155 ((150 -152):(-151 153)) u=2 vol=202.00
c
c  ***********************************************************************
c     ADRENALS
160    10 -1.04   162 (-160:-161) u=2 vol=15.70
c
c     BRAIN
180    10 -1.04  -111 u=2 vol=1370.00
c
c     BREAST
190    10 -1.04  11(-192:-193) u=2 vol =337.00
c
c     GALL BLADDER
200    10 -1.04  (-202 -200):(202 -201 -203) u=2 vol=63.70
c
c     ESOPHAGUS
212    10 -1.04  213 -212 322 -8 100 : -216 217 -218 210 350 100 u=2 vol=44.70
c     Air in Upper Esophagus
213    10 -1.04  -213 322 -8 u=2
c
c     STOMACH
210    10 -1.04  -210 u=2 vol=402.00
c
c     SMALL INTESTINE (exclude Ascending Colon, Transverse Colon,
c     and Descending Colon)
220    10 -1.04   -91 221 -222 223 -7 (232:230:-223)(240 :241 :-242 )
          (232:250:-223) u=2 vol=1060.00
c
c     ASCENDING COLON
230    10 -1.04   -230 231 -232 u=2 vol=187.50
c
c     TRANSVERSE COLON
240    10 -1.04    -240 -241 242 u=2 vol=248.00
c
c     DESCENDING COLON
250    10 -1.04   -250 251 -232 u=2 vol=191.90
c     SIGMOID COLON (Vol=106.0 cm^3)
280     1 -1.04   (-280 282 -251):(-281 -282 4) u=2 vol=106.0
```

```
c
c     HEART
c
290     1 -1.04 (290((-291 -292):(291 -293))):
              (-290((-291 -295):(291 -294))) u=2 vol=740.0
c
c     KIDNEYS
310    10 -1.04 (-310 282 -162):(-311 -313 -162) u=2 vol=288.00
c
c     LIVER
320    10 -1.04  -320 -321 7 -322 -132 u=2 vol=1830.00
c
c     LUNGS
330     3 -0.296  332 ((-331  (-335:336:334:-333)):
                    (-330  ( 339:338:337))) u=2 vol=3380.00
c
c     Ovaries
340    10 -1.04  -340:-341 u=2  vol=8.38
c
c     PANCREAS
350    10 -1.04  -350 351 (352:-282) u=2 vol=90.70
c
c     SPLEEN
360    10 -1.04  -360 u=2 vol=176.00
c
c     TESTICLES
370    10 -1.04  -370:-371 u=2 vol=37.60
c
c     THYMUS
380    10 -1.04  -380 u=2 vol=20.10
c
c     THYROID
390    10 -1.04  -390 391 -392 -393 8  u=2 vol=19.90
c
c     URINARY BLADDER
410    10 -1.04  -410 u=2 vol=248.70
c
c     UTERUS
420    10 -1.04  -420 421 u=2 vol=76.00
c
c     PENIS & SCROTUM
40     10 -1.04  -1 -4 47 -45 49 -48 37 38 370 371  u=2 vol=158.40  $ exclude Testicles
c
```

```
c
*************************************************************************
******
c
c  SKIN
c
c     Head & Neck Skin
22     10 -1.04  ((-21 22 9):(-20 23 -9 12))  u=2 vol = 259.26
28     10 -1.04  28 -27 8 -12  u=2 vol=58.74
c
c     Trunk Skin (exclude breast)
17     10 -1.04  (-8 18 20 -10):(4 -18 -10 11 192 193) u=2 vol=1440.00
c
c     Breast Skin
192    10 -1.04  10 ((-190 192):(-191 193)) u=2 vol 51.00
c
c     Penis & Scrotum Skin
41     10 -1.04  -1 -4  41 -42 43 -44 31 32 #40 370 371 u=2 vol=23.40  $ exclude Testicles
c
c     Legs Skin
34     10 -1.04 (-4 34 -31 36):(-31 33 -36) u=2 vol=605.00
35     10 -1.04 (-4 35 -32 36):(-32 33 -36)  u=2 vol=605.00
c
c
*************************************************************************
******
c
c     HEAD (exclude Skull & Brain, Face Bones, Spine & Thyroid)
20     10 -1.04 ((-22 9):(-23 -9 12)) 110 (-121:120:-122:1:123:-110)(105:-8:102)
            (390:-391:392:393:-8) u=2
c
c     NECK (exclude Spine &  Thyroid)
27     10 -1.04  -28 8 -12 105 (390:-391:392:393:-8) u=2
c
c     OUTER TRUNK-ARMS & SCAPULAE (excluded Scapulae and Arm Bones)
10     10 -1.04  4 131 -18 -11 (-131:156:-150:152:-154:155)
            (-131:156:151:-153:-154:155)(-4:71:73) (-4:72:73) u=2
c
c     UPPER TRUNK-ABOVE RIBS (exclude Spine, Clavicles, Upper Lungs,
c                         Thymus and Esophagus
11     10 -1.04  ((-18 -131 133):(-8 18 -20 -10)) (105:102:-8)(100:8:-133)
            (140:-141:143) (140:142:-144) (-133:330) (-133:331)
            380 #212 #213 u=2
c
```

```
c     UPPER RIB CAGE (exclude ribs 1-9
12     10 -1.04  -131 132 79 -133 (131:-132:133:-134) (131:-132:135:-136)
            (131:-132:137:-138) (131:-132:139:-74) (131:-132:75:-76)
            (131:-132:77:-78) u=2
c
c     LOWER RIB CAGE (exclude ribs 10-12)
13     10 -1.04  -131 132 -79 98 (131:-132:85:-86) (131:-132:87:-88)
            (131:-132:89:-98) (131:-132:79:-80) (131:-132:81:-82)
            (131:-132:83:-332) u=2
c
c     HIGH CHEST ORGANS (exclude Spine, Heart, Lungs, Thymus and Esophagus)
14     10 -1.04  -132 -133 332 (100:133:-332) #290 (330:133:-332:
            (-339 -338 -337)) (331:133:-332:(335 -336 -334 333))
            380 #212 #213 u=2
c
c     CHEST---LIVER LEVEL (exclude spine, Adrenals, Gall Bladder, Kidneys,
c                    Liver, Pancreas, Spleen, Esophagus & Stomach)
15     10 -1.04  (-132  -332   103  : -131  -103   7 ) ( 100  :  332
           : -7 ) ( 160  : -162 ) ( 161  : -162 ) ( 202  :  200
          ) (-202  :  201  :  203 ) ( 310  : -282 ) ( 311  :
           313 ) ( 320  :  321  : -7  :  322  :  132 ) ( 350
           : -351  : -352   282 )  360  (-213  :  212  : -322
           :  8  : -100 ) ( 216  : -217  :  218  : -210  :
          -350  : -100 ) ( 213  : -322  :  8 )  210  u=2
c
c     LOWER TRUNK (exclude Spine, Pelvis, Small Intestine, Ascending Colon
c               Descending Colon, Sigmoid Colon,Urinary Bladder, uterus
c               & ovaries)
16     10 -1.04  -131 4 -7 (100:-101:7) #90 (91:-221:222:-223:7) (232:230:-231)
            (232:250:-251)(280:-282:251) (281:282:-4) (420:-421) 340
            341  410 u=2
c
c     LEGS (exclude leg bones)
30     10 -1.04  -4 (-34:-35) 36 (4:51:-53) (4:52:-53) u=2 vol= 16790.00
c
c     SURROUNDING AIR exclude Head, Neck, Trunk and legs)
600     1  -0.001 -600
c          Exclude Head and Neck
            (21:-9) (20:9:-8)
c          Exclude Trunk
            (-4:10:8)
c          Exclude Breasts
             (-10:(190 191))
c          Exclude Legs
```

```
           (4:-33:(31 32))
c          Exclude Genitalia
           (1:4:-41:42:-43:44:-31:-32) #700 u=2
c
c     Air OUTSIDE of NECK
601    1  -0.001   -20 27 8 -12 u=2
c
c     Anterior Phantom Dosimetry Cell
700    1 -0.001  486 -485 -1 478 -470  u=2
c
c     Cylindrical cell for phantom universe
900    0  -500 1051 -502  fill=2
c
1099   0 1099  $ Outside world
c
c
*************************************************************************
******
c     END OF CELL CARDS
c
*************************************************************************
******

c
*************************************************************************
******
c     SURFACE CARDS
c
*************************************************************************
******
c
c Y
c
1001  py  -91.44
1002  py  -91.1225
1003  py  -78.105
1004  py  78.105
1005  py  91.1225
1006  py  91.44
1007  py  -98.7425
1008  py  -93.6625
1009  py  93.6625
1010  py  98.7425
1011  py  8.89
```

```
1012  py  35.56
1013  py  62.23
c
c Glove Ports - Front
1021  c/x -54.61 110.49 10.795
1022  c/x -16.61 110.49 10.795
1023  c/x  16.61 110.49 10.795
1024  c/x  54.61 110.49 10.795
c
c X
c
1031  px  -58.42
1032  px  -58.102
1033  px  47.9425
1034  px  58.1025
1035  px  58.42
1036  px  28.575
1037  px  55.245
1038  px  25.40
1039  px  52.07
1040  px  88.90
1041  px  93.98
1042  px  149.86
1043  px  154.94
c
c Z
c
1051  pz  0
1052  pz  76.2
1053  pz  90.17
1054  pz  90.4875
1055  pz  95.5675
1056  pz  99.06
1057  pz  121.92
1058  pz  172.72
1059  pz  176.2125
1060  pz  176.53
c
c Universe
c
1099  so  1000
c
c
```

```
c
**********************************************************************
******
c     Male Phanton Surfaces (Body Builder)
c
**********************************************************************
******
c     Planes used in several places
c
1     69  py  0
4     69  pz  0
332    69  pz  43.5000
7     69  pz  27.0000
8     69  pz  70.0000
9     69  pz  91.4500
12    69  pz  78.4000
c
c ******************************************
c     BODY SURFACE
c
c     HEAD
21    69  sq  1.54729 1 1.92586 0. 0. 0. -104.04 0 0 91.45
22    69  sq  1.5625 1 1.95609 0. 0. 0.  -100 0 0 91.45
20    69  sq  1.54729 1 0 0. 0. 0. -104.04 0 0 0
23    69  sq  1.5625 1 0 0. 0. 0. -100 0 0 0
c
c     NECK
27    69  cz  5.6000
28    69  cz  5.4000
c
c     TORSO
10    69  sq  1 3.92195 0 0. 0. 0. -408.04 0 0 0
11    69  sq  1 4 0 0. 0. 0. -400 0 0 0
18    69  pz  69.8000
c
c     LEGS
31    69  gq  1 1 0 0 0  -0.2000   -20.2000 0 0 0
32    69  gq  1 1 0 0 0   0.2000    20.2000 0 0 0
33    69  pz  -80.200
34    69  gq  1 1 0 0 0  -0.2000   -20.0000 0 0 0
35    69  gq  1 1 0 0 0   0.2000    20.0000 0 0 0
36    69  pz  -80.000
37    69  gq  1 1 0 0 0  -0.2000   -20.4000 0 0 0
38    69  gq  1 1 0 0 0   0.2000    20.4000 0 0 0
```

```
c
c     PENIS & SCROTUM
41     69  pz  -4.8
42     69  p   0 -10 -1 100
43     69  p   -10 0 1 -100
44     69  p   -10 0 -1 100
47     69  pz  -4.6
45     69  p   0 -10.1 -1 100
49     69  p   -10.1 0 1 -100
48     69  p   -10.1 0 -1 100
c
c
**********************************************************************
******
c     SKELETON
c     LEG BONES
51     69  gq  1 1  0.009069 0 0 -0.200501 -20.000000 0 1.785714  87.7500
52     69  gq  1 1  0.009069 0 0  0.200501  20.000000 0 1.785714  87.7500
53     69  pz  -79.8000
c
c     ARM BONES ( left/right) )
71     69  gq  0.510204    0.137174 0 0 0  0.010352
           -19.489796 0   -0.204969   185.877551
72     69  gq  0.510204    0.137174 0 0 0  -0.010352
           19.489796 0   -0.204969   185.877551
73     69  pz  69.0000
c
c     PELVIS
91     69  sq  1 1 0 0. 0. 0. -127.69 0 -3.8 0
92     69  sq  1 1 0 0. 0. 0. -144 0 -3 0
93     69  py  -3.0000
94     69  py  5.0000
95     69  pz  14.0000
c
c     SPINE
100    69  sq  1.5625 1 0 0. 0. 0 -6.25 0 5.5 0
105    69  sq  1.5625 1 0 0. 0. 0. -6.25 0 1.45 0
101    69  pz  22.0000
102    69  pz  84.8000
103    69  pz  35.1000
c
c     SKELETON
c     SKULL (head)
c     CRANIUM
```

```
110   69  sq  1.60444 1 2.04082 0. 0. 0. -90.25 0 0 91.45
111   69  sq  1.69789 1 2.23698 0. 0. 0. -73.96 0 0 91.45
c
c     FACIAL
120   69  sq  1.65306 1 0 0. 0. 0. -81 0 0 0
121   69  sq  1.84184 1 0 0. 0. 0. -57.76 0 0 0
122   69  pz  82.4000
123   69  pz  93.1300
c
c     RIBS
131   69  sq  1 3.00916 0 0. 0. 0. -289 0 0 0
132   69  sq  1 3.14776 0 0. 0. 0. -272.25 0 0 0
133   69  pz  67.3000
134   69  pz  65.9000
135   69  pz  64.5000
136   69  pz  63.1000
137   69  pz  61.7000
138   69  pz  60.3000
139   69  pz  58.9000
74    69  pz  57.5000
75    69  pz  56.1000
76    69  pz  54.7000
77    69  pz  53.3000
78    69  pz  51.9000
79    69  pz  50.5000
80    69  pz  49.1000
81    69  pz  47.7000
82    69  pz  46.3000
83    69  pz  44.9000
85    69  pz  42.1000
86    69  pz  40.7000
87    69  pz  39.3000
88    69  pz  37.9000
89    69  pz  36.5000
98    69  pz   35.1000
c
c     CLAVICLES
140   69  tz  0    11.1000    68.2500   20.0000   0.788300   0.788300
141   69  p   7.034200 1 0      11.100
142   69  p   7.034200 -1 0    -11.100
143   69  p   0.894150 1 0      11.100
144   69  p   0.894150 -1 0    -11.100
c
c     SCAPULAE
```

```
156   69  sq  1 3.75885 0 0. 0. 0. -361 0 0 0
150   69  p   0.2500 1 0 0
151   69  p   0.2500 -1 0 0
152   69  p   0.8000 1 0 0
153   69  p   0.8000 -1 0 0
154   69  pz  50.9000
155   69  pz  67.3010
c
c     ADRENALS
160   69  gq  37.298 25.202 0.5625 -48.5148
          0 0 -18.512 -82.2181 -42.75 1036.13
161   69  gq  37.298 25.202 0.5625 48.5148
          0 0 18.512 -82.2181 -42.75 1036.13
162   69  pz  38
c
c
c     BREASTS
c     left
190   69  sq  1 1.29489 1.4227 0. 0. 0. -24.5025 10 -8.6603 52
c     right
191   69  sq  1 1.29489 1.4227 0. 0. 0. -24.5025 -10 -8.6603 52
c
192   69  sq  1 1.31006 1.44608 0. 0. 0. -22.5625 10 -8.6603 52
193   69  sq  1 1.31006 1.44608 0. 0. 0. -22.5625 -10 -8.6603 52
c
c     GALL BLADDER
200   69  s   -4.5 -3.2 30 2.12
201   69  gq  0.924065 0.954066 0.0701124 -0.118118
          -0.413343 -0.531454 24.1414 18.1764
          -7.01399 171.417
202   69  p   0.268697 0.208982 0.940281 26.3306
203   69  p   0.268697 0.208982 0.940281 34.3306
c
c
c     ESOPAHGUS
212   69  sq  1 7.7602 0 0. 0. 0.
          -1.36905 0 2.575 0
213   69  sq  1 52.5625 0 0. 0. 0.
          -0.756944 0 2.575 0
216   69  gq  0.458169 0.633991 0.90784 0.890651
          -0.367322 0.446924 -21.1983 12.2727
          -75.8574 1588.09
217   69  p   0.736092 -0.604987 -0.303579 -14.2992
218   69  p   0.736092 -0.604987 -0.303579 -6.59922
```

```
c
c     STOMACH
210    69  sq  4 7.11111 1 0. 0. 0. -64 8 -4 35
c
c     SMALL INTESTINE
221    69  py  -4.8600
222    69  py  2.2000
223    69  pz  17.0000
c
c     ASCENDING COLON
230    69  sq  6.2500   6.2500 0 0 0 0  -39.0625  -8.5000  -2.3600 0
231    69  pz  14.4500
232    69  pz  24.0000
c
c     TRANSVERSE COLON
240    69  sq  0 1 2.77778 0. 0. 0. -6.25 0 -2.36 25.5
241    69  px  10.5000
242    69  px  -10.5000
c
c
c     DESCENDING COLON
251    69  pz  8.7200
250    69  gq  4.5369 3.5344 0.106435 0
           1.15654 -0.463191 -72.8161 -10.0851
           2.06701 283.329
c
c     SIGMOID COLON
282    69  px  3
280    69  ty  3 0 8.72
           5.72 1.57 1.57
281    69  ty  3 0 0
           3 1.57 1.57
c
c     HEART
290    69  p   0.675066 -0.4727 -0.566428 -26.7954
291    69  p   0.573592 0.819141 7.18977e-006 -0.900503
c Left Ventricle
292    69  gq  1946.76 1896.95 2854.33 -136.928
           -1284.71 1834.66 -95872.8 71201.4
           -289580 7.26092e+006
c Right Ventricle
293    69  gq  870.831 1369.38 559.799 1369.9
           -251.943 359.829 -17267.3 16157
           -56793.2 1.42524e+006
```

```
c Left Atrium
294   69  gq  409.659 572.418 267.401 447.228
            -21.4028 30.5767 -1543.14 2683.61
            -26809.2 666412
c Right Atrium
295   69  gq  1105.69 913.706 1363.44 -527.551
            -109.165 155.881 -10955 9275.13
            -136696 3.39551e+006
c
c     KIDNEYS
310   69  sq  1.49383 13.4444 1 0. 0. 0.
            -30.25 6 6 32.5
311   69  sq  1.49383 13.4444 1 0. 0. 0.
            -30.25 -6 6 32.5
312   69  px  3.0000
313   69  px  -3.0000
c
c     LIVER
320   69  sq  1 4.25391 0 0. 0. 0.
            -272.25 0 0 0
321   69  p   1935 1505 -1575 -67725
322   69  pz  43
c
c     Lungs
330   69  sq  23.0408 10.2404 1 0. 0. 0.
            -576.02 8.5 0 43.5
331   69  sq  23.0408 10.2404 1 0. 0. 0.
            -576.02 -8.5 0 43.5
333   69  px  -5.4000
334   69  py  1.5000
335   69  pz  46.0000
336   69  pz  54.0000
337   69  px  8.0000
338   69  py  1.0000
339   69  pz  55.0000
c
c     Ovaries
340   69  sq  4 16 1 0. 0. 0. -4 6 0 15
341   69  sq  4 16 1 0. 0. 0. -4 -6 0 15
c
c     PANCREAS
350   69  sq  1 177.778 23.5078 0. 0. 0. -256 -1 0 37
351   69  px  -1.0000
352   69  pz  37.0000
```

```
c
c     SPLEEN
360    69  sq  2.93878 9 1 0. 0. 0. -36 11 3 37
c
c     TESTICLES
370    69  sq  3.13018 2.35111 1 0. 0. 0. -5.29 1.3 -8 -2.3
371    69  sq  3.13018 2.35111 1 0. 0. 0. -5.29 -1.3 -8 -2.3
c
c     THYMUS
380    69  sq  7.11111 25 1 0. 0. 0. -16 0 -7.3 57
c
c     THYROID
390    69  c/z 0  -3.1500     2.2000
391    69  c/z 0  -3.1500     1.0000
392    69  py  -3.1500
393    69  pz  75.0000
c
c     URINARY BLADDER
410    69  sq  1 2.05572 2.05572 0. 0. 0. -24.5818 0 -4.5 8
c
c     UTERUS
420    69  sq  3.96952 1 11.0546 0. 0. 0. -27.2484 0 -2 14
421    69  py  -4.6200
c
c
c  Tally Dosimetry Lattice
c  "x" surface tally lattice coordinate
459    69  px  28
460    69  px  20
461    69  px  12
462    69  px   4
463    69  px  -4
464    69  px -12
465    69  px -20
466    69  px -28
c
c  "z" surface tally lattice coordinate
470    69  pz 78
c 8    69  pz 70
471    69  pz 62
472    69  pz 54
473    69  pz 46
474    69  pz 38
475    69  pz 30
```

```
476    69  pz 22
477    69  pz 14
478    69  pz 6
c
c  Dosimeter Cylinder Tally Cell
485    69  c/z 0 5.0 21.80  $ Outer surface
486    69  c/z 0 5.0 21.70  $ inner surface
487    69  pz 80
c
c
c    Phantom Cylinder
500    c/z 88.90 35.56 22.0  $ Cylinder for initial phantom
501    pz 0.01
502    pz 180
c
c
600    69  so 301
c
c
*************************************************************************
******
c     END OF SURFACE CARDS
c
*************************************************************************
******
c

c
c
*************************************************************************
******
c     MATERIAL CARDS
c
*************************************************************************
******
c
c
c     Dry air (density = 0.00098 g/cc at Los Alamos)
c     Reference: CRC Handbook of Chemistry and Physics and
c               CRC Handbook of tables for Applied Engineering Science
c     Nuclide composition in ATOM FRACTION
m1      7014     0.782315 $ Nitrogen  N14
        7015     0.002905 $ Nitrogen  N15
        8016     0.209966 $ Oxygen    O16
```

```
      8017     0.000080 $ Oxygen    O17
     18000.59c 0.004734 $ Argon     Ar-nat
     nlib=60c plib=02p elib=03e cond=0
c
c
c
c
c     Lead (density = 11.35 g/cc)
c     Nuclide composition in ATOM FRACTION
c     Reference:
c
m2    82000.42c 1.00     $lead       Pb-nat
     nlib=60c plib=02p elib=01e cond=0
c
c
c     Stainless Steel Type 304 Stainless Steel (density = 8.0 g/cc).
c     Nuclide composition in ATOM FRACTION
c     Reference: METALS HANDBOOK Tenth Edition pp. 843 & 871
m3     6000  0.003635  $ Carbon       C-nat
     14000  0.019431  $ Silicon      Si-nat
     15031  0.000793  $ Phosphorus   P31
     16000  0.000511  $ Sulfur       S-nat
     24050  0.008665  $ Chromium     Cr50
     24052  0.167091  $ Chromium     Cr52
     24053  0.018947  $ Chromium     Cr53
     24054  0.004716  $ Chromium     Cr54
     25055  0.019867  $ Manganese    Mn55
     26054  0.039181  $ Iron         Fe54
     26056  0.615060  $ Iron         Fe56
     26057  0.014204  $ Iron         Fe57
     26058  0.001890  $ Iron         Fe58
     28058  0.058551  $ Nickel       Ni58
     28060  0.022554  $ Nickel       Ni60
     28061  0.000980  $ Nickel       Ni61
     28062  0.003126  $ Nickel       Ni62
     28064  0.000796  $ Nickel       Ni64
     nlib=60c plib=02p elib=03e cond=1
c
c
c     Leaded Glass (density = 3.76 g/cc)
c     Nuclide composition in ATOM FRACTION
c     Reference: Askeland, Donald R., The Science and Engineering of Materials,
c                3rd ed., Table 14-2, p. 449 (1994) composition data
c               Dean, John A., Lange's Handbook of Chemistry, 14th ed.,
```

```
c               Table 3.2, pp. 3.12-3.63, McGraw-Hill Inc.(1992) density data
c      Approximate Thickness of glass (mm) per mm lead equivalent = 1.9
m4     8016     0.610814  $ oxygen     O16
       8017     0.000244  $ oxygen     O17
      11023     0.047148  $ sodium     Na23
      14000     0.271543  $ silicon    Si-nat
      19000     0.051704  $ potassium  K-nat
      82000.42c 0.018547  $lead        Pb-nat
      nlib=60c plib=02p elib=01e cond=0
c
c
c      Polyethylene (density = 0.92 g/cc).
c      Nuclide composition in ATOM FRACTION
c      Reference:Harmon II, Charles D., et al., "Criticality Calculations with
c               MCNP: A Primer", Appendix C, LANL, LA-12827-M, August 1994.
m5     1001  0.666584  $ Hydrogen     H1
       1002  0.000100  $ Hydrogen     H2
       6000  0.333316  $ Carbon       C-nat
      nlib=60c plib=02p elib=03e cond=-1
c
c
c
c      BodyBuilder Adult Tissue (density = 1.04 g/cc).
c      Nuclide composition in ATOM FRACTION
c      Reference:BodyBuilder Software, White Rock Science
m10    1001      0.63103424  $ Hydrogen     H1
       1002      0.00009467  $ Hydrogen     H2
       6000      0.11481305  $ Carbon       C-nat
       7014      0.01077719  $ Nitrogen     N-14
       7015      0.00004002  $ Nitrogen     N-15
       8016      0.24150173  $ Oxygen       O16
       8017      0.00009664  $ Oxygen       O17
      11023      0.00029644  $ Sodium       N23
      12000      0.00003255  $ Magnesium    Mg-nat
      14000      0.00006500  $ Silicon      Si-nat
      15031      0.00026325  $ Phosphorus   P-31
      16000      0.00038719  $ Sulfur       S-nat
      17000      0.00022827  $ Chlorine     Cl-nat
      19000      0.00032371  $ Potassium    K-nat
      20000      0.00003644  $ Calcium      Ca-nat
      26054      0.00000032  $ Iron         Fe-54
      26056      0.00000500  $ Iron         Fe-56
      26057      0.00000012  $ Iron         Fe-57
      26058      0.00000002  $ Iron         Fe-58
```

```
      30000.42c   0.00000279  $ Zinc        Zn-nat
      37085.55c   0.00000051  $ Rubidium    Rb-85
      37087.55c   0.00000020  $ Rubidium    Rb-87
      40000       0.00000067  $ Zirconium   Zr-nat
      nlib=60c plib=02p elib=03e cond=-1
c
c     BodyBuilder Skelton (density = 1.40 g/cc).
c     Nuclide composition in ATOM FRACTION
c     Reference:BodyBuilder Software, White Rock Science
m11     1001       0.55710523  $ Hydrogen    H1
        1002       0.00008358  $ Hydrogen    H2
        6000       0.16234404  $ Carbon      C-nat
        7014       0.01664370  $ Nitrogen    N-14
        7015       0.00006181  $ Nitrogen    N-15
        8016       0.22903186  $ Oxygen      O16
        8017       0.00009165  $ Oxygen      O17
        9019       0.00010072  $ Fluorine    F-19
       11023       0.00108539  $ Sodium      N23
       12000       0.00035271  $ Magnesium   Mg-nat
       14000       0.00000545  $ Silicon     Si-nat
       15031       0.01259075  $ Phosphorus  P-31
       16000       0.00041303  $ Sulfur      S-nat
       17000       0.00030874  $ Chlorine    Cl-nat
       19000       0.00029953  $ Potassium   K-nat
       20000       0.01946022  $ Calcium     Ca-nat
       26054       0.00000064  $ Iron        Fe-54
       26056       0.00001006  $ Iron        Fe-56
       26057       0.00000023  $ Iron        Fe-57
       26058       0.00000003  $ Iron        Fe-58
      30000.42c   0.00000585  $ Zinc        Zn-nat
      37085.55c   0.00000129  $ Rubidium    Rb-85
      37087.55c   0.00000050  $ Rubidium    Rb-87
      38000       0.00000262  $ Strontium   Sr
      82000.42c   0.00000037  $ Lead        Pb-nat
      nlib=60c plib=02p elib=03e cond=-1
c
c     BodyBuilder Lung (density = 0.296 g/cc).
c     Nuclide composition in ATOM FRACTION
c     Reference:BodyBuilder Software, White Rock Science
m12     1001       0.6331547  $ Hydrogen    H1
        1002       0.0000950  $ Hydrogen    H2
        6000       0.0536843  $ Carbon      C-nat
        7014       0.0128393  $ Nitrogen    N-14
        7015       0.0000477  $ Nitrogen    N-15
```

```
      8016      0.2980768  $ Oxygen      O16
      8017      0.0001193  $ Oxygen      O17
     11023       0.0005041  $ Sodium      N23
     12000       0.0000181  $ Magnesium   Mg-nat
     14000       0.0000135  $ Silicon     Si-nat
     15031       0.0001627  $ Phosphorus  P-31
     16000       0.0004420  $ Sulfur      S-nat
     17000       0.0004725  $ Chlorine    Cl-nat
     19000       0.0003125  $ Potassium   K-nat
     20000       0.0000141  $ Calcium     Ca-nat
     26054       0.0000024  $ Iron        Fe-54
     26056       0.0000383  $ Iron        Fe-56
     26057       0.0000009  $ Iron        Fe-57
     26058       0.0000001  $ Iron        Fe-58
     30000.42c   0.0000010  $ Zinc        Zn-nat
     37085.55c   0.0000005  $ Rubidium    Rb-85
     37087.55c   0.0000002  $ Rubidium    Rb-87
     nlib=60c plib=02p elib=03e cond=-1
c
c
c
*************************************************************************
******
c     END OF MATERIAL CARDS
c
*************************************************************************
******
c
c
c
*************************************************************************
******
c     SOURCE CARDS
c
*************************************************************************
******
c
c
mode    n
phys:n  20
cut:n   j 0
phys:p  100
cut:p   j 0.01
c
```

```
c      Neutron energy spectra for M-797 PuBe neutron source
c      Be - 7.86 g
c      Pu - 15.97 g
c      Dimensions of container: 1.02" o.d. x 1.46" high
c      Container material: Ta and SS
c      Thickness: Ta -
c      Calibrated 07 Nov 1961
c      Total neutron emission = 1.75E+06 neutrons/s
c
sdef   par=1 pos= 43.1025 35.56 94.1959 erg=d8
#       si8      sp8
         h        d
       1.00E-11  0.
       1.00E-02  1.47E+00
       2.00E-02  4.25E+00
       5.00E-02  2.53E+01
       1.00E-01  7.62E+01
       2.00E-01  2.29E+02
       4.00E-01  3.81E+03
       6.00E-01  1.57E+04
       8.00E-01  2.39E+04
       1.00E+00  2.59E+04
       1.30E+00  3.83E+04
       1.70E+00  3.87E+04
       2.10E+00  4.67E+04
       2.40E+00  4.65E+04
       2.70E+00  5.67E+04
       3.00E+00  9.16E+04
       3.30E+00  1.17E+05
       3.60E+00  1.10E+05
       4.00E+00  1.35E+05
       4.40E+00  1.23E+05
       5.00E+00  1.65E+05
       6.00E+00  1.65E+05
       7.00E+00  1.53E+05
       8.00E+00  1.73E+05
       9.00E+00  1.30E+05
       1.00E+01  7.86E+04
       1.20E+01  1.08E+04
       1.50E+01  7.41E-02
       2.00E+01  4.22E-03
c      Total     1.75E+06
c
c
```

```
c
**********************************************************************
******
c     END OF SOURCE CARDS
c
**********************************************************************
******
c
c
c
**********************************************************************
******
c     TALLY CARDS
c
**********************************************************************
******
c
c
**********************************************************************
******
c     NEUTRON
c
**********************************************************************
******
c
c
**********************************************************************
******
c     Simulated Dosimeter Lattice Tally
c
**********************************************************************
******
c
c     Multiplier for dose-rate conversion =
c     [(1.75E+06 src_neuts/s)/(kg Pu)] x [X tally_neuts/(src_neutron*cm^2)] x
c     [(Y*E-12 Sv cm^2)/(tally neut)]x(100 rem/Sv)x(3600 s/h)x(1000 mrem/rem) x
c      24 h = 1.512E+4*XY mrem
c
c     AP - Neutron Fluence-to Effective-Dose-Equivalent Conversion factors vs
c     Energy from ANSI/ANS-6.1.1-1977 for AP exposure geomertry.  Energy units
c     in MeV and conversion-factors units are 1.0e-12Sv-cm^2.
c     c
c     de0    2.50e-8 1.00e-7 1.00e-6 1.00e-5 1.00e-4 1.00e-3 1.00e-2 1.00e-1
c           5.00e-1 1.00e+0 2.50e+0 5.00e+0 7.00e+0 1.00e+1 1.40e+1 2.00e+1
```

```
c     df0    1.02e+1 1.02e+1 1.24e+1 1.26e+1 1.16e+1 1.04e+1 9.89e+0 6.03e+1
c            2.57e+2 3.67e+2 3.47e+2 4.33e+2 4.08e+2 4.08e+2 5.78e+2 6.31e+2
c     c
c
c
c*********************************************************************
******
c
fc2    mrem/source-particle-cm^2 averaged over tally surface area
f2:n   485
fs2    -464 -8 463 470
sd2    1 1 1 1 64
fm2    1.512E+4
fq2    e f
cf2    10 11 12 13 14 15 16 17 20 22 27 28 30 35 40 41 50 70 90 100
       101 102 110 130 140 150 160 180 190 192 200 210 212 213 220 230
       240 250 280  290 310 320 330  340 350 360 370 380
       390 410 420
e2     2.5e-8 1.0e-7 1.0e-6 1.0e-5 1.0e-4 1.0e-3
       0.01 0.02 0.05 0.1 0.2 0.4 0.6 0.8 1.0 1.3 1.7 2.1 2.4 2.7 3.0 3.3 3.6
       4.0 4.4 5 6 7 8 9 10 12 15 20
de2    2.50e-8 1.00e-7 1.00e-6 1.00e-5 1.00e-4 1.00e-3 1.00e-2 1.00e-1
       5.00e-1 1.00e+0 2.50e+0 5.00e+0 7.00e+0 1.00e+1 1.40e+1 2.00e+1
df2    1.02e+1 1.02e+1 1.24e+1 1.26e+1 1.16e+1 1.04e+1 9.89e+0 6.03e+1
       2.57e+2 3.67e+2 3.47e+2 4.33e+2 4.08e+2 4.08e+2 5.78e+2 6.31e+2
c
fc12   mrem/source-particle-cm^2 averaged over tally surface area
f12:n  485
fs12   -463 -8 462 470
sd12   1 1 1 1 64
fm12   1.512E+4
fq12   e f
cf12   10 11 12 13 14 15 16 17 20 22 27 28 30 35 40 41 50 70 90 100
       101 102 110 130 140 150 160 180 190 192 200 210 212 213 220 230
       240 250 280  290 310 320 330  340 350 360 370 380
       390 410 420
e12    2.5e-8 1.0e-7 1.0e-6 1.0e-5 1.0e-4 1.0e-3
       0.01 0.02 0.05 0.1 0.2 0.4 0.6 0.8 1.0 1.3 1.7 2.1 2.4 2.7 3.0 3.3 3.6
       4.0 4.4 5 6 7 8 9 10 12 15 20
de12   2.50e-8 1.00e-7 1.00e-6 1.00e-5 1.00e-4 1.00e-3 1.00e-2 1.00e-1
       5.00e-1 1.00e+0 2.50e+0 5.00e+0 7.00e+0 1.00e+1 1.40e+1 2.00e+1
df12   1.02e+1 1.02e+1 1.24e+1 1.26e+1 1.16e+1 1.04e+1 9.89e+0 6.03e+1
       2.57e+2 3.67e+2 3.47e+2 4.33e+2 4.08e+2 4.08e+2 5.78e+2 6.31e+2
c
```

```
fc22   mrem/source-particle-cm^2 averaged over tally surface area
f22:n  485
fs22   -462 -8 461 470
sd22   1 1 1 1 64
fm22   1.512E+4
fq22   e f
cf22   10 11 12 13 14 15 16 17 20 22 27 28 30 35 40 41 50 70 90 100
       101 102 110 130 140 150 160 180 190 192 200 210 212 213 220 230
       240 250 280  290 310 320 330  340 350 360 370 380
       390 410 420
e22    2.5e-8 1.0e-7 1.0e-6 1.0e-5 1.0e-4 1.0e-3
       0.01 0.02 0.05 0.1 0.2 0.4 0.6 0.8 1.0 1.3 1.7 2.1 2.4 2.7 3.0 3.3 3.6
       4.0 4.4 5 6 7 8 9 10 12 15 20
de22   2.50e-8 1.00e-7 1.00e-6 1.00e-5 1.00e-4 1.00e-3 1.00e-2 1.00e-1
       5.00e-1 1.00e+0 2.50e+0 5.00e+0 7.00e+0 1.00e+1 1.40e+1 2.00e+1
df22   1.02e+1 1.02e+1 1.24e+1 1.26e+1 1.16e+1 1.04e+1 9.89e+0 6.03e+1
       2.57e+2 3.67e+2 3.47e+2 4.33e+2 4.08e+2 4.08e+2 5.78e+2 6.31e+2
c
fc32   mrem/source-particle-cm^2 averaged over tally surface area
f32:n  485
fs32   -465 -471 464 8
sd32   1 1 1 1 64
fm32   1.512E+4
fq32   e f
cf32   10 11 12 13 14 15 16 17 20 22 27 28 30 35 40 41 50 70 90 100
       101 102 110 130 140 150 160 180 190 192 200 210 212 213 220 230
       240 250 280  290 310 320 330  340 350 360 370 380
       390 410 420
e32    2.5e-8 1.0e-7 1.0e-6 1.0e-5 1.0e-4 1.0e-3
       0.01 0.02 0.05 0.1 0.2 0.4 0.6 0.8 1.0 1.3 1.7 2.1 2.4 2.7 3.0 3.3 3.6
       4.0 4.4 5 6 7 8 9 10 12 15 20
de32   2.50e-8 1.00e-7 1.00e-6 1.00e-5 1.00e-4 1.00e-3 1.00e-2 1.00e-1
       5.00e-1 1.00e+0 2.50e+0 5.00e+0 7.00e+0 1.00e+1 1.40e+1 2.00e+1
df32   1.02e+1 1.02e+1 1.24e+1 1.26e+1 1.16e+1 1.04e+1 9.89e+0 6.03e+1
       2.57e+2 3.67e+2 3.47e+2 4.33e+2 4.08e+2 4.08e+2 5.78e+2 6.31e+2
c
fc42   mrem/source-particle-cm^2 averaged over tally surface area
f42:n  485
fs42   -464 -471 463 8
sd42   1 1 1 1 64
fm42   1.512E+4
fq42   e f
cf42   10 11 12 13 14 15 16 17 20 22 27 28 30 35 40 41 50 70 90 100
       101 102 110 130 140 150 160 180 190 192 200 210 212 213 220 230
```

```
      240 250 280  290 310 320 330  340 350 360 370 380
      390 410 420
e42   2.5e-8 1.0e-7 1.0e-6 1.0e-5 1.0e-4 1.0e-3
      0.01 0.02 0.05 0.1 0.2 0.4 0.6 0.8 1.0 1.3 1.7 2.1 2.4 2.7 3.0 3.3 3.6
      4.0 4.4 5 6 7 8 9 10 12 15 20
de42  2.50e-8 1.00e-7 1.00e-6 1.00e-5 1.00e-4 1.00e-3 1.00e-2 1.00e-1
      5.00e-1 1.00e+0 2.50e+0 5.00e+0 7.00e+0 1.00e+1 1.40e+1 2.00e+1
df42  1.02e+1 1.02e+1 1.24e+1 1.26e+1 1.16e+1 1.04e+1 9.89e+0 6.03e+1
      2.57e+2 3.67e+2 3.47e+2 4.33e+2 4.08e+2 4.08e+2 5.78e+2 6.31e+2
c
fc52  mrem/source-particle-cm^2 averaged over tally surface area
f52:n 485
fs52  -463 -471 462 8
sd52  1 1 1 1 64
fm52  1.512E+4
fq52  e f
cf52  10 11 12 13 14 15 16 17 20 22 27 28 30 35 40 41 50 70 90 100
      101 102 110 130 140 150 160 180 190 192 200 210 212 213 220 230
      240 250 280  290 310 320 330  340 350 360 370 380
      390 410 420
e52   2.5e-8 1.0e-7 1.0e-6 1.0e-5 1.0e-4 1.0e-3
      0.01 0.02 0.05 0.1 0.2 0.4 0.6 0.8 1.0 1.3 1.7 2.1 2.4 2.7 3.0 3.3 3.6
      4.0 4.4 5 6 7 8 9 10 12 15 20
de52  2.50e-8 1.00e-7 1.00e-6 1.00e-5 1.00e-4 1.00e-3 1.00e-2 1.00e-1
      5.00e-1 1.00e+0 2.50e+0 5.00e+0 7.00e+0 1.00e+1 1.40e+1 2.00e+1
df52  1.02e+1 1.02e+1 1.24e+1 1.26e+1 1.16e+1 1.04e+1 9.89e+0 6.03e+1
      2.57e+2 3.67e+2 3.47e+2 4.33e+2 4.08e+2 4.08e+2 5.78e+2 6.31e+2
c
fc62  mrem/source-particle-cm^2 averaged over tally surface area
f62:n 485
fs62  -462 -471 461 8
sd62  1 1 1 1 64
fm62  1.512E+4
fq62  e f
cf62  10 11 12 13 14 15 16 17 20 22 27 28 30 35 40 41 50 70 90 100
      101 102 110 130 140 150 160 180 190 192 200 210 212 213 220 230
      240 250 280  290 310 320 330  340 350 360 370 380
      390 410 420
e62   2.5e-8 1.0e-7 1.0e-6 1.0e-5 1.0e-4 1.0e-3
      0.01 0.02 0.05 0.1 0.2 0.4 0.6 0.8 1.0 1.3 1.7 2.1 2.4 2.7 3.0 3.3 3.6
      4.0 4.4 5 6 7 8 9 10 12 15 20
de62  2.50e-8 1.00e-7 1.00e-6 1.00e-5 1.00e-4 1.00e-3 1.00e-2 1.00e-1
      5.00e-1 1.00e+0 2.50e+0 5.00e+0 7.00e+0 1.00e+1 1.40e+1 2.00e+1
df62  1.02e+1 1.02e+1 1.24e+1 1.26e+1 1.16e+1 1.04e+1 9.89e+0 6.03e+1
```

```
     2.57e+2 3.67e+2 3.47e+2 4.33e+2 4.08e+2 4.08e+2 5.78e+2 6.31e+2
c
fc72   mrem/source-particle-cm^2 averaged over tally surface area
f72:n  485
fs72    -461 -471 460 8
sd72   1 1 1 1 64
fm72   1.512E+4
fq72   e f
cf72   10 11 12 13 14 15 16 17 20 22 27 28 30 35 40 41 50 70 90 100
     101 102 110 130 140 150 160 180 190 192 200 210 212 213 220 230
     240 250 280  290 310 320 330  340 350 360 370 380
     390 410 420
e72    2.5e-8 1.0e-7 1.0e-6 1.0e-5 1.0e-4 1.0e-3
     0.01 0.02 0.05 0.1 0.2 0.4 0.6 0.8 1.0 1.3 1.7 2.1 2.4 2.7 3.0 3.3 3.6
     4.0 4.4 5 6 7 8 9 10 12 15 20
de72   2.50e-8 1.00e-7 1.00e-6 1.00e-5 1.00e-4 1.00e-3 1.00e-2 1.00e-1
     5.00e-1 1.00e+0 2.50e+0 5.00e+0 7.00e+0 1.00e+1 1.40e+1 2.00e+1
df72   1.02e+1 1.02e+1 1.24e+1 1.26e+1 1.16e+1 1.04e+1 9.89e+0 6.03e+1
     2.57e+2 3.67e+2 3.47e+2 4.33e+2 4.08e+2 4.08e+2 5.78e+2 6.31e+2
c
fc82   mrem/source-particle-cm^2 averaged over tally surface area
f82:n  485
fs82   -465 -472 464 471
sd82   1 1 1 1 64
fm82   1.512E+4
fq82   e f
cf82   10 11 12 13 14 15 16 17 20 22 27 28 30 35 40 41 50 70 90 100
     101 102 110 130 140 150 160 180 190 192 200 210 212 213 220 230
     240 250 280  290 310 320 330  340 350 360 370 380
     390 410 420
e82    2.5e-8 1.0e-7 1.0e-6 1.0e-5 1.0e-4 1.0e-3
     0.01 0.02 0.05 0.1 0.2 0.4 0.6 0.8 1.0 1.3 1.7 2.1 2.4 2.7 3.0 3.3 3.6
     4.0 4.4 5 6 7 8 9 10 12 15 20
de82   2.50e-8 1.00e-7 1.00e-6 1.00e-5 1.00e-4 1.00e-3 1.00e-2 1.00e-1
     5.00e-1 1.00e+0 2.50e+0 5.00e+0 7.00e+0 1.00e+1 1.40e+1 2.00e+1
df82   1.02e+1 1.02e+1 1.24e+1 1.26e+1 1.16e+1 1.04e+1 9.89e+0 6.03e+1
     2.57e+2 3.67e+2 3.47e+2 4.33e+2 4.08e+2 4.08e+2 5.78e+2 6.31e+2
c
fc92   mrem/source-particle-cm^2 averaged over tally surface area
f92:n  485
fs92   -464 -472 463 471
sd92   1 1 1 1 64
fm92   1.512E+4
fq92   e f
```

```
cf92   10 11 12 13 14 15 16 17 20 22 27 28 30 35 40 41 50 70 90 100
       101 102 110 130 140 150 160 180 190 192 200 210 212 213 220 230
       240 250 280  290 310 320 330  340 350 360 370 380
       390 410 420
e92    2.5e-8 1.0e-7 1.0e-6 1.0e-5 1.0e-4 1.0e-3
       0.01 0.02 0.05 0.1 0.2 0.4 0.6 0.8 1.0 1.3 1.7 2.1 2.4 2.7 3.0 3.3 3.6
       4.0 4.4 5 6 7 8 9 10 12 15 20
de92   2.50e-8 1.00e-7 1.00e-6 1.00e-5 1.00e-4 1.00e-3 1.00e-2 1.00e-1
       5.00e-1 1.00e+0 2.50e+0 5.00e+0 7.00e+0 1.00e+1 1.40e+1 2.00e+1
df92   1.02e+1 1.02e+1 1.24e+1 1.26e+1 1.16e+1 1.04e+1 9.89e+0 6.03e+1
       2.57e+2 3.67e+2 3.47e+2 4.33e+2 4.08e+2 4.08e+2 5.78e+2 6.31e+2
c
fc102  mrem/source-particle-cm^2 averaged over tally surface area
f102:n 485
fs102  -463 -472 462 471
sd102  1 1 1 1 64
fm102  1.512E+4
fq102  e f
cf102  10 11 12 13 14 15 16 17 20 22 27 28 30 35 40 41 50 70 90 100
       101 102 110 130 140 150 160 180 190 192 200 210 212 213 220 230
       240 250 280  290 310 320 330  340 350 360 370 380
       390 410 420
e102   2.5e-8 1.0e-7 1.0e-6 1.0e-5 1.0e-4 1.0e-3
       0.01 0.02 0.05 0.1 0.2 0.4 0.6 0.8 1.0 1.3 1.7 2.1 2.4 2.7 3.0 3.3 3.6
       4.0 4.4 5 6 7 8 9 10 12 15 20
de102  2.50e-8 1.00e-7 1.00e-6 1.00e-5 1.00e-4 1.00e-3 1.00e-2 1.00e-1
       5.00e-1 1.00e+0 2.50e+0 5.00e+0 7.00e+0 1.00e+1 1.40e+1 2.00e+1
df102  1.02e+1 1.02e+1 1.24e+1 1.26e+1 1.16e+1 1.04e+1 9.89e+0 6.03e+1
       2.57e+2 3.67e+2 3.47e+2 4.33e+2 4.08e+2 4.08e+2 5.78e+2 6.31e+2
c
fc112  mrem/source-particle-cm^2 averaged over tally surface area
f112:n 485
fs112  -462 -472 461 471
sd112  1 1 1 1 64
fm112  1.512E+4
fq112  e f
cf112  10 11 12 13 14 15 16 17 20 22 27 28 30 35 40 41 50 70 90 100
       101 102 110 130 140 150 160 180 190 192 200 210 212 213 220 230
       240 250 280  290 310 320 330  340 350 360 370 380
       390 410 420
e112   2.5e-8 1.0e-7 1.0e-6 1.0e-5 1.0e-4 1.0e-3
       0.01 0.02 0.05 0.1 0.2 0.4 0.6 0.8 1.0 1.3 1.7 2.1 2.4 2.7 3.0 3.3 3.6
       4.0 4.4 5 6 7 8 9 10 12 15 20
de112  2.50e-8 1.00e-7 1.00e-6 1.00e-5 1.00e-4 1.00e-3 1.00e-2 1.00e-1
```

```
     5.00e-1 1.00e+0 2.50e+0 5.00e+0 7.00e+0 1.00e+1 1.40e+1 2.00e+1
df112  1.02e+1 1.02e+1 1.24e+1 1.26e+1 1.16e+1 1.04e+1 9.89e+0 6.03e+1
     2.57e+2 3.67e+2 3.47e+2 4.33e+2 4.08e+2 4.08e+2 5.78e+2 6.31e+2
c
fc122  mrem/source-particle-cm^2 averaged over tally surface area
f122:n 485
fs122  -461 -472 460 471
sd122  1 1 1 1 64
fm122  1.512E+4
fq122  e f
cf122  10 11 12 13 14 15 16 17 20 22 27 28 30 35 40 41 50 70 90 100
     101 102 110 130 140 150 160 180 190 192 200 210 212 213 220 230
     240 250 280  290 310 320 330  340 350 360 370 380
     390 410 420
e122   2.5e-8 1.0e-7 1.0e-6 1.0e-5 1.0e-4 1.0e-3
     0.01 0.02 0.05 0.1 0.2 0.4 0.6 0.8 1.0 1.3 1.7 2.1 2.4 2.7 3.0 3.3 3.6
     4.0 4.4 5 6 7 8 9 10 12 15 20
de122  2.50e-8 1.00e-7 1.00e-6 1.00e-5 1.00e-4 1.00e-3 1.00e-2 1.00e-1
     5.00e-1 1.00e+0 2.50e+0 5.00e+0 7.00e+0 1.00e+1 1.40e+1 2.00e+1
df122  1.02e+1 1.02e+1 1.24e+1 1.26e+1 1.16e+1 1.04e+1 9.89e+0 6.03e+1
     2.57e+2 3.67e+2 3.47e+2 4.33e+2 4.08e+2 4.08e+2 5.78e+2 6.31e+2
c
fc132  mrem/source-particle-cm^2 averaged over tally surface area
f132:n 485
fs132  -465 -473 464 472
sd132  1 1 1 1 64
fm132  1.512E+4
fq132  e f
cf132  10 11 12 13 14 15 16 17 20 22 27 28 30 35 40 41 50 70 90 100
     101 102 110 130 140 150 160 180 190 192 200 210 212 213 220 230
     240 250 280  290 310 320 330  340 350 360 370 380
     390 410 420
e132   2.5e-8 1.0e-7 1.0e-6 1.0e-5 1.0e-4 1.0e-3
     0.01 0.02 0.05 0.1 0.2 0.4 0.6 0.8 1.0 1.3 1.7 2.1 2.4 2.7 3.0 3.3 3.6
     4.0 4.4 5 6 7 8 9 10 12 15 20
de132  2.50e-8 1.00e-7 1.00e-6 1.00e-5 1.00e-4 1.00e-3 1.00e-2 1.00e-1
     5.00e-1 1.00e+0 2.50e+0 5.00e+0 7.00e+0 1.00e+1 1.40e+1 2.00e+1
df132  1.02e+1 1.02e+1 1.24e+1 1.26e+1 1.16e+1 1.04e+1 9.89e+0 6.03e+1
     2.57e+2 3.67e+2 3.47e+2 4.33e+2 4.08e+2 4.08e+2 5.78e+2 6.31e+2
c
fc142  mrem/source-particle-cm^2 averaged over tally surface area
f142:n 485
fs142  -464 -473 463 472
sd142  1 1 1 1 64
```

```
fm142  1.512E+4
fq142  e f
cf142  10 11 12 13 14 15 16 17 20 22 27 28 30 35 40 41 50 70 90 100
     101 102 110 130 140 150 160 180 190 192 200 210 212 213 220 230
     240 250 280  290 310 320 330  340 350 360 370 380
     390 410 420
e142   2.5e-8 1.0e-7 1.0e-6 1.0e-5 1.0e-4 1.0e-3
     0.01 0.02 0.05 0.1 0.2 0.4 0.6 0.8 1.0 1.3 1.7 2.1 2.4 2.7 3.0 3.3 3.6
     4.0 4.4 5 6 7 8 9 10 12 15 20
de142  2.50e-8 1.00e-7 1.00e-6 1.00e-5 1.00e-4 1.00e-3 1.00e-2 1.00e-1
     5.00e-1 1.00e+0 2.50e+0 5.00e+0 7.00e+0 1.00e+1 1.40e+1 2.00e+1
df142  1.02e+1 1.02e+1 1.24e+1 1.26e+1 1.16e+1 1.04e+1 9.89e+0 6.03e+1
     2.57e+2 3.67e+2 3.47e+2 4.33e+2 4.08e+2 4.08e+2 5.78e+2 6.31e+2
c
fc152  mrem/source-particle-cm^2 averaged over tally surface area
f152:n 485
fs152  -463 -473 462 472
sd152  1 1 1 1 64
fm152  1.512E+4
fq152  e f
cf152  10 11 12 13 14 15 16 17 20 22 27 28 30 35 40 41 50 70 90 100
     101 102 110 130 140 150 160 180 190 192 200 210 212 213 220 230
     240 250 280  290 310 320 330  340 350 360 370 380
     390 410 420
e152   2.5e-8 1.0e-7 1.0e-6 1.0e-5 1.0e-4 1.0e-3
     0.01 0.02 0.05 0.1 0.2 0.4 0.6 0.8 1.0 1.3 1.7 2.1 2.4 2.7 3.0 3.3 3.6
     4.0 4.4 5 6 7 8 9 10 12 15 20
de152  2.50e-8 1.00e-7 1.00e-6 1.00e-5 1.00e-4 1.00e-3 1.00e-2 1.00e-1
     5.00e-1 1.00e+0 2.50e+0 5.00e+0 7.00e+0 1.00e+1 1.40e+1 2.00e+1
df152  1.02e+1 1.02e+1 1.24e+1 1.26e+1 1.16e+1 1.04e+1 9.89e+0 6.03e+1
     2.57e+2 3.67e+2 3.47e+2 4.33e+2 4.08e+2 4.08e+2 5.78e+2 6.31e+2
c
fc162  mrem/source-particle-cm^2 averaged over tally surface area
f162:n 485
fs162  -462 -473 461 472
sd162  1 1 1 1 64
fm162  1.512E+4
fq162  e f
cf162  10 11 12 13 14 15 16 17 20 22 27 28 30 35 40 41 50 70 90 100
     101 102 110 130 140 150 160 180 190 192 200 210 212 213 220 230
     240 250 280  290 310 320 330  340 350 360 370 380
     390 410 420
e162   2.5e-8 1.0e-7 1.0e-6 1.0e-5 1.0e-4 1.0e-3
     0.01 0.02 0.05 0.1 0.2 0.4 0.6 0.8 1.0 1.3 1.7 2.1 2.4 2.7 3.0 3.3 3.6
```

```
     4.0 4.4 5 6 7 8 9 10 12 15 20
de162  2.50e-8 1.00e-7 1.00e-6 1.00e-5 1.00e-4 1.00e-3 1.00e-2 1.00e-1
     5.00e-1 1.00e+0 2.50e+0 5.00e+0 7.00e+0 1.00e+1 1.40e+1 2.00e+1
df162  1.02e+1 1.02e+1 1.24e+1 1.26e+1 1.16e+1 1.04e+1 9.89e+0 6.03e+1
     2.57e+2 3.67e+2 3.47e+2 4.33e+2 4.08e+2 4.08e+2 5.78e+2 6.31e+2
c
fc172  mrem/source-particle-cm^2 averaged over tally surface area
f172:n 485
fs172  -461 -473 460 472
sd172  1 1 1 1 64
fm172  1.512E+4
fq172  e f
cf172  10 11 12 13 14 15 16 17 20 22 27 28 30 35 40 41 50 70 90 100
     101 102 110 130 140 150 160 180 190 192 200 210 212 213 220 230
     240 250 280  290 310 320 330  340 350 360 370 380
     390 410 420
e172   2.5e-8 1.0e-7 1.0e-6 1.0e-5 1.0e-4 1.0e-3
     0.01 0.02 0.05 0.1 0.2 0.4 0.6 0.8 1.0 1.3 1.7 2.1 2.4 2.7 3.0 3.3 3.6
     4.0 4.4 5 6 7 8 9 10 12 15 20
de172  2.50e-8 1.00e-7 1.00e-6 1.00e-5 1.00e-4 1.00e-3 1.00e-2 1.00e-1
     5.00e-1 1.00e+0 2.50e+0 5.00e+0 7.00e+0 1.00e+1 1.40e+1 2.00e+1
df172  1.02e+1 1.02e+1 1.24e+1 1.26e+1 1.16e+1 1.04e+1 9.89e+0 6.03e+1
     2.57e+2 3.67e+2 3.47e+2 4.33e+2 4.08e+2 4.08e+2 5.78e+2 6.31e+2
c
fc182  mrem/source-particle-cm^2 averaged over tally surface area
f182:n 485
fs182  -465 -474 464 473
sd182  1 1 1 1 64
fm182  1.512E+4
fq182  e f
cf182  10 11 12 13 14 15 16 17 20 22 27 28 30 35 40 41 50 70 90 100
     101 102 110 130 140 150 160 180 190 192 200 210 212 213 220 230
     240 250 280  290 310 320 330  340 350 360 370 380
     390 410 420
e182   2.5e-8 1.0e-7 1.0e-6 1.0e-5 1.0e-4 1.0e-3
     0.01 0.02 0.05 0.1 0.2 0.4 0.6 0.8 1.0 1.3 1.7 2.1 2.4 2.7 3.0 3.3 3.6
     4.0 4.4 5 6 7 8 9 10 12 15 20
de182  2.50e-8 1.00e-7 1.00e-6 1.00e-5 1.00e-4 1.00e-3 1.00e-2 1.00e-1
     5.00e-1 1.00e+0 2.50e+0 5.00e+0 7.00e+0 1.00e+1 1.40e+1 2.00e+1
df182  1.02e+1 1.02e+1 1.24e+1 1.26e+1 1.16e+1 1.04e+1 9.89e+0 6.03e+1
     2.57e+2 3.67e+2 3.47e+2 4.33e+2 4.08e+2 4.08e+2 5.78e+2 6.31e+2
c
fc192  mrem/source-particle-cm^2 averaged over tally surface area
f192:n 485
```

```
fs192  -464 -474 463 473
sd192  1 1 1 1 64
fm192  1.512E+4
fq192  e f
cf192  10 11 12 13 14 15 16 17 20 22 27 28 30 35 40 41 50 70 90 100
       101 102 110 130 140 150 160 180 190 192 200 210 212 213 220 230
       240 250 280  290 310 320 330  340 350 360 370 380
       390 410 420
e192   2.5e-8 1.0e-7 1.0e-6 1.0e-5 1.0e-4 1.0e-3
       0.01 0.02 0.05 0.1 0.2 0.4 0.6 0.8 1.0 1.3 1.7 2.1 2.4 2.7 3.0 3.3 3.6
       4.0 4.4 5 6 7 8 9 10 12 15 20
de192  2.50e-8 1.00e-7 1.00e-6 1.00e-5 1.00e-4 1.00e-3 1.00e-2 1.00e-1
       5.00e-1 1.00e+0 2.50e+0 5.00e+0 7.00e+0 1.00e+1 1.40e+1 2.00e+1
df192  1.02e+1 1.02e+1 1.24e+1 1.26e+1 1.16e+1 1.04e+1 9.89e+0 6.03e+1
       2.57e+2 3.67e+2 3.47e+2 4.33e+2 4.08e+2 4.08e+2 5.78e+2 6.31e+2
c
fc202  mrem/source-particle-cm^2 averaged over tally surface area
f202:n 485
fs202  -463 -474 462 473
sd202  1 1 1 1 64
fm202  1.512E+4
fq202  e f
cf202  10 11 12 13 14 15 16 17 20 22 27 28 30 35 40 41 50 70 90 100
       101 102 110 130 140 150 160 180 190 192 200 210 212 213 220 230
       240 250 280  290 310 320 330  340 350 360 370 380
       390 410 420
e202   2.5e-8 1.0e-7 1.0e-6 1.0e-5 1.0e-4 1.0e-3
       0.01 0.02 0.05 0.1 0.2 0.4 0.6 0.8 1.0 1.3 1.7 2.1 2.4 2.7 3.0 3.3 3.6
       4.0 4.4 5 6 7 8 9 10 12 15 20
de202  2.50e-8 1.00e-7 1.00e-6 1.00e-5 1.00e-4 1.00e-3 1.00e-2 1.00e-1
       5.00e-1 1.00e+0 2.50e+0 5.00e+0 7.00e+0 1.00e+1 1.40e+1 2.00e+1
df202  1.02e+1 1.02e+1 1.24e+1 1.26e+1 1.16e+1 1.04e+1 9.89e+0 6.03e+1
       2.57e+2 3.67e+2 3.47e+2 4.33e+2 4.08e+2 4.08e+2 5.78e+2 6.31e+2
c
fc212  mrem/source-particle-cm^2 averaged over tally surface area
f212:n 485
fs212  -462 -474 461 473
sd212  1 1 1 1 64
fm212  1.512E+4
fq212  e f
cf212  10 11 12 13 14 15 16 17 20 22 27 28 30 35 40 41 50 70 90 100
       101 102 110 130 140 150 160 180 190 192 200 210 212 213 220 230
       240 250 280  290 310 320 330  340 350 360 370 380
       390 410 420
```

```
e212   2.5e-8 1.0e-7 1.0e-6 1.0e-5 1.0e-4 1.0e-3
       0.01 0.02 0.05 0.1 0.2 0.4 0.6 0.8 1.0 1.3 1.7 2.1 2.4 2.7 3.0 3.3 3.6
       4.0 4.4 5 6 7 8 9 10 12 15 20
de212  2.50e-8 1.00e-7 1.00e-6 1.00e-5 1.00e-4 1.00e-3 1.00e-2 1.00e-1
       5.00e-1 1.00e+0 2.50e+0 5.00e+0 7.00e+0 1.00e+1 1.40e+1 2.00e+1
df212  1.02e+1 1.02e+1 1.24e+1 1.26e+1 1.16e+1 1.04e+1 9.89e+0 6.03e+1
       2.57e+2 3.67e+2 3.47e+2 4.33e+2 4.08e+2 4.08e+2 5.78e+2 6.31e+2
c
fc222  mrem/source-particle-cm^2 averaged over tally surface area
f222:n 485
fs222  -461 -474 460 473
sd222  1 1 1 1 64
fm222  1.512E+4
fq222  e f
cf222  10 11 12 13 14 15 16 17 20 22 27 28 30 35 40 41 50 70 90 100
       101 102 110 130 140 150 160 180 190 192 200 210 212 213 220 230
       240 250 280  290 310 320 330  340 350 360 370 380
       390 410 420
e222   2.5e-8 1.0e-7 1.0e-6 1.0e-5 1.0e-4 1.0e-3
       0.01 0.02 0.05 0.1 0.2 0.4 0.6 0.8 1.0 1.3 1.7 2.1 2.4 2.7 3.0 3.3 3.6
       4.0 4.4 5 6 7 8 9 10 12 15 20
de222  2.50e-8 1.00e-7 1.00e-6 1.00e-5 1.00e-4 1.00e-3 1.00e-2 1.00e-1
       5.00e-1 1.00e+0 2.50e+0 5.00e+0 7.00e+0 1.00e+1 1.40e+1 2.00e+1
df222  1.02e+1 1.02e+1 1.24e+1 1.26e+1 1.16e+1 1.04e+1 9.89e+0 6.03e+1
       2.57e+2 3.67e+2 3.47e+2 4.33e+2 4.08e+2 4.08e+2 5.78e+2 6.31e+2
c
fc232  mrem/source-particle-cm^2 averaged over tally surface area
f232:n 485
fs232  -465 -475 464 474
sd232  1 1 1 1 64
fm232  1.512E+4
fq232  e f
cf232  10 11 12 13 14 15 16 17 20 22 27 28 30 35 40 41 50 70 90 100
       101 102 110 130 140 150 160 180 190 192 200 210 212 213 220 230
       240 250 280  290 310 320 330  340 350 360 370 380
       390 410 420
e232   2.5e-8 1.0e-7 1.0e-6 1.0e-5 1.0e-4 1.0e-3
       0.01 0.02 0.05 0.1 0.2 0.4 0.6 0.8 1.0 1.3 1.7 2.1 2.4 2.7 3.0 3.3 3.6
       4.0 4.4 5 6 7 8 9 10 12 15 20
de232  2.50e-8 1.00e-7 1.00e-6 1.00e-5 1.00e-4 1.00e-3 1.00e-2 1.00e-1
       5.00e-1 1.00e+0 2.50e+0 5.00e+0 7.00e+0 1.00e+1 1.40e+1 2.00e+1
df232  1.02e+1 1.02e+1 1.24e+1 1.26e+1 1.16e+1 1.04e+1 9.89e+0 6.03e+1
       2.57e+2 3.67e+2 3.47e+2 4.33e+2 4.08e+2 4.08e+2 5.78e+2 6.31e+2
c
```

```
fc242  mrem/source-particle-cm^2 averaged over tally surface area
f242:n 485
fs242  -464 -475 463 474
sd242  1 1 1 1 64
fm242  1.512E+4
fq242  e f
cf242  10 11 12 13 14 15 16 17 20 22 27 28 30 35 40 41 50 70 90 100
     101 102 110 130 140 150 160 180 190 192 200 210 212 213 220 230
     240 250 280  290 310 320 330  340 350 360 370 380
     390 410 420
e242   2.5e-8 1.0e-7 1.0e-6 1.0e-5 1.0e-4 1.0e-3
     0.01 0.02 0.05 0.1 0.2 0.4 0.6 0.8 1.0 1.3 1.7 2.1 2.4 2.7 3.0 3.3 3.6
     4.0 4.4 5 6 7 8 9 10 12 15 20
de242  2.50e-8 1.00e-7 1.00e-6 1.00e-5 1.00e-4 1.00e-3 1.00e-2 1.00e-1
     5.00e-1 1.00e+0 2.50e+0 5.00e+0 7.00e+0 1.00e+1 1.40e+1 2.00e+1
df242  1.02e+1 1.02e+1 1.24e+1 1.26e+1 1.16e+1 1.04e+1 9.89e+0 6.03e+1
     2.57e+2 3.67e+2 3.47e+2 4.33e+2 4.08e+2 4.08e+2 5.78e+2 6.31e+2
c
fc252  mrem/source-particle-cm^2 averaged over tally surface area
f252:n 485
fs252  -463 -475 462 474
sd252  1 1 1 1 64
fm252  1.512E+4
fq252  e f
cf252  10 11 12 13 14 15 16 17 20 22 27 28 30 35 40 41 50 70 90 100
     101 102 110 130 140 150 160 180 190 192 200 210 212 213 220 230
     240 250 280  290 310 320 330  340 350 360 370 380
     390 410 420
e252   2.5e-8 1.0e-7 1.0e-6 1.0e-5 1.0e-4 1.0e-3
     0.01 0.02 0.05 0.1 0.2 0.4 0.6 0.8 1.0 1.3 1.7 2.1 2.4 2.7 3.0 3.3 3.6
     4.0 4.4 5 6 7 8 9 10 12 15 20
de252  2.50e-8 1.00e-7 1.00e-6 1.00e-5 1.00e-4 1.00e-3 1.00e-2 1.00e-1
     5.00e-1 1.00e+0 2.50e+0 5.00e+0 7.00e+0 1.00e+1 1.40e+1 2.00e+1
df252  1.02e+1 1.02e+1 1.24e+1 1.26e+1 1.16e+1 1.04e+1 9.89e+0 6.03e+1
     2.57e+2 3.67e+2 3.47e+2 4.33e+2 4.08e+2 4.08e+2 5.78e+2 6.31e+2
c
fc262  mrem/source-particle-cm^2 averaged over tally surface area
f262:n 485
fs262  -462 -475 461 474
sd262  1 1 1 1 64
fm262  1.512E+4
fq262  e f
cf262  10 11 12 13 14 15 16 17 20 22 27 28 30 35 40 41 50 70 90 100
     101 102 110 130 140 150 160 180 190 192 200 210 212 213 220 230
```

```
      240 250 280  290 310 320 330  340 350 360 370 380
      390 410 420
e262   2.5e-8 1.0e-7 1.0e-6 1.0e-5 1.0e-4 1.0e-3
      0.01 0.02 0.05 0.1 0.2 0.4 0.6 0.8 1.0 1.3 1.7 2.1 2.4 2.7 3.0 3.3 3.6
      4.0 4.4 5 6 7 8 9 10 12 15 20
de262  2.50e-8 1.00e-7 1.00e-6 1.00e-5 1.00e-4 1.00e-3 1.00e-2 1.00e-1
      5.00e-1 1.00e+0 2.50e+0 5.00e+0 7.00e+0 1.00e+1 1.40e+1 2.00e+1
df262  1.02e+1 1.02e+1 1.24e+1 1.26e+1 1.16e+1 1.04e+1 9.89e+0 6.03e+1
      2.57e+2 3.67e+2 3.47e+2 4.33e+2 4.08e+2 4.08e+2 5.78e+2 6.31e+2
c
fc272  mrem/source-particle-cm^2 averaged over tally surface area
f272:n 485
fs272  -461 -475 460 474
sd272  1 1 1 1 64
fm272  1.512E+4
fq272  e f
cf272  10 11 12 13 14 15 16 17 20 22 27 28 30 35 40 41 50 70 90 100
      101 102 110 130 140 150 160 180 190 192 200 210 212 213 220 230
      240 250 280  290 310 320 330  340 350 360 370 380
      390 410 420
e272   2.5e-8 1.0e-7 1.0e-6 1.0e-5 1.0e-4 1.0e-3
      0.01 0.02 0.05 0.1 0.2 0.4 0.6 0.8 1.0 1.3 1.7 2.1 2.4 2.7 3.0 3.3 3.6
      4.0 4.4 5 6 7 8 9 10 12 15 20
de272  2.50e-8 1.00e-7 1.00e-6 1.00e-5 1.00e-4 1.00e-3 1.00e-2 1.00e-1
      5.00e-1 1.00e+0 2.50e+0 5.00e+0 7.00e+0 1.00e+1 1.40e+1 2.00e+1
df272  1.02e+1 1.02e+1 1.24e+1 1.26e+1 1.16e+1 1.04e+1 9.89e+0 6.03e+1
      2.57e+2 3.67e+2 3.47e+2 4.33e+2 4.08e+2 4.08e+2 5.78e+2 6.31e+2
c
fc282  mrem/source-particle-cm^2 averaged over tally surface area
f282:n 485
fs282  -465 -476 464 475
sd282  1 1 1 1 64
fm282  1.512E+4
fq282  e f
cf282  10 11 12 13 14 15 16 17 20 22 27 28 30 35 40 41 50 70 90 100
      101 102 110 130 140 150 160 180 190 192 200 210 212 213 220 230
      240 250 280  290 310 320 330  340 350 360 370 380
      390 410 420
e282   2.5e-8 1.0e-7 1.0e-6 1.0e-5 1.0e-4 1.0e-3
      0.01 0.02 0.05 0.1 0.2 0.4 0.6 0.8 1.0 1.3 1.7 2.1 2.4 2.7 3.0 3.3 3.6
      4.0 4.4 5 6 7 8 9 10 12 15 20
de282  2.50e-8 1.00e-7 1.00e-6 1.00e-5 1.00e-4 1.00e-3 1.00e-2 1.00e-1
      5.00e-1 1.00e+0 2.50e+0 5.00e+0 7.00e+0 1.00e+1 1.40e+1 2.00e+1
df282  1.02e+1 1.02e+1 1.24e+1 1.26e+1 1.16e+1 1.04e+1 9.89e+0 6.03e+1
```

2.57e+2 3.67e+2 3.47e+2 4.33e+2 4.08e+2 4.08e+2 5.78e+2 6.31e+2
c
fc292 mrem/source-particle-cm^2 averaged over tally surface area
f292:n 485
fs292 -464 -476 463 475
sd292 1 1 1 1 64
fm292 1.512E+4
fq292 e f
cf292 10 11 12 13 14 15 16 17 20 22 27 28 30 35 40 41 50 70 90 100
101 102 110 130 140 150 160 180 190 192 200 210 212 213 220 230
240 250 280 290 310 320 330 340 350 360 370 380
390 410 420
e292 2.5e-8 1.0e-7 1.0e-6 1.0e-5 1.0e-4 1.0e-3
0.01 0.02 0.05 0.1 0.2 0.4 0.6 0.8 1.0 1.3 1.7 2.1 2.4 2.7 3.0 3.3 3.6
4.0 4.4 5 6 7 8 9 10 12 15 20
de292 2.50e-8 1.00e-7 1.00e-6 1.00e-5 1.00e-4 1.00e-3 1.00e-2 1.00e-1
5.00e-1 1.00e+0 2.50e+0 5.00e+0 7.00e+0 1.00e+1 1.40e+1 2.00e+1
df292 1.02e+1 1.02e+1 1.24e+1 1.26e+1 1.16e+1 1.04e+1 9.89e+0 6.03e+1
2.57e+2 3.67e+2 3.47e+2 4.33e+2 4.08e+2 4.08e+2 5.78e+2 6.31e+2
c
fc302 mrem/source-particle-cm^2 averaged over tally surface area
f302:n 485
fs302 -463 -476 462 475
sd302 1 1 1 1 64
fm302 1.512E+4
fq302 e f
cf302 10 11 12 13 14 15 16 17 20 22 27 28 30 35 40 41 50 70 90 100
101 102 110 130 140 150 160 180 190 192 200 210 212 213 220 230
240 250 280 290 310 320 330 340 350 360 370 380
390 410 420
e302 2.5e-8 1.0e-7 1.0e-6 1.0e-5 1.0e-4 1.0e-3
0.01 0.02 0.05 0.1 0.2 0.4 0.6 0.8 1.0 1.3 1.7 2.1 2.4 2.7 3.0 3.3 3.6
4.0 4.4 5 6 7 8 9 10 12 15 20
de302 2.50e-8 1.00e-7 1.00e-6 1.00e-5 1.00e-4 1.00e-3 1.00e-2 1.00e-1
5.00e-1 1.00e+0 2.50e+0 5.00e+0 7.00e+0 1.00e+1 1.40e+1 2.00e+1
df302 1.02e+1 1.02e+1 1.24e+1 1.26e+1 1.16e+1 1.04e+1 9.89e+0 6.03e+1
2.57e+2 3.67e+2 3.47e+2 4.33e+2 4.08e+2 4.08e+2 5.78e+2 6.31e+2
c
fc312 mrem/source-particle-cm^2 averaged over tally surface area
f312:n 485
fs312 -462 -476 461 475
sd312 1 1 1 1 64
fm312 1.512E+4
fq312 e f

```
cf312  10 11 12 13 14 15 16 17 20 22 27 28 30 35 40 41 50 70 90 100
       101 102 110 130 140 150 160 180 190 192 200 210 212 213 220 230
       240 250 280  290 310 320 330  340 350 360 370 380
       390 410 420
e312   2.5e-8 1.0e-7 1.0e-6 1.0e-5 1.0e-4 1.0e-3
       0.01 0.02 0.05 0.1 0.2 0.4 0.6 0.8 1.0 1.3 1.7 2.1 2.4 2.7 3.0 3.3 3.6
       4.0 4.4 5 6 7 8 9 10 12 15 20
de312  2.50e-8 1.00e-7 1.00e-6 1.00e-5 1.00e-4 1.00e-3 1.00e-2 1.00e-1
       5.00e-1 1.00e+0 2.50e+0 5.00e+0 7.00e+0 1.00e+1 1.40e+1 2.00e+1
df312  1.02e+1 1.02e+1 1.24e+1 1.26e+1 1.16e+1 1.04e+1 9.89e+0 6.03e+1
       2.57e+2 3.67e+2 3.47e+2 4.33e+2 4.08e+2 4.08e+2 5.78e+2 6.31e+2
c
fc322  mrem/source-particle-cm^2 averaged over tally surface area
f322:n 485
fs322  -461 -476 460 475
sd322  1 1 1 1 64
fm322  1.512E+4
fq322  e f
cf322  10 11 12 13 14 15 16 17 20 22 27 28 30 35 40 41 50 70 90 100
       101 102 110 130 140 150 160 180 190 192 200 210 212 213 220 230
       240 250 280  290 310 320 330  340 350 360 370 380
       390 410 420
e322   2.5e-8 1.0e-7 1.0e-6 1.0e-5 1.0e-4 1.0e-3
       0.01 0.02 0.05 0.1 0.2 0.4 0.6 0.8 1.0 1.3 1.7 2.1 2.4 2.7 3.0 3.3 3.6
       4.0 4.4 5 6 7 8 9 10 12 15 20
de322  2.50e-8 1.00e-7 1.00e-6 1.00e-5 1.00e-4 1.00e-3 1.00e-2 1.00e-1
       5.00e-1 1.00e+0 2.50e+0 5.00e+0 7.00e+0 1.00e+1 1.40e+1 2.00e+1
df322  1.02e+1 1.02e+1 1.24e+1 1.26e+1 1.16e+1 1.04e+1 9.89e+0 6.03e+1
       2.57e+2 3.67e+2 3.47e+2 4.33e+2 4.08e+2 4.08e+2 5.78e+2 6.31e+2
c
c
*****************************************************************************
******
c      End of Simulated Dosimeter Lattice Tally
c
*****************************************************************************
******
c
c
*****************************************************************************
******
c      Phantom Organ/Tissue Tally Cells (rad to rem based on ANSI 1977)
```

```
c
**********************************************************************
******
c
c     Rad to rem conversion using ANSI/ANS-6.1.1-1977 Mean Quality Factors
c
c     Multiplier for rad-to-rem conversion =
c     [X MeV/g/basis] x [Y rem/rad] x [1 rad/6.242E+7 Mev/g] x [1000 mrem/rem]
c     = 1.602E-5 * XY mrem/h-basis
c
c     ANSI 1977 Mean Quality Factors
c     c
c     de0    2.5e-8   1.0e-7   1.0e-6   1.0e-5   1.0e-4   1.0e-3   1.0e-2   1.0e-1
c            5.0e-1   1.0      2.5      5.0      7.0      10.0     14.0     20.0
c     df0    2        2        2        2        2        2        2.5      7.5
c            11       11       9        8        7        6.5      7.5      8
c
c
**********************************************************************
******
c
fc306  Brain
f306:n 180
fm306  1.602e-5
e306   0.01 0.02 0.05 0.1 0.2 0.4 0.6 0.8 1.0 1.3 1.7 2.1 2.4 2.7 3.0 3.3 3.6
       4.0 4.4 5 6 7 8 9 10 12 15 20
de306  2.5e-8   1.0e-7   1.0e-6   1.0e-5   1.0e-4   1.0e-3   1.0e-2   1.0e-1
       5.0e-1   1.0      2.5      5.0      7.0      10.0     14.0     20.0
df306  2        2        2        2        2        2        2.5      7.5
       11       11       9        8        7        6.5      7.5      8
c
fc316  Thyroid
f316:n 390
fm316  1.602e-5
e316   2.5e-8 1.0e-7 1.0e-6 1.0e-5 1.0e-4 1.0e-3
       0.01 0.02 0.05 0.1 0.2 0.4 0.6 0.8 1.0 1.3 1.7 2.1 2.4 2.7 3.0 3.3 3.6
       4.0 4.4 5 6 7 8 9 10 12 15 20
de316  2.5e-8   1.0e-7   1.0e-6   1.0e-5   1.0e-4   1.0e-3   1.0e-2   1.0e-1
       5.0e-1   1.0      2.5      5.0      7.0      10.0     14.0     20.0
df316  2        2        2        2        2        2        2.5      7.5
       11       11       9        8        7        6.5      7.5      8
c
fc326  Thymus
f326:n 380
```

```
fm326  1.602e-5
e326   2.5e-8 1.0e-7 1.0e-6 1.0e-5 1.0e-4 1.0e-3
       0.01 0.02 0.05 0.1 0.2 0.4 0.6 0.8 1.0 1.3 1.7 2.1 2.4 2.7 3.0 3.3 3.6
       4.0 4.4 5 6 7 8 9 10 12 15 20
de326  2.5e-8   1.0e-7   1.0e-6   1.0e-5   1.0e-4   1.0e-3   1.0e-2   1.0e-1
       5.0e-1   1.0      2.5      5.0      7.0      10.0     14.0     20.0
df326  2        2        2        2        2        2        2.5      7.5
       11       11       9        8        7        6.5      7.5      8
c
fc336  Lungs
f336:n 330  T
fm336  1.602e-5
e336   2.5e-8 1.0e-7 1.0e-6 1.0e-5 1.0e-4 1.0e-3
       0.01 0.02 0.05 0.1 0.2 0.4 0.6 0.8 1.0 1.3 1.7 2.1 2.4 2.7 3.0 3.3 3.6
       4.0 4.4 5 6 7 8 9 10 12 15 20
de336  2.5e-8   1.0e-7   1.0e-6   1.0e-5   1.0e-4   1.0e-3   1.0e-2   1.0e-1
       5.0e-1   1.0      2.5      5.0      7.0      10.0     14.0     20.0
df336  2        2        2        2        2        2        2.5      7.5
       11       11       9        8        7        6.5      7.5      8
c
fc346  Heart
f346:n 290
fm346  1.602e-5
e346   2.5e-8 1.0e-7 1.0e-6 1.0e-5 1.0e-4 1.0e-3
       0.01 0.02 0.05 0.1 0.2 0.4 0.6 0.8 1.0 1.3 1.7 2.1 2.4 2.7 3.0 3.3 3.6
       4.0 4.4 5 6 7 8 9 10 12 15 20
de346  2.5e-8   1.0e-7   1.0e-6   1.0e-5   1.0e-4   1.0e-3   1.0e-2   1.0e-1
       5.0e-1   1.0      2.5      5.0      7.0      10.0     14.0     20.0
df346  2        2        2        2        2        2        2.5      7.5
       11       11       9        8        7        6.5      7.5      8
c
fc356  Adrenals
f356:n 160
fm356  1.602e-5
e356   2.5e-8 1.0e-7 1.0e-6 1.0e-5 1.0e-4 1.0e-3
       0.01 0.02 0.05 0.1 0.2 0.4 0.6 0.8 1.0 1.3 1.7 2.1 2.4 2.7 3.0 3.3 3.6
       4.0 4.4 5 6 7 8 9 10 12 15 20
de356  2.5e-8   1.0e-7   1.0e-6   1.0e-5   1.0e-4   1.0e-3   1.0e-2   1.0e-1
       5.0e-1   1.0      2.5      5.0      7.0      10.0     14.0     20.0
df356  2        2        2        2        2        2        2.5      7.5
       11       11       9        8        7        6.5      7.5      8
c
fc366  Kidneys
f366:n 310
```

fm366 1.602e-5
e366 2.5e-8 1.0e-7 1.0e-6 1.0e-5 1.0e-4 1.0e-3
0.01 0.02 0.05 0.1 0.2 0.4 0.6 0.8 1.0 1.3 1.7 2.1 2.4 2.7 3.0 3.3 3.6
4.0 4.4 5 6 7 8 9 10 12 15 20
de366 2.5e-8 1.0e-7 1.0e-6 1.0e-5 1.0e-4 1.0e-3 1.0e-2 1.0e-1
5.0e-1 1.0 2.5 5.0 7.0 10.0 14.0 20.0
df366 2 2 2 2 2 2 2.5 7.5
11 11 9 8 7 6.5 7.5 8
c
fc376 Liver
f376:n 320
fm376 1.602e-5
e376 2.5e-8 1.0e-7 1.0e-6 1.0e-5 1.0e-4 1.0e-3
0.01 0.02 0.05 0.1 0.2 0.4 0.6 0.8 1.0 1.3 1.7 2.1 2.4 2.7 3.0 3.3 3.6
4.0 4.4 5 6 7 8 9 10 12 15 20
de376 2.5e-8 1.0e-7 1.0e-6 1.0e-5 1.0e-4 1.0e-3 1.0e-2 1.0e-1
5.0e-1 1.0 2.5 5.0 7.0 10.0 14.0 20.0
df376 2 2 2 2 2 2 2.5 7.5
11 11 9 8 7 6.5 7.5 8
c
fc386 Gall Bladder
f386:n 290
fm386 1.602e-5
e386 2.5e-8 1.0e-7 1.0e-6 1.0e-5 1.0e-4 1.0e-3
0.01 0.02 0.05 0.1 0.2 0.4 0.6 0.8 1.0 1.3 1.7 2.1 2.4 2.7 3.0 3.3 3.6
4.0 4.4 5 6 7 8 9 10 12 15 20
de386 2.5e-8 1.0e-7 1.0e-6 1.0e-5 1.0e-4 1.0e-3 1.0e-2 1.0e-1
5.0e-1 1.0 2.5 5.0 7.0 10.0 14.0 20.0
df386 2 2 2 2 2 2 2.5 7.5
11 11 9 8 7 6.5 7.5 8
c
fc396 Pancreas
f396:n 350
fm396 1.602e-5
e396 2.5e-8 1.0e-7 1.0e-6 1.0e-5 1.0e-4 1.0e-3
0.01 0.02 0.05 0.1 0.2 0.4 0.6 0.8 1.0 1.3 1.7 2.1 2.4 2.7 3.0 3.3 3.6
4.0 4.4 5 6 7 8 9 10 12 15 20
de396 2.5e-8 1.0e-7 1.0e-6 1.0e-5 1.0e-4 1.0e-3 1.0e-2 1.0e-1
5.0e-1 1.0 2.5 5.0 7.0 10.0 14.0 20.0
df396 2 2 2 2 2 2 2.5 7.5
11 11 9 8 7 6.5 7.5 8
c
fc406 Spleen
f406:n 360

fm406 1.602e-5
e406 2.5e-8 1.0e-7 1.0e-6 1.0e-5 1.0e-4 1.0e-3
0.01 0.02 0.05 0.1 0.2 0.4 0.6 0.8 1.0 1.3 1.7 2.1 2.4 2.7 3.0 3.3 3.6
4.0 4.4 5 6 7 8 9 10 12 15 20
de406 2.5e-8 1.0e-7 1.0e-6 1.0e-5 1.0e-4 1.0e-3 1.0e-2 1.0e-1
5.0e-1 1.0 2.5 5.0 7.0 10.0 14.0 20.0
df406 2 2 2 2 2 2 2.5 7.5
11 11 9 8 7 6.5 7.5 8
c
fc416 Eosphagus
f416:n 212
fm416 1.602e-5
e416 2.5e-8 1.0e-7 1.0e-6 1.0e-5 1.0e-4 1.0e-3
0.01 0.02 0.05 0.1 0.2 0.4 0.6 0.8 1.0 1.3 1.7 2.1 2.4 2.7 3.0 3.3 3.6
4.0 4.4 5 6 7 8 9 10 12 15 20
de416 2.5e-8 1.0e-7 1.0e-6 1.0e-5 1.0e-4 1.0e-3 1.0e-2 1.0e-1
5.0e-1 1.0 2.5 5.0 7.0 10.0 14.0 20.0
df416 2 2 2 2 2 2 2.5 7.5
11 11 9 8 7 6.5 7.5 8
c
fc426 Stomach
f426:n 210
fm426 1.602e-5
e426 2.5e-8 1.0e-7 1.0e-6 1.0e-5 1.0e-4 1.0e-3
0.01 0.02 0.05 0.1 0.2 0.4 0.6 0.8 1.0 1.3 1.7 2.1 2.4 2.7 3.0 3.3 3.6
4.0 4.4 5 6 7 8 9 10 12 15 20
de426 2.5e-8 1.0e-7 1.0e-6 1.0e-5 1.0e-4 1.0e-3 1.0e-2 1.0e-1
5.0e-1 1.0 2.5 5.0 7.0 10.0 14.0 20.0
df426 2 2 2 2 2 2 2.5 7.5
11 11 9 8 7 6.5 7.5 8
c
fc436 Small Intestine
f436:n 220
fm436 1.602e-5
e436 2.5e-8 1.0e-7 1.0e-6 1.0e-5 1.0e-4 1.0e-3
0.01 0.02 0.05 0.1 0.2 0.4 0.6 0.8 1.0 1.3 1.7 2.1 2.4 2.7 3.0 3.3 3.6
4.0 4.4 5 6 7 8 9 10 12 15 20
de436 2.5e-8 1.0e-7 1.0e-6 1.0e-5 1.0e-4 1.0e-3 1.0e-2 1.0e-1
5.0e-1 1.0 2.5 5.0 7.0 10.0 14.0 20.0
df436 2 2 2 2 2 2 2.5 7.5
11 11 9 8 7 6.5 7.5 8
c
fc446 Ascending Colon
f446:n 230

```
fm446  1.602e-5
e446   2.5e-8 1.0e-7 1.0e-6 1.0e-5 1.0e-4 1.0e-3
       0.01 0.02 0.05 0.1 0.2 0.4 0.6 0.8 1.0 1.3 1.7 2.1 2.4 2.7 3.0 3.3 3.6
       4.0 4.4 5 6 7 8 9 10 12 15 20
de446  2.5e-8   1.0e-7   1.0e-6   1.0e-5   1.0e-4   1.0e-3   1.0e-2   1.0e-1
       5.0e-1   1.0      2.5      5.0      7.0      10.0     14.0     20.0
df446  2        2        2        2        2        2        2.5      7.5
       11       11       9        8        7        6.5      7.5      8
c
fc456  Transverse Colon
f456:n 240
fm456  1.602e-5
e456   2.5e-8 1.0e-7 1.0e-6 1.0e-5 1.0e-4 1.0e-3
       0.01 0.02 0.05 0.1 0.2 0.4 0.6 0.8 1.0 1.3 1.7 2.1 2.4 2.7 3.0 3.3 3.6
       4.0 4.4 5 6 7 8 9 10 12 15 20
de456  2.5e-8   1.0e-7   1.0e-6   1.0e-5   1.0e-4   1.0e-3   1.0e-2   1.0e-1
       5.0e-1   1.0      2.5      5.0      7.0      10.0     14.0     20.0
df456  2        2        2        2        2        2        2.5      7.5
       11       11       9        8        7        6.5      7.5      8
c
fc466  Descending Colon
f466:n 250
fm466  1.602e-5
e466   2.5e-8 1.0e-7 1.0e-6 1.0e-5 1.0e-4 1.0e-3
       0.01 0.02 0.05 0.1 0.2 0.4 0.6 0.8 1.0 1.3 1.7 2.1 2.4 2.7 3.0 3.3 3.6
       4.0 4.4 5 6 7 8 9 10 12 15 20
de466  2.5e-8   1.0e-7   1.0e-6   1.0e-5   1.0e-4   1.0e-3   1.0e-2   1.0e-1
       5.0e-1   1.0      2.5      5.0      7.0      10.0     14.0     20.0
df466  2        2        2        2        2        2        2.5      7.5
       11       11       9        8        7        6.5      7.5      8
c
fc476  Sigmoid Colon
f476:n 280  T
fm476  1.602e-5
e476   2.5e-8 1.0e-7 1.0e-6 1.0e-5 1.0e-4 1.0e-3
       0.01 0.02 0.05 0.1 0.2 0.4 0.6 0.8 1.0 1.3 1.7 2.1 2.4 2.7 3.0 3.3 3.6
       4.0 4.4 5 6 7 8 9 10 12 15 20
de476  2.5e-8   1.0e-7   1.0e-6   1.0e-5   1.0e-4   1.0e-3   1.0e-2   1.0e-1
       5.0e-1   1.0      2.5      5.0      7.0      10.0     14.0     20.0
df476  2        2        2        2        2        2        2.5      7.5
       11       11       9        8        7        6.5      7.5      8
c
fc486  Bladder
f486:n 410
```

```
fm486  1.602e-5
e486   2.5e-8 1.0e-7 1.0e-6 1.0e-5 1.0e-4 1.0e-3
       0.01 0.02 0.05 0.1 0.2 0.4 0.6 0.8 1.0 1.3 1.7 2.1 2.4 2.7 3.0 3.3 3.6
       4.0 4.4 5 6 7 8 9 10 12 15 20
de486  2.5e-8   1.0e-7   1.0e-6   1.0e-5   1.0e-4   1.0e-3   1.0e-2   1.0e-1
       5.0e-1   1.0      2.5      5.0      7.0      10.0     14.0     20.0
df486  2        2        2        2        2        2        2.5      7.5
       11       11       9        8        7        6.5      7.5      8
c
fc496  Testes
f496:n 370
fm496  1.602e-5
e496   2.5e-8 1.0e-7 1.0e-6 1.0e-5 1.0e-4 1.0e-3
       0.01 0.02 0.05 0.1 0.2 0.4 0.6 0.8 1.0 1.3 1.7 2.1 2.4 2.7 3.0 3.3 3.6
       4.0 4.4 5 6 7 8 9 10 12 15 20
de496  2.5e-8   1.0e-7   1.0e-6   1.0e-5   1.0e-4   1.0e-3   1.0e-2   1.0e-1
       5.0e-1   1.0      2.5      5.0      7.0      10.0     14.0     20.0
df496  2        2        2        2        2        2        2.5      7.5
       11       11       9        8        7        6.5      7.5      8
c
fc506  Genitalia
f506:n 40
fm506  1.602e-5
e506   2.5e-8 1.0e-7 1.0e-6 1.0e-5 1.0e-4 1.0e-3
       0.01 0.02 0.05 0.1 0.2 0.4 0.6 0.8 1.0 1.3 1.7 2.1 2.4 2.7 3.0 3.3 3.6
       4.0 4.4 5 6 7 8 9 10 12 15 20
de506  2.5e-8   1.0e-7   1.0e-6   1.0e-5   1.0e-4   1.0e-3   1.0e-2   1.0e-1
       5.0e-1   1.0      2.5      5.0      7.0      10.0     14.0     20.0
df506  2        2        2        2        2        2        2.5      7.5
       11       11       9        8        7        6.5      7.5      8
c
fc516  Skin
f516:n 22 28 17 41 34 35 192 T
fm516  1.602e-5
e516   2.5e-8 1.0e-7 1.0e-6 1.0e-5 1.0e-4 1.0e-3
       0.01 0.02 0.05 0.1 0.2 0.4 0.6 0.8 1.0 1.3 1.7 2.1 2.4 2.7 3.0 3.3 3.6
       4.0 4.4 5 6 7 8 9 10 12 15 20
de516  2.5e-8   1.0e-7   1.0e-6   1.0e-5   1.0e-4   1.0e-3   1.0e-2   1.0e-1
       5.0e-1   1.0      2.5      5.0      7.0      10.0     14.0     20.0
df516  2        2        2        2        2        2        2.5      7.5
       11       11       9        8        7        6.5      7.5      8
c
fc526  Bone
f526:n 50 70 90 100 101 102 110 130 140 150 T
```

```
fm526  1.602e-5
e526   2.5e-8 1.0e-7 1.0e-6 1.0e-5 1.0e-4 1.0e-3
       0.01 0.02 0.05 0.1 0.2 0.4 0.6 0.8 1.0 1.3 1.7 2.1 2.4 2.7 3.0 3.3 3.6
       4.0 4.4 5 6 7 8 9 10 12 15 20
de526  2.5e-8   1.0e-7   1.0e-6   1.0e-5   1.0e-4   1.0e-3   1.0e-2   1.0e-1
       5.0e-1   1.0      2.5      5.0      7.0      10.0     14.0     20.0
df526  2        2        2        2        2        2        2.5      7.5
       11       11       9        8        7        6.5      7.5      8
c
fc536  Breast
f536:n 190
fm536  1.602e-5
e536   2.5e-8 1.0e-7 1.0e-6 1.0e-5 1.0e-4 1.0e-3
       0.01 0.02 0.05 0.1 0.2 0.4 0.6 0.8 1.0 1.3 1.7 2.1 2.4 2.7 3.0 3.3 3.6
       4.0 4.4 5 6 7 8 9 10 12 15 20
de536  2.5e-8   1.0e-7   1.0e-6   1.0e-5   1.0e-4   1.0e-3   1.0e-2   1.0e-1
       5.0e-1   1.0      2.5      5.0      7.0      10.0     14.0     20.0
df536  2        2        2        2        2        2        2.5      7.5
       11       11       9        8        7        6.5      7.5      8
c
fc546  Ovaries
f546:n 340
fm546  1.602e-5
e546   2.5e-8 1.0e-7 1.0e-6 1.0e-5 1.0e-4 1.0e-3
       0.01 0.02 0.05 0.1 0.2 0.4 0.6 0.8 1.0 1.3 1.7 2.1 2.4 2.7 3.0 3.3 3.6
       4.0 4.4 5 6 7 8 9 10 12 15 20
de546  2.5e-8   1.0e-7   1.0e-6   1.0e-5   1.0e-4   1.0e-3   1.0e-2   1.0e-1
       5.0e-1   1.0      2.5      5.0      7.0      10.0     14.0     20.0
df546  2        2        2        2        2        2        2.5      7.5
       11       11       9        8        7        6.5      7.5      8
c
fc556  Uterus
f556:n 420
fm556  1.602e-5
e556   2.5e-8 1.0e-7 1.0e-6 1.0e-5 1.0e-4 1.0e-3
       0.01 0.02 0.05 0.1 0.2 0.4 0.6 0.8 1.0 1.3 1.7 2.1 2.4 2.7 3.0 3.3 3.6
       4.0 4.4 5 6 7 8 9 10 12 15 20
de556  2.5e-8   1.0e-7   1.0e-6   1.0e-5   1.0e-4   1.0e-3   1.0e-2   1.0e-1
       5.0e-1   1.0      2.5      5.0      7.0      10.0     14.0     20.0
df556  2        2        2        2        2        2        2.5      7.5
       11       11       9        8        7        6.5      7.5      8
c
```

```
c
**********************************************************************
******
c     End of Phantom Organ/Tissue Tally Cells
c
**********************************************************************
******
c
c
c
**********************************************************************
******
c     Mesh Tally - ANSI 1977
c
**********************************************************************
******
c
c     If mesh tally is used to correspond to the dosimeter tally plane of a
c     phantom, then the distance from the GB to the mesh tally is 13.68 and
c     has a width of 0.1 cm or is  16.8 cm toward GB from center line of
c     phantom (i.e. 149.86 - 16.8 = 133.06)
c
c     If the center line is at y' then set up the mesh tally in y direction to
c     be y'-m*8-4 (m+n)i y'+n*8+4
c     (i.e., to cover the front of the glove box need |y|> 91.44, which can
c     accomplish by n=8 and m=16 in this case.)
c
c     Should cover the z region as where the dosimeter can be normally worn.
c     With Z=0 is the ground floor that walk on, need zmin <= 82 and zmax>=162,
c     i.e., zmin=82-p*8 and zmax=162+q*8. If want to cover the z direction from
c     about the floor level to about the glove box height, then p=10 and q=2
c     in this case. (zmin (p+q+9)i zmax)
c
c
de1    2.50e-8 1.00e-7 1.00e-6 1.00e-5 1.00e-4 1.00e-3 1.00e-2 1.00e-1
       5.00e-1 1.00e+0 2.50e+0 5.00e+0 7.00e+0 1.00e+1 1.40e+1 2.00e+1
df1    1.02e+1 1.02e+1 1.24e+1 1.26e+1 1.16e+1 1.04e+1 9.89e+0 6.03e+1
       2.57e+2 3.67e+2 3.47e+2 4.33e+2 4.08e+2 4.08e+2 5.78e+2 6.31e+2
c
tmesh
rmesh1:n
  cora1  72.10 72.20
  corb1 -96.44 24i 103.56
  corc1    2 21i 178
```

```
endmd
fm1 1.512E+4
c
c
c
************************************************************************
******
c     End of Mesh Tally - ANSI 1977
c
************************************************************************
******
c
c
c
************************************************************************
******
c     END OF TALLY CARDS
c
************************************************************************
******
c
c
c
************************************************************************
******
c     Other Data Cards
c
************************************************************************
******
c
c     Phantom Transformation
tr69   88.90 35.56 80 0 1 0 1  0 0 0 0 1 1
c
dbcn   12j 137753
prdmp  j 5e7 j 1
ctme   9999
nps    3e7
print  10 40 50 60 110 140 160 161 162 170
imp:n  1 69r 0
```

Appendix L: Phantom Dose Estimates For NETL Glove Box Experiment

Table L-1: Phantom Dose Estimates at 1 ft using ICRP 26.

Male with breasts

Tissue	Testes	Breast	RBM	Lungs	Thyroid	NBS	Stomach	Transverse Colon	Gentalia	Thymus	Liver	EDE
mrem/b	1.67E+02	1.64E+02	3.90E+01	1.57E+00	7.14E+01	3.71E+01	1.71E+02	1.47E+02	1.31E+02	1.29E+02	1.29E+02	
fraction	0.25	0.15	0.12	0.12	0.03	0.03	0.06	0.06	0.06	0.06	0.06	
mrem/b	4.18E+01	2.47E+01	4.68E+00	1.88E-01	2.14E+00	1.11E+00	1.03E+01	8.80E+00	7.84E+00	7.76E+00	7.74E+00	1.17E+02

Male without breasts

Tissue	Testes	Breast	RBM	Lungs	Thyroid	NBS	Stomach	Transverse Colon	Gentalia	Thymus	Liver	EDE
mrem/b	1.67E+02	1.64E+02	3.90E+01	1.57E+00	7.14E+01	3.71E+01	1.71E+02	1.47E+02	1.31E+02	1.29E+02	1.29E+02	
fraction	0.25	0	0.12	0.12	0.03	0.03	0.06	0.06	0.06	0.06	0.06	
mrem/b	4.18E+01	0.00E+00	4.68E+00	1.88E-01	2.14E+00	1.11E+00	1.03E+01	8.80E+00	7.84E+00	7.76E+00	7.74E+00	9.24E+01

Female

Tissue	Ovaries	Breast	RBM	Lungs	Thyroid	NBS	Stomach	Transverse Colon	Gentalia	Thymus	Liver	EDE
mrem/b	3.95E+01	1.64E+02	3.90E+01	1.57E+00	7.14E+01	3.71E+01	1.71E+02	1.47E+02	1.31E+02	1.29E+02	1.29E+02	
fraction	0.25	0.15	0.12	0.12	0.03	0.03	0.06	0.06	0.06	0.06	0.06	
mrem/b	9.87E+00	2.47E+01	4.68E+00	1.88E-01	2.14E+00	1.11E+00	1.03E+01	8.80E+00	7.84E+00	7.76E+00	7.74E+00	8.51E+01

Table L-2: Phantom Dose Estimates at 1 ft using ICRP 60.

Male with breasts

Tissue	Testes	RBM	Colon	Lungs	Stomach	Bladder	Breast	Liver	Esophagus	Thyroid	Skin	NBS	Remainder	ED
mrem/b	1.67E+02	3.90E+01	8.82E+01	1.57E+00	1.71E+02	7.03E+01	1.64E+02	1.29E+02	5.65E+01	7.14E+01	6.50E+01	3.71E+01	5.54E+01	
fraction	0.2	0.12	0.12	0.12	0.12	0.05	0.05	0.05	0.05	0.05	0.01	0.01	0.05	
mrem/b	3.35E+01	4.68E+00	1.06E+01	1.88E-01	2.06E+01	3.52E+00	8.22E+00	6.45E+00	2.83E+00	3.57E+00	6.50E-01	3.71E-01	2.77E+00	9.79E+01

Male without breasts

Tissue	Testes	RBM	Colon	Lungs	Stomach	Bladder	Breast	Liver	Esophagus	Thyroid	Skin	NBS	Remainder	ED
mrem/hr-b	1.67E+02	3.90E+01	8.82E+01	1.57E+00	1.71E+02	7.03E+01	1.64E+02	1.29E+02	5.65E+01	7.14E+01	6.50E+01	3.71E+01	5.54E+01	
fraction	0.2	0.12	0.12	0.12	0.12	0.05	0	0.05	0.05	0.05	0.01	0.01	0.05	
mrem/b	3.35E+01	4.68E+00	1.06E+01	1.88E-01	2.06E+01	3.52E+00	0.00E+00	6.45E+00	2.83E+00	3.57E+00	6.50E-01	3.71E-01	2.77E+00	8.96E+01

Female

Tissue	Ovaries	RBM	Colon	Lungs	Stomach	Bladder	Breast	Liver	Esophagus	Thyroid	Skin	NBS	Remainder	ED
mrem/hr-b	3.95E+01	3.90E+01	8.82E+01	1.57E+00	1.71E+02	7.03E+01	1.64E+02	1.29E+02	5.65E+01	7.14E+01	6.50E+01	3.71E+01	5.63E+01	
fraction	0.2	0.12	0.12	0.12	0.12	0.05	0.05	0.05	0.05	0.05	0.01	0.01	0.05	
mrem/hr-b	7.89E+00	4.68E+00	1.06E+01	1.88E-01	2.06E+01	3.52E+00	8.22E+00	6.45E+00	2.83E+00	3.57E+00	6.50E-01	3.71E-01	2.82E+00	7.23E+01

Table L-3: Phantom Dose Estimates at 3 ft using ICRP 26.

Male with breasts

Tissue	Testes	Breast	RBM	Lungs	Thyroid	NBS	Thymus	Stomach	Liver	Pancreas	Esophagus	EDE
mrem/b	1.67E+01	4.58E+01	1.13E+01	5.27E-01	4.87E+01	1.07E+01	4.34E+01	2.71E+01	2.40E+01	1.85E+01	1.82E+01	
fraction	0.25	0.15	0.12	0.12	0.03	0.03	0.06	0.06	0.06	0.06	0.06	
mrem/b	4.18E+00	6.87E+00	1.35E+00	6.33E-02	1.46E+00	3.22E-01	2.60E+00	1.62E+00	1.44E+00	1.11E+00	1.09E+00	2.21E+01

Male without breasts

Tissue	Testes	Breast	RBM	Lungs	Thyroid	NBS	Thymus	Stomach	Liver	Pancreas	Esophagus	EDE
mrem/b	1.67E+01	4.58E+01	1.13E+01	5.27E-01	4.87E+01	1.07E+01	4.34E+01	2.71E+01	2.40E+01	1.85E+01	1.82E+01	
fraction	0.25	0	0.12	0.12	0.03	0.03	0.06	0.06	0.06	0.06	0.06	
mrem/b	4.18E+00	0.00E+00	1.35E+00	6.33E-02	1.46E+00	3.22E-01	2.60E+00	1.62E+00	1.44E+00	1.11E+00	1.09E+00	1.52E+01

Female

Tissue	Ovaries	Breast	RBM	Lungs	Thyroid	NBS	Thymus	Stomach	Liver	Pancreas	Esophagus	EDE
mrem/b	6.07E+00	4.58E+01	1.13E+01	5.27E-01	4.87E+01	1.07E+01	4.34E+01	2.71E+01	2.40E+01	1.85E+01	1.82E+01	
fraction	0.25	0.15	0.12	0.12	0.03	0.03	0.06	0.06	0.06	0.06	0.06	
mrem/b	1.52E+00	6.87E+00	1.35E+00	6.33E-02	1.46E+00	3.22E-01	2.60E+00	1.62E+00	1.44E+00	1.11E+00	1.09E+00	1.95E+01

Table L-4: Phantom Dose Estimates at 3 ft using ICRP 60.

Male with breasts

Tissue	Testes	RBM	Colon	Lungs	Stomach	Bladder	Breast	Liver	Esophagus	Thyroid	Skin	NBS	Remainder	ED
mrem/b	1.67E+01	1.13E+01	8.64E+00	5.27E-01	2.71E+01	1.07E+01	4.58E+01	2.40E+01	1.82E+01	4.87E+01	1.48E+01	1.07E+01	1.03E+01	
fraction	0.2	0.12	0.12	0.12	0.12	0.05	0.05	0.05	0.05	0.05	0.01	0.01	0.05	
mrem/b	3.35E+00	1.35E+00	1.04E+00	6.33E-02	3.25E+00	5.36E-01	2.29E+00	1.20E+00	9.09E-01	2.43E+00	1.48E-01	1.07E-01	5.16E-01	1.72E+01

Male without breasts

Tissue	Testes	RBM	Colon	Lungs	Stomach	Bladder	Breast	Liver	Esophagus	Thyroid	Skin	NBS	Remainder	ED
mrem/hr-b	1.67E+01	1.13E+01	8.64E+00	5.27E-01	2.71E+01	1.07E+01	4.58E+01	2.40E+01	1.82E+01	4.87E+01	1.48E+01	1.07E+01	1.03E+01	
fraction	0.2	0.12	0.12	0.12	0.12	0.05	0	0.05	0.05	0.05	0.01	0.01	0.05	
mrem/b	3.35E+00	1.35E+00	1.04E+00	6.33E-02	3.25E+00	5.36E-01	0.00E+00	1.20E+00	9.09E-01	2.43E+00	1.48E-01	1.07E-01	5.16E-01	1.49E+01

Female

Tissue	Ovaries	RBM	Colon	Lungs	Stomach	Bladder	Breast	Liver	Esophagus	Thyroid	Skin	NBS	Remainder	ED
mrem/hr-b	6.07E+00	1.13E+01	8.64E+00	5.27E-01	2.71E+01	1.07E+01	4.58E+01	2.40E+01	1.82E+01	4.87E+01	1.48E+01	1.07E+01	1.05E+01	
fraction	0.2	0.12	0.12	0.12	0.12	0.05	0.05	0.05	0.05	0.05	0.01	0.01	0.05	
mrem/hr-b	1.21E+00	1.35E+00	1.04E+00	6.33E-02	3.25E+00	5.36E-01	2.29E+00	1.20E+00	9.09E-01	2.43E+00	1.48E-01	1.07E-01	5.24E-01	1.51E+01

References

AGS. 1998. Guidelines for Gloveboxes, 2nd ed., American Glovebox Society Report AGS-G001-1998.Cristy, M., and Eckerman, K.F. 2003. The ORNL Mathematical Phantom Series, ORNL reports, available at http://homer.hsr.ornl.gov/.

ANS. 1977. Neutron and Gammy-Ray Flux-to-Dose-Rate Factors, ANSI standard, ANSI/ANS-6.1.1-1977.

ANS. 1991. Neutron and Gamma-Ray Fluence-to-Dose Factors, ANSI standard, ANSI/ANS-6.1.1-1991.

Bielajew, A.F. Fundamentals of the Monte Carlo Method for Neutral and Charged Particle Transport, Ann Arbor: University of Michigan.

Booth, T.E. 1985. A Sample Problem for Variance Reduction in MCNP, LANL report LA-10363-MS.

Briesmeister, J.F., ed. 2000. MCNP™ – A General Monte Carlo N-Particle Transport Code, LANL Report LA-13709-M, Version 4C.

Brown, T.H. 1997. Effect of Compositional Variation in Plutonium on Process Shielding Design, Transactions of the American Nuclear Society 77:320-322.

Carter, L.L., and Cashwell, E.D. 1975. Particle Transport Simulation with the Monte Carlo Method, Energy and Research Development Administration (ERDA) report, TID-26607.

Cross, W.G. and Ing, H. 1985. Conversion and Quality Factors Relating Neutron Fluence and Dosimetric Quantities, Radiation Protection Dosimetry 10(1-4):29-42.

Dargis, G. 2003. NS-3 with B4C, e-mail to A. Crawford including NS-3 Neutron and/or Gamma Shielding Material, Data Sheet, NAC International, 27 May 2003.

Dietze, G. 1998. Effective Dose – What Type of Quantity has been Created? (Editorial) Radiation Protection Dosimetry 76(3):131-133.

DOE. 1999. Title 10 Code Federal Regulations Part 835, Occupational Radiation Protection, U.S. Government Printing Office.

Dooley, D.E., and Kornreich, D.E. 1998. An MCNP Model of Glove Boxes in a Plutonium Processing Facility, Transactions of the American Nuclear Society 79:255-257.

Drake, P. and Bartlett, D.T. 1997. Neutron Dose Equivalent Rates Calculated from Measured Neutron Angular and Energy Distributions in Working Environments, Radiation Protection Dosimetry 70(1-4):235-239.

Drexler, G., Williams, G., and Zankl, M. 1985. The Meaning and the Principle of Determination of Effective Dose Equivalent in Radiation Protection, Radiation Protection Dosimetry 12(2):95-100.

Dupree, S.A., and Fraley, S.K. 2002. A Monte Carlo Primer. New York: Kluwer Academic/Plenum Publishers.

Endres, G.W.R., 1987. Tanner, J.E., Scherpelz, R.I., and Hadlock, D.E. 1987. Calculation Methods for Determining Dose Equivalent, Pacific Northwest Laboratory report, PNL-SA-14753.

Gauld, I.C., Hermann, O.W., and Westfall, R.M. 2002. ORIGEN-S: SCALE System Module to Calculate Fuel Depletion, Actinide Transmutation, Fission Product Buildup and Decay, and Associated Radiation Source Terms, ORNL Report, RONL/NUREG/CSD-2/V2/R7.

George, G.L. 1998. Neutron Correction Factor Measurements from a Reflected and a Non-Reflected Neutron Spectrum, LANL unpublished report.

George, G.L. and Shores, E.F. 2000. Methods for Effective Dose Equivalent Calculation, LANL report LA-UR-00-2816.

Hall, E.J. and Brenner, D.J. 1992. The Biological Effectiveness of Neutrons; Implications for Radiation Protection, Radiation Protection Dosimetry 44(1/4):1-9.

Healy, J.W. 1970. Los Alamos Handbook of Radiation Monitoring 1970, Los Alamos Scientific Laboratory Report LA-4400.

Hendricks, J.S., et al. 2003. MCNPX, Version 2.5C, LANL Report LA-UR-03-2202.

Hertz, M.R. 1961. Shipping Data Plutonium Neutron Source, Monsanto Research Corporation - Mound Laboratory shipping manifest, MWO 36901-119.

Hoffman, J. M. 1998. The LANL Model 8823 Whole-Body TLD and Associated Dose Algorithm, LANL Technical Basis Document, ESH4-PDO-TBD-02, R0.

Hoffman, J.M. and Mallett, M.W. 1999. The LANL Model 8823 Whole-Body TLD and Associated Dose Algorithm, Health Physics 77(Supplement 2):S96-S103.

Hollnagel, R.A. 1992. Calculated Effective Doses in Anthropoid Phantoms for Broad Neutron Beams with Energies from Thermal to 19 MeV, Radiation Protection Dosimetry 44(1/4):155-158.

Hollnagel, R.A., Alberts, W.G., and Dietze, G. 1994. On the Definition of the Remainder in ICRP 60 with respect to External Neutron Irradiation, Radiation Protection Dosimetry 55(2):93-97.

HPS. 1997. An American National Standard – Criteria for Performing Multiple Dosimetry, American National Standards Institute (ANSI), Inc. standard, HPS N13.41-1997.

ICRP. 1977. Recommendations of the International Commission on Radiological Protection, International Commission on Radiological Protection (ICRP) Publication 26, Annals of the ICRP 1(3).

ICRP. 1987. Data for Use in Protection Against External Radiation, ICRP Publication 51, Annals of the ICRP 17(2/3).

ICRP. 1991. 1990 Recommendations of the International Commission on Radiological Protection, Publication 60, Annals of the ICRP 21:(1-3), Pergamon Press, Oxford.

ICRP. 1996. Conversion Coefficients for Use in Radiological Protection, ICRP Publication 74, Annals of the ICRP 26(3/4).

Kalos, M.H., and Whitlock, P.A. 1986. Monte Carlo Methods Volume I: Basics. New York: John Wiley & Sons.

Kim, C.H., Reece, W.D., and Poston Sr., J.W. 1998. Effective Dose Equivalent and Effective Dose for Photon Dose Exposures from Point and Disk Sources on the Floor, Health Physics 75(2):170-178.

Kim, C.H., Reece, W.D., and Poston Sr., J.W. 1999, Calculation of Effective Doses for Broad Parallel Photon Beams, Health Physics 76(2):156-161.

Kim, C.H., and Reece, W.D. 2000. Overestimation of the Two-Dosimeter Approach and Movement of Radiation Workers During Exposure, Radiation Protection Management 17(6):17-25.

Kramer, R., and Drexler, G. 1982. On the Calculation of Effective Dose Equivalent, Radiation Protection Dosimetry 3(1-2):13-24.

Lehmer, D.H. 1951. Mathematical Methods in Large-Scale Computing Units, Ann. Comp. Lab., Harvard Univ. 26, 141 –146.

Lewis, E. E. and Miller Jr., W. F. 1993. Computational Methods of Neutron Transport, American Nuclear Society, La Grange Park, IL.

Lux, I. And Loblinger, L. 1991. Monte Carlo Particle Transport Methods: Neutron and Photon Calculations, Boca Raton: CRC Press.

McDonald, J.C., Schwartz, R.B., and Thomas, R.H. 1998. Neutron Dose Equivalent Conversion Coefficients Have Changed in the Last Forty Years… Haven't They?, Radiation Protection Dosimetry 78(2):147-149.

Mallet, M.W. 1997. Los Alamos National Laboratory Model 8823 Personnel Dosimeter Lower Limit of Detectability and Angular Dependence Studies, LANL memo ESH-4-MTS-97:047.

Meinhold, C.B. 1992. New Quantities for Use in Radiation Protection, Radiation Protection Dosimetry 44(1/4):151-154.

Morstin, K., Kopec, M., and Schmitz, T. 1992. Equivalent Dose Versus Dose Equivalent for Neutrons Based on New ICRP Recommendations, Radiation Protection Dosimetry 44(1/4):159-164.

NRC. 1991. Title 10 Code Federal Regulations Part 20, Standards for Protection Against Radiation, U.S. Government Printing Office.

O'Kelly, S, 2003. Personal communication. April 30.

Portal, G, and Dietze, G. 1992. Implications of New ICRP and ICRU Recommendations for Neutron Dosimetry, Radiation Protection Dosimetry 44(1/4):165-170.

Poston Sr., J.W. 2000. Dosimetry: Where We've Been, Where We Are, Where We're Going, American Nuclear Society Proceedings on the Topical Meeting on "Radiation Protection for our National Priorities: Medicine, the Environment, and the Legacy":630-636.

Prael, R.E. and Lichtenstein, H. 1989. User Guide to LCS: The LAHET Code System, LANL Report LA-UR-89-3014.

Profio, A.E. 1976. Experimental Reactor Physics, New York: Wiley.

Profio, A.E. 1979. Radiation Shielding and Dosimetry, New York: Wiley.

Reece, W.D., Poston Sr., J.W., and Xu, X.G. 1994. Determining the Effective Dose Equivalent for External Photon Radiation: Calculational Results for Beam and Point Source Geometries, Radiation Protection Dosimetry 55(1):5-21.

Reece, W.D., and Xu, X.G. 1997. Determining Effective Dose Equivalent for External Photon Radiation: Assessing Effective Dose Equivalent from Personal Dosimeter Readings, Radiation Protection Dosimetry 69(3):167-178.

Richards, J.R. 2003. Information concerning RSN-105S-M9: a proportional counter manufactured by Reuter-Stokes, Inc. A GE Power Systems Company, email message to author, May 14.

Shores, E.F. 1999. Calculated Dose Equivalent Rates from PuBe Source Neutrons, LANL report LA-UR-99-3595.

Siebert, R.L. and Thomas, R.H. 1997. Computational Dosimetry, Radiation Protection Dosimetry 70(1-4):371-378.Taylor, L.S. 1979. Organization for Radiation Protection – The Operations of the ICRP and NCRP, 1928-1974, Report, DOE/TIC-10124, National Technical Information Services, Springfield, VA 22161.

Sinclair, W.K. 1990. Quality Factor, Concepts and Issues, Radiation Protection Dosimetry 31(1/4):355-359.

Shultis, J.K., and Faw, R.E. 2000. Radiation Shielding, American Nuclear Society (ANS).

Tanner, J.E., Piper, R.K., Leonowich, J.A., and Faust, L.G. 1992., Verification of an Effective Dose Equivalent Model for Neutrons, Radiation Protection Dosimetry 44(1/4):171-174.

Taylor, L.S. 1981. The Development of Radiation Protection Standards (1925-1940), Health Physics 41:227-232.

Thomas, R.H. 1997. We Have Met the Enemy and He is Us", (Editorial) Radiation Protection Dosimetry 71(2):83-84.

Thomas, R.H. 1998. The Seven Deadly Sins of Dosimetry in Radiation Protection, (Editorial) Radiation Protection Dosimetry 78(2):87-90.

Van Dam, J., Beauduin, M., Gregoire, V., Gueulette, J., Laublin, G., and Wambersie, A. 1992. Variation of Neutron RBE as a Function of Energy for Different Biological Systems: A Review, Radiation Protection Dosimetry 44(1/4):41-44.

Van Riper, K.A. 2002. Body Builder User's Guide, White Rock Science.

Van Riper, K.A. 2002. MORITZ Geometry Tool, White Rock Science.

Wilson, W.B., Perry, R.T., Shores, E.F., Charlton, W.S., Parish, T.A., Estes, G.P., Brown, T.H., Arthur, E.D., Bozoian, M., England, T.R., Madland, D.G., and Stewart, J.E. 2002. SOURCES 4C: A Code for Calculating (α,n), Spontaneous Fission, and Delayed Neutron Sources and Spectra, LANL Report LA-UR-02-1617.

X-5 Monte Carlo Team. 2003. MCNP – A General Monte Carlo N-Particle Transport Code, Version 5, Volume 1: Overview and Theory, LANL report LA-UR-03-1987.

Zankl, M. and Drexler, G. 1995, An Analysis of the Equivalent Dose Calculation for the Remainder Tissues, Health Physics 69(3):346-355.

Zankl, M., Petoussi, N., and Drexler, G. 1992. Effective Dose and Effective Dose Equivalent – The Impact of the New ICRP Definition for External Photon Irradiation, Health Physics 62(5):395-399.

Zankl, M. 1999. Personal Dose Equivalent for Photons and its Variation with Dosimeter Position, Health Phys. 76(2): 162-170.

Vita

Arthur Bryan Crawford was born in Santa Fe, New Mexico on 17 March 1950, son of Harvey Elihu Crawford and Johnnie Lee Young of Holland, Georgia and Wichita Falls, Texas respectively. He was raised in Albuquerque, New Mexico and attended Bel Air Elementary, McKinley Jr. High, and Del Norte High School in Albuquerque, graduating in May 1968. He completed his Bachelor of Science in Physics and Mathematics at the University of New Mexico, Albuquerque in May 1972. He was accepted for graduate studies at the University of Illinois, Champaign-Urbana where he received Master of Science degrees in Physics and Nuclear Engineering in May 1974 and May 1979 respectively..

In June, 1979, he began work at Oak Ridge National laboratory in the Consolidated Fuel Reprocessing Program and then changed to the safety analysis arena when fuel reprocessing fell out of favor. In October 1983, he went to Los Alamos, where he has worked as a nuclear safety analyst for several different companies and for the University of California who operates Los Alamos National Laboratory. He currently works in the Radiation Protection Services group at Los Alamos doing radiological engineering design and analyses for different activities at Los Alamos and in the DOE complex.. He is a registered professional engineer in the State of New Mexico.

He has an interest in teaching. While at the University of Illinois, he taught different engineering physics classes for first and second year students He also has a teaching certificate and has taught mathematics and science at the secondary level in Santa Fe as circumstances allowed.

In the Washington DC Temple of the Church of Jesus Christ of Latter Day Saints, he married Pamela Elaine Stafford of Olney, Illinois on 19 December 1975 for time and

all eternity. They are blessed with 3 daughters: Charity Annalee Crawford and Roshana Shalene Crawford, of Urbana, Illinois, Amber Adrielle Crawford, of Oak Ridge, Tennessee, and a son, Caleb Bryan Eli Crawford, Los Alamos, New Mexico.

Publications and presentations include:

A. Crawford, Chaired Session 11.D – "Natural Phenomena Impacts to Doe Facilities", Eleventh Annual SAWG Workshop – American Nuclear Society Embedded Topical Meeting, Milwaukee, WI, June 14-21, 2001.

A. Crawford, "Authorization Basis Dose Assessment Calculations for a Hot Cell", Paper + presentation to Eleventh Annual SAWG Workshop – American Nuclear Society Embedded Topical Meeting, Milwaukee, WI, June 14-21, 2001.

Presented paper for T. Rudell, "The Cerro Grande Fire – From Wildfire Modeling through the Fire Aftermath", Eleventh Annual SAWG Workshop – American Nuclear Society Embedded Topical Meeting, Milwaukee, WI, June 14-21, 2001.

A. Crawford, Presentation and chair of session on "Design/QA Controls for SSCs", Authorization Basis Workshop, Las Vegas, NV, January 25, 2000.

G. Medford, et al, "Chemistry and Metallurgy Research (CMR) Facility Final Safety Analysis Report", LANL report CMR-FAC-95-291, October 1995.

J. L. LaChance, A. Kowaczkowski, A. Crawford, J. Holderness, and G. Medford, "A Risk Assessment and Management Tool for the Chemistry and Metallurgy Research Building," Proceedings of PSAM - II (March 20-25, 1994).

R. J. Romero et al, "The Chemistry and Metallurgy Research (CMR) Building Final Safety Analysis Report (FSAR)," Los Alamos National Laboratory draft report (February 1994).

J. H. Holderness, G. T. Medford, and A. B. Crawford, "Multidimensional Uncertainty Propagation for Process Event Trees," Proceedings of the International Topical Meeting on Probabilistic Safety Assessment (January 26-29, 1993).

R. J. Romero, et al, "The Chemistry and Metallurgy Research (CMR) Building Interim Safety Analysis Report (ISAR)," LANL report (March 23, 1992).

A. Kowaczkowski, et al, "DP Safety Survey Report, HB Line, Savannah River Site," U.S. DOE Office of Defense Programs draft report (January 1, 1992).

A. Kowaczkowski, et al, "DP Safety Survey Report, FB Line, Savannah River Site,"

U.S. DOE Office of Defense Programs draft report (January 1, 1992).

A. Kowaczkowski, et al, “DP Safety Survey Report, Building 12-42, South Vault, Pantex Plant,” U.S. DOE Office of Defense Programs draft report (January 1, 1992).

G. T. Medford, et al, “DP Safety Survey Report, Weapon Subsystem Laboratory TA-41-4 and Underground Vault TA-41-1, Los Alamos National Laboratory,” U.S. DOE Office of Defense Programs draft report (September 1991).

A. B. Crawford, “Comparison of ‘Requirements for the NMSF’ and the Approved Environmental Assessment (EA) with FONSI,” letter report to Dave Post, et al (July 1, 1991).

C. L. Faust, and A. B. Crawford, “Draft PSAR SNML Project,” LANL report SNML-89-021, Rev. B. (May 1990).

D. W. Stack, et al, “A Level One Probabilistic Risk Assessment of the N Reactor,” Vols. 1 and 2, LANL draft letter report (October 1987).

F. A. Guevara, L. G. Hoffman, W. A. Scoggins, C. M. Seabourn, C. C. Thomas, Jr., and A. B. Crawford, “Independent Safety Review of the E. I. du Pont de Nemours and Company Savannah River Plant Building 221 HB-Line Phase II Enhanced Neptunium Oxide Facility,” LANL letter report (July 1987).

C. A. Anderson, L. M. Carruthers, A. B. Crawford, G. F. Jones, and J. E. Hyder, “Independent Safety Review of the Teledyne Energy Systems Radioisotope Thermoelectric Generator Shipping Package,” LANL letter report (October 6, 1986).

A. B. Crawford and J. E. Hyder, “Independent Safety Review of the Foster Wheeler Energy Applications, Inc. Transportable Cesium Irradiator (TPCI),” LANL letter report (September 24, 1986).

A. B. Crawford, J. C. Elder, F. A. Guevara, W. A. Scoggins, C. M. Seabourn, and C. C. Thomas, “Independent Safety Review of the Martin Marietta Energy Systems, Inc. Thorium-Uranium Recycle Facility Californium Facility,” LANL letter report (February 20, 1986).

T. P. Suchocki, et al, “Savannah River Reactor Probabilistic Safety Assessment,” LANL classified draft letter report (January 1986).

A. B. Crawford, J. C. Elder, C. A. Linder, and C. C. Thomas, “Technical Evaluation Report Concerning the Proposed Renewal of the Operating License for the University of Lowell Research Reactor, Docket 50-223,” LANL letter report (October 16, 1985).

R. W. Andrae, A. B. Crawford, and J. E. Hyder, “Independent Safety Review of the Nuclear Packaging, Inc. Transportable Cesium Irradiator (TPCI) Shipping Cask,” LANL letter report (September 1985).

A. B. Crawford and J. E. Hyder, “Independent Safety Review of Rockwell International Rockwell Hanford Operation Proposed Plutonium Nitrate Transfer Between the PUREX Facility and the Plutonium Finishing Plant,” LANL letter report (August 8, 1985).

C. A. Linder, A. B. Crawford, and J. C. Elder, “Technical Evaluation Report Concerning the Proposed Construction Permit/Operating License for the University of Texas Triga Reactor, Docket 50-602,” LANL letter report (May 1985).

C. A. Linder and A. B. Crawford, “Technical Evaluation Report Concerning the Proposed Renewal of the Operating License for the Manhattan College Zero Power Reactor, Docket 50-199,” LANL letter report (January 1985).

C. C. Thomas, A. B. Crawford, J. E. Hyder, and C. A. Linder, “Technical Evaluation Report Concerning the Proposed Renewal of the Operating License for the University of Missouri-Rolla Research Reactor, Docket 50-123,” LANL letter report (January 1985).

A. B. Crawford, “Threat Assessment Book for the Vermont Yankee Nuclear Power Station,” LANL letter report (August 1984).

A. B. Crawford, J. E. Hyder, C. A. Linder, and C. C. Thomas, “Technical Evaluation Report Concerning the Proposed Renewal of the Operating License for the General Electric Nuclear Test Reactor, Docket No. 50-073,” LANL letter report (June 19, 1984).

A. B. Crawford, J. E. Hyder, and A. E. Sanchez-Pope, “Technical Evaluation Report Concerning the Proposed Renewal of the Operating License for the Westinghouse Nuclear Training Reactor, Docket No. 50-087,” LANL letter report (March 14, 1984).

A. B. Crawford, R. B. Gallagher, R. H. Guymon, K. H. Harrington, M. P. Johnson, G. T. Mays, and W. P. Poore, “Sequence Coding and Search System Coders Manual for the Licensee Event Reports, Vols. 1 and 2,” Oak Ridge National Laboratory (ORNL) report ORNL/NSIC-189 (March 1983).

M. L. Casada, A. B. Crawford, K. H. Harrington, and G. T. Mays, “Review of Operating Experience History of Yankee Rowe through 1980,” ORNL report ORNL/NSIC-204 (August 1982).

M. L. Casada, A. B. Crawford, K. H. Harrington, and G. T. Mays, “Review of Operating History of San Onofre-1 through 1980,” ORNL report ORNL/NSIC-201 (May 1982).

R. D. Hurt, S. J. Hurrel, J. W. Wachter, T. L. Hebble, and A. B. Crawford, “Experimental Demonstration of Microscopic Process Monitoring,” ORNL report ORNL/TM-7848 (January 1982).

A. B. Crawford, C. A. Kukielka, G. N. Lagerberg, and G. T. Mays, “Review of Operating Experience History of Dresden-2 through 1980,” ORNL report ORNL/NSIC-199 (September 1981).

R. D. Hurt, J. W. Wachter, T. L. Hebble, A. B. Crawford, and S. J. Hurrel, “Microscopic Process Monitoring,” Nuclear Materials Management Journal 9(1), 53-55 (Spring 1980).

Permanent address: 5 Juego Place, Santa Fe, NM 87508

This dissertation was typed by the author.